ΠΑΝΕΠΙΣΤΗΜΙΟ ΠΕΛΟΠΟΝΝΗΣΟΥ

ΣΧΟΛΗ ΟΙΚΟΝΟΜΙΑΣ ΚΑΙ ΤΕΧΝΟΛΟΓΙΑΣ

Τμήμα Πληροφορικής και Τηλεπικοινωνιών

ΔΙΔΑΚΤΟΡΙΚΗ ΔΙΑΤΡΙΒΗ:

An Electronic Nose System for Urban Search and Rescue Operations

Αντώνιος Ανυφαντής

Τρίπολη, Ιούνιος 2021

ΠΑΝΕΠΙΣΤΗΜΙΟ ΠΕΛΟΠΟΝΝΗΣΟΥ

ΣΧΟΛΗ ΟΙΚΟΝΟΜΙΑΣ ΚΑΙ ΤΕΧΝΟΛΟΓΙΑΣ

Τμήμα Πληροφορικής και Τηλεπικοινωνιών

An Electronic Nose System for Urban Search and Rescue Operations

ΔΙΔΑΚΤΟΡΙΚΗ ΔΙΑΤΡΙΒΗ του

Αντωνίου Ανυφαντή

Τριμελής συμβουλευτική επιτροπή: Σπυρίδων Μπλιώνας (επιβλέπων)
Δημήτριος Τσουκαλάς
Σταύρος Χατζανδρούλης

Υποστηρίχθηκε την 28η Ιουνίου 2021 ενώπιον της Επταμελούς Εξεταστικής Επιτροπής:

.... Σπυρίδων Μπλιώνας Αναπληρωτής Καθηγητής του τμήματος Πληροφορικής και Τηλεπικοινωνιών του Πανεπιστημίου Πελοποννήσου	.... Σταύρος Χατζανδρούλης Ερευνητής του Ινστιτούτου Νανοεπιστήμης και Νανοτεχνολογίας Δημόκριτος	.... Δημήτριος Τσουκαλάς Καθηγητής του τομέα Φυσικής της Σχολής Εφαρμοσμένων Μαθηματικών και Φυσικών Επιστημών του ΕΜΠ
.... Δημήτριος Βλάχος Αναπληρωτής Καθηγητής του τμήματος Πληροφορικής και Τηλεπικοινωνιών του Πανεπιστημίου Πελοποννήσου	.... Νικόλαος Σαγιάς Αναπληρωτής Καθηγητής του τμήματος Πληροφορικής και Τηλεπικοινωνιών του Πανεπιστημίου Πελοποννήσου	.... Γρηγόρης Καλτσάς Καθηγητής του τμήματος Ηλεκτρολόγων και Ηλεκτρονικών Μηχανικών του Πανεπιστημίου Δυτικής Αττικής
	.... Γιώργος Κορνάρος Επίκουρος Καθηγητής του τμήματος Ηλεκτρολόγων Μηχανικών και Μηχανικών Υπολογιστών του Μεσογειακού Πανεπιστημίου	

Επιτελική σύνοψη

Σε αυτή τη διδακτορική διατριβή παρουσιάζεται η επιτυχημένη δοκιμή ενός συστήματος ηλεκτρονικής μύτης, καθώς και όλη η έρευνα που χρειάστηκε για να προκύψει αυτή, και η οποία έχει ως σκοπό την ανίχνευση παγιδευμένων ανθρώπων καθώς και επικίνδυνων ατμοσφαιρικών καταστάσεων στα ερείπια κτηρίων σε περιπτώσεις επιχειρήσεων έρευνας και διάσωσης σε αστικά περιβάλλοντα. Εισαγωγικά παρουσιάζεται το πεδίο εφαρμογής στο οποίο προσπαθεί να δώσει λύσεις αυτή η εργασία, οι υπάρχουσες λύσεις και μέθοδοι με ή χωρίς αισθητήρες αερίων, καθώς επίσης αναλύεται το περιβάλλον από τη σκοπιά της ανίχνευσης. Παρουσιάζονται οι τεχνολογίες ανίχνευσης και οι δυνατότητές τους. Επίσης παρουσιάζονται οι τυπικές και αναμενόμενες ουσίες/αέρια που είναι δείκτες της ανθρώπινης παρουσίας και παράγεται μια εκτίμηση για την δυνατότητα ανίχνευσής τους με κάποιους δεδομένους περιορισμούς στους οποίους πρέπει να ακολουθεί η λύση ώστε αυτή να μπορεί να χρησιμοποιηθεί πρακτικά σε πραγματικές συνθήκες. Η έρευνα έγινε με σταδιακή εμβάθυνση στο πρόβλημα, αρχικά επιβεβαιώνοντας, πρώτα θεωρητικά και μετά εργαστηριακά, την βιωσιμότητα της προτεινόμενης προσέγγισης - τη χρήση αισθητήρων για τη μέτρηση συγκέντρωσης αερίων, θερμοκρασίας, υγρασίας και ατμοσφαιρικής πίεσης. Μετά την επιτυχημένη δοκιμή της ακολουθούμενης προσέγγισης, σχεδιάστηκε και δοκιμάστηκε επιτυχημένα σε κλειστούς χώρους με συνθήκες αρκετά κοντινές στις πραγματικές, ένα σύστημα ηλεκτρονικής μύτης που έχει τη δυνατότητα ανίχνευσης της ανθρώπινης παρουσίας. Η μέθοδος της δοκιμής επιβεβαίωσε τη δυνατότητα ανίχνευσης ανθρώπινης παρουσίας με μέθοδο αναζήτησης από την επιφάνεια των ερειπίων. Δεδομένης αυτής της επιτυχίας, σχεδιάστηκε και δοκιμάστηκε σε σχεδόν πραγματικές συνθήκες νέο σύστημα ηλεκτρονικής μύτης το οποίο τοποθετήθηκε πάνω σε ρομποτική πλατφόρμα η οποία έχει τη δυνατότητα να κινείται μέσα στα ερείπια. Αυτή η ηλεκτρονική μύτη έχει τη δυνατότητα να ανιχνεύει ανθρώπινη παρουσία καθώς επίσης και διάφορες τυπικές επικίνδυνες ατμοσφαιρικές καταστάσεις μέσα στα ερείπια. Ταυτόχρονα, με την μείωση του όγκου της νέας και τελικής ηλεκτρονική μύτης και την αύξηση των δυνατοτήτων ανίχνευσης, βελτιώθηκε δραστικά η διεπαφή του χειριστή του συστήματος με την υλοποίηση και ενσωμάτωση λογικής που παράγει απλές εξόδους/ενδείξεις για τις ανιχνευόμενες καταστάσεις. Τέλος, μελετούνται άλλες περιπτώσεις χρήσης αυτής της ηλεκτρονικής μύτης καθώς και οι απαραίτητες προσαρμογές που θα χρειάζονταν για κάθε περίπτωση. Το κείμενο της διατριβής είναι στην Αγγλική γλώσσα.

Executive summary

In this thesis the successful testing of an electronic nose system is presented, as well as all the required research to achieve that goal. This electronic nose is intended to detect the presence of trapped humans in confined spaces and, also, air-related hazardous conditions in collapsed buildings during search and rescue operations in an urban environment. Initially, the field of interest for which this work provides a solution is presented. Existing methods, with and without gas sensors, are presented and the environment in which the electronic nose is intended to work in is investigated from a measurement and detection perspective. Various sensing technologies and their capabilities are presented. Also, the anticipated target gases/compounds which are indicators of human presence are listed and an estimation regarding the feasibility of detecting them is produced, given some specific constraints that must be met in order for the end result to be practically usable in real conditions. The research and resulting developments were performed incrementally by first confirming, theoretically and then experimentally, the feasibility of the proposed approach – which is to use sensors for the measurement of gas concentrations, temperature, humidity and air pressure. After the successful completion of the feasibility test of the proposed approach, an electronic nose system capable of detecting human presence in confined spaces was designed and successfully tested under near realistic conditions. The testing method of this system confirmed the ability of the system to detect human presence by performing a search on the surface of the building debris. Given this success, a new electronic nose system, which was designed and tested under realistic conditions, was installed on a robotic platform capable of moving inside collapsed building structures. This system can detect human presence and many typical air related hazards inside building rubble. While the functionality of the system was increased and its volume reduced, the operator interface was drastically improved with the introduction and implementation of logic that produces simple outputs/indicators regarding the detected conditions. Finally, alternative uses of the system are investigated, as well as the required adjustments in each case.

Acknowledgements

I would like to thank my esteemed supervisor Dr. Spyridon Blionas for his invaluable supervision and support during the course of my PhD degree. I also thank Dr. Stavros Chatzandroulis and Prof. Dimitris Tsoukalas for their “steering” reviews. Additionally, I would like to thank my colleague Thanasis Silis for our excellent cooperation and his contribution to this work. My gratitude extends to the INACHUS consortium without which this research outcome would not be possible. My appreciation also goes out to my family and friends for their encouragement and support all through my studies.

This work was supported by the European Commission under INACHUS, a collaborative project part of the FP7 for research, technological development and demonstration (Grant Agreement No 607522).

Publications

Conferences

[1] Athanasiou, G., Amditis, A., Riviere, N., Makri, E., Bartzas, A., **Anyfantis, A**., ... & Schaap, M. (2015). INACHUS: Integrated wide area situation awareness and survivor localisation in search and rescue operations. In *5th International Conference on Earth Observation for Global Changes (EOGC) and the 7th Geo-information Technologies for Natural Disaster Management (GiT4NDM)*.

[2] **Anyfantis, A.**, & Blionas, S. (2019, November). Indoor air quality monitoring sensors for the design of a simple, low cost, mobile e-nose for real time victim localization. In *2019 Panhellenic Conference on Electronics & Telecommunications* (PACET) (pp. 1-6). IEEE.

[3] **Anyfantis, A.**, & Blionas, S. (2020, May). Design and development of a mobile e-nose platform for real time victim localization in confined spaces during USaR operations. In *2020 IEEE International Instrumentation and Measurement Technology Conference* (I2MTC) (pp. 1-6). IEEE.

Journals

[1] **Anyfantis, A**., & Blionas, S. (2020). Proof of concept apparatus for the design of a simple, low cost, mobile e-nose for real-time victim localization (human presence) based on indoor air quality monitoring sensors. *Sensing and Bio-Sensing Research*, 27, 100312.

[2] **Anyfantis, A.**, & Blionas, S. (2021). An analysis on the performance of a mobile platform with gas sensors for real time victim localization. *Sensors*, 21(6), 2018.

[3] **Anyfantis, A**., Silis, A., & Blionas, S. (2021). A low cost, mobile e-nose system with an effective user interface for real time victim localization and hazard detection in USaR operations. *Measurement: Sensors*, 100049.

This work has received funding from the European Union's Seventh Framework Programme for research, technological development and demonstration under the INACHUS project, grant agreement no 607522

LIST OF FIGURES......10

LIST OF TABLES......15

LIST OF ABBREVIATIONS......17

INTRODUCTION......19

1. DETECTION TARGETS FOR HUMAN PRESENCE INDICATION......23

1.1. OVERVIEW......23
1.2. AIR COMPOSITION......23
1.2.1. Dry Air Composition......*24*
1.2.2. Water vapor content......*25*
1.2.3. Volatile Organic Compounds (VOCs) with biogenic origin......*25*
1.2.4. Volatile Organic Compounds (VOCs) with anthropogenic origin......*26*
1.3. GASES/COMPOUNDS EMITTED FROM THE HUMAN BODY......26
1.3.1. Composition of exhaled human breath......*26*
1.3.2. Gases originating from body fluids......*27*
1.4. SENSOR TECHNOLOGIES AND CAPABILITIES......30
1.4.1. Gas sensing technologies......*30*
1.5. CONCLUSIONS – DISCUSSION......34

2. REQUIREMENTS......36

2.1. OVERVIEW......36
2.2. REQUIREMENTS......36

3. ELECTRONIC NOSE SYSTEM......38

3.1. OVERVIEW......38
3.2. ENVISIONED E-NOSE SYSTEM – EARLY VERSION......38
3.2.1. Hardware architecture of the e-nose......*38*
3.2.2. E-nose firmware and software architecture......*40*
3.1. COMPONENT SELECTION......42
3.2. SYSTEM DESIGN......47
3.2.1. Core system......*47*
3.2.2. Core system specifications......*48*
3.3. SUMMARY OF THE E-NOSE PROTOTYPE DEVICES PRESENTED IN THE FOLLOWING CHAPTERS......51

4. FIRST PROTOTYPE, PROOF OF CONCEPT APPARATUS AND TESTS......54

4.1. OVERVIEW......54
4.2. ELECTRONICS OF THE 1ST PROTOTYPE......55
4.3. SOFTWARE OF THE 1ST PROTOTYPE......57
4.4. PROOF OF CONCEPT TESTING APPARATUS – INITIAL EXPERIMENTS AND RESULTS......57
4.5. SENSOR READINGS STABILITY OF THE 1ST E-NOSE PROTOTYPE UNDER STATIC CONDITIONS......61

5. THEORETICAL ANALYSIS AND EXPERIMENTS TO EVALUATE SELECTED CO_2 AND O_2 SENSORS......63

5.1. THEORETICAL ANALYSIS......63
5.2. EXPERIMENT TO EVALUATE SELECTED SENSORS......64
5.3. DISCUSSION......68

6. THEORETICAL ANALYSIS FOR NON STATIC CONDITIONS – HUMAN PRESENCE AND FRESH AIR INPUT......69

6.1. OVERVIEW......69
6.2. LIMIT OF DETECTION OF SELECTED CO_2 AND O_2 SENSORS......69
6.3. EXHALED AIR FLOW RATE......69
6.4. MODELING REALISTIC CONDITIONS......70
6.5. APPLYING THE MODEL......73
99......*76*

Extr. small cavity *76*
0.5 .... *76*
adult male *76*
6.3 .... *76*
20.734 .... *76*
141 .... *76*
10 .... *76*
(average person's head and upper body) *76*
6.6. ELABORATING ON THE MODEL 76
6.6.1. Maximum fresh air flow rates *76*
6.6.2. Final gas concentration for several scenarios *77*
6.6.3. Time delay for gas concentration to enter "detectable" zone *78*
6.6.4. Time delay to reach saturation concentration *79*
6.7. CONCLUSIONS - FINDINGS 79
6.8. EXPECTED E-NOSE PERFORMANCE DEPENDING ON DETECTION PARAMETERS 81

7. SECOND PROTOTYPE, VERIFICATION AND VALIDATION TESTS 84

7.1. OVERVIEW 84
7.2. ELECTRONICS OF THE 2ND PROTOTYPE 85
7.3. MECHANICAL ASPECTS OF THE 2ND PROTOTYPE 89
7.4. SOFTWARE OF THE 2ND PROTOTYPE 93
7.4.1. Firmware running on the Microcontroller *94*
7.4.2. Software running on the host computer - KST plot *95*
7.4.3. Software running on the host computer - Advanced logic unit Software *96*
7.5. VERIFICATION - SETUPS AND TESTS FOR THE 2ND PROTOTYPE 99
7.5.1. Office room experiments *99*
7.5.2. Closet experiments with controlled opening(s) *101*
7.5.3. Closet experiment with controlled fresh air flow– fans *110*
7.5.4. Guard post experiment with controlled opening(s) *119*
7.5.5. Controlled conditions urine detection test *127*
7.6. VALIDATION – FIRST FIELD TEST P1 129
7.7. CONCLUSIONS 132

8. THIRD PROTOTYPE, VERIFICATION AND VALIDATION TESTS 134

8.1. OVERVIEW 134
8.2. ELECTRONICS OF THE 3RD PROTOTYPE 139
8.3. MECHANICAL DESIGN OF THE 3RD PROTOTYPE 148
8.3.1. Manifold design *148*
8.3.2. Enclosure design *152*
8.3.3. Assembly of the 3rd prototype *156*
8.4. INDICATORS - INTEGRATED INTERFACE CONCEPT 159
8.5. SOFTWARE OF THE 3RD PROTOTYPE 162
8.5.1. Firmware *163*
8.5.2. Advanced logic unit *166*
8.5.3. Sensor Indicator types *170*
8.5.4. Calibration *173*
8.5.5. Gas Sensor Types *174*
8.5.6. Global Indicators – calculation *187*
8.5.7. Extended GUI of the 3rd prototype *191*
8.6. ELECTRONIC NOSE TESTING (VERIFICATION) 198
8.6.1. Victim localization tests *198*
8.6.2. Hazardous conditions in the air detection tests *203*
8.7. SECOND FIELD TESTS P3 – END-USER VALIDATION 207
8.8. THIRD FIELD TESTS P4 – FINAL VALIDATION 225

9. ALTERNATIVE USES OF THE E-NOSE 238
9.1. FIXED POSITION STAND-ALONE E-NOSE SYSTEM 238
9.2. PORTABLE STAND-ALONE ELECTRONIC NOSE 239
9.2.1. Power supply 239
9.2.2. User interface and Advanced Logic Unit 239
9.2.3. Suitable components 240
9.3. PEOPLE DETECTOR 241
9.3.1. Fixed position people detector 241
9.3.2. Portable people detector 242
9.4. SMOKING DETECTOR 242
9.5. CAPNOGRAPHY 242
10. CONCLUSIONS 243
11. REFERENCES 244
12. APPENDIX: ATMOSPHERIC AIR CONSTITUENTS –SUPPLEMENTARY DATA 248
12.1. CONVERSION FACTORS FOR CONVERTING PARTS PER MILLION FOR SOME CONSTITUENTS 248
13. APPENDIX: ADVANCED LOGIC UNIT - LOGIC TABLES 249
14. APPENDIX: ELECTRONIC NOSE SENSOR POISONS AND CONTAMINANTS 255
15. APPENDIX: A COST ESTIMATION FOR THE E-NOSE DEVICE 256

LIST OF FIGURES

Figure 1: The high level block diagram of the electronic nose which is intended to be placed in a robotic platform. 38
Figure 2: Top level block diagram of the e-nose's air system. 39
Figure 3: Sensor modules connected in series (implemented). 39
Figure 4: Sensor modules connected in parallel. 39
Figure 5: Information and control flow 40
Figure 6. The selected CO_2 sensor with a very fast response fitted with a flow-through adapter 43
Figure 7. The selected O_2 sensor. 43
Figure 8. The selected NH_3 sensor 44
Figure 9. The selected humidity sensor. The sensor also includes a temperature sensor. 44
Figure 10. A stand-alone temperature sensor 45
Figure 11. The selected hydrophobic filter 45
Figure 12. The selected pump suitable for moving air 46
Figure 13. The selected heating resistor type 46
Figure 14. The selected ARM based embedded computing platform 47
Figure 15. The core system implementing the bare minimum mandatory requirements. 47
Figure 16. The component placement inside the e-nose compartment. 50
Figure 17. The arrangement of the sensors in the custom manifold. 51
Figure 18. The 1st prototype system is built around the O_2 and CO_2 sensors so that the measurements can be viewed in plots. 55
Figure 19. The first prototype. On the left is the CO_2 (top), O_2 sensor (bottom) and a fan (black). In the center are two USB to serial converters stacked on each other. On the right is the custom power supply PCB. 57
Figure 20. The experiment setup with the rapid prototype system. 58
Figure 21. Inside the gas chamber of the experimental setup. 59
Figure 22. Plot of CO_2 concentration versus time. 60
Figure 23. Plot of O_2 concentration versus time. 60
Figure 24 : Operation concept of the apparatus for air mixing and sensor measurements. The sample and relief containers are plastic bags that can easily be manipulated by hand to move the air inside them. 64
Figure 25. Breath sampling and introduction into apparatus 65
Figure 26 : Air mixing and measurements. 65
Figure 27 : The Experimental Apparatus for the Sensor Measurements. 66
Figure 28 : A graphical comparison between the target CO_2 concentration cases listed in Table 1 and the measured CO_2 concentration when using the apparatus listed in Table III. Concentration axis is plotted in a logarithmic scale. For fresh air, the target concentration is assumed to be 400ppm. 67
Figure 29 : A graphical presentation of the measured O_2 concentrations (listed in Table III) when using the apparatus. 68
Figure 30: Model of an ideal sealed room with single person in it. Arrows depict air direction to and from air sources / sinks (i.e. human and environment) 70
Figure 31: CO_2 concentration response of a person in a room where air is refreshed at a rate of 500lt/min 72
Figure 32: O_2 concentration response in the 1st 10 minutes that a person is in a room where air is refreshed at a rate of 500lt/min. 73
Figure 33. The core system implementing the bare minimum mandatory requirements. 84
Figure 34. The system is implemented with off-the-shelf components and evaluation boards. 86
Figure 35. Schematic/Interconnection diagram the 2nd e-nose prototype 87
Figure 36. Schematic diagram of the printed circuit boards for the 2nd prototype 88
Figure 37. The layout of the various PCBs for the 2nd prototype 89
Figure 38. The assembled PCB that host the gas sensors 89
Figure 39. The lightweight and heat conductive custom manifold 89
Figure 40. The assembled sensor cluster 90
Figure 41. The assembled readout and control PCB stackup of the 2nd prototype 90
Figure 42. The 2nd prototype of the e-nose 91
Figure 43: CAD of the Prototype 2 enclosure. The base, cover and two sides of the cover are shown 92

Figure 44. The Plexiglas enclosure (left) and the complete 2nd e-nose prototype. 93
Figure 45. Flow chart for the firmware of the 2nd prototype 94
Figure 46. A caption of the e-nose measurements when exhaling directly in front the input port. 96
Figure 47: The main loop for data acquisition, processing and indicator updating of the 2nd e-nose prototype . 97
Figure 48: Conceptual design - color coding of the user-friendly information (indicators) in the GUI 98
Figure 49. Room with two people, CO_2 and O_2 test measurements. 100
Figure 50. Various tests with different ventilation positions. Ventilation opening is 20x20cm (red shape). 102
Figure 51. Testing different locations of the e-nose and a larger ventilation opening size 20x60cm 102
Figure 52: CO_2 concentration response and threshold indicator graphs in closet with ventilation opening 103
Figure 53: CO_2 trend indicator graph in closet with ventilation opening 104
Figure 54: O_2(%) concentration response and threshold and trend indicator graphs in closet with ventilation opening 105
Figure 55:O_2 partial pressure (mbar) concentration response in closet with ventilation opening 106
Figure 56: O_2 partial pressure (mbar) trend indicator in closet with ventilation opening 106
Figure 57: NH_3 (0.1ppm) concentration response and threshold indicator graphs in closet with ventilation opening 107
Figure 58: Humidity (RH%) response and trend indicator in closet with ventilation opening 108
Figure 59: External and internal temperature (°C) signals and trend indicator graphs in closet with ventilation opening 109
Figure 60: Barometric pressure (mbar) level trend indicator graphs in closet with ventilation opening 109
Figure 61. Air fans to control fresh air flow rate 111
Figure 62. Left: All fans OFF ventilation openings open. Right: All fans ON ~ 1750 LPM. 111
Figure 63. Left to right: 4 fans ON ~ 1250LPM. 3 fans ON ~ 750LPM. 2 fans ON~ 250LPM 112
Figure 64. Left: 1 fan ON ~ 50LPM. Right: No fans ON, only 20x20cm opening. 112
Figure 65. First to last row, [left to right: CO_2 (ppm), O_2 (%,mbar) and NH_3 (0.1ppm) sensor readings]. Thresholds. Derivative of trend. Trends. 113
Figure 66. First to last row, {left to right: Humidity (RH%), temperature[external(°C), internal(°C), O_2 sensor(°C)]} and pressure(mbar) sensor readings. Derivative of trend. Trends. 113
Figure 67. CO_2 (ppm) concentration response during the closet with fans experiment. Both filtered (CO2rawCV) and raw (CO2rawCVR) values are shown 114
Figure 68: O_2 (%) concentration response during the closet with fans experiment. Both filtered (O2pctCV) and raw (O2pctCVR) values are shown 115
Figure 69: NH_3 (0.1ppm) concentration response during the closet with fans experiment. Both filtered (NH3CV) and raw (NH3CVR) values are shown 116
Figure 70. Left 2 fans ON~ 250lpm Right 4 fans ON ~ 1250lpm. 117
Figure 71. Extended office storage closet with one person test measurements. 117
Figure 72: CO_2 (ppm) spike concentration response during the closet with fans experiment. Both filtered (CO2rawCV) and raw (CO2rawCVR) values are shown. E-nose approaches victim, then goes away. 118
Figure 73: O_2 (%) spike concentration response during the closet with fans experiment. Both filtered (O2pctCV) and raw (O2pctCVR) values are shown. E-nose approaches victim, then goes away. 119
Figure 74. Left to right: Guard post with door and windows. Door and window used as ventilation openings. 120
Figure 75. Left: e-nose and control interface computer. Right: e-nose and sampling tube 120
Figure 76. Left: sampling fresh air. Right: different ventilation parameter via different window opening 120
Figure 77: CO_2, O_2 (%) and O_2 (partial pressure, mbar) columns showing the current value (*CV), threshold (*TH) and trend (*TRD) indicators in three rows for the guard post large filter window experiment 121
Figure 78: NH_3 (0.1ppm) concentration and threshold indicator for the guard post large filter experiment 122
Figure 79: CO_2 (ppm) concentration response for guard post short filter experiment 123
Figure 80: CO_2, O_2 (%) and O_2 (partial pressure, mbar) columns showing the current value (*CV), threshold (*TH) and trend (*TRD) indicators in 3 rows for the guard post short filter window experiment 124
Figure 81. Left: guard post with door and windows. Right: detector device with the sampling tube and the entire measurement setup. 125
Figure 82. Guard post test measurements. 126
Figure 83. Heater plate with temperature controller, digital sensor, and heating resistor. Right: cloth inside bag 127

Figure 84. Left: Interface PC collecting raw measurements, 2nd prototype of the e-nose, bag, and heated plate. Right: The e-nose's input interface is placed inside the bag to take samples/measurements. 128
Figure 85. Left to Right: Heated plate partially inside glove, glove after experiment, cloth after experiment.. 128
Figure 86. Right to left: ammonia measurement and detection, system temperature, humidity levels 128
Figure 87. Headspace measurement of ammonia over fresh urine. 129
Figure 88. The increase of the relative humidity does not affect the NH_3 sensor significantly. 129
Figure 89: Confined space test site for the electronic nose during first field test P1 130
Figure 90: Anticipated response of the electronic nose when moving close to the opening of the void 131
Figure 91: Left, The e-nose test site. Right, the compartment separator with a ventilation opening 131
Figure 92: Inserting the sampling tube's end in the void with a victim inside 131
Figure 93: Blowing/exhaling in front of the sampling tube's end 132
Figure 94: First peak is 20cm outside the void's ventilation opening. The second peak is inside the void 132
Figure 95: All the measurements of that demonstration + the response of the ammonia sensor to fumes originating from a low concentration ammonia solution. 132
Figure 96. Interconnection diagram the 3rd e-nose prototype 141
Figure 97. Schematic diagram of the analog board for the 3rd prototype 142
Figure 98: Schematic diagram of the power electronics located on the microcontroller board for the 3rd prototype 143
Figure 99: Schematic diagram of the microcontroller board for the 3rd prototype 144
Figure 100: Schematic diagram of the connectors on the microcontroller board for the 3rd prototype 145
Figure 101: Schematic diagram of all the custom sensor breakout boards for the 3rd prototype 146
Figure 102: The layout of the PCB for the 3rd prototype 147
Figure 103: 3D view of the main, CO_2, O_2 and humidity PCBs with the corresponding sensors. On the bottom left corner the interface cable connector will connect the main PCB to the outside world. 149
Figure 104: 3D view of the main PCB accompanied by the daughter PCBs 149
Figure 105: Side view (cross section) of the main and daughter PCBs. 149
Figure 106: Manifold cross section of the primary airway. Air-redirection walls are used to force air turbulence above the sensor drums. 150
Figure 107: 3D view of the manifold with the external components only attached (2x resistors, a temperature relay (red) and the temperature PCB (green) with a temperature sensor mounted on. 151
Figure 108: Bottom 3D view of the manifold showing the sensor hangars. 151
Figure 109: Rendered bottom 3D view of the manifold with all the internal and external components mounted. Only the bottom cover has been removed. 152
Figure 110: The enclosure top and bottom parts. All internal mounting holes (for enclosure cover and manifold stands). 153
Figure 111: 3D view of the enclosure with the manifold included along with its most bulky components. 154
Figure 112: 3D view of the microcontroller PCB mounted on the manifold with 10mm standoffs. 155
Figure 113: 3D view of the pneumatic parts as fit in the available space of the enclosure. 155
Figure 114: Bottom view of manifold with sensor inserts visible (left) and the PCB panel (right). 156
Figure 115: The humidity board installed (left) and the CO_2 sensor installed on top (right). 156
Figure 116: From left to right: heater, thermal protection, temperature sensor and heater. 156
Figure 117: The analog PCB populated with sensors (O_2, NH_3, CO, H_2S, combustibles). 157
Figure 118: The assembled manifold with the control board attached to it 157
Figure 119: From left to right: machined air interface parts, custom assembly jig, assembled interfaces. 157
Figure 120: The assembled e-nose without the enclosure. 158
Figure 121. The completed e-nose - 3rd and final prototype 159
Figure 122: Mock-up of the interface of the robotic platform of the e-nose alarms and indicators 161
Figure 123: Flow diagram of 3rd prototype's firmware 163
Figure 124: Main loop execution during training and normal modes 169
Figure 125: Processing of Threshold sensor type on sampled data during normal execution 171
Figure 126: Processing of Threshold Indicator Type at the end of a training cycle 171
Figure 127: Processing of Trend sensor type on sampled data during normal execution 172
Figure 128: Processing of Trend Indicator Type at the end of a training cycle 172
Figure 129: Processing of point of interest sensor type on sampled data during normal execution 172
Figure 130: Graph depicting the CO_2 threshold levels 175

Figure 131: Graph depicting the O_2(%) threshold levels 176
Figure 132: Graph depicting the NH_3 threshold levels 177
Figure 133: Graph depicting the manifold temperature threshold levels 178
Figure 134: Graph depicting the environmental temperature threshold levels 179
Figure 135: Graph depicting the O_2 temperature threshold levels 180
Figure 136: Graph depicting the barometric pressure threshold levels 181
Figure 137: Graph depicting the manifold humidity threshold levels 182
Figure 138: Graph depicting the environmental humidity threshold levels 183
Figure 139: Graph depicting the carbon monoxide threshold levels 184
Figure 140: Graph depicting the hydrogen sulphide threshold levels 185
Figure 141: Graph depicting the combustibles and derivatives threshold levels 186
Figure 142: Global indicators start-up operation 188
Figure 143: Global indicators runtime operation 188
Figure 144: ENALU GUI main window layout 191
Figure 145: "Set Graph Range" menu allows time window of graphs to be changed 192
Figure 146: "view graph" menu, which allows zooming in on a specific graph 192
Figure 147: Combustible selection graph, which allows selection of the primary flammables monitoring %LEL gas 193
Figure 148: Currently monitored combustibles gas indicator 193
Figure 149: Notification board containing only INFO graded messages 193
Figure 150: Notification board containing WARNING (orange) graded messages 194
Figure 151: Notification board containing ERROR (red) graded messages 194
Figure 152: Buttons to clear log messages, or clear the background color of the notification board 194
Figure 153: Detailed view of the quick access button and global indicators 194
Figure 154: Enlarged sensor graph 195
Figure 155: Typical sensor widget 195
Figure 156: Hover with the mouse to find the current values at the x-axis location of the mouse 196
Figure 157: Disengaging the auto-shifting of the real-time graph in order to manually pan and zoom 197
Figure 158. The confined space and breath-based victim localization test for the 3rd prototype of the e-nose 198
Figure 159. Human presence and approaching indicator triggered when moving inside the confined space ... 199
Figure 160. E-nose system output when crossing the ventilation opening of a human-occupied confined space with the electronic nose. 200
Figure 161. Apparatus for creating a small, steady and controlled exhaled air flow. 201
Figure 162. Results summary for the experiment of detecting a Hot Spot 201
Figure 163. E-nose system output when momentarily exposed to high human presence air conditions. 202
Figure 164. CO, H_2S and NH_3 sensor response to ammonia gas (mosquito bite stick) 202
Figure 165. Ammonia containing product used for testing 202
Figure 166. Left to right: Response of the CO, H_2S and Combustibles sensors to exhaled cigarette smoke 203
Figure 167. Left to right: Response of the CO_2, O_2 and NH_3 sensors to exhaled cigarette smoke 203
Figure 168. Left to right: Response of the CO, H_2S and Combustibles sensors to cigarette lighter gas 204
Figure 169. Left to right: Response of the CO_2, O_2 and NH_3 sensors to cigarette lighter gas 204
Figure 170. A portable e-nose configuration for scanning and acquiring measurements 205
Figure 171. Ampoule with ammonium sulfide for H_2S testing 205
Figure 172. H_2S detection test apparatus 206
Figure 173. The CO, H_2S and NH_3 sensors response from exposure to a stink ampoule (ammonium sulfide solution) 206
Figure 174. The CO_2, H_2S and Humidity sensors response from exposure to a stink ampoule (ammonium sulfide solution) 206
Figure 175. The CO, H_2S and NH_3 sensors response from exposure to a stink ampoule (ammonium sulfide solution) 206
Figure 176. The CO_2, H_2S and Humidity sensors response from exposure to a stink ampoule (ammonium sulfide solution) 206
Figure 177. The victim's survival space used to test the e-nose victim localization capabilities. 207
Figure 178. The volunteer "victim" while entering the confined space 20 minutes before the e-nose test and demonstration. 208

Figure 179. The e-nose demonstration for victim localization and hazardous conditions detection capabilities. 209
Figure 180. All test scenario measurements are illustrated in this e-nose interface screenshot. 210
Figure 181. Case (2). Scanning far away from the survival space 213
Figure 182. Case (2). Scanning the entrance and then inside the survival space. Approaching indicator is triggered 214
Figure 183. Case (2). Continuing to sample from inside the survival space. A weak Human presence is triggered. 215
Figure 184. Case (2). Sampling inside the survival space. Human presence indicator is still weak but the O_2 sensor is converging. This maintains the Approaching indicator 216
Figure 185. Case (2). With the sampling tube inside the survival space, a strong Human presence indicator is triggered. 217
Figure 186. Case (3). H_2S detection with the Toxic indicator being triggered. 220
Figure 187. Case (4). Combustible atmosphere detected, with the Combustibles indicator being triggered. ... 221
Figure 188. Case (5). Air input sampling/Filter blockage detection with an error status indicator being triggered. 222
Figure 189. Case (6). A Toxic indicator being triggered by high levels of CO_2 from undiluted exhaled breath... 223
Figure 190. Case (7). Toxic indicator triggered from CO gas originating from exhaled cigarette smoke. 224
Figure 191. The location of the training site – Gordolon Worksite marked with a black X on the bottom centre of the map. 225
Figure 192. The test location with various rubble piles with hidden “survivors”. On the bottom right, the robotic platform is entering the rubble with a goal of reaching the area seen on the bottom left. 226
Figure 193. The search location. Entering the rubble pile, the e-nose is located on the central compartment. The air input and output interfaces can be distinguished on the side of the e-nose compartment. 227
Figure 194. The robotic platform's control interface. On the right is the output of the e-nose, from top to bottom: Human indicator (red = strong indicator, person detected), Approaching indicator, Hot-spot indicator, Toxic indicator, Combustible indicator, Status indicator. 228
Figure 195. Carbon monoxide detection test. 228
Figure 196: Human detection data with the e-nose mounted on the robotic platform. The robotic platform moved under the rubble to and then away from the victim. 231
Figure 197: Human detection data with the e-nose mounted on the robotic platform. A weak approaching global indicator is triggered. 232
Figure 198: Human detection data with the e-nose mounted on the robotic platform. A weak Human (global) indicator is triggered, the weak Approaching (global) indicator is active, a weak Point of interest (global) indicator is triggered. 233
Figure 199: Human detection data with the e-nose mounted on the robotic platform. A strong human (global) indicator is triggered while the approaching (global) indicator is still weak. 234
Figure 200: Human detection data with the e-nose mounted on the robotic platform. A strong human (global) indicator is active while the approaching (global) indicator is zero. 235
Figure 201: Human detection data with the e-nose mounted on the robotic platform. A strong Human (global) indicator is active while the Approaching (global) indicator is weak - moving away. 236
Figure 202: Human detection data with the e-nose mounted on the robotic platform. A weak Human (global) indicator is triggered while the Approaching (global) indicator is weak - moving away... 237
Figure 203. The system implementing the basic functionality but independently from the snake robot 238
Figure 204: From left to right, battery holder, keypad, speaker, LCD screen, LED indicator, ON/OFF push button. 240
Figure 205. Block diagram of a fixed point people detector with IoT and multi-source capabilities based on the e-nose. 241
Figure 206. Block diagram of the implementation of the multi-source sampling solution for the fixed point people detector based on the e-nose. 242

LIST OF TABLES

Table 1: Dry air composition 24
Table 2: Concentration of hydrocarbons in the remote continental boundary layer 24
Table 3: Saturation vapor pressure of pure water in various temperatures 25
Table 4. Major constituents of exhaled air. 26
Table 5. Sensors for the MultiRAE gas monitor of RAE systems and their capabilities 34
Table 6. The victim localization detection targets 35
Table 7. Alarm thresholds proposed to the end-users 36
Table 8. Comparison of the prototype e-nose device versions 51
Table 9. ROOM CO_2 CONCENTRATION AFTER 5 HOURS 63
Table 10. Calculated Quantities of Fresh and Exhaled Air for Mixing 64
Table 11. Measurements 67
Table 12: Minimum exhaled flow rate for individuals of both sexes and of different age groups. 69
Table 13: Maximum exhaled flow rate for individuals of both sexes and of different age groups. 70
Table 14: Maximum fresh air flow rate and 3τ time-to-reach detectable CO_2 concentration for various room size and exhaled air flow rates. 74
Table 15: Maximum fresh air flow rate and 3τ time-to-reach detectable O_2 concentration for various room size and exhaled air flow rates. 75
Table 16: maximum fresh air flow rate (lt/min) for which CO_2 detection is possible 76
Table 17: maximum fresh air flow rate (lt/min) for which O_2 detection is possible 77
Table 18: Maximum CO_2 concentration (in ppm) for several scenarios of fresh air vs. exhaled air flow(i.e. people) 77
Table 19: Minimum O_2 concentration (in %) for several scenarios of fresh air vs. exhaled air flow(i.e. people) . 77
Table 20: Time for CO_2 footprint to enter detectable zone (Vroom = 26250lt) for various flow rate scenarios .. 78
Table 21: Time for O_2 footprint to enter detectable zone (Vroom = 26250lt) for various flow rate scenarios..... 78
Table 22: Time for CO_2 footprint to enter detectable zone (Vroom = 5000lt) for various flow rate scenarios 78
Table 23: Time for O_2 footprint to enter detectable zone (Vroom = 5000lt) for various flow rate scenarios....... 78
Table 24: 3τ time (in minutes) for CO_2 footprint to approach saturation levels in various room sizes and for various trapped people 79
Table 25: 3τ time (in minutes) for O_2 footprint to approach saturation levels in various room sizes and for various trapped people 79
Table 26. Estimation of maximum total possible area of large openings in voids (Urban/Suburban). 81
Table 27. Estimation of maximum total possible area of openings in voids (Stack effect). 82
Table 28. Estimation of maximum total possible area of openings in voids (Wind and Stack effect, z=2m, T_f-T_C=5°). 83
Table 29. The e-nose connection parameters of the COM port 94
Table 30. The e-nose command interface 94
Table 31. Description of the identifiers in the e-nose's measurements stream 95
Table 32: Training session statistical data in closet with non-forced air experiment 103
Table 33: Data from the closet with fans experiment 112
Table 34: Training session statistical data for guard post experiment with filter window size 240 seconds...... 120
Table 35: Training session statistical data for the short filter guard post experiment 122
Table 36. Alarm thresholds proposed to the end-users 136
Table 37: Indicator and Alarm color coding - general 161
Table 38: Status wording and color coding per alarm and indicator (preview view) 161
Table 39: Labels and units of e-nose output. 164
Table 40: Status – STA bit interpretation. Note that the status is printed in Hexadecimal (0x00xx) 164
Table 41: Control command for the e-nose firmware 165
Table 42: Gas sensor name identifiers as perceived by the E-nose applications 166
Table 43: Layout of the input data stream basic element 168
Table 44: Layout and order of 168
Table 45: Explanation of the parameters accepted when setting a user-defined threshold 170
Table 46: Zero concentration values for calibrate-able sensors 173

Table 47: Calibration command parameters ... 174
Table 48: CO_2 Thresholds and threshold zones ... 174
Table 49: O_2(%) Thresholds and threshold zones ... 175
Table 50: Partial pressure O_2 Thresholds and threshold zones ... 176
Table 51: NH_3 Thresholds and threshold zones ... 177
Table 52: Manifold temperature thresholds and threshold zones ... 177
Table 53: Environmental temperature thresholds and threshold zones ... 178
Table 54: O_2 temperature thresholds and threshold zones ... 179
Table 55: Barometric pressure thresholds and threshold zones ... 180
Table 56: Manifold humidity thresholds and threshold zones ... 181
Table 57: Environmental humidity thresholds and threshold zones ... 182
Table 58: Carbon monoxide thresholds and threshold zones ... 183
Table 59: Hydrogen sulphide thresholds and threshold zones ... 184
Table 60: combustibles and derivatives thresholds and threshold zones ... 185
Table 61: Flammable Gas Coefficients for calculation of target gas %LEL based on methane % concentration 186
Table 62: Typical global indicator state table ... 187
Table 63: Layout of the main sensors screen ... 193
Table 64. Results summary for the experiment of going into a confined space via a ventilation tube ... 199
Table 65. Results summary for the experiment of crossing a ventilation opening ... 199
Table 66. Power consumption in various operating modes ... 207
Table 67. Summary of results for case (2): Searching outside the cavity and then moving inside. NH_3 readings did not measure significant change. ... 212
Table 68. Summary of detection results for cases 3-7. ... 219
Table 69. Summary of victim detection results when inside an occupied confined space. ... 230
Table 70: Implemented logic for generating the Human Indicator ... 250
Table 71: Implemented logic for generating the Approaching (Trend) Indicator ... 251
Table 72: Implemented logic for generating the Hot spot (Edge) indicator. ... 252
Table 73: Implemented logic for generating the Toxic Alarm ... 252
Table 74: Implemented logic for generating the Combustibles Alarm. ... 253
Table 75. e-nose cost estimation ... 256

LIST OF ABBREVIATIONS

ABBREVIATION	DESCRIPTION
ABL	Atmospheric Boundary Layer
AC	Alternating Current
AIMS	Aspiration Ion Mobility Spectrometry
API	Application Programming Interface
ARM	type of central processing unit
ASR	Assessment, Search and Rescue
CAD	Computer Aided Design
CAN bus	Controller Area Network
CBRN	Chemical, Biological, Radiological, Nuclear
CO	Carbon Monoxide
CO_2 (or CO2)	Carbon Dioxide
DC	Direct Current
EC	Electro Chemical
ENALU (or enalu)	e-nose advanced logic unit
ENSAIS	Electronic Nose Sensor Array Intelligent System
H_2S (or H2S)	Hydrogen Sulphide
HAZMAT	HAZardous MATerials
i^2c bus(or i2c bus)	inter integrated circuit bus
LEL	Lower Explosive Limit
LNG	Liquid Natural Gas
LPG	Liquid Petroleum Gas
LPM	Liters Per Minute
NDIR	NonDispersive Infra Red
NH_3 (or NH3)	Ammonia
O_2 (or O2)	Oxygen
PBL	Planetary Boundary Layer
PC	Personal Computer
PCB	Printed Circuit Board
PID	Photo Ionization Detector
PM	Particulate Matter
ppm	parts per million
RH	Relative Humidity
Rpm	rounds per minutes
RRD	Round Robin Database
RSP	Rapid System Prototyping
TTL	Transistor to Transistor Logic. Also defines voltage levels (3,3V or 5V)
USB	Universal Serial Bus
USaR	Urban Search and Rescue
VOC	Volatile Organic Compound

INTRODUCTION

Urban search and rescue (USaR) operations are rescue operations that take place in an urban environment after some type of catastrophe has damaged building structures resulting in the entrapment of humans – victims inside them. The collapse of a building could be partial or complete and the cause could be a natural disaster such as an earthquake, an accident such as a gas leak explosion, or an act of terror. USaR operations are carried out by trained personnel, professionals, for example the Greek fire service [1] or volunteers, or the Hellenic Rescue Team [2], and are organized with a hierarchical command structure that can be compatible with INternational Search And Rescue Advisory Group (INSARAG) [3]. Rescue operations are performed in stages (Assessment, Search, and Rescue (ASR) stages 1-4) depending on the scale of the catastrophe and carried out by USaR teams. The USaR team members are also referred to as rescuers, or first responders. During ASR stages 3 and 4, USaR team members use various methods and tools to detect trapped victims. Established methods include the utilization of search dogs (canines or K9), microphones/geophones, and equipment for digging, cutting, stabilizing and lifting building materials. Personal protective equipment is also used, such as helmets, boots, gloves, securing equipment and also gas detectors for air-related hazard detection. New detection technologies are being evaluated and introduced to USaR teams that complement [4], or even replace the trained search and rescue dog. This equipment can be part of systems for large scale disaster management or stand-alone detection tools. The e-nose system of this work is intended to be part of a large scale disaster management system but can be used independently as a stand-alone victim localization tool. Other detection technologies available are surface radars [5], seismic or acoustic sensor clusters, optical cameras in the visible and IR spectrum [6], LIDARs, Cellphone base stations (IMSI catchers), cellphone detectors, gas sensors [7] and robots for searching when in the rubble, have also been proposed [8]. All technologies have their advantages and limitations. Radar can detect small movement under/inside the rubble and infer human presence. It has difficulty penetrating (or its penetration depth is reduced) by metallic objects, heavily reinforced concrete, water, and wet or even damp materials. Seismic/acoustic sensor cluster technologies can locate the source of a vibration/sound that could be generated by a trapped victim. They require some degree of silence to detect and their localization capabilities are susceptible to the unknown structural patterns of the rubble pile that affect the sound/vibration path. Optical methods require a line of sight, while dust and building debris make victim identification difficult, especially when only some body parts might be exposed. Cellphone-based detection technologies require that a victim has a cellphone on/next to him and that the cellphone signal can penetrate the rubble. An IMSI catcher can remotely activate a phone to communicate, ring or transmit. The victim can be instructed to perform actions that help determine his position, or for his device to be located (triangulation or search with a handheld cellphone power meter) although multipath effects make this difficult in some types of building materials. Also, short cellphone battery life time with modern smart phones is a factor that reduces the operating time window. Air/gas-based victim detection detects characteristic gases/compounds that are produced by humans somewhat like the nose of a K9. It only requires an airway (air path) between the victim and detection device. No line of sight is required and the type of building material is not critical as long as there is some airway to the victim. A search pattern must be executed so that the point where the maximum response is generated can be found. Air-based detection is susceptible to local weather conditions, mainly wind speed and interference by other sources that also emit the detection targets (gases and compounds). With proper training/experience the operator can evaluate the effect of these conditions onsite, factor them in and, in many cases, eliminate them with proper deployment.

It makes sense for the gas/chemical in the air-based identification of human presence to be performed with a method that can be automated and the results transmitted electronically. Although there might be other alternatives, the approach here is to build an electronic system that can perform the tasks at hand. Since the device is essentially a nose for detecting human presence, it was thought appropriate to call the device an electronic nose or e-nose. The term e-nose is used to refer to the device that is developed in the scope of this work without implying it is as equally capable as the biological ones. The e-nose in this context is a purpose-built machine with specific capabilities that, in some very particular cases, is “better” than, but not as versatile as biological sensors found in nature. The natural counterpart of the e-nose is the trained search and rescue dog or the mosquito [9]. The e-nose is not intended to replace the search and rescue dog, but rather to work complementarily and assist urban search and rescue teams where the dogs might not perform well: narrow spaces too small for dogs to enter, areas that are too hazardous for living beings, harsh environments, contaminated areas with chemicals that block the scent from the dogs, large search areas and thus long operation times are some scenarios where the e-nose could be more effective than dogs. Sensitivity and speed of detection are not currently comparable, based on the state of the art. This is the main reason the e-nose is specifically targeted for use in confined and narrow spaces where the detecting conditions are more favorable for the e-nose. To operate in confined spaces, the e-nose is intended to be mounted on a robotic platform that can go under the rubble.

The goal of this work is to provide a sensing solution that can give an indication of the presence of humans in narrow spaces. Ideally, for any detection solution, the certainty of the system's output must be high: weak positive output (there might be a human) or weak negative output, is not very helpful when it comes to prioritizing limited resources in a crisis. The optimal solution would be to combine a plethora of different sensing solutions based on completely independent physical properties so that all location specific peculiarities are covered. The combined evaluation of all sensing solution outputs together can greatly improve the accuracy of the final decision (whether or not a human is present). The operating concept of the victim localization e-nose is based on sampling of the surrounding air and the measurement of its composition for the detection of concentration levels of specific target gases which are indicators of a human presence [10].

The feasibility of using a low-cost and simple gas/chemical detection approach for victim localization is evaluated and explored in [11], and in more detail in [12]. A first prototype system was built [13], addressing only the entrapped victim localization aspect and was tested by itself, from the surface, under realistic conditions. That system was not capable of addressing detection under many hazardous conditions and the search was performed by probing from the surface, via a flexible air sampling tube, through openings to find survival spaces with victims. The system in [13] could provide enough sensor information to infer victim detection but was too complicated for actual use in the field [13]. Capable devices presented previously have limitations. In [14] an e-nose for the measurement and identification of three volatile organic compounds (VOCs) in a mixture is presented. The system employs commercial MOS sensors and uses the transient sensor response to produce near real-time results. It is intended to operate as an open sampling system with forced air flow and to measure Acetone, Isopropyl Alcohol and Ethanol. The system employs a neural network which needs to be trained for these targets. This work is indicative of the challenges met when utilizing this type of sensor. In [15] a sensor array for the detection of human presence is presented which can measure Acetone, Isoprene and Ammonia at very low (ppb) concentrations. It accomplishes this by utilizing three tailor-made metal oxide gas sensors. The system is capable of indicating human presence just by detecting skin emissions, even without the influence of breath emissions. It also employs a COTS CO_2 and humidity sensor for breath-based detection. It was tested in tightly controlled laboratory conditions and the effect of typical hazardous gases was not investigated.

The usage scenarios for the e-nose system presented here also include conditions that may be hazardous. The system has the capability of detecting common air-related hazards associated with entry into a confined space. These include explosive atmospheric hazards, asphyxiation hazards and toxic/poisoning hazards. Rescuers are familiar with such tools which are typically carried by them, either hand-held or strapped to them. Adding such functionality to the e-nose device increases situational awareness in the earlier stages of a rescue operation with lower risk and less effort. It also complements victim localization efforts from a perspective of survivability in the rubble cavities. The developed system of [13] did not have such capabilities.

This research work improves on the current state of the art of interface design in many aspects; the end-user of the e-nose system is the technical search specialist of a rescue team. This team member operates the detection tools used during a rescue operation which can be more than one at a time. In parallel, the operator must communicate with his team, be aware of the shifting surrounding conditions – rubble pile- and navigate the robotic platform. Examining the e-nose sensor outputs in an office environment could be enough to determine human presence or a hazardous condition, but its complexity is not practical for use in the field. The interfacing of the e-nose with the operator and the algorithm/logic that prepares the information based on the raw sensor data is also part of the e-nose system. This is implemented as software components that run on the robotic platform's processor and on the operator's control interface. The interface is optimized, not only to present the detection of various conditions, but also to assist in the execution of the search with only a periodic glimpse of it. Other aspects are its simplicity in areas such as training, maintenance and deployment. The interface of the developed system of [13] did not have such capabilities.

The research and development of this e-nose system was also validated by end-users who proposed interesting features for the graphical user interface (GUI).

The e-nose system of this research work, is partially based on the results and outcomes of the presented work of FIRST [7][16], a large backpack system combined with an air sampling and probing handheld stick for searching on the surface of the rubble for indications of a human presence, much like a search dog would. Our research improves on that method and system of detection by searching inside the rubble and by simplifying the sensor requirements, as well as reducing the size and complexity of the system. Our approach takes advantage of the limited air refreshing rate in the confined spaces of the rubble. This condition allows for the existence of large variations in the target gases when a human is present in a survivable space. The operator of the robotic platform fitted with such an e-nose system, can find the position of a victim using the e-nose, by performing a search, much like a search dog would, assisted by the helpful e-nose outputs. For such an e-nose system, proper selection of the target gases/substances to be detected is crucial and this work is presented in [13]. The selected sensors of our approach are not as sensitive as in [15], but the system has been designed to operate in a broader range of operational conditions, including the presence of hazardous atmospheres. In this work, the system is tested in more realistic conditions, including natural air being refreshed through relatively large openings, and with the presence of various sources of interference present, such as generators and other combustion motors. The e-nose of the presented work is intended for USaR operations involving collapsed structures and aims to fulfill a different set of operational requirements compared to [17]. In that work, a robot for USaR operations where fire and smoke are involved is presented. It is fitted with various sensors including an e-nose system, capable of detecting and identifying hazardous gases. It is capable of operating in near real time and can produce relative concentration maps of the detected gases. To achieve this, and to reduce the computational power requirements, output calculation is performed only when sensor input events are identified. Regarding hazard detection, information about the presence of potential hazards is useful, but absolute concentration values are preferred. This is because clearly defined safe levels exist for various hazards. The e-nose of this work employs selective sensors for the toxic target gases and a nonspecific sensor for combustible gas detection. The operator only has to select the type of combustible gas to be detected in order for the correct gas concentration and safety thresholds to be applied. This information can, in many cases, be acquired by the operators during the survey of the worksite from secondary information, common practices and experience with similar cases.

For an air sampling e-nose system to operate, only a portion of the surrounding air is sampled and analyzed, that which is near the air sampling input interface of the e-nose system, and it is assumed that the result applies for most of the air in the confined space under investigation. This, however, is an approximation and can only be used for victim localization. For air-related hazard detection this is not the case. Vertical scanning must be performed [18], which is partially supported by the robotic platform hosting the e-nose via active joints capable of raising the air sampling interface.

The e-nose presented in this work is a low-cost system, considering many factors which contribute to the cost of owning and maintaining a system operational. For USaR applications such factors are not just the cost of purchasing the device, but also all aspects that affect the organization adopting a “system”. The prominent parameters in mind are training and maintenance costs. Another aspect when comparing systems is to do so properly by carefully evaluating their capabilities. When compared to other air-based human detection methodologies for USaR, this e-nose system can be considered mostly complete, at least from a hardware perspective; it can operate in harsh environments, includes its own air sampling mechanism and only requires a hosting robotic platform which provides power input and operator interfacing. Operating in potentially explosive atmospheres requires an ATEX compatible design and component selection which increases the device’s cost considerably. Regarding the maintenance of the system, sensor aging does not affect any system training and decision making logic, as long as the sensors are two point calibrated. Sensor calibration can be performed with standard calibration procedures and tools that are typically available at organizations performing USaR operations. Sensor selection in this work favored devices with a longer lifetime in terms of expiry date and usage in detection conditions to reduce the frequency of sensor replacement, if any. Training personnel to operate and maintain the system does not require much effort for those already familiar with gas sensors and air-related hazard detection. All the aforementioned parameters influenced this research effort. The e-nose prototype device cost was in the order of €3500, excluding calibration (see 15. APPENDIX). This figure includes expensive prototype mechanical parts and approximately half of that is the cost of purchasing single quantity COTS sensors. In this regard, this e-nose is a low-cost solution compared to a trained canine. All these aspects are considered to be significant advantages for its adoption by organizations that perform USaR operations. This e-nose is not intended to replace the trained canine, but to economically help increase (build) USaR response capacity; in a major crisis where too many hot spots appear at once, there might not be enough search dogs to cover all the disaster sites. The availability of many such e-nose systems that can be stored for long periods of time and be deployed within a few hours can dramatically increase USaR response capacity especially when trained volunteers are involved in operations.

For the e-nose, proper selection of the target gases/substances to be detected is crucial in order to minimize uncertainty.

One set of selection criteria is to select gases/substances that do not have a high background measurement level and are emitted by humans, or are not present in fresh air, or at least their measured level increases substantially in the collapsed site's cavity when someone is trapped inside. Also, these gases should not be emitted by other sources near the sensor working environment. For these reasons, the atmosphere's composition is investigated in some detail and compared with the composition of exhaled human breath.

Another set of selection criteria is to select gases/substances depending on the method of detection. It is most desirable to have a real-time measurement system that is not cumulative (output zeroes when the gas/substance is not present any longer), compact, and lightweight. The response time of the e-nose affects the speed at which the search pattern can be performed by moving around and consequently the area of the site that can be covered. The noncumulative measurement scheme implies that the sensors are capable of performing multiple measurements without having to re-functionalize them. Also, various technologies have different limits of detection, ranges of operation, sampling methods, and measurement procedures. For these reasons, a survey of sensing technologies was performed to aid in target gas/substance selection based on the characteristics of the sensors or instruments required to detect candidate gases/substances at the anticipated amounts. Their characteristics must be compatible with USaR operations and first responder requirements.

The metrics for describing how much of a gas is present in a gas mixture is concentration. For gases, volume concentration is used and is defined as the volume of the target gas divided by the volume of the gas solution.

$$\text{Volume concentration} = \text{Volume of target gas}/\text{Volume of gas mixture} \tag{1}$$

The field of deployment for the e-nose is in building ruins caused by disasters such as earth quakes, equipment failure, or a terrorist action. The mobile sensor platform carrying the e-nose is sent into collapsed sections of the disaster site where access to human or dog rescue team members is not possible or safe. Survivors are expected to be found in cavities with a confined space and little air renewal. These harsh conditions increase the likelihood of detecting survivors with the electronic nose because the concentration of the target gases/compounds is expected to be higher than that of the atmosphere.

A human can be considered a source, or sink, of a target gas by producing or consuming the target gas, thus changing the concentration. The volume of the cavity can be considered the same, but not sealed (in the general case), allowing the escape of target particles and the renewal of the solution (air). Under various constraints, the concentration of various compounds can be above detection limits, thus information about the presence of victims can be extracted.

The detection of gases emitted from a human in a confined space is influenced by the following parameters

- Target gas sources (number of victims in cavity, victim’s size such as male, female or child)
- Ventilation of cavity (expressed in air flow rate changes).

The ventilation of a cavity is influenced by the following aspects:

- Openings of the cavity with air sources outside examined cavity (could be fresh air or from adjacent cavity).
- Weather conditions- wind, local weather conditions.
- Other airflows caused by temperature difference (stack effect).

The effects of these parameters on the detection performance of the e-nose were studied in [19] and the conducted verification tests performed as part of this work and are presented in [section 7, 2nd e-nose prototype].

In summary, the main contributions of this research work are to the system design which combines victim detection with hazard detection capabilities, and the capability of operation in harsh and hazardous environments by broadening the research goals. It also contributes to the detection methodology of human presence from inside the rubble. A major contribution is the e-nose interface designed for this specialized USaR application and the associated algorithmic aspects regarding the generation of the information provided. Finally, the low-cost aspects of this system can potentially contribute to creating more USaR response capacity. The latest and most complete developments of this work are published in [20].

1. DETECTION TARGETS FOR HUMAN PRESENCE INDICATION

1.1. Overview

Determining the detection targets or human presence indicators for the e-nose requires a fair knowledge of the field of operation when no human is present, the disturbances that can be caused to that state by human presence and finally the capabilities of the sensor technology detecting the disturbances. The field of operation for the e-nose is the environment and conditions the e-nose is expected to operate in. Typically the environment is an urban building construction that has been severely damaged. From the e-nose perspective, the condition of the air in the search site is of interest to assist in determining suitable detection targets for human presence indication. This includes the air composition, the air temperature, atmospheric pressure, and humidity. The air conditions of the site when no human is present could be roughly approximated to the atmospheric conditions. These conditions are the base onto which human presence, as a source or a sink, makes changes. Human breath rapidly changes the composition of the air in confined spaces. The atmosphere is also influenced by human body fluids such as sweat, saliva, tears, mucus and, in the case of entrapment, urine will most probably be excreted and influence the air composition with blood and faeces being less expected. Analysis of this information produces a first set of the candidate detection targets. This set is drastically reduced in size when the detection technology capabilities and other technical constraints are taken into account when producing the final candidates.

1.2. Air composition

The air composition of the atmosphere is examined in this section to acquire the baseline conditions in which the e-nose must operate and use them as a definite reference having no human presence. Air suitable for sustaining human life is found in nature in Earth's troposphere. It is the lowest layer of atmosphere that extends, on average, approximately 17km above the Earth’s surface. The air composition in the troposphere can be considered uniform except for the water vapor content, while air density varies with altitude. The lowest part of the atmosphere that extends a few hundred meters up to 2Km from the earth’s surface is referred to as the planetary boundary layer and is the portion of the atmosphere that is considered in this work. The planetary boundary layer (PBL), or else atmospheric boundary layer (ABL), is directly influenced by its contact with the planet’s surface affecting various physical quantities such as air flow velocity, temperature, moisture content, etc. The most critical quantities from the e-nose point of view are temperature (affecting moisture content), moisture content, and wind velocity (affecting air renewal in narrow spaces and aerosols). Due to the high variability of moisture content, the composition of the atmospheric air is given as dry air composition. The maximum moisture content can be calculated from the conditions present at a specific location. Local pollutants and aerosols also have to be considered.

$$Air\ composition = Dry\ Air\ composition\ (unpolluted) + Water\ Vapour\ Content + Local\ Pollutants + Aerosols \tag{2}$$

Aerosols, in this work, are small particles suspended in air. The particles must have a lifetime of minutes at least and are grouped as particles below a certain diameter. Particulate Matter, by definition, is the total mass of aerosols per unit of volume. PM-X is the mass of aerosol particles with a diameter of X micrometers or smaller. Aerosols can be primary (pollen, dust, ash) or secondary when they are formed by a conversion in the atmosphere. Aerosols, initially at least, are not considered as target compounds for sensor detection due to the high level of complexity regarding the sampling of them in conjunction with limitations introduced by requirements on the mobile sensor platform (robotic platform on which the e-nose can be installed). The most important limitation is the waterproof requirement set for all modules on the mobile sensing platform. The waterproofing of the e-nose system requires special filters that block a considerable amount of particle matter even for particles with a diameter smaller than that of the filter's nominal pore diameter. The local pollutants, in this context, are all substances that are not included in the dry air composition. They can occur naturally (nonanthropogenic) e.g. from plant activity or can be a result of human activities (anthropogenic) [21]. The most representative and common case of interest are hydrocarbons and volatile organic compounds. The following subsections are intended to identify the major constituents and their anticipated quantities that are at the same time emitted by the human body.

1.2.1. Dry Air Composition

The following table lists the composition of dry unpolluted air by volume at sea level [22].

Table 1: Dry air composition

Gas	Concentration
Nitrogen	78.084%
Oxygen	20.946%
Argon	0.934%
Carbon dioxide	360ppm (variable)
Neon	18.18ppm
Helium	5.24ppm
Methane	1.6ppm
Krypton	1.14ppm
Hydrogen	0.5ppm
Nitrous Oxide	0.3ppm
Xenon	0.078ppm

Note that the carbon dioxide, or CO_2, content listed as 360ppm is equivalent to 0.036%. This value is steadily increasing every year and since the publication of the source has reached 0.040% or 400ppm [23]. This value is not to be taken blindly because it is influenced by many local factors. The value measured at each site depends on the local conditions and activities, including both anthropogenic and nonanthropogenic. Since local conditions change, a constant value should not be assumed, even for the same exact location. For example, in densely populated urban locations pollution as well as the weather conditions affect the CO_2 concentration. Also, in lightly populated semi-urban locations that include or are near vegetation, such as forests, the CO_2 concentration can be influenced by vegetation's (metabolic) activity and variations should be anticipated between day and night. This uncertainty of the baseline value of the CO_2 concentration should be accounted for if it is used as an indicator. The design of the e-nose must anticipate small variations of the CO_2 concentration during deployment at a site by supporting the easy and frequent update of baseline-reference measurements, as well as an increased immunity to these variations that can be modeled as noise. Similar considerations apply for the oxygen concentration. These O_2 variations, though, will not be much noticed because they are not very high if expressed as a percentage of the O_2 concentration value.

The following table lists the concentration of hydrocarbons in the remote continental boundary layer [22].

Table 2: Concentration of hydrocarbons in the remote continental boundary layer

Hydrocarbon	Concentration (ppb)
Methane	1600
Ethane	1-6
Ethene	0.2-3.2
Ethyne (acetylene)	0.3-2.4
Propane	0.1-2.7
Propene	0.2-0.8
n-Butane	0.1-1.9
1-Butane	0.1-0.7
n-Pentane	0.1-0.7
Benzene	0.2-1.2
Toluene	0.1-1.0
Isoprene	0.6-2.3
α-Pinene	0.033-1.5
β-Pinene	0.1-0.43

The concentrations listed are very low and are not considered to be a great influence in case these gases are selected as indicators. However, as in all cases, local sources and conditions can greatly affect these values. The Methane concentration value could be an exception since it is in the low ppm range (1ppm is 1000ppb). Its occurrence at high levels should be anticipated since it is the major constituent of natural gas, liquefied natural gas (LNG) and is also a product of the anaerobic decay of organic matter. Methane is flammable and is used as fuel in many cities. In an urban setting, it can be the primary cause of a disaster, such as an explosion from a (natural) gas leak. It can also be a safety hazard in a disaster site since it can fuel a fire or cause an explosion. It can also be a cause for asphyxiation if it displaces enough of the air's oxygen in a confined space. The methane concentration levels in the atmosphere are very low compared to the levels considered hazardous, so there is no interference if methane is monitored for safety reasons.

1.2.2. Water vapor content

The metric for describing water vapor content in the atmosphere is humidity. Humidity is quantified in three ways:

$$\text{Absolute Humidity} = \text{mass of water vapour / volume of air and water vapour mixture} \tag{3}$$

$$\text{Relative Humidity} = (\text{partial pressure of water vapour in air/} \\ \text{saturation vapour pressure of water at the same temperature}) * 100\% \tag{4}$$

Relative Humidity can also be calculated as = Absolute Humidity/Absolute Humidity when air saturated in the current conditions.

$$\text{Specific Humidity} = \text{mass of water vapour / total mass of moist air [24]} \tag{5}$$

Absolute Humidity is the metric more useful for quantifying the amount of water vapor present in air. Relative Humidity is the metric more suitable for estimating human comfort and air quality. It is very helpful in understanding the water vapor carrying potential of air in certain conditions of temperature, pressure, and absolute humidity. Humidity is a parameter that has to be controlled inside the e-nose instrumentation because the complete range is not supported by all the sensing technologies used. The following table lists the saturation vapor pressure of pure water at various temperatures [22].

Table 3: Saturation vapor pressure of pure water in various temperatures

Conditions	Set 1	Set 2	Set 3	Set 4	Set 5	Set 6
Temperature (°C)	0	5	10	15	20	25
Pressure (Pa)	610	872	1228	1705	2338	3167
Water content (g/m3)	4.847	6.797	9.399	12.83	17.30	23.05

A more detailed table regarding relative humidity and temperature can be calculated at [25] from the equations given at [26][27].

An important observation is that when the temperature increases, so does the water carrying capacity of the air. This also implies that when the temperature decreases, so does the water carrying capacity. A critical observation is that if the air is saturated with humidity (100% RH) at a specific temperature and then the temperature drops, the excess humidity forms water droplets. This condition is described as condensation and is a condition in which electronic components are not typically specified to operate in.

1.2.3. Volatile Organic Compounds (VOCs) with biogenic origin

The volatile organic compounds considered in this section are mostly the ones produced by plants. The following short chain oxygenated VOCS, or else oxVOCs, play many roles in plant physiology and ecology: Formic and acetic acids, acetone, formaldehyde, acetaldehyde, methanol, and ethanol. Plants, under non-stressed conditions can emit all of them at fluxes ranging from 0.2 up to 4.8ug(C)g-1 (leaf dry weight)h-1. These rates increase several orders of magnitude when the plants are under stress. Due to their relatively long atmospheric half-lives they can reach considerable concentration in the atmosphere in the range of ppbv [28].

Isoprene occurs naturally and is widely present in the environment at low concentrations [29]. It is emitted from plants and trees and it is estimated that the contribution of isoprene to the total nonmethane emissions from the biosphere is about 50% [30]. The global annual foliar emission of isoprene was estimated to be about 400 million tons [31]. Isoprene is produced endogenously by humans (as the major endogenous hydrocarbon), probably from mevalonic acid, a precursor of cholesterol biosynthesis. The production rate of isoprene was calculated to be 0.15 pmol/kg and the quantity exhaled per day was estimated to be 2-4 mg/kg [32][33].

1.2.4. Volatile Organic Compounds (VOCs) with anthropogenic origin

Isoprene is present in roasted coffee and is formed in combustion processes (detected in automobile and turbojet exhaust and in the gas phase of tobacco smoke) and during wood pulping and rubber abrasion [33]. An investigation into the traffic-related fraction of isoprene at an urban location is presented in [34]. This study concludes that in the winter isoprene and the other measured hydrocarbons are of anthropogenic, vehicle motor origin. In the summer, a strong biogenic origin of isoprene was pointed out, conforming to similar works. The concentrations of Isoprene are not steady throughout the year and vary during the seasons and the time of day as can be seen in [35].

1.3. Gases/compounds emitted from the human body

This section examines the gases and compounds emitted from the human body through breath, sweat, tears, saliva, mucus and other body fluids such as urine and blood. Faeces are not examined because they are not generally anticipated to be produced during entrapment. Most interest is focused on breath and urine-oriented sources because they have the most potential to generate practically measurable concentration changes.

1.3.1. Composition of exhaled human breath

The composition of exhaled human breath is examined in this section to acquire information on the disturbances caused to the atmospheric baseline composition which could be detected and thus be used as human presence indicators. The composition of human breath, and more precisely, the composition of the exhaled air has similarities to the composition of the inhaled air. The major constituents are present but have slightly different concentrations, with the only exception that of water vapor content, which is always near 100% relative humidity.

“Full saturation of the exhaled air is essential because it minimizes airway drying and local increases in the concentrations of solutes in the fluid lining the airway that could damage the pulmonary epithelium and interfere with gas exchange.” [36]

The most apparent changes can be observed in the concentrations of oxygen and carbon dioxide as a result of the main human metabolic activity: energy consumption. The ratios of input/output oxygen and input/output carbon dioxide are not the same among all humans and, in fact, vary greatly. The efficiency of each individual in absorbing oxygen, and thus emitting carbon dioxide, depends on many factors. Physical health and fitness level can be considered the most influential. In any case, oxygen absorption is not 100% efficient. Human metabolism is very complicated and that can explain the plethora of emitted compounds. The content of these other compounds in the exhaled air of healthy humans is dramatically different among individuals and can be partially attributed to environmental factors, such as exposure to pollution, different metabolic activity, and nutrition composition. A recent research work suggests that every individual has his own unique breath chemical pattern [37]. Various health conditions have an effect on the composition of the exhaled air as shown in various publications [38][39]. Typically, a substance's concentration increases or new compounds are present, without greatly affecting the core composition of the exhaled breath. Thus, the detectability of healthy/ill individual is not distinguishable if specific compounds are not monitored.

A fair approximation of the exhaled air content regarding the major breath constituents is included in the following table:

Table 4. Major constituents of exhaled air.

Component	Concentration (by Volume)
Nitrogen	78.04%
Oxygen	13.6% - 16%
Carbon dioxide	4% - 5.3%
Argon, Helium, Neon, and other gases	1%
Water vapor	5%

Other traces of gases (Carbon monoxide, Hydrogen, etc)	In the ppm level
Other non methane carbohydrates , Volatile Organic compounds (Ammonia, Acetone, Methanol, Ethanol, etc)	In the ppm level
Aerosols	

Human breath is vapor content saturated and has a relative humidity of 100%. The margin of ambient humidity to 100% humidity could give an indication of human presence: humidity is elevated. Under conditions, such as low environment temperatures and confined spaces, the exhaled humidity can create condensing humidity conditions that are not tolerated very well by many electronic components. It is anticipated that the e-nose will operate in such conditions and special care (design features) should be taken.

Comparing the information of the concentration of the atmosphere and the exhaled breath, it is evident that oxygen and carbon dioxide have a great margin for producing detectable variations in a confined space occupied by a human. Thus far, the concentrations of CO_2, O_2 and humidity can be used as indicators of human presence. Another aspect not obvious in the data is that the exhaled air has a relatively fixed temperature close to that of the human body. Again, if the temperature of the environment is different, this could also be detected and used as a human presence indicator.

Concentrations of VOCs in human breath emissions in various situations can be found in table 1 of [40]. Also, the results of a simple box model used to calculate steady-state VOC concentrations resulting from a few common, if confined, situations can be found in table 2 of [40]. The measured VOC levels for similar spaces are provided, where available, for comparison. Due to large uncertainties these comparisons should be regarded as qualitative. According to the authors of the referenced work, “when people congregate indoors, human emissions are likely to be a significant fraction (e.g., >10–20%) of the source of TVOC. In some cases, human emissions may dominate other sources of VOCs.”

The volatile organic compounds emitted by human breath listed in [40] are in the ppb range and their detection depends on the sampling techniques and sensing technology employed. Current requirements and the state of the art of the sensing technologies do not allow, for the near future, the utilization of other identified ubiquitous compounds as victim localization indicators. This is because the anticipated detection range is wide due to the large variations between individuals. Some individuals fall below the detection thresholds, thus not all people will be detected with these indication criteria. The resulting and anticipated false negatives will only be increased when applied at real disaster sites where sampling conditions might not be known and cannot be controlled, producing unfavorable conditions for victim detection.

1.3.2. Gases originating from body fluids

This section presents the potential gas targets that could be detected from various body fluids.

The metrics for quantifying the presence of a specific gas/compound is concentration. For fluids, ideally, the concentration of gases/compounds is measured in the headspace of the fluid. For laboratory analysis of the headspace of a liquid, a specified volume of the fluid is placed in a specified fluid container leaving a specified air volume above the surface of the fluid. The air of the container is sampled and compounds are detected in it. These sampling conditions are known and the same for all samples. In the electronic nose field of operation, the sampling conditions are neither steady nor known in most cases. One aspect is almost certain: The conditions are not favorable for the accumulation of large, easily detectable, concentrations due to rubble gap/void conditions such as ventilation, material absorption/adsorption and large ratio of fluid sample to air volume. Thus, the concentrations reported by the various studies referenced in this work, must be used with caution, as they should be interpreted as the maximum values in the best-case scenario (concentration wise) conditions for the electronic nose. When no data is available about the headspace concentration of gases over a liquid, the composition of the fluid itself is studied. A rough estimation of the possible gases that could be emitted in the air in some cases is produced based on assumptions. Again, the assumptions can be fairly optimistic and the results indicating best-case scenario conditions (concentration wise) for the electronic nose.

The work mainly focuses on urine since this is the most anticipated body fluid to be excreted producing detectable ammonia levels depending on various conditions. Faeces are not examined because they are not much anticipated in trapped human situations. Other body fluids such as saliva, tears, sweat and mucus are not examined independently since they are examined in the Trapped Human Experiment work [41][42], where a person was placed in a chamber and the air sampled and measured. Their contribution to the overall result is not considered because for the entrapment case they cannot be found separately (breath vs. sweat, tears, mucus, saliva). The cause (gas substances) of metallic blood odor was investigated in literature. The metallic odor humans can smell after a fresh cut is in fact the by-product of decomposition of substances found on human hands and skin when they come in contact with ferrous ions (Fe^{2+}) of the blood [43]. This reaction is rapid and the released compounds are aldehydes and ketones. The key odorant is 1-octen-3-one. The supporting table lists the odorants contribution to the characteristic smell.

The maximum concentration of the detection threshold of the critical odor component is 1.12ug/m3. This is equal to 0.00022ppm or 0.22ppb. This value indicates a very high sensitivity of the human olfactory system to this substance. The detection of this substance requires GC – MS sensing techniques and probably under nonlaboratory conditions is not feasible. Furthermore, the detection of this compound requires that the ferrous ions of blood react with substances located on human hands and skin.

$$\text{ppm} = (\text{mg/m3 value})(24.45)/(\text{molecular weight}) \tag{6}$$

$$\text{mg/m3} = (\text{ppm value})(\text{molecular weight})/24.45 \tag{7}$$

24.45 is a conversion factor that represents the volume of one mole of gas.

To determine the molecular weight of a particular substance, add the atomic weights (refer to the MSDS of the particular substance) of each atom present in the chemical formula of that particular substance.

Note: this calculation assumes a temperature of 25°C (77°F) and a pressure of 1 atmosphere (760 torr or 760 mm Hg).

1-Octen-3-one molecular weight is 126.20g/mol

Urine constituents and detection

Urine is a body fluid that is anticipated to be excreted during entrapment of human victims in building rubble voids. Detection of urine is an indicator of both healthy and injured victims. Its detection cannot indicate the current status of the person who produced it, if he/she is still alive. The examination of urine as a human presence indicator for the e-nose is promising since the typical volume excreted is in the ml-l range and contains a large number of compounds/substances some of which are in high concentrations. Furthermore, some of the substances are even volatile or produce gases that can be detected in the air. A limiting factor is that the detectable contents in urine are not released/ produced at once and greatly depend on many conditions, of the victim and of the environment.

Liquid contents in human urine

A list of compounds present in the human urine can be found in [44]. The amount of ammonia present in the typical urine sample is very high, though it is not released in the air but is rather diluted. Its origin might not be from the human body. The potential source of ammonia in the air is from the large quantities of urea when decomposed by bacteria.

Volatile organic compounds in human urine

A list of the volatile compounds present in human urine can be found in [45]. These compounds are measured in the air above urine samples (headspace). That work includes the compounds identified in the referenced work, as well as compounds identified with other methods from other research groups. Note that not all of the compounds were found in all test subjects. Also, many of the compounds were not found with all of the sampling/detection methodologies. From all the compounds listed, only the following are found in all samples independent of pH conditions and can be considered for detecting human urine: acetone, methylene chloride, 4-heptanone, 2-pentanone, 2-butanone.

The following section has a more relevant, to this work’s case, setup and the reported concentrations for the target compounds are in the lower ppb range. Using sensor detectors that are not strictly sensitive to a specific compound, but rather sensitive to groups of compounds, could increase the effective concentration.

Permeation profiles of urine volatile compounds

In [46], a simulation of a void in rubble was created to study the permeation profiles of twenty-two volatile compounds occurring from urine samples. The apparatus was built around a custom-made container that could hold various types of rubble suspended above a urine sample. A light air flow was maintained over the urine surface and the air above the rubble. The air over the rubble was sampled at regular intervals. That research includes a table that lists the retention times (R t), LODs (ppb), RSDs (%), correlation coefficients (R 2), linear ranges (ppb) and qualifier–quantifier ion ratios used for identification of monitored urine species. It also includes tables that list the incidence and maximal concentrations of urine-borne compounds obtained for different materials investigated within that study. Another interesting table lists the average time constants (τ) representing the removal rate of the urine-borne compounds from the chamber and the average peak times (times of the maximal concentrations measured from the time of the urine injection). This work and results suggest that poorly soluble substances are released early after the urine is excreted and probably disappear relatively quickly from the victim's surroundings. Among those substances is acetone, which exhibits very high concentrations compared to the other compounds yet in the ppb range.

Ammonia creation from the hydrolysis of urea

Urease is an enzyme that catalyzes the hydrolysis of urea into carbon dioxide and ammonia [47][48][49][50]. The reaction occurs as follows:

$$(NH_2)2CO + H_2O \rightarrow CO_2 + 2NH_3$$

The kcat/Km of urease in the processing of urea is 10^{14} times greater than the rate of the uncatalyzed elimination reaction of urea. Ureases are found in many bacterial species and are used in the detection of various urease generating pathogens such as: Proteus mirabilis and Proteus vulgaris, Ureaplasma urealyticum (a relative of Mycoplasma spp.), Nocardia, Corynebacterium urealyticum, Cryptococcus spp. (an opportunistic fungus), Helicobacter pylori, Brucella, Staphylococcus saprophyticus, and certain enteric bacteria including Proteus spp., Klebsiella spp., Morganella, Providencia, and possibly Serratia spp.

The biochemistry of urease [49] indicates that other compounds can be affected by urease: The enzymatic decomposition pathway catalyzed by urease features kcat/Km approximately 10^{15} times higher than the rate of the uncatalyzed reaction [51]. The observed values of Km fall in the 1–100 mM range and are largely independent of pH, while kcat strongly depends on this parameter. Typical bell-shaped pH profiles for urease activity are observed, with pKa values of 6.5 for a general base that must be deprotonated, and ca. 9.0 for a general acid that must be protonated. The maximum of activity is detected at pH 7.5–8, with maximal values of kcat and kcat/Km of ~3,000 s−1 and ~1,000 s−1 mM−1, respectively. Enzyme inactivation at pH < 5 is due to irreversible protein denaturation and loss of the essential nickel ions. Urea is not the only substrate for the enzyme, and hydrolytic activity also involves formamide, acetamide, N-methylurea, N-hydroxyurea, N,N′-dihydroxyurea, semicarbazide, and different kinds of phosphoric acid amides. The values of kcat for these alternative substrates are two orders of magnitude lower than that observed for urea.

The most interesting substances are ammonia and acetone due to their ability to be in a gas form at ambient temperatures. Acetone is also emitted from the human body by breath and sweat, but the amount produced, indicated by the urine content, is not high enough to be detectable by acetone gas sensors. Ammonia, on the other hand, is produced in larger quantities, though what is very interesting is the production of ammonia from bacteria which consume urea.

A study reports that the mean odor detection threshold (ODT) for NH_3 is 2.6 parts per million [52]. This information is very useful and helps determine the potential concentrations that can be encountered if combined with the following observation. Places where urine is deposited and not cleaned, like urinals (waterless or even flushed ones), back alleys, walls, a body with poor personal hygiene, used diaper [53] bins, develop the distinct urine smell of ammonia. Since the ammonia can be smelled even in the outdoor cases, it can be assumed that the emissions are adequate to produce concentrations way above the limit of detection. Also, ammonia is exhaled when breathing. For these reasons, ammonia is the only gas/compound that has the potential to be accumulated in a confined space in concentrations at the ppm level and thus be detected by a small ammonia gas sensor.

Other urine constituents that could be potentially detected in the air are the volatile organic compounds present in it if state-of-the-art sensing technologies miniaturize substantially. Most of the volatiles detected in the referenced study are detected after the urine sample is mixed with an acid or a base. Only five compounds were ubiquitous independent of pH: acetone, methylene chloride, 4-heptanone and 2-pentanone and 2-butanone. These compounds represent the compounds emitted directly from the urine without any interactions with the environment. When urine is released into the environment, which is typically not sterile, chemical or biological interactions occur that produce or consume volatile compounds. Anyhow, the concentrations of these volatile organic compounds are in the ppb range and it is not very likely that gas sensors can detect them.

1.4. Sensor technologies and capabilities

The initial concept when inventing the term e-nose was that of an artificial system that could perform as the mammalian olfactory system for detecting smells. Great effort has been put into the subject over the years but the resulting devices are still outperformed by their natural counterparts in most cases. Only in specific, very well defined and controlled conditions, do e-noses perform well, by automating specific processes, providing round-the-clock detection services and reducing cost [54]. Nowadays, the e-nose terminology is also used for gas detection systems that can detect gases not sensed by the mammalian olfactory system. An example of a highly specific task, where e-nose systems perform well, is the detection of flammable natural gas in mining operations. An example of a highly complex problem, where e-nose systems have not yet reached maturity, is quality control testing of food specimens via odor sensing. The state of the e-nose technology is affected by the underlying detection/sensor capabilities, the equivalent of the biological receptors, in terms of detectability and selectivity of various target elements. Many technologies exist, each having their advantages and disadvantages. Many configurations are possible but most of them require many sensing receptors, as do the natural ones. Some approaches use a number of standard gas chemical sensors. Others use custom-made clusters of sensing elements. No single technology can yet be considered the prevailing one, although chromatography coupled with mass spectrometry-based solutions exhibit high sensitivity and selectivity at the expense of time, space, simplicity and cost. The objective in this case dictates many constraints effectively reducing the suitable e-nose or sensor choices. For example, any e-nose system larger than 20x20cm is not considered simply because it is too large. The following section will briefly present the technology of various types of gas sensors (receptors). Having a basic notion of the underlying detection technology will assist in the evaluation and suitability of the currently available e-nose products and sensors for creating them.

1.4.1. Gas sensing technologies

Gas sensing technologies are categorized according to the physical properties they use in order to convert the gas concentration information into a computer measurable property. Each detection technology will be evaluated according to its advantages and disadvantages. The criteria for the sensing technologies are sensitivity, selectivity, response time, energy consumption, reversibility, long-term stability, cost, size, and if the detection is destructive.

The following gas sensing technologies are considered suitable and some of them are utilized in the e-nose prototype devices.

Metal Oxide Sensor – MOX, Metal Oxide Semiconductor sensors MOS

The MOX or MOS sensor is a commonly used sensor. This sensor utilizes a layer of metal oxide over a semiconductor in order to detect redox reactions of the target gas with the metal oxide. The detection process is the following: 1) Redox reactions occur on the surface of the metal oxide (for example between the O- in a SnO_2 metal oxide sensor) distributed on the surface and the molecules of the target gas. 2) The redox reaction creates an electronic variation that changes the conducting state of the semiconductor. This change can be interpreted with the readout circuits. The redox reaction is influenced by the reaction temperature of the oxidizer (O-) which is typically high. The high working temperature of the sensor is typically maintained with a heated filament. Various gases have different optimum working temperatures, thus selectivity of the sensor depends on the air sample mixture. Advantages: low cost, medium sensitivity, possibility of detecting more than one target by changing the temperature, fast reaction time, small, reversible. Disadvantages: higher power consumption, selectivity depends on sample mixture.

NonDispersive Infrared sensor –NDIR [55][56][57]

In this detection technology, infrared light from an infrared source is guided to pass through two sample chambers. Infrared detectors are located where the light exits at each chamber. The gas in the chambers causes absorption of specific frequencies according to the Beer-Lambert law. According to the attenuation measured by the detectors, the gas concentration can be determined. The one chamber is typically sealed with a known concentration of a gas and is used as reference to cancel out external gas-related measurement noise.

Other thermal background noise is removed by modulating the infrared source (simplest form is ON/OFF). Also, the selection of specific frequencies is assisted by the utilization of various optical filters. This type of sensor is very popular for detecting CO_2. Advantages: small, medium price range, selective, fast response, good long-term stability, small to medium energy consumption. Disadvantages: sensitivity not greatly influenced by low selectivity at low concentrations of target gas.

Fluorescence-based optical sensor

In this detection technology, the principle of fluorescence quenching by the target gas is used. An example of this type of sensor is an oxygen sensor. These sensors have low power consumption but at the same time have a longer lifetime compared to electrochemical sensors due to the nondepleting sensing principle. These sensors can operate in a wide range of environmental conditions and are very stable and robust. Also, they do not contain hazardous materials and can have negligible cross-sensitivity to other gases. Advantages: small size, medium price range, selective, good long-term stability, low energy consumption, long lifetime. Disadvantages: response time.

Electrochemical Cells – EC sensors

Single compounds in a gas mixture are usually detected with electrochemical cells. These cells are isolated from the environment by a selective diffusion barrier. Only the target gas is, theoretically, able to reach the electrochemical cell. The target gas is detected in an EC cell via the oxidization or reduction of the gas. The cell typically contains 3 electrodes that are used to perform amperometric or potentiometric measurements. The current/potential is correlated directly with the concentration of the gas in the cell and therefore in the sample. Advantages: good selectivity- not perfect due to nonperfect diffusion barrier, small, relatively cheap, long-term stability, low power. Disadvantages: sensitivity, response time, destructive detection, electrochemically active compounds.

The following list includes the sensing technologies considered for utilization in the e-nose but were deemed unsuitable.

Bulk Acoustic Wave – BAW, Surface Acoustic Wave – SAW [58][59]

The acoustic wave sensors are capable of sensing by detecting differences in the propagation of sound/mechanical waves. The differences are commonly the change of mass of the surrounding air or of a polymer coating that absorbs target gases. Sound waves are typically produced by a piezoelectric transducer and received by another one. The propagation mechanism of the wave determines if the sensor is a surface acoustic wave or a bulk acoustic wave device. For sensing one gas, typically, there are two pairs of transducers: one that is exposed to the measured mixture, and one that is not and serves as a reference. For e-nose applications, a cluster of transducers is assembled, but each detection cell has a different sorptive coating. The selectivity of the sensor depends on the properties of the coating. Advantages: small, inexpensive, low power, sensitivity. Disadvantages: selectivity, sensitive to particles and water condensation.

Metal Oxide Field Effect Transistor – MOSFET [60]

In a CCFET setup (Capacitive Coupled Field Effect Transistor), a gas-sensitive layer is applied to a suspended gate that is mounted on top of a silicon chip. If this layer comes into contact with molecules of the target gas it responds with a change of its surface potential. The gas-sensitive layer is capacitively coupled to a large floating electrode which is connected to the floating gate of a conventional MOSFET (Metal Oxide Semiconductor Field-Effect Transistor).

Photo-acoustic Infrared Spectroscopy

In this method, a modulation of the intensity of an IR source causes a temperature variation and the resulting expansion and contraction of the gas is measured with a microphone as audible frequencies. Alternatively, the absorbed energy of a narrow band- pass infrared beam is measured in filter-based infrared spectroscopy. Commercially available devices (e.g., MIRAN SapphIRe from Thermo Scientific [61]) are used mostly for absolute measurements of concentration either in detection of a single compound which has a unique absorbance wave-length or by analysis at multiple wavelengths for a known gas mixture. However, where the constituents of the gas mixture are unknown, these instruments can also be combined with pattern recognition and used as an e-nose. Advantages: good selectivity performance in known gas mixture, response time, no reversibility issues, good stability in the long term. Disadvantages: Sensitivity is not very high. An instrument capable of detecting various gases is expensive and its size is not very small.

Mass Spectrometry [62][63]

Mass spectrometers are typically used in analytical chemistry for the determination of the amount and type of chemicals present in a sample. This is achieved by ionizing chemical compounds to generate charged molecules, or even fragments, and measure their mass-to-charge ratios. The mass-to-charge ratio is measured by accelerating the charged molecules/fragments and then deflecting them in an electric or magnetic field. The induced deflection is higher when the mass is smaller and the charge is larger. The detection of the deflection can be done by a properly positioned electron multiplier. Many configurations exist for deflecting, filtering and detecting. A common disadvantage of all mass spectrometers is that their operation requires a vacuum. Mass spectrometers are often fed the output of gas chromatographers. In e-nose applications though, no separation is performed and each mass-to-charge ratio can be treated as a virtual sensor further analyzed with pattern recognition algorithms. Advantages: very good sensitivity, very good selectivity. Disadvantages: high cost, requires vacuum, requires ionization of sample, complex power supply, relatively long response time.

Gas Chromatography [64]

Gas chromatography is used in analytical chemistry for separating and analyzing compounds that can be vaporized without decomposition. The separation process is followed by some type of detection of the separated compounds. Various detectors are used depending on the target gases and solutions. Gas chromatography is performed with the following process: the sample is vaporized and mixed with an inert or nonreactive gas- the mobile phase. During the static phase the mixture is passed through a long tube or column coated with a liquid or polymer. The sample compounds interact differently during the static phase as they travel through the column at different times, thus separating. The detector then can detect individual compounds. The measurement is the intensity of the output of the detector over time. Various compounds are indicated with peaks in the diagram. The area of each peak determines the concentration of the compound in the sample. The time at which each compound exits the column is detected and can be used to infer what compound it is according to known reference outputs. In e-nose applications, the detector output at various output windows can be integrated and considered the output of a virtual sensor. Advantages: sensitivity depends on detector type, very good selectivity. Disadvantages: requires an inert or nonreactive gas; heating the column increases power consumption; response time depends on length of column -not instant; device can’t be miniaturized beyond a point.

Flame Photometry Detector – FPD [65]

The flame photometry detector (FPD) is based on the decomposition of any organic compounds in a hydrogen flame. If phosphorus or sulphur is present, light of a specific wavelength will be emitted. After the other wavelengths are masked out through filters, a photomultiplier detects the concentration of one of the elements. Because phosphorus and sulphur are present in classical nerve gases, this technology is often used in the military/security application field. Advantages: capable of detecting specific phosphorous and sulphur-based compounds, long-term stability, quick response. Disadvantages: requires hydrogen gas flame; limited sensitivity; not miniaturized - though portable; cost; destructive detection.

Photo Ionization Detector PID -without coupling to an Ion Mobility Spectrometer [66][67]

This detection mechanism uses a UV light source to ionize the target gas mixture. It is capable of detecting compounds with an ionization potential equal or lower than that of the UV light. This method is a broad range method without great selectivity since it detects all the compounds in the solution that can be ionized with the particular UV source. Detection is performed with an electron multiplier and the output of the device is a current measurement. This sensing method is produced as a handheld portable and is used in a wide range of applications due to its high sensitivity. Advantages: good sensitivity, fair long-term stability, nondestructive detection, reversible, fast response. Disadvantages: not good selectivity, medium price range, portable but not miniature.

Flame Ionization Detector – FID [68]

For a nonspecific determination of flammable compounds, flame ionization detectors (FIDs) are used. In a hydrogen- oxygen flame the compounds are burned in an electric field, and the ion increases are detected as an electrical current via two specially shaped electrodes. Because all organic compounds are detectable, flame ionization detectors are often used in gas chromatographs, but they are available as stand-alone devices as well. Advantages: high measuring range, long-term stability, fast response time. Disadvantages: not selective, unable to detect inorganic substances, require flame, destructive detection, relatively low-medium cost, portable not miniature.

Thermal Conductivity Detector – TCD [69]

In this type of sensor, the different thermal conductivities of various gases are exploited. A chamber is heated to steady conditions. A temperature sensor (RTD, Thermocouple, Thermistor) is located within the chamber. Under normal conditions the temperature reading is constant, but when a gas with a different thermal conductivity enters the chamber, the temperature of the sensor changes. This type of sensor is nondestructive but does not have great selectivity since many gas mixtures could exhibit similar thermal conductivity. Nevertheless, it is ideal in determining the ratio of a two gas mixture when the gases have different thermal conductivities. This type of detector is typically used as a detector for low end gas chromatography instruments as it is robust and cheap, even though it does not provide the best available sensitivity. Advantages: low cost, nondestructive, fast response, good long-term stability, good selectivity for gas mixtures of two known gases with dissimilar thermal conductivities, relatively small, reversible. Disadvantages: sensitivity, selectivity, power requirements for heater.

Carbon Nanotubes based sensors

Carbon nanotube based sensors can employ different working principles similar to other types of gas sensors (e.g. variable resistance, carbon nanotube field effect transistor) [70]. Their advantage is better sensitivity even at room temperatures for specific target gases and the miniaturization due to the very good physical properties of the carbon nano tubes. The disadvantage is that although they have been developed for quite some time, there do not seem to be any commercially available sensors. Advantages: high sensitivity at room temperatures, miniaturized. Disadvantage: for research only, no sensors commercially available.

Conductive Polymer – CP [71]

A typical type of conductive polymer sensor is the chemresistive type. In this sensor configuration, the polymer material changes its conductance when exposed to substances that react with it. The polymer can be customized to be sensitive to different substances. The sensor is not very selective but exhibits different responses for a wide range of substances. Creating an array with multiple chemiresistors that have differentiated polymer materials is a popular way to create an e-nose. The reaction of the entire array when exposed to a substance creates an identifiable pattern. Different substances each produce a unique pattern. Unfortunately, each substance to be detected must be chosen in advance and the system trained. This fact also limits the use cases of this type of sensor to detecting only one gas target at a time. If more than one target gases are present at the same time their patterns are mixed, the response of the sensor depends on the concentration of each gas. The concept of this sensor was proposed decades ago and many sensor devices have been published in research results. Few commercial products are advertised and even those have not yet reached maturity. Advantages: sensitivity to some gases is very high, low power, small, portable, non-cumulative, low price (promised in the long term but not yet). Disadvantages: not great selectivity, although this is exploited in arrays; reversibility issues; lifespan issues; destructive detection; sensitivity to humidity; price (now as prototypes); commercial products are not widely advertised.

AIMS (Aspiration Ion Mobility Spectrometry) [72]

This sensor works in the following way: the sample gas is ionized. This is done with alpha particles from Am-241 sources which are similar in smoke detectors. The original ions react with the analyte and form ions which are transported with gas flowing to the measurement area. The measurement area is a narrow, flat channel with electrodes on both sides of the channel. These electrodes are used to create an electric field which is perpendicular to the flow. The ions are transported via the channel with the flow and towards the electrodes by the forces caused by the electric field and ions' charge. The movement depends on the characteristics of the ion: high mobility ions go fast and drop to the first electrodes while low mobility ions travel a long time with the flow and reach the latter electrodes. When the ion hits the electrode, the ion loses its charge. The charges hitting the electrodes are measured as current and the current is used as an indication of the existence of certain types of ions. The sensor is a somewhat compacted mass spectrometer that can work without a vacuum with atmospheric air. It is portable and can be considered to be a large handheld device. Its performance is orders of magnitude better than the single detector sensors like EC, MOS, MOX sensors but is not as sensitive as Mass Spectrometry. Advantages: high sensitivity, selectivity, measurement speed. Disadvantages: high cost to acquire and maintain, portable but not compact, heavy weight, cannot be used to detect CO_2, contains nuclear source, very difficult to transport due to nuclear source.

Specifications of various sensor types from a portable handheld instrument

The following table lists sensors for the MultiRAE gas monitor of RAE systems and is provided as an indicator of the current capabilities of some of the sensor technologies [73].

Table 5. Sensors for the MultiRAE gas monitor of RAE systems and their capabilities

Sensor type	Range	Resolution
PID Sensors	Range	Resolution
VOC 10.6 eV (Ext. Range)	0 to 5,000 ppm	0.1 ppm
Combustible Sensors	Range	Resolution
Catalytic LEL	0 to 100% LEL	1% LEL
NDIR (0-100% LEL Methane)	0 to 100% LEL	1% LEL
NDIR (0-100% Vol. Methane)	0 to 100% Vol.	0.1% Vol.
Carbon Dioxide Sensor	Range	Resolution
Carbon Dioxide (CO_2) NDIR	0 to 50,000 ppm	100 ppm
Electrochemical Sensors	Range	Resolution
Ammonia (NH_3)	0 to 100 ppm	1 ppm
Carbon Monoxide (CO)	0 to 500 ppm	1 ppm
Carbon Monoxide (CO), Ext. Range	0 to 2,000 ppm	10 ppm
Carbon Monoxide (CO), H_2 -comp.	0 to 2,000 ppm	10 ppm
Carbon Monoxide (CO) +	0 to 500 ppm	1 ppm
Hydrogen Sulfide (H_2S) Combo	0 to 200 ppm	0.1 ppm
Chlorine (Cl_2)	0 to 50 ppm	0.1 ppm
Chlorine Dioxide (ClO_2)	0 to 1 ppm	0.03 ppm
Ethylene Oxide (EtO-A)	0 to 100 ppm	0.5 ppm
Ethylene Oxide (EtO-B)	0 to 10 ppm	0.1 ppm
Formaldehyde (HCHO)	0 to 10 ppm	0.05 ppm
Hydrogen Cyanide (HCN)	0 to 50 ppm	0.5 ppm
Hydrogen Sulfide (H_2S)	0 to 100 ppm	0.1 ppm
Methyl Mercaptan (CH_3-SH)	0 to 10 ppm	0.1 ppm
Nitric Oxide (NO)	0 to 250 ppm	0.5 ppm
Nitrogen Dioxide (NO_2)	0 to 20 ppm	0.1 ppm
Oxygen (O_2)	0 to 30% Vol.	0.1% Vol.
Phosphine (PH_3)	0 to 20 ppm	0.1 ppm
Sulfur Dioxide (SO_2)	0 to 20 ppm	0.1 ppm

1.5. Conclusions – discussion

The composition of the atmosphere in conjunction with the composition of the air around and near a trapped victim contains many properties that can be used as human presence indicators. From these candidates though, only a small fraction can be practically utilized in real, nonlaboratory, conditions. This is because of the following reasons: The concentration of most of the compounds produced by humans is very low, in the low ppb range. The reported values are the concentrations of the source. These concentration values are reduced by order(s) of magnitude when the source mixture is diluted in the air of a particular space. The source or even the number of sources is unknown. The detection and quantification of most of these compounds, at the low ppb concentration range, require steady and known sampling conditions, complex calibration procedures and large measurement instruments. The robotic platform that hosts the e-nose has severely constrained requirements on its physical dimensions and thus can only host a finite payload of size, weight and power. The AIMS detector, even in case the size and weight were acceptable, was rejected because of the included nuclear source that restricts transportation and usage. This was the only feasible ppb capable detector that is mature enough to be used. The PID detector or a conductive polymer sensor arrays might seem to be good candidates for detecting multiple compounds at first glance but are not suitable for our purposes. The PID detector is not specific and quantification of a substance requires that only one be present at a time and that its ID is known. The conductive polymer sensor array can perform better since it can identify the gas, if it has been trained for it, but not in a mixture of unknown gases. The conductive polymer array can detect substances that are members of certain chemical classes that can interact with the polymer. Finally, some gases cannot be detected with generic sensors and require a specialized sensor (e.g. CO_2).

The detection target candidates remaining after taking into account the suitable detection technologies, the requirements listed in the next chapter and ethical constraints are: the exhaled, when breathing, detectable gas mixture and its properties. This includes only elevated levels of CO_2, humidity, temperature and reduced levels of O_2. Another target is the NH_3 gas that could potentially be produced from the bacterial consumption of the contained urea in urine. All other candidates are not detectable with the current state-of-the-art technology for a large portion of potential victims in this application. Only for a small portion of potential victims and under very ideal and possibly unusual conditions (e.g. acetone) could more detection targets be used.

The victim localization detection targets are listed in the following table:

Table 6. The victim localization detection targets

Detection Target (detection technology)	Description
CO_2 (NDIR)	Originating from exhaled breath. Increased levels anticipated
O_2 (Fluorescence)	Originating from exhaled breath. Decreased levels anticipated
NH_3 (Electrochemical)	Originating from urine. Detectable levels anticipated
Air temperature	Originating from body heat. Increased levels anticipated
Humidity	Originating from exhaled breath. Increased levels anticipated

The CO_2 and O_2 levels are also critical for the safety of the rescue crews when operating in confined spaces and can be used as indicators for survivability in those spaces, too.

Note that for breath analysis and detection of potential health problems, suitable detection technologies are available and can detect some of the ppb range substances for a number of reasons: The sampling method and procedure can be strictly determined and constrained in order to acquire the most concentrated and undiluted samples directly from the source. The sampling can even be optimized to acquire alveolar exhaled air which contains the most useful air mixture. The sampling conditions, like temperature, pressure and humidity, can be controlled. Also, the person providing the sample is known and particular physical parameters of the person can be accounted and compensated for if necessary. Another critical element is that the health issue indicator is most likely an elevated level (concentration) of a compound or set of compounds. The measurement result does not have to be delivered in real-time. The sampling and measurement apparatus does not have to be small, lightweight or even portable. The power consumption of the sampling and measurement system is not so critical.

For these reasons the sensor array is composed of individual sensors with different detection principles. A conductive polymer array is not the best solution for the purpose of victim localization. The sensors selected are fairly selective and do not require training in order to identify their target. Instead of training, periodic calibration is required to compensate for ageing, and functional testing (challenging or bump testing) should be performed before use. Training of the system is required on site just before deployment into the rubble for the purpose of determining the background concentrations and automatically determining some of the thresholds.

2. REQUIREMENTS

2.1. Overview

This research work is a step forward in victim localization technology. The primary goal was to improve the SoTA (state of the art) in the detection methodology and tools for air-based human presence detection. Beyond the primary research objective it is desired, if possible, that this work or portions of it to be practically utilized and provide a noticeably positive impact in society specifically by improving disaster management and mitigation methods and tools – contribute to saving lives. For this reason it was decided to study what aspects of a potential solution would make it (or not) more appealing for utilization. These aspects are included in the requirements some of which are a product of interaction with end-users. The e-nose is intended to be used by Search and Rescue crews, otherwise known as rescuers or first responders. The USaR team member responsible for operating tools like the e-nose is the Technical Search Specialist. They are the "End-users" of the e-nose system and it must satisfy, as much as possible, their requirements. These requirements cover a wide range of topics and with varying levels of abstraction. The requirements listed in this chapter are examined in order to determine the feasibility of implementing them, as well as how that will be achieved, in the chapter describing the 3rd and final e-nose system. Interaction with end-users was achieved through end-user workshops and interviews that were conducted for this purpose, and also on other less formal occasions. This research information is very valuable for anyone interested in developing tools for USaR crews. The requirements are prioritized into 3 levels: mandatory, Important and Interesting. Some of the requirements listed here are concerned with the training requirements of the personnel handling the e-nose. Although addressing them is outside the scope of this work, the resulting e-nose system and the required training material shall be compatible with these requirements. If not, that is an indicator of the high complexity of the system which is a hindering factor in its adoption, assuming it is otherwise successful. Most of the mandatory technical requirements are implemented in the second prototype system. Almost all technical requirements are implemented with the third prototype system.

2.2. Requirements

Technical Requirements

Sensors and output

- *The system must detect oxygen levels to aid in indicating human presence, or the presence of hazardous levels of oxygen* (Mandatory).
- *The system must detect carbon dioxide, to aid in indicating human presence or the presence of hazardous levels of carbon dioxide* (Mandatory).
- *The system must detect ammonia, to aid in indicating human presence related to body fluids* (Mandatory).
- *The system must detect flammable gases* (Interesting).
- *The system must detect toxic gases (like H_2S and CO)* (Interesting).
- *The systems' feedback must be presented in a user-friendly format* (Mandatory).
- *Sensors' false alarms cannot be more than 10%* (Important).
- *The system's accuracy must be in the range of one to two meters* (Interesting).
- *Sensor data must be archived* (Important).
- *Data format must be qualified for sharing* (Important).
- *The system must trigger an alert/alarm on the user interface when air is detected that is above/below a particular threshold* (Mandatory). The alarm thresholds, proposed to the end-users, for various gases are listed in the following table.

Table 7. Alarm thresholds proposed to the end-users

Compound	CO	CO_2	O_2	H_2S	Combustible gas
Threshold	> 50 ppm	>1%	< 20%	>5 ppm	>10 %

Operational conditions and controls

- *The e-nose device must not contain flammable and nuclear substances, in order to avoid explosion in confined spaces and transportation issues* (Mandatory).
- *The e-nose device must work in extreme temperatures* (Important).
- *The e-nose device must be able to be remotely powered ON/OFF* (Interesting).
- *The e-nose device must be water resistant* (Important).
- *The e-nose device must work in various types of USaR environments* (Important).
- *The e-nose device must be able to work in various weather conditions* (Important).
- *The set up time of the e-nose system on the disaster site should be within 15 minutes, including sensor calibration time* (Important).
- *The e-nose device should be serviceable. For example, access is needed to the dust filter of the e-nose sensor for cleaning purposes* (Mandatory).
- *The e-nose system should be able to be transported on commercial flights* (Mandatory).
- *The e-nose system should be developed to comply with INSARAG Guidelines* (Mandatory).

Ethical Requirements

- *The e-nose system should be developed allowing privacy by design/by default (Mandatory).*
- *The e-nose system should have sufficient accuracy of the data on the victims (Important). Data to be collected and stored on trapped victims (sensors, voice, pictures) should be accurate and detailed enough for medical people to estimate the health situation of the victim, as well as for rescue people to take into consideration cultural aspects of dignity (e.g. when rescuing Muslim women or dead people).*
- *Good understanding on the features and restrictions of the system (Mandatory). The system should provide various users with general information on its various features and restrictions (not only the information on how to use it).*

Training Requirements

- End-users require that there be training material for the e-nose system. This training material must *be tool specific, oriented to the role of the end-user it is intended for (Technical Search specialist), allow for training delivery both in face-to-face learning in classroom setting, and as e-learning (on-line training), with different types of training material, including instructional 'how-to' videos for training on the use of technical tools. Training and user guides to be developed must be as simple as possible, with graphics, clear symbols and easy-to-understand language. Pocket-sized instructions on the use of the e-nose must also be created. The training material for Technical Search Specialists and Maintenance teams must include tool documentation (in order to fully understand functionality, to be able to diagnose problems in case of malfunctioning and to be able to carry out basic 'instrument resets' and/or repairs). Users prefer shorter training over longer training (such as half a day training instead of training that takes a week).*

3. ELECTRONIC NOSE SYSTEM

3.1. Overview

The development methodology/approach for the electronic nose is a modified waterfall methodology with rapid system prototyping (RSP) for the hardware elements (mechanical, electronics) and a spiral methodology for the various software components (firmware, embedded software, e-nose system control, data analysis, and communications). This implies that there is more flexibility for changes of the software components in a late stage of the design while it is very difficult and expensive for changes to be made in the hardware. The first version of the envisioned system is included in the first prototype section, while the second version of the envisioned system is in the second prototype. The first prototype, also called a rapid prototype, was built to function as a proof of concept for the proposed human detection scheme. This was deemed necessary to reduce the risk in case this scheme was not a viable detection method. For the second prototype, mainly off-the-shelf components like evaluation platforms were used and some small custom-made prototype interconnection printed circuit boards were designed. The focus was on developing an e-nose system with all the functionality. Most of the firmware and large portions of the embedded software were developed on this platform that was designed in a way so that most of the components, hardware and software, would be used in the final system. The final design- the 3rd prototype is a miniaturized version of the second prototype with the ability to detect more target gases (CO, H_2S, LPG/LNG). The miniaturization process involved designing a custom PCB that includes the required functionality of most of the development/evaluation platforms and the mechanical design of the e-nose compartment including a custom air manifold with air conditioning capabilities.

3.2. Envisioned e-nose system – early version

A preliminary design of the hardware system of the e-nose was performed, an initial system design. A number of user requirements were examined and their implementation considered from a high level of abstraction. The chapter presents the various capabilities, advantages, disadvantages, tradeoffs, and compromises associated with each possibility.

3.2.1. Hardware architecture of the e-nose

The electronic nose is realized as a cluster of chemical gas sensors. Air is sampled through an opening, passed over the sensors and is returned to the environment. The following block diagram illustrates the concept. All the functionality is built around the cluster of gas sensors. Auxiliary components are other sensors, actuators, electronics, and mechanical aspects required for the system to operate as specified.

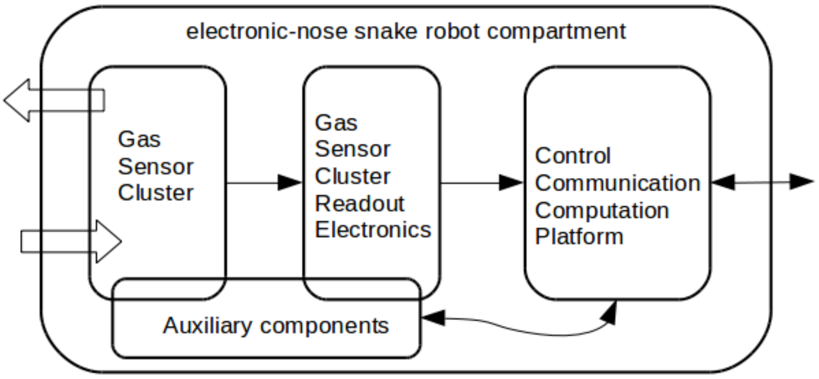
electronic-nose snake robot compartment
Gas Sensor Cluster
Gas Sensor Cluster Readout Electronics
Control Communication Computation Platform
Auxiliary components

Figure 1: The high level block diagram of the electronic nose which is intended to be placed in a robotic platform.

For a waterproof system, the air input and output must be waterproofed with a filter that blocks water and allows gases to pass through. Diffusion of the chemicals through the filter is not very fast so a pump is required to move air in and out. The connectivity of the various sensors is affected by the nature of the sensors: If they detect various gases by consuming/destroying chemicals, they have to be at the end of the chain or in separate parallel branches of the sampled air distribution system. After the readout of the sensors, the sampled data is processed for human detection. The system functions under the control of the control and communications module. The control and communications module is also responsible for sending sensor data and data analysis results to the robotic platform operator and for accepting and acting on control and configuration commands sent to the e-nose. The following pictures illustrate the concepts. The air sample is pumped into the system with a pump through a water blocking filter. The sample passes through the sensor cluster and then exits the system after going through another water blocking filter.

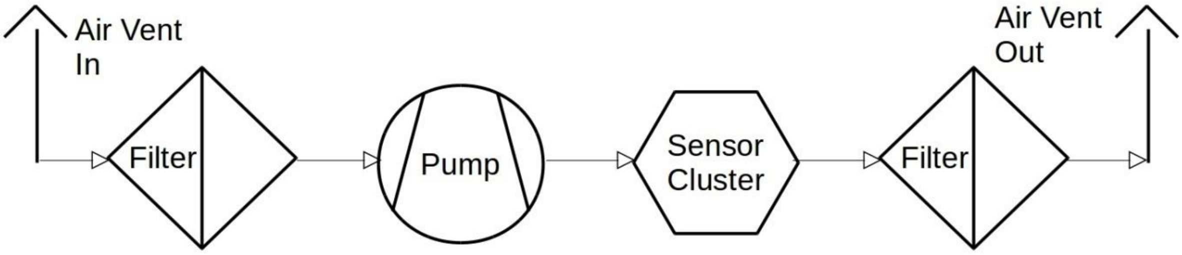

Figure 2: Top level block diagram of the e-nose's air system.

The Sensor cluster could be a combination of series and parallel connected sensor modules. The following drawing illustrates sensors connected in series. All the sensors, except for the last one, in this configuration must not alter the composition of the sampled air.

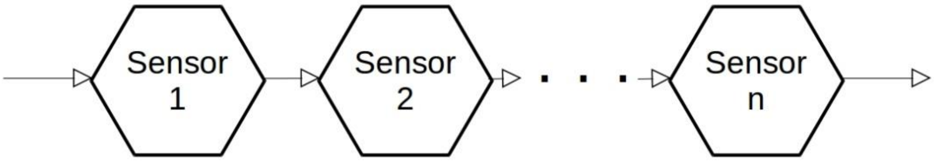

Figure 3: Sensor modules connected in series (implemented).

The following drawing illustrates sensors connected in parallel. All the sensor modules have their own air supply so they can consume/ alter the composition of the air sample.

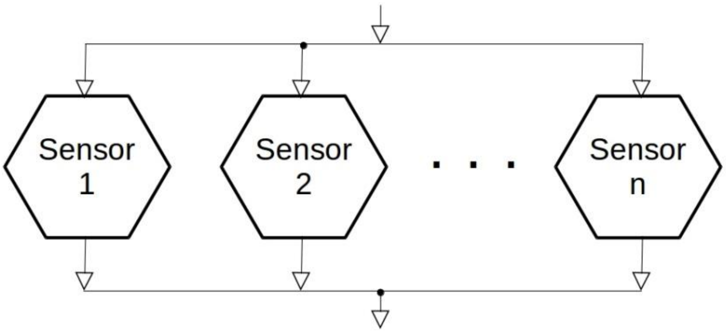

Figure 4: Sensor modules connected in parallel.

Victim localization is possible by measuring the variation of the concentration of chemicals/gases that are human indicators. The Concentration variation is calculated based on a reference reading. Concentration of the chemical/gas depends on many factors, most critical are:
The number of victims in a cavity
The ventilation conditions of the cavity

Other factors that influence the type and concentration of human presence gas/chemical indicators are the following:

- The amount of time the victims are trapped in the void
- The physical condition of the trapped victims (under stress or not)
- The existence of body fluids in the void

Factors that reduce the accuracy of the e-nose readings and could lead to false positives are the following:

- The contamination of the area with the same detection targets used for human detection. These could be caused by various conditions
    - Fires
    - Leaks of household chemicals
- The operation of the e-nose in extreme conditions:
    - High humidity levels (condensation)
    - High temperature
- Factors that reduce the accuracy of the e-nose readings and could lead to false negatives are the following:
    - Operation in high temperature environment(reduced absolute concentration)
    - Operation in nonstandard or unanticipated environments where detection targets could be absorbed

3.2.2. E-nose firmware and software architecture

The electronic nose sensor array is placed at the source end of the chain of sensory inputs that need to be provided to the intelligence unit (operator). Between the sensors and the operator monitoring tools, information will need to be processed in the electronic control and advanced logic unit, travel along with information from other sensors of the robotic platform and finally arrive at the operators monitor unit.

Information and control flow

The information/data flow of the electronic nose is the following: The information is sampled from the sensors, stored in a database for processing and keeping historical data and finally, presented to the operator. The general flow of information and control is as follows:

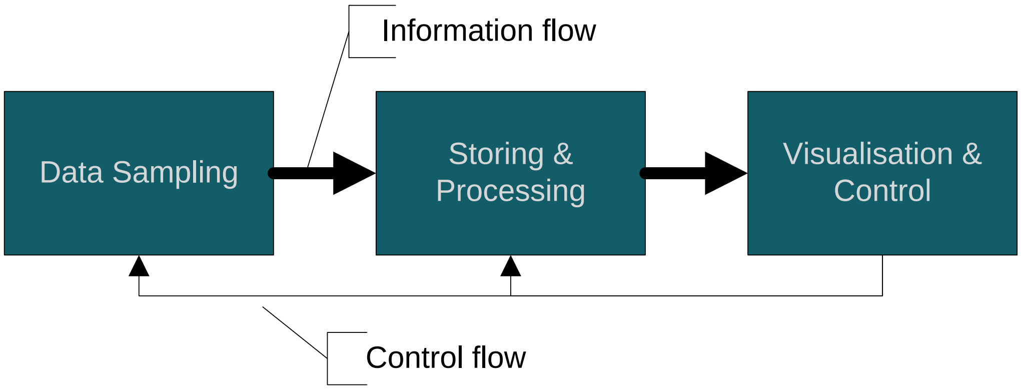

Figure 5: Information and control flow

The gas sensors are sampled at regular intervals providing values for the gas concentrations of several monitored gases. This information is collected and stored in a time series database. Storing the information provides access to historical data, as well as feeding the processing algorithms. At the other end of the chain, the processed data is presented in an orderly and concise fashion to the operator of the system, who is also responsible for any sort of configuration that needs to be done prior to or during operation of the robotic platform.

Constraints

In order avoid pitfalls and possible re-development of the firmware and software involved, the system architecture took into account the following constraints

Sensor and actuator interfaces

There is a multitude of sensory input that needs to be gathered by the electronic nose. Each of these sensors uses a different interface to provide the sampled data. Serial devices, i^2c components and even some analog sensors all need to be read into a gathering database and processing unit.

Actuators also need to be driven. Heating elements are utilized to prohibit humidity from condensing in the sensors, while an air pump forces air circulation to the sensor via a sensor manifold. ON/OFF or PWM is the driving method.

User interface

During search and rescue operations all operator tasks are performed under stressful conditions and under time constraints that push for continuous operation during the available time frames (i.e. the few hours/days after a catastrophic event). All feedback provided to the operator should be clear and concise. This includes using less text and as many visually clear and distinctive outputs as possible.

As a result, a number of human- computer interaction decisions are made at an early stage. All data that are acquired from the sensors is processed in order to provide analyzed information to the operator. Additionally, historical data are also presented in graphical form. Indicators produced by the electronic nose advanced logic unit are color coded. All this is done with the aim of aiding the operators in quickly identifying key information that could help detect humans in proximity to the robotic platform's path.

Advanced Logic unit

The conditions under which the operator needs to work require intensive supervision of the sensory input at all times during each of the system's missions. In many search and rescue operations, work may also need to continue for extended periods of time, while the chances of trapped people being alive are still high. Therefore, it is necessary to provide meaningful results to the end-user instead of presenting numerical values and expecting the stressed operator to draw their own conclusions based solely on what they observe. This is especially true for the electronic nose which is a nonstandard set of sensor equipment with nonstandard sensory output, as opposed to other sensors such as a camera, where visual perception of a video feed is a familiar concept. The sensor inputs are processed in order to identify key features in the data that can then be used to detect with a high degree of certainty, the existence of living humans in the ruins.

The subsystem responsible for processing the raw data and provide notifications to the operator about potential living humans in the vicinity is the advanced logic unit. In essence this is the analysis and decision algorithm that processes the electronic nose inputs according to sets of rules that are fed into the system from extended testing that has been carried out on the electronic nose in order to characterize its behavior.

Such rules include the following cases:

- Sudden changes in the gas concentrations of the monitored gases.
- Correlation of sensor responses to expected responses for several basic scenarios.
- Steady rate trends in the gas concentrations.
- Threshold levels within human survival limits.
- Existence of characteristic concentrations of specific gases. For example, the existence of NH_3 can be related to urine. High concentrations though, could indicate spillage of ammonia-based cleaning products.

With constant monitoring of the raw data inputs and grading – weighting the concentrations with respect to the aforementioned rules, deterministic output is generated and this is provided as a notification to the user.

Compartment limitations

Creating a robotic platform that is able to pass effectively through small openings in ruins presents some implications for the overall design and imposes some restrictions with respect to the available space for electronics and actuators. CAD design was required to model and verify that all components fit in the system, but also to minimize the overall required volume.

Because of these volumetric restrictions, the design of the electronics of the e-nose was indirectly affected; several components, driving electronics and actuators were too large, physically, for the available space. As a result, the software and hardware architecture needed to remain flexible and portable before the final design was produced. Hardware is tailor-made incorporating only the necessary components; consequently the low level software driving the electronics is also developed specifically for this system. Additionally, the analysis and decision algorithms are portable in order to be able to run on a platform that is not necessarily the same as the one where development was carried out.

Communication across systems

A significant number of architecture decisions both for the robotic platform and the e-nose had not been finalized when the design started. As far as the electronic nose information path is concerned, that meant that the information flow from the sensors all the way to processing and data visualization on the operator's monitor was largely carried out through/on unknown systems.

Initial System Architecture

Considering the characteristics of the system, as well as the constraints imposed, a number of design decisions were made:

Data collection is implemented in a custom hardware solution. The electronic nose device is a single compartment with interfaces to the outside world. These interfaces will be a least one of serial, USB, Ethernet. With careful PCB design, the volumetric footprint of the system was minimized, thus conforming to the robotic platform requirements.

In the intermediate step the data is stored in a simple database, along with timestamps. The reason is to be able to visualize historical data during the operation. The historical data is available for further processing by the electronic nose data analysis unit. Processing power and storage are necessary to implement these steps. (The following design approach is only true for the 1st prototype and was abandoned in the following prototypes due to power and space design constraints.) To avoid interoperability and communication issues it was decided to avoid sharing processing power and storage capacity with other sensors within the robotic platform. Instead, every system – electronic nose included – is self-sustained in an attempt to minimize potential integration problems. As a result, the electronic nose database and analysis logic is implemented in a dedicated computer module.

Originally this module was to be located in the e-nose, since unifying the electronic nose components created a very portable and easy-to-operate device. However, design took into account the possibility that all the logic involved might be moved to a dedicated environment in the operator's console/PC system. There are a number of factors which may prove that adding a computer module in the robotic platform affects operation of other critical systems. For example, space considerations and power supply limitations were a determining factor in the location of storage and processing. Considering space and power limitations it was proposed that a relatively low-power development board be used for providing enough power to carry out data sampling, storing, processing and visualization.

With enough processing power available on the computer on module (CoM) it would be possible to further minimize the interaction with other systems (i.e. the operator's monitoring station) of which little was known at the time and to make integration easier. There will be one operator controlling the robotic platform and evaluating the data input, but there may be additional viewers who need to have read-only access to the data for training purposes. In such case a system that is able to serve the content to more than one destination must be implemented. It was thought very useful, at the time, to add a Web server that serves not only the historical data to the users, but also provides the means to control the functionality of the e -nose.

3.1. Component selection

In order to verify that the system is within specifications, individual components are selected for implementation. The overall system specifications depend on the specifications of the selected components but are not always limited by these specs. For example, the humidity specification is very hard to meet, requiring the system to operate in high humidity environments reaching 100% relative humidity and even condensing conditions. None of the selected components themselves meet such specs, but the design ensures that the components are not exposed to conditions harmful for them.

Core system component selection

The main components for the electronic nose are the following:

CO_2 sensor, O_2 sensor, NH_3 sensor, Humidity sensor, Temperature sensor, Air filter, Pump, Heating resistor, Computing platform

CO_2 sensor

The selected CO_2 sensor is based on NDIR – optical detection technology. The CO2F-W is a high speed (20 Hz) CO 2 sensor, ideally suited for applications which require the capture of rapidly changing CO_2 concentrations, including metabolic assessment and analytical instrumentation.

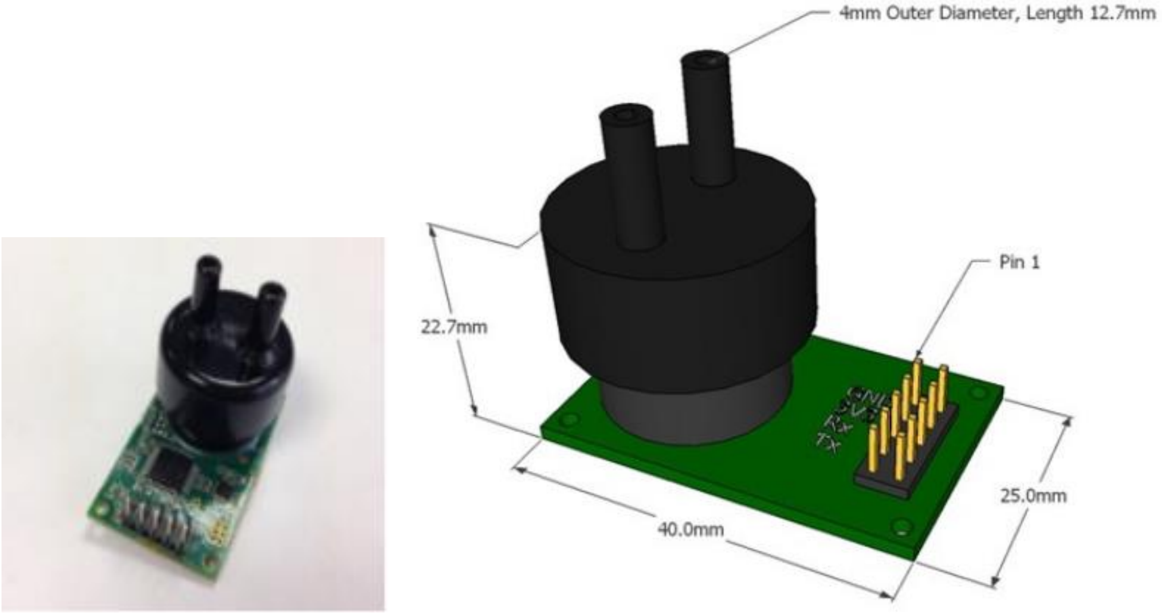
4mm Outer Diameter, Length 12.7mm
Pin 1
22.7mm
GND
5V
RX
TX
25.0mm
40.0mm

Figure 6. The selected CO_2 sensor with a very fast response fitted with a flow-through adapter

O_2 sensor

The selected O_2 sensor is a LuminOX LOX-01 Fluorescence-based Optical Oxygen Sensor. The sensor module also includes a barometric sensor and a temperature sensor. The barometric sensor can be used to detect filter blockage if the pump is placed near the output air port.

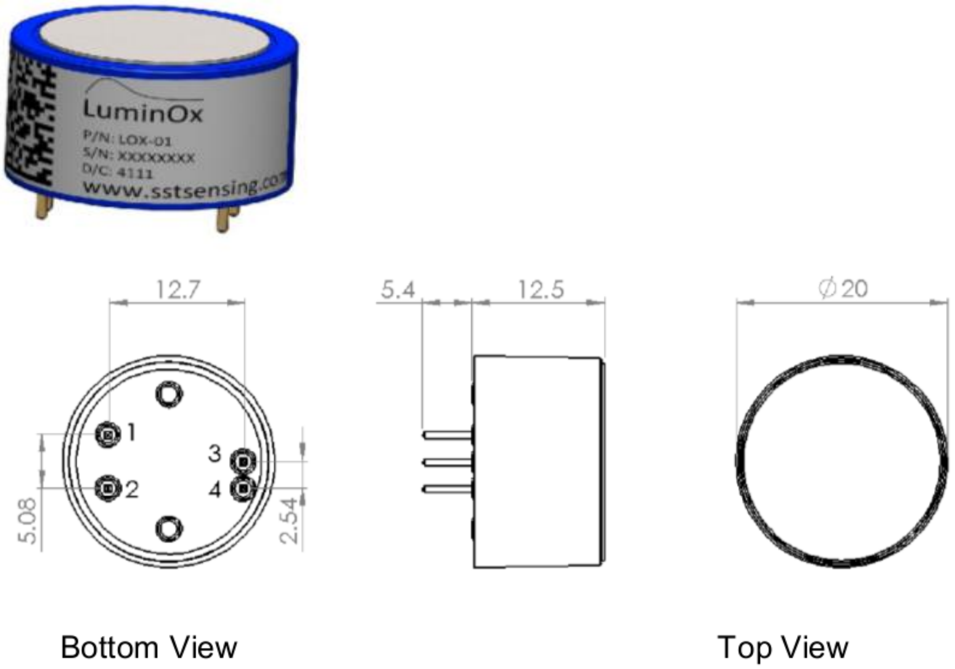
LuminOx
P/N: LOX-01
S/N: XXXXXXXX
D/C: 4111
www.sstsensing.com
12.7
1
2
3
4
5.08
2.54
5.4
12.5
∅20
Bottom View
Top View

Figure 7. The selected O_2 sensor.

NH_3 sensor

The selected NH_3 sensor, the AirSence NH3-B1 is an electrochemical-based Sensor.

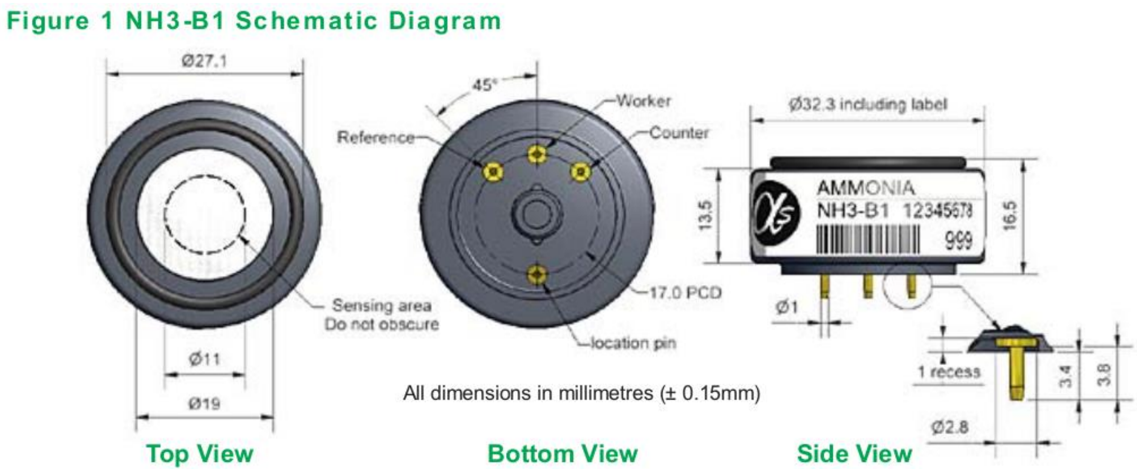
Figure 1 NH3-B1 Schematic Diagram
Ø27.1
45°
Worker
Reference
Counter
Ø32.3 including label
13.5
AMMONIA
NH3-B1 12345678
999
16.5
Sensing area
Do not obscure
17.0 PCD
Ø1
location pin
1 recess
3.4
3.8
Ø11
Ø19
All dimensions in millimetres (± 0.15mm)
Ø2.8
Top View
Bottom View
Side View

Figure 8. The selected NH_3 sensor

Humidity sensor

The selected humidity sensor is the HIH8120 Honeywell HumidIcon TM Digital Humidity/Temperature Sensors

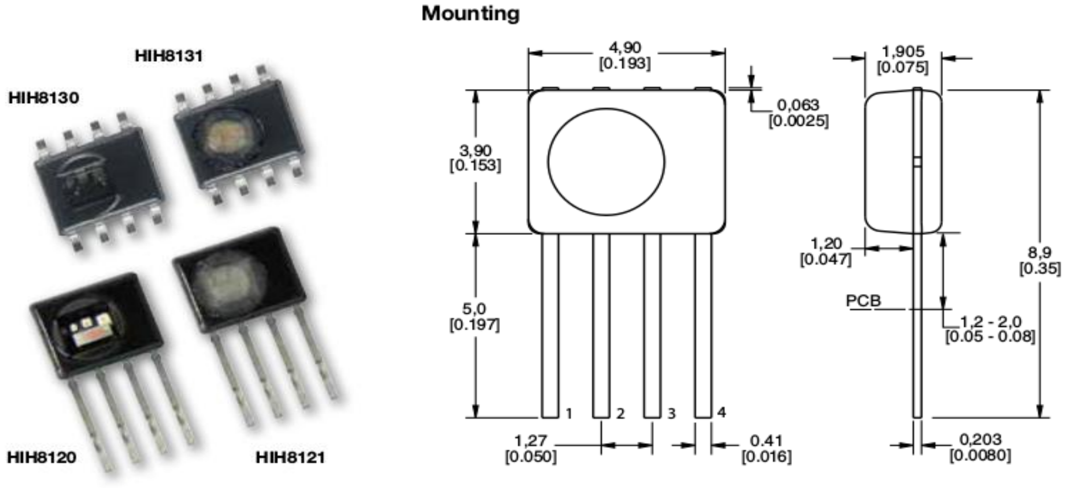
Mounting
HIH8131
HIH8130
HIH8120
HIH8121
4,90
[0.193]
0,063
[0.0025]
1,905
[0.075]
3,90
[0.153]
1,20
[0.047]
8,9
[0.35]
PCB
5,0
[0.197]
1,2 - 2,0
[0.05 - 0.08]
1
2
3
4
1,27
[0.050]
0.41
[0.016]
0,203
[0.0080]

Figure 9. The selected humidity sensor. The sensor also includes a temperature sensor.

Temperature sensor

The selected temperature sensor is the LM35 Precision Centigrade Temperature Sensor.

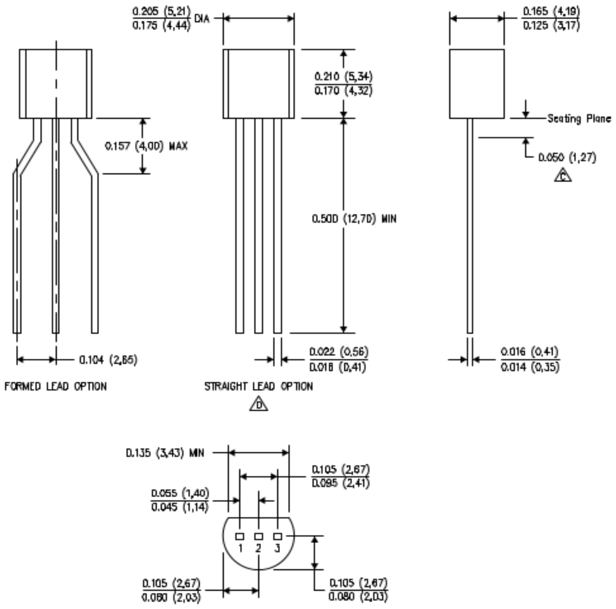
0.205 (5,21)
0.175 (4,44) DIA
0.165 (4,19)
0.125 (3,17)
0.210 (5,34)
0.170 (4,32)
Seating Plane
0.157 (4,00) MAX
0.050 (1,27)
C
0.500 (12,70) MIN
0.104 (2,65)
0.022 (0,56)
0.018 (0,41)
0.016 (0,41)
0.014 (0,35)
FORMED LEAD OPTION
STRAIGHT LEAD OPTION
D
0.135 (3,43) MIN
0.105 (2,67)
0.095 (2,41)
0.055 (1,40)
0.045 (1,14)
1
2
3
0.105 (2,67)
0.080 (2,03)
0.105 (2,67)
0.080 (2,03)

Figure 10. A stand-alone temperature sensor

Air filter

The selected air filter is the Qosina 28213 hydrophobic filter with female luer lock inlet, male luer lock outlet.

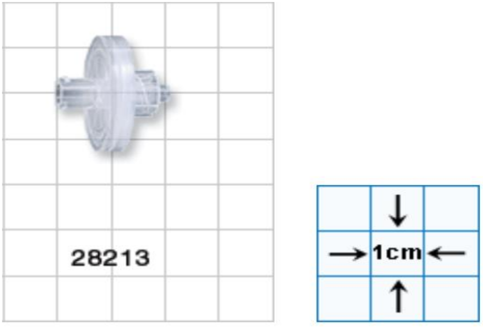

Figure 11. The selected hydrophobic filter

Air pump

The selected pump is a Parker micro diaphragm pump capable of pumping air and gas. The motor of the pump is a PMDC (permanent magnet DC) Iron Core Brush Motor (eCompact).

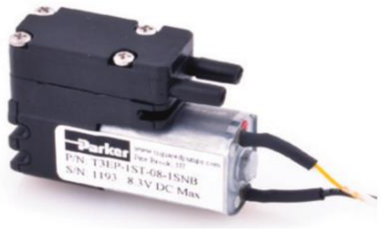
Parker
P/N T3EP-1ST-08-1SNB
S/N 1193 8.3V DC Max

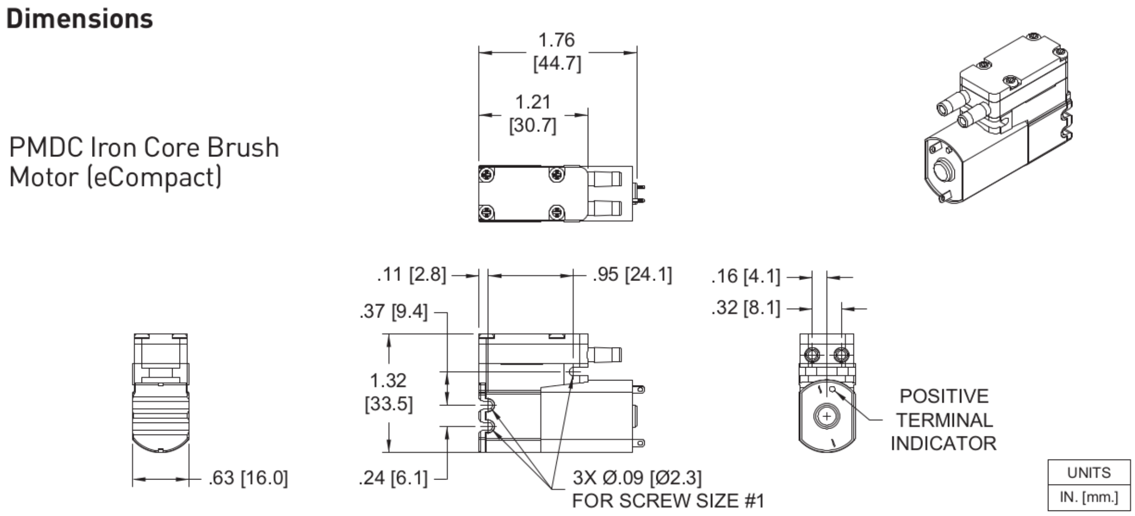
Dimensions
PMDC Iron Core Brush
Motor (eCompact)
1.76
[44.7]
1.21
[30.7]
.11 [2.8]
.95 [24.1]
.37 [9.4]
1.32
[33.5]
.24 [6.1]
.63 [16.0]
3X Ø.09 [Ø2.3]
FOR SCREW SIZE #1
.16 [4.1]
.32 [8.1]
POSITIVE
TERMINAL
INDICATOR
UNITS
IN. [mm.]

Figure 12. The selected pump suitable for moving air

Heating resistor

The selected heating resistor type is a VISHAY wire-wound, industrial, power, aluminum housed, chassis mount resistor.

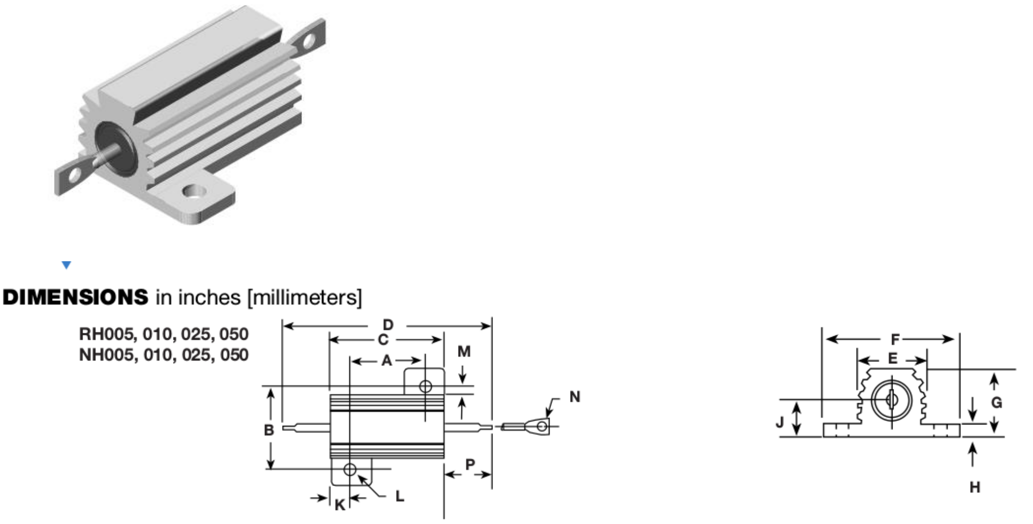
DIMENSIONS in inches [millimeters]
RH005, 010, 025, 050
NH005, 010, 025, 050
D
C
A
M
N
B
P
K
L
F
E
J
G
H

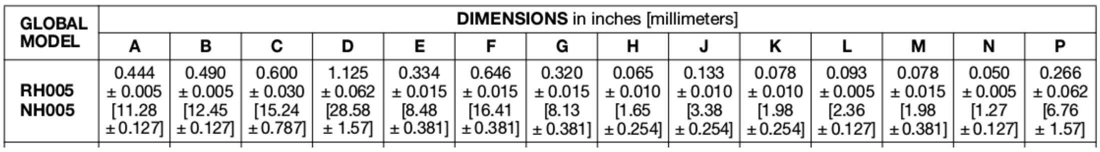

GLOBAL MODEL	A	B	C	D	E	F	G	H	J	K	L	M	N	P
RH005 NH005	0.444 ± 0.005 [11.28 ± 0.127]	0.490 ± 0.005 [12.45 ± 0.127]	0.600 ± 0.030 [15.24 ± 0.787]	1.125 ± 0.062 [28.58 ± 1.57]	0.334 ± 0.015 [8.48 ± 0.381]	0.646 ± 0.015 [16.41 ± 0.381]	0.320 ± 0.015 [8.13 ± 0.381]	0.065 ± 0.010 [1.65 ± 0.254]	0.133 ± 0.010 [3.38 ± 0.254]	0.078 ± 0.010 [1.98 ± 0.254]	0.093 ± 0.005 [2.36 ± 0.127]	0.078 ± 0.015 [1.98 ± 0.381]	0.050 ± 0.005 [1.27 ± 0.127]	0.266 ± 0.062 [6.76 ± 1.57]

DIMENSIONS in inches [millimeters]

Figure 13. The selected heating resistor type

Computing and classification platform

The selected platform is the WANDBOARD which includes a Freescale i.MX6 Cortex-A9 ARM processor. The platform is a low-cost, open source development board.

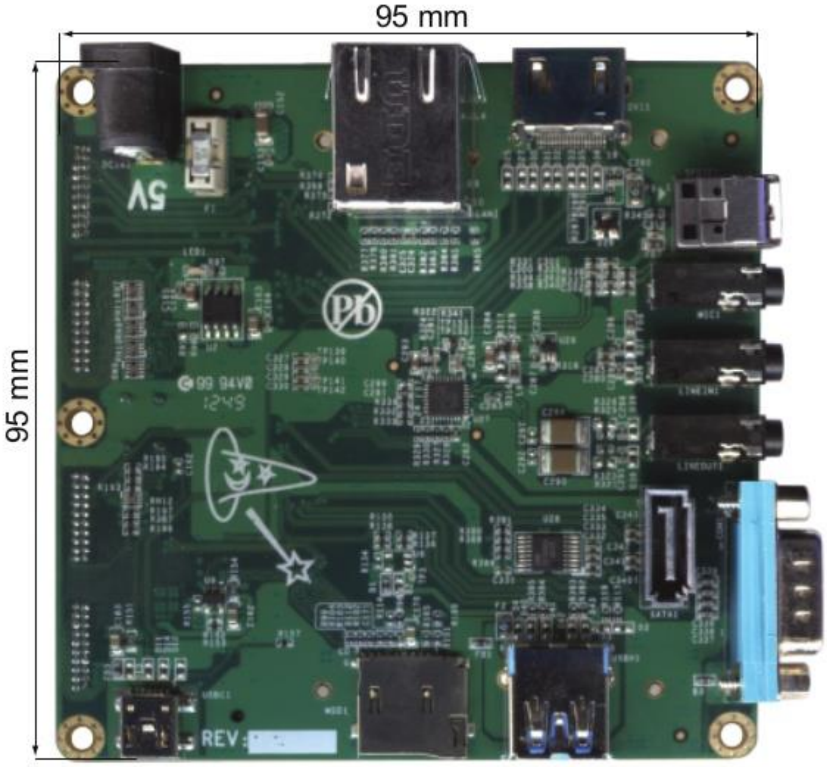
95 mm
95 mm
5V
REV

Figure 14. The selected ARM based embedded computing platform

3.2. System design

This section presents the system configuration that was considered feasible to implement while covering the most critical requirements. The resulting core system configuration is one of the high-level system designs (conceptual designs) that occurred during this phase of the research. It also contains the initial component selection.

3.2.1. Core system

The following block diagram illustrates the required components for implementing the core functionality. The picture on the right illustrates the approximate volume and position of the various components. The external dimensions required with the component selection are 10x10x10cm.

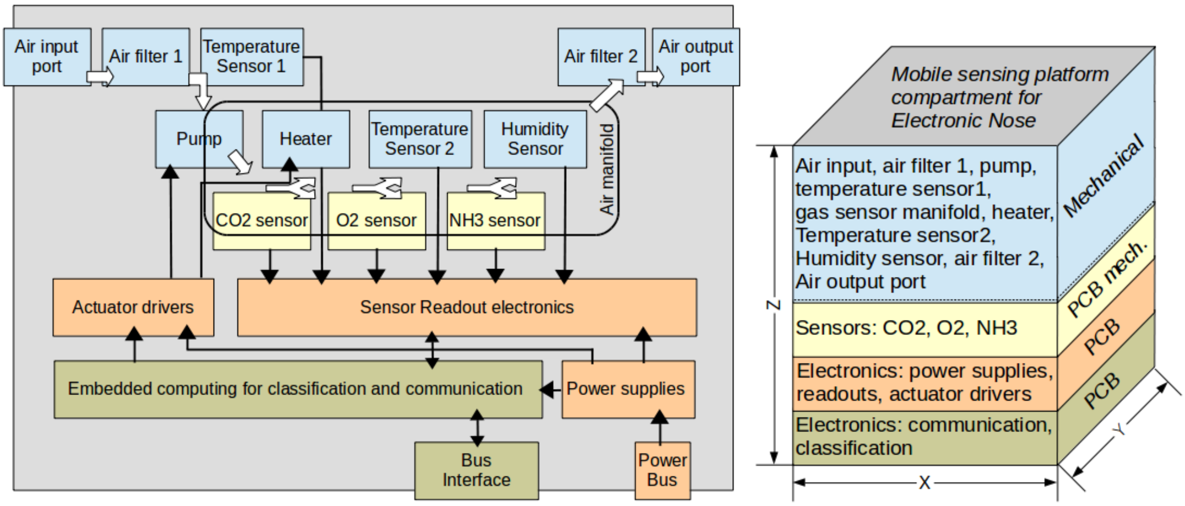
Air input port
Air filter 1
Temperature Sensor 1
Air filter 2
Air output port
Pump
Heater
Temperature Sensor 2
Humidity Sensor
Air manifold
CO2 sensor
O2 sensor
NH3 sensor
Actuator drivers
Sensor Readout electronics
Embedded computing for classification and communication
Power supplies
Bus Interface
Power Bus
Mobile sensing platform compartment for Electronic Nose
Air input, air filter 1, pump, temperature sensor1, gas sensor manifold, heater, Temperature sensor2, Humidity sensor, air filter 2, Air output port
Sensors: CO2, O2, NH3
Electronics: power supplies, readouts, actuator drivers
Electronics: communication, classification
Mechanical
PCB mech.
PCB
PCB
Z
X
Y

Figure 15. The core system implementing the bare minimum mandatory requirements.

3.2.2. Core system specifications

The specifications of the core system components are the following:

The following table lists the specifications of each component of the system.

Component	Interface	Voltage	Current	Power	Xdim	Ydim	Zdim	Weight	Humidity	Temperature	Accuracy	Price	From	Notes
CO_2 sensor	TTL – RS232	3.3V	100mA	35mW	40mm	25mm	22.7mm+12.7mm		0-95% non-condensing	0-50	+- 70ppr or +-5% of reading		sst	
O_2	3.3 TTL RS232	5V	20mA	7.5mA	20mm	20mm	12.5mm		0-99% non condensing	-30_+60	0,10%		sst	response time <30s
NH_3	electrochemical -analog				32.3	32.3	16.5	13g	15-90%	-30_+50			Alphasense	response time <60s
Humidity	i^{2}c	2.3-5.5V	750uA		4.9mm	3.9mm	1,95		10-90%	-40_+125	-+2%rh		Honeywell	response time <6s @ 20LPM high flow rate
Temperature	analog	4-30V	60uA		5.1mm	4.19mm	5.34mm			-55_+150	0,5		TI	
Pressure sensor														
Heating resistor	analog			1W @ 5V	29mm	16.41mm	8.13mm			X			Vishay'	
Pump	analog	8V		2.5W	44.7 mm	33.5mm	16.0mm	33g	5-95%	0-50			Parker	Diaphragm pump min noise 45dB
Air filter					25mm	25mm	20mm			X			Qosina	.2u filter 17mm diameter
Computation/communication		5V	0.5 – 1.2A	3W typical	82.55 mm	82.55mm	20mm		20-90%	0-70			Farnell – sabrelite Quad core	
Computation/communication					86mm	52mm	17mm						Raspberry pie	

Notes: Interface types are the ones intended to be used. Current consumption is what is listed by manufacturer, or in the case of the communications board, experimentally measured. The humidity range is the operational range specified by the manufacturer. The total system will be able to work in a wider range due to controlled conditions inside the gas compartment via a closed control loop. Prices are very approximate and underestimated in many cases, not including VAT, shipping, handling fees and customs.

Mechanical design – component placement

The selected components were modeled and arranged in order to acquire a fairly accurate estimation of the required space for the e-nose. The arrangement of the components also took into account the extra materials required to hold the components in place, interconnect them, as well as provide thermal management such as insulation (manifold) or heat removal (ARM board). Voids or gaps seen in the following model are places where such structures will reside. The most important structure is the custom manifold which is responsible for guiding the sampled air in the sensors and heating the sensors and air to the target temperature setting. A large area of the compartment will be consumed by the structure, providing easy access to the air filters, so they can be changed without much effort. The following picture illustrates the design of the e-nose compartment that has external dimensions of 10x10x10cm. Note that the orientation of the compartment is rotated in respect to the block diagrams seen in previous sections. The three flat surfaces on the left are the ARM PCB, a conduction cooling plate for the ARM microprocessor, and the PCB containing the readout, power conversion, temperature control and actuator drivers. The air pump is located in the center in front of the 2 round air filters. On the bottom right is the custom air manifold.

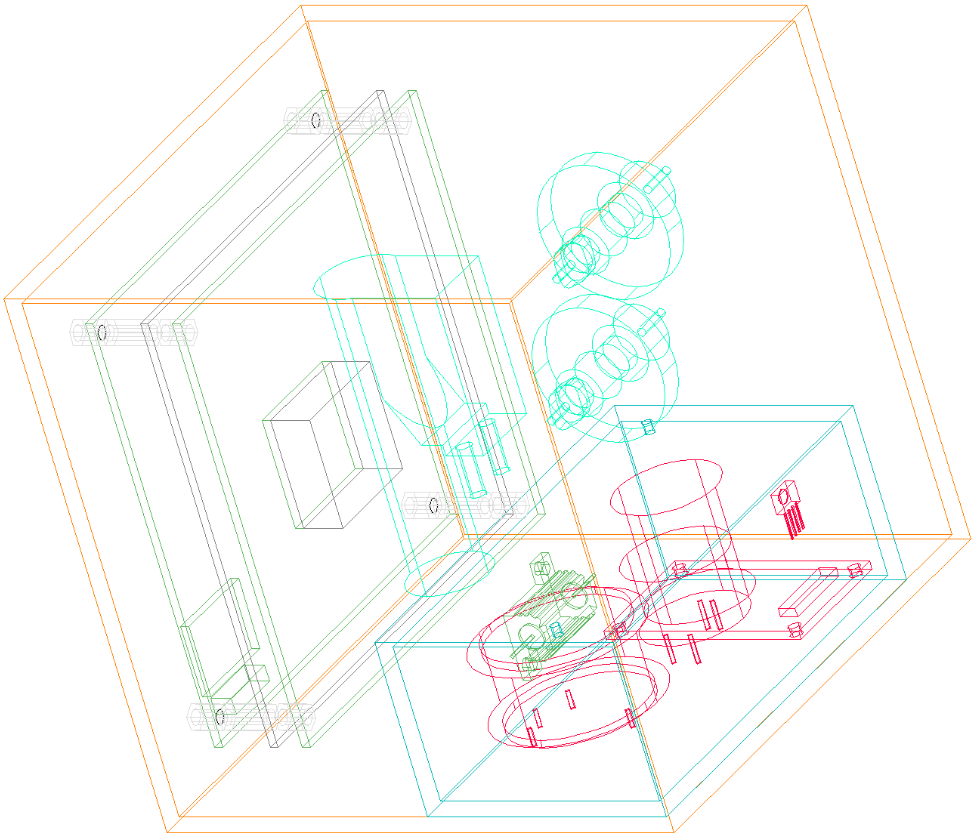

Figure 16. The component placement inside the e-nose compartment.

The following picture illustrates the custom manifold. The actual pattern for the air flow has not yet been designed but will connect the sensors in a series. The air manifold contains the CO_2 sensor (left), the O_2 sensor (top-center), the NH_3 sensor (right), the humidity sensor (top-left) and the heating resistor (center-bottom).

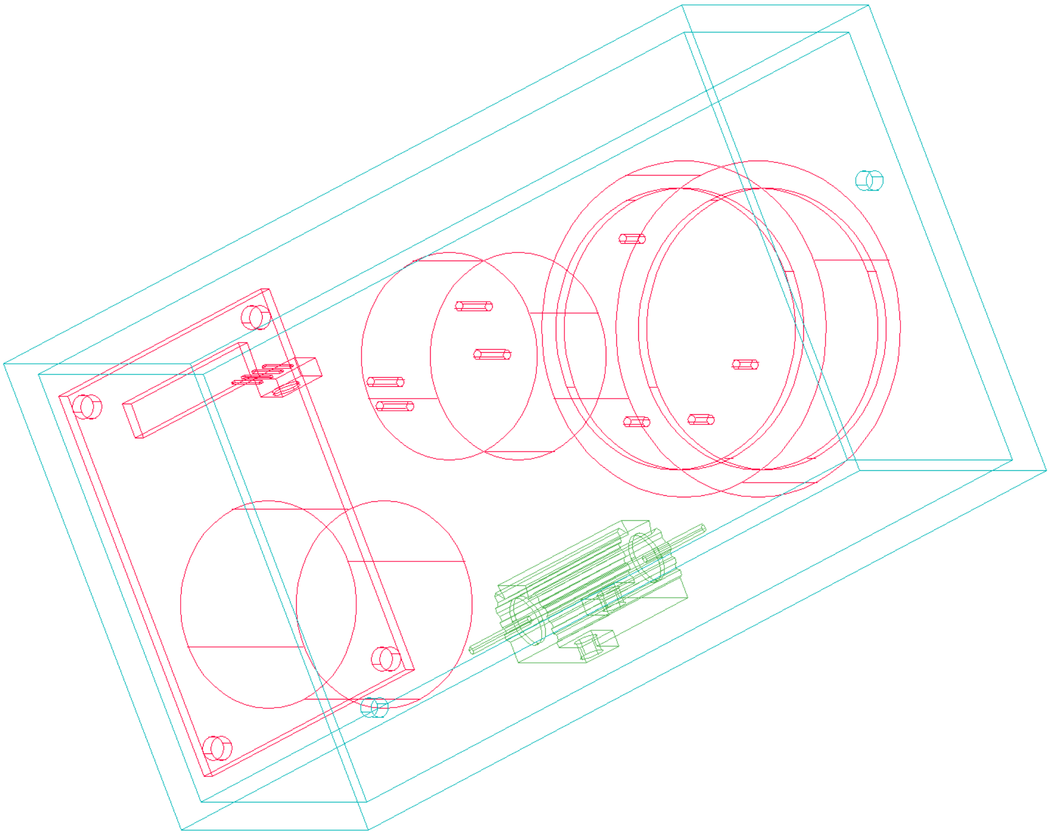

Figure 17. The arrangement of the sensors in the custom manifold.

The air manifold design is challenging since it must fulfill multiple requirements at the same time:

- Guide the sampled air inside the sensors, not only over the sensors opening.
- Heat the sampled air to the target temperature.
- Heat the sensors to the target temperature.
- Have small air volume so the measurement delay is minimized.
- Exhibit low air flow resistance.
- Be low weight.
- Exhibit a uniform temperature as much as possible.

3.3. Summary of the e-nose prototype devices presented in the following chapters

Table 8. Comparison of the prototype e-nose device versions

Features	First prototype	Second prototype	Third prototype
Picture	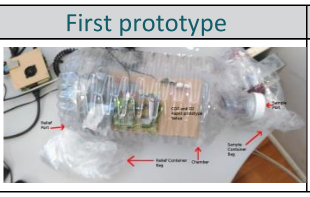 Relief Port CO2 and O2 Rapid prototype Setup Sample Port Sample Container Bag Relief Container Bag Chamber	INACHUS e-nose	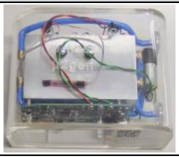

Features	First prototype	Second prototype	Third prototype
General description	A bench-top apparatus for acquiring and storing measurements of breath based samples with controlled and known conditions.	A portable device capable of operating in uncontrolled conditions.	A portable device capable of operating in uncontrolled conditions. Increased capabilities at a slightly reduced size. ~130x170x70mm
Detection targets	CO_2 and O_2	CO_2, O_2, NH_3, humidity, internal and external temperature, (barometric) pressure	CO_2, O_2, NH_3, CO, H_2S, combustibles, humidity, internal and external temperature, (barometric) pressure
Operating conditions and sampling	Typical lab environment conditions. Special sampling procedure in order not to harm the sensors.	Air system can operate in wide range of conditions due to: air sampling pump, air filters and humidity control. No special sampling procedure required.	Air system can operate in wide range of conditions due to: air sampling pump, air filters and humidity control. No special sampling procedure required.
Interface configuration	Web-based technologies for presenting and storing measurements. No configuration of HW possible.	Scientific data plots (KST) of all outputs. Command line interface for configuration and control.	Application with simple outputs (indicators), detailed outputs (plots) and control/ configuration buttons
Uses	Proof of concept for victim localization strategy envisioned with the e-nose. Measurements used for the performance analysis (theoretical analysis).	For victim localization purposes and very limited air related hazards.	For victim localization purposes. Confined space entry air related hazards.
Design and implementation files	Electrical diagram of interconnections. Minimal readout software, webpage and database configuration.	Electrical diagram of interconnections. PCB design files. CAD for enclosure. Firmware for readout and control. Real-time analysis software. Configuration of interfacing plots.	For complete system.
Assembly time	Assembly and development at the same time.	Long assembly time due to handmade air manifold and assembly of PCB by hand.	7 days by 1 person. Can be improved.
Cost	Low cost. Implemented using available tools where possible.	Low to medium cost due to the utilization of evaluation boards where possible.	Medium cost due to increased sensor count and its cost. Increased requirements for fabrication (machine shops, PCB fab.)
Tests performed	Initial measurements in static and known conditions. Successful.	Verification tests. End-user validation at field test P1. Successful.	Verification and validation tests. Successful.
Compatibility for integration in robotic platform	Not compatible for integration.	No, but with a few minor adaptations on the hardware and more firmware and software development it could become compatible.	Yes. Interface designed, information/data already computed.

Features	First prototype	Second prototype	Third prototype
Fulfillment of end-user requirements	Not adequate.	End-user requirements: All mandatory*, many important, some interesting.	All, within the limits of the feasibility analysis described in the 3rd prototype.

*The hardware supports them. Software and material created for the third prototype can be adjusted for the second prototype, but extra effort is required.

4. FIRST PROTOTYPE, PROOF OF CONCEPT APPARATUS AND TESTS

4.1. Overview

The first prototype of the e-nose is designed and built with the aim of performing initial tests for the proof of concept of the detection strategy followed. The apparatus/setup is built around the selected CO_2 and O_2 sensors with a minimum of other components. This reduces the capabilities of the setup to only the basic functionality. Operation in extended ranges of environmental conditions is not possible and the setup is planned to work in a controlled lab environment with special sampling and measuring procedures in place to protect the sensors from conditions that in the final design will not be of concern (e.g. humidity condensation). Although the setup has only two sensor elements, the effort to implement a working and convenient prototype tool requires both hardware configuration and software development.

The functionality provided by the hardware/software setup is the following:

1) Initiate the sensors for reading – start acquiring measurements.
2) Periodically read the sensors to acquire measurements.
3) Store the read values.
4) Send the read values to a computer so the results can be visualized and evaluated in real time.

This functionality is implemented with an ARM-based embedded computer that runs a web server, serving the results as measurement plots. The embedded computer platform is connected to a wired network and all the computers on it can view the results in real time. The sensors are connected to the embedded platform via modified USB adaptors. A custom power supply board is assembled to provide the required voltage rails from a common 12V power supply.

4.2. Electronics of the 1st prototype

The setup is built around the O_2 and CO_2 sensors so that the measurements can be viewed as plots in real time. Both sensors' output is transferred to the ARM based embedded computer platform via a modified USB to serial converters. This is because each sensor board has an rs232 TTL level communication port to communicate configuration parameters and the measurement results. The embedded computer platform does not display the measurements directly but serves measurement plots to web browsers connected to the same network, via an Ethernet port. Alternatively, the sensors can be connected to the PC directly via the USB to serial converters where the measurements are stored, processed and then plotted (KST plot or libreoffice Calc). The following figure illustrates the block diagram of the rapid prototype system:

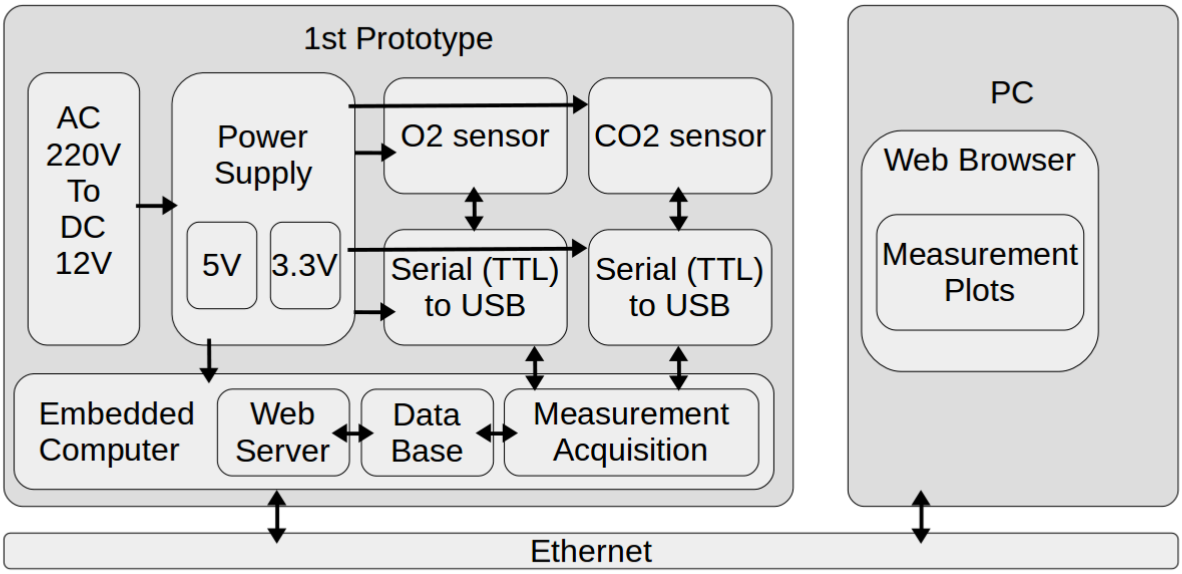

Figure 18. The 1st prototype system is built around the O_2 and CO_2 sensors so that the measurements can be viewed in plots.

The following figure illustrates a high-level schematic connection diagram of the rapid prototype system. This configuration is the final development of the first prototype. Not all tests and measurements were performed with it, namely the fan for creating air circulation at the top left of the schematic diagram or the ARM board. On the bottom right of the schematic diagram, the power supplies are illustrated. Their input is AC mains 220V and their output is 5V for the one and 12V for the other one. The 5V power is supplied to the ARM board and the 12V power is supplied to the custom power supply illustrated on the top center of the schematic diagram. The custom power supply is used to produce DC voltages of 3.3V and 5V from the 12V input with off-the-shelf, 3pin, L78XX pin and mechanically compatible, DC/DC converter modules. The O_2 sensor and its connections are illustrated at the left middle of the diagram. This sensor is operated with a 5V power supply and 5V serial interface levels. The CO_2 sensor and its connections are illustrated at the bottom left of the diagram. This sensor is operated with a 3.3V power supply and 3.3V serial interface levels. Both sensors are connected with a USB to serial FTDI based converters. The RX pin of the sensor is connected to the TX pin of the FT232r chip and the TX pin of the sensor is connected to the RX pin of the FT232r chip. No flow control pins are used for the communication. The FTDI based converters are ARDUINO based boards where the Atmega microcontroller was removed. Wires were soldered onto the bottom side of the IC socket to connect cables with 2.54mm pin sockets on the other end. Standard off-the-shelf USB 2.0 type A to B 1.2m cables were used to connect the USB converters with the ARM board (or the computer). Figure 19 illustrates the implemented electronics which have a similar layout to the one illustrated in the schematic diagram (AC power supplies, ARM board and computer are not illustrated).

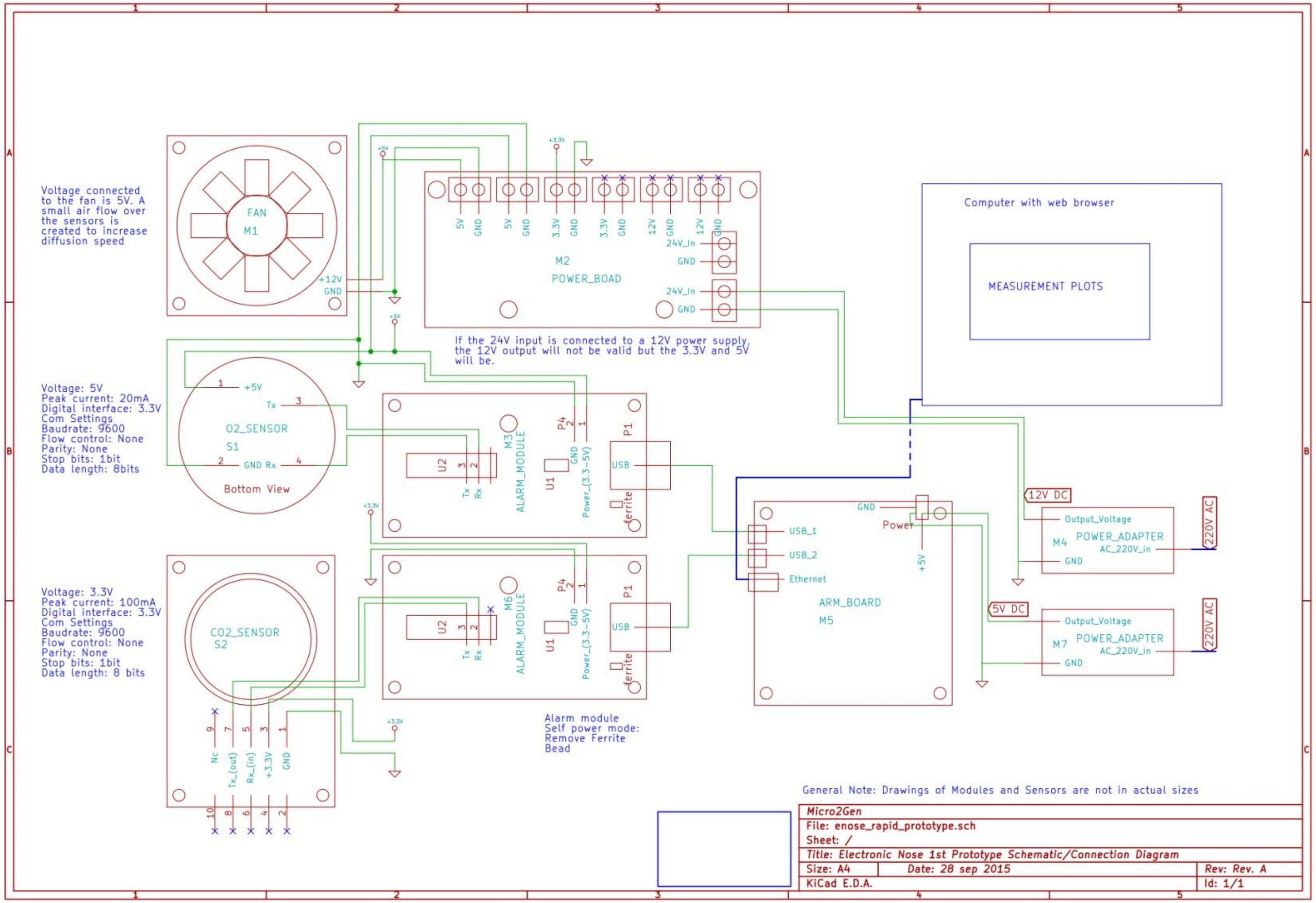
FAN
M1
+12V
GND
5V
GND
5V
GND
3.3V
GND
3.3V
GND
12V
GND
12V
GND
24V_In
GND
24V_In
GND
M2
POWER_BOAD
+3.3V
+5V
Computer with web browser
MEASUREMENT PLOTS
+5V
Tx
O2_SENSOR
S1
GND Rx
Bottom View
U2
Tx
Rx
M3
ALARM_MODULE
U1
P4
GND
Power_(3.3-5V)
P1
USB
ferrite
GND
Power
+5V
USB_1
USB_2
Ethernet
ARM_BOARD
M5
12V DC
Output_Voltage
M4
POWER_ADAPTER
AC_220V_in
GND
220V AC
5V DC
Output_Voltage
M7
POWER_ADAPTER
AC_220V_in
GND
220V AC
CO2_SENSOR
S2
U2
Tx
Rx
M6
ALARM_MODULE
U1
P4
GND
Power_(3.3-5V)
P1
USB
ferrite
Nc
Tx_(out)
Rx_(in)
+3.3V
GND
+3.3V
1
2
3
4
5
A
B
C

Voltage connected to the fan is 5V. A small air flow over the sensors is created to increase diffusion speed

If the 24V input is connected to a 12V power supply, the 12V output will not be valid but the 3.3V and 5V will be.

Voltage: 5V
Peak current: 20mA
Digital interface: 3.3V
Com Settings
Baudrate: 9600
Flow control: None
Parity: None
Stop bits: 1bit
Data length: 8bits

Voltage: 3.3V
Peak current: 100mA
Digital interface: 3.3V
Com Settings
Baudrate: 9600
Flow control: None
Parity: None
Stop bits: 1bit
Data length: 8 bits

Alarm module
Self power mode:
Remove Ferrite
Bead

General Note: Drawings of Modules and Sensors are not in actual sizes

Micro2Gen
File: enose_rapid_prototype.sch
Sheet: /
Title: Electronic Nose 1st Prototype Schematic/Connection Diagram
Size: A4 | *Date: 28 sep 2015* | *Rev: Rev. A*
KiCad E.D.A. | *Id: 1/1*

The following picture illustrates the implemented hardware:

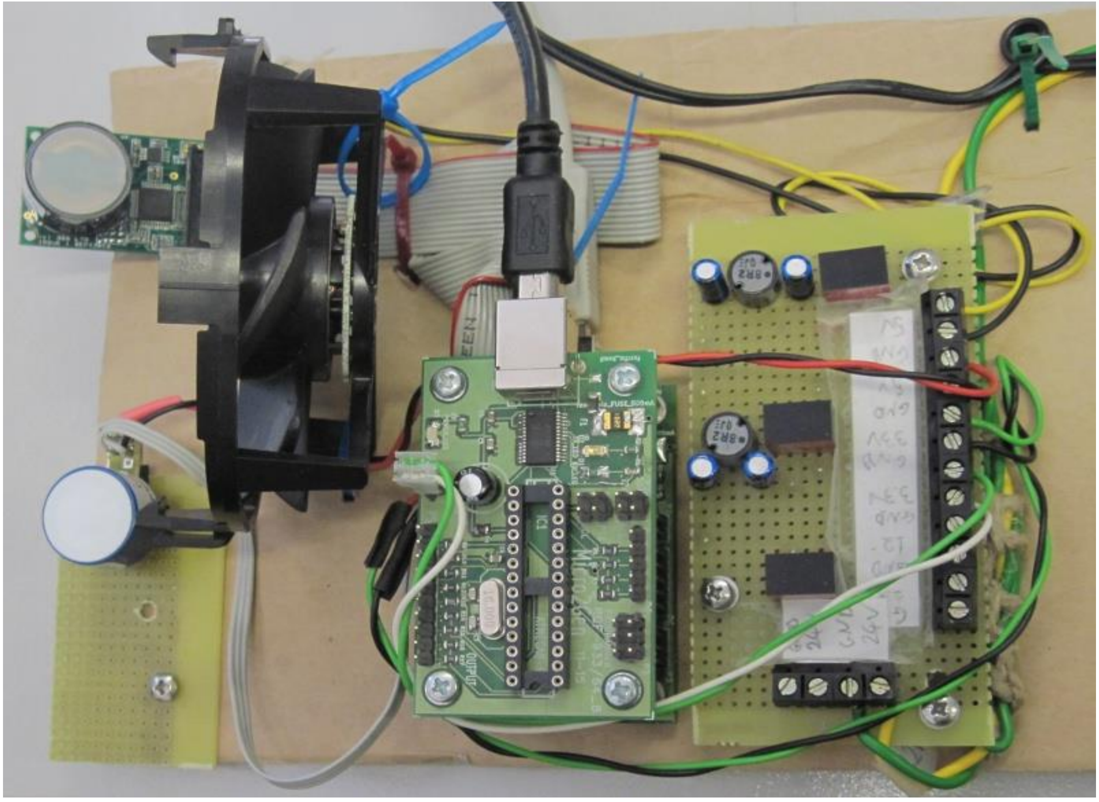

Figure 19. The first prototype. On the left is the CO_2 (top), O_2 sensor (bottom) and a fan (black). In the center are two USB to serial converters stacked on each other. On the right is the custom power supply PCB.

4.3. Software of the 1st prototype

This section describes the alternative setup where the sensors are connected to the PC via the USB to serial converters. To acquire measurements with this hardware configuration two instances of a terminal emulation program such as *gtkterm* or *minicom* are opened. Each instance of the application is connected to the assigned virtual com port of a USB to serial convert which corresponds to a sensor. The sensors were configured in a mode to continually produce measurements. (This setting is retained between power cycles.). The terminal application was configured to log the data – measurements to a file. The data file format is as seen on the terminal window and is compatible with CSV format (space delimited format) and can be processed with a spread sheet application, such as libreoffice Calc.

4.4. Proof of concept testing apparatus – initial experiments and results

This section includes a description of the setup and the method used to evaluate the setup and function as a proof of concept for the detection strategy of the e-nose.

Setup

The experimental setup is based on creating an air chamber in which air can enter and then be removed. The rapid prototype setup with the sensors is placed inside the chamber. The chamber has two ports. Each port can function as an input, output, or be blocked. When one port is used as an input (air is placed in the chamber), the other port acts as an output releasing air so the pressure does not increase in the chamber. At the one port, an air relief container is permanently connected. The other port can be connected to an air sample container or the atmosphere.

Method

The rapid prototype setup is evaluated by monitoring the sensors' outputs while placing a gas mixture of (approximately 1.3l exhaled air = 5exhales) known volume and concentration of the target gases in the chamber. This is performed with the following sequence of steps: A predefined number of exhaled breaths are placed in the sampling container, thus providing a rough estimation of the air volume and its concentration of CO_2 and O_2 gases (The volume of the chamber is known; the relief chamber is empty; the air in the chamber is assumed to be clean atmospheric). The sampled air is left in the sampling container for three minutes with the air circulating in the container so that it reaches the environmental temperature and any condensing humidity droplets sit on the chamber walls not harming the sensors. The sample is placed in the chamber and at the same time air moves to the relief chamber. Air is oscillated between the sample chamber and the relief chamber so that the air mixes. Finally, the sample chamber is emptied and the sample port is sealed. The new concentrations should be steady in the chamber (and in the relief container). After five minutes the air in the chamber is renewed with atmospheric air. This is performed with the following sequence of steps. The chamber's sample port is opened and the relief container is emptied. Atmospheric air is placed in the sample container and placed in the chamber as if it was an ordinary sample, including the mixing steps. The insertion of atmospheric air is repeated three times, with a fully loaded sample container, effectively surpassing two air changes. The sample port entrance is left open for a complete balance of atmospheric versus chamber concentrations to occur.

Ethical issues

The setup and experiment procedure do not cause any harm to the well-being of the person that provides the sample. There are no means of discriminating or extracting information regarding the status of the person who provides the sample. No written consent was acquired from the person who provided the sample. The test sample was generated by a member of the team that designed and implemented the setup.

Results

The experimental setup is illustrated in the following picture.

- The chamber is a 10l plastic bottle with two openings.
- The sample and relief containers are plastic bags that can be manipulated by hand.
- The sensors are covered with bags to provide some protection although they increase the response time.
- Sample input is five exhaled breaths with an approximate volume of 1.3l produced from a male who only performed work on a computer for at least three hours prior to sampling.

The following picture illustrates the experimental setup. The components placed in the gas chamber are the sensors, the USB to serial communication converters and the power supply board. The ARM embedded computing platform (upper left corner) and the AC mains power adaptors were left outside since they were not needed inside and would consume chamber volume. The fan listed in the schematics was not placed in the setup because the protective covers on the sensors would block the air.

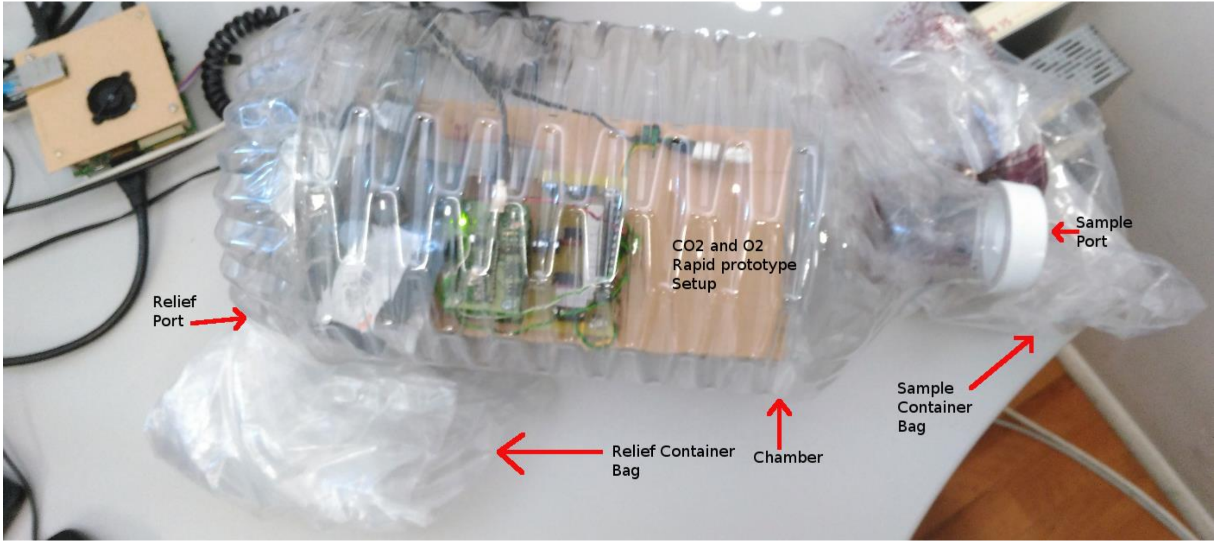

Figure 20. The experiment setup with the rapid prototype system.

The following picture illustrates a different view of the experimental setup.

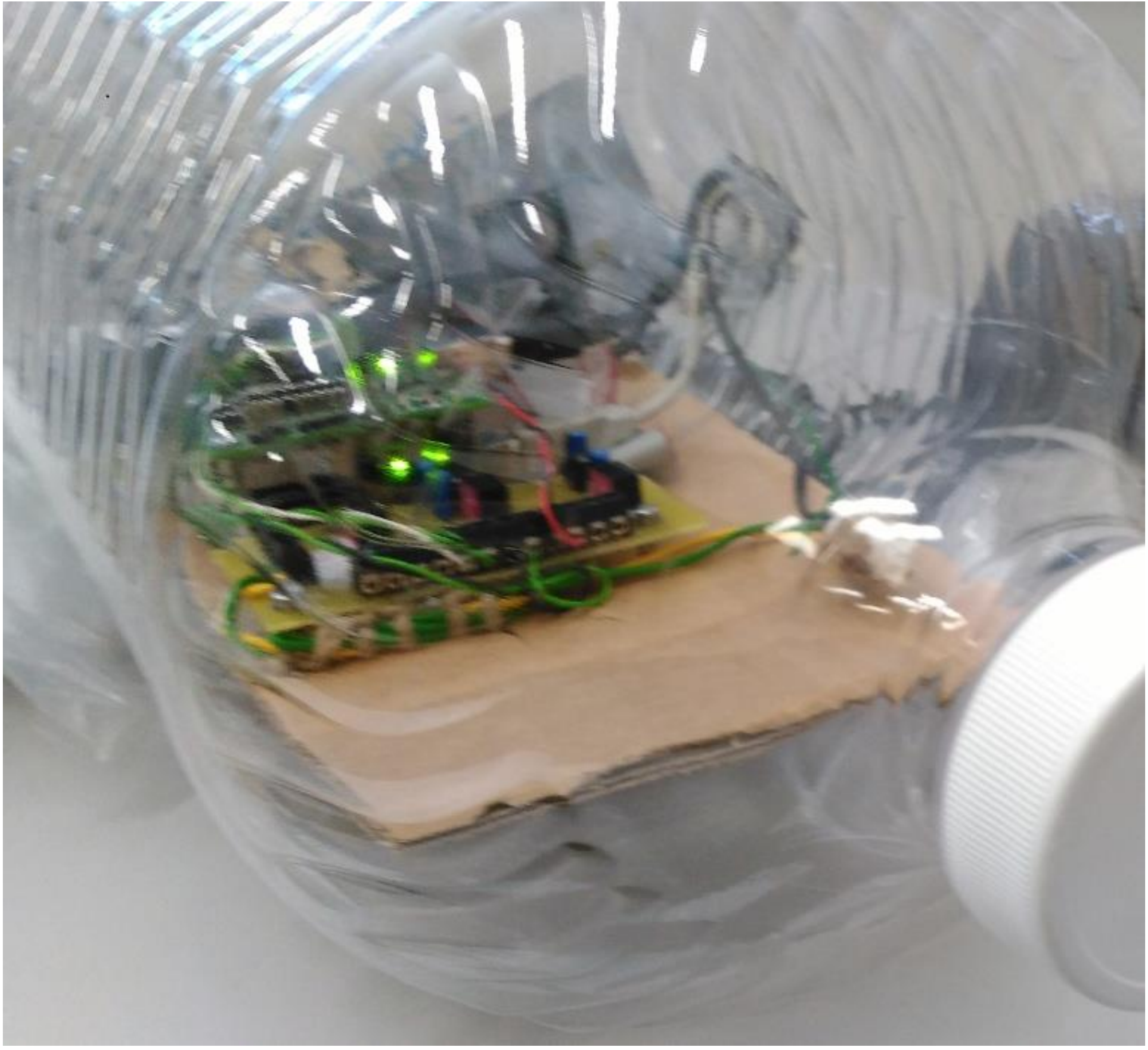

Figure 21. Inside the gas chamber of the experimental setup.

The following two plots visualize the measurement results acquired during the execution of the experiment for the CO_2 and O_2 sensors.

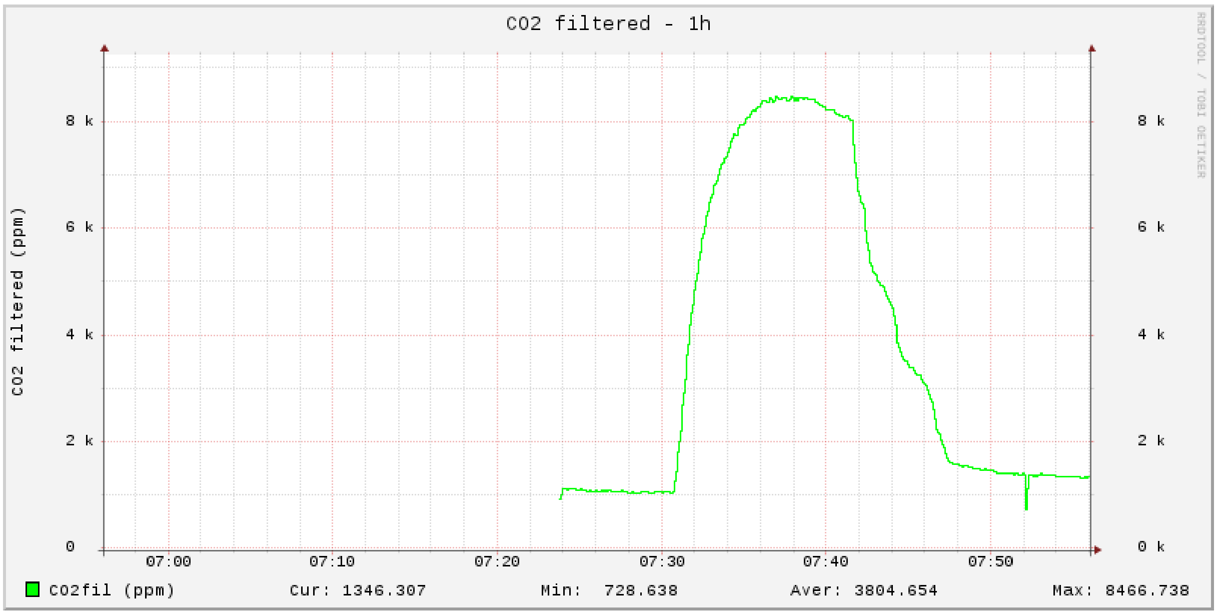

Figure 22. Plot of CO_2 concentration versus time.

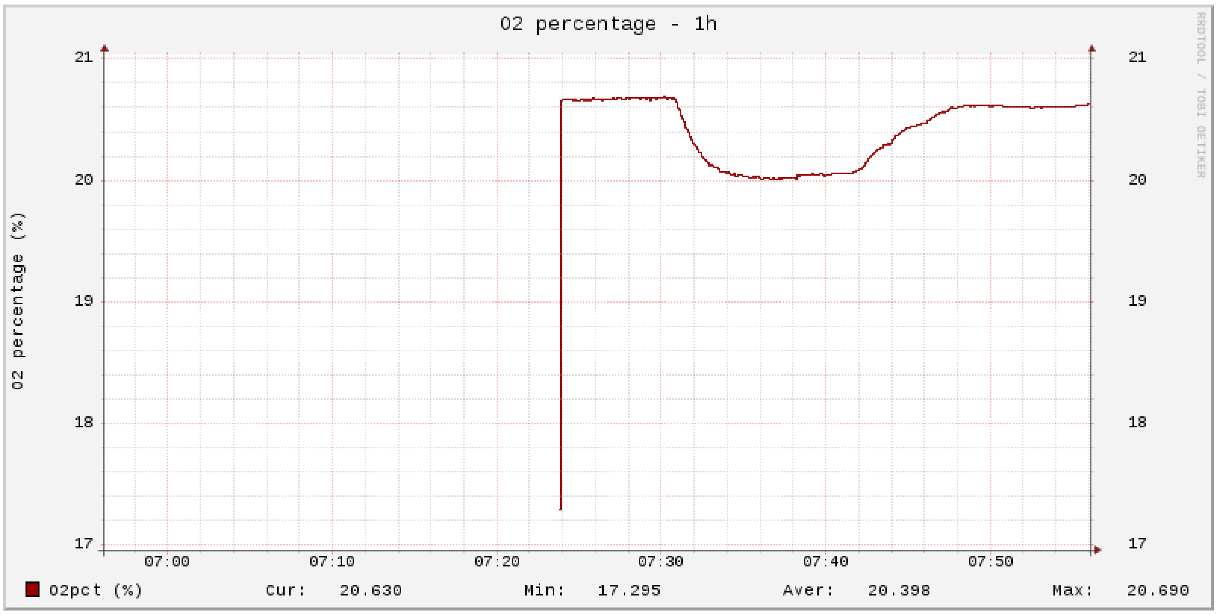

Figure 23. Plot of O_2 concentration versus time.

Phases of the experiment execution that can be seen in the graphs:

The air mixture was introduced into the chamber.
The relief chamber was emptied, output left open.
Atmospheric air was introduced as sample #1.
Atmospheric air was introduced as sample #2.
Atmospheric air was introduced as sample #3.
The sample port was left open.

Note that the setup was not optimized for a fast response; it was only intended as a proof-of-the-detection concept. The sensors responses are slow because the air mixture in the chamber has to diffuse through the sensors filters. No air manifold was used to force air through the sensor filters. An improved response could be achieved by placing a fan over the sensors inputs. Also, the CO_2 sensor was not calibrated at the beginning of the experiment so the fresh air level was not correct.

Conclusions

The sensors' responses are very indicative of the application and removal of the test subject's exhaled breath. The levels of CO_2 and O_2 produced with the addition of the sample can be easily distinguished from the fresh atmospheric air levels. Also, the removal of those levels until reaching the atmospheric level with the dilution of the air mixture reveals a step response that is visible in the graphs.

Even though the experiment was not thorough and exhaustive, these results are considered successful and the approach followed for the e-nose is viable. There is room for improvement in the detection speed (latency) domain but this will be of concern in the next version of the prototype e-nose system.

4.5. Sensor readings stability of the 1st e-nose Prototype under static conditions

The aim of the experiment is to evaluate the detection sensitivity and response of the first prototype of the e-nose under static conditions. The effectiveness of the two available sensors (CO_2 and O_2) is evaluated against the composition of the exhaled breaths of a human test subject. The primary means to achieve the objective is to measure CO_2 and O_2 levels for a variable amount of exhales. Secondarily, the speed of data delivery is logged in order to identify the overall responsiveness of the system.

To complete the main objectives a number of secondary tasks were undertaken. This includes testing the sensors, sizing the apparatus air chambers (sample chamber, relief chamber and gas chamber) and quantifying the exhaled volume of air at unit time of the human subject.

Sensor calibration is tested and the noise of the sensors was measured. This way the sensor operation was fully determined when the experiments commenced.

It is assumed that the metabolic function is associated with the tidal volume of a human test subject, which is the volume of exhaled air at rest. This is used in order to calculate concentrations of CO_2 and O_2 in the mixed exhaled + environment "fresh" air.

Compared to the previous tests with the 1st electronic nose prototype, this setup includes:

- A fan for circulating and mixing the air
- Exposed sensors in the airflow of the circulation fan (covers have been removed).
- Sensors have been calibrated, with the aid of an auto-calibration function based on fresh air composition measurements.

Experiment summary - conclusions

Initially, the noise of the sensors was recorded, in order to acquire statistical data for the mean and the standard deviation of the available sensors. The CO_2 sensor gave 5.87% noise on its unfiltered output and 1.32% on the filtered one, while the O_2 sensor provided a noise measurement of less than 0.02%.

Additionally, in order to approximately know the amount of air quantities that would be mixed, the source bag and exhaled air volume had to be measured. It turned out that the minimum exhaled air that could be taken from a single expiration was approximately 650ml. Additionally, 20 exhales were required to fill the source bag with exhaled air. Overall, the exhaled air in the bottle could be in the range 6% to 57% of the final volume of mixed air. This translates to approximately 3200ppm – 26300ppm of CO_2 and 20.78% - 18% of O_2. It is possible to measure lower concentrations, but a different setup should be used in order to be more accurate.

Measurements provided the means to evaluate how the concentration is expected to vary with an increasing portion of exhaled air volume in a known constant volume of fresh air: the general trend is that the measured and expected values follow the same direction. More accurate results could be drawn if the experiment is repeated with an apparatus where the source bag, bottle and exhaled air volumes can be measured with more accuracy.

As expected, the CO_2 sensor provides a fast response following a change in CO_2 concentration which is typically two seconds, while the O_2 has a propagation delay of six seconds. Both delays are not related to the time an acquired value needs to appear on a graph; however, graphs are only used for human monitoring supervision. The actual processing of the data in order to identify potential conditions of a trapped human will be done by acquiring values directly from the sensors. As a result, the delay of two seconds for the CO_2 sensor and that of six seconds for the O_2 sensor are within normal operating limits and adequately “real time” for the speed of a search and rescue operation.

5. Theoretical analysis and experiments to evaluate selected CO_2 and O_2 sensors

5.1. Theoretical analysis

In this section, a theoretical analysis is presented of the anticipated CO_2 and O_2 gas concentrations in a space with a human trapped inside. CO_2 and O_2 concentrations (m^3/m^3), in exhaled breath, as mentioned in literature [74][75][76], vary and depend on many parameters. For the scope of this work, it is adequate to compromise with the approximation, that in comparison with fresh air, the decrease of the concentration of O_2 is equal to the increase of CO_2 concentration. Thus, in this section only CO_2 anticipated concentrations are calculated and this value may be used as well for the trend of the decrease of O_2 concentration from the 21% reference value in fresh air.

A typical scenario is investigated involving a room/space with a single opening. The size of the opening is the input parameter affecting the concentration of the space after 5 hours. All other factors are considered steady.

The analysis is based on the following assumptions: Experiments are conducted at sea level (atmospheric pressure 1atm = 101,325pa), the environmental temperature is 20^0C, space temperature is 28^0C, its volume is cubic $8m^3$, the trapped human produces CO_2 at a rate of $0.05m^3/h$ and according to the aforementioned approximation consumes O_2 also at a rate of $0.05m^3/h$, and the opening is a square window (h meters*h meters) that is fully open. It also assumes that entrapment occurs in a space that has a single opening and that the buoyancy forces are those that drive the air exchange with the environment.

First, the air flow Q is calculated, given the aforementioned conditions /assumptions and using equation 11 of [77],

$$Q = \frac{1}{3} c_d A_{eff} \sqrt{{(gh\Delta T)}/{T_{out}}} \qquad (8)$$

where C_d is the discharge coefficient = 0.6, A_{eff} is the effective flow area of the opening (h^2 m^2), g is acceleration of gravity, h is the square window dimensions in meters (m), ΔT is the temperature difference between the environmental and room/space temperatures and T_{out} is the environmental temperature.

The model assumes relatively large openings. The opening sizes listed in Table 9 are assumed to be relevant for the application. The smaller opening sizes might not be so compatible with the original assumption in [77] but nevertheless will provide an indication of the anticipated levels, although not very accurate.

Table 9. ROOM CO_2 CONCENTRATION AFTER 5 HOURS

Case	**Calculated room CO_2 concentration after 5 hours**			
	Opening size	***Volume flow rate(m3/s)***	***Concentration after 5 Hours(ppm)***	***Notes***
A	0.1mX0.1m	0.0004	20000	Not final concentration
B	0.15mX0.15m	0.0012	11000	Almost final concentration
C	0.2mX0.2m	0.0025	6000	Final concentration
D	0.3mX0.3m	0.0069	2400	Final concentration
E	0.5mX0.5m	0.0247	1000	Final concentration

Then the air changes (shifts) per hour are calculated given the room/space size. The CO_2 concentration is calculated after 5 hours using equation 9 from [78], assuming the initial CO_2 concentration in the room to be same as the environment.

$$c = (q/nV)[1-(1/e^{nt})] + (c_0 - c_i)\,(1/e^{nt}) + c_i \;\; (1) \qquad (9)$$

Where c is CO_2 concentration in the room (m^3/m^3), q is CO_2 supplied to the room (m^3/h) from the entrapped human, V is volume of the room (m^3), e is Euler's number, n is number of air shifts per hour (h^{-1}), t is time (h), c_i is CO_2 concentration in the incoming atmospheric air (m^3/m^3) and c_0 is CO_2 concentration in the room at the start, t = 0 (m^3/m^3).

The calculated concentrations are listed in Table 9. For evaluating via testing the selected sensors, the calculated concentrations for each opening are fed to the sensors. These concentrations are created by mixing known volumes of fresh air and exhaled air.

The calculation of the mixing volumes is based on the following assumptions and conditions: Experiments are conducted at sea level (1atm), the environmental temperature is 36^{0}C, exhaled breath temperature is the same, and it is saturated with humidity (100%RH), the flexible air containers used (plastic bags), always have atmospheric pressure, air compounds follow ideal gases law and Dalton's law for partial pressures, and finally that a trapped human produces CO_2 at a rate of 0.05m^3/h.

Fresh air gas concentrations and exhaled air concentrations listed in literature are dry air concentrations, without humidity. Ideal gas law and Dalton's law of partial pressures are used to calculate concentrations of CO_2 in fresh air with 50%RH and exhaled breath saturated with humidity at 36°C.

$$P = P_a + P_w \tag{10}$$

$$P_w = RH\, P_{ws}/100 \tag{11}$$

Where P is the total pressure of the air mixture, P_a is the partial pressure of dry air, P_w is the partial pressure of the water vapor, P_{ws} is the partial pressure of saturated water vapor in atmospheric air at the given conditions (temperature and pressure). At the examined conditions (with 50%RH), it is calculated that for environmental air, P_w=2973.98pa (P_{ws} = 5947.96pa) and for the exhaled breath case $P_w = P_{ws}$.

With the CO_2 concentrations (and partial pressures) of the two samples known, the equation of the CO_2 partial pressure of their mixture, given the assumptions, can be written as:

$$P_{F+E} = (P_F V_F + F_E V_E)/(V_F + V_E) \tag{12}$$

Where P_{F+E} is the partial pressure of the mixture of fresh air volume V_F with CO_2 partial pressure P_F and exhaled air volume V_E with CO_2 partial pressure P_E. Solving the equation to find V_E is possible because all other quantities are known or assumed. Table 10 lists the required mixing volumes to proceed with the tests and it includes the calculated V_E in column 4, given V_F in column 3 and target CO_2 concentration in column 2.

Table 10. Calculated Quantities of Fresh and Exhaled Air for Mixing

Case	**Calculated fresh and exhaled air quantities required to be mixed to acquire target CO_2 concentration**		
	CO_2 concentration(ppm)	***Fresh air volume(ml)***	***Exhaled air volume(ml)***
A	20000	10000	11100
B	11000	10000	4000
C	6000	10000	1770
D	2400	10000	570
E	1000	10000	170

5.2. Experiment to evaluate selected sensors

The rapid prototype readout setup of the apparatus, shown in Figure 19 was evaluated by monitoring the sensors' outputs while placing a gas mixture, listed in Table 10, of known volume and concentration of the target gases, in an experimental chamber setup including two additional containers. In Figure 24 the operation concept of the apparatus is illustrated.

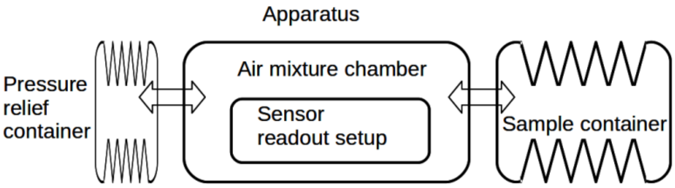

Figure 24 : Operation concept of the apparatus for air mixing and sensor measurements. The sample and relief containers are plastic bags that can easily be manipulated by hand to move the air inside them.

The preparation, mixing and measurements were performed with the following sequence of steps: A predefined volume of exhaled breath was placed in a flexible sampling container bag (Figure 24 on the right), thus providing a rough estimation of the air volume and its concentration of CO_2 and O_2 gases. The exhaled air was produced by and sampled from a normally breathing healthy male who was performing office work (no heavy physical activities that increase CO_2 concentration). This breath sample container is connected to the main air mixture chamber, (Figure 24 the middle), but not immediately so that humidity has time to condense on the walls of the sample bag. The volume of the main experimental chamber is known, and initially it is assumed to be filled with normal atmospheric air. In order to be able to manipulate the air samples without having to handle much larger than atmospheric pressures, another flexible bag, the relief bag, is used to relieve the pressure when inserting the sample in the experimental chamber (Figure 24 on the left). After the introduction of the exhaled air sample into the air mixture chamber (Figure 25), air is transferred back and forth between the sample container and the relief container to mix well before taking measurements (Figure 26).

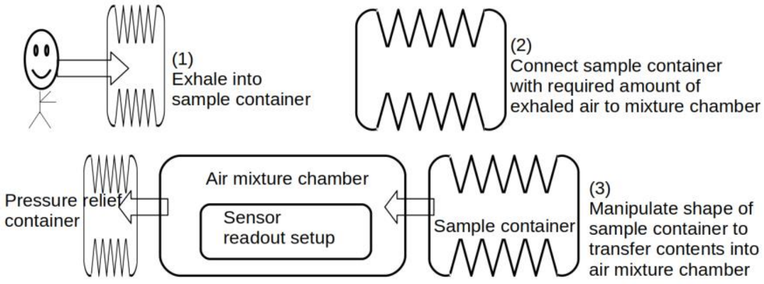
(1)
Exhale into
sample container
(2)
Connect sample container
with required amount of
exhaled air to mixture chamber
Pressure relief
container
Air mixture chamber
Sensor
readout setup
Sample container
(3)
Manipulate shape of
sample container to
transfer contents into
air mixture chamber

Figure 25. Breath sampling and introduction into apparatus

Manipulation by hand of both the relief bag and the sample bag, as shown in Figure 26, allows for easy mixing of the air in the system.
It must be mentioned that the apparatus and experiment procedure do not place the well-being of the person who provides the sample in any danger. There are no means of identifying, discriminating, or extracting information regarding the status of the person who provides the sample.

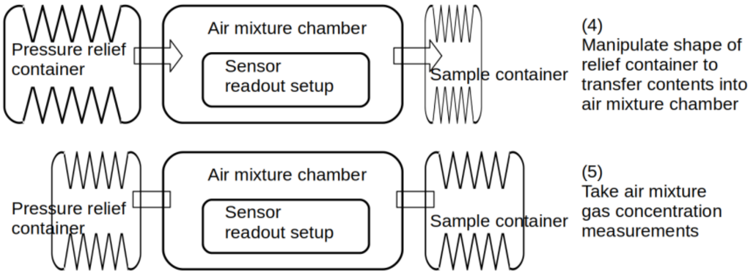
Pressure relief
container
Air mixture chamber
Sensor
readout setup
Sample container
(4)
Manipulate shape of
relief container to
transfer contents into
air mixture chamber
Pressure relief
container
Air mixture chamber
Sensor
readout setup
Sample container
(5)
Take air mixture
gas concentration
measurements

Figure 26 : Air mixing and measurements.

The actual experimental apparatus is illustrated in Figure 27. The 10 liter plastic bottle is the main gas chamber where the readout setup is placed. The bottle has two extra openings, one for interfacing the relief chamber (bag) on the left and one for cable entry. Sample entry is at the bottle entry opening where the sample container (bag) is attached. The base of the bottle was cut off in order to place the readout setup and then it was carefully reattached with clear adhesive tape.

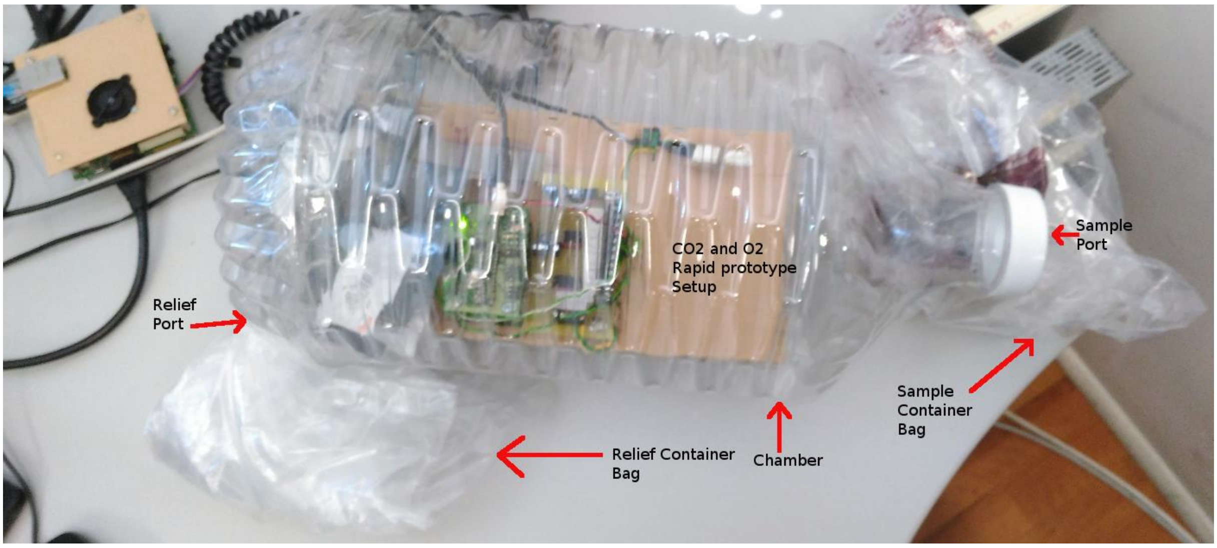

Figure 27 : The Experimental Apparatus for the Sensor Measurements.

The captured raw sensor values were processed off-line. Using the known fresh air concentrations, offset correction was performed, as if single point sensor calibration had been performed. Gain correction was not performed since a second reference was not available. Another reason was that for the application of human presence detection, accurate concentration measurements are not required. The listed average concentration and standard deviation are calculated on the range of values when the sensor output is in plateau.

Table 11 lists the captured measurement statistics. Note that the readout setup and apparatus were not optimized for a fast sensor response. Also note that the apparatus and execution of the experiment were not intended to acquire very accurate air volumes since there exist important fluctuations of compounds concentrations in fresh air in a period of a few days or in different nearby places [79], and of the exhaled air depended on the person's characteristics and physical condition [74]. The readout setup and apparatus were only intended as a proof of the detection concept. The sensors' responses are slow because the air mixture in the chamber has to diffuse through the sensors' filters. No air manifold is used to force air through the sensor filters. After the tests were finished, an improved response time was achieved by placing a fan over the sensors' inputs as illustrated in Figure 19.

The sensors' responses are very indicative of the application. The levels of CO_2 and O_2 produced as soon as the exhaled air sample was added could be easily distinguished from the fresh atmospheric air levels. Even the case with the smallest CO_2 concentration, which corresponds to the largest opening/window of 0.5m by 0.5m, seems to be easily detectable.

Table 11. Measurements

Case	Measured CO_2 and O_2 concentrations			
	Gas	*Average Concentration (CO_2-ppm, O_2-%)*	*Standard Deviation*	*Notes*
Fresh Air	CO_2	450	125	24minutes of samples
Fresh Air	O_2	20.86	0.011	24minutes of samples
E	CO_2	733,	40	30-60 samples
E	O_2	20.83	0.009	30-60 samples
D	CO_2	1891	172	30-60 samples
D	O_2	20.79	0.01	30-60 samples
C	CO_2	4635	533	30-60 samples
C	O_2	20.67	0.05	30-60 samples
B	CO_2	8327	546	30-60 samples
B	O_2	20.42	0.03	30-60 samples
A	CO_2	33722	1245	30-60 samples
A	O_2	18.72	0.03	30-60 samples

Figure 28 includes a graphical comparison between the target CO_2 concentrations listed in Table 9 and the measured CO_2 concentrations acquired with the apparatus listed in Table 11. Concentration axis is plotted in a logarithmic scale. For fresh air, the target concentration is assumed to be 400ppm. Horizontal category axis shows the target cases that correspond to the various openings (window size), of the confined space where an assumed victim is entrapped. Vertical axis presents the CO_2 concentration in ppm. It is evident that target and measured concentrations are in accordance.

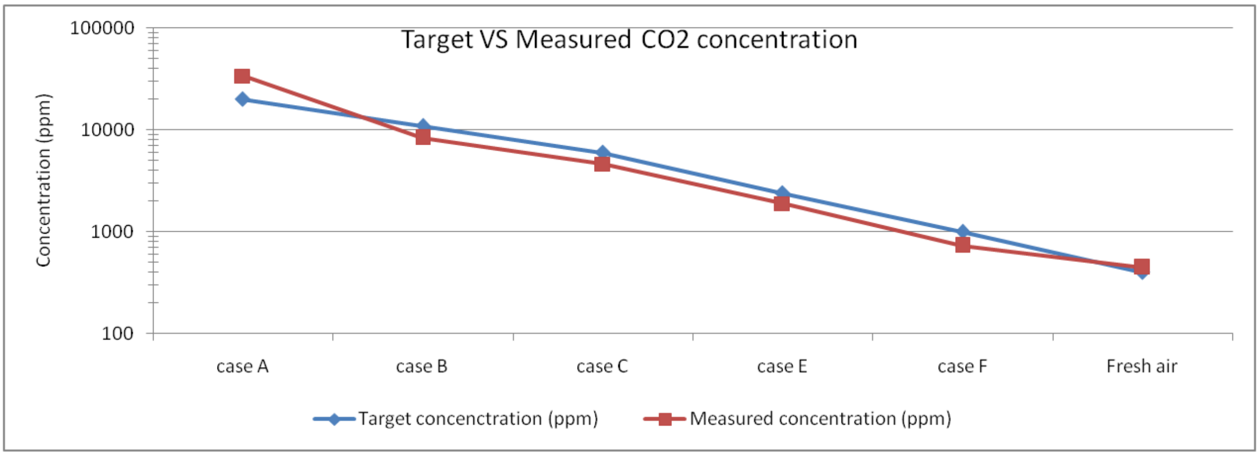

Figure 28 : A graphical comparison between the target CO_2 concentration cases listed in Table 1 and the measured CO_2 concentration when using the apparatus listed in Table III. Concentration axis is plotted in a logarithmic scale. For fresh air, the target concentration is assumed to be 400ppm.

Figure 29 presents the measured O_2 concentrations acquired with the apparatus and are listed in Table 11. Horizontal category axis shows the various air-mixture cases. Vertical axis presents the O_2 concentration in percentage (%). Oxygen measurements show that higher accuracy is needed to distinguish the various cases, especially those that correspond to large window openings. Nevertheless, the selected sensors for the apparatus sufficiently cover the required sensitivity. Case A measurement (18.72%), is omitted from Figure 29, in favor of cases C-E that are very tightly spaced.

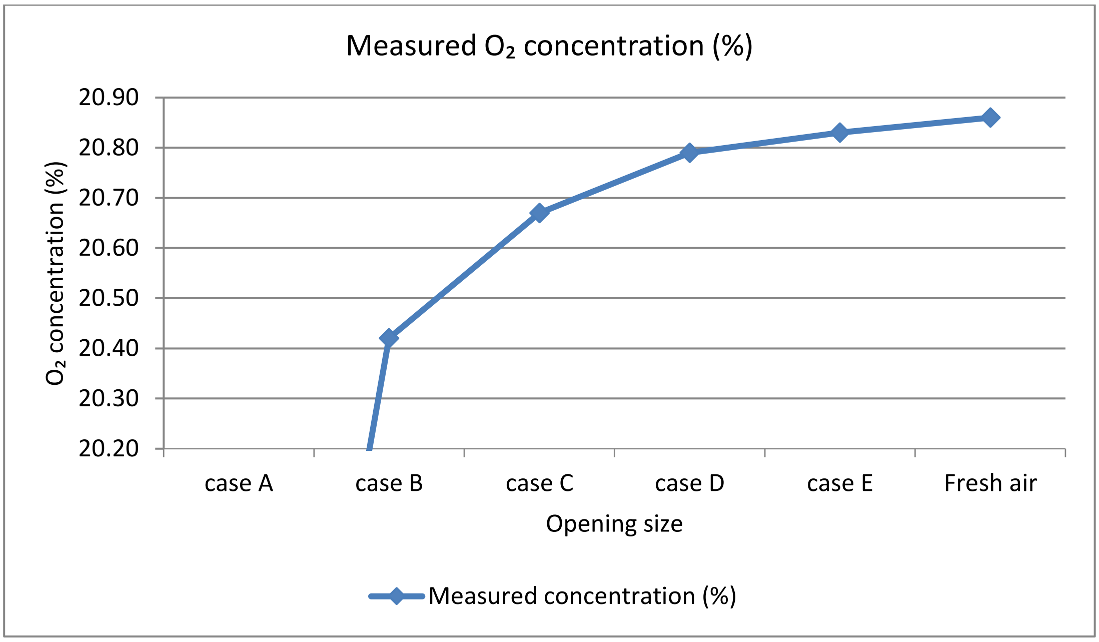

Figure 29 : A graphical presentation of the measured O_2 concentrations (listed in Table III) when using the apparatus.

5.3. Discussion

Even though the experiment was not thorough or exhaustive, these results are considered successful and the approach followed for the e-nose currently in development is viable. There is room for improvement in the detection speed (latency) domain, and this has already been taken into account in the current development of the e-nose system.

6. THEORETICAL ANALYSIS FOR NON STATIC CONDITIONS – HUMAN PRESENCE and FRESH AIR INPUT

6.1. Overview

In this chapter, a theoretical analysis of the anticipated gas concentration to be found in a void is presented. For this, a model was created and various conditions were examined. The concentration in the void is not static, but dynamic, because of the existence of the human sources and ventilation that constantly affect them. The human sources are the numbers of trapped victims, as well as their breathing capacity. The ventilation condition is the fresh air flow that refreshes the air of the void with atmospheric air. Other parameters examined are the effect of the void's volume in respect to the steady state gas concentrations and the time required to reach that steady state. Also, based on the static condition measurements (proof of concept measurements), the limit of detection for the selected sensors was determined. Another outcome of this study is the maximum fresh air flow entering the void that allows for victim detection with the selected sensors.

6.2. Limit of detection of selected CO_2 and O_2 sensors

The proof of concept experiments were carried out under static and sealed conditions. This is an ideal situation in which no fresh air circulates from the outside environment, leaving only exhaled air to affect the mixed air composition. If fresh air circulation is taken into account, then there exists a maximum fresh air refresh rate for which CO_2 and O_2 concentration changes are still observable based on the assumption that only one measurement would have to suffice to produce human presence indicators. To be observable they need to be clearly differentiated from the average gas and noise concentration.

Bearing Table 1 and Table 4 in mind, it is clear that in order for someone to be detectable under present conditions, the raw value acquired from the sensor should be **at least two standard deviations away from the mean**. Using the daily mean, which is higher, the target CO_2 concentration should be at minimum 820ppm. Similarly the maximum O_2 concentration should be lower than 20.734%. These values are the worst-case scenario. If more than one measurement are used for the decision making with filtering/averaging performed on a window of values, the limit of detection can be significantly reduced. The costs are response time and consequently in search/scanning speed.

6.3. Exhaled Air flow rate

For adults the respiratory rate is usually 12-18 breaths per minute [80] and this is the case with the human test subject used in this experiment. Elderly people may have a slower breathing rate (10-30 breaths per minute). Younger children have a faster breathing frequency reaching up to 30-60 breaths per minute for infants.

In the worst case the average human test subject will exhale ten times per minute which essentially gives the following flow rate of exhaled air:

$$FRexh\ (l/min) = \text{number of breaths}\ (\#\ breaths/min) * \text{tidal volume}\ (liters) \qquad (13)$$

Where volume of the average breath (tidal volume) has been calculated to 660ml for the test subject, but for the average population it is approximately 500ml for men and 390 for women. This gives an approximate minimum flow rate FRexh=0.39lt/breath * 10breaths/min = 3.9lt/min, which we can use to determine the maximum fresh air flow rate for O_2 and CO_2 concentration.

However, in absolute terms, the amount of air a person needs is determined by their mass. On average a person requires 7ml/kg of body mass [81]. So an average male adult weighing 75kg would have a tidal volume of 0.525lt and, as such, an exhaled air flow rate of FRexh= 6.3lt/min. Below are calculated the exhaled air flow rates for individuals at different ages.

Table 12: Minimum exhaled flow rate for individuals of both sexes and of different age groups.

description of individual	weight (kg) [82]-[87]	minimum number of breaths / min [81]	tidal volume (lt)	Minimum FRexhaled (lt/min)
adult male (35yo , 25% percentile)	75	12	0.5	6.3
adult female (35yo, 25% percentile)	57	12	0.4	4.8

child (10 years old)	33	15	0.2	3.5
child (3 years old)	14	20	0.1	2.0
baby (6 months old)	7.5	25	0.1	1.3
elderly male (>80yo, 25% percentile)	72	10	0.5	5.0
elderly female (>80yo, 25% percent.)	52	10	0.4	3.6

Table 13: Maximum exhaled flow rate for individuals of both sexes and of different age groups.

description of individual	weight (kg) [82]-[87]	max number of breaths / max [81]	tidal volume (lt)	Maximum FRexhaled (lt/min)
adult male (35yo , 25% percentile)	75	20	0.5	10.5
adult female (35yo, 25% percentile)	57	20	0.4	8.0
child (10 years old)	33	20	0.2	4.6
child (3 years old)	14	30	0.1	2.9
baby (6 months old)	7.5	40	0.1	2.1
elderly male (>80yo, 25% percentile)	72	18	0.5	9.1
elderly female (>80yo, 25% percent.)	52	18	0.4	6.6

This information will be used as input to identify the maximum fresh air flow rate (ventilation) in a closed space (i.e. a room). To do that a model of a system needs to be generated.

6.4. Modeling realistic conditions

In this case the closed cavity (room) is modeled ideally as a completely sealed space. There exist only two pairs of inflow-outflow points. The first pair is the external inflow-outflow, where fresh air with flow rate *FRfresh (FRf)* enters into the room and room air with the same flow rate flows out of the room. The second pair is the expiratory cycle of a human test subject placed adjacent (or in) the room, where looking in from the room's perspective there is outflow of air that goes into the human's lungs and inflow of their exhaled air, which is done at the human's exhaled flow rate *FRexhaled (FRe)*. Of course, inflowing volume of air should have the opposite sign from any outflowing volume of air.

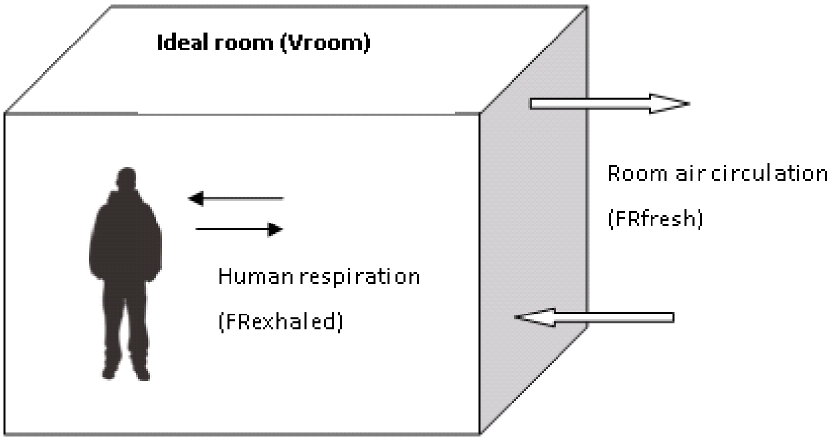

Figure 30: Model of an ideal sealed room with single person in it. Arrows depict air direction to and from air sources / sinks (i.e. human and environment)

The equation that relates the flow rates of O_2 and CO_2 concentrations with the room size should take into account the flow rates of fresh and exhaled air and should be the sum of all inflowing and outflowing air sources. From gas mixing theory the relevant equation is of the form:

Rate of change of gas in air =

inflow rate of air with specific gas concentration

outflow rate of air with gas at room concentration. (14)

Where, the rate of change of gas(Q) in the air is the volume of the gas, and it is related to the concentration of that gas as

$$C_{room}(t) = \frac{Q(t)}{V_{room}} \tag{15}$$

Keeping that in mind, the differential equation that describes the room system is shown below. It is noted that the assumption that air mixes evenly and immediately in the room is still used:
:

$$\frac{dQ}{dt} = F_e C_e - F_i C_{room} + F_f C_f - F_o C_{room} \tag{16}$$

Where *Fe = exhaled air flow rate (lt of air / min)*
Fi = inhaled air flow rate (lt of air / min) = Fe
Ff = inflowing fresh air flow rate (lt of air / min)
Fo = Outflowing air flow rate (lt of air / min) = Ff
Ce = gas (CO_2 or O_2) concentration in exhaled air (lt of gas / lt of air)
Cf = gas concentration in fresh air (lt of gas / lt of air)
Croom = gas concentration in the room (lt of gas / lt of air)

Solving this differential equation provides the following gas concentration in the room as a function of time, the room size, the concentrations and flow rates of gases that act on the system. Equation (17) calculates the concentration of a gas in a room when two gas sources-sinks mix in the same room.

$$C_{room}(t) = \frac{F_e C_e + F_f C_f}{F_e + F_f} + k e^{-\frac{F_e + F_f}{V_{room}} t} \tag{17}$$

Equation1: Equation that mixes two gas sources-sinks in the same room

Where k can be determined at time t=0 minutes and is given by equation (18),

$$k = C_{room}(0) - \frac{F_e C_e + F_f C_f}{F_e + F_f} \tag{18}$$

Croom(0) is the initial concentration of the gas, Fe is the exhaled flow rate, Ce is the concentration of the gas in the exhaled air, Ff is the fresh air flow rate, Cf is the concentration of the gas in the fresh air and Vroom is the volume of the entrapement cavity.

The equations are based on the following assumptions:

- A room in which air mixture through convection is immediate and uniform.
- Flow rates are constant through time.
- Pressure and temperature remain constant at the time intervals when calculations are performed.

It is important to note that **the size of the room is not important for the final equilibrium concentration** (as time t takes large values) and that the V_{room}/F_e+F_f value is the time constant τ of the system.

What is more, in any unsealed space, pressure and temperature are expected to be constant and the same as the surroundings. As a result, for any new molecule of fresh air (CO_2, O_2, or any other) another molecule must leave the cavity or either pressure or temperature should increase due to the laws of thermodynamics. Keeping the number of molecules of each gas in the cavity/room also translates to keeping the volume that each gas occupies constant for a given cavity size. This is due to the law of partial pressures (and volumes), which states that the ratio of molecules of a gas, compared to the total number of molecules in a cavity equals the ratio of volume that this gas occupies compared to the volume of the cavity. Equation (19) captures Dalton's law of partial pressures with the extension of Amagat's law of additive volumes.

$$\frac{n_{gas\,molecules}}{n_{molecules\,in\,room}} = \frac{V_{gas}}{V_{room}} = \frac{P_{gas}}{P_{room}} \tag{19}$$

The above equation provides the means to examine the model from the perspective of volume whilst maintaining mass conservation, which is proportional to the number of molecules. Plotting Equation1, and specifically the gas concentration versus time, will produce the following graphs (for given values of Fe, Ce, Ff and Cf). Note that the only differences between the two graphs are the initial and exhaled gas concentrations for CO_2 and O_2 respectively.

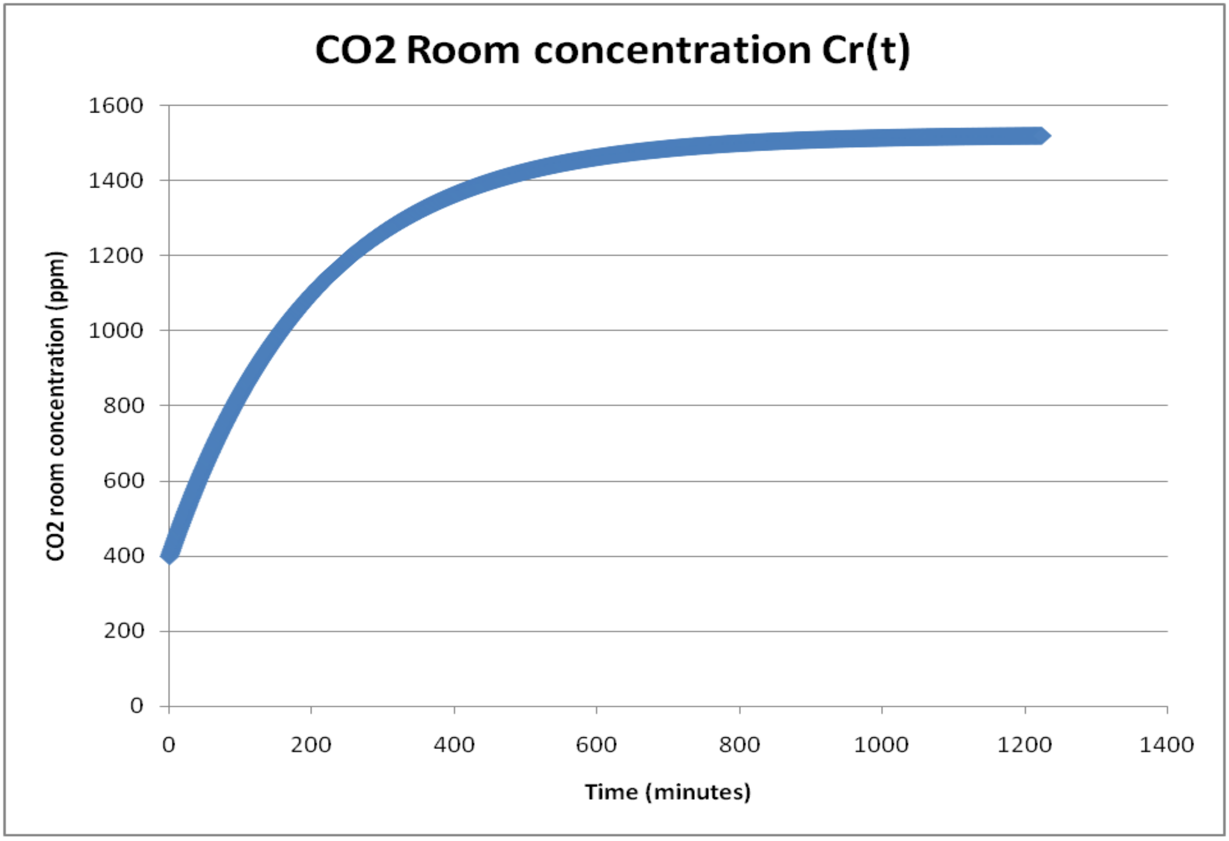

Figure 31: CO_2 concentration response of a person in a room where air is refreshed at a rate of 500lt/min

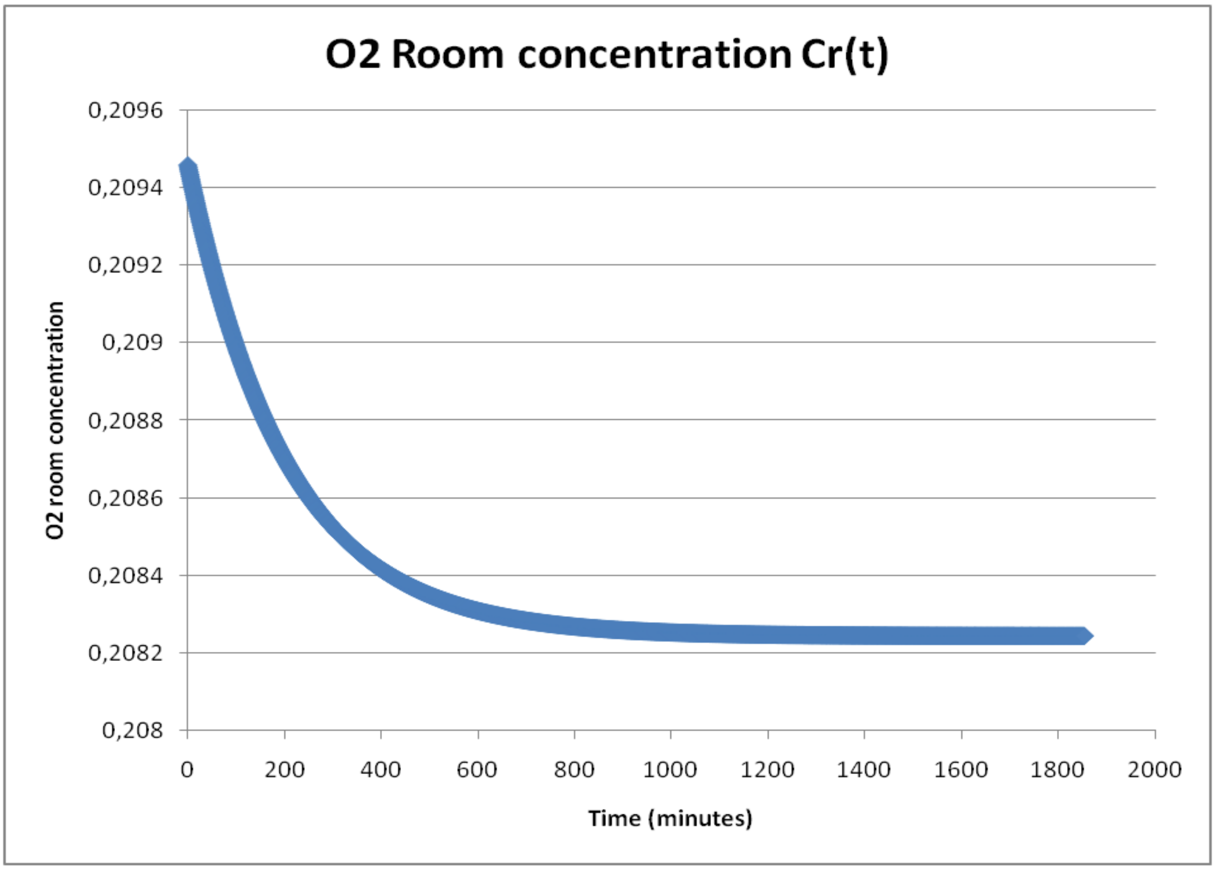

Figure 32: O_2 concentration response in the 1st 10 minutes that a person is in a room where air is refreshed at a rate of 500lt/min.

An observation that can be made from the graphs is that some time after the beginning of air mixing, an equilibrium gas concentration is reached. Also, for this room size it takes approximately 800 minutes for the equilibrium state to be reached.

This analysis has been carried out for several exhaled flow rates and room sizes. In these, the **maximum fresh air flow rate** and corresponding **final equilibrium concentration** have been calculated and presented in the following table. Note that only the terminal conditions, when the gas concentrations are just barely within the detectable zone, are shown. This "detectable zone" was calculated earlier from sensor noise analysis in the introduction of this chapter. Their values are **820ppm** or higher concentration for CO_2 and **20.734%** or lower for O_2.

6.5. Applying the model

The calculations are summarized in the following two tables – one of CO_2 and the other for O_2. The two left column groups contain typical numerical inputs along with a description. On the rightmost column group the results are presented; the calculated final equilibrium concentration, the maximum sustained flow rate of fresh air for which detection is possible and the 3τ time of the system. **3τ time is considered sufficient for the purpose of this work;** for CO_2 it is the time required for the gas concentration to reach 95% of its equilibrium concentration. This percentile was chosen in order to account for the slow progression once the gas has nearly reached its equilibrium values due to its naturally asymptotic behavior. The selection of 2σ distance from the atmospheric concentration for the decision threshold of the concentration and time 3τ where it is assumed equilibrium concentration is reached is not ideal: It does not ensure that at 3τ time after entrapment all measurement values will fall within the detection zone but it is the point at which positive detection measurements will start to be more frequent.

Note that for the cases of *very small* and *extremely small* cavities, no (2x) adult male scenario has been calculated. This is intentional since physically it is impossible for 2 people to fit in such small spaces.

Additionally, in the following table only the **boundary conditions** are shown, because it was deemed necessary to focus on the **worst-case scenarios**. The fresh air's concentrations of gases are assumed as follows: CO_2 F_f=400ppm and O_2 Ff=20.946%. The exhaled air's concentrations of gases are assumed as follows: CO_2 F_e=40000ppm and O_2 F_e=16%. In these scenarios the time required until the CO_2 levels are detectable/distinguishable for a given minimum exhaled air flow rate, as well as maximum fresh air flow rate that permits detection are calculated to aid end users in their work: CO_2 limit is 820ppm and O_2 limit is 20.734% which are assumed to be the equilibrium concentrations.

Table 14: Maximum fresh air flow rate and 3τ time-to-reach detectable CO_2 concentration for various room size and exhaled air flow rates.

room description	room size (m3)	human description	flow rate of exhaled air (lt/min)	equilibrium CO_2 (ppm)	Flow rate of fresh air (lt/min) adequate for CO_2 detection	t (min) 3τ time for CO_2 detection
typical room	**52.5**	2x adult male	12.6	820	1175	133
		adult male	6.3	820	588	265
		adult female & elderly male	4.8	820	448	348
		child and elderly female	3.5	820	327	477
		child 3 years old	2	820	187	835
		baby 6 months old	1.3	820	121	1285
small room	**26.25**	2x adult male	12.6	820	1175	66
		adult male	6.3	820	588	133
		adult female & elderly male	4.8	820	448	174
		child and elderly female	3.5	820	327	239
		Child 3 years old	2	820	187	418
		baby 6 months old	1.3	820	121	642
large cavity	**10**	2x adult male	12.6	820	1175	25
		adult male	6.3	820	588	51
		adult female & elderly male	4.8	820	448	66
		child and elderly female	3.5	820	327	91
		child 3 years old	2	820	187	159
		baby 6 months old	1.3	820	121	245
medium cavity	**5**	2x adult male	12.6	820	1175	13
		adult male	6.3	820	588	25
		adult female & elderly male	4.8	820	448	33
		child and elderly female	3.5	820	327	45
		child 3 years old	2	820	187	80
		baby 6 months old	1.3	820	121	122
small cavity (average person in stretched position but with room to turn around)	**2**	2x adult male	12.6	820	1175	5
		adult male	6.3	820	588	10
		adult female & elderly male	4.8	820	448	13
		child and elderly female	3.5	820	327	18
		child 3 years old	2	820	187	32
		baby 6 months old	1.3	820	121	49
very small cavity (average person in	**1**	adult male	6.3	820	588	5
		adult female & elderly male	4.8	820	448	7

sitting position)		child and elderly female	3.5	820	327	9
		child 3 years old	2	820	187	16
		baby 6 months old	1.3	820	121	24
Extr. small cavity (average person's head and upper body)	**0.5**	adult male	6.3	820	588	3
		adult female & elderly male	4.8	820	448	3
		Child and elderly female	3.5	820	327	5
		child 3 years old	2	820	187	8
		child 6 months old	1.3	820	121	12

Here it is clearly visible that the larger the room and the lower the exhaled air flow rate, the more time is necessary for the CO_2 concentration to reach the equilibrium value. For example, one can say that **an adult female subject with an exhaled air flow rate 4.8lt/min, who has *just* been trapped in a medium sized cavity 5m^3, with a fresh air flow of 448 lt/min, will be detectable after 33 minutes from entrapment due to the CO_2 footprint she exhales.**

This will be the case provided the fresh air is not circulated at a very high rate in the room/cavity and mixing of exhaled air with the surrounding air happens evenly across the room.

Similarly, it is apparent that **the room size does not affect the amount of fresh air flow rate which determines the final equilibrium concentration** – only the exhaled air flow rate plays a role in that, leaving room size to affect only *how quickly* the detectable concentration will be reached.

The female subject will not be detectable at all (not after 33 minutes, or however much more time is allowed to pass) if the fresh air circulation happens at a rate of more than 448lt/min.

Similarly, for O_2 the table summarizes the threshold O_2 concentration below which human presence may be in close proximity, the maximum fresh air flow rate that allows detection of humans and the minimum time required for concentration levels to pass the O_2 threshold that will enable detection.

Note that due to the reduction of O_2 during human breathing, the O_2 trend approaches the asymptote of the equilibrium with a negative slope and 3τ is used to measure to the time to equilibrium.

Table 15: Maximum fresh air flow rate and 3τ time-to-reach detectable O_2 concentration for various room size and exhaled air flow rates.

room description	room size (m3)	human description	flow rate of exhaled air (lt/min)	equilibrium O_2 (%)	Flow rate of fresh air (lt/min) adequate for O_2 detection	t (min) 3τ time for O_2 detection
typical room	**52.5**	2x adult male	12.6	20.734	281	536
		adult male	6.3	20.734	141	1072
		adult female & elderly male	4.8	20.734	107	1406
		child and elderly female	3.5	20.734	78	1929
		child 3 years old	2	20.734	45	3375
		baby 6 months old	1.3	20.734	29	5193
small room	**26.25**	2x adult male	12.6	20.734	281	268
		adult male	6.3	20.734	141	536
		adult female & elderly male	4.8	20.734	107	703
		child and elderly female	3.5	20.734	78	964
		child 3 years old	2	20.734	45	1688
		baby 6 months old	1.3	20.734	29	2597
large cavity	**10**	2x adult male	12.6	20.734	281	102
		adult male	6.3	20.734	141	204
		adult female & elderly male	4.8	20.734	107	268

		child and elderly female	3.5	20.734	78	367
		child 3 years old	2	20.734	45	643
		baby 6 months old	1.3	20.734	29	989
medium cavity	**5**	2x adult male	12.6	20.734	281	51
		adult male	6.3	20.734	141	102
		adult female & elderly male	4.8	20.734	107	134
		child and elderly female	3.5	20.734	78	184
		child 3 years old	2	20.734	45	321
		baby 6 months old	1.3	20.734	29	495
small cavity (average person in stretched position but with room to turn around)	**2**	2x adult male	12.6	20.734	281	20
		adult male	6.3	20.734	141	41
		adult female & elderly male	4.8	20.734	107	54
		child and elderly female	3.5	20.734	78	73
		child 3 years old	2	20.734	45	129
		baby 6 months old	1.3	20.734	29	198
very small cavity (average person in sitting position)	**1**	adult male	6.3	20.734	141	20
		adult female & elderly male	4.8	20.734	107	27
		child and elderly female	3.5	20.734	78	37
		child 3 years old	2	20.734	45	64
		baby 6 months old	1.3	20.734	29	99
Extr. small cavity (average person's head and upper body)	**0.5**	adult male	6.3	20.734	141	10
		adult female & elderly male	4.8	20.734	107	13
		child and elderly female	3.5	20.734	78	18
		child 3 years old	2	20.734	45	32
		baby 6 months old	1.3	20.734	29	49

O_2 detection is far slower compared to CO_2. This is due to the much higher concentration of O_2 that exists in the atmosphere and the much smaller difference of O_2 concentration between atmospheric air and exhaled air (as opposed to CO_2 % change). In fact, the same female in the same 5m^3 can be detected by her O_2 footprint only after 134 minutes (as opposed to 29 minutes from CO_2 footprint), and this is only possible if the fresh air refresh rate does not increase more than 107 lt/min (as opposed to 448lt/min for the CO_2 footprint).

6.6. Elaborating on the model

Even though Table 14 and Table 15 contain all the necessary information they are a little difficult to follow. As a result the information has been split into the following tables in different groupings.

6.6.1. Maximum fresh air flow rates

Detection of humans in a cavity is governed by gas mixing theory and has an upper limit when the air is refreshed in that cavity. This limit differs for people of different masses exhaling in that cavity. It also differs between CO_2 and O_2.

Table 16: maximum fresh air flow rate (lt/min) for which CO_2 detection is possible

human presence	Exhaled air flow rate (lt/min)	maximum fresh air flow rate (lt/min) for which CO_2 detection is possible
2x adult male	12.6	1175

adult male	6.3	588
adult female & elderly male	4.8	448
child and elderly female	3.5	327
child 3 years old	2	187
baby 6 months old	1.3	121

Table 17: maximum fresh air flow rate (lt/min) for which O_2 detection is possible

human presence	Exhaled air flow rate (lt/min)	maximum fresh air flow rate (lt/min) for which O_2 detection is possible
2x adult male	12.6	281
adult male	6.3	141
adult female & elderly male	4.8	107
child and elderly female	3.5	78
child 3 years old	2	45
baby 6 months old	1.3	29

6.6.2. Final gas concentration for several scenarios

It is useful to have a reference for the **maximum concentration that can be reached in several scenarios for trapped humans and fresh air circulation conditions**. The CO_2 is in ppm units and the O_2 is in % units. Marked with red color are the undetectable levels, while marked with green color are the detectable ones. Note that for CO_2 the threshold is set to 820ppm and for O_2 it is set to 20.734%

Table 18: Maximum CO_2 concentration (in ppm) for several scenarios of fresh air vs. exhaled air flow(i.e. people)

Person \ Ff(lt/min)->	1500	1000	500	250	100	50	20
2x adult male	730	893	1373	2300	4831	8371	15706
adult male	566	648	893	1373	2747	4831	9886
adult female & elderly male	526	589	777	1146	2214	3869	8065
child and elderly female	492	538	675	947	1739	2991	6298
child 3 years old	453	479	558	714	1176	1923	4000
baby 6 months old	434	451	503	605	908	1404	2817

Table 19: Minimum O_2 concentration (in %) for several scenarios of fresh air vs. exhaled air flow(i.e. people)

Person \ f(lt/min)->	1500	1000	500	250	100	50	20
2x adult male	20.905	20.884	20.824	20.709	20.393	19.95	19.034
adult male	20.925	20.915	20.884	20.824	20.653	20.393	19.761
adult female & elderly male	20.93	20.922	20.899	20.853	20.719	20.513	19.989
child and elderly female	20.934	20.929	20.912	20.878	20.779	20.622	20.209
child 3 years old	20.939	20.936	20.926	20.907	20.849	20.756	20.496
baby 6 months old	20.942	20.94	20.933	20.92	20.883	20.821	20.644

Again, it is easy to see that the CO_2 concentration increases and the O_2 concentration decreases the lower the fresh air flow rate and/or the more mass the person has.

Note that the volume of the room/cavity is not important in any of these scenarios as final concentration is independent of the size of the room.

6.6.3. Time delay for gas concentration to enter “detectable” zone

The time it takes for the gas concentration to enter detectable zone in a cavity is directly related to Table 18 and Table 19 above. These times depend on all 3 factors (room size and fresh and exhaled air flow rates) and cannot be presented in a two dimensional table. Instead, two typical room sizes (26250lt and 5000lt) have been selected and the relevant times are presented in the following tables. The first 2 tables present the time (minutes) for a room of size 26250lt for gases CO_2 and O_2 accordingly.

Table 20: Time for CO_2 footprint to enter detectable zone (Vroom = 26250lt) for various flow rate scenarios

Person \ Ff(lt/min)->	1500	1000	500	250	100	50	20
2x adult male	-	50	29	25	23	23	22
adult male	-	-	99	58	49	46	45
adult female & elderly male	-	-	-	85	66	62	60
child and elderly female	-	-	-	151	95	87	83
child 3 years old	-	-	-	-	200	163	148
baby 6 months old	-	-	-	-	454	277	235

Table 21: Time for O_2 footprint to enter detectable zone (Vroom = 26250lt) for various flow rate scenarios

Person \ Ff(lt/min)->	1500	1000	500	250	100	50	20
2x adult male	-	-	-	224	113	100	95
adult male	-	-	-	-	317	225	197
adult female & elderly male	-	-	-	-	688	322	265
child and elderly female	-	-	-	-	-	522	379
child 3 years old	-	-	-	-	-	-	761
baby 6 months old	-	-	-	-	-	-	1493

While the following 2 tables present the time (minutes) for a room of size 5000lt.

Table 22: Time for CO_2 footprint to enter detectable zone (Vroom = 5000lt) for various flow rate scenarios

Person \ Ff(lt/min)->	1500	1000	500	250	100	50	20
2x adult male	-	9	6	5	4	4	4
adult male	-	-	19	11	9	9	9
adult female & elderly male	-	-	-	16	13	12	11
child and elderly female	-	-	-	29	18	17	16
child 3 years old	-	-	-	-	38	31	28
baby 6 months old	-	-	-	-	86	53	45

Table 23: Time for O_2 footprint to enter detectable zone (Vroom = 5000lt) for various flow rate scenarios

Person \ Ff(lt/min)->	1500	1000	500	250	100	50	20
2x adult male	-	-	-	43	21	19	18
adult male	-	-	-	-	60	43	37
adult female & elderly male	-	-	-	-	131	61	50
child and elderly female	-	-	-	-	-	100	72
child 3 years old	-	-	-	-	-	-	145
baby 6 months old	-	-	-	-	-	-	284

6.6.4. Time delay to reach saturation concentration

The 3τ time it takes for the gas concentration to approach saturation level in a cavity for various cavity sizes is shown below for CO_2 and O_2 respectively.

Table 24: 3τ time (in minutes) for CO_2 footprint to approach saturation levels in various room sizes and for various trapped people

person\Vr(m3)	0.5	1	2	5	10	26.25	52.5
2x adult male			5	13	25	66	133
adult male	3	5	10	25	51	133	265
adult female & elderly male	3	7	13	33	66	174	348
child and elderly female	5	9	18	45	91	239	477
child 3 years old	8	16	32	80	159	418	835
baby 6 months old	12	24	49	122	245	642	1285

Table 25: 3τ time (in minutes) for O_2 footprint to approach saturation levels in various room sizes and for various trapped people

person\Vr(m3)	0.5	1	2	5	10	26.25	52.5
2x adult male			20	51	102	268	536
adult male	10	20	41	102	204	536	1072
adult female & elderly male	13	27	54	134	268	703	1406
child and elderly female	18	37	73	184	367	964	1929
child 3 years old	32	64	129	321	643	1688	3375
baby 6 months old	49	99	198	495	989	2597	5193

It is clear that a person in a larger room will take more time to alter the gas concentration in the room in order for the latter to be clearly separated from the noise and reach a “detectable” level.
Additionally, the smaller the mass of the person, the less the gas that is deposited by each exhale into the atmosphere and consequently, the slower the change of the gas concentration will be.

6.7. Conclusions - findings

A horizontal analysis of the CO_2 and the O_2 results leads to some very interesting conclusions that affect the way e-nose sensors readings are interpreted.
Human physiology generates a much clearer CO_2 footprint that has a much larger exhaled air to fresh air concentration ratio, compared to O_2. Therefore, it is apparent that the O_2 human footprint can be detectable under a narrower set of possibilities. For the same example case, it only takes 107 lt/min of fresh air to disrupt the results of the O_2 sensor and prevent detection of human adult presence, whereas it takes approximately 5 times more fresh air to disrupt the detection capability of the CO_2 sensor.
Additionally, the time it takes for the O_2 concentration to surpass the securely detectable thresholds is multiple times as long as that of the CO_2 concentration. Even though time between a catastrophe and robotic platform’s deployment will normally exceed a few hours, there will always be a comparative advantage for the CO_2 sensor.
On the other hand, the higher noise sensitivity of the CO_2 sensor can render its result less trustworthy, in which case the O_2 sensor will be a valuable addition to be sure of the readings. One possible way to improve on the CO_2 readings is to apply a filter to suppress parts of the noise.
Regardless of the specific details of the sensor, application of the model has led to two important conclusions. The size of the room does not play a role in the equilibrium concentration of either CO_2 or O_2 and consequently in the detectability of human presence. Instead room (or cavity) size determines how quickly the gas

concentration will be changed. In contrast, the amounts of exhaled and fresh air flow rates both contribute to the level of gas concentration and the detectability of human presence.

For a typical cavity of size $5m^3$, an adult female, and detection thresholds for CO_2 and O_2 at 820ppm and 20.73% respectively, it is calculated that it will take 33 minutes after entrapment for CO_2 detection to be possible and 134 minutes for O_2 detection. Naturally, larger room sizes will require more time for detection to be possible as can be seen in Table 20 and Table 21.

An important matter that needs to be raised is the inevitable variation of fresh air flow rate that can weaken or even completely prevent human presence detection – at least by the e-nose sensor. It is clear from the results that the sensor readings can vary by a large factor the smaller the human footprint is and the larger the room (cavity) size is.

To increase the "hits" (true positive results) rate of the e-nose it is advised that readings should always be performed at the small cross section entrances and exits that the robotic snake goes through. The reason is because the air sinks (small openings where cavity air flows out of the cavity) of each cavity should be checked for changes in gas concentrations. It would also help if the robotic platform scans every large surface area from side to side and along the perimeter as that would help reduce significantly any chances of failing to detect human presence.

What is more, scanning air concentration at higher ground – if the conditions allow the snake to climb to a high point in the cavity - would help eliminate chances of missing detection. This is due to the fact that exhaled air is usually warmer than surrounding air and will tend to collect at the ceiling of a cavity rather than at the bottom.

Additionally, it is expected that approaching a human-occupied cavity, will register as a gradual change in the read concentrations as less fresh and exhaled air have enough time to mix. Of course, this will be the case provided that the fresh air circulation is not above the set limits.

However, as a general rule and due to lack of adequate data for each and every potential confined space that the robotic platform will go through in search and rescue operations around the globe, it is best if exact conditions are not programmed in the electronic nose data processing and decision unit. Instead, other features such as trends identified by the experiments carried out or interpolation of the analyzed results with a large variable factor will be used to help detect human presence. For example, sudden changes in concentration as opposed to steadily change over the course of time. Additionally, coordinated sensory input from other sensors which are more tuned to human physiology (such as NH_3 sensors) may also prove to be able to secure even further positive and correct detections by the electronic nose.

In this part of the analysis, the concentrations of CO_2 and O_2 of a confined space are calculated given the air refreshment rate without examining the conditions required to cause this air exchange. In [19] a model is proposed which can provide information about the air exchange given the geometry and weather conditions for a much broader range of cases compared to the model used in the proof of concept section of this work. The 2nd e-nose prototype of this work was used to validate the applicability of this model by examining some typical cases which are, among others, presented in the following chapter.

6.8. EXPECTED E-NOSE PERFORMANCE DEPENDING ON DETECTION PARAMETERS

Overview

In the previous section, the analysis determined the atmospheric air flow rate at which the e-nose can detect victims without examining the cause and conditions that create the air flow. This section briefly lists the mechanisms responsible for air flow in the anticipated USaR environments, the available formulas for quantifying their effect and some specific calculations illustrating the anticipated performance limits of this specific e-nose.

Cause of air flow

Air flow in rubble voids is caused by two mechanisms. The first, more obvious mechanism, is wind and the associated pressure differences that cause air flow inside the rubble. The second mechanism is the temperature difference (stack effect) between the fresh air outside the cavity and the air inside the cavity. Air at different temperatures has different densities. The presence of gravity allows for the existence of buoyancy effects, pressure differential and air flow.

The following equation, (eq 18) of [19] calculates the pressure differential caused by wind between entrance opening ‘i’ and exit opening ‘j’ of a rubble pile in an urban/suburban environment.

$$\Delta p_{W_{f}{}_{\text{”}\ i-j\text{”}}} = 0.5\rho_f \left(C_{p_i} - C_{p_j}\right)\left(C_R v_{ref}\right)^2 \tag{20}$$

Where C_R is the roughness coefficient for the examined area, v_{ref} is the reference regional wind speed, ρ_f is the density of fresh air, C_{p_i} is the wind pressure coefficient for the surface of opening ‘i’, and $C_{p_j}$is the wind pressure coefficient for the surface of opening ‘j’.

The following equation, (eq 19) of [19] calculates the, wind generated, volumetric flow rate between entrance opening ‘i’ and exit opening ‘j’ of a rubble pile caused by the pressure deferential between those two openings

$$F_{W_{f}{}_{\text{”}\ i-j\text{”}}} = C_{d_i} A_i \sqrt{\frac{2\Delta p_{W_{f}{}_{\text{”}\ i-j\text{”}}}}{\rho_f}} \tag{21}$$

Where C_{d_i} is the discharge coefficient ≈ 0.61, A_i is the area of the opening ‘I’ on the surface of the void that “directly” faces the wind, and ρ_f is the density of air.

The following table (Table 6) from [19] lists the maximum opening area for which the e-nose can detect a person when air flow is caused only by the indexed wind speeds. The calculations do include a number of assumptions but provide indicative figures for the anticipated performance of the system when attempting to detect victims using the CO_2 sensor by itself or when using both O_2 and CO_2 sensors.

Table 26. Estimation of maximum total possible area of large openings in voids (Urban/Suburban).

Wind Speed m/s	Description of Entrapped Human	A_i (m^2) for Max. $\Delta p_{W_{f}{}_{\text{”}\ i-j\text{”}}}$ CO_2 Sensor	A_i (m^2) for Min. $\Delta p_{W_{f}{}_{\text{”}\ i-j\text{”}}}$ CO_2 Sensor	A_i (m^2) for Max. $\Delta p_{W_{f}{}_{\text{”}\ i-j\text{”}}}$ CO_2 & O_2 Sensors	A_i (m^2) for Min. $\Delta p_{W_{f}{}_{\text{”}\ i-j\text{”}}}$ CO_2 & O_2 Sensors
0.25	child 3 y	0.2199	0.9653	0.1248	0.5480
	adult male	0.7476	3.2820	0.4244	1.8634
3	child 3 y	0.0183	0.0814	0.0104	0.0462
	adult male	0.0623	0.2768	0.0353	0.1571
5	child 3 y	0.0110	0.0488	0.0062	0.0277
	adult male	0.0374	0.1661	0.0212	0.0943
10	child 3 y	0.0055	0.0244	0.0031	0.0139
	adult male	0.0187	0.0830	0.0106	0.0471

The following equation (eq 20) of [19] calculates the pressure deferential between entrance opening ‘i’ and exit opening ‘j’ of a rubble pile caused by temperature difference between the two openings

$$\Delta p_{S_{fc"}\ _{i-j"}} = \left(\rho_f - \rho_C\right) g z_{"\ i-j"} \tag{22}$$

Where $z_{"i-j"}$ is the vertical distance between openings ‘i’ and ‘j’, ρ_f is the air density outside the cavity, ρ_C is the air density inside the cavity, and g is the gravitational acceleration.

The following equation (eq 21) of [19] calculates the, temperature-caused, volumetric flow rate between entrance opening ‘i’ and exit opening ‘j’ of a rubble pile caused by the pressure deferential between those two openings

$$F_{fc_{S"\ i-j"}} = C_{d"\ i-j"} A_i \sqrt{\frac{2\left|\Delta p_{S_{fc"}\ _{i-j"}}\right|}{\rho}} \tag{23}$$

Where $C_{d_{"i-j"}}$ is the discharge coefficient for the airflow, A_i is the area of the opening ‘I’ and ρ is the air density.

The following equation (eq 24) of [19] calculates the total incoming air flow rate from all openings when $T_f < T_c$.

$$F_{fc_{S_{sum}}} \approx 0.61 A_{sum} \sqrt{\frac{2\left|\left(T_C - T_f\right) g z\right|}{T_f + 273}} \tag{24}$$

and following equation (25) of [19] calculates the total outgoing air flow rate from all openings when Tf>Tc

$$F_{fc_{S_{sum}}} \approx 0.61 A_{sum} \sqrt{\frac{2\left|\left(T_f - T_c\right) g z\right|}{T_c + 273}} \tag{25}$$

Where A_{sum} is the total area of all openings, T_f is the temperature in Celsius degrees of the air outside the cavity, T_c is the temperature in Celsius degrees of the air inside the cavity, g is the gravitational acceleration, and z is the assumed vertical distance between input and output openings.
The following table (Table 7) from [19] lists the maximum opening area for which the e-nose can detect a person when air flow is caused only by the indexed temperature difference. The calculations do include a number of assumptions but provide indicative figures for the anticipated performance of the system when attempting to detect victims using the CO_2 sensor by itself or when using both O_2 and CO_2 sensors.

Table 27. Estimation of maximum total possible area of openings in voids (Stack effect).

$T_C - T_f$°C	Description of Entrapped Human	A_{sum} (m^2) CO_2 & O_2 Sensors z = 1 m	A_{sum} (m^2) CO_2 & O_2 Sensors z = 2 m	A_{sum} (m^2) CO_2 & O_2 Sensors z = 3 m
3	child 3 y	1.1664	0.8248	0.6734
	adult male	3.9658	2.8043	2.2897
5	child 3 y	0.9035	0.6389	0.5216
	adult male	3.0719	2.1722	1.7736
10	child 3 y	0.6389	0.4518	0.3689
	adult male	2.1722	1.5360	1.2541
15	child 3 y	0.5216	0.3689	0.3012
	adult male	1.7736	1.2541	1.0240

It is shown that under the conditions that exist at rubble piles, with both wind and temperature conditions acting concurrently, the total incoming air flow rate can be approximated with the following equation (eq 36) of [19]

$$F_{(W+S)_{sum}} \approx 0.61 A_{sum} \sqrt{\Delta C_p \left(C_R v_{ref}\right)^2 + 2\frac{\left(T_c - T_f\right) g z}{T_f + 273}} \tag{26}$$

Where 0.61 is the assumed discharge coefficient of all openings, A_{sum} is the total area of all openings, $\Delta C_p = C_{p_i} - C_{p_j}$, C_{p_i} is the assumed wind pressure coefficient of the incoming air openings , C_{p_j} is the assumed wind pressure coefficient of the outgoing air openings, T_f is the temperature in Celsius degrees of the air outside the cavity, T_c is the temperature in Celsius degrees of the air inside the cavity, g is the gravitational acceleration, and z is the assumed vertical distance between input and output openings.

By requiring a $2\underline{\sigma}$ decision threshold value above the fresh air's concentration for a particular gas, and utilizing the formula for calculating the equilibrium concentration, it is shown in [19] (eq 38 and eq 39) that for detecting a person the following must be true:

$$\frac{F_{(W+S)_{sum}} C_{(CO_2)f} + F_e C_{(CO_2)e}}{F_{(W+S)_{sum}} + F_e} \geq \left(\overline{C_{(CO_2)f}} + 2stdev_{\overline{C_{(CO_2)f}}}\right) \tag{27}$$

$$\frac{F_{(W+S)_{sum}} C_{(O_2)f} + F_e C_{(O_2)e}}{F_{(W+S)_{sum}} + F_e} \leq \left(\overline{C_{(O_2)f}} - 2stdev_{\overline{C_{(O_2)f}}}\right) \tag{28}$$

The following table (Table 8) from [19] lists the maximum opening area for which the e-nose can detect a person when air flow is caused by the indexed wind speed and the concurrent action of a 5°C temperature difference and a 2m height difference between input/output openings. The calculations do include a number of assumptions but provide indicative figures for the anticipated performance of the system when attempting to detect victims using the CO_2 sensor by itself or when using the O_2 sensor.

Table 28. Estimation of maximum total possible area of openings in voids (Wind and Stack effect, z=2m, T_f-T_C=5°).

Wind Speed v_{ref} (m/s)	**Description of Entrapped Human**	**$\Delta C_{p_{max}} = 1.51$ CO_2 Sensor Max. A_i (m^2)**	**$\Delta C_{p_{min}} = 0.44$ CO_2 Sensor Max. A_i (m^2)**	**$\Delta C_{p_{max}} = 1.51$ O_2 Sensor Max. A_i (m^2)**	**$\Delta C_{p_{min}} = 0.44$ O_2 Sensor Max. A_i (m^2)**
0.25	child 3 y	0.0645	0.0673	0.0366	0.0382
	adult male	0.2194	0.2289	0.1245	0.1300
3	child 3 y	0.0177	0.0520	0.0100	0.0295
	adult male	0.0601	0.1766	0.0341	0.1003
5	child 3 y	0.0108	0.0396	0.0062	0.0225
	adult male	0.0369	0.1345	0.0209	0.0764
10	child 3 y	0.0055	0.0230	0.0031	0.0130
	adult male	0.0186	0.0781	0.0106	0.0443

The above tables provide promising indications regarding the detection capabilities of the e-nose even in harsh weather. For the most difficult of the examined cases, the maximum equivalent square opening for detecting a single 3-year-old child with the $C0_2$ sensor is approximately 7x7cm (0.0055m^2 opening area). These estimations are produced after a number of assumptions and simplifications are applied which might have reduced the accuracy of the estimations compared to the actual conditions. This is not detrimental for the research as the estimations only serve as a quick and easy method to establish potential boundaries for following experiments and tests.

7. SECOND PROTOTYPE, VERIFICATION and VALIDATION TESTS

7.1. Overview

The purpose of building the second prototype was to have a system with the complete victim localization functionality (three gas sensors) of the electronic nose in order to carry out tests with a mobile platform. The time for implementing this prototype was minimized by using off-the-shelf components and limiting custom-made hardware to a minimum. Also, the design of the final setup was assisted by selecting components that would/could later be integrated in the custom PCB and by designing the setup so that the software and firmware could be reused with little or no modification. This approach was also followed to reduce risks involved with a one-off final design. The downside of this approach is that the size of the second prototype does not allow for it to fit on the robotic platform. Additionally, functionality regarding the detection of flammable/combustible gases (LPG and LNG) and toxic gases (CO and H_2S) is not implemented in this prototype as it does not participate in the actual localization of victims but rather in the detection of hazardous environments.

The following picture illustrates the updated high level block diagram. Minor changes were made in the original conception including the placement of the air pump after the sensor cluster so that the barometric pressure sensor of the O_2 sensor can also be utilized as a blockage detection mechanism. Also, a different ammonia sensor was selected that is smaller and has better characteristics (optimized for a more steady zero level output current). The external dimensions required for the components selected for the localization solution were initially 10x10x10cm. This size specification reflects the achievable size target for the final design when only three gas sensors are utilized, not the size of the 2nd prototype. New developments (after hardware of 2nd prototype was designed) originating from the robotic platform's design mandated a different e-nose compartment: The volume for the e-nose was increased by widening the design to 130x170mm, but at the same time the height was reduced from 10cm to 7cm (not all the volume can be utilized). A floor plan of the system indicated that the additional sensors for safety could also fit in the e-nose compartment. It was decided that the sensors concerned with safety be implemented directly in a 3rd/final prototype so that development and testing of the second prototype was not delayed.

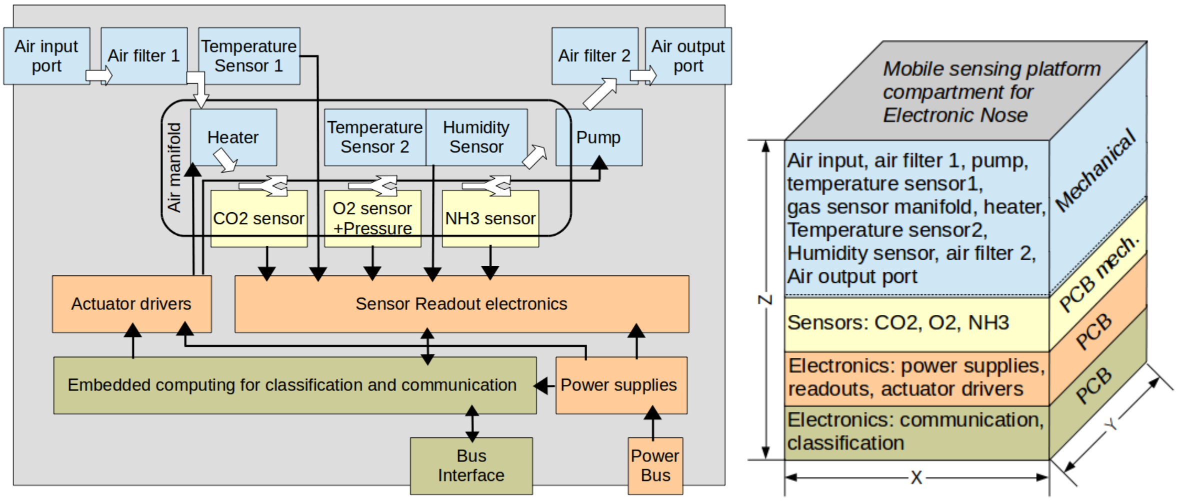
Air input port
Air filter 1
Temperature Sensor 1
Air filter 2
Air output port
Air manifold
Heater
Temperature Sensor 2
Humidity Sensor
Pump
CO2 sensor
O2 sensor +Pressure
NH3 sensor
Actuator drivers
Sensor Readout electronics
Embedded computing for classification and communication
Power supplies
Bus Interface
Power Bus
Mobile sensing platform compartment for Electronic Nose
Air input, air filter 1, pump, temperature sensor1, gas sensor manifold, heater, Temperature sensor2, Humidity sensor, air filter 2, Air output port
Sensors: CO2, O2, NH3
Electronics: power supplies, readouts, actuator drivers
Electronics: communication, classification
Mechanical
PCB mech.
PCB
PCB
Z
X
Y

Figure 33. The core system implementing the bare minimum mandatory requirements.

The e-nose can be controlled via terminal (since the commands are single characters and the measurements are in a readable format) and the measurements can be read directly from the terminal or be plotted in real-time with the program KST plot.

Selected sensors

The selected CO_2 sensor is based on NDIR technology because of the aforementioned competitive advantages of these sensors, taking also into account the low sensitivity required. The CO2F-W from SST Sensing Ltd, is a compact and high speed (20 Hz) CO_2 sensor, ideally suited for applications which require the capture of rapidly changing CO_2. This CO_2 sensor is the fastest NDIR CO_2 sensor available in the world, requiring on average less than 15mA current at 3.3 V, provides digital TTL output and detects CO_2 levels in the range 0–200,000 ppm (0-20%), with an accuracy of ±50ppm. The O_2 sensor LuminOx (LOX-02) that was chosen is a compact Fluorescence-based Optical Oxygen Sensor. It requires less than 7.5mA current at 3.3V, provides digital TTL output and detects O_2 levels in the range 0-25%, with a resolution of 0.01%. The Ammonia NH3-3E-100-SE of City Technology, is an Amperometric electrochemical 3 electrode sensor cell, designed for NH3 detection. It shows a sensitivity of 100-160 na/ppm NH_3, at a bias voltage of 0 mV and with a resolution of less than 1 ppm (optimized for a steady zero level output current).

The selected gas sensors presented above need to function under certain conditions of humidity and temperature. Thus additionally, these 2 parameters of the sampled air will be monitored with separate sensors to verify the reliability of the gas measurements. Humidity and temperature have to be measured for air inside the e-nose system and outside as it is explained in a next section. For inside and outside humidity, the selected sensor is the Honeywell HumidIcon HIH8120-021, 10-90 range, accuracy ±2%, 14 bits resolution I2C digital output, consuming 1 mA at 3.3 V. For inside temperature measurements the PCT2075 NXP's sensor was chosen. It is a temperature sensor with range -25 ^{o}C -+100 ^{o}C, accuracy ±1^{o}C, 11 bits digital output through I2C interface, consuming 70 μA at 5 V when sampling and 1μA when not. A sampling period may range from 100 milliseconds to 3.1 seconds. For external temperature TI's TMP112A temperature sensor was selected, featuring accuracy ±1^{o}C at a range -40 ^{o}C -+125 ^{o}C, 12 bits digital output through I2C interface, consuming 10 μA at 3.6 V when sampling and 1μA when not. A sampling period can range from 125 milliseconds to 4 seconds.

7.2. Electronics of the 2nd prototype

The hardware architecture of the proposed e-nose system consists, as shown in Figure 34, of four evaluation boards and six designed custom-made prototype interconnection printed circuit boards, connected to the sensors and to the pump and heater. The air pump is a Parker's T2-03 micro diaphragm pump, with flow up to 2.5 lpm, operating at 0-8.4 V with a current 25-390 mA, and the heating resistor a 25 Watts 18 Ohm operated at 0-5V and up to 278mA, capable of increasing the temperature of the sensors' enclosure at a speed of 10^{o}C/min, up to 40 degrees, ensuring RH humidity is less than 100% in this temperature range. As a side effect, a better NH_3 sensor sensitivity is achieved. Evaluation Boards 3 and 4 are for providing controllable DC voltage, up to a 2A output from an input voltage source of 3.5-28 V, to the air pump and heating resistor of the e-nose system. Evaluation Board 1 is the ATMEL's (Microchip) ATEVK1101, it includes its AT32UC3B0256 32-bit AVR RISC-based microcontroller, that is a complete System-On-Chip microcontroller, based on the 32 bit AVR32 UC RISC micprocessor core running at the frequency of 60 MHz, with on-chip, 128KB flash memory, 32KB SRAM, 3 USART ports, ADC, PWM controller and a Master/Slave Two-Wire Interface (TWI), 400kbit/s (I2C-compatible). Evaluation board 2 is made by TI (LMP91000EVM/NOPB), and it incorporates the programmable LMP91000 Sensor Analog Front End potentiostat chip. It functions as the readout for the selected NH_3 Electrochemical sensor. It provides an output voltage proportional to the current required to maintain the configured cell bias voltage of the NH_3 sensor. The LMP91000 supports Programmable Cell Bias Voltages and gas sensitivities over a range of 0.5 nA/ppm to 9500 nA/ppm and it also allows for a conversion of current ranges from 5 μA to 750 μA full scale. It operates over a voltage range of 2.7 to 5.25 V and has a total current consumption less than 10 μA. Adjustable cell bias and transimpedance amplifier (TIA) gain are programmable through the I2C interface. The readout output voltage from the NH_3 potentiostat is sampled by an ADC that is connected to the SPI bus. Evaluation boards 3 and 4 are both the TPS54231 device of TI incorporating a low RDS (on) high-side MOSFET for implementing a nonsynchronous (diode) DC-DC buck converter with 570-kHz Switching Frequency. They both accept 3.5- to 28 V Input Voltage Range and they provide an output for the pump 0.8-8.4 V and for the heater 0.8-5 V respectively, both up to 2 A continuous current.

The implementation of the system is achieved mainly with off-the-shelf components. The following picture depicts the portions of the system that can be built with evaluation boards, namely for the microcontroller, the ammonia sensor analog front end and the power drivers for the actuators.

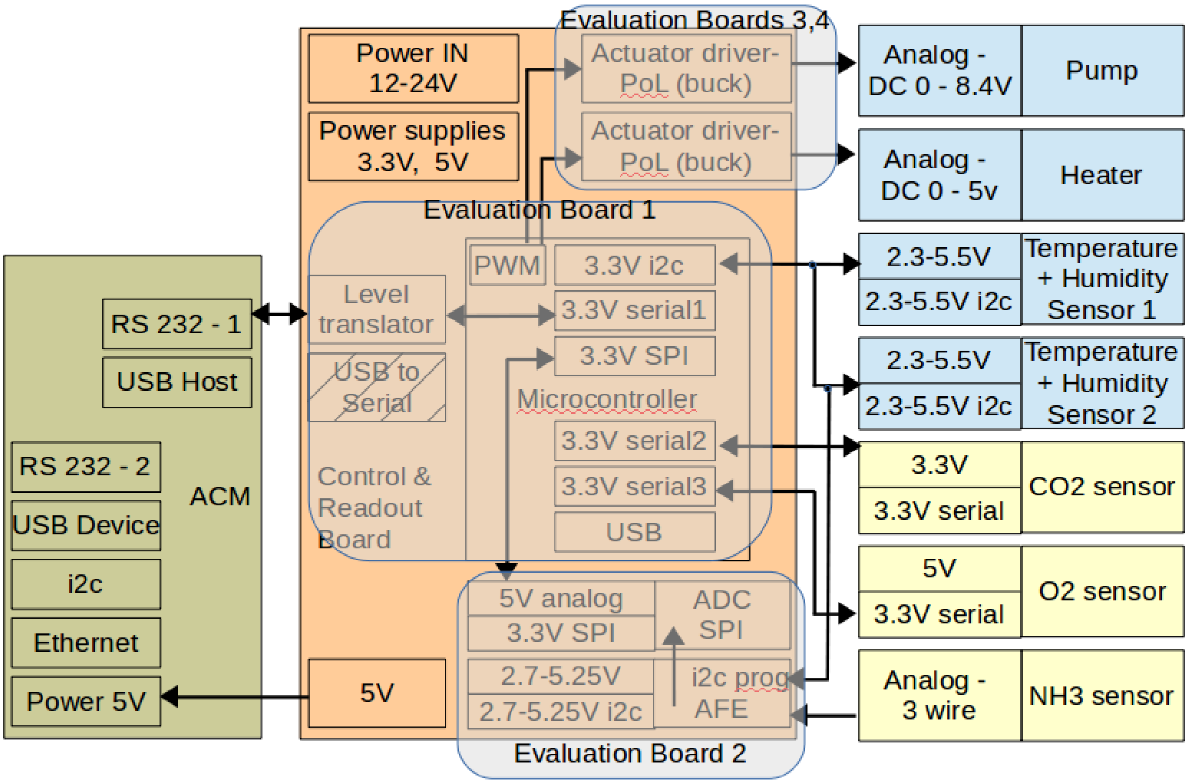
Evaluation Boards 3,4
Power IN 12-24V
Power supplies 3.3V, 5V
Actuator driver-PoL (buck)
Actuator driver-PoL (buck)
Analog - DC 0 - 8.4V
Pump
Analog - DC 0 - 5v
Heater
Evaluation Board 1
PWM
3.3V i2c
3.3V serial1
3.3V SPI
Microcontroller
3.3V serial2
3.3V serial3
USB
Level translator
USB to Serial
Control & Readout Board
2.3-5.5V
2.3-5.5V i2c
Temperature + Humidity Sensor 1
2.3-5.5V
2.3-5.5V i2c
Temperature + Humidity Sensor 2
3.3V
3.3V serial
CO2 sensor
5V
3.3V serial
O2 sensor
Analog - 3 wire
NH3 sensor
RS 232 - 1
USB Host
RS 232 - 2
USB Device
i2c
Ethernet
Power 5V
ACM
5V
5V analog
3.3V SPI
ADC SPI
2.7-5.25V
2.7-5.25V i2c
i2c prog AFE
Evaluation Board 2

Figure 34. The system is implemented with off-the-shelf components and evaluation boards.

In Figure 34 the block diagram of the electronics of the system is illustrated. The functionality that is included in evaluation boards is marked with the transparent "bubbles". Black arrows indicate the direction of data or current flow. The color coding of the modules indicates their position and role in the e-nose as described in the block diagram of the system as illustrated in Figure 33. The green block which corresponds to the ACM module is not mandatory and was not used in the assembled system tested during the field tests. Its functionality was supplemented with a standard laptop computer. All the sensors are connected through breakout boards to the main interconnection board named control and readout board or directly to readout board (NH_3 sensor). The CO_2, O_2 sensors are connected to the microcontroller with dedicated serial buses. The temperature and humidity sensors are connected to the microcontroller via the shared i2c bus. The biasing of the NH_3 sensor is performed with an AFE IC which is configured via the i2c bus. The readout voltage is sampled with an ADC which has an SPI bus interface. The control and readout board also includes power supplies that convert the 12-24V input to the required 5V and 3.3V voltage rails. The 12-24V input is also fed into the buck converters that drive the heater element and the pump. Initially these power supplies were controlled as configurable power supplies (POL). It was found that configurable and accurate output was not required from these actuators so they were configured to operate in ON/OFF mode before being replaced by simple power MOS transistors. The heating resistor is powered by the 12-24 power input while the pump is powered by the 5V net. This design choice has minor implications in the time required for the system to reach operational temperature when a low input voltage (12V) is supplied but is a convenient compromise for the flexibility of using various power supply options.

The following pictures illustrate the interconnection diagram of the 2ndprototype and the schematic diagram of the 2ndprototype custom PCBs:

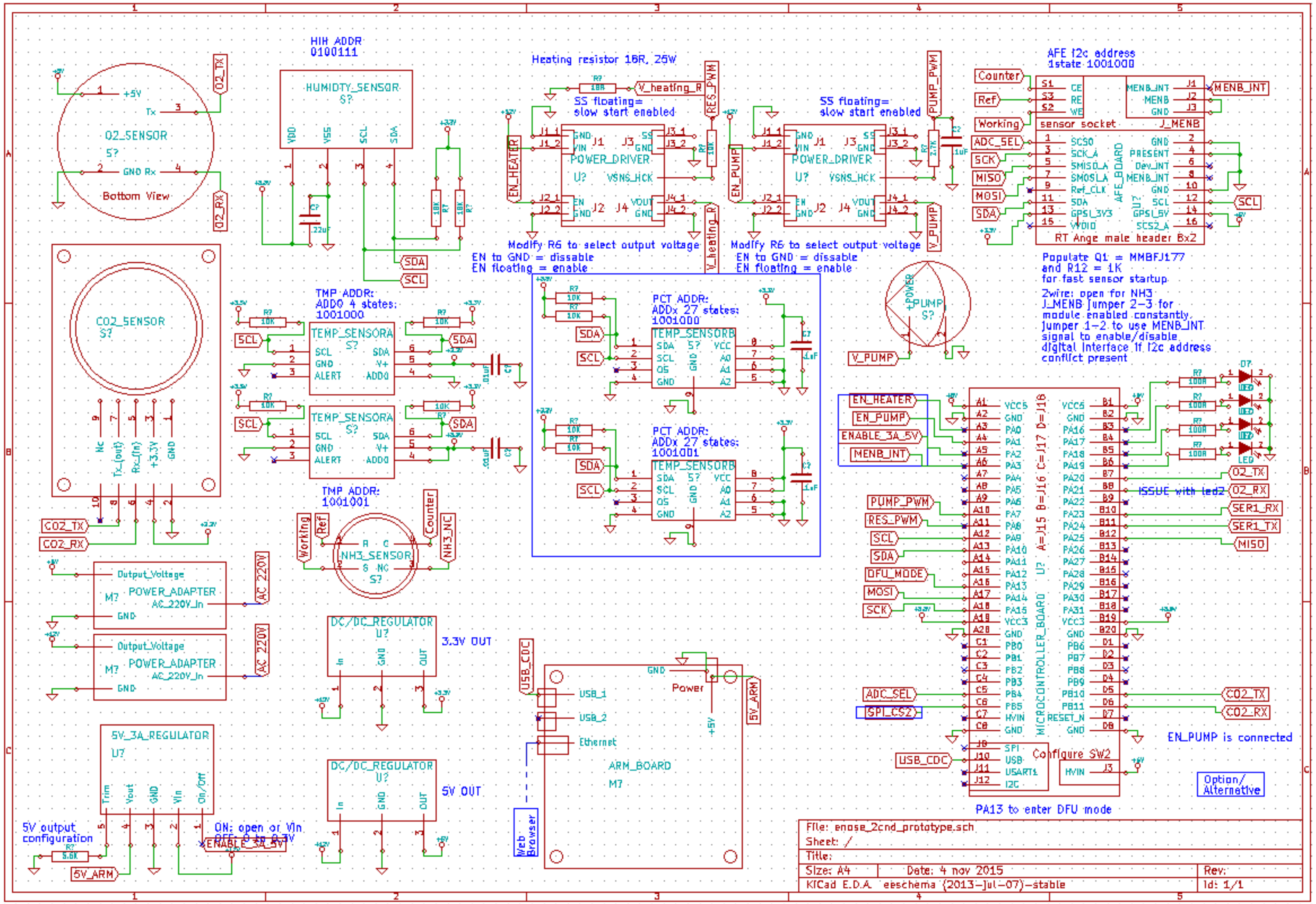
HIH ADDR 0100111
HUMIDTY_SENSOR S?
O2_SENSOR S?
Bottom View
O2_TX
O2_RX
CO2_SENSOR S?
CO2_TX
CO2_RX
Heating resistor 18R, 25W
V_heating_R
RES_PWM
PUMP_PWM
SS floating= slow start enabled
POWER_DRIVER U?
EN_HEATER
EN_PUMP
V_heating_R
V_PUMP
Modify R6 to select output voltage
EN to GND = dissable
EN floating = enable
TMP ADDR: ADD0 4 states: 1001000
TEMP_SENSORA S?
TMP ADDR: 1001001
PCT ADDR: ADDx 27 states: 1001000
PCT ADDR: ADDx 27 states: 1001001
TEMP_SENSORB S?
NH3_SENSOR S?
Working
Ref
Counter
NH3_NC
PUMP S?
AFE I2c address 1state 1001000
sensor socket
AFE_BOARD U?
J_MENB
RT Ange male header 8x2
MENB_INT
SCL
SDA
ADC_SEL
SCK
MISO
MOSI
Populate Q1 = MMBFJ177 and R12 = 1K for fast sensor startup
2wire: open for NH3 J_MENB jumper 2-3 for module enabled constantly. Jumper 1-2 to use MENB_INT signal to enable/disable digital interface if I2c address conflict present
EN_HEATER
EN_PUMP
ENABLE_3A_5V
MENB_INT
MICROCONTROLLER_BOARD U? A=J15 B=J16 C=J17 D=J18
ISSUE with led2
SER1_RX
SER1_TX
DFU_MODE
SPI_CS2
USB_CDC
Configure SW2
EN_PUMP is connected
PA13 to enter DFU mode
Option/ Alternative
Output_Voltage
POWER_ADAPTER M?
AC_220V_In
AC 220V
DC/DC_REGULATOR U?
3.3V OUT
5V OUT
5V_3A_REGULATOR U?
5V output configuration
ON: open or Vin OFF: 0 to 0.3V
ENABLE_3A_5V
5V_ARM
USB_1
USB_2
Ethernet
Power
ARM_BOARD M?
Web Browser
File: enose_2cnd_prototype.sch
Sheet: /
Title:
Size: A4
Date: 4 nov 2015
Rev:
KiCad E.D.A. eeschema (2013-jul-07)-stable
Id: 1/1

Figure 35. Schematic/Interconnection diagram the 2nd e-nose prototype

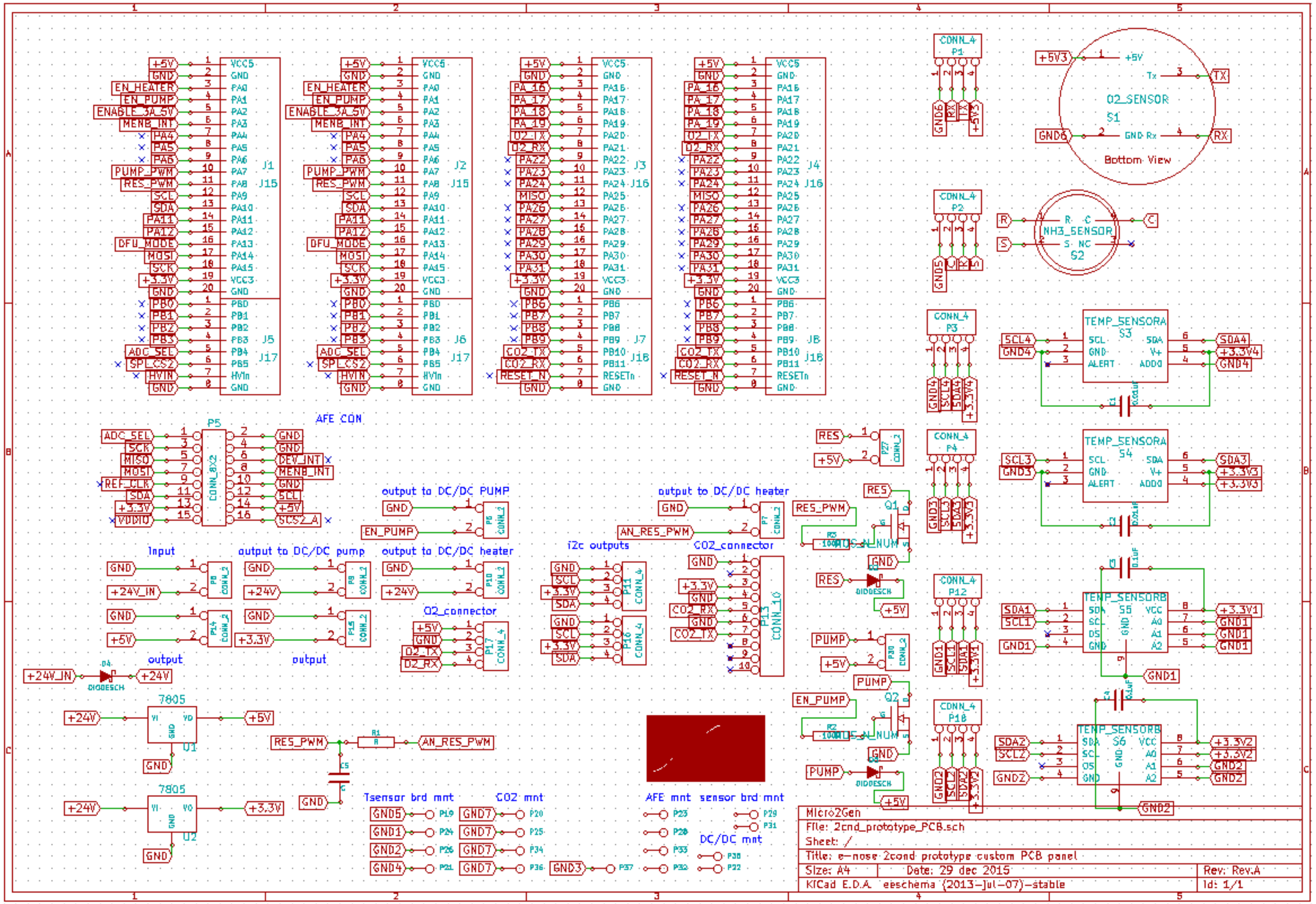
J1
J15
J2
J3
J16
J4
J5
J17
J6
J7
J18
J8
P5
AFE CON
CONN_8X2
output to DC/DC PUMP
output to DC/DC heater
Input
output to DC/DC pump
i2c outputs
CO2_connector
O2_connector
output
7805
U1
U2
R1
Tsensor brd mnt
CO2 mnt
AFE mnt
sensor brd mnt
DC/DC mnt
CONN_4
P1
P2
P3
P4
P12
P18
O2_SENSOR
S1
Bottom View
NH3_SENSOR
S2
TEMP_SENSORA
S3
S4
TEMP_SENSORB
S5
S6
Q1
Q2
DIODESCH
Micro2Gen
File: 2cnd_prototype_PCB.sch
Sheet: /
Title: e-nose 2cond prototype custom PCB panel
Size: A4
Date: 29 dec 2015
Rev: Rev.A
KiCad E.D.A. eeschema (2013-jul-07)-stable
Id: 1/1

Figure 36. Schematic diagram of the printed circuit boards for the 2nd prototype

The following picture illustrates the layout of the second prototype PCBs. The layout is a custom-made panel that includes six different PCBs: The four narrow boards on the left are temperature sensor boards. The board on the bottom hosts the gas sensors and the board on the top right provides mounting and interconnection interfaces, glue logic, power supplies, power electronics and distribution.

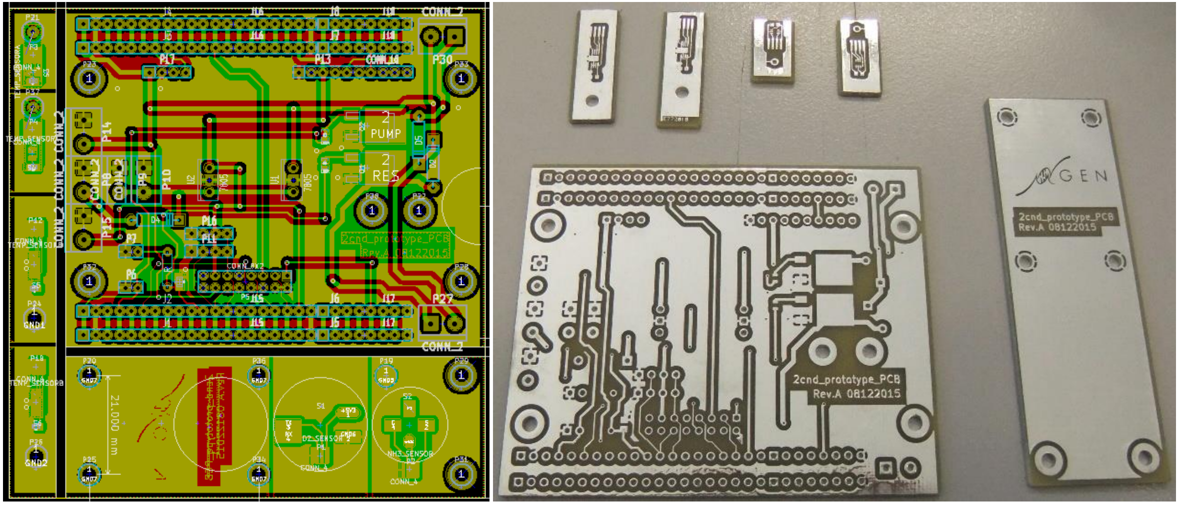
CONN_2
PUMP
RES
2cnd_prototype_PCB
Rev.A 08122015
GEN
2cnd_prototype_PCB
Rev.A 08122015
21.000 mm
O2_SENSOR
NH3_SENSOR
TEMP_SENSOR
GND1
GND2

Figure 37. The layout of the various PCBs for the 2^{nd} prototype

The following picture illustrates the assembled sensor PCB. On the left is the CO_2 sensor, in the centre is the O_2 sensor and on the right is the NH_3 sensor.

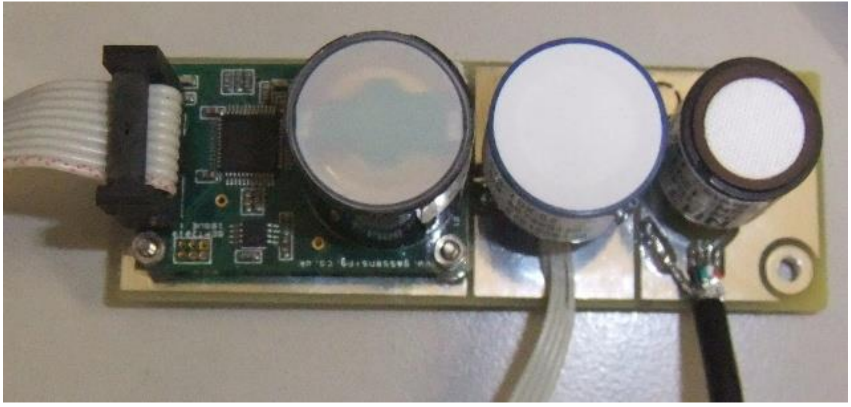

Figure 38. The assembled PCB that host the gas sensors

7.3. Mechanical aspects of the 2^{nd} prototype

Manifold

The following picture illustrates the custom gas manifold. From left to right the sensor interfaces are the air input tube adapter, humidity sensor socket, CO_2 sensor socket, O_2 sensor socket, NH_3 sensor socket and the output tube adapter.

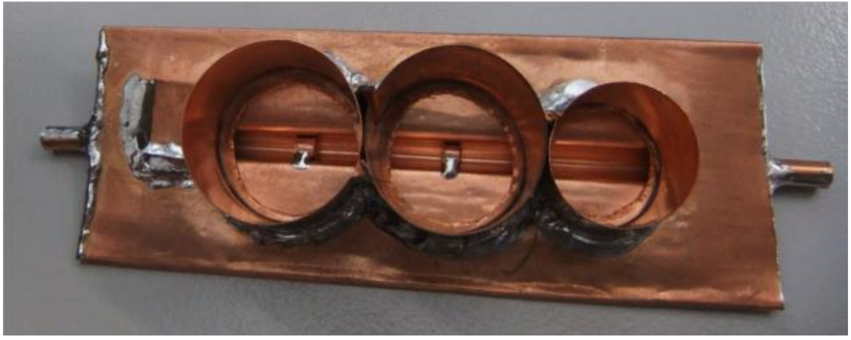

Figure 39. The lightweight and heat conductive custom manifold

The following picture illustrates the assembled sensor cluster. Notice the heating resistor and a temperature sensor PCB mounted on the top of the air manifold.

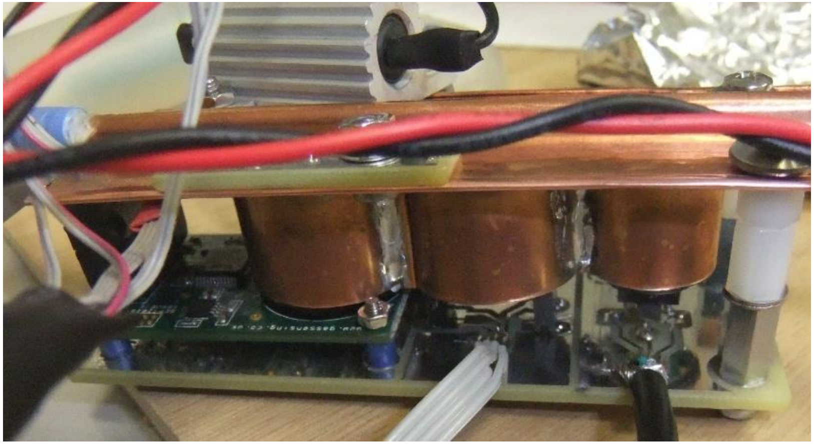

Figure 40. The assembled sensor cluster

The following picture illustrates the readout and control PCB stack. On the bottom is the microcontroller board, on the top is the analog front end for the NH_3 sensor and in between is the custom "glue" PCB.

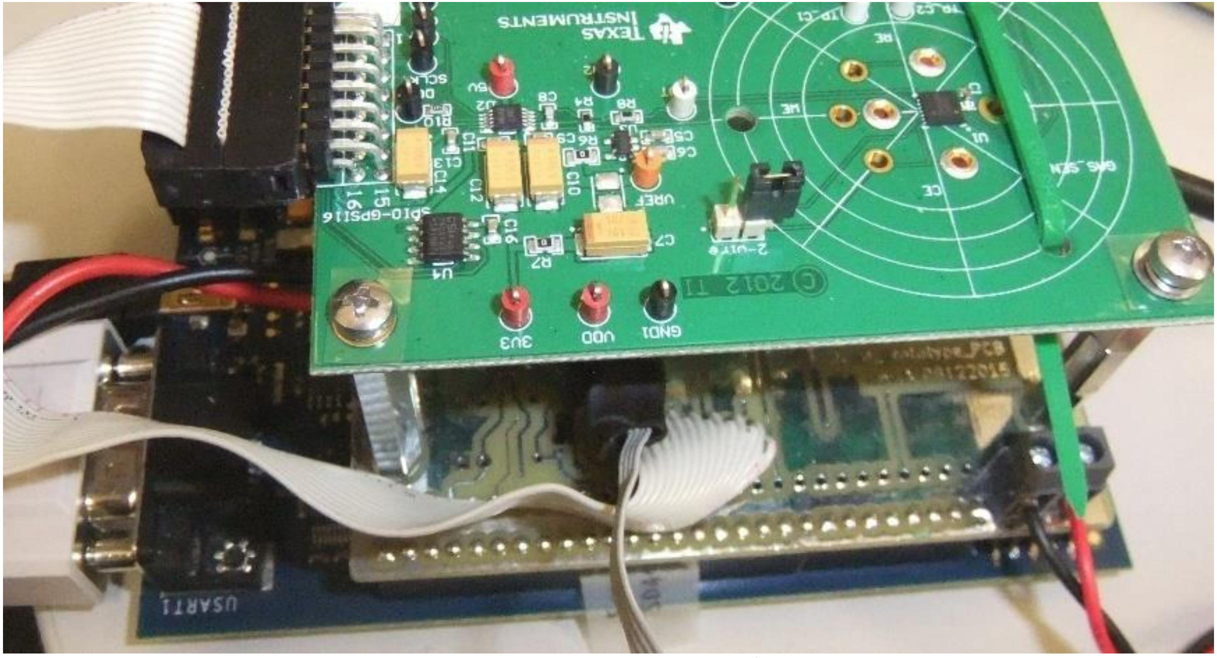

Figure 41. The assembled readout and control PCB stackup of the 2nd prototype

The following picture illustrates the second prototype of the e-nose. The sensor cluster (right) has been wrapped in thermal conductive material, wrapped with air sealing material. The sensor cluster is also wrapped in heat insulation material (not seen in this picture). The pump is located in the centre, the air filters (white disks) are connected to the pump and sensor cluster with the blue air tubing. The readout and control PCB stack is connected to a computer to display results and accept commands/configuration via connections on the bottom left.

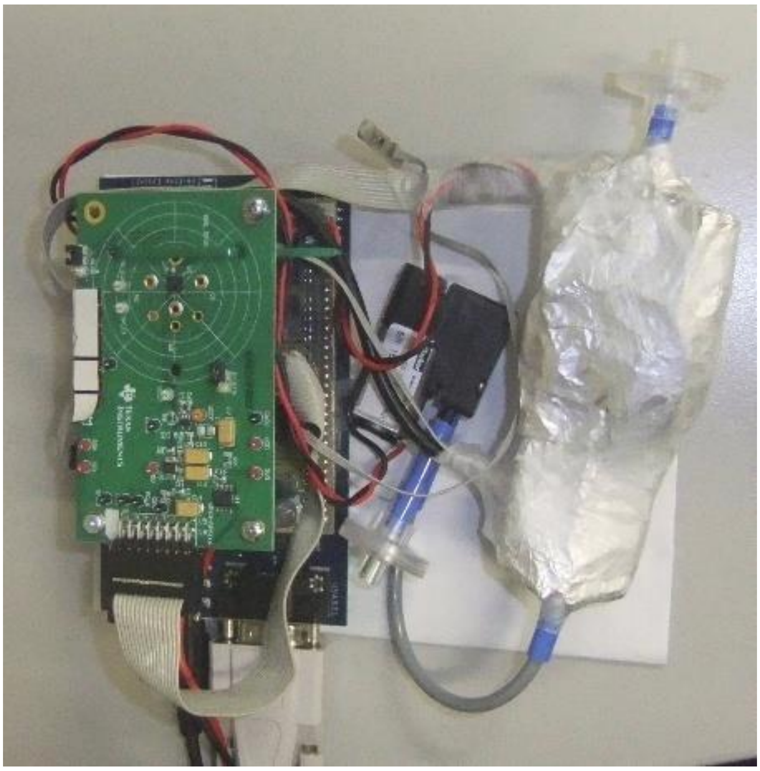

Figure 42. The 2nd prototype of the e-nose

Enclosure design

The primary concern in the second prototype instrument is to create a portable device; one that can be transported in the field (albeit in nondangerous for the e-nose locations) and simulate detection as if mounted on top of the snake robot. The aim is to obtain results from the outdoor operation and evaluate it.

To this extent, a durable, light-weight and protective enclosure needed to be created. Due to the portability requirements a low cost design was proposed. What is more, this design resembles the compartment of the robotic platform.

The connections to the outside world have been minimized to just two wires (power and data) and a pneumatic inlet and outlet connection which need to be included. The electronic boards are designed to support the primary functions of the e -nose that are CO_2, O_2 and NH_3 detection, as well as all the supporting sensors that monitor the condition of the e-nose during operation. Additionally, one air inlet and one air outlet are required. It is better if the air ports are located on opposite sides of the enclosure to avoid sampled air re-entering the system.

To accommodate these requirements a large opening was created on the side of the cover of the enclosure. Additionally, since it was not planned for the construction to be mounted in the snake robot in its current state, it was comprised only of a base where the electronics and sensor were mounted and a protective cover. The generated CAD design of the case is shown in the following picture:

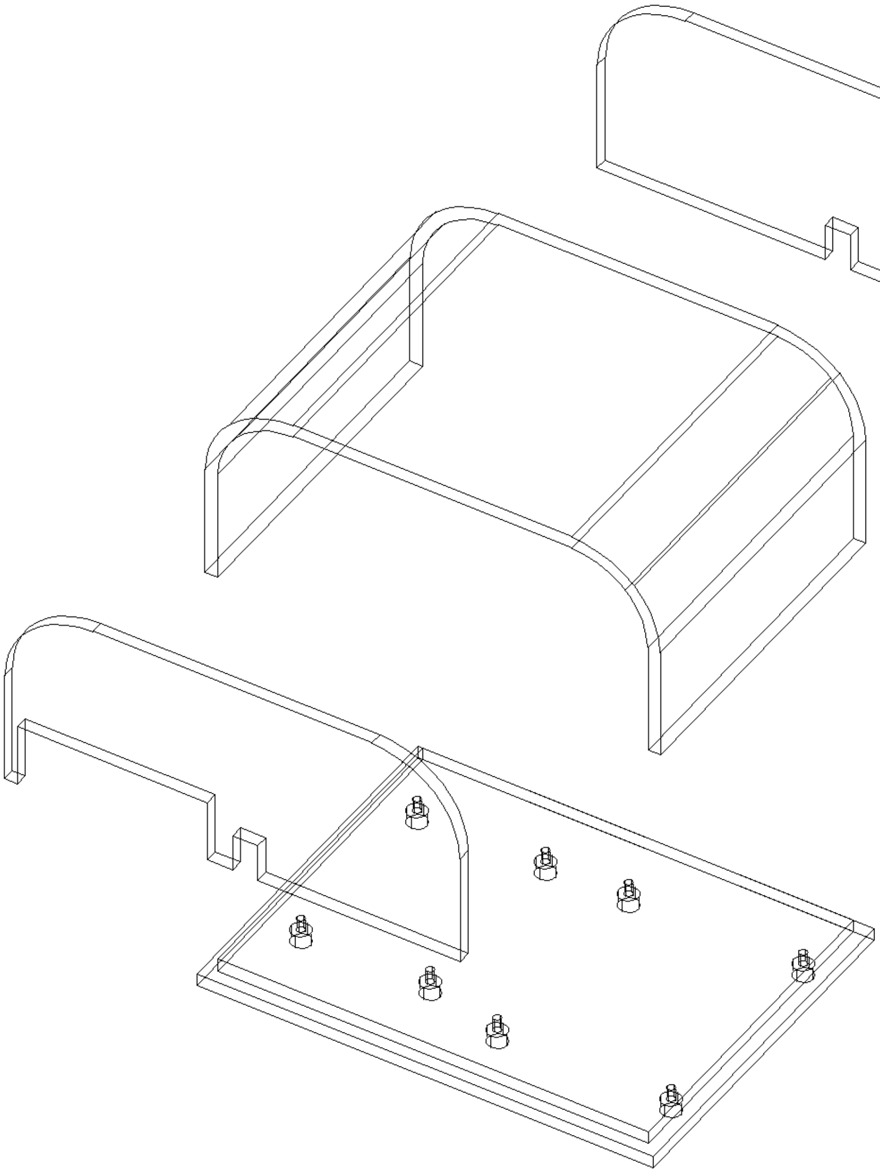

Figure 43: CAD of the Prototype 2 enclosure. The base, cover and two sides of the cover are shown

Note that a double base (two slabs) is used for two reasons. First, a “staircase” is created if the top base slab has a slightly smaller surface compared to the bottom base slab. This allows a secure fit of the cover so that is does not slide and fall off. Secondly, holes have been opened in both slabs. The holes in the top slab have a smaller diameter than those in the bottom slab. The reason is to place mounting screws firmly in order to hold the electronics in place. Finally, it is noted that the side walls are glued onto the main cover frame, thus minimizing the assembly to just two parts, base and cover. This simplifies opening and accessing the electronics for demonstration purposes.

The enclosure was manufactured with Plexiglas (PMMA) material which allows easy manipulation of material to create the bent corners of the cover’s main frame. This reduces construction time and costs for the amount of covers that needed to be created (exactly one). Moreover, it provides visibility to the internal components of the e-nose which render it ideal for demonstration purposes. The manufactured enclosure can be seen in the following picture:

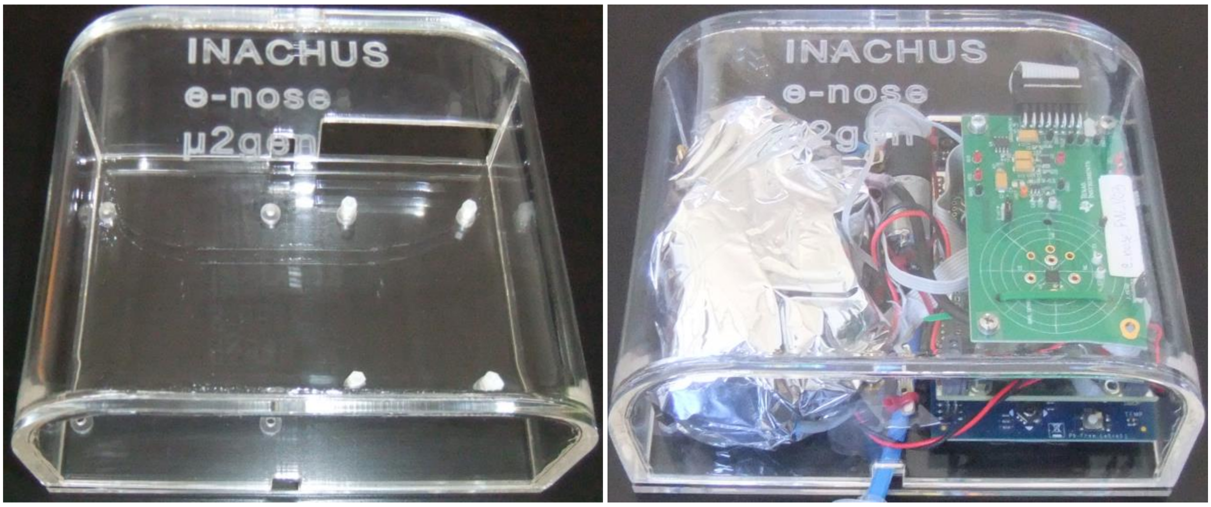

Figure 44. The Plexiglas enclosure (left) and the complete 2nd e-nose prototype.

7.4. Software of the 2nd prototype

The software of the 2nd prototype can be put in two categories: firmware running on the microcontroller of the e-nose and software running on the host computer (KST plots and advanced logic unit). For visualizing the measurements of the 2nd e-nose device prototype, KST plot was configured to perform this task. KST plot can plot the captured measurements "as is" or can apply various filters. Another option is to pre-process the captured measurements from the e-nose device on the host computer with a customized program and then feed the output to KST plot. This pre-processing is performed with the advanced logic unit software. The advanced logic unit software used in the 2nd e-nose device prototype was a transitional development in the sense that only small portions of the functionality implemented for the 3rd e-nose device prototype were available or even conceived. The 2nd prototype was used as an initial testing platform for some aspects of the final development (the individual indicators calculated for each sensor). Some of the outputs of the advanced logic unit, such as the Indicators, were placed in separate plots since there was no way to represent them in the same plot with the respective measurements. This made understanding their meaning difficult for people other than the developers of the system which lead to their use only for development purposes.

A high level block diagram of the firmware is illustrated in the following figure. The firmware is a stand-alone program (no OS) which performs the sensor sampling, handles communication and runs the control loop(s).

7.4.1. Firmware running on the Microcontroller

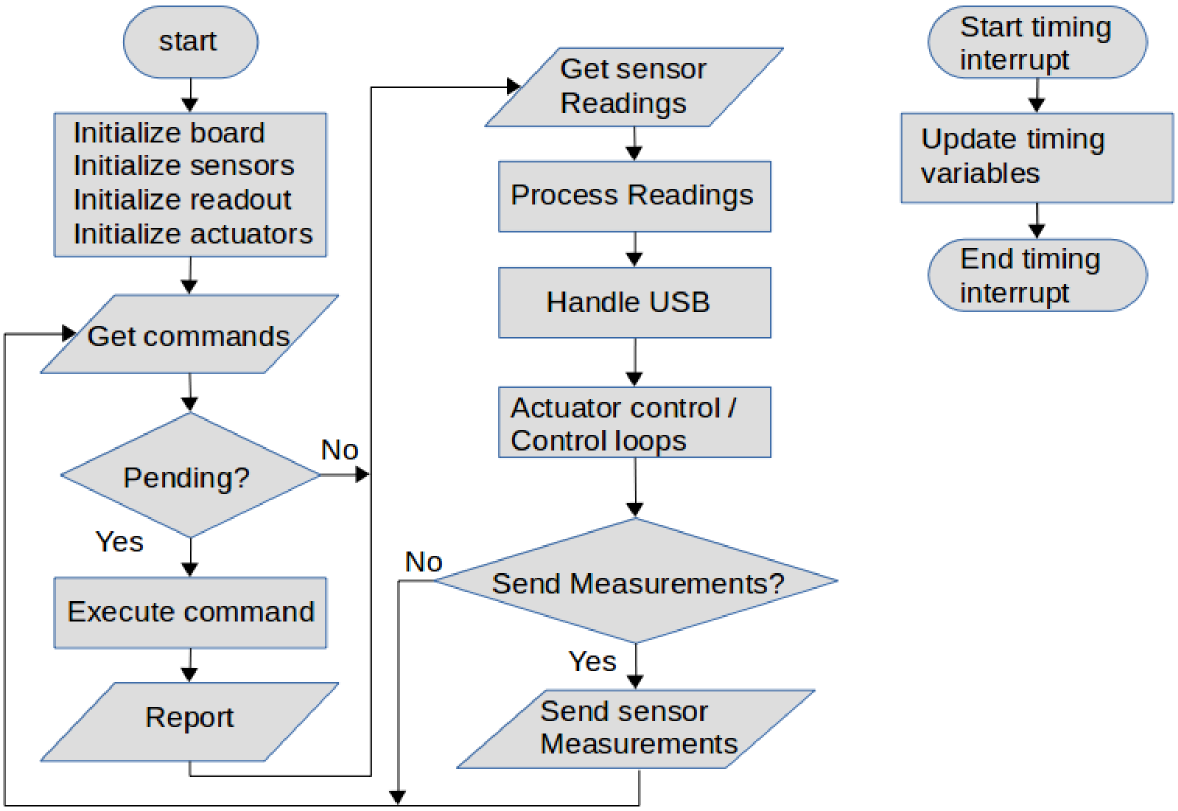
start
Initialize board
Initialize sensors
Initialize readout
Initialize actuators
Get commands
Pending?
No
Yes
Execute command
Report
Get sensor Readings
Process Readings
Handle USB
Actuator control / Control loops
Send Measurements?
No
Yes
Send sensor Measurements
Start timing interrupt
Update timing variables
End timing interrupt

Figure 45. Flow chart for the firmware of the 2nd prototype

The command interface, as well as the data interface of the e-nose, is implemented via the USB connection. The microcontroller implements the USB CDC device class and thus a virtual COM port is created when the e-nose is connected to a compatible computer. The COM port settings are the following:

Table 29. The e-nose connection parameters of the COM port

Parameter	Value
Baud Rate	57600
Parity	None
Data bits	8
Stop bits	1
Flow control	None

The commands supported by the firmware that are exposed to the user interface are listed in the following table:

Table 30. The e-nose command interface

Command name	Command sequence	Description
Start Pump	'P'	The command turns the pump ON, the command sequence is echoed back. The power up state of the e-nose has the pump at the OFF state
Stop Pump	'p'	The command turns the pump OFF, the command sequence is echoed back.

Perform CO_2 auto calibration	‘G’	The command sets the current reading of the sensor at 400ppm assuming that the sensor is exposed in clean fresh air. The command sequence is echoed back.
Start Heater	‘H’	The command turns the heater ON, the command sequence is echoed back. The power up state of the e-nose has the heater at the ON state. (NOT implemented yet)
Stop Heater	‘h’	The command turns the heater OFF, the command sequence is echoed back. (NOT implemented yet)
Start Reading	‘R’	The command enables the e-nose to send measurements, the command sequence is echoed back. The power up state of the e-nose has the e-nose streaming measurements. (NOT implemented yet)
Stop Reading	‘r’	The command stops the e-nose from streaming measurements, the command sequence is echoed back. (NOT implemented yet)

Every second, the measurements are sent in a burst.
The data format of the e-nose measurements is the following:
The character ‘r’ followed by a space ‘ ’ followed by the information regarding each sensor
The information regarding each sensor has the following format:
3character sensor identifier followed by a space character ‘ ‘ followed by a status character ‘0’ followed by a space character ‘ ’ followed by the 6character value. This sequence is identical and printed for all the sensors in a single line. An example of output is the following:

```
“r co2 0 001000 pO2 0 020.85 nh3 0 +000.4 H2O 0 025.03 iTe 0 +26.00
  eTe 0 +24.88 oO2 0 0206.6 tO2 0 +25.90 bO2 0 000991”
```

The following table lists the meaning of the identifiers.

Table 31. Description of the identifiers in the e-nose’s measurements stream

Identifier	Units	Description
co2	ppm	The CO_2 sensor result
pO2	%	The O_2 sensor result
nh3	ppm	The NH_3 sensor result
H2O	%	The humidity sensor result in relative humidity
iTe	°C	The internal temperature value
eTe	°C	The external temperature value
oO2	mbar	The O_2 sensor result in O_2 partial pressure
tO2	°C	The temperature of the O_2 sensor
bO2	mbar	the barometric pressure reading from the O_2 sensor

Note that the status character concerning each measurement has not been implemented yet.

7.4.2. Software running on the host computer - KST plot

The following example plot was acquired by exhaling directly in front of the air input sampling port. Note that the measurements are not thoroughly filtered and conditioned, though a clear indication is acquired just from the plot. This case can be characterized as ideal since the change in the concentrations is rapid and the base level of measurements and the acquired level of the measurement vary greatly (for the sensors that should). The index is in sample number. Since one sample per second is acquired in this case, the index is also in seconds.

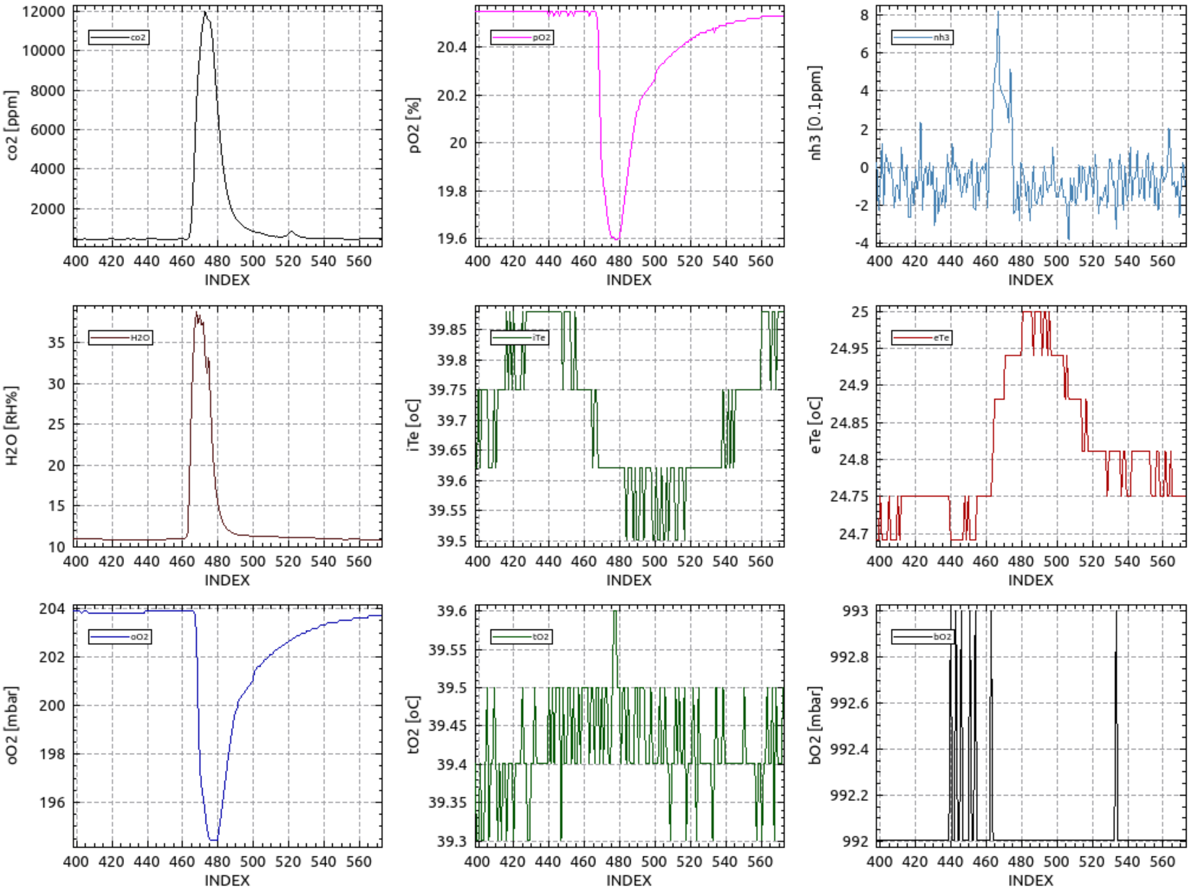

Figure 46. A caption of the e-nose measurements when exhaling directly in front the input port.

7.4.3. Software running on the host computer - Advanced logic unit Software

There are a large number of sensors incorporated in the second version of the prototype. This leads to a need to process the raw information arriving in the e-nose advanced logic unit in order to present it to the e-nose operator in a manner that can be easily followed during highly stressful search and rescue operations. Information extraction in the form of indicators is thus necessary from the raw data available. Indicators are explained in detail in the section of the third prototype. Indicators concept and implementation in the third prototype are significantly advanced compared to the second prototype.

Technology that was already used in the first prototype has been reused in this prototype. Data acquisition from the sensor readout board is implemented over a serial line as well, so it has been reused. Data presentation is also still carried out independently from the final GUI application. That is, the RRD database has been reused as well. However, an additional presentation mechanism – with KST plot- has been added. The reason is that only a single screen will be used for monitoring and the KST method offers slightly faster updates than the RRD one. Both will continue to be available until final integration of the dedicated GUI allows control of the e-nose configuration parameters as well.

Extraction of meaningful information takes many forms, but in this case it focuses on identifying abrupt and unexpected changes in the read values. Statistical analysis is carried out in the e-nose advanced logic unit to identify these unexpected changes, but in order for it to work, a practice session is required. This is so as to generate the initial statistical sample set which in turn is used as the statistical basis against which analysis is carried out. The main loop for data acquisition, training mode (possibly), processing and indicator updating is shown below:

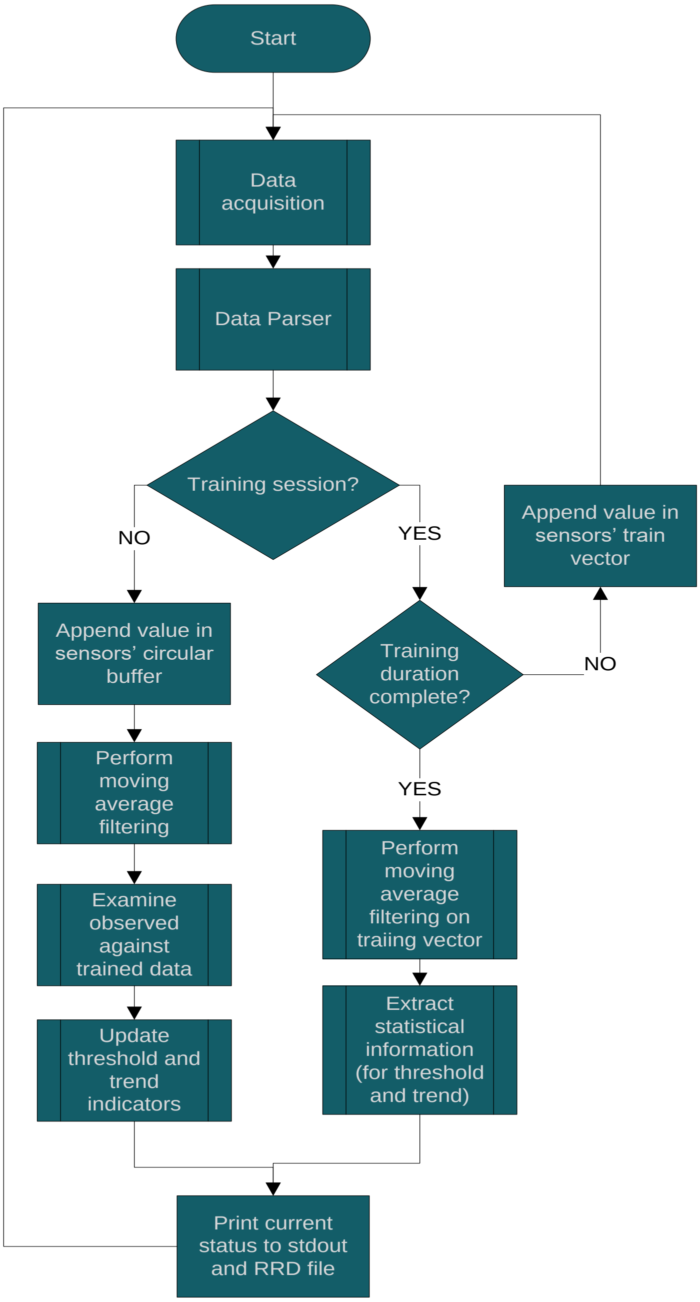
Start
Data acquisition
Data Parser
Training session?
NO
YES
Append value in sensors' circular buffer
Perform moving average filtering
Examine observed against trained data
Update threshold and trend indicators
Training duration complete?
NO
Append value in sensors' train vector
YES
Perform moving average filtering on traiing vector
Extract statistical information (for threshold and trend)
Print current status to stdout and RRD file

Figure 47: The main loop for data acquisition, processing and indicator updating of the 2nd e-nose prototype

Further introducing the new features, the statistical analysis performs filtering of the input stream. Each stream is considered to be a signal originating in each sensor, and thus primarily each filtering operation aims to filter out noise and calculate trending characteristics. These include the expected value, the standard deviation, the upper and lower threshold zones, as well as other useful characteristics for each signal. A training session is used to obtain initial values for the characteristics. Based on this information the e-nose is then able to perform detection operations in which the threshold level and trend of each signal are monitored. The resulting indicators categorize the threshold and trend of each signal accordingly:

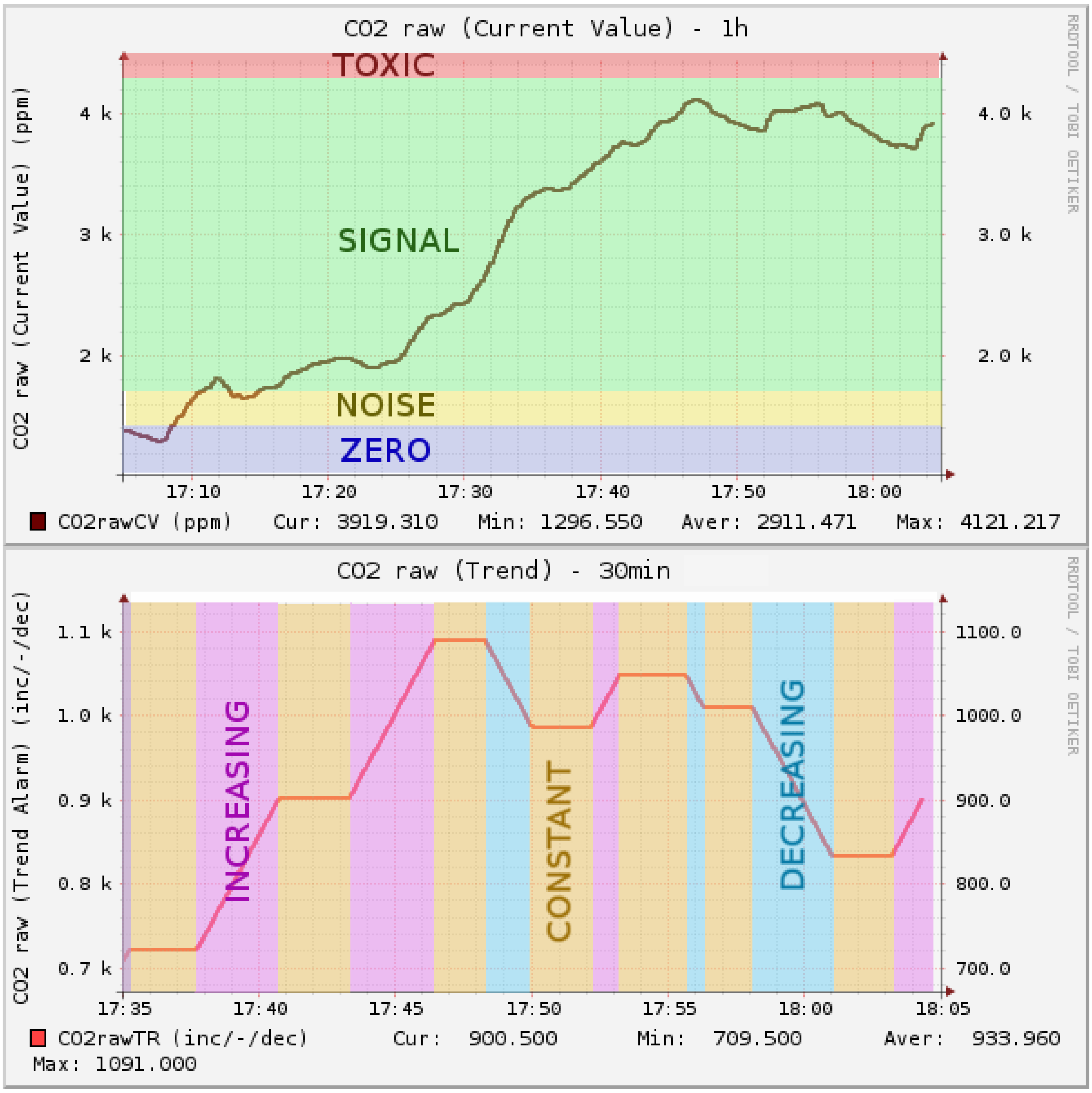

Figure 48: Conceptual design - color coding of the user-friendly information (indicators) in the GUI

Incidentally, these charts do not depict the current state of the GUI; however, this is a mock-up of how the final GUI will look. Currently the separate indicators appear as separate statuses rather than a properly color coded plot as shown above.

The e-nose advanced logic unit performs an additional set of tasks that ease the operation during development and testing. These include:

- Reading user commands from standard input
- Reading and writing configuration values and training statistical data from/to file
- Reading debugging and important configuration values as parameters to program start
- Using a signaling mechanism to trigger reading any updated configuration values
- Performing moving average filtering
- Using a decision algorithm to update the threshold and trend indicators
- Using execution threads to parallelize and avoid blocking code execution

Overall, the advanced electronic nose logic unit produces independent indicators that notify the operator of abrupt changes in the sampled air. This greatly reduces the time that the operator needs to spend looking at graphs and an overwhelming load of information in order to extract meaningful information. Currently the operator can rely on the system to notify them, thus diverting the precious SaR time to other tasks and other sensors' observations. In future versions of the e-nose advanced logic unit, a qualitative analysis of the current indicators across all sensors will be used to produce a weighted analysis of whether indications from different sensors are meaningful with respect to human presence or not.

7.5. Verification - setups and tests for the 2nd prototype

The operation and performance of the 2nd e-nose prototype was tested with a series of experiments. The main objectives of the tests were to determine the detection capability of the system in controlled but nonlaboratory conditions and to validate the theoretical model calculations. For this reason the e-nose was tested in various confined spaces with actual human subjects. Ethical considerations were taken into account during the design and planning of the experiments with the main focus on not putting the test subject (one of the design engineers) in hazardous and frustrating conditions. For these reasons:

- There was always a ventilation opening adequate for maintaining non-hazardous air conditions inside the confined space.
- The test subject was allowed to stop the experiment at any moment. He could exit the void on his own.
- The test subject was always supervised.
- The test subject was seated and allowed to work on a laptop, tablet, or smart phone.
- The confined space, and the test subject, had good lighting and a view of the outside.

The experiments were carried out in the office, a guard post and a closet. The following sections have more details regarding the tests and results.

7.5.1. Office room experiments

Objectives

A room on the office premises has suitable dimensions to perform one of the large cavity experiments as calculated in the theoretical analysis. It is expected that few cavities in real life scenarios will be larger than a room of approximately 50m^3 in volume. Additionally, the immediate availability of the location rendered it a frequent testing apparatus. Focus was given in the following factors:

- Perform frequent tests during the development cycle of the e-nose.
- Verify the validity of the theoretical results and identify potential discrepancies for the case of no fresh air circulation (no openings, sealed cavity) in a large room
- Check the sensor output for e-nose health monitoring sensors

Method

With given room size and room openings (a door and a window) not much variation could be tested on the fresh air circulation. Instead, the aim was oriented to the exhaust air flow rate; that is, the number of people in the room. Moreover, the large volume of the room would lead to a long time required for the actual air mixture to be changed. Thus, no changes were performed on the initial conditions of the room. Typically, each test involved the following:

1. Have two people in the room (those working in the room).
2. Open windows and door for 5-10 minutes, so as to let fresh air in and minimize effect of exhaled human breath inside the room.
3. Train the e-nose - acquire air samples from outside the windows (so 100% fresh air).
4. Bring the e-nose air sampling inlet in and close door and window.
5. Start monitoring and logging.
6. Stop monitoring when enough data has been obtained (usually after 1-2 hours).

Results

The first test took place on office premises, in a room of suitable dimensions (3.2 m × 5.5m × 2.7 m), emulating a large cavity. It is expected that few cavities in real life scenarios will be larger than such a room of approximately 47.5 m^3 in volume. Additionally, the immediate availability of this specific room rendered it a frequent testing "apparatus". This office room allowed us to perform frequent tests during the development cycle of the system with gas sensors, to verify the validity of the theoretical results and identify potential discrepancies in various cases of fresh air circulation in a large room and to check the system's gas sensors outputs. The openings of the room (an interior door 1.89 m^2, and an outdoor south facing window with a maximum opening of 1 m^2 and a minimum of 0.005 m^2), allowed us to control the fresh air circulation during this first test. An additional aim of this test was to verify the time for equilibrium, according to the exhaust air flow rate, for a large volume void such as this room.

When the test started at 11:45 the air in the room was refreshed by leaving the window and the door wide open for 60 min, to let fresh air in and minimize the effect of the exhaled human breath from within the room. During part I of the test (11:45–12:45), "calibration" of the system took place by sampling the outdoor air just outside the outdoor window of the room. As may be seen in Figure 2, the system with gas sensors revealed a mean concentration value for CO_2 in the fresh atmospheric air of $\overline{C_{(CO_2)f}} = 405$ ppm (left vertical axis) and for O_2 $\overline{C_{(O_2)f}} = 20.61\%$ (right vertical axis) with standard deviations $stdev_{\overline{C_{(CO_2)f}}} = 12.31$ ppm and $stdev_{\overline{C_{(O_2)f}}} = 0.0057\%$ respectively. By applying these values in Equations (27) and (28) and assuming that the concentrations in the exhaled breath are for CO_2 40000 ppm (the minimum [88]-[91]) and the maximum in O_2 16% [88]-[91], results show that the fresh air flow rate should be $F_f > \approx 956\ F_e$ for it to be possible for the CO_2 sensor to detect the human presence in the room and $F_f < \approx 328\ F_e$ must be true for it to be possible for the O_2 sensor to detect human presence.

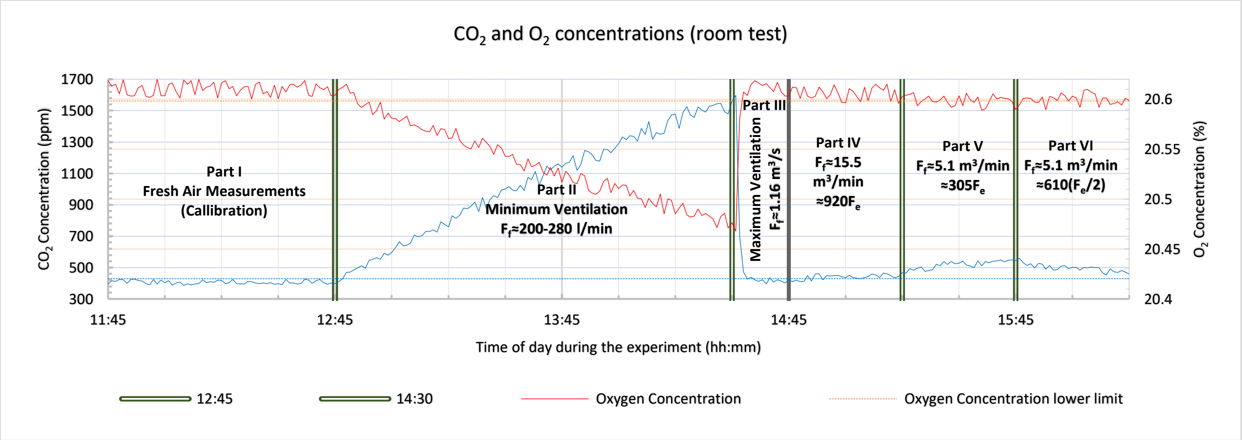

Figure 49. Room with two people, CO_2 and O_2 test measurements.

Part II of the experiment started at 12:45 when we adjusted the window opening to just 0.5 cm wide, allowing fresh air to enter through an area of just 50 cm^2 and 2 adult male persons entered the room. The large volume of the room would take a long time for the actual air mixture to change and reach equilibrium concentrations and for that reason it was convenient that two people were working in the room. Weather data for the day of the experiment showed a SE wind of v_{ref}=10 km/h and the outdoor temperature was measured T_f =20 °C. At the beginning of the experiment the temperature in the room was T_c = T_f = 20 °C, but slowly T_c started to rise during part II of the test and after an hour it had risen to 25° C. By applying (26) (A_{sum} = 0.005 m^2 g=9.81 m/sec^2, z = 2.7 m, C_R = 0.35,
v_{ref} ≈ 2.78 m/sec, ΔC_p = 0.44 - 1.51, T_f = 20 °C, and T_c = 25 °C), the expected fresh air flow rate was estimated to be F_f ≈ 200 – 280 L/min. We assumed, from Table 12 and Table 13, that the exhaled airflow rate for the 2 adult males would have an average value of F_e=16.8 L/min. Then it was calculated according to section 3.4 and by using Equation (17) that the expected equilibrium concentration would be reached in 17.5 h and would be on average for CO_2 3335 ppm and for O_2 20.27%. We decided to limit the duration of part II of this test to 14:30 (105 min duration), and according to our calculations, we could thus reach a concentration ranging between 1593 – 2650 ppm for CO_2 and 20.47 – 20.48% for oxygen. The actual measurements taken at the end of part II were 1590 ppm for CO_2 and 20.47% for oxygen, (Figure 49), verifying the theoretical expected values.

Part III of the first test was planned to last for 15 min with the openings of the room at their maximum. The expected airflow rate on average 1.16 m^3/s completely cleaned the indoor air, and the concentrations became the same as they were for the fresh atmospheric air.

Part IV of the test started at 14:45 and lasted 30 min. We closed the window halfway at 50 cm letting an opening with an area of A_{sum} = 0.5 m^2. At the beginning of this part of the test the temperature in the room was measured and was found to be

$T_c = T_f$ = 20.5 °C, but slowly T_c started to rise and at the end of part IV of the first test it had risen to T_c = 21.5 °C. By applying (26) (A_{sum} = 0.5 m^2, g = 9.81 m/sec^2, z = 2.7 m, C_R = 0.35, $v_{ref} \approx$ 0.83 m/sec, ΔC_p = 0.44-1.51, T_f = 20.5 °C, and T_c = 21.5 °C), we calculated that the expected fresh air flow rate at that point would be about 15.5 m^3/min i.e. $F_f \approx 920F_e$ and, according to the theoretical expectations from Equation (27) it required $F_f \leq 956F_e$, the CO_2 sensor should identify human presence. In Figure 49, it can be seen that the CO_2 sensor is clearly differentiated beyond its upper limit, indicating a human presence as expected theoretically from (27), with a value of 444 ppm. The oxygen sensor is within its noise zone with an average value of 20.6%, near the measured fresh air O_2 concentration (20.61%).

Part V started at 15:15 and the duration was again 30 min. We continued by closing the window to a 15 cm opening, with an area of A_{sum} = 0.15 m^2. At the beginning of the experiment the temperature in the room was measured and was found to be T_c = 21.5 °C, and slowly started to rise and at the end of part V of the first test it had risen to 22.5° C. By applying (26) (A_{sum} = 0.15 m^2 g = 9.81 m/sec^2, z = 2.7 m, C_R = 0.35, $v_{ref} \approx$ 0.83 m/sec, ΔC_p = 0.44 - 1.51, T_f = 21 °C, and T_c = 22.5 °C), we calculated that the expected fresh air flow rate at that point would be about 5.1 m^3/min i.e. $F_f \approx 305\ F_e$ and according to the theoretical expectations from (27) and (28) (CO_2 sensor $F_f \leq 956\ F_e$ and for O_2 sensor $F_f \leq 328\ F_e$), both CO_2 and O_2 sensors should identify human presence. In Figure 49, it can be seen that the CO_2 sensor is more clearly differentiated beyond its upper limit indicating a human presence, as expected theoretically from (27), with a value of 520 ppm. The oxygen sensor also reveals a human presence, as expected theoretically from (28), with an average value of 20.58%.

This first test had an additional sixth phase. In this last part of the first test the ventilation remained the same, but one of the two people left the room and the exhaled air flow rate decreased to $F_e \approx$ 8.4 L/min, the fresh air flow rate remained unchanged

(F_f = 5.1 m^3/min), thus their relationship became $F_f \approx 610\ F_e$. In Figure 2, it may be seen that the CO_2 sensor is still clearly differentiated beyond its upper limit indicating human presence, as expected theoretically from (27), with a value of 471 ppm. The oxygen sensor no longer shows human presence, as expected theoretically from (28), since the average value was 20.60% i.e. within the noise zone of the specific sensor used in the system with gas sensors used for the measurements.

During the experiment execution the other sensors behaved as follows: The NH_3 sensor reading was about 0 ppm and can be considered steady, started at about 0.04ppm and reached a maximum of 0.08ppm. The external air temperature started at about 24° C and reached a maximum of about 26° C influenced by the fresh air's cooler temperature. The internal temperature sensor had a constant average value of 39.7° C with a 0.3° C control loop setpoint (40° C) error. The barometric pressure sensor of the O_2 sensor was almost constant in the range [972.0-973.2 mbar].

Conclusion 1: All parts of the first room test confirmed the theoretical expectations and verified the analysis presented in this work.

The absent humidity sensor will be incorporated in the next stage of the experiments and is expected to show a shape similar to the NH_3 one.

7.5.2. Closet experiments with controlled opening(s)

Objectives

A closet was used as a confined space by sealing it with food wrap. The objectives of this series of experiments were to:

- Measure the air conditions inside the simulated void for known/controlled ventilation parameters. In this case the ventilation parameter is the size of a single opening.
- Test the response of the electronic nose (sensors) when inserting and removing it from the space (or the sampling probe) where it is known that a human subject is present.
- Test the response of the electronic nose (interface, indicators and triggers) when inserting and removing it from the space (or the sampling probe) where it is known that a human subject is present.

Method

The closet's volume was extended by keeping the doors open with appropriate support. The closet was gradually sealed in order to control the fresh air entering the interior of the space. The procedure for closing the human subject in the space is listed and is designed in such a way that there is no chance of suffocation. Also the materials for creating a closed space and sealing the tube section can easily be removed by hand. The sequence is the following:

1. Place human subject in the space
2. Seal the top half of the space with film
3. Install the means of ventilation in the installed film
4. Test the ventilation installation
5. Place one paper cutter inside the space
6. Seal the bottom half of the space with film
7. Seal the bottom and top sections to make the complete space sealed. The experiment can now commence, measurements should be acquired for all the monitored attributes.

The following pictures illustrate the confined space used and the various tests executed.

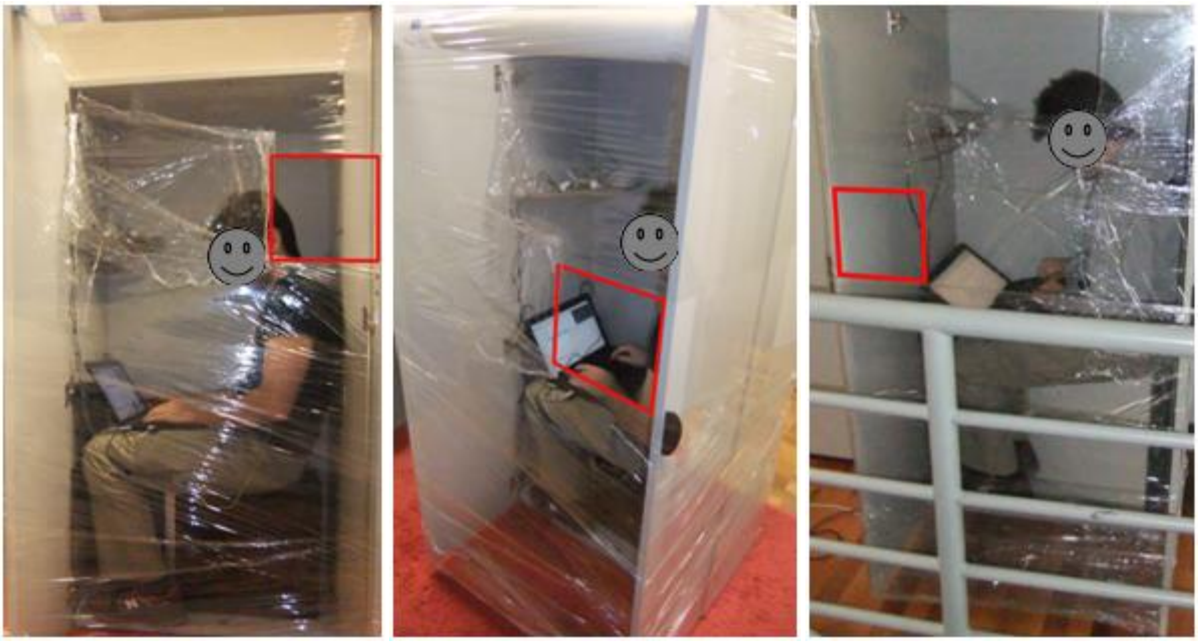

Figure 50. Various tests with different ventilation positions. Ventilation opening is 20x20cm (red shape).

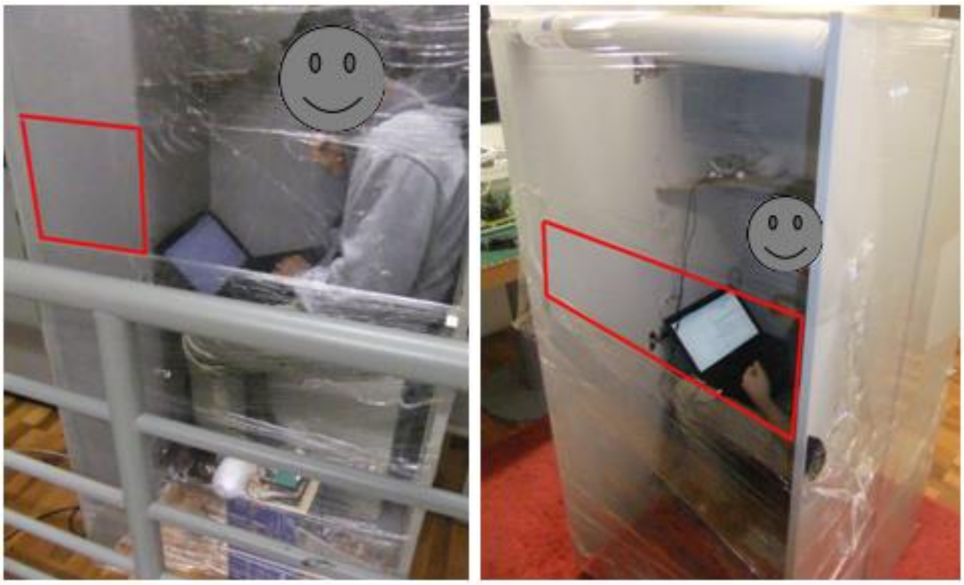

Figure 51. Testing different locations of the e-nose and a larger ventilation opening size 20x60cm

Results

The training session ended providing the following statistical data

Table 32: Training session statistical data in closet with non-forced air experiment

		CO_2 (ppm)	O_2 (%)	O_2 (mbar)	NH_3
thresh	**Signal**	1506.41932	20.45659	201.91730	4.12735
Trend	**Decr**	-0.93492	-0.00082	-0.00098	-
	Incr	0.93492	0.00082	0.00098	-

The CO_2 increased to a maximum of approximately 3500ppm as a result of the human subject being sealed in the closet. Afterwards (point A ->B in graph below) the e-nose was inserted into the closet and left to monitor the variations caused from the opening of 20x20cm that was left open. During operation air currents in the room where the closet was located (due, for example, to door or windows being opened) caused fluctuations around the 3500ppm mark (points C in graph below). In the end it was removed (point D) so that the gas concentrations would once again reach fresh air levels (point E).

Starting with the CO_2, the following response was recorded:

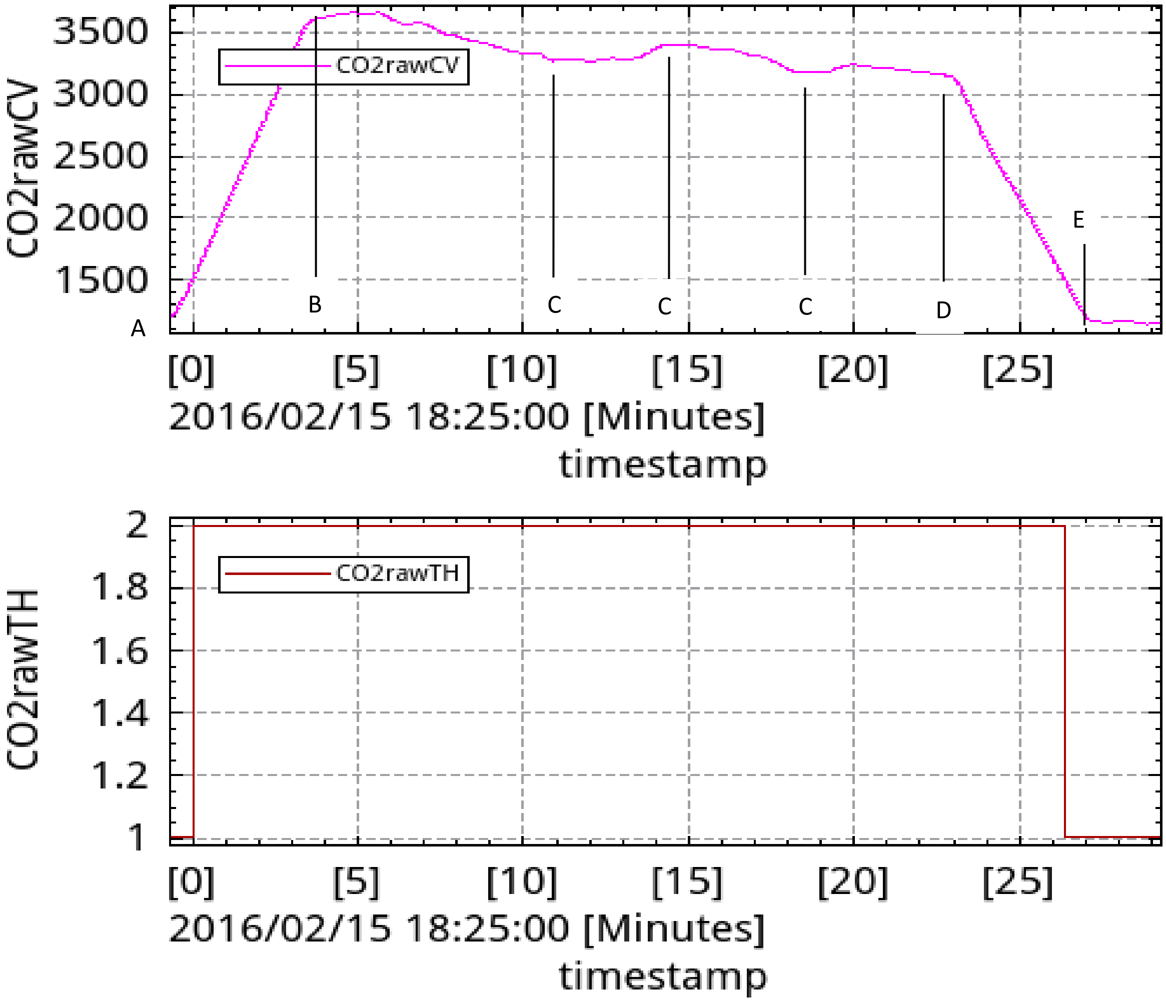

Figure 52: CO_2 concentration response and threshold indicator graphs in closet with ventilation opening

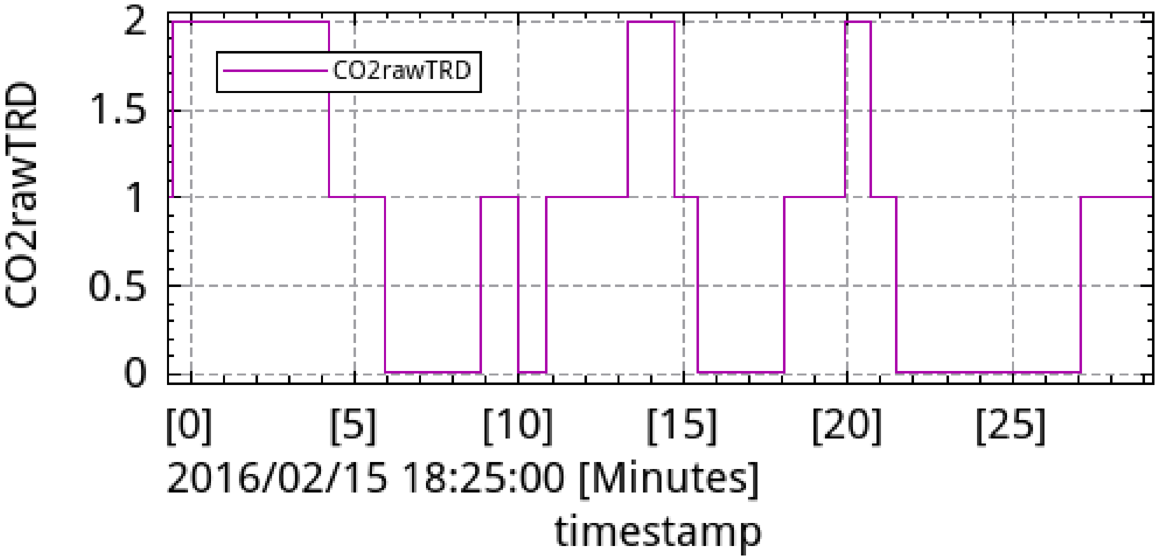

Figure 53: CO_2 trend indicator graph in closet with ventilation opening

It is clear that the maximum CO_2 concentration fluctuated but was always well within the signal level of the threshold indicator (CO2rawTH), where a value of 1 means that the signal (CO2rawCV) is at noise level and cannot be identified as signal, or it is moved to value 1 for all the time that the e-nose is in the closet with the human test subject. Moreover, the trend of the initial increase (points A -> B), final fall (points D -> E), and intermediate fluctuations (points C) are registered in the trend indicator (CO2rawTRD), where a value of 1 means that the value of CO2rawCV was steady, a value of 0 means that it was decreasing and a value of 2 that it was increasing. Note that both CO2rawTH and CO2rawTRD will be incorporated as color codes in the signal graph (CO2rawCV) and corresponding trend indicator as shown in Figure 48.
Continuing a similar but mirrored signal was given by the O_2 sensor

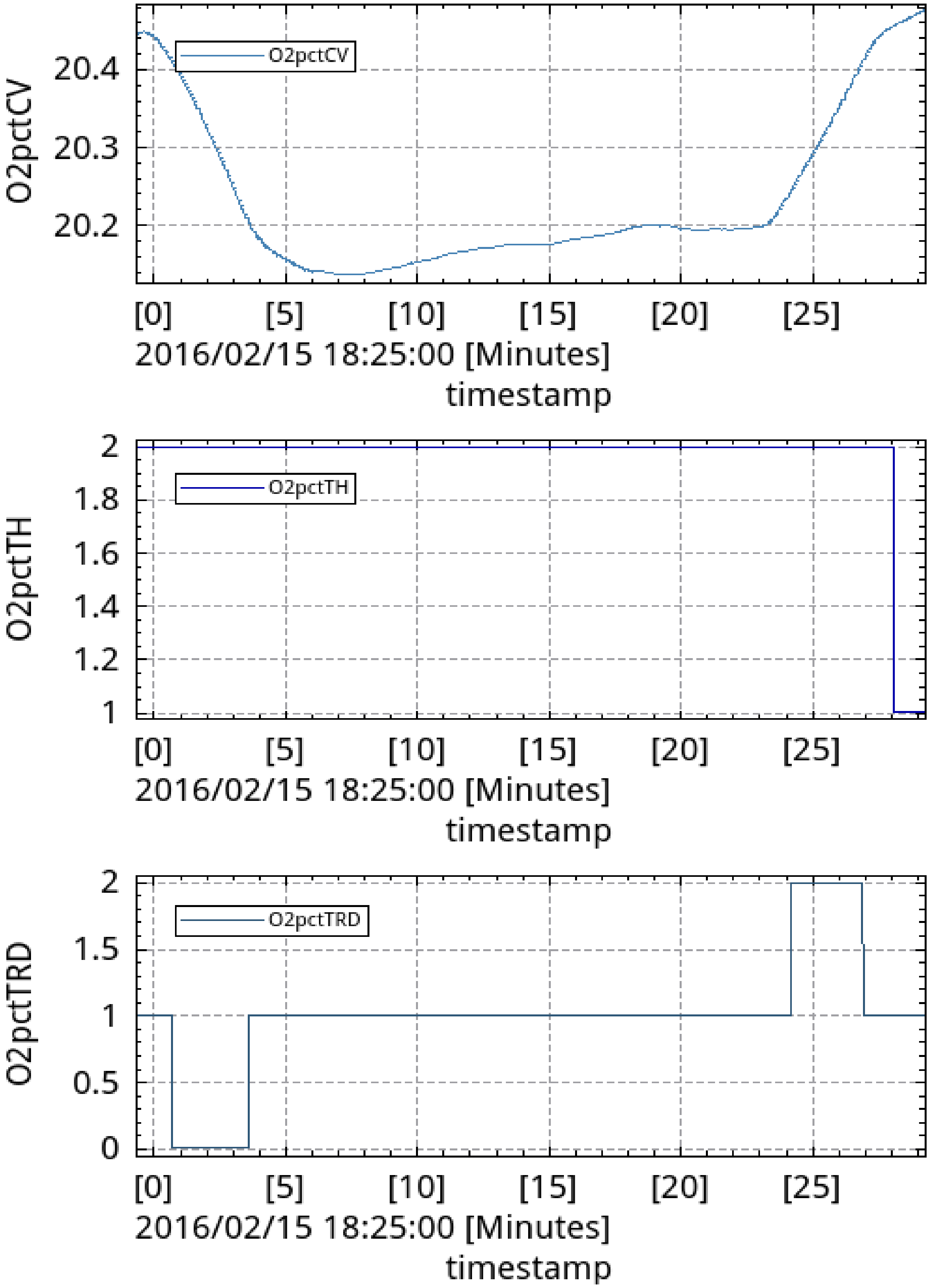

Figure 54: O_2(%) concentration response and threshold and trend indicator graphs in closet with ventilation opening

The O_2 response looked similar, albeit mirrored, to the CO_2 response. Once again, the threshold indicator correctly indicated human presence (O2pctTH has value 2) while the O_2 had dropped from the fresh air level.

Towards the end of the test, the threshold indicator is shown to return to the noise level (value of 1), i.e. the level which cannot be separated from the fresh air levels.

Simultaneously, the trend indicator would identify the significant drop and rise of the O_2 level. It does not identify the fluctuations however. This is due to the low precision of the percentage O_2 signal. If instead the O_2 partial pressure reading is used, the signal response is the same, but due to the higher precision, the trend response is more detailed.

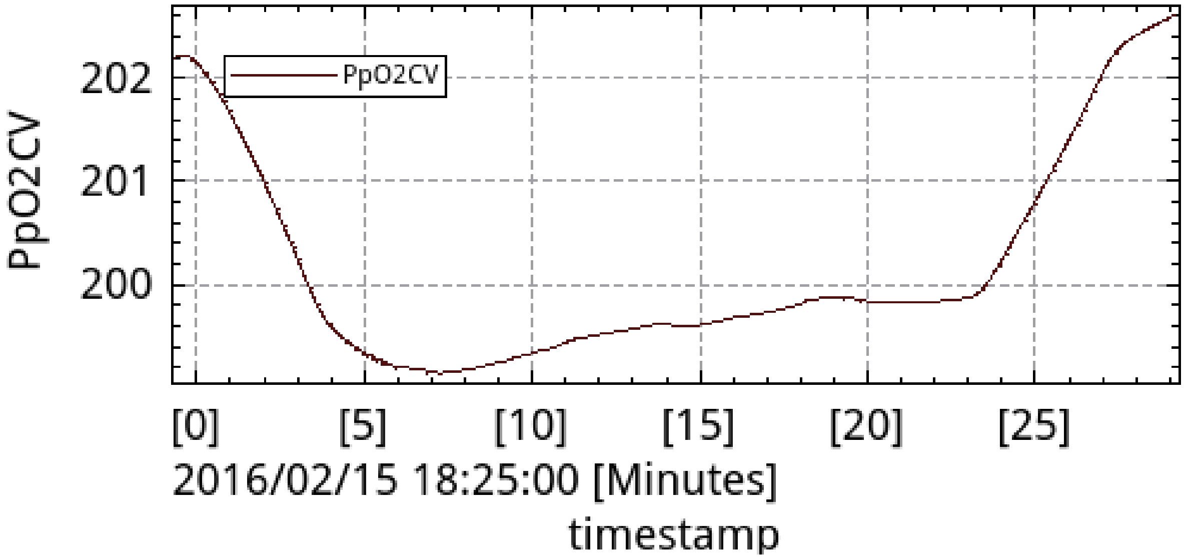

Figure 55:O_2 partial pressure (mbar) concentration response in closet with ventilation opening

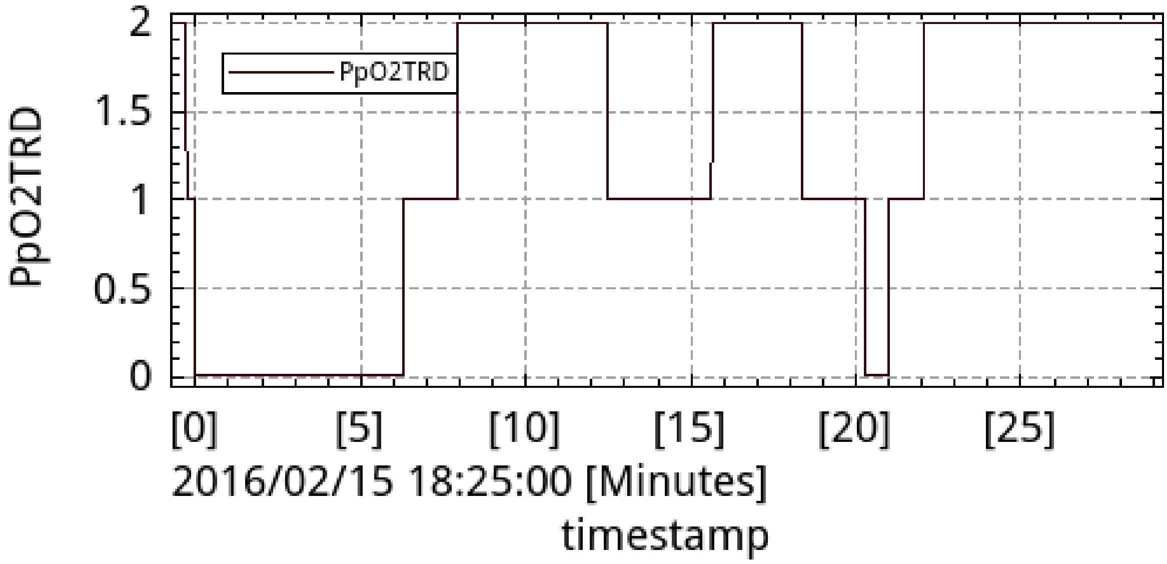

Figure 56: O_2 partial pressure (mbar) trend indicator in closet with ventilation opening

At the same time the NH_3 did not change significantly. Of course, a slight increase was registered. However, this is due to the increase in humidity in the closet and not to the increase of NH_3 itself. Regardless, the threshold indicator of the NH_3 correctly did not pick up this increase and remained at value 1 (i.e. noise level, no difference from the fresh air conditions) for the duration of this experiment.

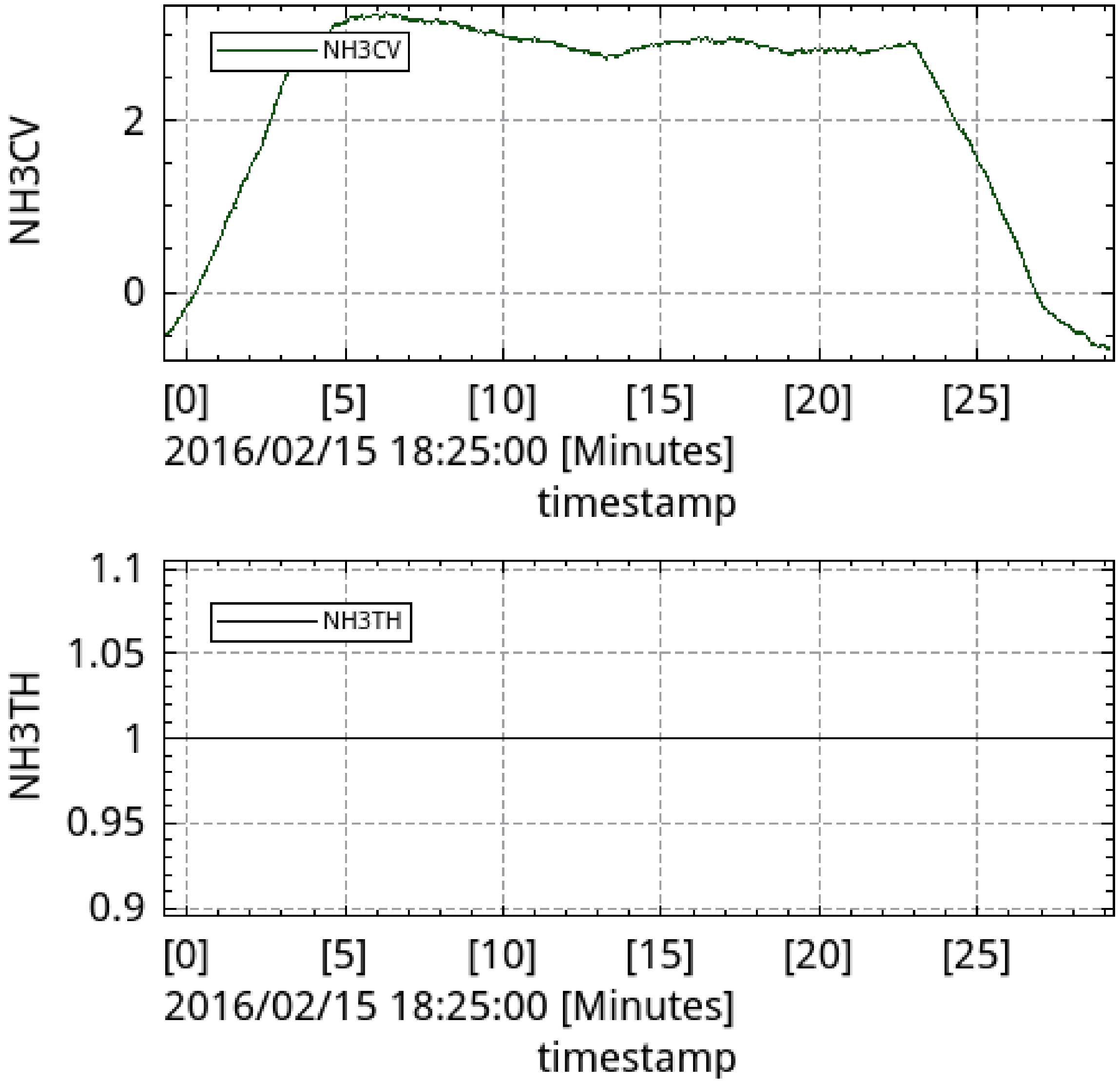

Figure 57: NH_3 (0.1ppm) concentration response and threshold indicator graphs in closet with ventilation opening

Similarly, the humidity (HumCV) had the following response, which resembles the NH_3 and CO_2 responses. This is expected as all the quantities originate from the same exhalation source and are all proportional to the exhaled air flow rate. The humidity's trend indicator (HumTRD) followed closely the fluctuations in humidity where a value of 0 denotes a decrease in the HumCV signal, 1 denotes a steady signal and 2 denotes an increasing signal.

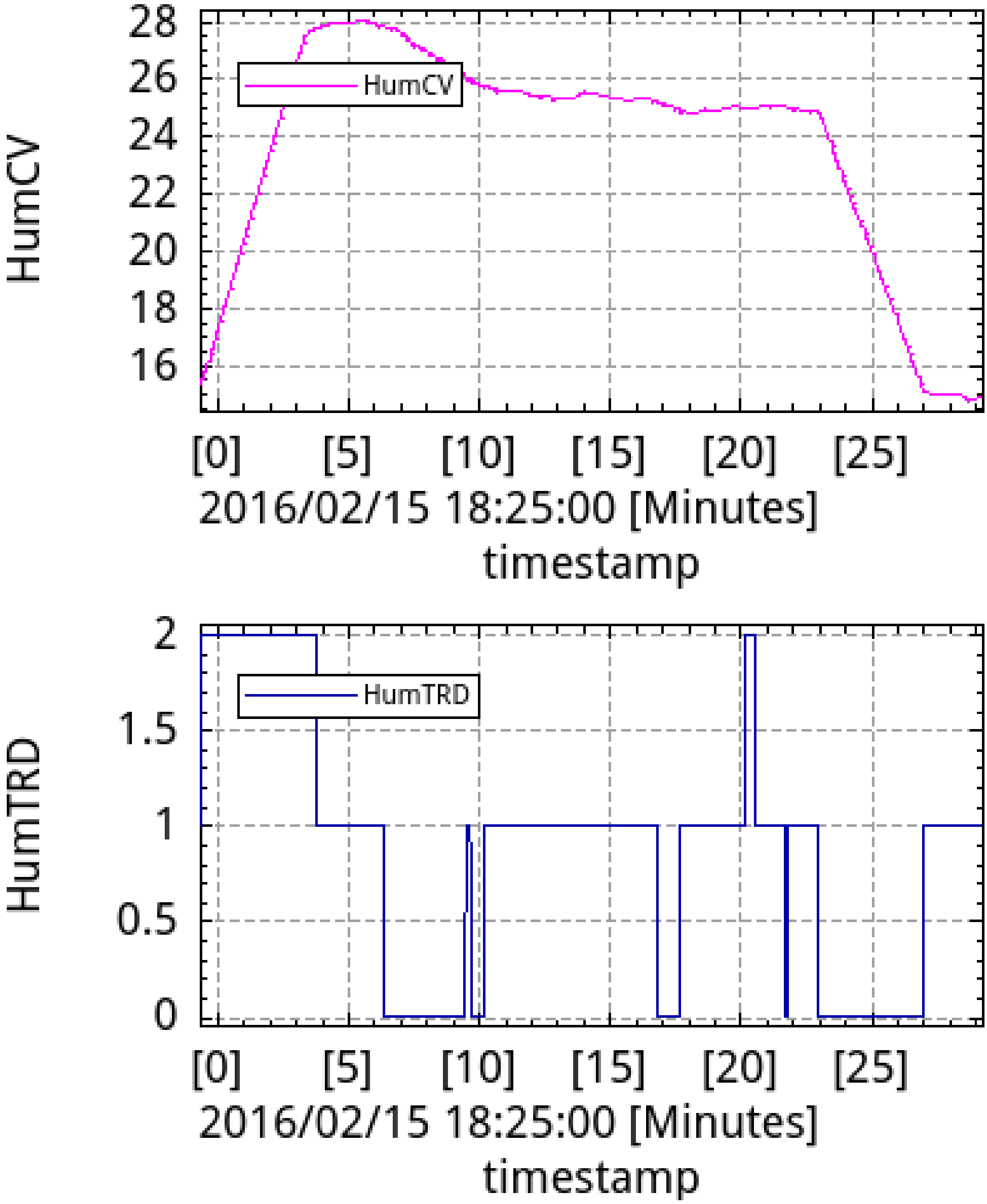

Figure 58: Humidity (RH%) response and trend indicator in closet with ventilation opening

Finally, the rest of the signals from the system's health monitoring are shown as additional demonstrations of the correct operation of the trend indicators:

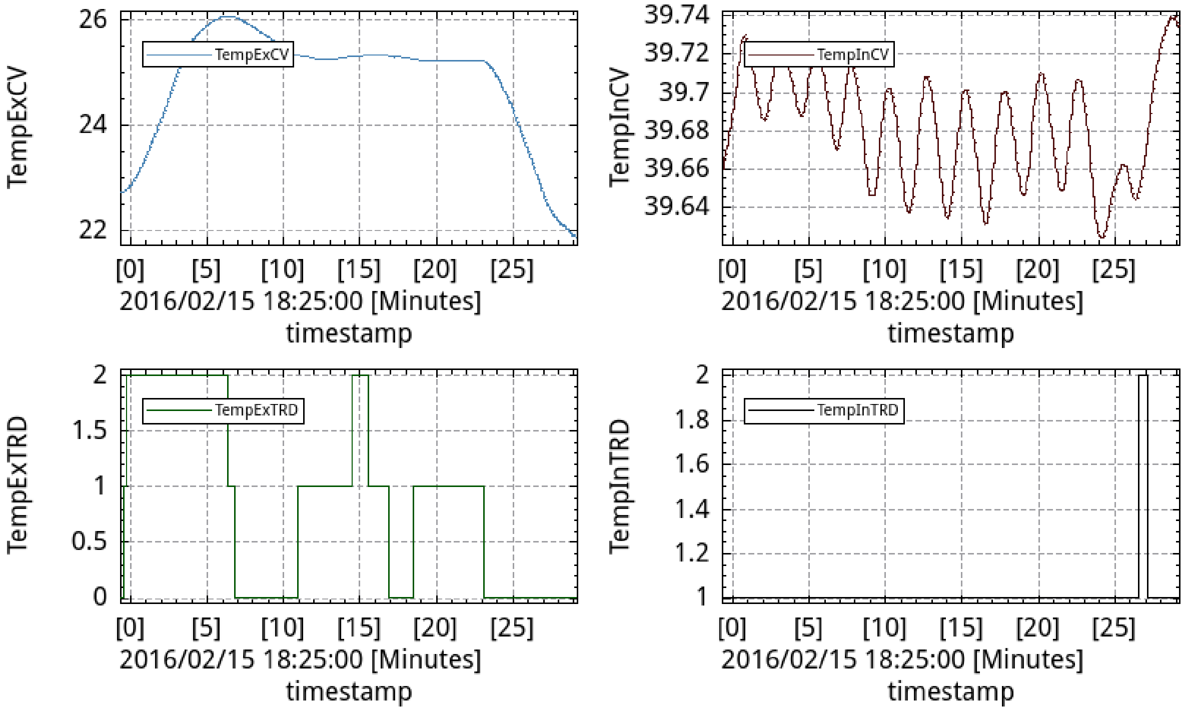

Figure 59: External and internal temperature (°C) signals and trend indicator graphs in closet with ventilation opening

The external temperature (TempExCV) altered according to the CO_2, NH_3 and humidity concentrations, while its trend indicator correctly followed the temperature changes.

It is interesting to note that the internal temperature signal (TempInCV) fluctuated frequently, but after a training session its trend indicator TempInTRD correctly did not follow these ripples. It did, however, follow the increase in temperature that appears at the end of the measurement window.

Similarly, the barometric pressure was also recorded

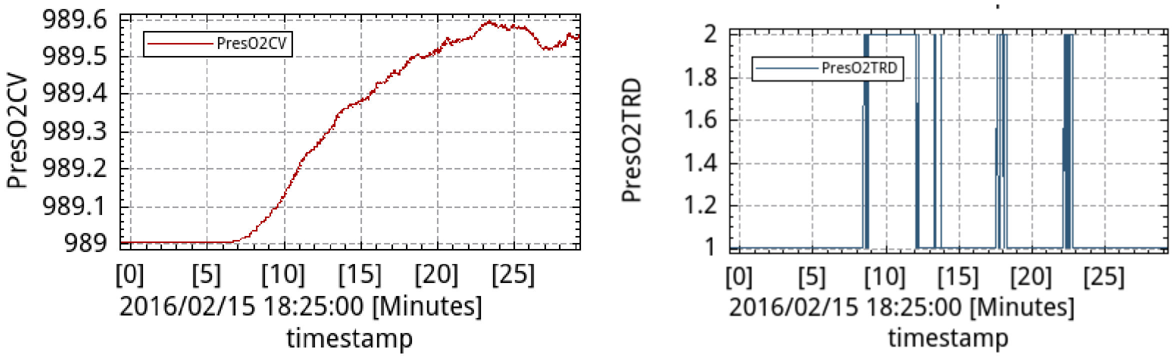

Figure 60: Barometric pressure (mbar) level trend indicator graphs in closet with ventilation opening

The barometric pressure (PresO2CV) did not change significantly or abruptly enough to cause its trend indicator (PresO2TRD) to register the whole change. It may be the case that slight tweaking of the pressure filtering mechanism is necessary in order to fix the trend indicator to show the correct value (of 1 = steady, no significant change) all the time.

Discussion

An opening large enough to fit at least the cross section of the forward moving snake robot was assumed. It was expected that the opening would affect the concentrations introducing some unforced fresh air circulation. As it turned out, the opening allowed fluctuations in the saturation concentration of the gases and other characteristics, such as humidity and temperature in the closet. These were created even by slight air currents occurring outside the closet and included opening doors and windows in the room where the closet was located, walking quickly in front of the closet opening etc. Thus, the opening allows changes outside the closet to propagate inside it. Nevertheless, these changes did not render the e-nose unable to identify the human presence as all the victim localization threshold indicators correctly operated in the “signal presence” region, having a value of 2.

It is noted that all the threshold and trend indicators which currently appear as independent graphs, will be converted into color coded ranges and status indicators respectively in the final version of the e-nose prototype device.

Additionally, the threshold and trend indicators were thoroughly tested and showed that after a training session would correctly identify current levels and trends (i.e. increasing, steady or decreasing) during operations. Minor discrepancies in the barometric pressure trend indicator will be corrected for the next part of the prototype. It is thus concluded that the experiment objectives were fulfilled and the electronic nose system met the tested requirements.

7.5.3. Closet experiment with controlled fresh air flow– fans

A closet was used as a confined space by sealing it with food wrap. The objectives of this series of experiments were to:

- Measure the air conditions inside the simulated void for known/controlled ventilation parameters. In this case the ventilation parameter is the air flow controlled with a cluster of fans with known air flow.
- Test the response of the e-nose (sensors) when inserting and removing it from the space (or the sampling probe) where it is known a human subject is present.
- Test the response of the e-nose (interface, indicators and alarm triggers) when inserting and removing it from the space (or the sampling probe) where it is known a human subject is present.
- Validate the theoretical model calculations.

The closet’s volume was extended by keeping the doors open with appropriate support. The closet was gradually sealed in order to control the fresh air entering. The procedure for closing the human subject in the space is listed and is designed in such a way so that there is no chance of suffocation in the event the mechanical ventilators do not work for any amount of time. Also, the materials for creating a closed space and sealing the tube section can easily be removed by hand. The sequence is the following:

7. Place human subject in the space.
8. Seal the top half of the space with film.
9. Install the means of ventilation.
10. Test the ventilation installation.
11. Place one paper cutter inside the space.
12. Turn ON the ventilation fans.
13. Seal the bottom half of the space with film.
14. Seal the bottom and top sections so that the space is completely sealed. The experiment can now commence, measurements should be acquired for all the monitored attributes.

During the experiment, the fans were switched ON or OFF to produce several different amounts of fresh air flow circulations (different scenarios). Pairing these with the volume of the sealed cavity and the exhaled air flow rate of the test subject is expected to alter the CO_2 and O_2 concentration in the cavity. These concentration changes were monitored and recorded.

In this section, pictures illustrate the confined space used, the ventilation fan set-up used and the various tests executed.

The following picture illustrates the air fan cluster to control fresh air flow rate. Each fan is controlled by an ON/OFF switch and the total flow is assumed to be the sum of the flow of each fan that is enabled. The fans present are:

- 1 x 50 liters per minute fan (LPM)
- 1 x 200 liters per minute fan
- 3 x 500 liters per minute fans

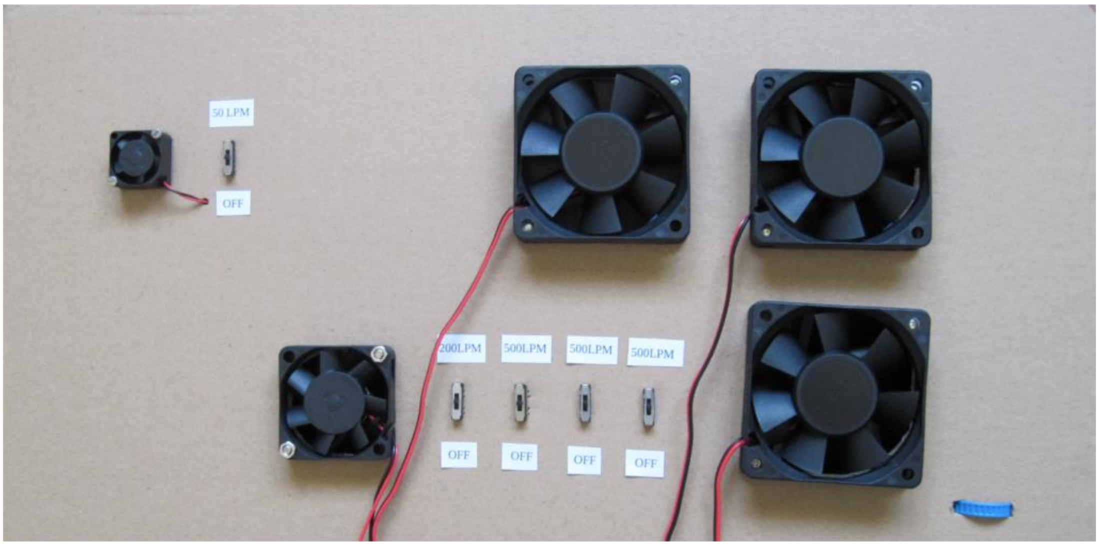
50 LPM
OFF
200LPM
500LPM
500LPM
500LPM
OFF
OFF
OFF
OFF

Figure 61. Air fans to control fresh air flow rate

The following pictures illustrate the tested configurations: different air flows and different sampling positions via sampling tube:

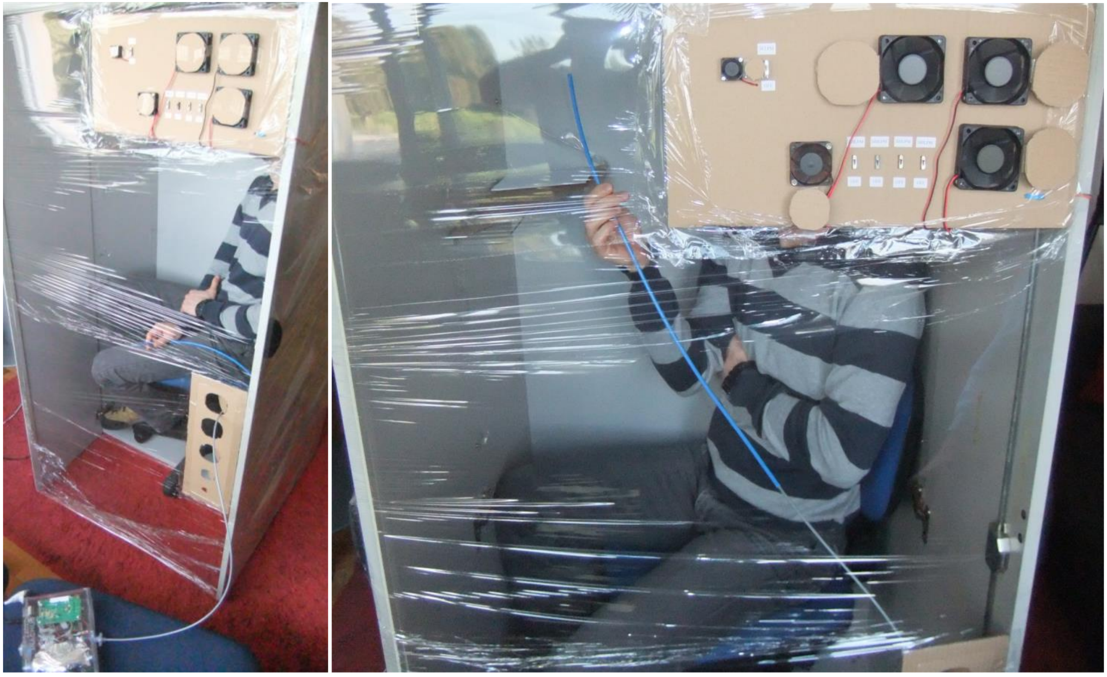

Figure 62. Left: All fans OFF ventilation openings open. Right: All fans ON ~ 1750 LPM.

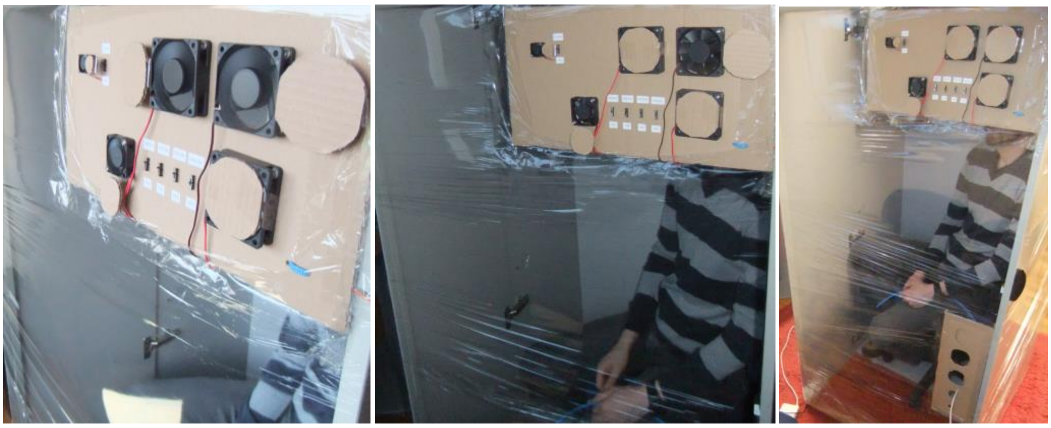

Figure 63. Left to right: 4 fans ON ~ 1250LPM. 3 fans ON ~ 750LPM. 2 fans ON~ 250LPM

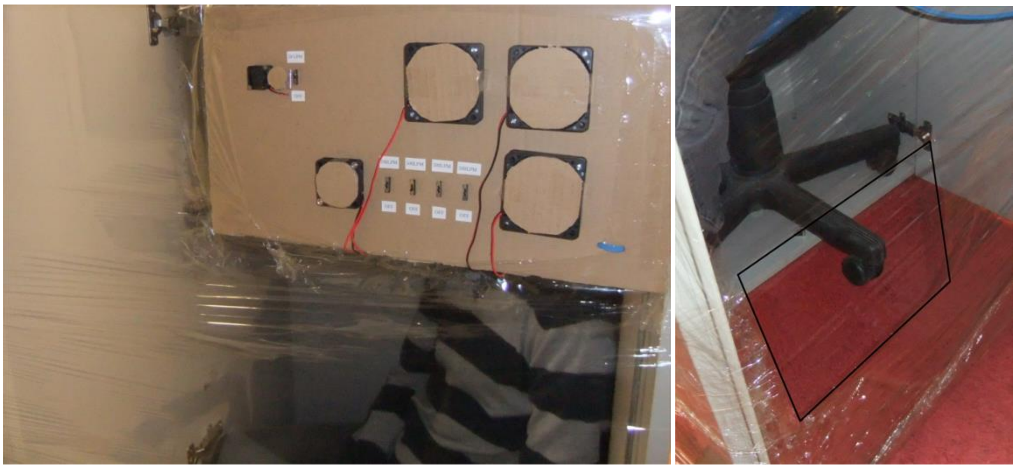

Figure 64. Left: 1 fan ON ~ 50LPM. Right: No fans ON, only 20x20cm opening.

Results

Following the training session, the obtained statistical data are the following:

Table 33: Data from the closet with fans experiment

		CO_2 (ppm)	O_2 (%)	O_2 (mbar)	NH_3
thresh	**signal**	866.77629	20.39384	198.22583	0.81509
trend	**decr**	-0.36894	-0.00116	-0.00116	-
	incr	0.36894	0.00116	0.00116	-

The threshold signal is the threshold above or below which a detected signal will enter the “signal zone”. This signal zone is above the mentioned threshold for CO_2 and NH_3 since both are expected to rise in the presence of a human, while it is below for O_2 since this is expected to drop in the presence of a human. Likewise, due to noise in the incoming raw signal, a “zero” trending zone is allowed between the “incr” to “decr” range. This means that any filtered signal that does not change abruptly enough (i.e. line outside the decr-incr range), will be considered as steady and the indicator will tag it as such. If it changes in the positive direction (> incr), then it will be considered that the signal is increasing , while if the signal drops below “decr” the trend indicator will register it as “decreasing”.

The experiment results are included in the following graphs. The first one includes the measurements of the most importance to the user- the main sensors and various calculations. The second one includes the measurements of other sensors not so interesting for the users, but important for system health monitoring. The third one displays the CO_2 measurements with annotation regarding the phases of the experiment.

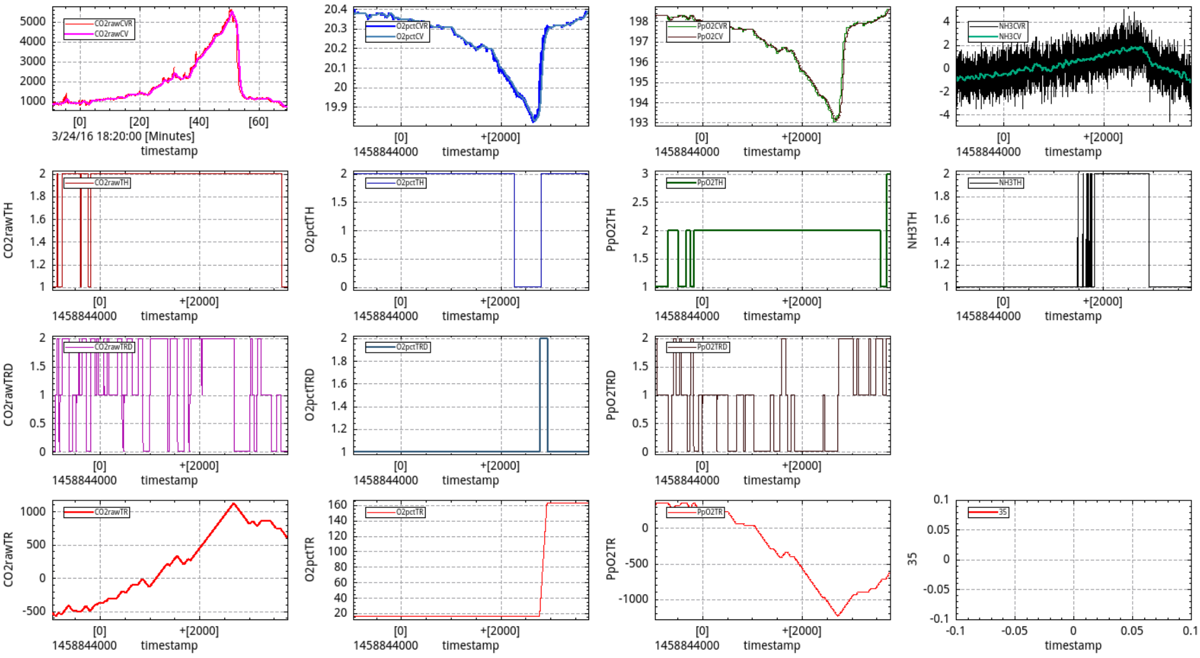

Figure 65. First to last row, [left to right: CO₂ (ppm), O₂ (%,mbar) and NH₃ (0.1ppm) sensor readings]. Thresholds. Derivative of trend. Trends.

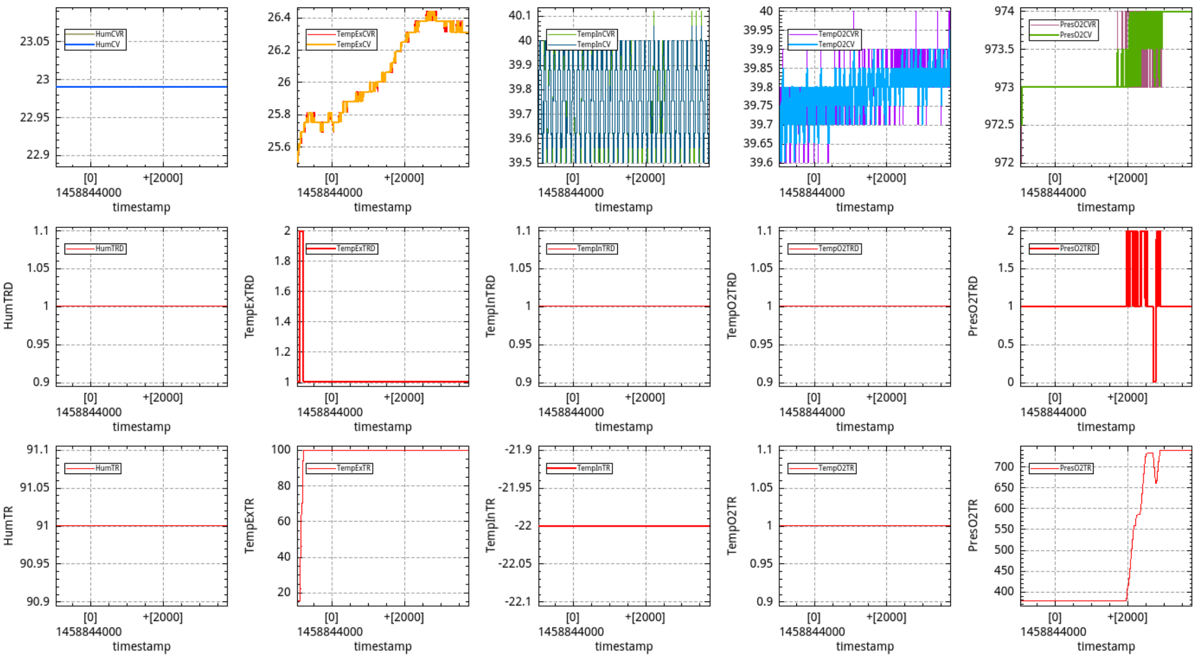

Figure 66. First to last row, {left to right: Humidity (RH%), temperature[external(°C), internal(°C), O₂ sensor(°C)]} and pressure(mbar) sensor readings. Derivative of trend. Trends.

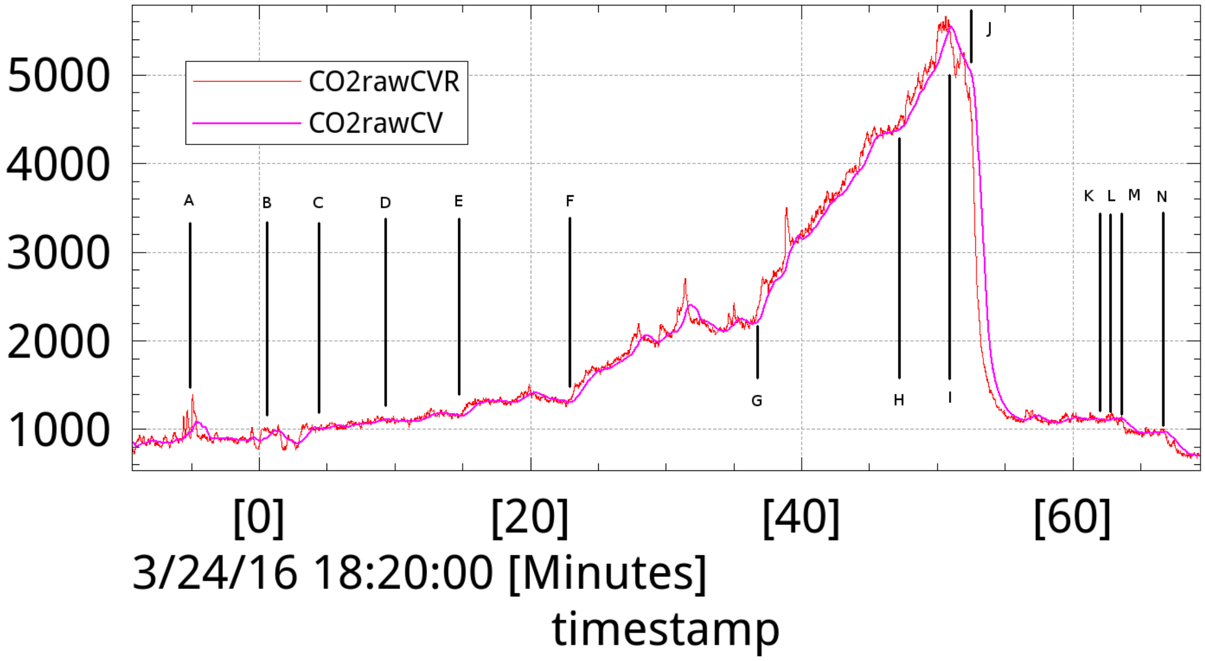

Figure 67. CO_2 (ppm) concentration response during the closet with fans experiment. Both filtered (CO2rawCV) and raw (CO2rawCVR) values are shown

The measurements can be analyzed in the following stages with actions at the indicated positions:

- START: All fans ON. Sampling input placed near ventilation window of room. Range 800-900ppm. Semi noise-signal
- **A**: Moved sampling input to 20cm close to closet's ventilation window. Range 900-950ppm
- **B**: Brought sampling input in front of closet's opening. Range 950 – 1000ppm
- **C**: Moved sampling input into the closet at knee level. Raised to 1000 – 1080ppm
- **D**: Turned OFF 1st 500lt/min fan. Range 1060 – 1200ppm
- **E**: Turned OFF 2nd 500lt/min fan. Range 1250 – 1350ppm. Measurements rose from 1150 to 1300ppm. No action taken, but CO_2 slightly rose again, possibly as a result of the air mixing. The unexpected change was undone.
- **F**: Turned OFF 3rd 500lt/min fan. Measurements rose from 1300 to 1700ppm within 2 minutes, and then rose again from 1800 to 2kppm after mixing. Measurements continued to rise, from about 2000 to 2400ppm over 4 minutes. Measurements fell back down to 2200ppm. Approximately steady.
- **G**: Turned OFF 1x 200lt/min fan. Measurements rose from 2200 to 3200ppm in 4 minutes, up to 4400ppm after 11 minutes.
- **H**: Turned OFF last fan - 50lt/min. Measurements started rising immediately.
- **I**: Made large ventilation opening approx 20x20cm.
- **J**: Turned ON all fans. After 8 minutes measurements reached 1050 – 1150ppm
- **K**: Moved sampling input to large opening. No change
- **L**: Moved sampling input outside the large opening (outside closet). Approx. 15cm. No change
- **M**: Moved sampling input on chair. Approx. 30 cm. Measurements dropped from 1100 to 975ppm. Range 950-1000ppm. Indicators calculate there is still a signal present
- **N**: Moved sampling input out of the ventilation window of the room. Measurements dropped to below 800ppm. No indicators triggered any more.
- End

At the same time the CO_2 behaved as is shown in Figure 67, while the O_2 behaved in approximately the opposite (mirrored) way. This is expected as the relative consumption of O_2 by the same human respiratory sink will produce corresponding amounts of CO_2.

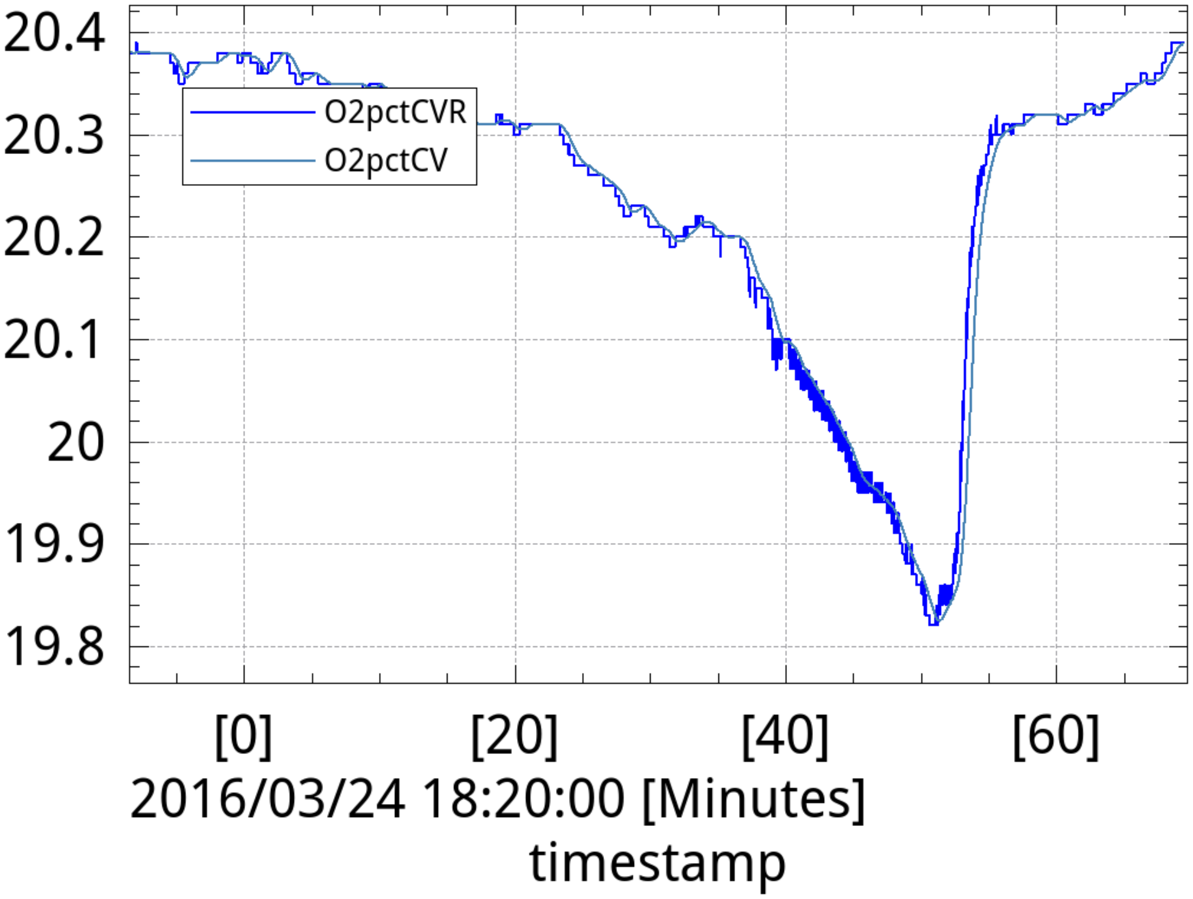

Figure 68: O_2 (%) concentration response during the closet with fans experiment. Both filtered (O2pctCV) and raw (O2pctCVR) values are shown

At the same time, the NH_3 remained, as expected, almost at idle levels. Any minimal variations are caused by the change in humidity of the exhaled air. This NH_3 change will be potentially present in a poorly ventilated space, but will usually be negligible and unable to produce a valuable above the signal detection threshold.

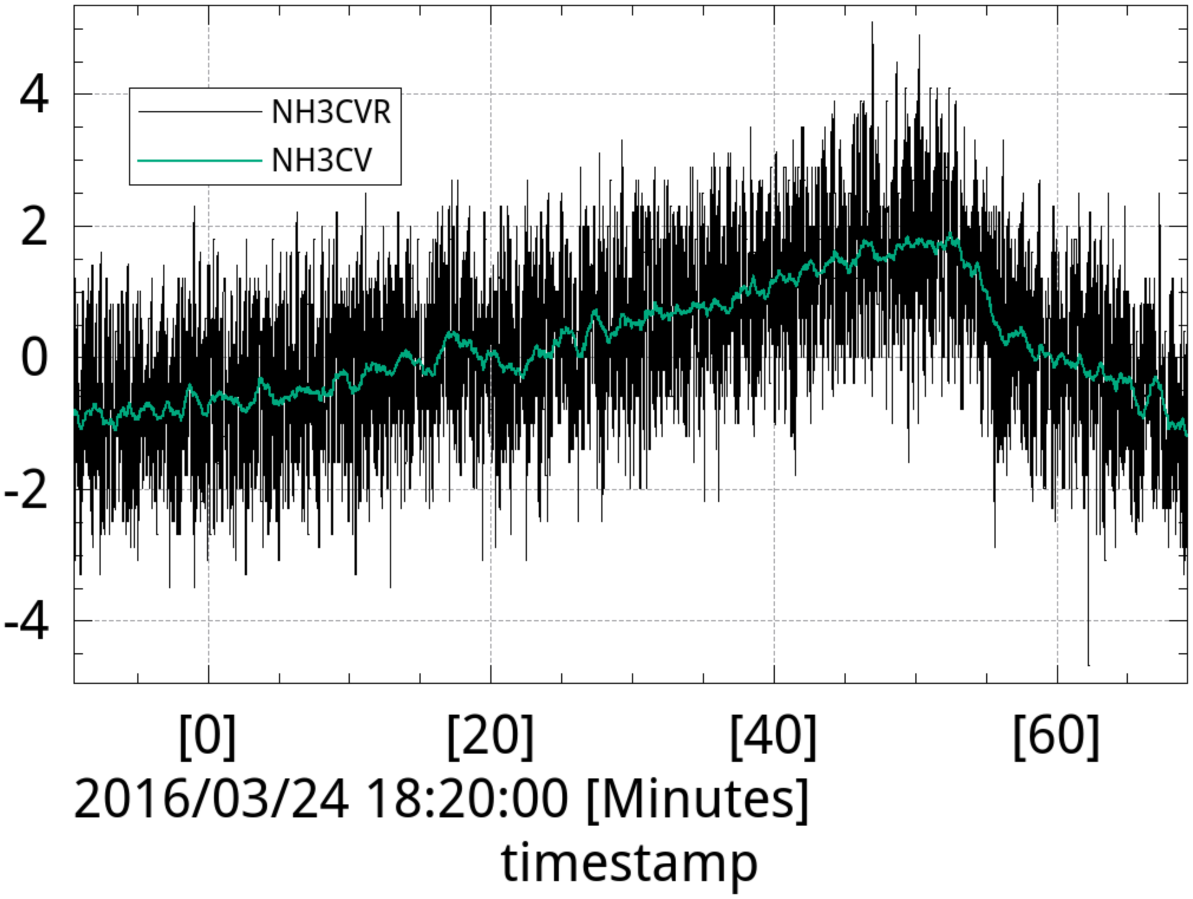

Figure 69: NH_3 (0.1ppm) concentration response during the closet with fans experiment. Both filtered (NH3CV) and raw (NH3CVR) values are shown

Office storage closet test to verify the theoretical model

For the second test, a confined space was created by sealing an office storage closet with food wrap and adding a cluster of fans with known airflow rate capability to adjust the incoming “fresh” airflow rate. Therefore, air conditions inside the closet were expected to simulate a rubble void with controlled fresh air flow by switching fans on and off and actually simulating a controlled wind effect. The office storage closet volume was extended by keeping the doors open with appropriate support, Figure 70, and was then gradually sealed in order to control the fresh air entering the interior of the space and a procedure was adopted for closing the human subject inside the space, designed in such a way that there was no chance of suffocation. Also, the materials for creating the closed space and sealing the tube section could very easily be removed by hand. First, the human subject was placed in the space equipped with a paper cutter for an emergency exit. Next, the top half of the setup was sealed with film, including the top section, and then an opening of 20 cm × 20 cm was created in the installed film to host the fan setup. The installation and testing of the means of ventilation (fans), on the already installed film, followed. After installing and testing the fans through a panel in the top half of the test setup, the bottom half of the space was then also sealed with film without including the bottom section of the setup that was facing the floor in order to create a way-out for the incoming air from the fans. Thus, we created a sealed space that allowed airflow coming in from the fans and exiting from the bottom of the closet setup.

The measurements of the gas concentrations inside the simulated void were related to known/controlled ventilation values. During the test, the fans were switched ON or OFF to produce the required amounts of fresh air flow circulations during different parts of the test. Figure 70 illustrates this closet test setup, including the ventilation fan setup. On the top right of the closet space, the air fan cluster is positioned to control the “fresh” air flow rate. Each fan is controlled by an ON/OFF switch and the total flow is assumed to be the sum of the flow of each fan that was enabled. There were five fans in the cluster. Three of them had an airflow capability of 2000 L/min, one of 1500 L/min and one of 75 L/min. The total air flow ideally was 7.575 m^3/min.

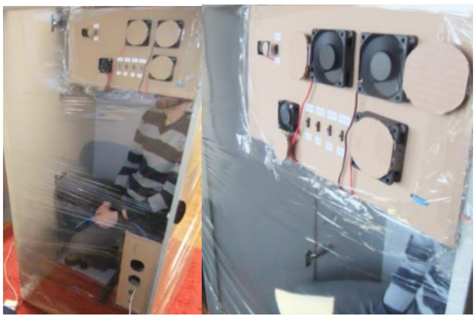

Figure 70. Left 2 fans ON~ 250lpm Right 4 fans ON ~ 1250lpm.

The office storage closet was placed in a large corridor and the test measurements started at 10:00. During the preparation of the closet setup, “calibration” of the system with gas sensors took place by sampling the air in the corridor and the measured concentration mean values were $\overline{C_{(CO_2)f}} = 866\ \text{ppm}$ and $\overline{C_{(O_2)f}} = 20.39\%$, with standard deviations $stdev_{\overline{C_{(CO_2)f}}} = 23.57\ \text{ppm}$ and $stdev_{\overline{C_{(O_2)f}}} = 0.0051\%$. Applying these values in (27) and (28) and assuming that the concentrations in the exhaled breath are for CO_2 40000 ppm (the minimum) and for O_2 16% (the maximum) [88]-[91], shows that that the fresh air flow rate should be $F_f \leq 414\ F_e$ to be possible for the CO_2 sensor to detect a human presence in the office storage closet and $F_f \leq 215\ F_e$ should hold for it to be possible for the O_2 sensor to detect a human presence. According to those measurements in part I the dotted orange line in Figure 71, represents the fresh air oxygen average concentration-2stdev (20.38%), measured by the O_2 sensor and the light blue line similarly represents the fresh air carbon dioxide average concentration + 2stdev (912 ppm) for the CO_2 sensor. The oxygen sensor measurements must be below this limit to detect entrapped victims in a cavity with enough certainty and without creating false alarms for the rescue teams, and similarly, the CO_2 sensor measurements have to be below the estimated limit. Figure 71 displays the CO_2 and O_2 measurements with annotation regarding the phases of the experiment.

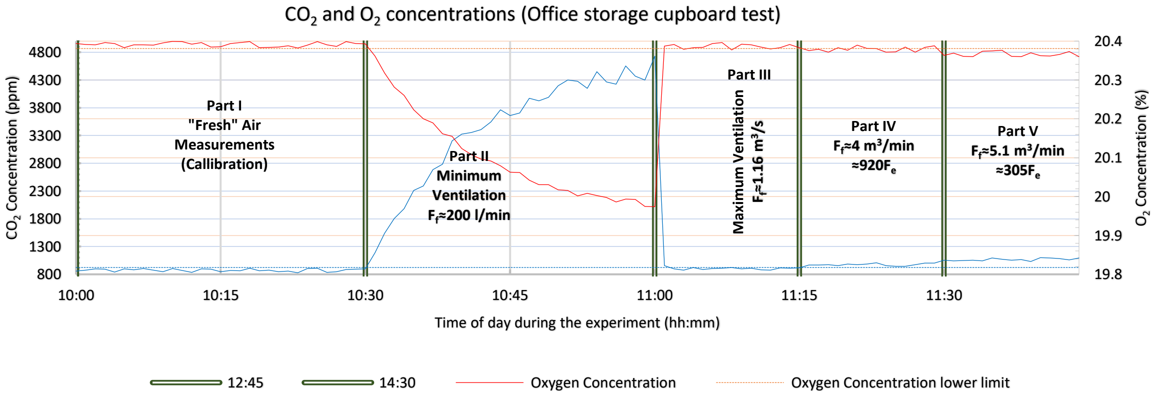

Figure 71. Extended office storage closet with one person test measurements.

When the sealing of the closet was finished at 10:30, part II of the test started. The volume of the sealed created cavity was calculated as $V_c = 0.93\ m^3$, and the exhaled air flow rate of the test subject (an adult male) $Fe \approx 8.4$ L/min. It was calculated that with only the 75 L/min fan activated, and by using Equation (17), the expected equilibrium concentration would be reached in 55 min and would be on average 4808 ppm for CO_2 and 19.95% for O_2. We decided to limit the duration of part II of this test to 30 min, and according to our estimations we could reach a concentration of about 4569 ppm for CO_2 and 19.97% for oxygen. The actual measurements during part II of the test as may be seen in Figure 71 reached 4612 ppm for CO_2 and 19.98% for oxygen, verifying the theoretical expected values.

Part III of the closet test was planned to last for 15 min with all the fans switched ON (expected airflow rate on average 7.575 m^3/min), to clean the air going into the closet enough and force the concentrations to become almost the same as the concentrations of the air in the corridor. The measured concentrations during part III reached

910 ppm for CO_2 and 20.39% for oxygen, thus neither sensor detected a human presence because the high airflow rate forced them under and over their limits respectively (both calculated in part I of this test).

Part IV of the test followed and lasted for another 15 min. We left just two of the fans switched ON to adjust the airflow at F_f = 3500 L/min, thus, $F_f = 417F_e$ (Fe ≈ 8.4 L/min). According to our calculations in part I of this test the theoretical “demand” from (27), for the CO_2 sensor to detect a human presence is $F_f \leq 414\ F_e$. For oxygen similarly from (28) and the part I measurements, $F_f \leq 215\ F_e$ should hold. As can be seen in Figure 71, the carbon dioxide sensor conclusively detected a human presence (values about 912 ppm over the threshold- light blue dotted line). For the oxygen sensor, this was not possible since the result was still in the noise zone of 20.38%.

The last part of this test was part V with a duration again of 15 min. Just two of the fans were left switched ON in order to adjust the airflow to F_f = 1575 L/min, thus $F_f = 188F_e$ (Fe = 8.4 L/min). According to the calculations in part I of this test the theoretical “demand” from (28), for the O_2 sensor to detect a human presence is that $F_f \leq 215F_e$ should hold true. As can be seen in Figure 4, both the oxygen and, certainly, the carbon dioxide sensor obviously detected a human presence. The value of the O_2 concentration was 20.38% under the threshold orange dotted line and the CO_2, 1002 ppm, was over the threshold light blue dotted line.

Conclusion 2: The office storage closet test also fully confirmed the theoretical expectations

A special case

While constantly monitoring a human subject will produce a similar slowly increasing response in CO_2 concentration and a correspondingly slow decreasing response in the O_2 concentration, a different set of responses is expected when the e-nose approaches and moves away from a cavity containing a human. In this case the width of the spike is in direct connection to the time the e-nose spent passing close to the respective cavity, but will always have abruptly increasing and decreasing slopes.

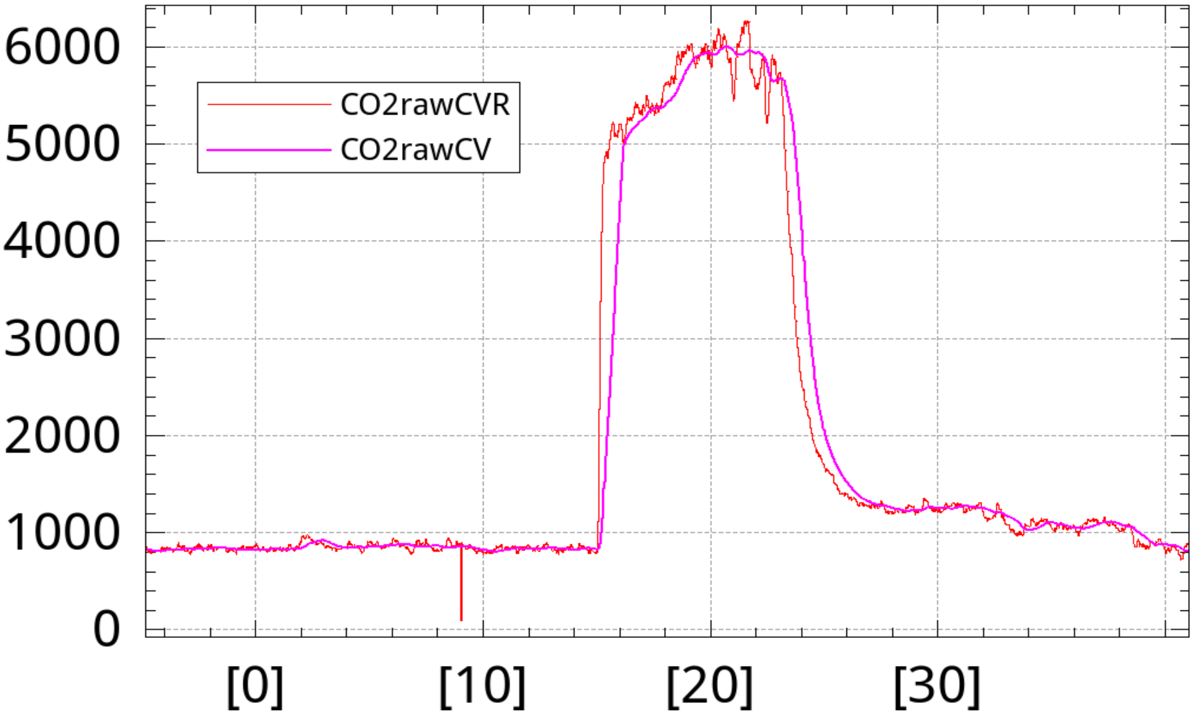

Figure 72: CO_2 (ppm) spike concentration response during the closet with fans experiment. Both filtered (CO2rawCV) and raw (CO2rawCVR) values are shown. E-nose approaches victim, then goes away.

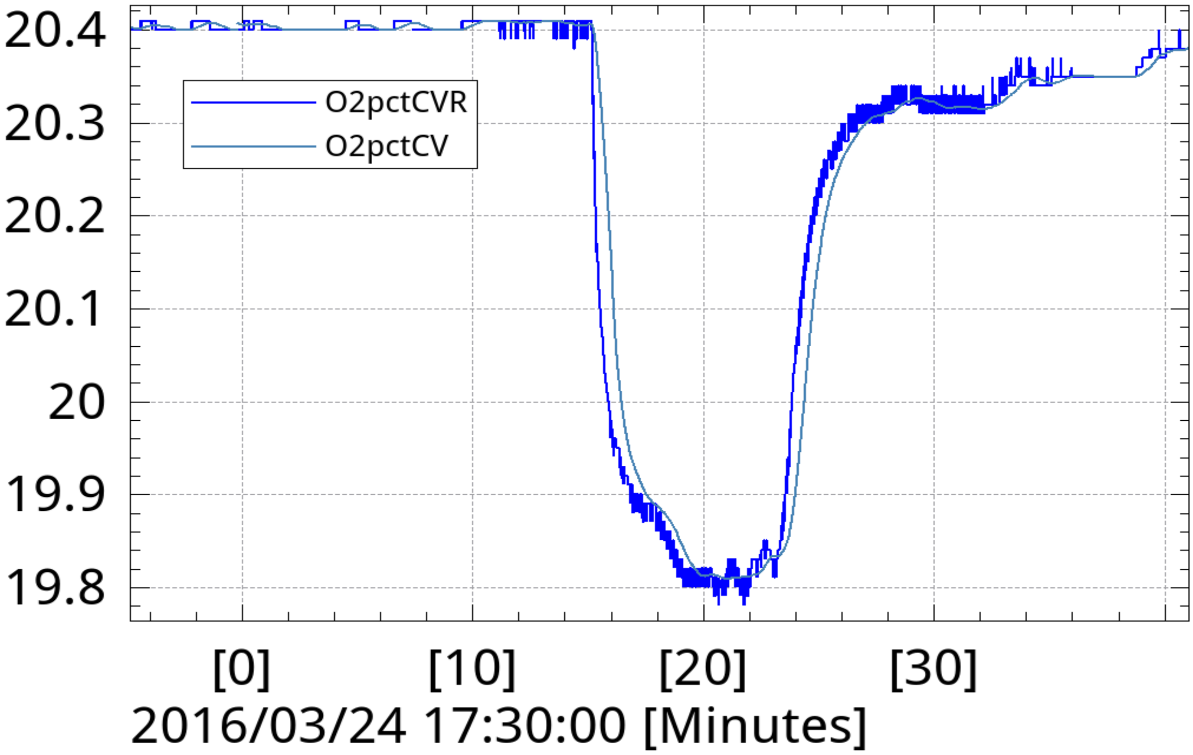

Figure 73: O_2 (%) spike concentration response during the closet with fans experiment. Both filtered (O2pctCV) and raw (O2pctCVR) values are shown. E-nose approaches victim, then goes away.

Discussion

The measurement procedure and the results are fairly accurate for at least the lower half of the fresh air flow rates. The high flow rates are probably not very accurate because parallelizing the fans in a sealed container (even with relief openings) renders the flow characteristics different than "free flow" where the fan specifications are valid. Nevertheless, it does not seem to have a considerable effect since the measurements are not very different when the flow is eased with an additional large 20x20 ventilation opening. The actual measurement values do provide indicative information regarding anticipated concentrations when there is a considerable air flow refreshing the air in a void.

In all cases, when changing the air refresh rate, there was a detectable difference in the CO_2 concentration and a corresponding difference in the mirrored O_2 concentration. In contrast, the NH_3 concentration did not alter accordingly. This is to be expected since no NH_3 is exhaled by human test subjects.

This experiment also indicates there is a chance the e-nose can detect CO_2 differences even outside the void, but very close to the opening (detection near the opening is similar to scanning on the surface of the rubble), though the conditions in this case were fairly favorable since there was no external air flow (the wind that caused the fresh air flow in void at the first place). The experiment is considered successful. The operation of the 2nd prototype is found to be sufficient for fulfilling the victim localization requirements from a sensor's capabilities perspective. The operation of the 2nd prototype's user interface and mainly the calculation of various indicators are successful. Additional work is required for the interface so that a combined view of the indicators with the measurements is presented to the operator.

7.5.4. Guard post experiment with controlled opening(s)

Objectives and Method

The objective of this experiment was similar to the experiment in the closet with the main differences being that

- Two human subjects were inside to increase the speed of gas concentration changes.

- Two ventilation openings were tested, where unforced fresh air was allowed to flow through the room (guard post) through the openings, with only environmental conditions determining its flow rate.
- Test variable filter sizes to identify optimal filters for the e-nose threshold and trend graphs.

The following pictures illustrate the test location (guard post):

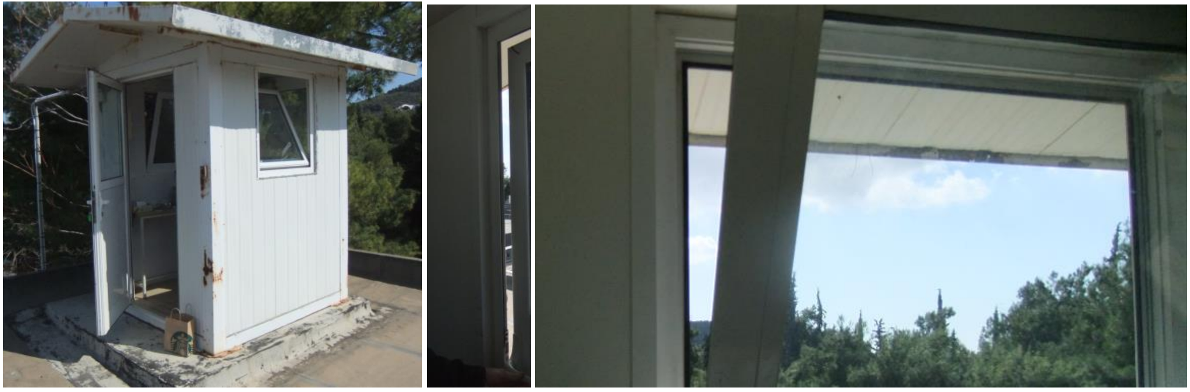

Figure 74. Left to right: Guard post with door and windows. Door and window used as ventilation openings.

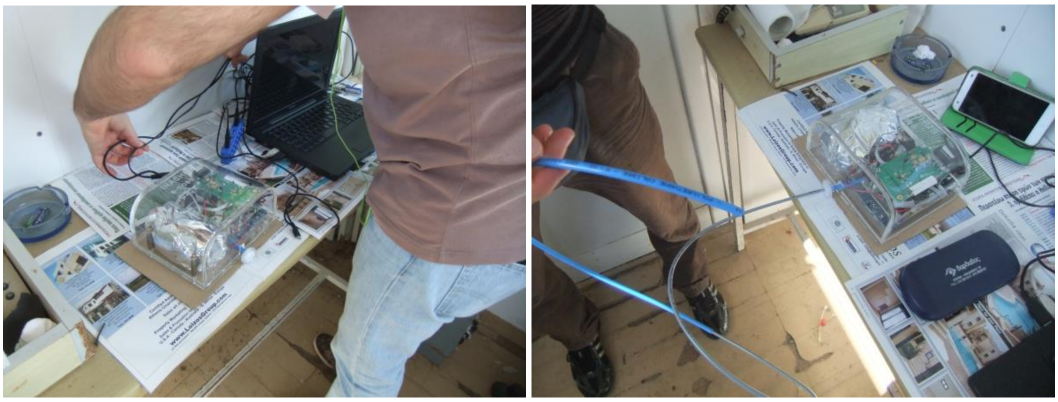

Figure 75. Left: e-nose and control interface computer. Right: e-nose and sampling tube

Figure 76. Left: sampling fresh air. Right: different ventilation parameter via different window opening

Results with filter window of 240 seconds

Similarly to previous experiments, the two openings were open and gas concentrations were monitored to see if human presence would be identified. First, a training session commenced which yielded the following results:

Table 34: Training session statistical data for guard post experiment with filter window size 240 seconds

	CO_2 (ppm)	O_2 (%)	O_2 (mbar)	NH_3
thresh signal	1323.97540	20.49457	201.43168	2.59100
trend decr	-0.35051	-0.00082	-0.00127	-

incr	0.35051	0.00082	0.00127	-

Then human test subjects were brought into the room and with the openings closed, the gas concentrations changed quickly. For CO_2 it reached a maximum of 4000ppm approximately, while for O_2 it dropped to almost 20.00%. Following that, the openings were opened to approximately one snake robot cross section width each and fresh air was allowed for a long period of time to clear the air inside the room. As the following graphs show, the CO_2 and O_2 threshold indicators correctly identified human presence (CO2rawTH, O2pctTH and PpO2TH have a threshold value of 2) even after the signals CO2rawCV, O2pctCV and PpO2CV respectively had settled into their final mixed free and exhaled air equilibrium.

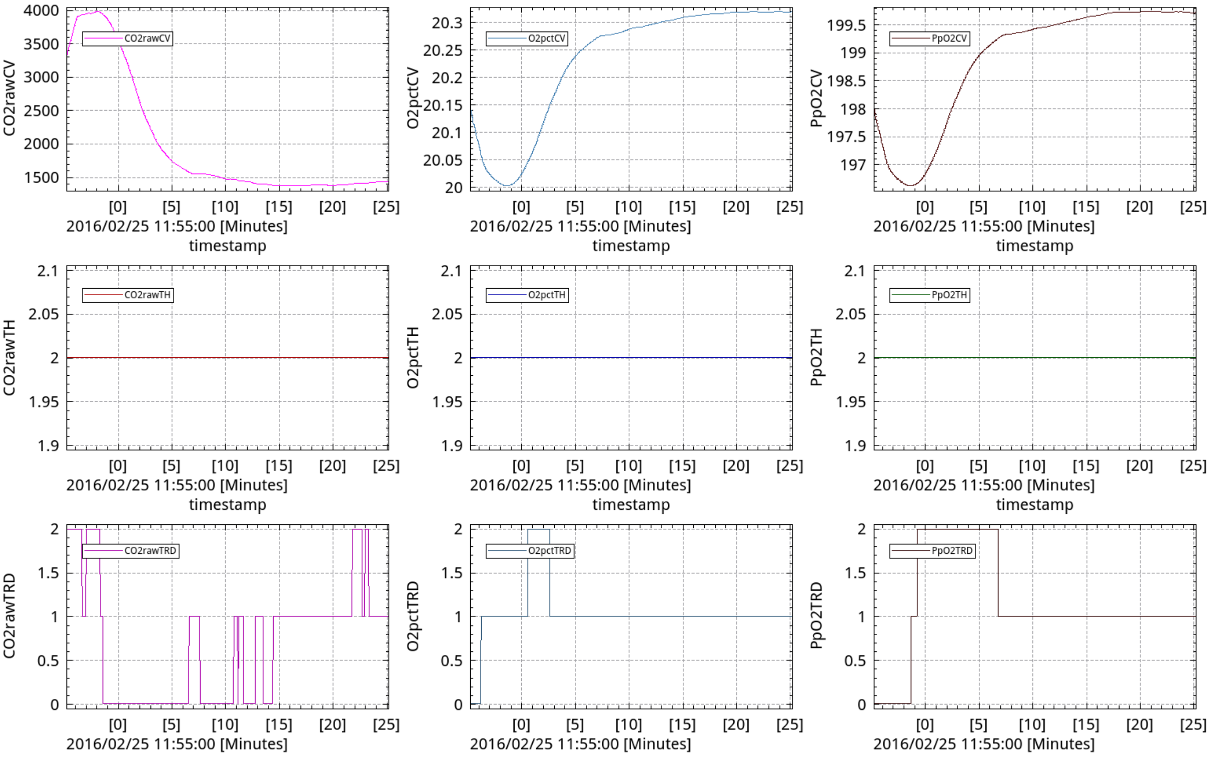

Figure 77: CO_2, O_2 (%) and O_2 (partial pressure, mbar) columns showing the current value (*CV), threshold (*TH) and trend (*TRD) indicators in three rows for the guard post large filter window experiment

Additionally, the trend indicators CO2rawTRD, O2pctTRD and PpO2TRD have followed closely the trend (slopes) of the signals CO2rawCV, O2pctCV and PpO2CV respectively.
It is stated that the NH_3 sensor correctly did not track any NH_3 presence as shown in the following graph by the threshold indicator of the NH_3 (NH3TH), even though some increase in the NH_3 was registered.

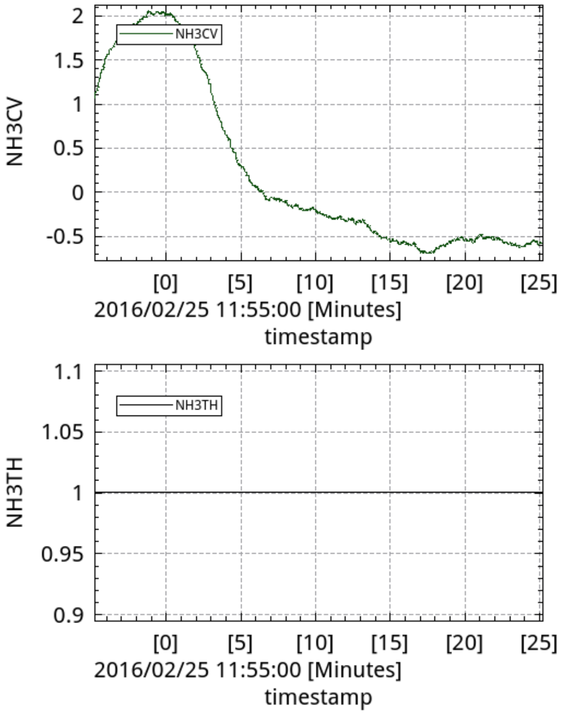

Figure 78: NH_3 (0.1ppm) concentration and threshold indicator for the guard post large filter experiment

Finally, the rest of the sensors including humidity, temperature sensors and barometric pressure produced expected results that secured the operation of the e-nose free of/ unhampered by errors.

Results with filter window of 15 seconds

To test the practical difference a filter would make in the measurements, a fairly short filter size was selected in order to test the result threshold and trend operator responses. It is noted that from filter theory, a smaller sized filter will, compared to a larger one, offer:

- faster response to changes
- allow more noise to pass through

Again, a new training session produced the following statistical analysis:

Table 35: Training session statistical data for the short filter guard post experiment

		CO_2 (ppm)	O_2 (%)	O_2 (mbar)	NH_3
thresh	**signal**	1125.13447	20.36532	200.24716	1.03805
trend	**Decr**	-3.81556	-0.00116	-0.00566	-
	Incr	3.81556	0.00116	0.00566	-

In this case the e-nose monitored (point A onward) the gas concentration changes with closed openings and at some point (B) the air sampling tube of the e-nose was removed from a small opening of the guard post so as to sample fresh air from outside of the guard post. At that point (B) gas levels dropped to a state the e-nose correctly categorized as "no human presence". Then the air sampling tube was reinserted (point C) where it reached the maximum change (CO_2 peaked at almost 3000ppm, point D). Soon after the openings (point E) were opened and fresh air mixed with the exhaled air in the guard post. After a while the air mixture settled at a level at which the e-nose still indicated human presence.

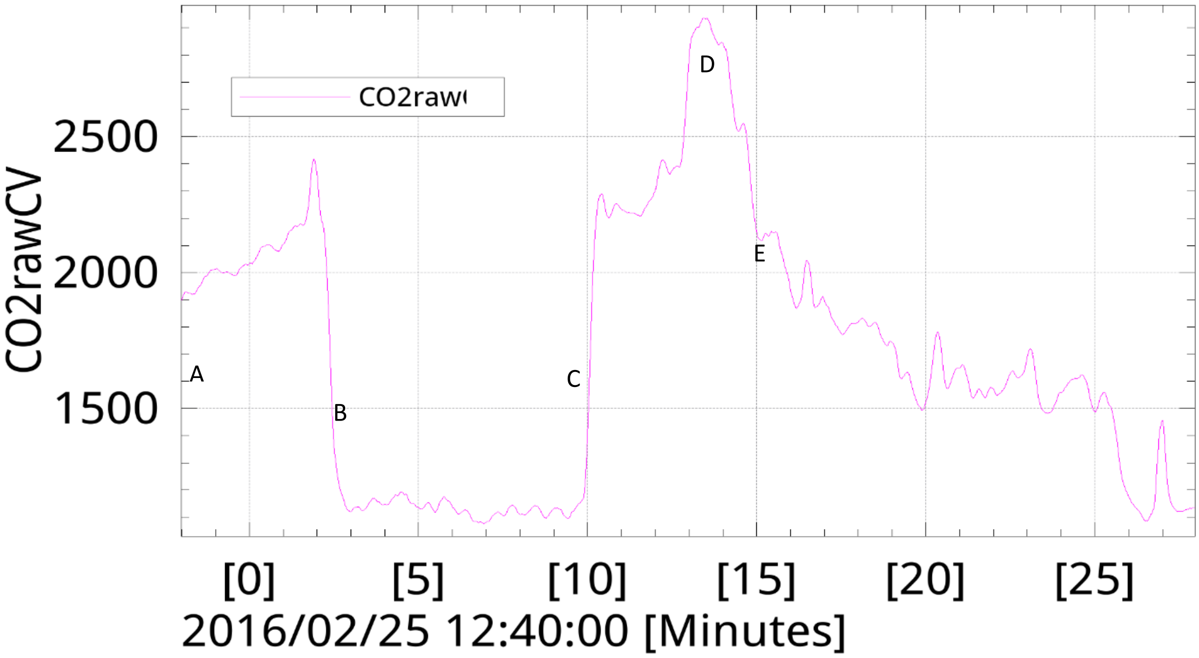

Figure 79: CO_2 (ppm) concentration response for guard post short filter experiment

Based on the measurements of the graph above, the data analysis plots can be generated (see following graph). In this case, the threshold indicators in row #2, when the e-nose air sampling tube was placed outside a small opening the indicator, showed a drop from signal – human presence value (2), to value 1 – denoting that no human presence can be identified. In fact, the edge of the tube was only slightly extended from the guard post opening so the value of threshold jumped from 1 to 2 and back, but remained mostly at value 2. However, by extending the tube even further outside the guard post opening, a tendency to remain at value 1 most of the time is shown. This discrepancy is observed mostly in the CO_2, as the O_2 is more steady at a value of 1 throughout the time frame (points B – C) where the air sampling tube sampled air from outside the guard post.
It is noted that the effects of small filter sizes, as this one, produce rapid alterations of values in the threshold indicators. These add confusion and do not allow the operator to quickly "see" where the indicator tends to settle. The confusion is even greater with the trend indicators (3^{rd} row in the following graph) where noisy input is passed through and there are more spikes with trends (slopes), rather than firm indicators of the general trend of each corresponding signal. Thus, a larger filter size is always preferable.

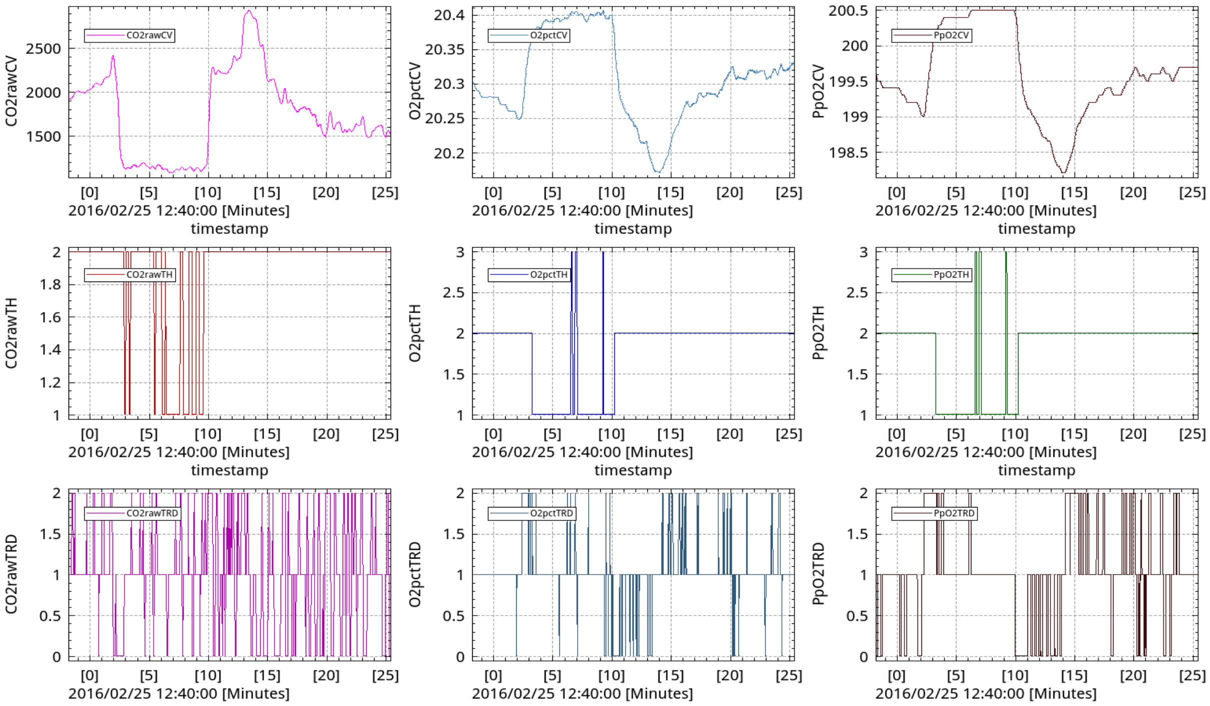

Figure 80: CO_2, O_2 (%) and O_2 (partial pressure, mbar) columns showing the current value (*CV), threshold (*TH) and trend (*TRD) indicators in 3 rows for the guard post short filter window experiment

Discussion

In this experiment the performance of the e-nose was evaluated in a medium sized cavity with two human subjects and two air openings. This configuration could allow fresh air flow paths and make it more difficult to successfully identify human presence. The size of each opening was approximately 1 robotic platform cross section so as to depict a situation where the robotic platform would enter from one opening and exit from the other. More importantly, the air would, also.

From the analysis of the results it turns out that the e-nose can successfully identify human presence even in scenarios where ventilation pathways are present, whereas it correctly identifies as “no human presence” situations when air is sampled from the environment (and not from inside the space with the subject). This is crucial for the correct operation of the e-nose in a large number of scenarios where the cavity will have multiple air ventilation holes.

As far as the filter size is concerned, it is suggested larger filter sizes be used that will produce more stable threshold and trend indicators. That is, there will be fewer fluctuations and less quick and repeated changes between indicator levels. However, too large filter sizes may affect the responsiveness of the system. As a result, a compromise must be made for the filter size. A suggestion that can conveniently be used with the e-nose is approximately four minutes of filter size. This creates non-spike-like changes in the indicator states and will also be able to respond timely in the chance that a human subject is found in the rubble. This response time has been measured to be approximately five seconds which is deemed adequately fast for the estimated robotic platform’s speed of travel.

Outdoor guard post experiment to validate theoretical model

The outdoor guard post with controlled openings (a door and three windows), allowed us to examine the influence of fresh airflow rate on concentration measurements according to the equations presented in section 6.8.

The photographs in Figure 81 illustrate the guard post test location. The dimensions of the guard post were 1.2 m × 1.2 m × 2.3 m (V_c = 2.3 m^3), simulating a medium-small cavity. The openings of the guard post were on the north side.

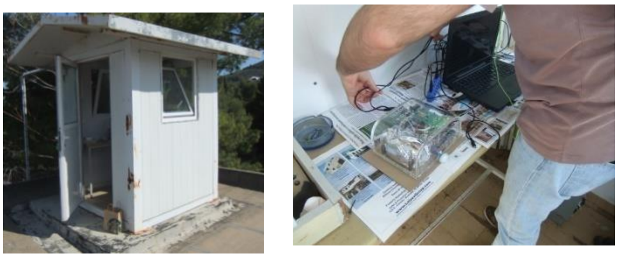

Figure 81. Left: guard post with door and windows. Right: detector device with the sampling tube and the entire measurement setup.

Part I: As in the last test, the “calibration session” commenced by taking measurements with the air sampling tube placed further from the openings of the guard post. The processed measurements yielded averaged concentrations for CO_2 and O_2, $\bar{C}_{(CO_2)f}$ =418 ppm with a standard deviation of 12.22 and $\bar{C}_{(O_2)f}$ = 20.75% with a standard deviation of 0.006 (Figure 82). At the same time the air inside the guard post was refreshed by leaving all the windows and the door wide open for 30 min, to let fresh air in and reset the concentrations within the room. By applying the values in Equations (27) and (28) and assuming that the concentrations of the exhaled breath are 40000 ppm for CO_2 (minimum) and for O_2 16% (maximum) [88]-[91], showing that the fresh air flow rate should be $F_f \leq 808\ F_e$ for the CO_2 sensor to detect a human presence in the room and $F_f \leq 324F_e$ should hold true for the O_2 sensor respectively.

Part II: This part of the test was performed with the door closed and with two human subjects inside the guard post (adult males with an expected average $F_e \approx 16.8l/min$). At the end of part I, the air sampling tube was inserted into the guard post to start the measurements for part II. The outdoor temperature was 21 °C and the wind about 8 km/h, in a northerly direction (weather report on the day and at the time of the experiment). At the beginning of the experiment, the temperature in the interior of the guard post was $T_c = T_f$ = 21 °C, but at the end it had risen to 23 °C. With the openings of the windows adjusted approximately to 100 cm^2 (A_i = 0.01 m^2), and taking into account the wind and temperature data, (26), (A_{sum} = 0.01 m^2 g = 9.81 m/sec^2, Z = 0.7 m, C_R = 0.35, v_{ref} ≈ 2.22 m/sec, ΔC_p= 0.44 - 1.51, T_f = 21 °C, and T_c = 23 °C) was applied, and an expected fresh air flow rate through the guard post of $F_f \approx 144 - 433\ l/min$ and $F_f \approx 8.62 - 25.83\ F_e$ was estimated. Then, it was calculated by using Equation (17) that the expected equilibrium concentration would be reached in 37–102 min and would be, on average, 1895–4534 ppm for CO_2 and for O_2 20.26–20.57%. It was decided to limit the duration of part II of this final test to 30 min duration, and according to our calculations, concentrations ranging between 1863–3570 ppm for CO_2 and 20.36–20.58% for oxygen could be reached. After 30 min $C_{(CO_2)c}$ reached a maximum of approximately 2604 ppm, while for O_2 the concentration dropped to almost 20.49% as shown in Figure 82, which was in accordance with our theoretical expectations.

Part III: As in the first test there was a break of 15 min duration and the window openings of the guard post were open to their maximum (expected airflow rate on average 0.84 m^3/min), which almost completely cleared the indoor air when the CO_2 concentration was reduced to 433 ppm and the oxygen concentration became 20.75%, both concentrations reaching those of the fresh atmospheric air.

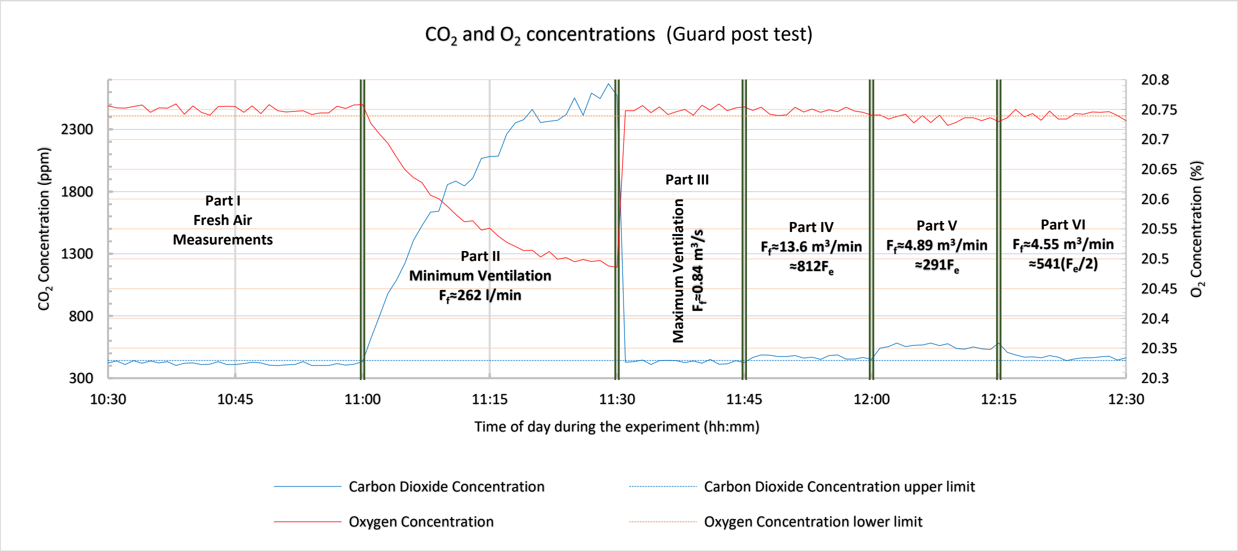

Figure 82. Guard post test measurements.

Part IV: This lasted for 15 min. The windows were closed leaving an opening with an area of A_{sum} = 0.6 m^2. At the beginning of this part of the test the temperature in the guard post was measured and was found to be T_c = T_f = 21 °C, but it slowly started to rise and at the end of this part of the test it had risen to 21.5 °C. By applying (26) (A_{sum} = 0.6 m^2, g = 9.81 m/sec^2, z = 0.7 m, C_R = 0.35, v_{ref} ≈ 0.83 m/sec, ΔC_p = 0.44 - 1.51, T_f = 21 °C, and T_c = 21.5 °C), it was calculated that the expected fresh air flow rate at that point would be about 13.65 m^3/min i.e., $F_f \approx 812\ F_e$ and according to the theoretical expectations from (27) ($F_f \leq 808\ F_e$), the CO_2 sensor should identify a human presence. In Figure 82 it can be seen that the CO_2 sensor is clearly differentiated beyond its upper limit indicating a human presence, which was theoretically expected from (28), with a value of 462 ppm. The oxygen sensor is within its noise zone with an average value 20.75%, equal to the measured fresh air O_2 concentration (20.75%).

Part V: This once again lasted for 15 min. The window was adjusted by leaving an opening with an area of A_{sum} = 0.20 m^2. At the beginning of this part of the last test the temperature in the room was measured and was found to be T_c = 21.5 °C, and slowly started to rise until at the end of part V of the first test it had risen to 22 °C. By applying (26) (A_{sum} = 0.20 m^2 g = 9.81 m/sec^2, z = 0.7 m, C_R = 0.35, v_{ref} ≈ 0.83 m/sec, ΔC_p = 0.44 - 1.51, T_f = 21 °C, and T_c = 22 °C), the expected fresh air flow rate at that point was calculated to be about 4.89 m^3/min i.e. $F_f \approx 291\ F_e$ and according to the theoretical expectations from (27) and (28) ($F_f \leq 808\ F_e$ for the CO_2 sensor and $F_f \leq 324\ F_e$ for the O_2 sensor), both the CO_2 and O_2 sensors should identify a human presence. In Figure 82, it can be seen that the CO_2 sensor is more clearly differentiated beyond its upper limit indicating a human presence, as was expected theoretically from (27), with a value of 547 ppm. The oxygen sensor also reveals a human presence, which was expected theoretically from (28), with an average value 20.73%.

Part VI: This third and last test had a sixth phase. For this last part, the openings remained the same as in the previous part, but one of the two people inside the guard post left and the exhaled air flow rate decreased to F_e ≈ 8.4 L/min. At the beginning of this part of the test, the temperature inside was measured and found to be T_c = 22 °C, which then slowly started to fall and at the end, it had fallen to 21.5 °C. By applying (26) (A_{sum} = 0.2 m^2 g = 9.81 m/sec^2, z = 0.7 m, C_R = 0.35, v_{ref} ≈ 0.83 m/sec, ΔC_p = 0.44 - 1.51, T_f = 21 °C, and T_c = 21.5 °C), we calculated that the expected fresh air flow rate at that point would be about 4.55 m^3/min i.e. $F_f \approx 541\ F_e$ thus $F_f \approx 542\ F_e$. In Figure 82, it can be seen that the CO_2 sensor is still clearly differentiated beyond its upper limit indicating a human presence, confirming the theory in (27), with a value of 464 ppm. The oxygen sensor does not however, show a human presence, which was expected from the theory in (28), since the average value was 20.74%, within the noise zone of the specific sensor used in the system with gas sensors used for these measurements.

Conclusion 3: This third and last test in the guard post confirmed the theoretical expectations and verified the analysis presented in work.

7.5.5. Controlled conditions urine detection test

The following test was performed to verify the urine detection concept. The e-nose's NH_3 sensor capability to detect and measure NH_3 is tested in a different, simple test: exposure to an NH_3 mosquito pain relief stick – and is successful. In this experiment, a confined space was created and conditions similar to human presence were simulated. In brief, the urine detection is based on detecting the ammonia generated by the bacterial decomposition of the urea contained in the urine. For this, real human urine was used. To simulate human entrapment and create more favorable detection conditions, the experiment assumes that in entrapment conditions the victim will have to excrete urine on his clothing, being unable to remove or unbutton anything. This puts a large amount of the urine in the victims clothing. Even if the victim can remove clothing, it is very possible that amounts or urine will reach the ground and then transfer back to the clothing of the victim. This soaking in the clothing aspect of the experiment is crucial because it provides key elements for ammonia generation:

1. Clothing will hold a large amount of urine and urea to "fuel" ammonia creation by bacteria.
2. Clothing in contact with human skin, especially near body cavities, is not sterile and could host the bacterial species required for ammonia generation
3. The clothing soaked with urine on the human body is a humid and warm place - very good conditions for bacterial growth

For these reasons, the test apparatus was configured to simulate these conditions as much as possible, without having to entrap an actual human, since the process could take more than a day, and the conditions would be very harsh and unpleasant for the test subject. The following characteristics of the apparatus mimic human presence in the sense mention previously:

1. A cloth was used to hold the urine sample that was tested for detection.
2. The cloth was not sterile. It could be considered spiked with many types of bacteria.
3. The cloth was held on a small temperature controlled plate. The temperature setting configured was 36.6 but the layout allowed for a nonuniform temperature distribution (is considered a positive aspect for acquiring a result, not ideal for determining the optimal conditions).
4. The cloth was not in contact with the metallic plate (heat distribution) but with a latex glove (semper care latex powder-free) that covered the heated plate. This was performed so that the conditions are more like that of human skin.
5. The ventilation conditions were reduced for the sake of reaching a detection result faster. The bag was not sealed. A small opening was left so that air could be exchanged with the environment.

The following pictures illustrate the temperature controlled plate and the plate inside a glove covered by the urine soaked cloth inside the bag used to create a confined space.

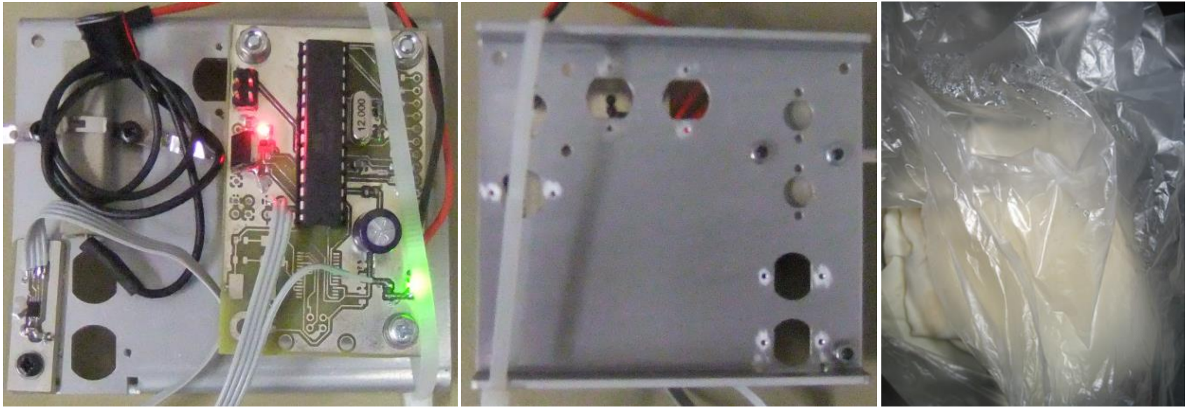

Figure 83. Heater plate with temperature controller, digital sensor, and heating resistor. Right: cloth inside bag

The following pictures illustrate the test apparatus

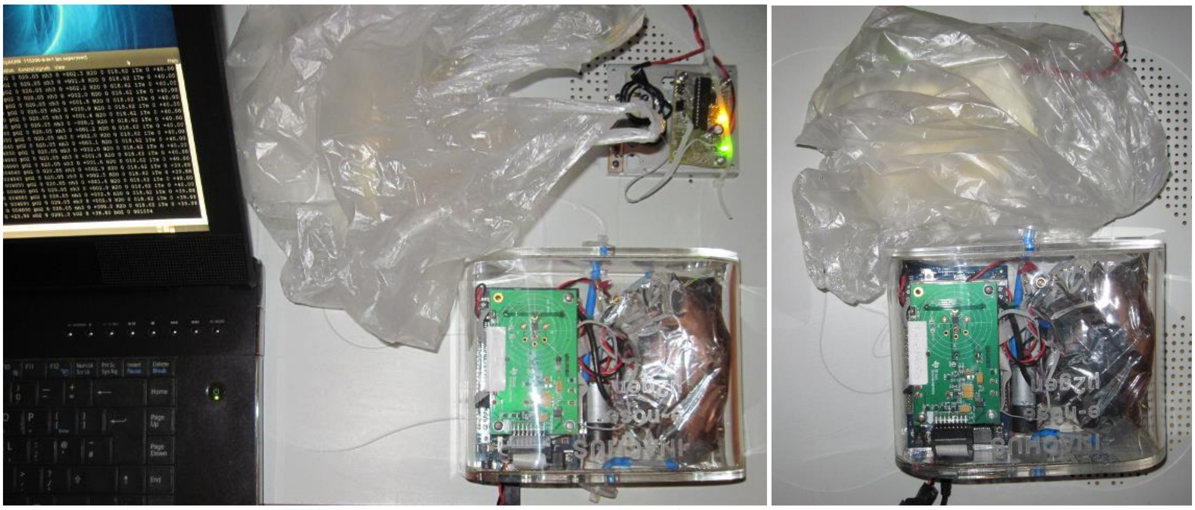

Figure 84. Left: Interface PC collecting raw measurements, 2nd prototype of the e-nose, bag, and heated plate. Right: The e-nose's input interface is placed inside the bag to take samples/measurements.

The following pictures illustrate the heated plate inside a glove and the cloth after use.

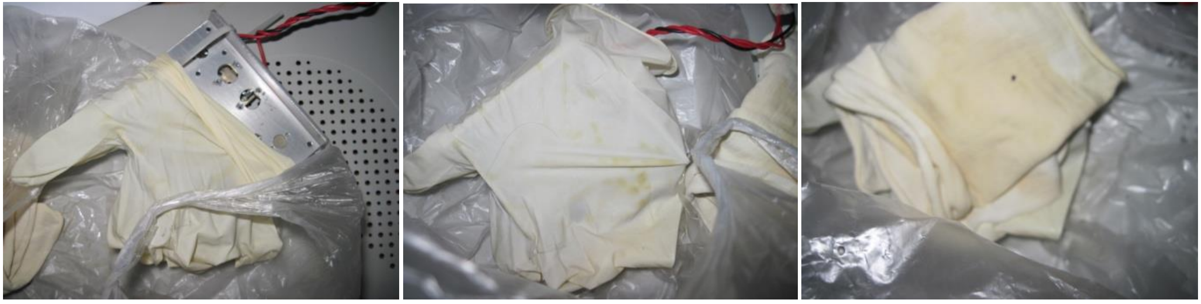

Figure 85. Left to Right: Heated plate partially inside glove, glove after experiment, cloth after experiment

The methodology for testing was the following: The temperature controlled heated plate was inserted into a latex glove, exposing only the power cable. The covered heated plate was placed in the bag. The urine soaked cloth was placed on the heated plate and the bag was closed leaving a small opening for air exchange. The progress of the air inside the bag was periodically checked by smelling (via odor). No signs of odor /malodor were detected after two days. After the third day, some odor developed but was not considered significant at the time. The cloth was re-soaked with fresh urine. After a whole week, the odor was not yet considered significant but measurements were taken.

The following picture illustrates the results of exposing the sensor to the air contents of the bag that held urine for a long period of time.

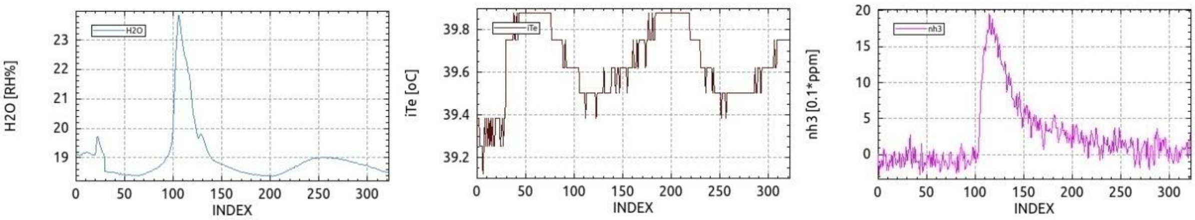

Figure 86. Right to left: ammonia measurement and detection, system temperature, humidity levels

Note that the index is the sample number and it also corresponds to seconds. Also the ammonia (NH_3) measurements are in 0.1ppm units. The peak value measured is almost 20 = 2ppm. The actual concentration is less because the sensor is operated in conditions that allow the electrochemical sensor to exhibit the largest gain (high temperature indicated by iTe measurement). The humidity content of the bag was larger than that of the environment.

For reference, the following graph illustrates the results of exposing the sensor to the headspace air of fresh urine (no PH alterations or heating performed)

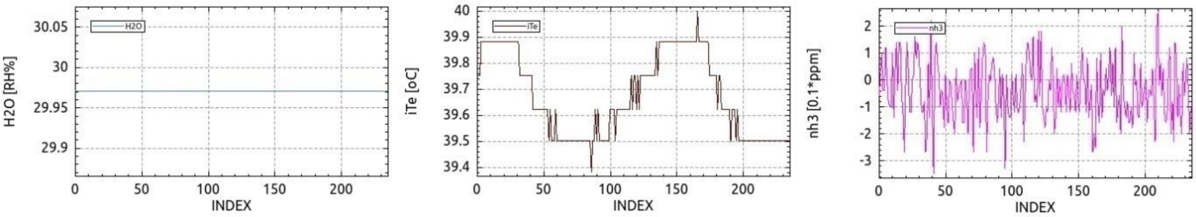

Figure 87. Headspace measurement of ammonia over fresh urine.

No ammonia was detected or measured over fresh urine with the same sensor. Note that the humidity measurements were not captured correctly (flat line) but this does not affect the ammonia measurement.

The effect of the humidity increase on the NH_3 sensor was tested by exhaling air into the air input interface of the e-nose. The following graph illustrates the results:

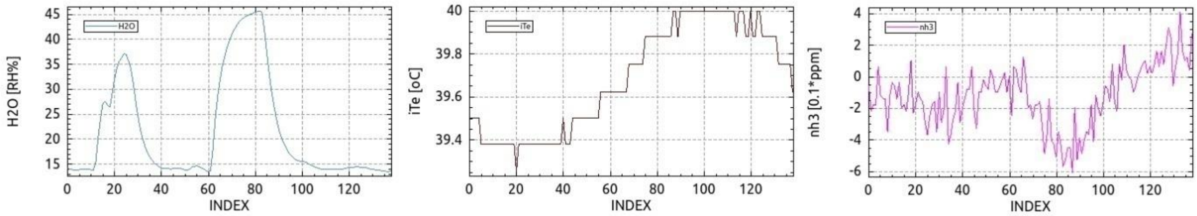

Figure 88. The increase of the relative humidity does not affect the NH_3 sensor significantly.

The momentary increase of the humidity does not affect the NH_3 sensor output significantly, thus the response from the ammonia sensor when exposed to the atmosphere of the bag with urine was caused by one or more chemical compounds.

Conclusions and Discussion: The e-nose measurement results of the ammonia sensor revealed that ammonia was present and in detectable levels inside the bag and on the cloth. Testing via odor did not reveal a hint of ammonia scent. This could be attributed to two factors. The first one is that the observer's ammonia detection threshold is higher than 2ppm, a very possible scenario since the average detection threshold for humans is reported to be 2.6ppm. Another factor could be that ammonia was not the only compound produced and that the sensor exhibits cross-sensitivity to the other compounds generated.

The e-nose's capability to detect urine as described was verified with this proof of concept test. The performance of the e-nose itself is considered to be very good. The urine detection concept with ammonia detection in this particular experiment took too long to develop since the survivability of most of the entrapped victim cases is within a smaller time frame. It is worth noting that, based on the smell testing (via odor) of the bag, the odor on the seventh day was present on the fourth day, as well, but unfortunately was not considered for measurement. Nevertheless, this was the first execution of this experiment and it was successful. Improving the (time) performance of this experiment would not contribute any significant value. Ammonia-based malodor can definitely be produced much faster (bathroom urine spills, diaper bin smell, people with urine incontinence), but such conditions were not present in this test. Measurements from actual entrapment cases should be acquired. In general, this detection concept relies on many uncontrollable factors. This is only one of the reasons why, from the conception of the e-nose's architecture, urine detection is not considered as one of its primary victim localization factors. Among the most important reasons is the fact that urine presence does not necessarily signify a live victim. Given the field of operation for the e-nose, the end-user and technical requirements and the current state of the art for ammonia detection, this, for now, is the best solution that can be provided. The limitations of the urine - ammonia detection method are clearly stated to the end-users, and are part of the specifications of the e-nose.

7.6. VALIDATION – First field test P1

The electronic nose was tested in the first field test P1, that took place in the Ågesta Rescue Centre, Sweden, at a training facility of INACHUS partner SBFF. The location had a pile of rubble that could be configured according to the needs of the tests. The objective of the e-nose test during the first field test P1 was to demonstrate its victim localization/detection functionality in favorable and realistic conditions. Such conditions are found in a poorly ventilated, confined space. To demonstrate the detection and the increase of the indicator signals, an access path was constructed leading to the confined space that contained a human. The electronic nose sampling input was introduced in the rubble at the opening of the access path and moved progressively into the confined space containing the human. The indicator signals increased when approaching the chamber opening, mostly near the opening, affected by local wind conditions. In front of the chamber opening and inside the chamber the indicator signals were the strongest and reached maximum. The indicator signals decreased when moving away from the chamber opening. In the access path, both when approaching and leaving the opening, the way the concentration was distributed depended on the wind conditions and was non-linear. The same procedure was demonstrated when no human was present in the confined space to demonstrate correctly the no detection scenario.

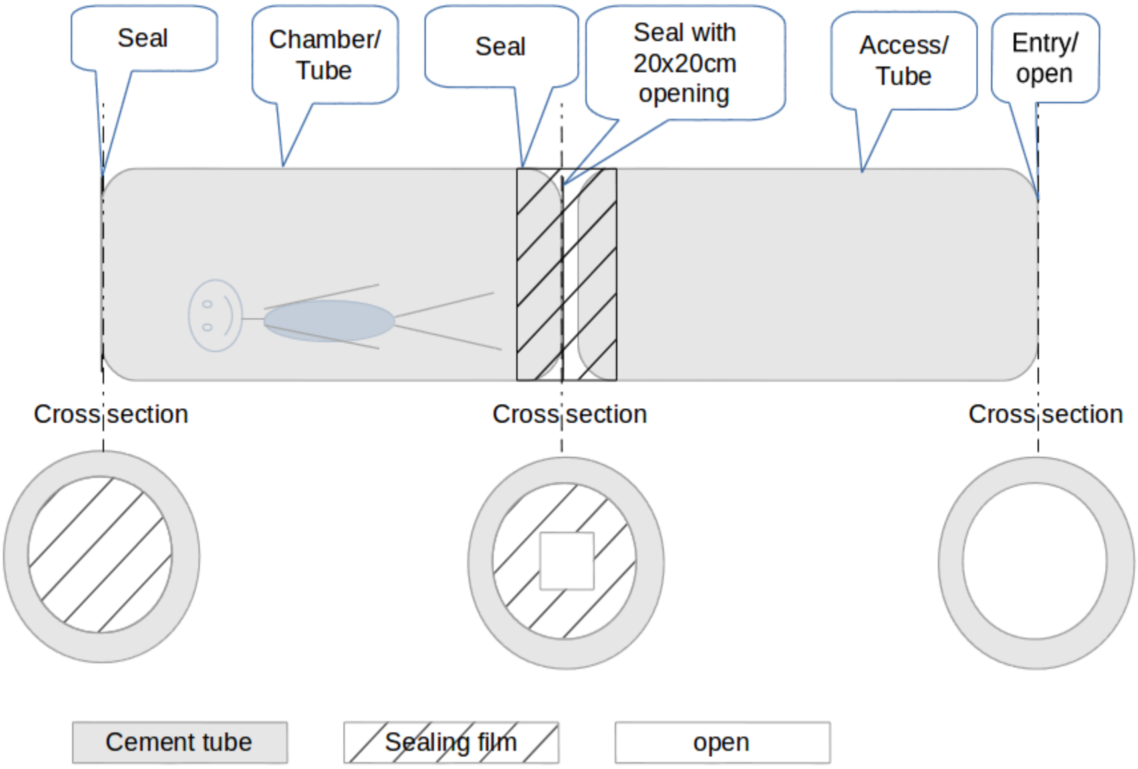

Figure 89: Confined space test site for the electronic nose during first field test P1

For this scenario the following spaces were created:

1) Chamber for the human/victim
2) Access path/tunnel to chamber

The chamber and access path were each formed within a long cement tube. The chamber had the following characteristics:

- Sealed from external air flow influences. The one end was closed (achieved with a nylon sheet held in place with a bicycle inner tube).
- An air opening of about 20x20 cm with the access path, an opening formed by a sheet of plywood.

The access path had the following characteristics:

- The connection of the chamber and the access path was sealed by using a single, long tube divided in two by a plywood barrier.

Notes:

- The length and diameter of the access tube (in the described configuration) influenced the fresh air exchange in the chamber, and reduced the effects of air flows (wind). The worst-case scenario for the e-nose is if there is no access path and the chamber opening is directly exposed to the fresh air and wind (similar to the closet experiment).
- The size of the chamber does not influence the detection because the saturation concentrations are independent of the chamber size.

- The size of the chamber influences only the time required to reach saturation concentrations.
- The size of the chamber opening influences the detection. Larger openings reduce the signal span between environment and confined space.
- The seals mentioned above were not perfect.

The following picture illustrates the anticipated response of the sensors.

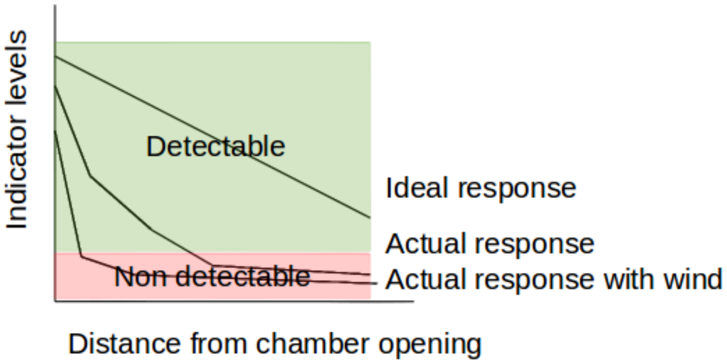

Figure 90: Anticipated response of the electronic nose when moving close to the opening of the void

The following pictures illustrate the field test site for the electronic nose. This long tube section is separated into two spaces by a wooden separator, loosely wedged in place without an airtight seal.

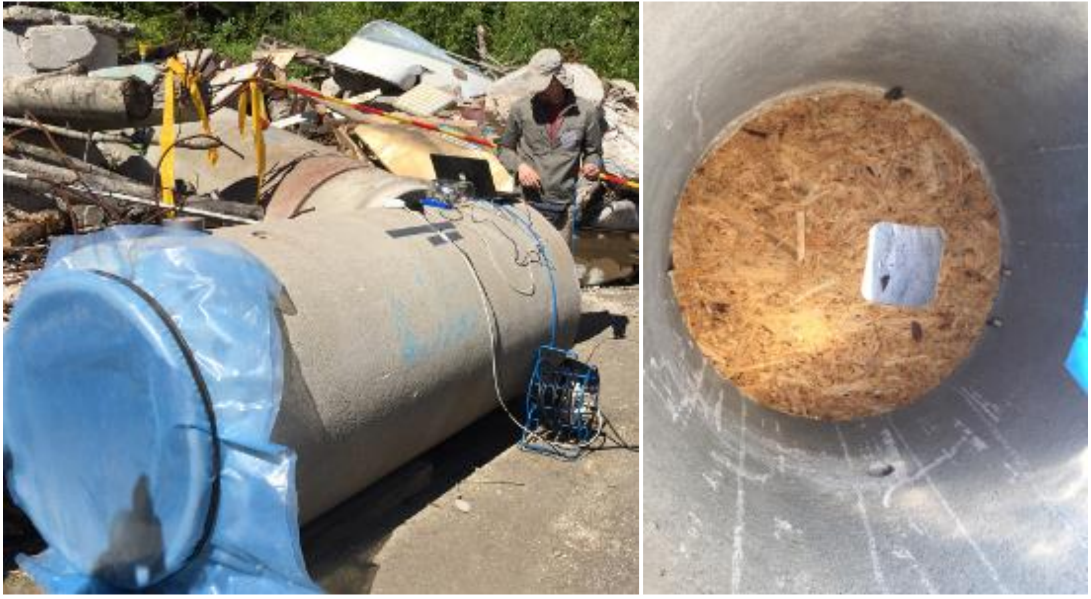

Figure 91: Left, The e-nose test site. Right, the compartment separator with a ventilation opening

A person entered the tube section, and then he was "trapped" by the nylon sheet. In case of any discomfort, the nylon could easily be pushed off by the person inside and he could exit on his own. The air sampling tube (blue) was moved towards the opening and also placed inside the compartment with the human. The response of the electronic nose was more like the one anticipated with windy conditions.

The following plots illustrate the actual response of the electronic nose during one of the tests. Reported values, from left to right: CO_2 in ppm, O_2 in %, O_2 in mbar, NH_3 in 0.1ppm

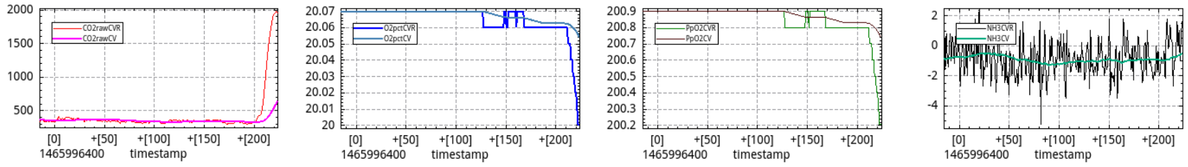

Figure 92: Inserting the sampling tube's end in the void with a victim inside

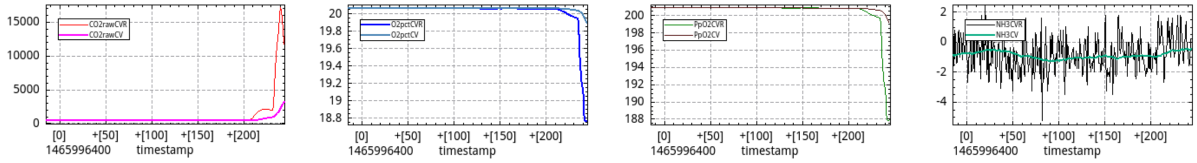

Figure 93: Blowing/exhaling in front of the sampling tube's end

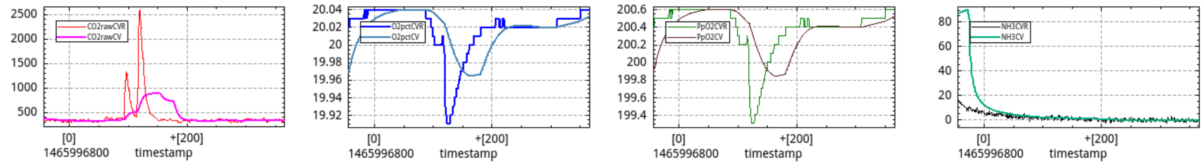

Figure 94: First peak is 20cm outside the void's ventilation opening. The second peak is inside the void

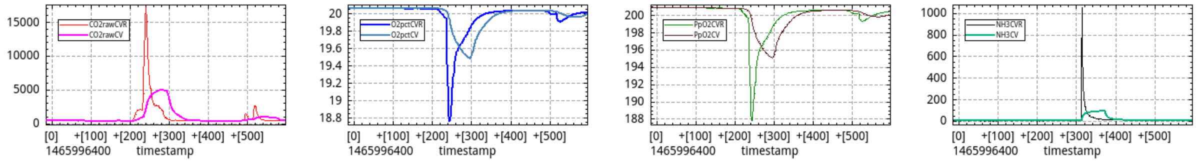

Figure 95: All the measurements of that demonstration + the response of the ammonia sensor to fumes originating from a low concentration ammonia solution.

Discussion on first field test P1 results

The victim localization capabilities of the electronic nose were successfully demonstrated in non-laboratory conditions. End-users were satisfied with that aspect of the electronic nose. The response time of some of the sensors when listed as a specification troubled them, but explaining that the response would start to develop almost immediately was adequate for their needs. End-users would have appreciated it more if the ammonia test was performed with actual urine and not with a low concentration ammonia solution. The issues and justification for not testing with actual urine are the following:

- Urine contains small amounts of ammonia, not detectable by the type of sensor utilized. The ideal (based on detection performance) sensor candidate (AIMS) was rejected due to space, weight and hazardous materials (beta particle – nuclear source) constraints.
- Urine can be detected indirectly when the urea contained in it is consumed/ decomposed into ammonia by bacteria.
- The bacterial decomposition greatly depends on the conditions present at the site.
- Simply spilling urine in the rubble is not a representative test case for entrapment conditions and the case of no detection would not have significant value. It most probably would fail for two reasons:
- Bacteria species that are capable of decomposing the urea must be present. These bacterial species are more likely to be present on a human body. Examples of such cases are: the odor people with urine incontinence might have or diaper bin odor. In both cases, the urine has been at least "spiked" with bacteria of a person.
- Bacteria thrive in warm and humid conditions such as present on or very close to a live human.
- Thus, the experiment should be performed with an actual human that urinates on himself.
- The experiment (and the human entrapment) would have to last for many hours.

The end-users did not like the very early version of the user interface that was used for the tests because it was considered too complex and too scientific but preferred the proposed mock-ups that were presented to them and described the envisioned interface at the end of the e-nose development. Based on the user input regarding the interface, the design of the control interface of the electronic nose was subjected to another design cycle to further simplify it (see 3rd prototype).

7.7. Conclusions

The 2nd prototype which was tested in non-laboratory conditions demonstrated its ability to detect human presence in the specified operating conditions. The sensor selection and system configuration proved successful for victim localization purposes and was deemed a good basis for the 3rd and final prototype. The logic (software) that processes the raw output from the electronic nose functioned properly and generated helpful output providing good indicator signals. The presentation and control interface (software), that accompanied the 2nd prototype, which was not intended to be released in that form to the end-users, served its purpose well by exposing all the system's output in a structured and compact view. It facilitated the development of the electronic nose, as well as the execution of the experiments and the quick and easy analysis of the results in real-time.

8. THIRD PROTOTYPE, VERIFICATION and VALIDATION TESTS

8.1. Overview

The latest e-nose system configuration was tested with the 3rd e-nose prototype device developed and is integrated in a robotic platform. The development of the robotic platform is not part of this work. Only the aspects of the user control interface of the robotic platform were influenced by the e-nose GUI design. The e-nose device is designed to include all the technically feasible requirements in the constrained space of the robotic platform. For these reasons, a completely custom designed device was built using only a few off-the-shelf components. The electronics and mechanical design were made from scratch. The design of the electronics started before the mechanical design, but the completion of both of them required constant exchange of information. The mechanical dimensions of the boards are a result of the allocated space and mounting positions assigned from the mechanical design. The allocated size for the boards in the mechanical design depends on the circuit complexity and the electronic component selection. Software design is relatively independent of the hardware design with the exception of the low level firmware: its design requires a completed schematic diagram and its implementation is most favorable when at least the assembled PCBs are available. The control interface software of the electronic nose that is hosted on the control interface tablet of the robotic platform is only proposed in this work. A stand-alone interface is available and used for testing purposes which includes the implementation of a heuristic algorithm for providing simple output to the operator.

The 3rd prototype's design is based on the sensor selection and system architecture of the successful 2nd prototype and implements the nonmandatory requirements that deal with safety aspects. The safety aspects that are implemented are the detection of some specific toxic and combustible atmospheres and require the addition of three extra sensors, for CO, H_2S and combustibles. The CO and H_2S sensors are two discrete sensors so that there is the flexibility, in the future, of building different configurations that can detect other gases by installing different gas sensors. The implementation of the nonmandatory safety aspects is considered to be added value for the electronic nose especially by the end-users. This added value comes with a significant cost which can be understood by the end-users in many aspects of the tool: size, weight, volume, training, operating, servicing and certification are affected. For the 3rd prototype, replacing the sensors in the field is not an option. The storage of the e-nose does not require the presence of a power source to keep the sensors biased. A combination of sensor selection and circuit design keeps the electrochemical sensors biased even without power. Little or no recovery time is needed for the sensors to be operational after storage.

Some design features were included, mainly in the electronics that would allow for the configuration of a stand-alone e-nose with the utilization of some additional modules. These features allow the connection of external devices to serve as the user interface. A tablet could be connected to one of the serial communication ports or a low-cost dedicated interface with buttons, LED indicators and a buzzer could be connected to the exposed General Purpose Input/Output pins available at an expansion header and the extra actuator output (speaker). The possibility of implementing a stand-alone e-nose sensor was investigated and a high level solution was proposed, but it was partially implemented just for collecting data during hazardous gas measurements.

A detailed description of the hardware and software of the 3rd prototype is included in the following sections.

The material is presented in the following order: Initially, the feasibility analysis of the requirements is presented. Then, the hardware aspects are presented and after that the software aspects. Hardware is considered to be the electronic circuit boards and the mechanical design and manufacturing. Software is considered to be the low level firmware running on the circuit boards, the advanced logic unit (generating the indicators) and the GUI running on the interface PC. Finally, the various tests are presented. These include verification tests and field tests. The field tests are the validation tests because the functionality of the e-nose was validated by end-users in realistic conditions.

Requirements feasibility analysis and implementation

Sensors and output

The system must detect oxygen levels to aid in indicating human presence, or the presence of hazardous levels of oxygen (Mandatory). The e-nose includes an O_2 sensor that can measure in the range: 0-25%

The system must detect carbon dioxide, to aid in indicating human presence or the presence of hazardous levels of carbon dioxide (Mandatory). The e-nose includes a CO_2 sensor that can measure in the range: 0-20%. Higher concentrations of CO_2 gas will not harm the sensor. In this case the sensor will return the maximum output value.

The system must detect ammonia, to aid in indicating human presence related to body fluids (Mandatory). The e-nose includes an electrochemical NH_3 sensor that can measure in the range 1-100ppm for indirect urine detection: The urea in the urine has to undergo bacterial decomposition producing the by-product of NH_3. The effectiveness of the process has a strong dependence on the conditions inside the rubble.

The system must detect flammable gases (Interesting). The e-nose includes a combustibles gas sensor that can detect both LPG and LNG and is sensitive to other combustible gases. To acquire reliable measurements, the sensor must be operated as a typical combustible gas detector (calibration, bump testing, and search pattern). The target gas must be selected by the operator so that the correct concentration is reported and the correct alarm threshold is used. The electronic nose cannot name the type of combustible gas that is activating the combustibles sensor's output.

The system must detect toxic gases (like H_2S and CO) (Interesting). The e-nose includes an electrochemical CO gas sensor and an electrochemical H_2S gas sensor. To acquire reliable measurements these sensors must be operated as a typical toxic gas detector (calibration, bump testing, and search pattern).

The systems' feedback must be presented in user-friendly format (Mandatory). The e-nose's advanced control logic provides plots of the measurements of the sensors up to the current time frame. It also features real-time data analysis logic to generate indicators to assist in the search.

The system's false alarms cannot be more than 10% (Important). The quality of the e-nose output signals depends on the quality of the search pattern, the alarm trigger thresholds set by user and the operation in specified conditions. This requirement is enforced by filtering the sensor outputs to smooth out noise. A single sensor value exceeding the threshold will not trigger an alarm. Taking into consideration the nature of gas sensing, alarm conditions occur when the concentration is above (or below) a threshold and maintains this state for some consistent number of samples. Gas sensing alarms for safety reasons, from an instrument's point of view, are not an event that can be missed if the sampling rate is not fast enough. They are conditions that are constant and observed over long periods in time. In some cases, though, there is a possibility of false negatives meaning that the alarm is not triggered while the alarm condition is present in the void but not in the sampled air. An example for this situation is when a gas leak of Liquid Petroleum Gas (LPG) does not mix with the air because it is heavier and moves towards the ground. A good search pattern must scan/sample from the ground to the ceiling, in the specified speed due to sensor response time, to properly clear the area. Performing a scan by simply going through the void or even scanning the e-nose in the vertical axis too fast might not detect the condition. Even if a slow scan is performed, there is still a chance of a correct negative explosive atmosphere output when the atmosphere is completely filled with an otherwise flammable gas. This is true because in most cases oxygen is required for combustion. Also, the sensors must be properly calibrated. Before deployment in the rubble, a bump test should be performed. Failing to do so affects the validity of the sensor outputs. Such cases are beyond the control of the e-nose and are not considered as false alarms.

The system's accuracy must be in the range of one to two meters (Interesting). This requirement is not feasible or applicable to the e-nose. Localization accuracy is not applicable to the e-nose because it can only provide information about the air it samples like a search dog does. The localization information is inferred during/after the search is performed, as is the case with the search dogs. The maximum (or minimum) concentration of a gas can be detected and indicated. It is the operator's responsibility to interpret the results into localization information based on his understanding of the situation/conditions at the search site, again as is the case with the search dogs.

The sensor data must be archived (Important). All the input/output to/from the electronic nose is logged in a human readable format. The logs are maintained by the electronic nose's Advanced Logic Unit software.

Data format must be qualified for sharing (Important). The data output (measurements) format of the e-nose is in a readable text format, although this is not required. Readings can be opened with spreadsheet software. All the input/output to/from the electronic nose is logged in a human readable format.

The e-nose device must not contain flammable and nuclear substances, in order to avoid explosion in confined spaces and transportation issues (Mandatory). This requirement is met by selecting sensing technologies and sampling methods that do not involve nuclear or flammable substances. This has implications for the performance. The suitable technologies do not perform the same, mostly affecting the sensitivity and limit of detection for some gases/chemicals. More specifically, this technical requirement bans the use of AIMS (Aspiration Ion Mobility Spectrometry) because it has a beta particle emitter source, and narrows down the target gases/chemicals that can be used as indicators of human presence.

The system must trigger an alert/alarm on the user interface when it detects air that is above/below a particular threshold (Mandatory). The alarm thresholds according to literature and proposed to the end-users, for various gases are listed in the following table.

Table 36. Alarm thresholds proposed to the end-users

Compound	CO	CO_2	O_2	H_2S	Combustible gas
Threshold	> 50 ppm	>1%	< 20%	>5 ppm	>10 %

The implementation of this general requirement is feasible. The advanced control logic of the e-nose is capable of detecting the alarm conditions and triggering the appropriate user interface alarm mechanism.

Operational conditions and controls

The e-nose device must work in extreme temperatures (Important). This requirement is met by selecting components that can work in extreme temperature conditions, at least the ones critical for start up. After start-up, the e-nose has a heater and temperature sensors that operate in a closed control loop to maintain the temperature at a constant set-point. The e-nose system can work in extremely cold conditions this way. Maintaining a constant temperature at extremely hot conditions is not possible. All the components can operate up to temperatures of 45°C with the exception of the NH_3 electrochemical sensor that is rated to a temperature of 40°C. Sensors with a higher temperature rating exist but do not offer the same performance for sensitivity and zero point stability. The electrolyte of the sensor is more hydrated and the filter more permeable, rendering it more sensitive and, at the same time, susceptible to electrolyte evaporation if operated for a prolonged period in high temperatures. Theoretically, the sensor can operate for a short time, such as a USaR operation, in higher temperatures, but this requires negotiation with the sensor manufacturer to determine its performance.

The e-nose device must be able to be remotely powered ON/OFF (Interesting). This requirement is fulfilled by implementing various stand-by modes. In each mode, a number of functions within the e-nose are stopped. It is implemented this way because completely powering OFF the e-nose might require the execution of many of the start-up procedures performed before deployment inside the rubble.
The functions that can be powered OFF without causing too much interference are:

- The sampling of air by stopping the pump while sampling of sensors is active,
- The sampling of air by stopping the pump and the sampling of the sensors.

The functions that can be powered OFF but can cause a great deal of delays are:

- The temperature control loop by turning off the heating resistor. This will allow the sensor cluster to cool down if the external temperature is low and will require some time before the sensor can function after it is powered ON again.

Completely powering OFF can cause some irregularities in the output of some sensors because they contain internal logic that has to settle/converge.
The e-nose is designed to be able to recover its operation if power is cut and then powered ON again. The penalty in this case is a delay until the e-nose heats up and can safely sample air again and some irregular sensor readings from some sensors.

The e-nose device must be water resistant (Important). The e-nose has water protective filters on the air interfaces to meet this requirement. The e-nose pump should not be operating when large quantities of water are anticipated to splash the air sampling port, in order to avoid filter blockage. If a blockage occurs, the e-nose is capable of detecting it, but it is not possible to resolve the issue without user intervention. If a blockage occurs the filters should be changed.

The e-nose device must work in various types of USaR environments (Important). The e-nose cannot operate in environments that have contaminants, because it samples air. If the e-nose is contaminated (0.2 Micron filters) all the air components must be decontaminated or discarded. Components that can not be decontaminated include the sensors and possibly the pump depending on the decontamination protocol required. The e-nose can be operated in these conditions, but the operation cost could be high since all the air components might have to be changed. This is not an issue because the cost is within acceptable limits (estimation). Such environments are HAZMAT and CBRN environments that have contaminants. All the air components must be changed in such cases so that any contaminants absorbed in one deployment are not released somewhere else. Special handling and servicing procedures must be followed because contaminants can be inside the air system. Operation in radiological and nuclear environments is not reliably possible because the electronics are not radiation-hardened. Operation in environments with very low oxygen levels is possible but some sensor outputs will not be valid. This condition will be detected and the operator will be informed. Operation in environments with fires or smoldering fires is possible, but victim localization features will have reduced performance. Operation in environments where oily substances are anticipated to flood the air sampling interfaces is not possible. Also, the presence of fires, including smoldering ones, can interfere with sensors directly or indirectly. Many of the sensors require the presence of oxygen for them to provide a correct output because the principle of operation is based on the target gas being oxidized. The e-nose includes an oxygen sensor and can detect when there are low levels of oxygen, indicating (with an alarm) that other readings are not valid.

The e-nose device must be able to work in various weather conditions (Important). The e-nose operation should be within specified temperature conditions. Operation of the sampling pump should be stopped when it is anticipated that the e-nose air sampling interfaces will be submerged in filter clogging quantities of substances. The e-nose will not be damaged in these cases, but its functionality will temporarily be impaired, until the filters are changed. This condition is detected by the e-nose. Particles above 0.2um can be stopped by the filters. Smaller particles cannot be filtered.

The set-up time of the e-nose system on the disaster site should be within 15 minutes, including sensor calibration time (Important). The fulfillment of this requirement might not always be feasible in extreme conditions. The e-nose requires time to warm up after it is turned ON. After it warms up, some time is required to perform sensor bump tests, auto-calibration and reference measurements acquisition.

The warm-up time is required to heat the gas sensor cluster manifold from the environment's temperature to the preset temperature setting. The time required, where no user intervention is needed after turn ON, depends on the initial temperature. In very cold weather this time is long, in warm weather this time might even be zero. The warm-up time is also affected by some design choices (compromises) made. The heating power is kept low to maintain the e-nose's power requirements low. Another factor for this decision is the stability of the temperature control loop.

After the e-nose has warmed up, the user has to perform bump tests of the sensors to ensure that the system provides valid measurement readings. The e-nose's air input sampling port has to be connected via a tube to a sample holding chamber (or bag). For each sensor, a known concentration of the target gas is placed inside the sample chamber and sampled by the e-nose. The target gas sample is provided by either breaking an ampoule inside the chamber or flushing/filling it from a compressed canister (spray). The measurement observed for each execution must be within the acceptable tolerance limits for the sensor. This time can be shortened by omitting the bump test of some sensors if their output is not required.

The e-nose device should be serviceable. For example, access is needed to the dust filter of the e-nose sensor for cleaning purposes (Mandatory). The e-nose provides field access only for changing the air filters. Access to the gas sensors is not provided during deployment. All sensors are included in the e-nose and there are not any other sensor types that can be installed. Installation of new sensors (of the same type already installed) is possible.

The e-nose system should be able to be transported on commercial flights (Mandatory). For the e-nose, calibration gas mixtures in compressed canisters might not be allowed (depending on the target gas). Ampoules for bump testing mixtures can be the solution, but the allowed quantity could be an issue.

The e-nose system should be developed to comply with INSARAG Guidelines (Mandatory). The system is a research prototype development, not a commercial product. It does not hold any certifications but was designed considering the requirements for ATEX certification.

Ethical Requirements

The e-nose system should be developed following privacy by design/by default (Mandatory). Privacy and data protection issues were taken into account already in the design phase of the system. Data generated from the e-nose does not contain private data or data that can be used to discriminate.

The e-nose system should have sufficient accuracy of the data on the victims (Important). Data to be collected and stored on trapped victims (sensors, voice, pictures) should be accurate and detailed enough for medical people to estimate the health situation of the victim, as well as for rescue people to take into consideration cultural aspects of dignity (e.g. when rescuing Muslim women or dead people). No health information can be provided by the electronic nose in the way it is used.

The features and restrictions of the system should be clearly stated (Mandatory). The system should provide various users general information on its various features and restrictions (not only the information how to use it). The feasibility analysis of the requirements clarifies the actual capabilities of the system and tries to identify end-user expectations that could be misinterpreted.

Training Requirements

End-users require that there is training material for the e-nose system. This training material must *be tool specific, oriented to the role of the end-user it is intended for (Technical Search specialist), allow for training delivery both in face-to-face learning in classroom setting, and as e-learning (on-line training), with different types of training material, including instructional 'how-to' videos for training on the use of technical tools. Training and user guides to be developed must be as simple as possible, with graphics, clear symbols and easy-to-understand language. Pocket-sized instructions on the use of the e-nose must also be created. The training material for Technical Search Specialists and Maintenance teams must include tool documentation (in order to fully understand functionality, to be able to diagnose problems in case of malfunctioning and to be able to carry out basic 'instrument resets' and/or repairs). Users prefer shorter training over longer training (such as half day training instead of training that takes a week).*

It is estimated that the required training for the e-nose system can fulfill most of these requirements with the exception of the short training duration example of half a day. This is because of the requirement of training for servicing and troubleshooting the e-nose system which is a complex system.

Feasibility analysis conclusions

The design and implementation of the e-nose has taken into account all the requirements and aimed at fulfilling all of them, even the ones characterized as interesting. The fulfillment of all the requirements for the e-nose was very difficult because many of the requirements are antagonistic and a working combination/compromise has to be found. For the final e-nose system prototype, even though no cost/price requirement is set, effort has been made so that the resulting designs and materials are manufacturable with typical manufacturing processes and the assembly is not complex. The cost for operating the e-nose system depends on the conditions. There are a number of consumables that have to be replaced, including some of the sensors, as well as various accessories for bump testing and calibration. The e-nose is based on industry-proven sensor technologies that mandate specific procedures in order to ensure readings are valid. There is no way around these procedures, especially if the e-nose is also utilized for safety purposes, in addition to victim localization. There is a trade-off between the capabilities and number of features on the one hand, and the ease of use, training time and cost on the other.

8.2. Electronics of the 3rd prototype

The design of the electronics for the 3rd prototype was based completely on custom PCB boards because the integration of off-the-shelf boards was not feasible; none exist that can fulfill the requirements. The design approach for the 3rd prototype electronics was based on the following general requirements:

- Minimize the noise susceptibility of the analog signals – sensors so that the system can achieve the performance goals.
- Minimize the size of boards and at the same time
- Facilitate the overall size reduction by providing more easy-to-place board sizes for the mechanical design.
- Place all the components of the electronic nose in a single compartment.
- ATEX compatible.

The resulting scheme involved breaking up the main functionality into two boards, namely Analog PCB and Digital PCB (or control or microcontroller) PCB. It was also deemed necessary to design some other small boards that host mainly sensors and provide mechanical support and electrical connectivity. Interconnection between the various components is performed with ribbon cables when the power requirement allows for it.

Component selection

The selected CO_2 sensor is based on NonDispersive InfraRed (NDIR) technology, because of the several competitive advantages of these sensors and taking into account the lenient sensitivity requirements. They are small, in the low-medium price range, selective, have a very fast response, a good long-term stability, low power consumption, and fair sensitivity. The CO2F-W from SST Sensing Ltd is a compact and high speed (20 Hz) CO_2 sensor ideally suited for applications which require the capture of rapidly changing CO_2 concentrations. This CO_2 sensor requires on average less than 15mA of current at 3.3 V. It provides digital TTL output and detects CO_2 levels in the range 0–200,000 ppm (0-20%), with an accuracy of ±50ppm @400ppm. Fluorescence-based optical sensors are usually used for oxygen detection, are small in size, available in the low-medium price range, have a good long-term stability and lifetime, exhibit low power consumption and negligible cross-sensitivity to other gases. Other oxygen measurement sensor types exist but do not offer a digital interface, faster response time, or long operating lifetime. The selected LuminOx LOX-02 O_2 sensor is a compact Fluorescence-based Optical Oxygen Sensor. It consumes less than 7.5mA of current at 3.3 V, provides digital TTL output and detects O_2 levels in the range 0-25%, with a resolution of 0.01%. The NH3-3E-100-SE from City Technology is an Amperometric electrochemical 3 electrode sensor cell designed for NH3 detection. It has a sensitivity of 100-160 nA/ppm NH_3, a bias voltage of 0 mV, and a resolution of less than 1 ppm is typical. The H_2S sensor is the AC200-800 3 terminal, 20mm diameter, electrochemical cell H_2S 4H CiTiceL gas sensor. It is rated for operating in the 0-100ppm concentration range, can handle a maximum overload of 500ppm, has a 30s response time and a 0.1ppm typical resolution. The CO sensor is the 2112B2055R 3 terminal, 20mm diameter, electrochemical cell, 4CM CiTiceL CO gas sensor. It is rated for operating in the 0-2000ppm concentration range, has a 10s response time, a 90s recovery time, a 1ppm resolution is typical, and has an acid gas filter rated for 20000ppm hours. The combustibles sensor is the PM493-000 PELLISTOR 4P75 combustible gases sensor. It functions in the 0-100%LEL range for a variety of combustible gases and includes an H_2S filter rated for 1000ppm hours. For measuring humidity the Honeywell HumidIcon HIH8120-021 is used. It operates in the 10-90% RH range and has a ±2% accuracy. Its interface is an i2c digital output with up to 14 bits of resolution and consumes 1 mA of current at 3.3 V. For measuring the temperature inside the device, NXP's PCT2075 sensor was chosen. It is capable of measuring temperatures in the range -25 ^oC to +100 ^oC with an overall accuracy of ±1^oC. It has an i2c digital interface with 11 bits of resolution and consumes 70 μA at 5 V when sampling and 1μA in standby. For the external air temperature measurement TI's TMP112A temperature sensor was selected, featuring an accuracy of ±1^oC in the -40 ^oC -+125 ^oC temperature range. It has 12 bits of resolution and the digital output is communicated via an i2c interface, consuming 10 μA at 3.6 V when sampling and 1μA in standby. The air pump used to force air through the air filters and over the sensors is Parker's T2-03 micro diaphragm pump, with a free flow rate of up to 2.5 LPM. It can operate in the 0-8.4 V range with a current consumption in the range of 25-390 mA. The THS2518RJ 25 Watts 18 Ohm wire-wound, chassis mountable, power resistor is used as a heater and is operated at 0-5V. The hydrophobic air filters used to protect the sensors from dust, debris, and water are the Qosina 28213 17mm diameter 0.2 Micron PTFE inline air filters. The barometric pressure measurement capability of the O_2 sensor is also used to detect filter blockage. The control microcontroller is the AT32UC3B0256 32 bit microcontroller from Microchip with 256KB flash memory and 32KB ram memory and a plethora of peripherals. Ethernet communication is provided by the Lantronix xpp1003000-02r Ethernet to serial device networking module.

Electronics description

Block diagram of Figure 96 illustrates the main functional blocks of the electronics. Each rectangular block represents a single PCB. The Microcontroller board hosts the control microcontroller (Figure 99), the Ethernet module, the required power supplies and the power electronics for controlling the actuators (Figure 98). The analog board hosts the analog gas sensor biasing and readout electronics (Figure 97). It also facilitates their mechanical support. For the electrochemical analog gas sensors a potentiostat Analog Front End (AFE) IC is used to bias each sensor. The combustibles sensor is pellistor-based and a fine tunable, via a multiturn potentiometer, voltage divider is used as a reference voltage for the readout. A multichannel ADC is used to read the output voltages of the readout circuits. AFE configuration is performed over the i2c bus while the ADC communicates through the SPI bus. Interconnection between boards is achieved with flex cables and connectors when possible (Figure 100). The analog board is used as a pass through path for the communication busses of the digital sensors that are located inside the air manifold.

The following pictures illustrate the schematic diagram of the custom boards of the 3rd prototype:

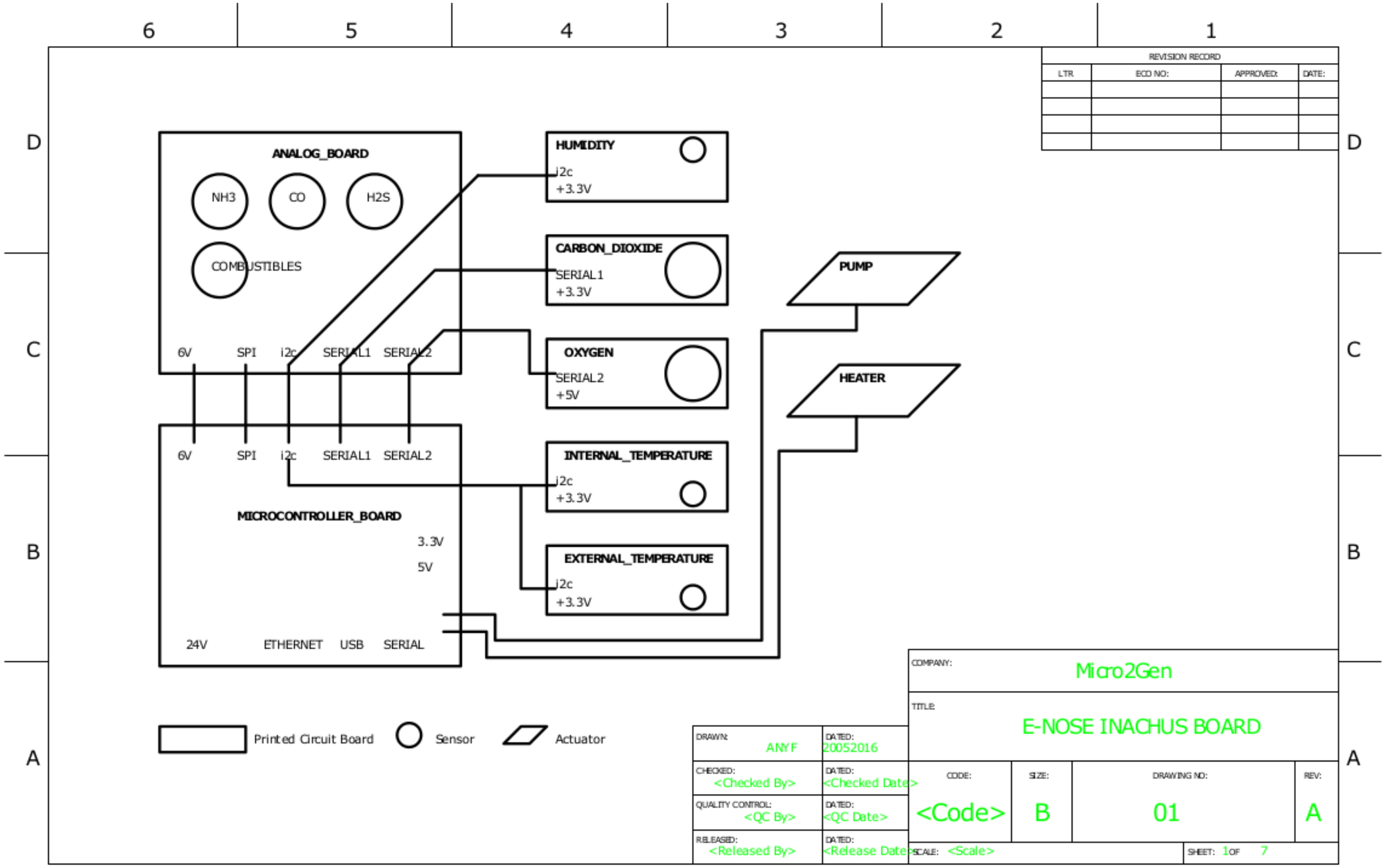
6
5
4
3
2
1
D
C
B
A
REVISION RECORD
LTR
ECO NO:
APPROVED:
DATE:
ANALOG_BOARD
NH3
CO
H2S
COMBUSTIBLES
6V
SPI
i2c
SERIAL1
SERIAL2
MICROCONTROLLER_BOARD
3.3V
5V
24V
ETHERNET
USB
SERIAL
HUMIDITY
i2c
+3.3V
CARBON_DIOXIDE
SERIAL1
+3.3V
OXYGEN
SERIAL2
+5V
INTERNAL_TEMPERATURE
i2c
+3.3V
EXTERNAL_TEMPERATURE
i2c
+3.3V
PUMP
HEATER
Printed Circuit Board
Sensor
Actuator
COMPANY:
Micro2Gen
TITLE:
E-NOSE INACHUS BOARD
DRAWN:
ANYF
DATED:
20052016
CHECKED:
<Checked By>
DATED:
<Checked Date>
QUALITY CONTROL:
<QC By>
DATED:
<QC Date>
RELEASED:
<Released By>
DATED:
<Release Date>
CODE:
<Code>
SIZE:
B
DRAWING NO:
01
REV:
A
SCALE:
<Scale>
SHEET:
1 OF 7

Figure 96. Interconnection diagram the 3rd e-nose prototype

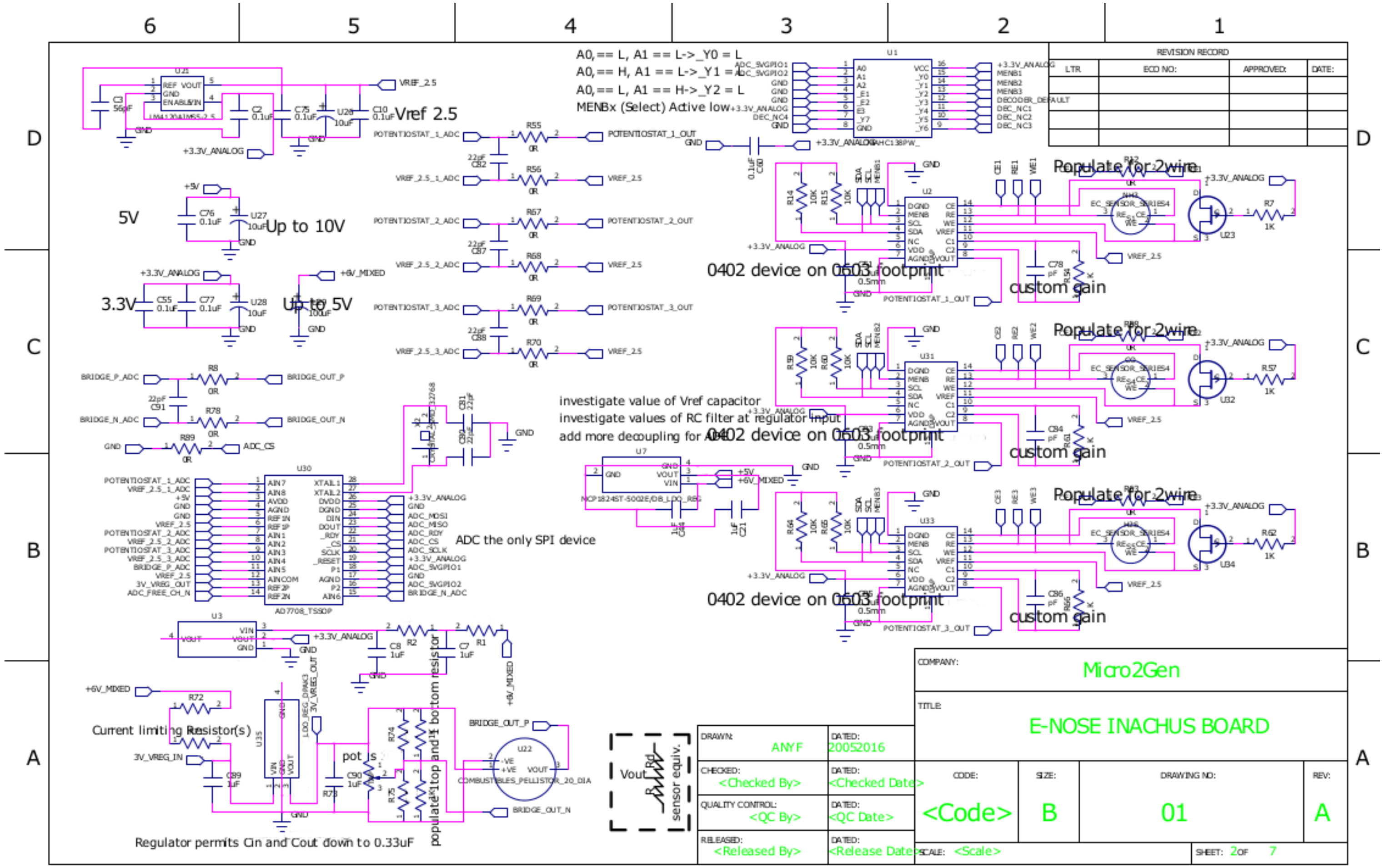
6
5
4
3
2
1
D
C
B
A
A0, == L, A1 == L->_Y0 = L
A0, == H, A1 == L->_Y1 = L
A0, == L, A1 == H->_Y2 = L
MENBx (Select) Active low
Vref 2.5
5V
Up to 10V
3.3V
Up to 5V
Populate for 2wire
0402 device on 0603 footprint
custom gain
investigate value of Vref capacitor
investigate values of RC filter at regulator input
add more decoupling for ADC
ADC the only SPI device
AD7708_TSSOP
MCP1824ST-5002E/DB_LDO_REG
Current limiting Resistor(s)
pot is
populate top and bottom resistor
Vout
sensor equiv.
COMBUSTIBLES_PELLISTOR_20_DIA
Regulator permits Cin and Cout down to 0.33uF
REVISION RECORD
LTR
ECO NO:
APPROVED:
DATE:
COMPANY:
Micro2Gen
TITLE:
E-NOSE INACHUS BOARD
DRAWN:
ANYF
DATED:
20052016
CHECKED:
<Checked By>
DATED:
<Checked Date>
QUALITY CONTROL:
<QC By>
DATED:
<QC Date>
RELEASED:
<Released By>
DATED:
<Release Date>
CODE:
<Code>
SIZE:
B
DRAWING NO:
01
REV:
A
SCALE:
<Scale>
SHEET:
2 OF 7

Figure 97. Schematic diagram of the analog board for the 3rd prototype

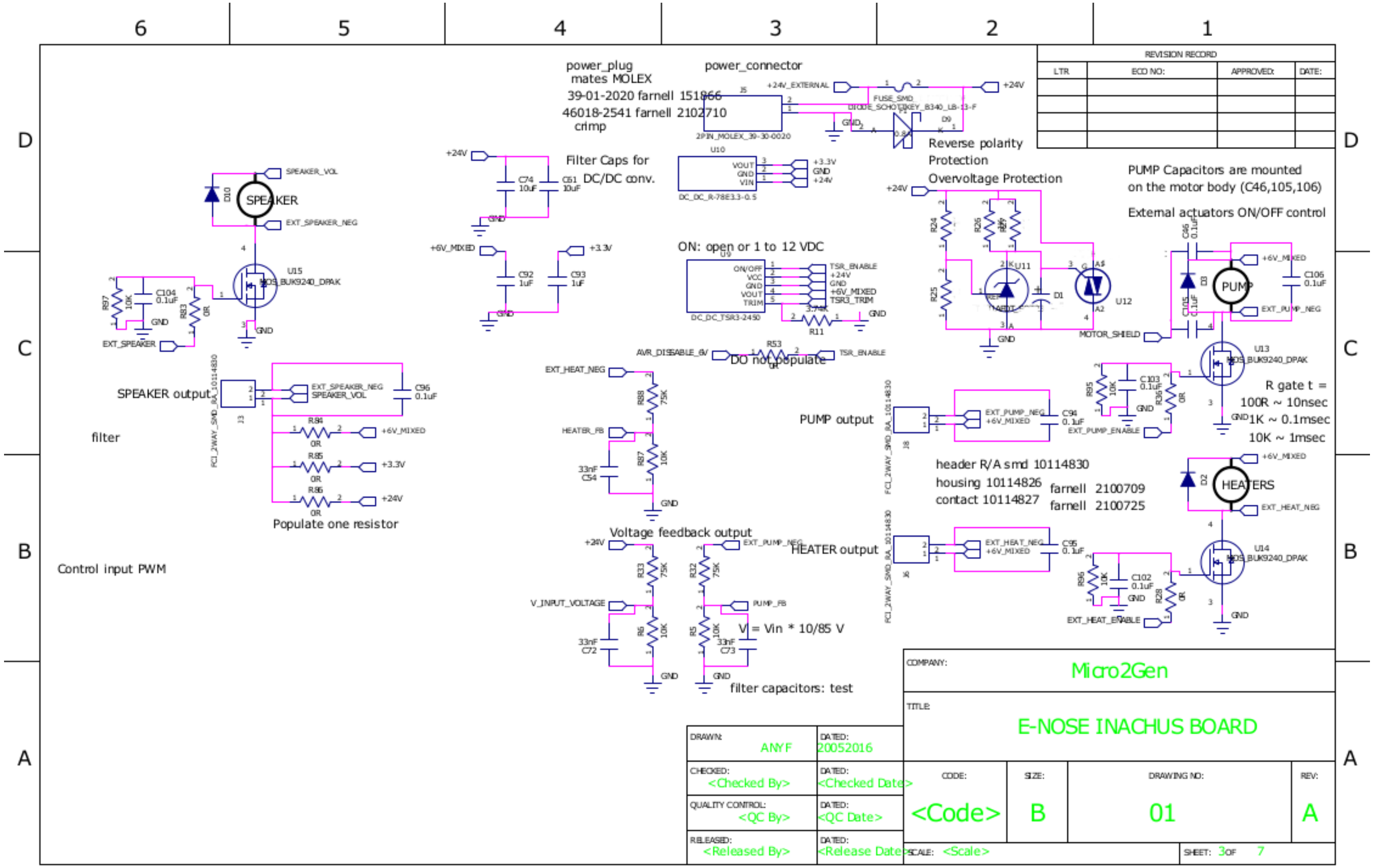
6
5
4
3
2
1
D
C
B
A
REVISION RECORD
LTR
ECO NO:
APPROVED:
DATE:
power_plug
mates MOLEX
39-01-2020 farnell 151866
46018-2541 farnell 2102710
crimp
power_connector
+24V_EXTERNAL
+24V
FUSE_SMD
DIODE_SCHOTTKY_B340_LB-13-F
D9
2PIN_MOLEX_39-30-0020
J5
GND
Reverse polarity
Protection
Overvoltage Protection
U10
VOUT
GND
VIN
+3.3V
GND
+24V
DC_DC_R-78E3.3-0.5
Filter Caps for
DC/DC conv.
+24V
C74
10uF
C61
10uF
GND
+6V_MIXED
C92
1uF
C93
1uF
+3.3V
GND
ON: open or 1 to 12 VDC
U9
ON/OFF
VCC
GND
VOUT
TRIM
TSR_ENABLE
+24V
GND
+6V_MIXED
TSR3_TRIM
DC_DC_TSR3-2450
3.74K
R11
GND
AVR_DISABLE_6V
R53
0R
DO not populate
TSR_ENABLE
SPEAKER_VOL
D10
SPEAKER
EXT_SPEAKER_NEG
U15
MOS_BUK9240_DPAK
R97
10K
C104
0.1uF
GND
R83
0R
EXT_SPEAKER
GND
SPEAKER output
J3
FCI_2WAY_SMD_RA_10114830
EXT_SPEAKER_NEG
SPEAKER_VOL
C96
0.1uF
filter
R84
0R
+6V_MIXED
R85
0R
+3.3V
R86
0R
+24V
Populate one resistor
Control input PWM
EXT_HEAT_NEG
R88
75K
HEATER_FB
33nF
C54
R87
10K
GND
Voltage feedback output
+24V
EXT_PUMP_NEG
R33
75K
R32
75K
V_INPUT_VOLTAGE
PUMP_FB
33nF
C72
R6
10K
R5
10K
33nF
C73
V = Vin * 10/85 V
GND
GND
filter capacitors: test
+24V
R24
R26
R27
U11
REF
ANODE
D1
U12
R25
GND
MOTOR_SHIELD
PUMP Capacitors are mounted
on the motor body (C46,105,106)
External actuators ON/OFF control
C46
0.1uF
D3
PUMP
+6V_MIXED
C106
0.1uF
C105
0.1uF
EXT_PUMP_NEG
U13
MOS_BUK9240_DPAK
R95
10K
C103
0.1uF
R36
0R
GND
EXT_PUMP_ENABLE
GND
R gate t =
100R ~ 10nsec
1K ~ 0.1msec
10K ~ 1msec
PUMP output
J8
FCI_2WAY_SMD_RA_10114830
EXT_PUMP_NEG
+6V_MIXED
C94
0.1uF
header R/A smd 10114830
housing 10114826
contact 10114827
farnell 2100709
farnell 2100725
+6V_MIXED
D2
HEATERS
EXT_HEAT_NEG
HEATER output
J6
FCI_2WAY_SMD_RA_10114830
EXT_HEAT_NEG
+6V_MIXED
C95
0.1uF
U14
MOS_BUK9240_DPAK
R96
10K
C102
0.1uF
GND
R28
0R
EXT_HEAT_ENABLE
GND
COMPANY:
Micro2Gen
TITLE:
E-NOSE INACHUS BOARD
DRAWN:
ANYF
DATED:
20052016
CHECKED:
<Checked By>
DATED:
<Checked Date>
QUALITY CONTROL:
<QC By>
DATED:
<QC Date>
RELEASED:
<Released By>
DATED:
<Release Date>
CODE:
<Code>
SIZE:
B
DRAWING NO:
01
REV:
A
SCALE:
<Scale>
SHEET: 3 OF 7

Figure 98: Schematic diagram of the power electronics located on the microcontroller board for the 3rd prototype

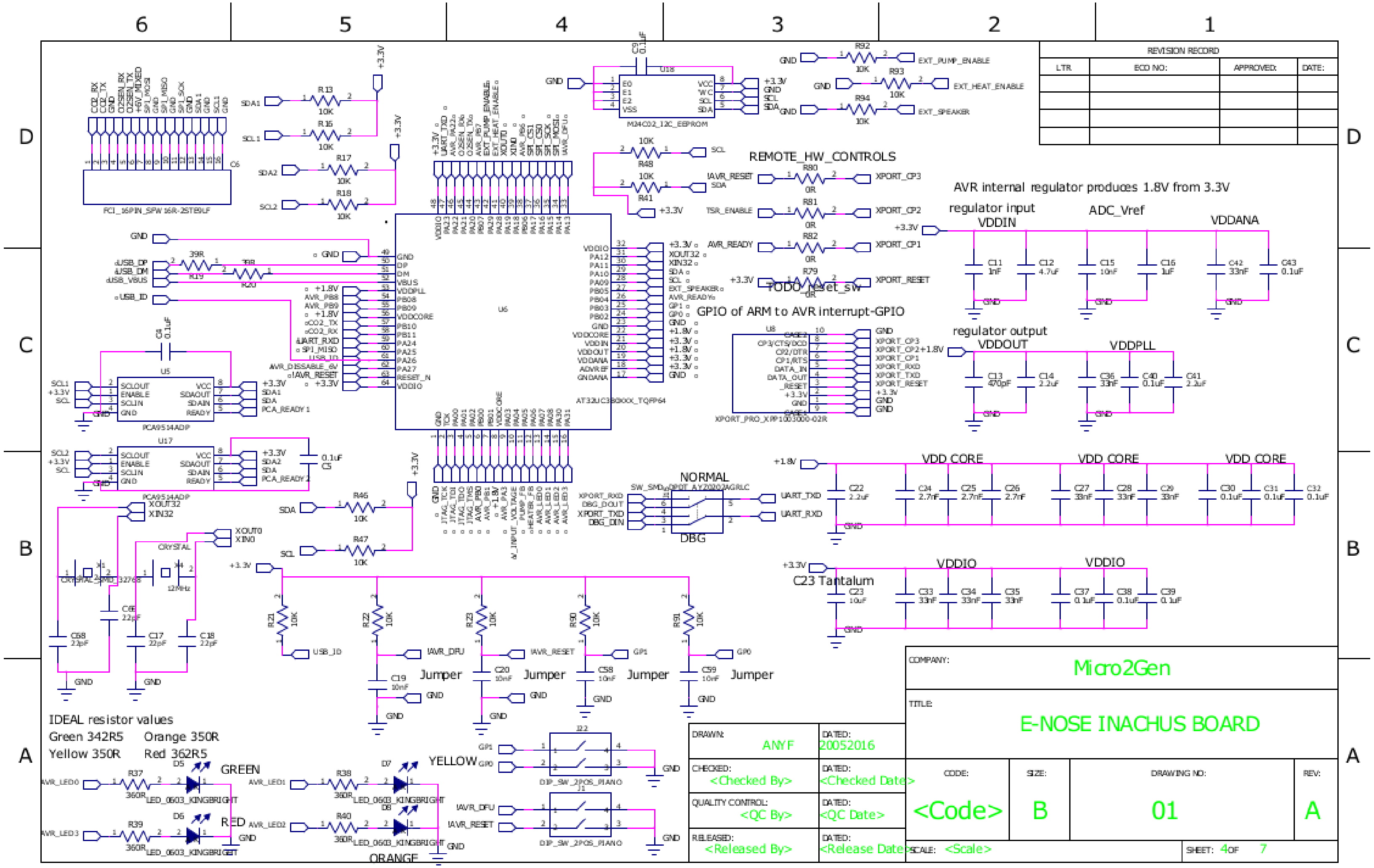
REVISION RECORD
LTR
ECO NO:
APPROVED:
DATE:
REMOTE_HW_CONTROLS
AVR internal regulator produces 1.8V from 3.3V
regulator input
VDDIN
ADC_Vref
VDDANA
regulator output
VDDOUT
VDDPLL
GPIO of ARM to AVR interrupt-GPIO
TODO: reset_sw
VDD CORE
VDDIO
C23 Tantalum
NORMAL
DBG
M24C02_I2C_EEPROM
AT32UC3BXXXX_TQFP64
XPORT_PRO_XPP1003000-02R
PCA9514ADP
FCI_16PIN_SFW16R-2STE9LF
CRYSTAL
12MHz
Jumper
IDEAL resistor values
Green 342R5
Orange 350R
Yellow 350R
Red 362R5
GREEN
YELLOW
RED
ORANGE
LED_0603_KINGBRIGHT
DIP_SW_2POS_PIANO
COMPANY:
Micro2Gen
TITLE:
E-NOSE INACHUS BOARD
DRAWN:
ANYF
DATED:
20052016
CHECKED:
<Checked By>
<Checked Date>
QUALITY CONTROL:
<QC By>
<QC Date>
RELEASED:
<Released By>
<Release Date>
CODE:
<Code>
SIZE:
B
DRAWING NO:
01
REV:
A
SCALE:
<Scale>
SHEET: 4 OF 7

Figure 99: Schematic diagram of the microcontroller board for the 3rd prototype

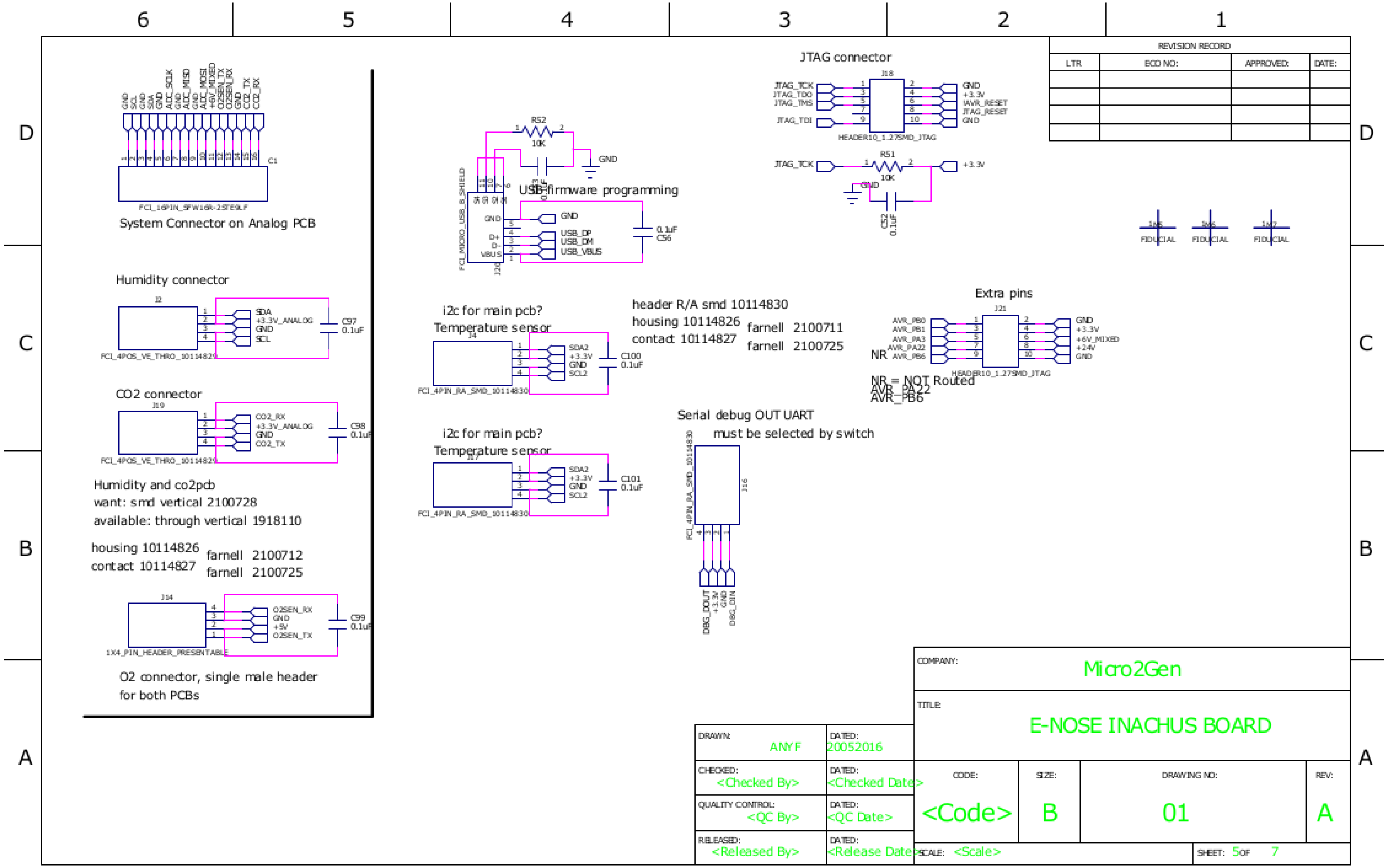
6
5
4
3
2
1
D
C
B
A
GND SCL GND SDA GND ADC_SCLK GND ADC_MISO GND ADC_MOSI +6V_MIXED O2SEN_TX O2SEN_RX GND CO2_TX CO2_RX
C1
FCI_16PIN_SFW16R-2STE9LF
System Connector on Analog PCB
Humidity connector
J2
SDA
+3.3V_ANALOG
GND
SCL
C97
0.1uF
FCI_4POS_VE_THRO_10114829
CO2 connector
J19
CO2_RX
+3.3V_ANALOG
GND
CO2_TX
C98
0.1uF
FCI_4POS_VE_THRO_10114829
Humidity and co2pcb
want: smd vertical 2100728
available: through vertical 1918110
housing 10114826
contact 10114827
farnell 2100712
farnell 2100725
J14
O2SEN_RX
GND
+5V
O2SEN_TX
C99
0.1uF
1X4_PIN_HEADER_PRESENTABLE
O2 connector, single male header
for both PCBs
R52
10K
GND
USB firmware programming
FCI_MICRO_USB_B_SHIELD
J20
GND
D+
D-
VBUS
USB_DP
USB_DM
USB_VBUS
0.1uF
C56
i2c for main pcb?
Temperature sensor
J4
SDA2
+3.3V
GND
SCL2
C100
0.1uF
FCI_4PIN_RA_SMD_10114830
i2c for main pcb?
Temperature sensor
J17
SDA2
+3.3V
GND
SCL2
C101
0.1uF
FCI_4PIN_RA_SMD_10114830
header R/A smd 10114830
housing 10114826
contact 10114827
farnell 2100711
farnell 2100725
JTAG connector
J18
JTAG_TCK
JTAG_TDO
JTAG_TMS
JTAG_TDI
GND
+3.3V
!AVR_RESET
JTAG_RESET
GND
HEADER10_1.27SMD_JTAG
R51
JTAG_TCK
10K
+3.3V
GND
C52
0.1uF
Extra pins
J21
AVR_PB0
AVR_PB1
AVR_PA3
AVR_PA22
AVR_PB6
NR
GND
+3.3V
+6V_MIXED
+24V
GND
HEADER10_1.27SMD_JTAG
NR = NOT Routed
AVR_PA22
AVR_PB6
Serial debug OUT UART
must be selected by switch
FCI_4PIN_RA_SMD_10114830
J16
DBG_DOUT
+3.3V
GND
DBG_DIN
FIDUCIAL
FIDUCIAL
FIDUCIAL
REVISION RECORD
LTR
ECO NO:
APPROVED:
DATE:
COMPANY:
Micro2Gen
TITLE:
E-NOSE INACHUS BOARD
DRAWN:
ANYF
DATED:
20052016
CHECKED:
<Checked By>
DATED:
<Checked Date>
QUALITY CONTROL:
<QC By>
DATED:
<QC Date>
RELEASED:
<Released By>
DATED:
<Release Date>
CODE:
<Code>
SIZE:
B
DRAWING NO:
01
REV:
A
SCALE:
<Scale>
SHEET: 5 OF 7

Figure 100: Schematic diagram of the connectors on the microcontroller board for the 3rd prototype

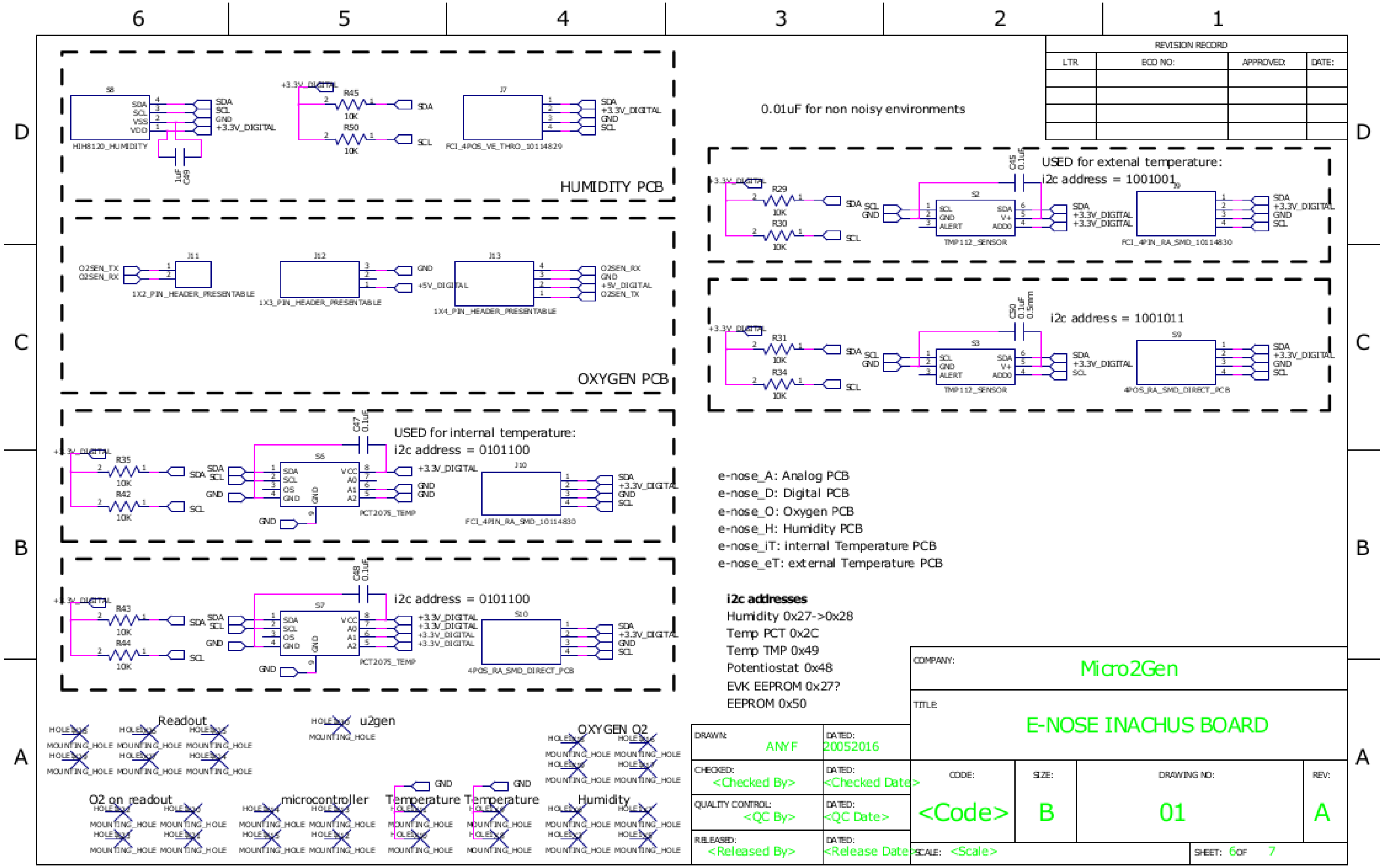
6
5
4
3
2
1
D
C
B
A
REVISION RECORD
LTR
ECO NO:
APPROVED:
DATE:
S8
HIH8120_HUMIDITY
SDA
SCL
VSS
VDD
GND
+3.3V_DIGITAL
1uF
C49
+3.3V_DIGITAL
R45
10K
R50
10K
SDA
SCL
J7
FCI_4POS_VE_THRO_10114829
HUMIDITY PCB
0.01uF for non noisy environments
USED for extenal temperature:
i2c address = 1001001
C45
0.1uF
R29
10K
R30
10K
S2
TMP112_SENSOR
ALERT
ADD0
V+
J9
FCI_4PIN_RA_SMD_10114830
J11
O2SEN_TX
O2SEN_RX
1X2_PIN_HEADER_PRESENTABLE
J12
1X3_PIN_HEADER_PRESENTABLE
+5V_DIGITAL
J13
1X4_PIN_HEADER_PRESENTABLE
OXYGEN PCB
i2c address = 1001011
C50
0.1uF
0.5mm
R31
10K
R34
10K
S3
TMP112_SENSOR
S9
4POS_RA_SMD_DIRECT_PCB
USED for internal temperature:
i2c address = 0101100
C47
0.1uF
R35
10K
R42
10K
S6
PCT2075_TEMP
VCC
A0
A1
A2
OS
J10
FCI_4PIN_RA_SMD_10114830
i2c address = 0101100
C48
0.1uF
R43
10K
R44
10K
S7
PCT2075_TEMP
S10
4POS_RA_SMD_DIRECT_PCB
Readout
u2gen
OXYGEN O2
O2 on readout
microcontroller
Temperature
Temperature
Humidity
HOLE
MOUNTING_HOLE
COMPANY:
Micro2Gen
TITLE:
E-NOSE INACHUS BOARD
DRAWN:
ANYF
DATED:
20052016
CHECKED:
<Checked By>
DATED:
<Checked Date>
QUALITY CONTROL:
<QC By>
DATED:
<QC Date>
RELEASED:
<Released By>
DATED:
<Release Date>
CODE:
<Code>
SIZE:
B
DRAWING NO:
01
REV:
A
SCALE:
<Scale>
SHEET: 6 OF 7

e-nose_A: Analog PCB
e-nose_D: Digital PCB
e-nose_O: Oxygen PCB
e-nose_H: Humidity PCB
e-nose_iT: internal Temperature PCB
e-nose_eT: external Temperature PCB

i2c addresses
Humidity 0x27->0x28
Temp PCT 0x2C
Temp TMP 0x49
Potentiostat 0x48
EVK EEPROM 0x27?
EEPROM 0x50

Figure 101: Schematic diagram of all the custom sensor breakout boards for the 3rd prototype

Figure 102 illustrates the layout of the third prototype's PCBs. The layout is a custom-made panel that includes all the printed circuit boards combined into one. All the layers are visible including the mechanical/assembly one. The PCB is a 4 layer PCB and was fabricated at Eurocircuits using the default 1.6mm PCB thickness layer stackup with the "PCB proto" service and with a 6D classification. The two internal layers are used as ground (return) plane and power plane. The component selection, their placement and their footprint were intentionally designed so that the boards could be assembly by hand.

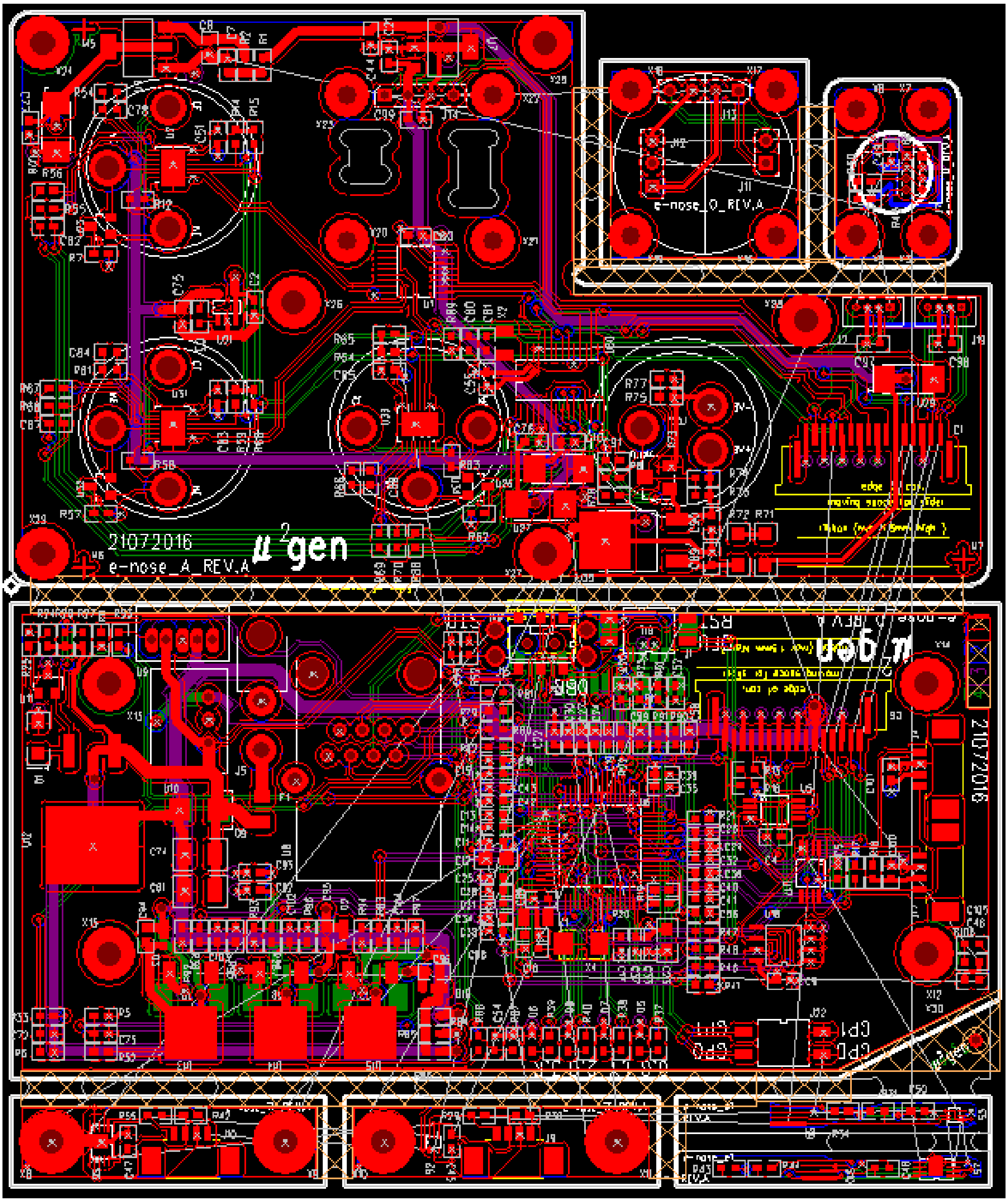

Figure 102: The layout of the PCB for the 3rd prototype

The electronics are built around a microcontroller which is responsible for managing the system. A number of features are built in the electronics to make them more robust and expandable. A reverse polarity diode is present at the power input. Also, a crowbar circuit is present to protect the system from an input overvoltage paired with an input fuse. The purpose of this circuit is to create a short circuit when a voltage anomaly is detected and burns the fuse. As is, the circuit is too sensitive to transient voltages occurring when installed in the robotic platform and was not used. A surge suppressor, or stopper, that continues to provide power to the load would be a more appropriate solution for the integrated device. Even without the crowbar circuit, the electronics are adequately protected since the power supply modules used have a sufficiently large input voltage rating.

The actuators control electronics are capable of providing ON/OFF functionality or low frequency PWM. A single N channel power MOSFET is used for each actuator to close the circuit of power return (GND). A (freewheeling) diode is placed across the load connection terminals so that inductive loads can be driven.

The board includes an i2c eeprom so that sensor calibration data and system configuration parameters can be stored and retrieved from the e-nose device. This functionality has not been implemented in the FW but in the software as this system is a research prototype.

The electronics also include an expansion header that exports multiple microcontroller GPIOs and system voltage rails. There is also an extra actuator output. These provisions were made to support the potential implementation and connection of the required interfacing components for making a completely stand-alone, portable, or even hand-held, e-nose device. For more information regarding the control aspects of the microcontroller, see the firmware sub-section under software section of this chapter.

8.3. Mechanical Design of the 3rd prototype

8.3.1. Manifold design

Architecture - Concept

The air manifold is the central block of the e-nose. It holds the e-nose sensor array and the necessary analog to digital converter electronics circuitry. The sensors are mounted on a main (core) PCB and all together are inserted in the manifold. The latter is a heat conducting enclosure, made of aluminum, for the sensors and electronics so that they are kept at a relatively high temperature compared to the surroundings. The reason for the elevated temperature lies in preventing environmental humidity from condensing in the sensors, an outcome that would result in the quick deterioration of the sensor longevity and significantly affect the accuracy of the measured values.

The manifold architecture implements a configurable air connection path. The sensors are grouped in two categories, namely, human identification capability and hazardous gasses detection. The former group is considered the core sensor group and it includes the CO_2, O_2, NH_3 and humidity sensors. It works independently from the other secondary, optional group of hazardous gas detectors. To achieve this goal a two lane airway is implemented in the manifold. Each airway runs through one group of sensors thereby supplying them with sampled air in order to perform gas concentration measurements. Each airway has independent inflow and outflow orifices where flexible pipes can be mounted.

The independent inlets and outlets allow two different connection topologies to be realized. A series connection of the two lanes is implemented when all sensors are present, where the outlet of the primary airway is connected to the inlet of the secondary lane. The second lane can be completely bypassed when the secondary set of hazardous gas detectors is not installed. A parallel connection of the two lanes is also possible.

To ensure that airflow is effectively diffused in the sensor drums, forced turbulence is created on top of the sensors. This is achieved by changing the geometry of the airway on top of the sensors input interface. Additional strengthening of the air flow through all sensors is achieved by sealing the airway so that sampled air does not escape from the airway path and flow towards the outer bottom side of the sensor drums and the main PCB. This is enforced by using elastomeric gaskets (~1mm thickness) that secure the sensors in place when the sensors and main PCB are mounted in the manifold.

To design the two parallel airways in the manifold a number of as similar as possible sensors have been selected. These have the same diameter of 20mm and, where possible, the same height. Irrespective of the height, however, all sensor input interfaces have been designed to be on the same plane parallel to the surface of the main PCB, thus avoiding unnecessary bending of the airways. With the sensors all set in place, the main

PCB that is large enough to host all of them was designed. Consequently, the daughter PCBs are mounted onto the main PCB using off-the-shelf standoffs, screws and nuts or extension cables. Extra care was taken to include the outline of bulky components and identify the dead zones i.e. zones where no components are placed. Finally, the manifold was designed to host all the components, whilst keeping the smallest footprint possible.

Main PCB, sensors, CO_2, O_2 PCB and screw-washer-nuts

A representation of the layout and placement of the sensors on the breakout PCBs can be seen in the following figures:

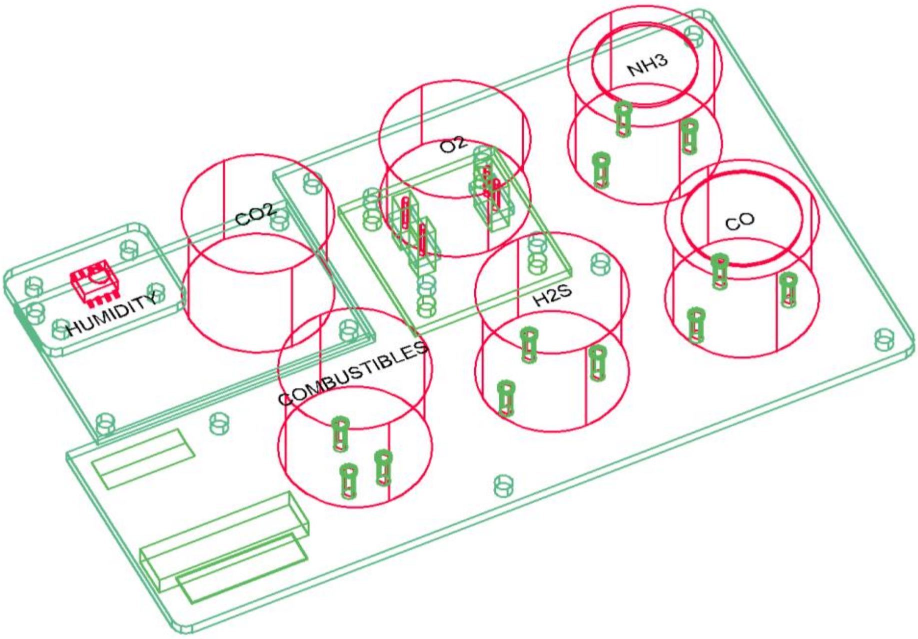

Figure 103: 3D view of the main, CO_2, O_2 and humidity PCBs with the corresponding sensors. On the bottom left corner the interface cable connector will connect the main PCB to the outside world.

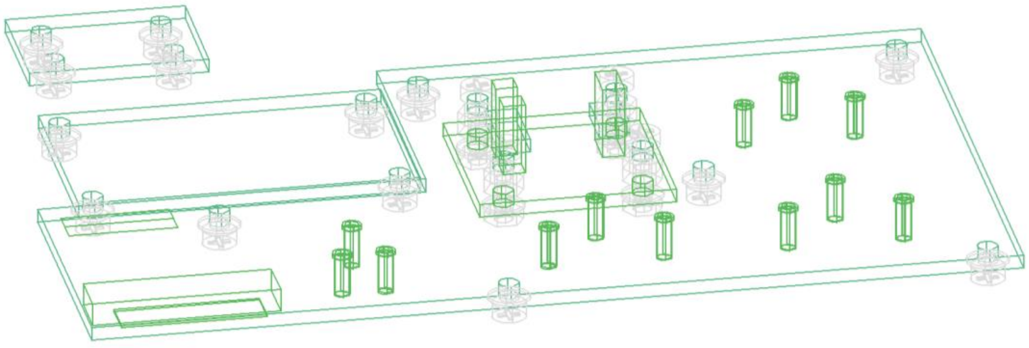

Figure 104: 3D view of the main PCB accompanied by the daughter PCBs

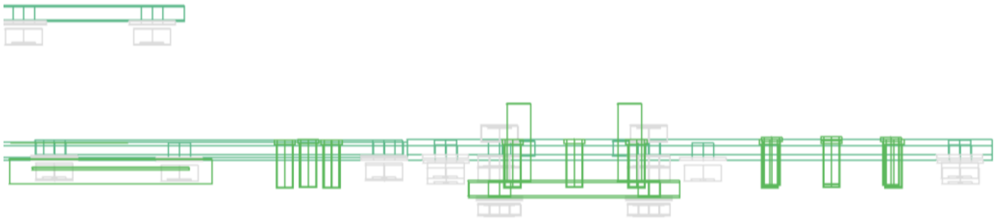

Figure 105: Side view (cross section) of the main and daughter PCBs.

Manifold

The manifold consists of two parts. The part which simply acts as a cover for the bottom side of the main PCB and the central and main manifold which:

- houses the sensors
- provides mount points (screw sockets) for the main PCB
- provides mount points for the bottom cover
- contains the air delivery system (air path) that directs sampled air onto the sensor drums.

Hangars and their wall thickness

The sensor drums are inserted in the sensor drum hangars. The hangars have a diameter of 20.9mm. This is deemed the minimum adequate diameter taking into account sensor component manufacturing tolerances, sensor sticker thicknesses and manufacturing (milling process) tolerances. The walls of these hangars should have at minimum 2mm thickness in order to provide adequate heat capacity for transferring heat to the sensor drums whilst maintaining their own. The hangar walls have a safety clearance of 1mm away from the top surface of the main PCB.

Hangar Dome and airway

At the top end of the hangars a dome acts as a junction between the sensor top surfaces and the airway that transports the sampled air across the sensors. The dome provides a “step” for the elastomeric ring to “sit” on. The clearance between the sensor drum top and the dome’s step is 0.8mm. Additionally, the dome provides air insulation and also has a 4mm circular opening that traverses the domes and implements the air path. A M5 thread is inscribed at the ends of the traversing airway. According to manufacturing requirements a M5 opening (depending on fitting) should have a diameter of 4.14 – 4.33mm. Such M5 openings are incorporated at the inflow and outflow ends of the manifold and are used to connect the e-nose sensor array to the pump and filtering system.

Air redirection walls for Domes

To improve air turbulence in the dome and thus increase the amount of air that travels into the sensor drum, air redirection walls are implemented in the dome. These force the air to move towards the sensor drums before going to the dome’s outflow orifice. The wall thickness is 2mm.
M5 screw holes at the top of the dome enable a screw to adjust the amount of turbulence.

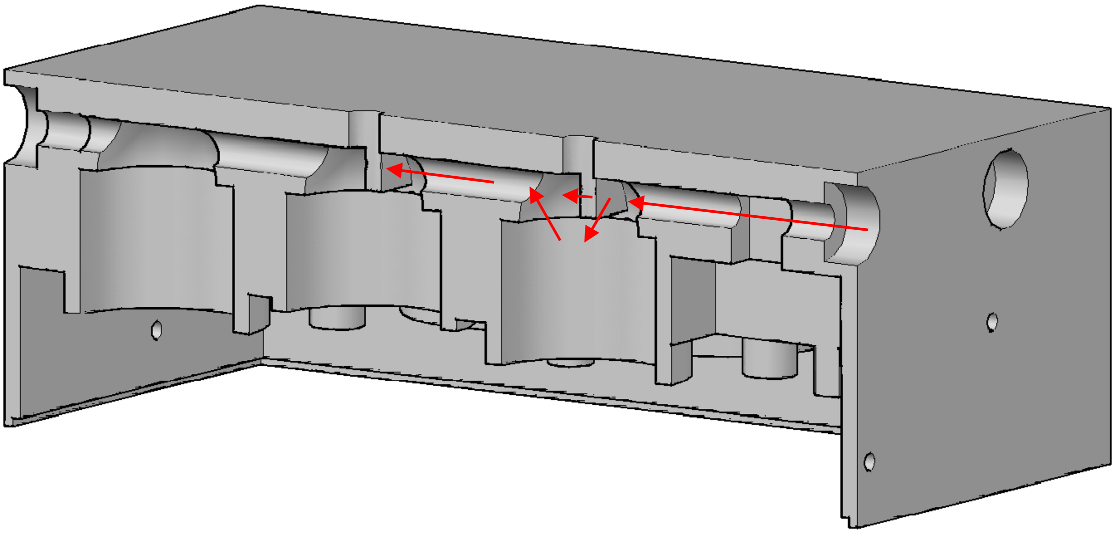

Figure 106: Manifold cross section of the primary airway. Air-redirection walls are used to force air turbulence above the sensor drums.

Assembled manifold

The complete manifold with the external components mounted is shown below. All the externally mounted equipment is mounted with M2.5 screws. Caution has been exercised to prevent the external equipment mounting screws from intervening with the main PCB and other internal equipment.

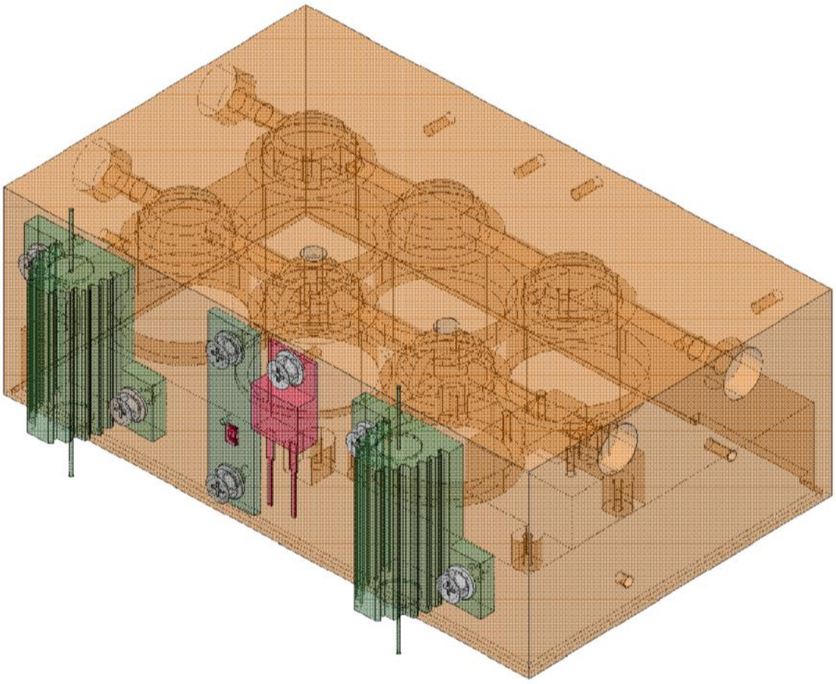

Figure 107: 3D view of the manifold with the external components only attached (2x resistors, a temperature relay (red) and the temperature PCB (green) with a temperature sensor mounted on.

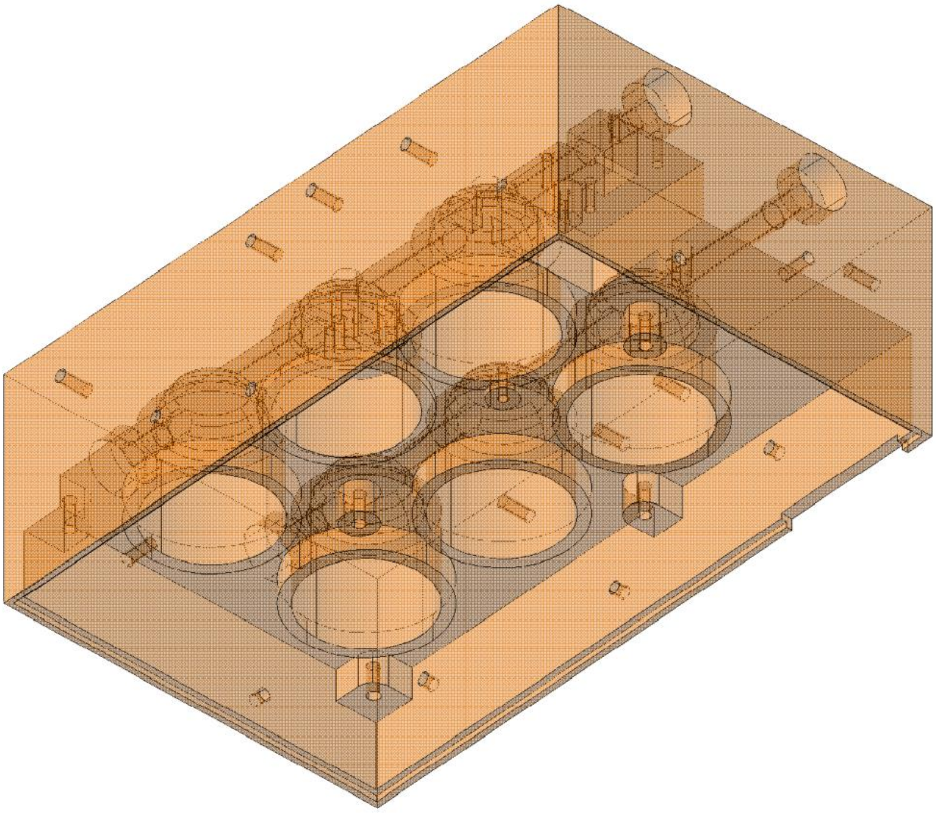

Figure 108: Bottom 3D view of the manifold showing the sensor hangars.

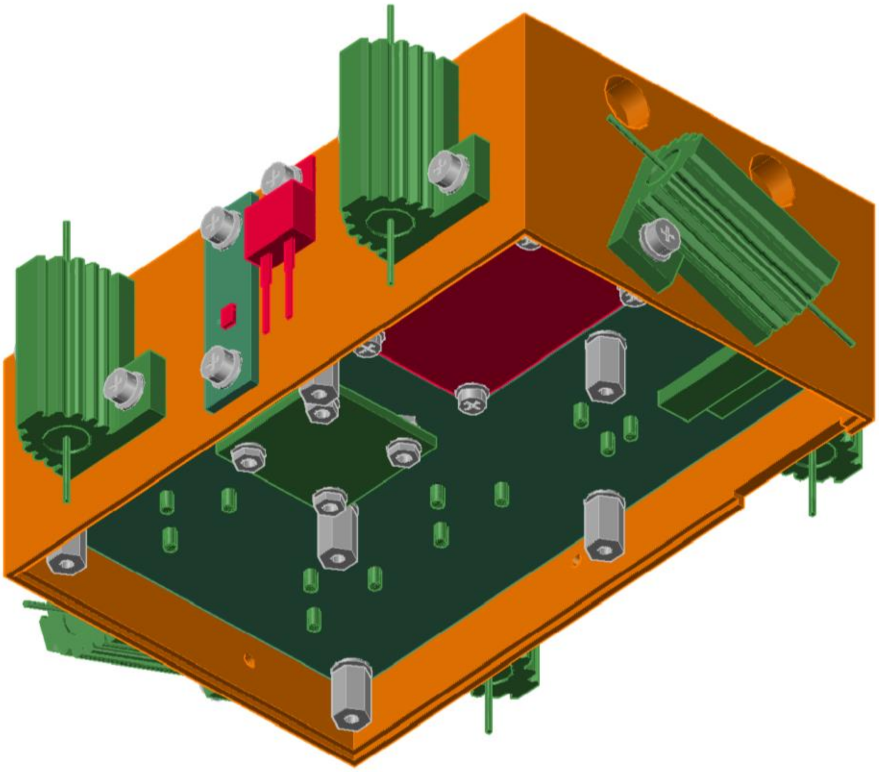

Figure 109: Rendered bottom 3D view of the manifold with all the internal and external components mounted. Only the bottom cover has been removed.

The volume of the manifold (without the electronics, sensors and mounting screws) is approximately 156,848 mm^3. When aluminum is used for manufacturing the manifold, the expected weight of the manifold is 0.424kg (aluminum density used is 2.7 x 10^{-6} kg / mm^3 [92]).

8.3.2. Enclosure design

Architecture - concept

The enclosure allows the e-nose unit to be portable, as well as be compatible for mounting it on the robotic platform. Therefore, it was important to create a design suitable to work both as a stand-alone unit, but which provides the necessary mounting points to be integrated in the robotic platform.

The main subsystems inside the enclosure are the

- e-nose manifold: which houses the sensors and the readout electronics
- pneumatic system: including air pump, filters and piping
- the microcontroller PCB
- the filter compartment: an easily accessible space that houses the two hydrophobic filters and allows their easy replacement.

As far as the compartment design is concerned, it must fulfill the following requirements:

- Keep the filters separated from the rest of the electronics. This means air holes should be designed. Alternatively, openings through which the pipe can go through can also be used.
- Allow easy access to the filters. Hatch access could be with screws. The hatch should ideally be similar to those used in the battery compartments of remote controls. Alternatively, a screw-hatch can be used.
- Provide all the necessary piping while avoiding abrupt corners for the pipes that could block unobstructed air flow.

Enclosure dimensions

The external dimensions (170 x 130 x 70mm) of the enclosure are mandated by the allocated space of the robotic platform for the e-nose. Depending on the material used, the internal dimensions vary. For example, aluminum sheet of thickness 2mm may be used which is durable and thin enough to allow 166 x 126 x 66 mm internal dimensions. This solution would be relatively heavy, however, due to the widespread use of aluminum material. Similarly a 3D printed part needs to be thicker (4mm) allowing slightly less internal dimensions, but at the benefit of a lighter construction combined with more design freedom. To be on the safe side, the minimum internal volume of 162 x 122 x 62 was assumed.

Enclosure parts

The enclosure is comprised of two parts: the bottom base and the top cover. The latter includes the four side walls as well. The top part is mounted in the bottom part through a series of M3 screws (6x) as shown below:

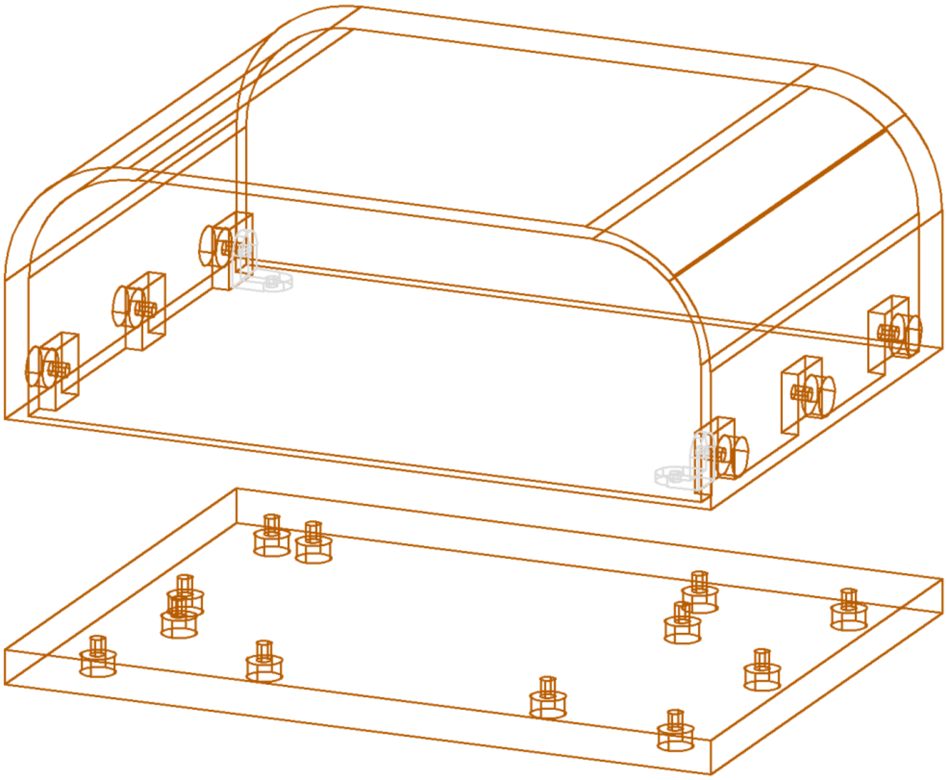

Figure 110: The enclosure top and bottom parts. All internal mounting holes (for enclosure cover and manifold stands).

Component placement - E-nose manifold

The e-nose manifold is the most important, complex and bulky part placed inside the enclosure. It has a number of components externally attached to it: namely a temperature sensor, a temperature safety relay and two heating resistors.

The combined part could be wrapped in thermal insulating material in order to avoid heat escaping to the surroundings, thus improving the energy efficiency of the system. Overall, the dimensions of the manifold with its external components is 115 x 85 x 41mm. 10mm of insulation on each dimension have been allocated.

Due to the large dimension of the manifold (115mm + 10mm) exceeding the 122mm inner dimension of the enclosure, the manifold is placed along the large dimension of the enclosure.

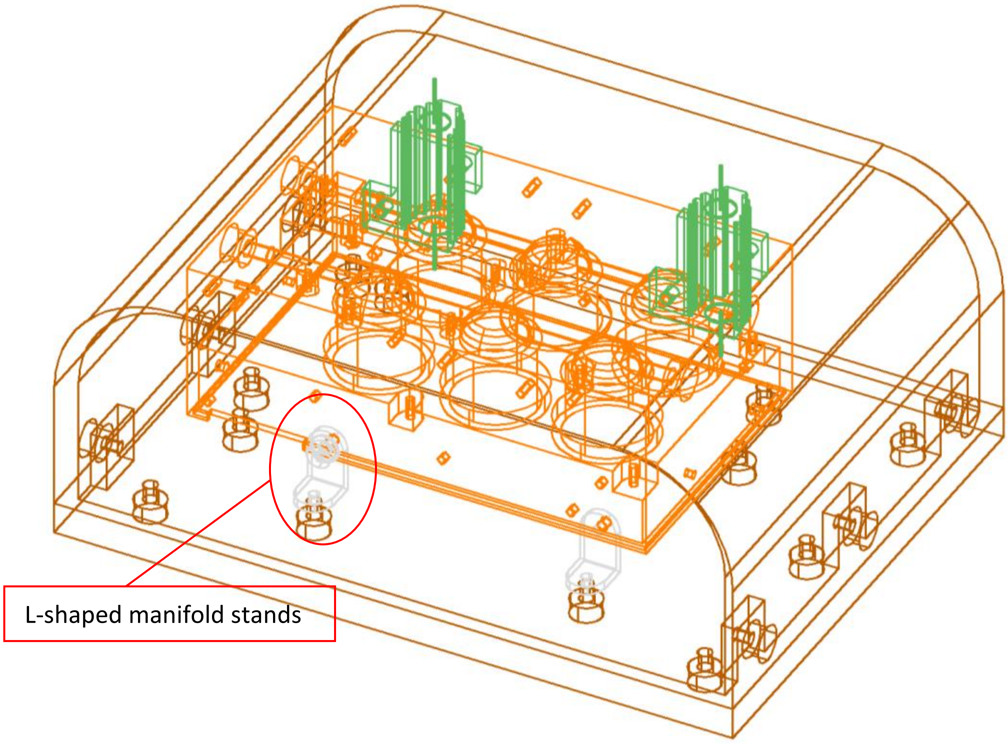

Figure 111: 3D view of the enclosure with the manifold included along with its most bulky components.

Microcontroller PCB (sensor read-out board)

The microcontroller PCB gathers signals from the manifold main PCB and prepares them for transmission through an Ethernet interface. Additionally, it controls the air pump and the external components of the manifold directly.

The top left side of the PCB is intentionally cut out so that it can fit in a vertical posture in the enclosure whilst using the available space efficiently. The overall dimensions of the PCB are 110mm x 53mm.

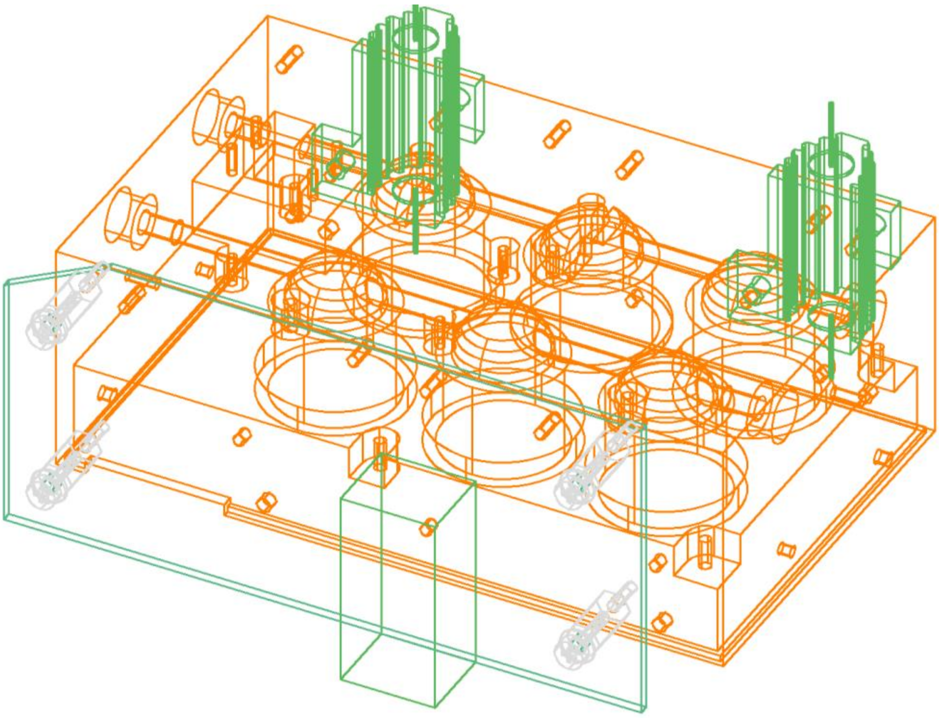

Figure 112: 3D view of the microcontroller PCB mounted on the manifold with 10mm standoffs.

Pneumatic parts

The remaining available space in the enclosure is used to fit the air pump and air filters. These have no solid mounting points and are secured in place by flexible means so that the pump vibrations are not fully transferred to the rest of the structure.

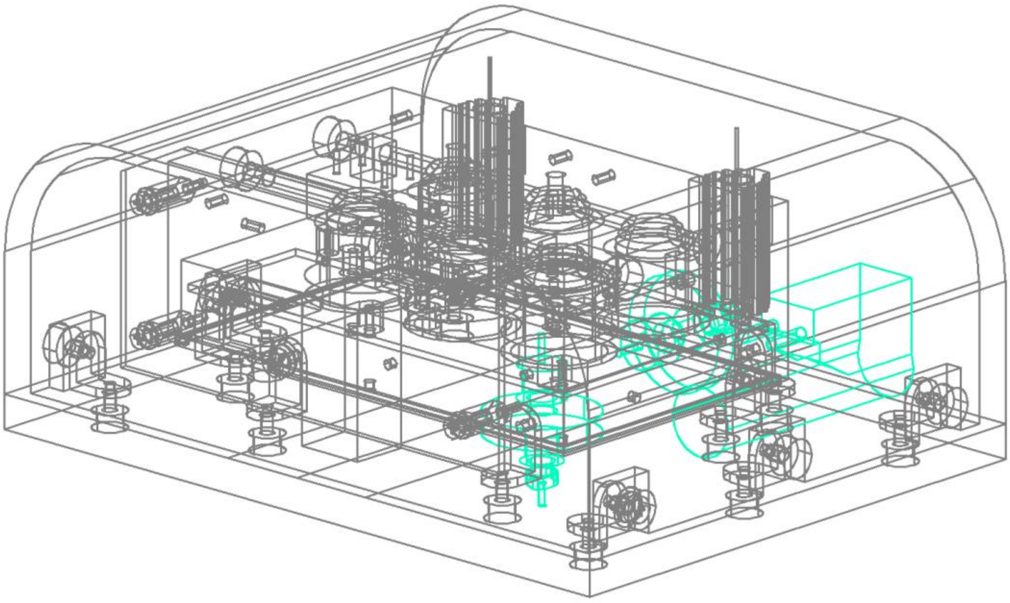

Figure 113: 3D view of the pneumatic parts as fit in the available space of the enclosure.

8.3.3. Assembly of the 3rd prototype

The components of the third prototype were successfully assembled without encountering noteworthy issues. In the following sections, pictures illustrate the most critical assembly steps. The assembly of the manifold is mostly comprised of installing the sensors in it. Some sensors are installed separately on their own PCB while others are first mounted on the analog readout PCB and then installed inside.

The following picture illustrates the machined aluminum manifold without components and the printed circuit board panel for the 3rd prototype:

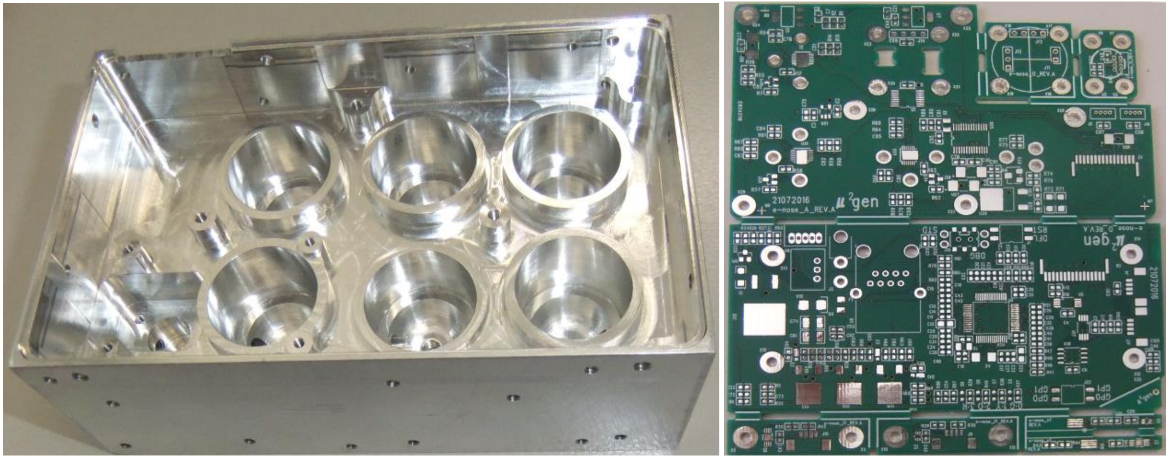

Figure 114: Bottom view of manifold with sensor inserts visible (left) and the PCB panel (right).

The following picture illustrates the installed humidity sensor on its printed circuit board. The board provides mechanical support as well as an airtight seal. The CO_2 sensor is installed near the humidity sensor and its board covers the humidity board.

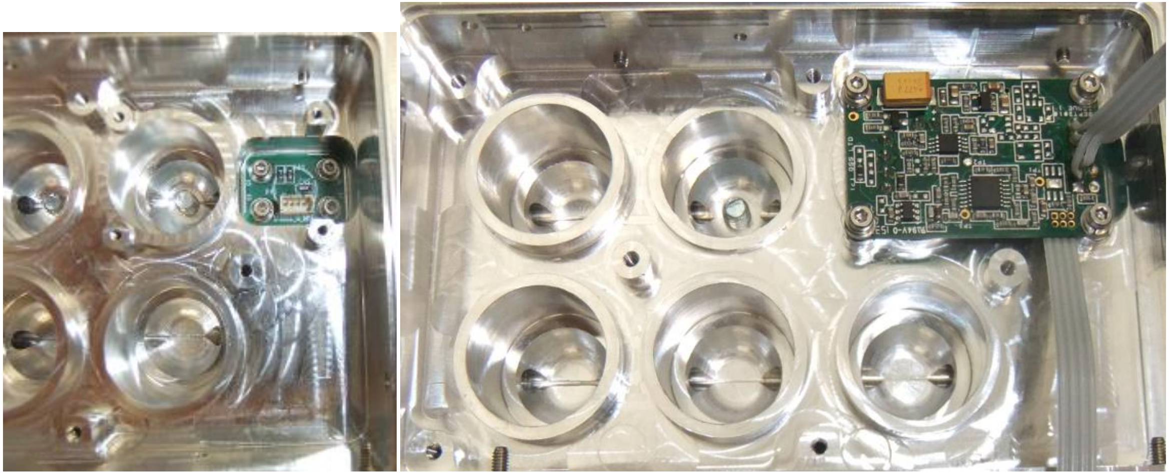

Figure 115: The humidity board installed (left) and the CO_2 sensor installed on top (right).

The following picture illustrates the installed components for temperature sensing, heating and over-temperature cut-off:

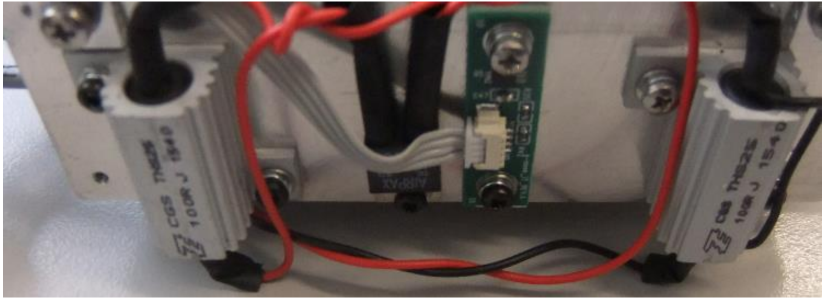

Figure 116: From left to right: heater, thermal protection, temperature sensor and heater.

The following pictures illustrate the analog sensor board, populated with the sensors, next to the manifold. The sensors extend from the surface of the analogue PCB socket in the manifold.

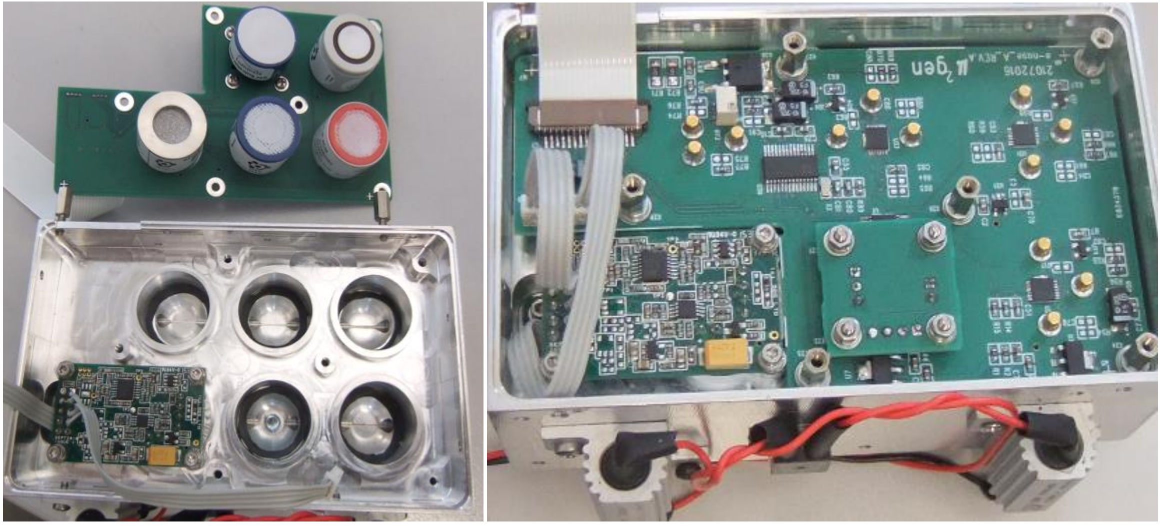

Figure 117: The analog PCB populated with sensors (O_2, NH_3, CO, H_2S, combustibles).

The manifold cover and the L shaped supports are screwed on. The control (microcontroller) board is installed on the free long side (top in the pictures) of the manifold.

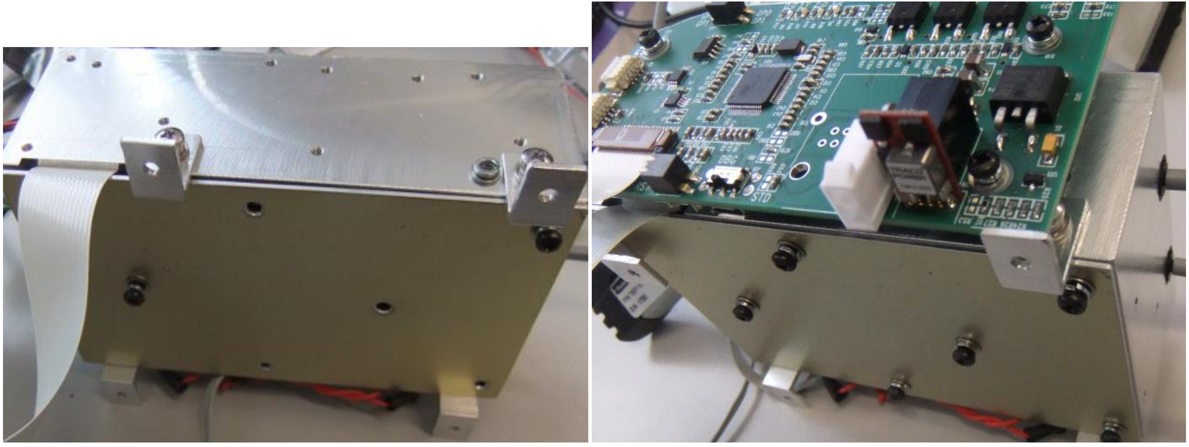

Figure 118: The assembled manifold with the control board attached to it

Connecting the air pump, air filters and heat insulation concludes the assembly of the system required for the e-nose to function.
Custom elbow air interfaces were built to connect the air tubing with the manifold. They were machined in two pieces that were soldered together (PB free solder). In the following pictures part of the assembly can be seen.

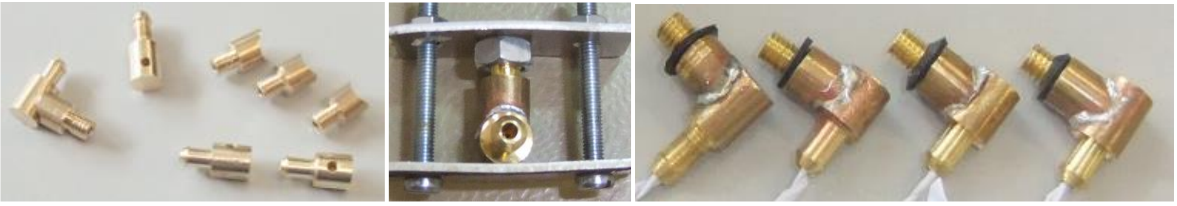

Figure 119: From left to right: machined air interface parts, custom assembly jig, assembled interfaces.

The air system was completed by installing the air interfaces on the manifold and connecting the air pump and air filters. The following picture illustrates the completed electronic nose without the electronic nose enclosure.

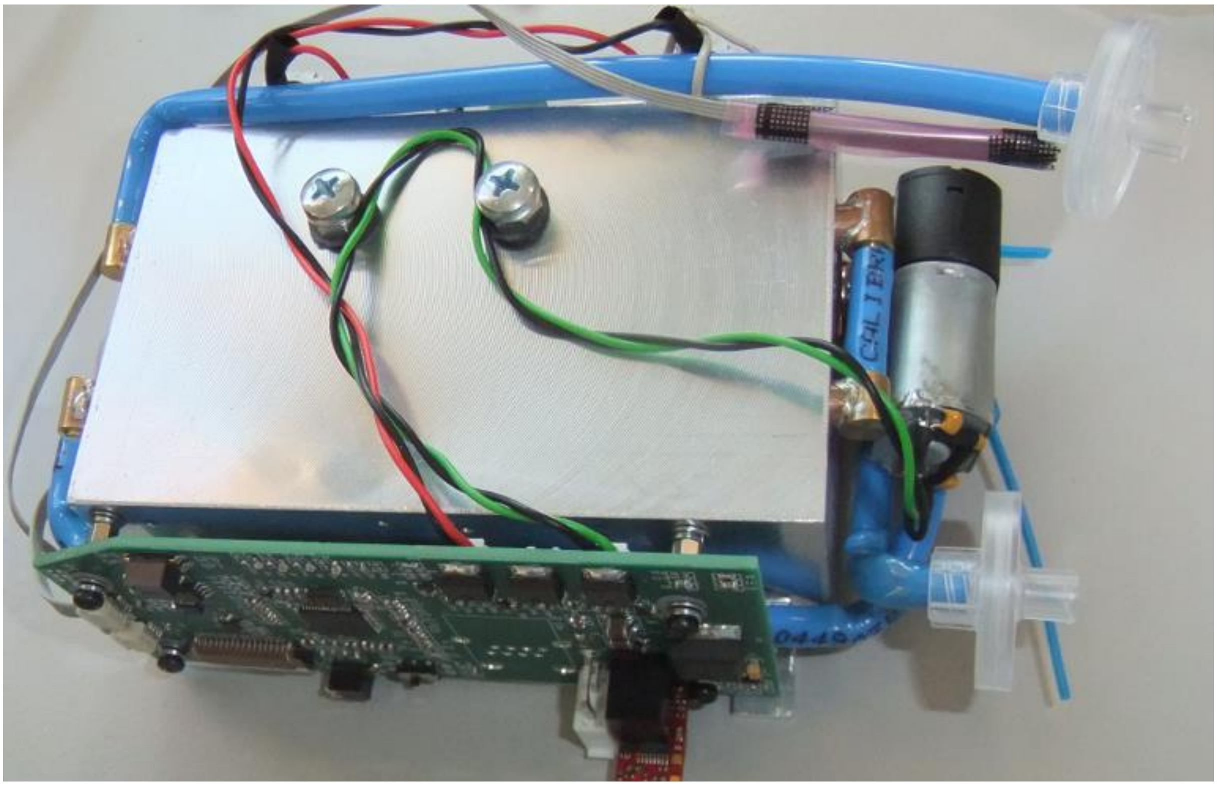

Figure 120: The assembled e-nose without the enclosure.

The following picture illustrates the electronic nose installed in a Plexiglas enclosure.

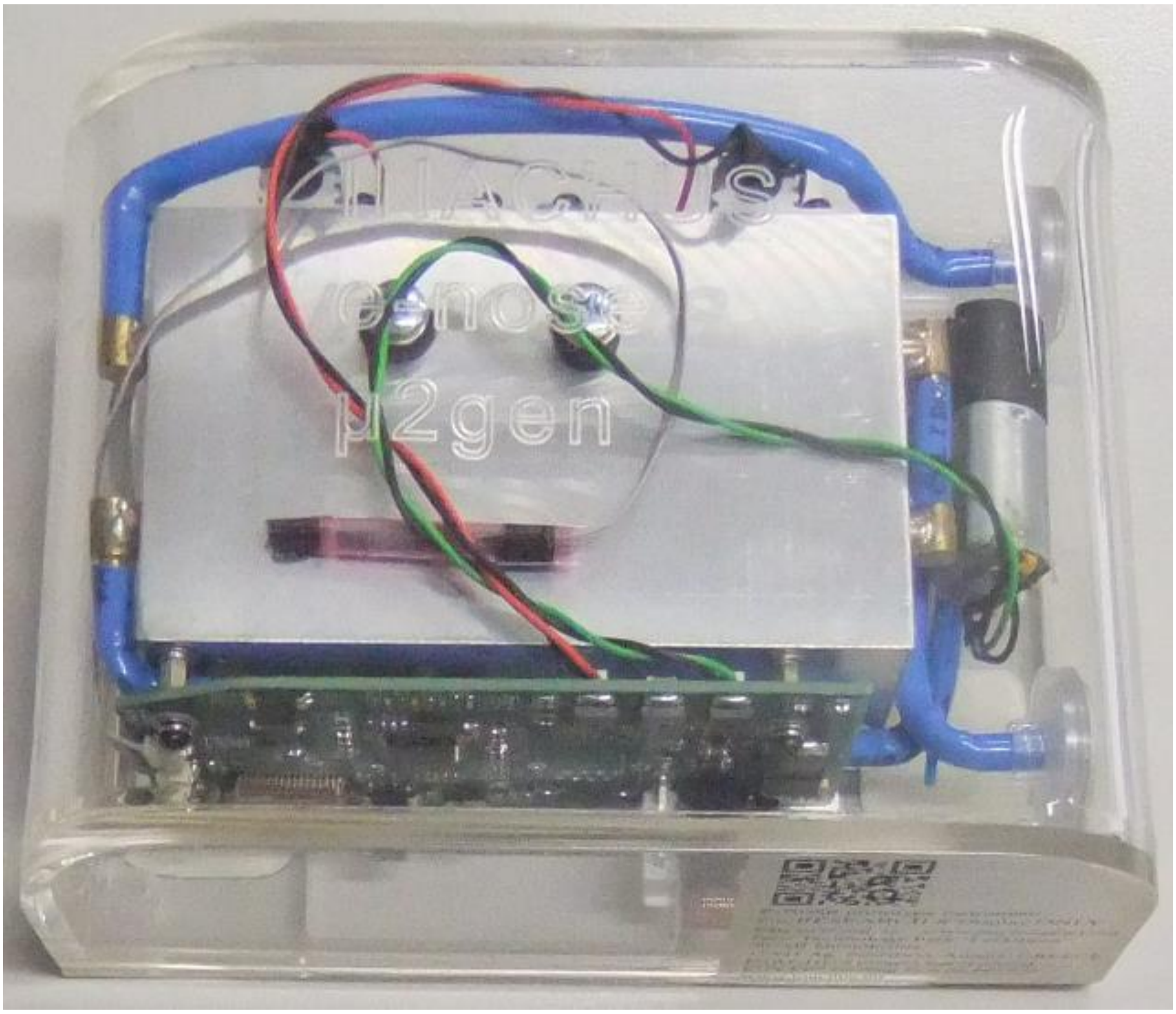

Figure 121. The completed e-nose - 3rd and final prototype

8.4. INDICATORS - Integrated interface concept

Detection scenario

The main detection scenario the e-nose is envisioned to operate in is the following. The robotic platform will enter the rubble and start moving inside. The operator will be looking at the optical cameras of the interface and the outputs of the IR camera and the e-nose. Periodically or whenever it is deemed necessary, the robotic platform will be kept stationary and measurements with the radar will be taken. The e-nose will produce six main outputs. Three of the outputs are for victim localization, two are for hazardous conditions detection and one is about the electronic nose's status. The victim localization outputs should be used in the following way: the Human indicator indicates when Human presence indicators are at detectable levels in the air. The Approaching indicator indicates when the Human presence indicators are getting stronger or weaker, thus inferring that the e-nose is approaching or moving away from a victim. The Hot Spot indicator indicates when a place with elevated human presence indicators was detected and from which the e-nose is now moving away.

The detection of a victim in a confined space is associated with high Human presence indicators. The actual values cannot be determined in uncontrolled conditions and with unknown victims. This means that specific values cannot be assigned as thresholds and maximum values. The operator of the robotic platform and the e-nose has to find the maximum value by performing a search pattern. To assist in the execution of the search pattern, the e-nose produces the Approaching indicator which informs the operator if he is moving in the correct direction (when approaching) or in the wrong direction (when moving away). A maximum (local or global) can be found by observing "approaching indicator" status followed by a "moving away" indicator status. Since the e-nose is not the only system the operator has to attend to, there is a chance he might miss this sequence. The Hot Spot indicator provides an output for such cases, indicating a maximum (local or global cannot be distinguished). Once a Hot Spot is indicated, the robotic platform has to backtrack to reposition itself at the position of maximum signal strength and execute a more thorough search using the other available sensors.

GUI Concept

This section provides information regarding the user interface (integrated GUI) of the e-nose that is integrated in the control tablet of the robotic platform. The concept and design of the integrated GUI is substantially different from that of the stand-alone GUI. This is because of the limited available space on the interface but more importantly the reduced attention of the operator allocated for the e-nose, because it is just one of the many instruments that have to be monitored and controlled by him. For these reasons the integrated GUI has only one view: a view that is permanently visible but occupies a very small section of the screen and provides alarms and indicators. These alarms and indicators facilitate the operator’s decision making. They also provide general information which is enough for the operator to gain a good situation awareness (regarding the e-nose).

In both cases, effort has been put in the design so that the interface is very easy to operate. The following key design features lead to the fulfillment of that goal:

- The operator does not have to know measurement values. All the output from the e-nose is coded in states. For example, for toxic hazards the states are coded to nothing toxic, low toxic, highly toxic, based on defined thresholds (system provider, user modification is possible).
- The operator does not have to read (words or numbers) to gain good awareness of the situation since information is color-coded. Stated values are color-coded. Green was selected for states that indicate all good or no change, yellow for states that indicate some potential issue and red for states that indicate problem or change.
- Color coding is universal. For all types of output the color coding is the same. In this way, just a glimpse of the e-nose’s interface is enough to see if there is something that is interesting or requires special attention. Any type of information can be spotted by color.
- Most important information for situation awareness is always visible. Just a glimpse at the always visible view is enough. The view has output (color-coded states) that combine the output of multiple sensors based on the output of the advanced logic unit of the e-nose. This way, the operator can focus most of his attention on operating the robotic platform, evaluating output from other sensors, coordinating with his team and filing reports.

Indicators and Alarms

The information provided to the operator, that is easily interpreted, is by Indicators and Alarms.

- **Alarms** are used to provide information about **Safety** (Hazards). Alarms are based on well defined and known thresholds. For example, one of OSHA’s criteria for a hazardous atmosphere in a confined space is when the concentration of oxygen is outside the [19.5%-23.5%] range.
- **Indicators** are used to provide information about **Victim localization**. Alarms cannot be provided for victim localization because no threshold can be defined. Indicators are not based on fixed thresholds. Some thresholds can be produced on site with automatic training, but they alone are not enough to provide the most helpful information for finding victims. A search pattern has to be performed to determine the point where the indicators show a maximum – just like a search dog is trained to do.

The following Alarms and Indicators are provided:

- Human indicator: indicates if human presence signs are in detectable limits
- Trend indicator: indicates if the robot is approaching or moving away from human indicators- getting “warmer” or “colder” while searching/moving
- Edge indicator: indicates if there is a point of interest- human indicators peaked
- Toxic Alarm: goes off if any sensor reads a toxic concentration
- Combustibles Alarm (Flammables): Alarms if the combustible sensor measures a combustible atmosphere (based on the selected target gas. The type of target gas has to be configured by the user; it is not determined by the electronic nose.)
- Status Alarm: indicates the system is properly set up and operational

Color coding

The indicators and alarms have the same color coding but a different style so that they can be distinguished. Green is used to show that nothing is found, yellow is used to show something is found but it is weak and red is used to show something is found and it is strong. The following table illustrates the concept.

Table 37: Indicator and Alarm color coding - general

INDICATOR	ZERO	WEAK	STRONG
ALARM	OK	WEAK	STRONG

The following table shows the status words and color coding per indicator and alarm (preview view). Note that all color coding and naming is debatable so that it is accepted and understood by the end-users. The general idea is that when nothing is worth mentioning, every alarm and indicator will be green. When a condition is detected, but it is not certain or it is weak, it will be colored yellow. When a condition is detected with a level of confidence or it is strong, it will be colored red. Actions could be associated with the color scheme: Green – Nothing, Yellow – Could do something, Red – Should do something.

Table 38: Status wording and color coding per alarm and indicator (preview view)

Human Ind	Trend ind	Edge ind	Combustible Alarm	Toxic Alarm	Status Alarm
No indicators	zero(steady)	zero(steady)	zero (OK)	zero (OK)	zero (OK)
weak indicators	weak(colder)*	weak (no point)	weak (issue)	weak (issue)	weak (issue)
strong indicators	strong(warmer)	strong(point of interest)	strong (Toxic)	strong (Combustible)	strong (malfunction)

* Colder and warmer color coding should be the same.

The following picture illustrates a mock-up of the robotic platform control interface with the e- nose's GUI on the right.

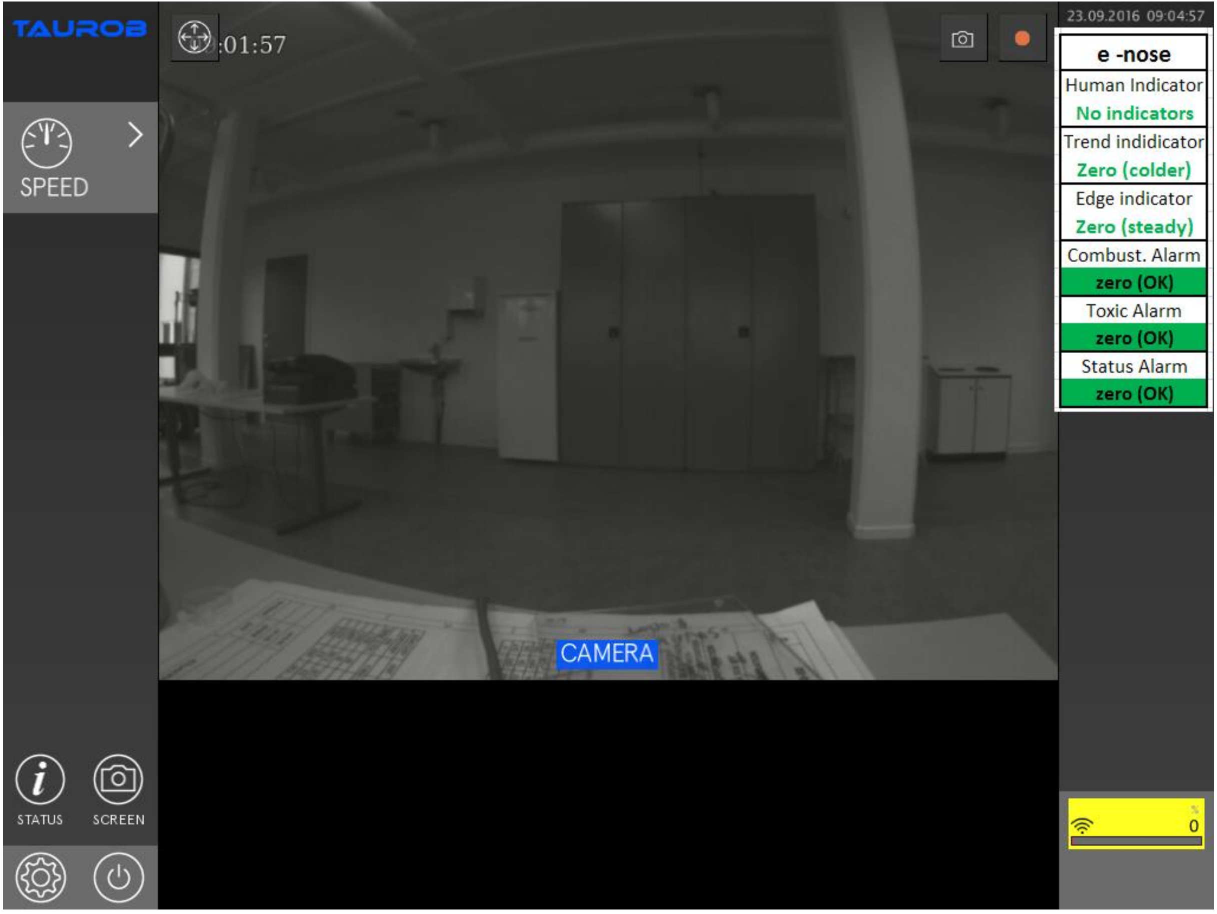

e -nose
Human Indicator
No indicators
Trend indidicator
Zero (colder)
Edge indicator
Zero (steady)
Combust. Alarm
zero (OK)
Toxic Alarm
zero (OK)
Status Alarm
zero (OK)

Figure 122: Mock-up of the interface of the robotic platform of the e-nose alarms and indicators

The operator can also control the e-nose. The available control operations are the following:

- Enable/disable the air sampling pump (sleep mode 1). This could be desired when going through an area that has an increased likelihood of clogging the air filters if the pump is ON. Another reason could be to reduce noise sources in order for the two-way communication system to operate better.
- Enable/disable the heater (sleep mode 2). This could be desired when trying to minimize power consumption when the working environment conditions allow for it. It could also be used for training purposes in order to use the electronic nose, but not put the thermal (and cycling) stress on the sensors. The downside is a reduced accuracy of the sensor readings.
- Enable/disable printing results (sleep mode 3).
- Auto-calibrate the sensors that support this function.
- Perform auto-training for the electronic nose to determine the thresholds of some of the sensors taking into account the background concentrations at the field of operation.
- Select the combustible gas target for which the system will report %LEL results. Not selecting the correct gas can in most cases lead to incorrect readings regarding the combustible environment (DANGER).

Feedback from end-users about the integrated GUI

Feedback was requested from end-users of the system (USAR.NL, EPLFM, SBFF). The concept and information displayed by the GUI to the operator was considered good and was accepted. Based on their recommendations, though, the following changes were performed when implementing the integrated interface:

- There is no distinction between alarms and indicators. All high level output is referred to as "Indicators" and the color coding of the formerly named alarms is used.
- The naming of the alarms was changed. The Trend indicator was renamed to Approach indicator and the Edge indicator was renamed to Hot Spot indicator.
- The color coding of the indicators was adapted to comply with the scheme that was utilized in the robotic platform's interface.

The advanced logic unit is responsible for converting the raw sensor readings into meaningful outputs for the operator. This involves converting each numeric measurement value into the pre-defined and color-coded sensor ranges. The most important functionality is that of evaluating the outputs of each sensor and generating the general alarms and indicators. The logic for performing this operation is based on logic operations between the sensor ranges. "APPENDIX: ADVANCED LOGIC UNIT - LOGIC TABLES" includes a portion of the logic tables that are implemented. The states for each sensor value are defined in the section "INDICATORS - Integrated interface" and details about their calculation can be found in the following section.

8.5. Software of the 3rd prototype

The software of the electronic nose can be distinguished in three different modules: The firmware running in the e-nose, the software running on the host platform that mainly implements the advanced logic functions of the e-nose and the user interface. For the user interface, two versions are designed:

- A complete graphical user interface (GUI) for stand-alone system testing, training and possibly deployment.
- A simple and yet powerful interface integrated in the robotic platform's control interface tablet.

8.5.1. Firmware

The following flow diagram depicts the high level operation of the firmware running in the e-nose.

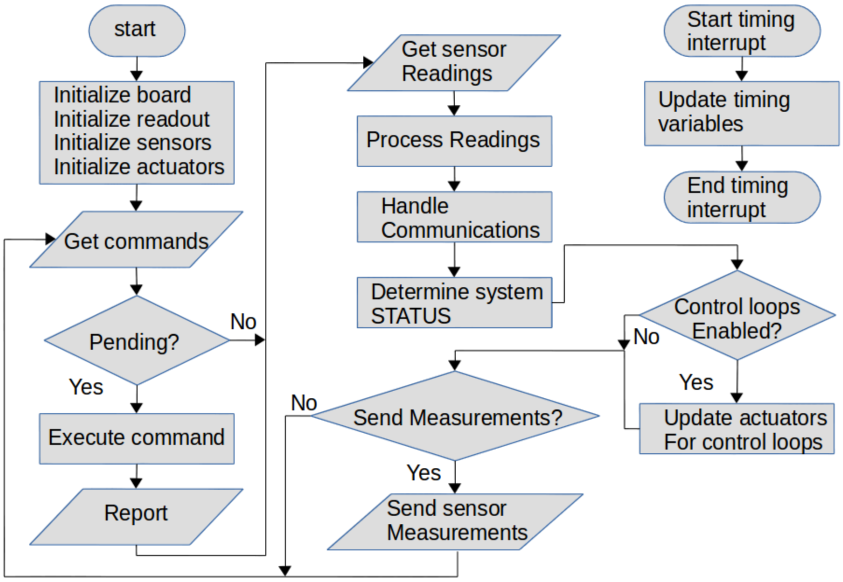
start
Initialize board
Initialize readout
Initialize sensors
Initialize actuators
Get commands
Pending?
No
Yes
Execute command
Report
Get sensor Readings
Process Readings
Handle Communications
Determine system STATUS
Send Measurements?
No
Yes
Send sensor Measurements
Start timing interrupt
Update timing variables
End timing interrupt
Control loops Enabled?
No
Yes
Update actuators For control loops

Figure 123: Flow diagram of 3rd prototype's firmware

The firmware runs on a 32bit microcontroller. It is a single program (stand-alone application) and runs without an operating system.

Firmware operation

Serial communication from the O_2 and CO_2 sensors is managed by the DMA controller with little involvement of the CPU when servicing the overflow interrupt service routines of the ping pong buffers. The output of the device is also handled by the DMA controller to the appropriate output serial port and USB CDC port of the uC. This allows enough time for the CPU to read the ADC channels and the other "slow" i2c temperature sensors and perform basic arithmetic calculations/conversions on the acquired values to produce the human readable output stream of data.

For the conversion of the analog sensor values, the datasheet sensitivity values are used (and also incorporating the current to voltage conversion and the ADC configuration parameters) and a zero offset is assumed since the sensor response is linear in the specified range. These values are corrected with 2 point calibration. Calibration is not performed on the firmware of the e-nose device but on the higher level software application named ENALU, analyzed in a following section. Readings from the CO_2 and O_2 sensors are provided in human readable values and no conversion is required. For all sensor values, the values accumulated over one second are averaged and packaged in the output stream.

At startup the complete e-nose device is initialized. The analog front end potentiostats for the electrochemical sensors are configured with the biasing parameters of the connected sensors. The i2c connected temperature sensors are also configured to output the temperature in the required resolution/accuracy. The GPIOs of the microcontroller are configured in the correct direction (input or output) and for the outputs the correct value is set. Initial values are applied to all state holding variables and data variables. Hardware peripherals of the microcontroller are initialized and enabled. Finally all interrupts are enabled just before entering the main loop.

When in the main loop and a timing interrupt is triggered and served, the corresponding state variables are updated. The appropriate action is performed in the main loop. The same principle is applied for servicing control commands. The input data stream is monitored for valid commands and when one is detected the corresponding state variable is updated. The execution of the appropriate action is performed in the main loop.

When the temperature control loop is activated, its execution is also handled in the main loop. Due to the large mass of the manifold, which has a large thermal capacity, and the relatively small power available to the heating resistors there is a slow response to input changes. Taking also into account the relaxed temperature accuracy and stability requirements, a simple ON/OFF control mechanism with a small hysteresis is implemented.

Sampling the voltage output from the readout electronics of the analogue sensors is performed with a multichannel ADC. This ADC has a single converter with an analog switch connected before its input for selecting the ADC channel to be sampled and converted. Depending on the conversion accuracy, the required time varies. The firmware in each loop execution monitors the status of the conversion (non blocking) and changes the input channel when the converted value is acquired in order to sample the next sensor.

Output format

The output of the electronic nose is the following:

```
r co2 0 000980 pO2 0 020.39 nh3 0 +000.6 H2O 0 042.18 iTe 0 +29.88 eTe 0 +27.00 oO2 0 0200.3 tO2 0 +29.80 bO2 0 000982 COm 0 +005.4 H2S 0 +003.3 FLA 0 -004.1 STA 0 0x00ae
```

The format has the following properties:

- Starts with the character ‘r’.
- Single line terminated with the character ‘\r’ (not \r\n or \n).
- Has a fixed length if no errors have occurred.
- Each measurement is indicated by a label that is followed by a valid character (not implemented yet, always reads as zero ‘0’).
- The measurement field is fixed length, even for value zero.

Output units and label definition

The output of the e-nose values has the following units:
i,co2,0, ppm,pO2,0, %,nh3,0, 0.1ppm,H2O,0, RH%,iTe,0, oC,eTe,0, oC,oO2,0, mbar,tO2,0, oC,bO2,0, mbar,COm,0, ppm,H2S,0, ppm,FLA,0, %CH4,STA,0,

Table 39: Labels and units of e-nose output.

Label	Gas name	Units	Comments
co2	CO_2 – Carbon Dioxide	Ppm	
pO2	O_2 – Oxygen (percentage)	%	
Nh3	NH_3 – Ammonia	0.1ppm	
H2O	Relative Humidity	%RH	
iTe	Internal Temperature	°C	
eTe	External air temperature	°C	
oO2	O_2 – Oxygen (partial pressure)	Mbar	
tO2	Temperature of Oxygen sensor	°C	
bO2	Barometric pressure – from Oxygen sensor	Mbar	
Com	CO – Carbon Monoxide	Ppm	
H2S	H_2S – Hydrogen Sulfide	Ppm	
FLA	Flammables / Combustible gases	%methane	
STA	Status	In Hexadecimal format	See following table for details

Table 40: Status – STA bit interpretation. Note that the status is printed in Hexadecimal (0x00xx)

bit #	15	14	13	12	11	10	9	8	7	6	5	4	3	2	1	0
Function	6V enabled	Heater FB	Pump FB	24V OK	LED 3	LED 2	LED 1	LED 0	Humidity OK	Pressure OK	FLA volt. ok	iTe OK	Heater Stat.	Heater Enable	Print	Pump
Val.									1=OK		1=OK	1=OK	1=On	1=On	1=On	1=On

bit #	15	14	13	12	11	10	9	8	7	6	5	4	3	2	1	0
implemented	No	No	No	No	No	No	No	No	Yes	No	Yes	Yes	Yes	Yes	Yes	Yes
Notes		Red	Orange	Yellow	Green											

An output example of the status (STA) is the value (0x00ae). The status value in binary representation is 10101110. The status indicates that:

- Humidity is within operational levels.
- Pressure.
- Voltage of the flammable / combustible gases is OK – valid output from the sensor.
- The internal temperature has not reached operational target; output should not be used for search.
- Heater is ON.
- Heating is enabled.
- Printing / returning measurements is enabled.
- Pump is OFF.

Control commands

The following commands are implemented for controlling the e-nose via the serial (Ethernet) or USB (CDC class) interface. Note that only the character has to be sent – pressed. Enter does not have to be pressed when connected to a terminal.

Table 41: Control command for the e-nose firmware

Command	Command description	Operands	Comments
‘P’	Turn Pump ON		
‘p’	Turn Pump OFF		
‘R’	Start printing Measurements		
‘r’	Stop printing Measurements		Only affects serial (Ethernet) interface. USB is always on.
‘H’	Enable Heating		
‘h’	Disable Heating		
‘G’	Calibrate CO_2 to 400ppm		
‘S’	-		Reserved

Start-up behavior

The start-up behavior when power is applied to the e-nose is controlled by the state of the GP0 and GP1 input switches located on the control PCB.

- When GP0 is **not** pressed towards the PCB surface, then the e-nose will print measurements after power up. If GP0 is pressed, the measurements will not be sent to the output. The output can be enabled after power up with the ‘R’ command.

- When GP1 is **not** pressed towards the PCB surface, then the e-nose will be set to reach operational temperature when powered up. The heater will probably turn ON. If GP1 is pressed, the e- nose will not attempt to reach operational temperature. The e-nose can be commanded to reach operational temperature after power up with the ‘H’ command.

By default, after power up the air sampling pump is OFF.

The output can be sent to the Ethernet port when the switch is at the STD position or to the serial port (debug port) when the switch is at the DBG position.

Calibration

The calibration options for the e-nose are two: single point calibration or zeroing and two point calibration, or simply calibration. In one point calibration or zeroing, it is assumed that the gain of the sensor is correct and any discrepancies are due to a fixed error offset. In two point calibration, or calibration, it is assumed that both the gain and the offset need to be determined. In practice, two point calibration is executed by performing a zeroing of the sensors and then a calibration with a calibration gas (one for every sensor – worst-case). These two steps provide the two required data points, but require only one calibration gas (per sensor) with the assumption that clean air has a well-defined concentration value.

The calculation of the correct output of a gas detector that is meant for hazard detection must be performed on the hardware. For this e-nose which is a research prototype and not a market ready device, the calculation will not be performed on the hardware where the sensors are placed.

The calculation of the correct concentration value from the reported value is the following:

$$G(y(x) = Ay(x) + B \tag{29}$$

Where y(x) is the concentration value reported by the e-nose, and G(y(x)) is the corrected concentration value. For zeroing (1 point calibration), A = 1 and B are determined by solving the equation when substituting the following values:

G(y(x)) is substituted with the assumed clean air value for the sensor. For example, the CO_2 value is 400ppm and the H_2S value is zero. y(x) is substituted with the actual value reported by the e-nose when exposed to the assumed clean air. For example, the CO_2 value could be 501ppm and the H_2S value could be 1pmm.

For calibration (2point calibration), values A and B are calculated by using the two known data points: one for clean air and one with the calibration gas mixture. Note that both A and B must be calculated, the B value of a sensor zeroing cannot be used.

$$A = (G\big(y(x2)\big) - G(y(x1))/(y(x2) - y(x1)) \tag{30}$$

$$B = G\big(y(x1)\big) - Ay(x1) \tag{31}$$

8.5.2. Advanced logic unit

The electronic nose's advanced logic unit (ENALU or enalu) core software component is the data sampling, processing, logical analysis and logging unit of the electronic nose. It can work independently of user interaction using default or preconfigured values and will constantly report individual statistics for each sensor, as well as monitor for human presence, flammable and toxic gases and even its own hardware's good health. It runs on an external from the e-nose computing platform.

Sensor

A "sensor", in this context, is a software object representing the hardware equivalent present in the e-nose manifold. It is the recipient of the sampled values from the specific hardware sensor and holds methods to process them. Specifically, the sensor object:

- Stores incoming samples in an internal buffer.
- Performs calibration on the input samples.
- Performs training of the session thresholds based on historical data.
- Processes current and historical data to produce useful statistics and trends regarding the state of the gas monitored by the sensor.
- Stores and recalls session thresholds, calibration data and other configuration data from file.

The last feature is especially useful as it enables full resumption of a terminated (but saved) session.

There are several sensors on the e-nose hardware and each has a specific identifier so that commands can be used to update specific features of every one of them. These identifiers are listed in the following table:

Table 42: Gas sensor name identifiers as perceived by the E-nose applications

#	Gas sensor name	Description
1	"CO2"	Carbon dioxide sensor
2	"O2PER"	Oxygen sensor (percentage reading)
3	"PPO2"	Oxygen sensor (partial pressure reading)
4	"NH3"	Ammonia sensor

#	Gas sensor name	Description
5	“TIN”	Manifold temperature sensor (internal)
6	“TEX”	Environment temperature sensor (external)
7	“HUM”	Manifold humidity sensor (internal)
8	“HUMEX”	Environmental humidity sensor (external)
9	“TO2”	Temperature of the Oxygen sensor
10	“BO2”	Barometric pressure sensor
11	“CCO”	Carbon monoxide sensor
12	“H2S”	Hydrogen sulphide sensor
13	“CMB”	Combustibles (=flammables) sensor (methane % concentration reading)
13.1	“Methane”	Combustibles - Methane % LEL reading
13.2	"Propane"	Combustibles - Propane % LEL reading
13.3	"Butane"	Combustibles - Butane % LEL reading
13.4	"Pentane"	Combustibles - Pentane % LEL reading
13.5	"Hexane"	Combustibles - Hexane % LEL reading
13.6	"Heptane"	Combustibles - Heptane % LEL reading
13.7	"Octane"	Combustibles - Octane % LEL reading
13.8	"Methanol"	Combustibles - Methanol % LEL reading
13.9	"Ethanol"	Combustibles - Ethanol % LEL reading
13.10	"Isopropyl"	Combustibles - Isopropyl % LEL reading
13.11	"Acetylene"	Combustibles - Acetylene % LEL reading
13.12	"Butadiene"	Combustibles - Butadiene % LEL reading
13.13	"CarbonMonox"	Combustibles - CarbonMonox % LEL reading
13.14	"Acetone"	Combustibles - Acetone % LEL reading
13.15	"MethylEthylKetone"	Combustibles - MethylEthylKetone % LEL reading
13.16	"Toluene"	Combustibles - Toluene % LEL reading
13.17	"EthylAcetate"	Combustibles - EthylAcetate % LEL reading
13.18	"Hydrogen"	Combustibles - Hydrogen % LEL reading
13.19	"Ammonia"	Combustibles - Ammonia % LEL reading

#	Gas sensor name	Description
13.20	"Cyclohexane"	Combustibles - Cyclohexane % LEL reading

Please note that the whole family of combustible sensors that return a %LEL reading, as well as the external humidity sensor, are virtual sensors that exist only in software. They return a modified result based on the samples derived from sensors “CMB” and “HUM” respectively.

Input data stream

The core application has been developed to accept input streams from the e-nose hardware for either a serial or an Ethernet port. In either case the data is delivered in a separate thread that stores input in the internal buffer. The worker thread picks up the data and performs the necessary processing. The data have the following layout:

```
r co2 0 001300 pO2 0 019.80 nh3 0 +001.1 H2O 0 014.53 iTe 0 +39.88 eTe 0 +33.81 oO2 0
0196.1 tO2 0 +39.50 bO2 0 000990 COm 0 +001.9 H2S 0 -000.0 FLA 0 -000.1 STA 0 0x00b6
```

An update message with new values for all the sensors will always start with the letter “r”, while the separator is a single space character. What follows is each separate hardware sensor, in turn, along with 2 values as discussed in the following table:

Table 43: Layout of the input data stream basic element

Parameter	Description
Co2	Sensor name
0	Validity of the value (0 = valid)
001300	The updated value (in unit described in the sensor manual)

All sensor elements follow this pattern. This includes the following sensors

Table 44: Layout and order of

Parameter	units	Description
co2	ppm	CO_2 sensor
pO2	%	Oxygen sensor (% reading)
nh3	0.1 * ppm	Ammonia sensor
H2O	%	Humidity sensor
iTe	°C	Manifold (internal) temperature sensor
eTe	°C	Environmental (external) temperature sensor
oO2	mbar	Oxygen sensor (partial pressure reading)
tO2	°C	Oxygen sensor temperature reading
bO2	mbar	Oxygen sensor barometric pressure reading
COm	ppm	Carbon monoxide sensor
H2S	ppm	Hydrogen sulphide sensor

Parameter	units	Description
FLA	%	Combustibles (flammables) sensor

Finally, the last parameter that is sent to the core ENALU application is the hardware status ("STA") message. It is a 2 byte value containing the status of all hardware parts. For a detailed view on this 2 byte value, please see Table 40.

Sensor operation

In the main loop of execution the sensor simply receives samples for input (Ethernet or serial connection), stores them in an internal buffer (a circular buffer suffices for time series data in this case) and performs processing on that buffer according to the Sensor Indicator types (see chapter 8.5.3). At the end of the main loop the sensor makes the results of this processing available upstream.

When training is performed the process differs slightly. The data are stored in a training buffer (rather than the usual circular buffer). The reason behind that is that training time will always be larger than the observation (detection) window that the circular buffer has been configured to operate upon. Additionally, sensor indicators are not updated during training duration – this is to avoid reporting transient results to the user interface.

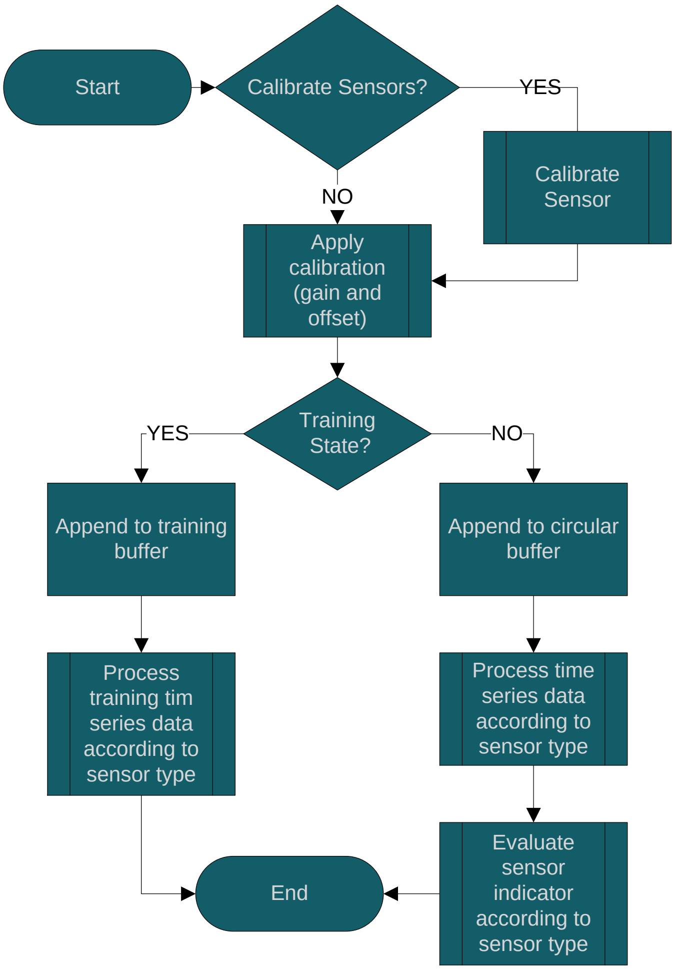
Start
Calibrate Sensors?
YES
Calibrate Sensor
NO
Apply calibration (gain and offset)
Training State?
YES
NO
Append to training buffer
Append to circular buffer
Process training tim series data according to sensor type
Process time series data according to sensor type
Evaluate sensor indicator according to sensor type
End

Figure 124: Main loop execution during training and normal modes

However, other commands may be required to be executed in parallel or instead of the commands of the main loop. Specifically, it is possible that the user will request that a calibration is performed or even training.

Training

For correct runtime operation the e-nose application must be trained every time, before performing gas detection in the field. This happens so that a number of internal variables can be tweaked according to the local conditions. Such conditions include not only local temperature and pressure, but also background gas levels. For example, CO_2 levels vary during the day and from place to place (often this tends to be in higher levels in densely populated areas).

To perform the training process the user must send to the core application the command

```
tr <training duration in seconds>
```

Which stands for “training”. When training initializes a similar procedure to normal main loop, execution is followed (see Figure 124). However, there are two main differences, which need to be mentioned:

1) No evaluation of the sampled data is carried out.
2) A specific training buffer is used to hold samples.

Evaluation is not carried out because it could lead to reporting false results to the user during this transient period, while a separate buffer secures that training can be performed in a much larger than the usual buffer size used during normal operation.

At the end of the training cycle the training buffer is used by the sensor indicator types (see chapter 8.5.3) to set the training values which will be used as references for the normal operation evaluation tests.

8.5.3. Sensor Indicator types

Useful information is expected to be extracted by processing the data in the sensor buffer. For example, a noise-free version of the incoming signal, a trend about whether the signal (i.e. the gas concentration) is generally increasing or decreasing, local (i.e. quick and intense) peaks in the gas concentration will help the user determine the current gas state around the e-nose.

In order to provide different feature extraction functionality, several different sensor types have been developed, all of which work with a set of values acquired from training or are user-defined. A mechanism has been created so that the user is able to view all values related to sensor indicator types and set the user-defined ones during runtime. The “view thresholds” command, which can be typed in directly during runtime to the running session of the core e-nose application is

```
pr thr
```

which stands for “print thresholds”. Alternatively, to set one of the user defined values, one should type in the command

```
upd <gas sensor name> <sensor type name> <threshold name> <new value>
```

All fields are necessary and each field should contain a value. For possible values see the following table:

Table 45: Explanation of the parameters accepted when setting a user-defined threshold

Parameter	Value
Gas sensor name	Please see Table 42.
Sensor type name	“thres” = for threshold type, “trend” = for trend (a.k.a. approaching) sensor type, “edge” = for POI sensor type.
Threshold (i.e. value) name	Please see individual “threshold” tables in each gas sensor type in 8.5.5, because each sensor accepts different thresholds.
New value	A floating point value.

Please note that the thresholds will be saved to file along with other data during a saving operation, thus a loading operation (or “recall”) will reinstate those thresholds that were previously saved in a file.

Threshold sensor indicator

The most important indicator type is the averaging sensor type. It works as time-series moving average filter that allows suppression of the noise in the signal. Averaging works based on a preconfigured window size which may be smaller than or equal to the input buffer size. It is always the latest data samples that are used in the averaging process.

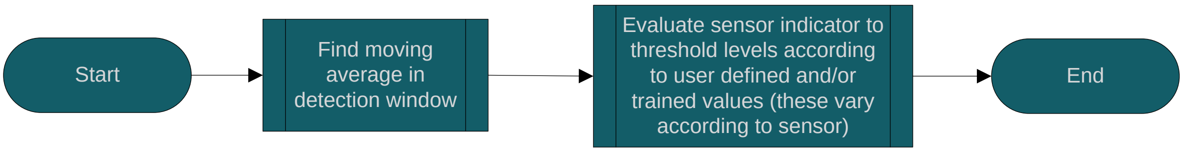
Start
Find moving average in detection window
Evaluate sensor indicator to threshold levels according to user defined and/or trained values (these vary according to sensor)
End

Figure 125: Processing of Threshold sensor type on sampled data during normal execution

Once the average value has been determined, it is used along with the average calculated on the last training session to determine the threshold range in which the current concentration lies. The thresholds that separate the threshold ranges differ from sensor to sensor and can be either user-defined or calculated during training or both. The entire set of user-defined thresholds is: *"zero", "low", "signal", "normal", "warning", "high", "dangerous"* and *"toxic"*, but all sensors use a subset of this set (see the following chapter for details). The set of training related thresholds are: “mid”, “midh” (for “mid - high”) and “midl” (for mid-low). Again, each sensor only uses a sub-set of these if training is performed on the sensor. Ultimately, the current value of the signal falls within one of these threshold “zones” (or ranges) and this is what is reported on output.
To set the threshold level, a user should send the following command to the e-nose

```
upd <gas sensor name> thres <threshold name> <new value>
```

Please note that even the training thresholds can be updated after a training operation (and thus be user-defined).

Training of threshold sensor indicator type
The aim of the training period is to determine the average (mean) and standard deviation of the incoming signal.

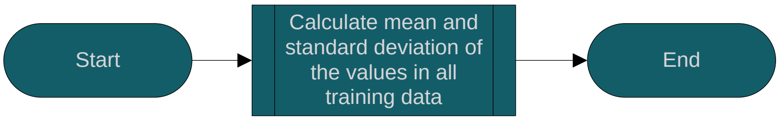
Start
Calculate mean and standard deviation of the values in all training data
End

Figure 126: Processing of Threshold Indicator Type at the end of a training cycle

This leads to a definition of the “range” of values which constitute the “noise” level, i.e. a level for which the specific signal is considered to be at “quiescent” or background value. This range is **normally** calculated as

```
"Noise" threshold zone = Mean +/- factor * standard deviation
```

Where, the factor is set independently for each sensor and is user-defined. Using a factor of 1, means that approximately 66% of the training sampled values will fall within the “noise” range and thus be considered as such. Instead of trying to include more than 99% of the trained values in the noise range, a value of 3 is used as a default. Using the minimum and maximum values to determine the noise range has been avoided in order to ensure that any training spikes will not help determine the noise range.
Alternatively, on occasions where the standard deviation of a signal is expected to be very small or even zero (such as the oxygen sensor and the barometric pressure signal), there is little use in using the standard deviation as it will create a very thin noise range, which is practically useless. In such cases it is more useful to have a **fixed** range and the calculation that takes place then is the following

```
"Noise" threshold zone = Mean +/- factor
```

That is, the range is set as 2 * factor and biased at the calculated “mean” level. To set the factor, a user should send the following command to the e-nose

```
upd <gas sensor name> thres range <new value>
```

Where “range” is the value of the factor that needs to be set.

Trend sensor (a.k.a. proximity tendency, approach – move away sensor) indicator

The trend indicator is used to identify the gradient or “slope” of the samples within the detection window. To do that “data fitting” is carried out in order to obtain a linear first order trend line (y=ax+b). Specifically, the least square method is used from the *GNU Scientific library (GSL)* in order to carry out the tedious calculation. Once the gradient has been obtained it is used, along with the trend levels calculated during the last training session, to categorize the current trend to “steady”, “decreasing” (i.e. moving away), or “increasing” (i.e. approaching).

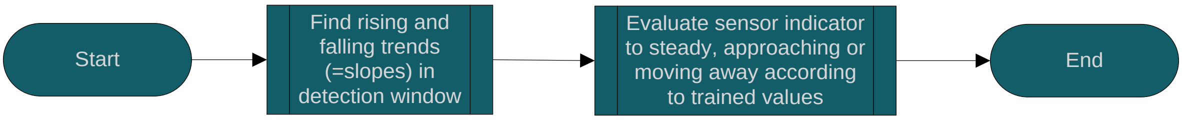
Start
Find rising and falling trends (=slopes) in detection window
Evaluate sensor indicator to steady, approaching or moving away according to trained values
End

Figure 127: Processing of Trend sensor type on sampled data during normal execution

During training the training buffer samples are used to determine the average gradient across a moving window that "runs" across all the data. This is possible as the training data sample number will always be more (= has a larger buffer size) than the detection window size. Thus "many" detection windows will exist within the training data set and the gradient in each of these windows is calculated. In the end, the average and standard deviation of these gradients is calculated and this is what will be used as a reference during normal operation

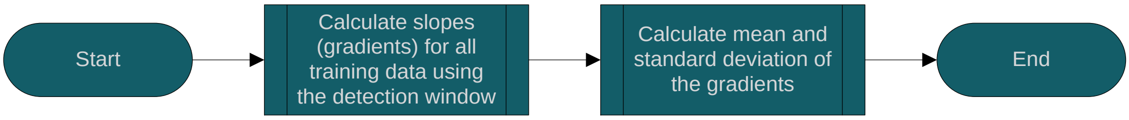
Start
Calculate slopes (gradients) for all training data using the detection window
Calculate mean and standard deviation of the gradients
End

Figure 128: Processing of Trend Indicator Type at the end of a training cycle

As in the Threshold indicator type's case, it is again possible to have a **normal** or **fixed** range in which the value of the gradient within the detection window is supposed to remain "steady". These are calculated respectively as

```
        "Steady" trend zone = +/- factor * gradient's standard deviation
        "Steady" trend zone = +/- factor
```

Where the factor is again user-defined. One can observe that the mean is not used for trend calculation. This is so as to avoid adding a bias that would disrupt the symmetry of the trend.

To update the trend range one can send the command

```
        upd <gas sensor name> trend range <new value>
```

Obviously, a gradient value greater than *+factor * std. dev.* will be reported "increasing" or "approaching" , while a gradient value smaller than *-factor * std. dev.* will be reported as "decreasing" or "moving away".

Point of Interest sensor indicator

When moving within a cavity in the rubble it is possible that the human presence will already have been there for a long time. In such a case the exhaled breath may have saturated the cavity thus leading to the approaching indications remaining at "steady" level. To continue to have a "close proximity" indication or "point of interest" ("POI") indication when the robotic platform passes close to a human in the cavity, the point of interest indicator has been implemented. Its purpose is to detect transient peaks (or troughs in the case of O_2 sensor) which last very little, but could help pinpoint a local gas source (or sink) even within a saturated cavity.

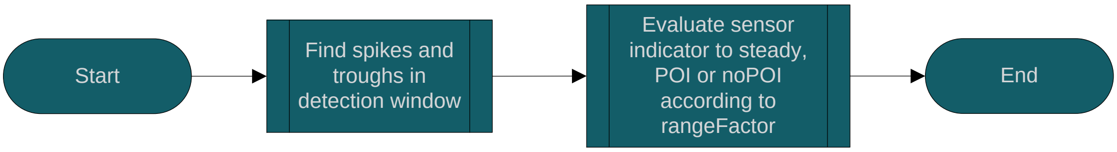
Start
Find spikes and troughs in detection window
Evaluate sensor indicator to steady, POI or noPOI according to rangeFactor
End

Figure 129: Processing of point of interest sensor type on sampled data during normal execution

To do this the most recent maximum or minimum value (within the detection window) is checked against the average value again within the detection window. Then any large deviations from the average are registered as "POI" ("peaks" or "troughs", depending on what the sensor considers as significant), or otherwise "no POI". Additionally, when signal is in "noise" zone, no transient peaks will trigger the specific indicator.

The actual calculation for "peaks" is

```
        factor = recent maximum - average value
```

If "factor" is larger than the user-defined factor value then the algorithm produces the output of having a local point of interest. The default user-defined value in this case is 2.

Similarly for the "troughs" the actual calculation is:

```
        factor = recent minimum - average value
```

In this case the user-defined factor is a negative value and if the calculated "factor" is smaller than the user-defined factor value then the "POI" indicator is triggered.

To update the value of the factor, the user must send the following command to e-nose:

```
upd <gas sensor name> edge factor <new value>
```

8.5.4. Calibration

Calibration for the sensors aims to correct any drifts in the reported value due to aging of the sensors. It is expected to be linear and attempts to calculate correction factors (offset and gain) used during normal operation. Two calibration procedures are supported by the e-nose algorithm:

- Two point calibration, where both gain and offset are calculated and applied,
- Zero calibration, where only the offset is calculated and applied to the incoming data.

During normal operation incoming data are modified in the following way

```
Buffered value = incoming value * gain + offset
```

Where by default gain = 1 and offset = 0.

For “Zero calibration” the offset is calculated as

```
Offset = zero concentration – average value
```

Where the average value is just the average of the last 10 sampled values and zero concentration values are as follows

Table 46: Zero concentration values for calibrate-able sensors

Gas Sensor Identifier	Zero Concentration Value
CO2	400 ppm [93]
O2PER	20.95% [94]
PPO2	213.32mbar [95]
NH3	0.0057ppm [96]
BO2	1013.25mbar
CCO	0.1ppm [97]
H2S	0.00047ppm [98]
CMB	0.0001834% [99]

Note that the sensors that are not shown in table above are not able to be calibrated.

For “Two point calibration” 2 datasets are used to solve the equations, where the average value is once again the average of the last 10 sampled values and the “known concentration” is provided at runtime by the user.

Equations:

```
Buffered value = incoming value * gain + offset
```

Two datasets for two point calibration:

Zero dataset:

```
Zero concentration = average value1 * gain + offset
```

Calibration gas mixture dataset:

```
User input value = average value2 * gain + offset

Offset = zero concentration – average value1 * gain   (32)

Gain = (user input value – offset) / average value2   (33)
```

Substitute equation (32) in equation (33) and calculate gain.

With equation (32) and known gain calculate offset.

In order to perform a calibration the user should send the following command to e-nose

```
cal <gas sensor name> <calibration type> [known concentration]
```

Where

Table 47: Calibration command parameters

Parameter	Value
Gas sensor name	Please see Table 42.
Calibration type	"zero" = for zero calibration, "2pt" = for two point calibration, "none" = to reset to: gain =1 and offset = 0
known concentration	A floating point value. Required only if "calibration type" above is "2pt".

Please note that if calibration is performed, the sensors will require retraining.

8.5.5. Gas Sensor Types

Especially for the thresholds (and partially for the trends) of each sensor smaller or larger variations needed to be implemented. These are explained in the following section

CO_2 threshold sensor type:

The carbon dioxide sensor has the following three thresholds, which separate 4 threshold zones.

Table 48: CO_2 Thresholds and threshold zones

Threshold name	Default Value (ppm)	User - Defined / obtained from Training	zone	zone color	Zone Description
zero	360	user - defined	zero	red	Faulty sensor
			noise	grey	training range
mid	-	both			
			signal	orange	CO2 source
toxic	5000	user - defined			
			toxic	red	

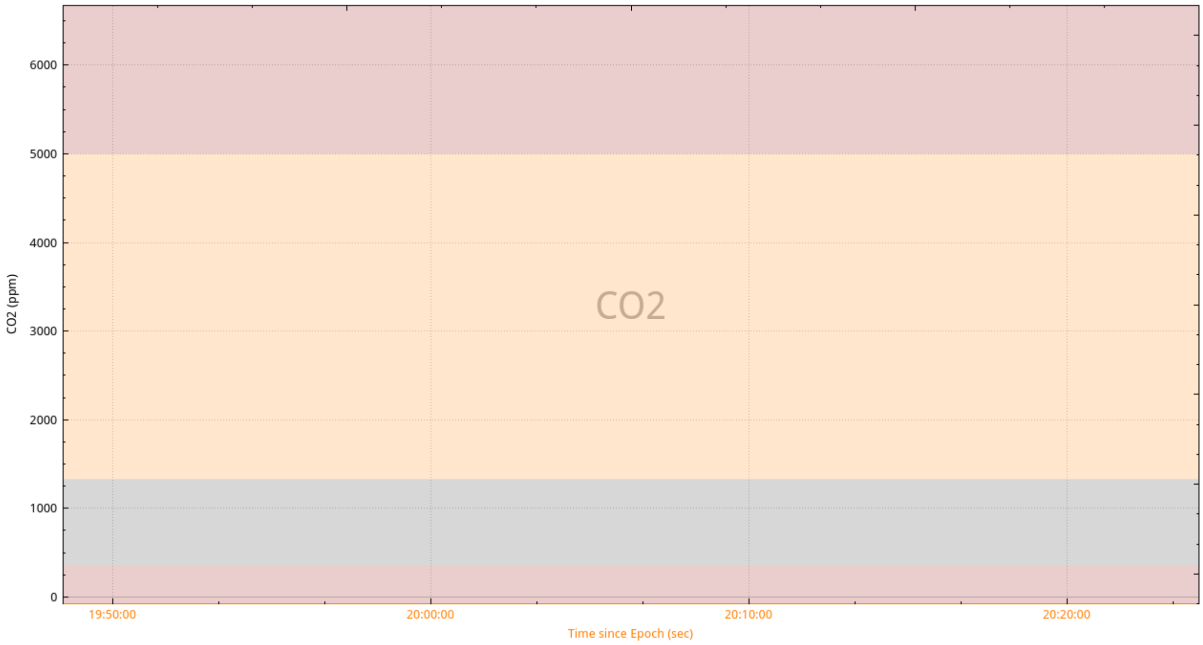

Figure 130: Graph depicting the CO_2 threshold levels

It is expected that after training the sensor concentration will remain in the “noise” zone until human presence (or other CO_2 generating sources) will let it go into “signal” or even “toxic” zone. Going into “zero” zone during normal operation is considered as a fault condition.

O_2 threshold sensor type:

The oxygen sensor has the following 5 thresholds, which separate 6 threshold zones.

Table 49: O_2(%) Thresholds and threshold zones

Threshold name	Default Value (%)	User - Defined / obtained from Training	zone	zone color	Zone Description
elecchem	19.4	user - defined	zero	red	untrustworthy accuracy of readings
low	19.5	user - defined	low	red	unsafe for human presence
midl	-	both	signal	orange	Oxygen sink
midh	-	both	noise	gray	training range
toxic	23.5	user - defined	warning	orange	Oxygen source
			toxic	red	

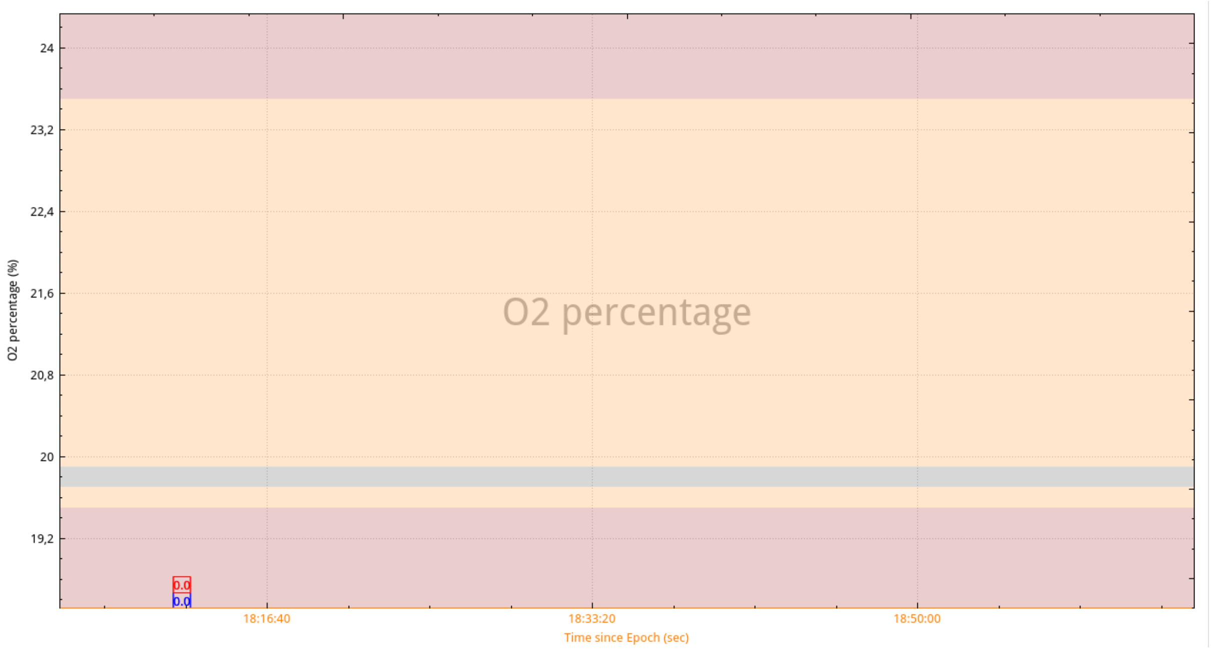

Figure 131: Graph depicting the O_2(%) threshold levels

In this case a lowering of the normal value (from noise level) will signify an oxygen sink (human presence or otherwise). The user-defined “low” and “toxic” thresholds are provided. The warning threshold zone is never expected to be visited unless an oxygen source exists in the vicinity.
Note than the O_2 sensor has been set to have a fixed range due its low standard deviation value as obtained at the end of a training session.

Similarly, for partial pressure oxygen sensor the threshold values are:

Table 50: Partial pressure O_2 Thresholds and threshold zones

Threshold name	Default Value (mbar)	User - Defined / obtained from Training	zone	zone color	Zone Description
elecchem	167.22	user - defined	zero	red	untrustworthy accuracy of reading
			low	red	unsafe for human presence
low	178.23	user - defined	signal	orange	O2 sink
midl	-	both	noise	gray	training range
midh	-	both	warning	orange	O2 source
toxic	238.9	user - defined	toxic	red	

The default values have been determined by using the assumptions that:

- The air is dry, thus at sea level 1 mm Hg =1.33322368 mbar
- 16% O_2 corresponds to 122 mmHg

Then O2(mbar) = O_2(%) * 122mmHg / 16%.

NH_3 threshold sensor type:

The ammonia sensor has the following threshold which separates the following 2 threshold zones

Table 51: NH_3 Thresholds and threshold zones

Threshold name	Default Value (ppm)	User - Defined / obtained from Training	zone	zone color	Zone Description
signal	-	user - defined or obtained from training	low	gray	training range
			signal	orange	NH3 source

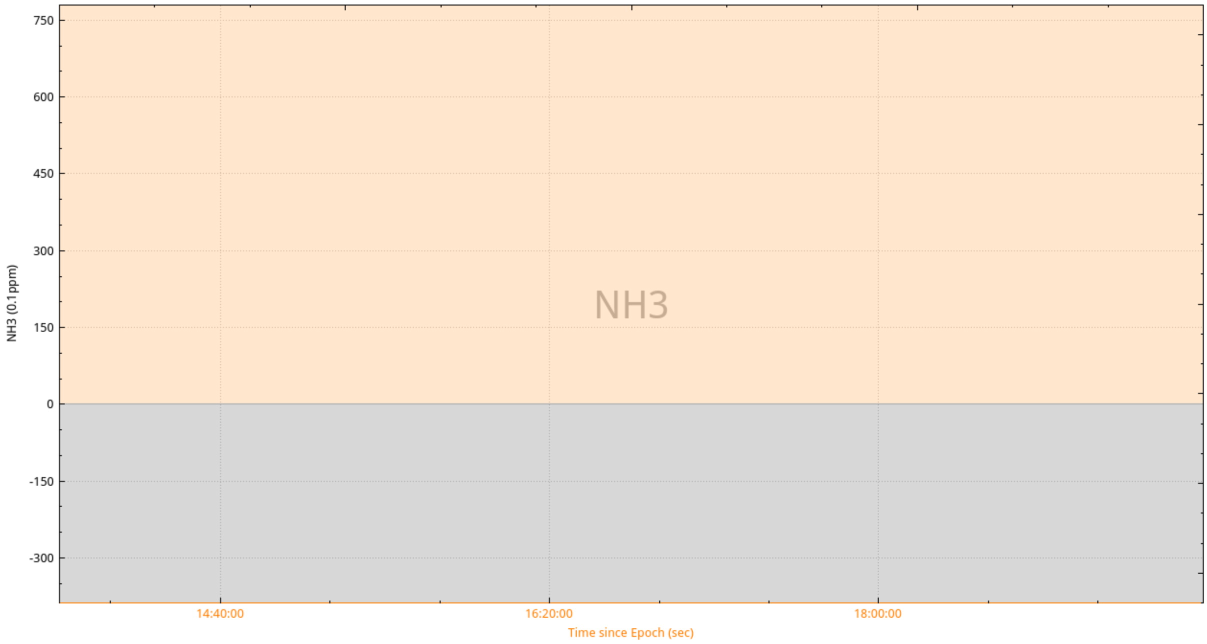

Figure 132: Graph depicting the NH_3 threshold levels

Due to the extremely low background value of ammonia in a normal environment it is possible that the trained value will be too low and trigger "signal" indications often even though it is only noise. In such a case the user can send the command

```
upd <gas sensor name> thres signal <new value>
```

Then this specific sensor will start using this new user-defined value as a "signal" threshold. If the user wants to move back to using the trained value, then the command

```
upd <gas sensor name> thres sysValue 1.0
```

should be sent to the sensor.

Manifold temperature threshold sensor type

The manifold temperature sensor has the following 2 thresholds, which separate the following 3 threshold zones

Table 52: Manifold temperature thresholds and threshold zones

Threshold name	Default Value (°C)	User - Defined / obtained from Training	zone	zone color	Zone Description
low	38.5	user - defined	low	orange	
			normal	green	
high	41	user - defined	high	red	

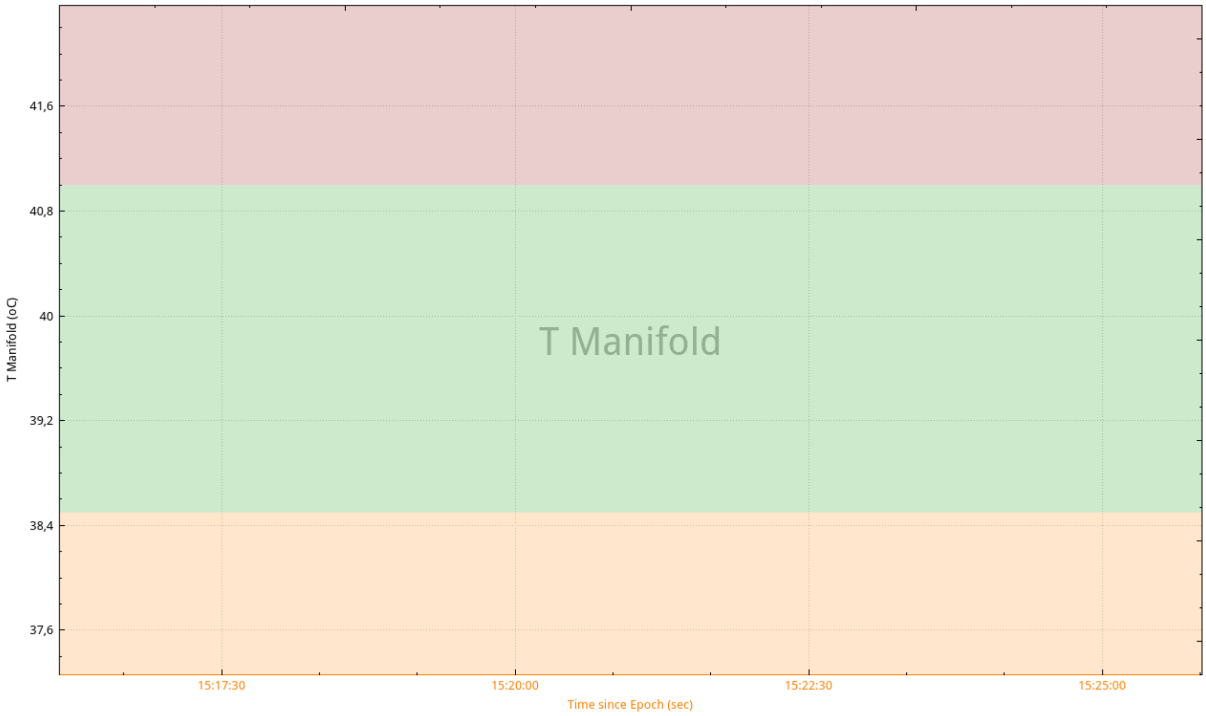

Figure 133: Graph depicting the manifold temperature threshold levels

During normal operation (and after the heating up stage during booting) the manifold temperature should be around 39.9 +/- 0.25 °C.

Environmental Temperature thresholds sensor type
The Environmental temperature sensor has the following 3 thresholds, which separate the following 4 threshold zones

Table 53: Environmental temperature thresholds and threshold zones

Threshold name	Default Value (°C)	User - Defined / obtained from Training	zone	zone color	Zone Description
low	0	user - defined	low	orange	
			normal	green	
high	40	user - defined			
			high	orange	
danger	45	user - defined	dangerous	red	

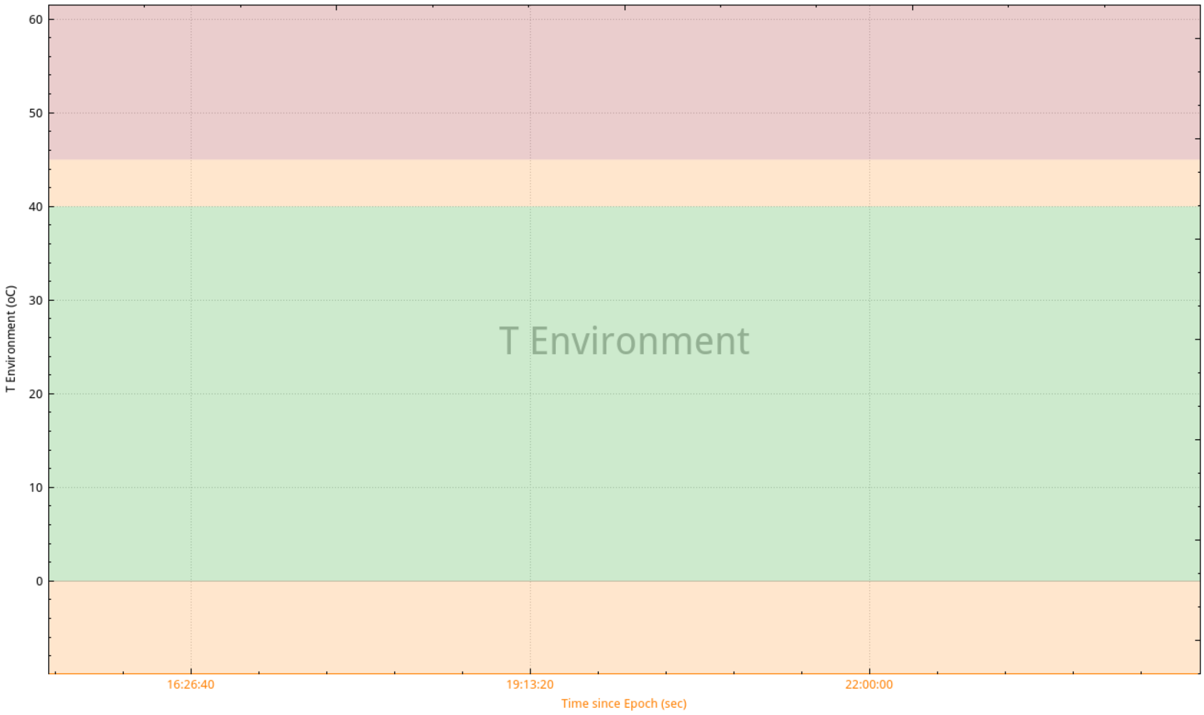

Figure 134: Graph depicting the environmental temperature threshold levels

Normally the environment temperature should be between 0 and 40°C. The e-nose should never be used in locations with a higher than 45°C environmental temperature.
Please note that if the e-nose is to be operated in environments where temperatures of 40°C are normal and expected, then the high threshold may need to be increased to account for that.

O_2 temperature threshold sensor type
The O_2 temperature sensor has the following two thresholds, which separate the following 3 threshold zones

Table 54: O_2 temperature thresholds and threshold zones

Threshold name	Default Value (°C)	User - Defined / obtained from Training	zone	zone color	Zone Description
low	38.0	user - defined	low	orange	
			normal	green	
high	42	user - defined	high	red	

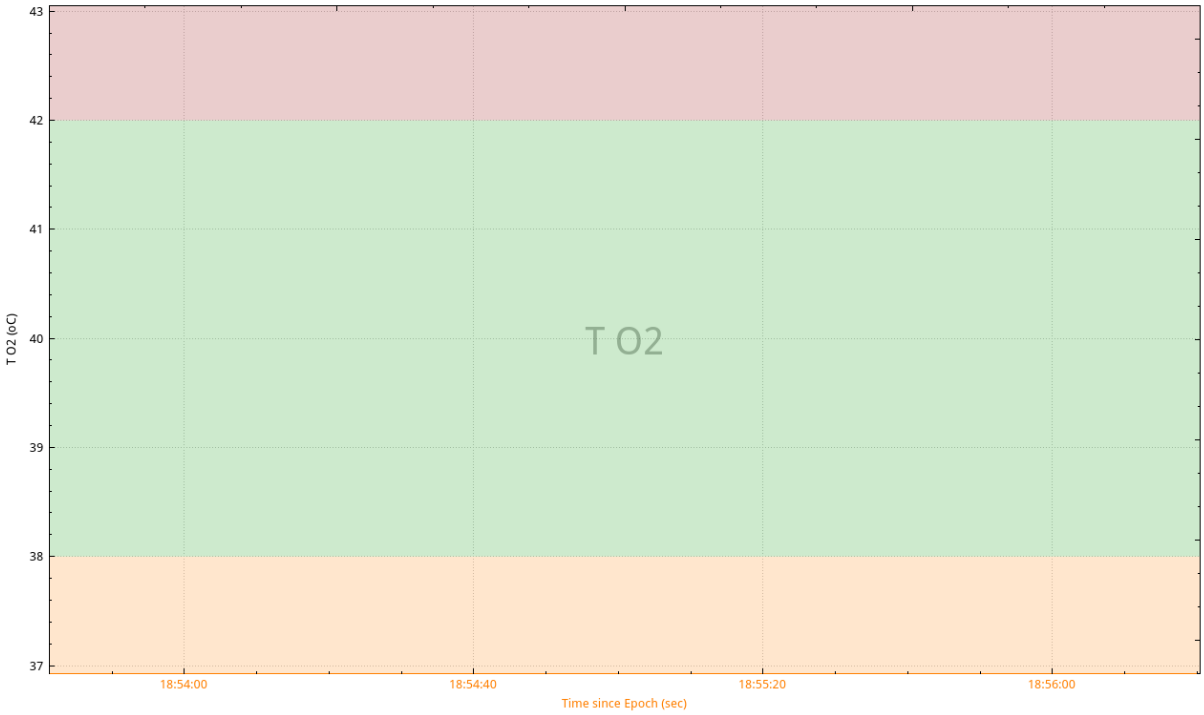

Figure 135: Graph depicting the O_2 temperature threshold levels

The temperature of the sensor should be very close to that of the manifold temperature sensor and is generally used as a secondary sensor.

Barometric pressure threshold sensor type

The barometric pressure sensor has the following 4 thresholds, which separate the following 5 threshold zones

Table 55: Barometric pressure thresholds and threshold zones

Threshold name	Default Value (mbar)	User - Defined / obtained from Training	zone	zone color	Zone Description
zero	900	user - defined	zero	red	
			low	orange	
midl	-	both			
			normal	green	
midh	-	both			
			high	orange	
danger	1100	user - defined			
			dangerous	red	

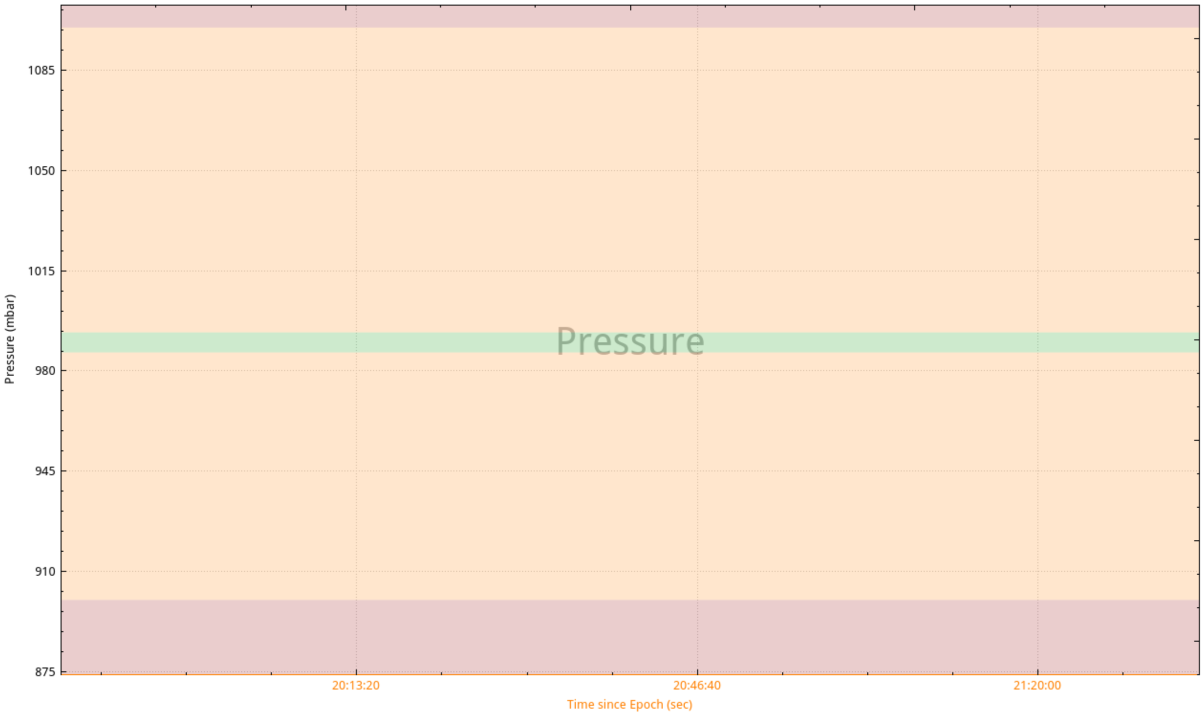

Figure 136: Graph depicting the barometric pressure threshold levels

The training range between midl and midh is used along with a fixed range factor of +/-3mbar to enable detection of input or output of the pneumatic system of the e-nose, while the user-defined thresholds are used to secure that the sensor operates within a sensible range.

Manifold humidity threshold sensor type

The manifold humidity sensor has the following 2 thresholds, which separate the following 3 threshold zones

Table 56: Manifold humidity thresholds and threshold zones

Threshold name	Default Value (%)	User - Defined / obtained from Training	zone	zone color	Zone Description
low	3	user - defined	low	orange	
			normal	green	
high	90	user - defined			
			high	red	

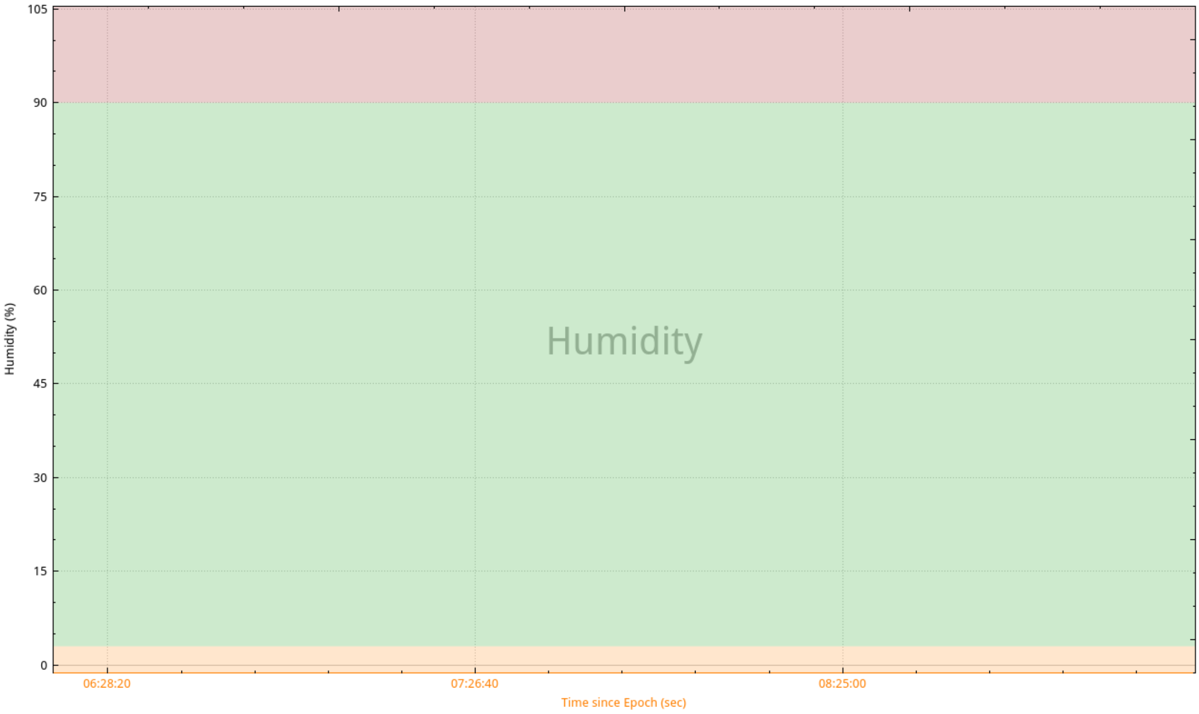

Figure 137: Graph depicting the manifold humidity threshold levels

The manifold humidity is calculated by a sensor within the manifold and takes normal values between 3% and 90%.

Environmental humidity threshold sensor type

The environmental humidity sensor has the following 2 thresholds, which separate the following 3 threshold zones

Table 57: Environmental humidity thresholds and threshold zones

Threshold name	Default Value (%)	User - Defined / obtained from Training	zone	zone color	Zone Description
low	3	user - defined	low	orange	
			normal	green	
high	90	user - defined	high	red	

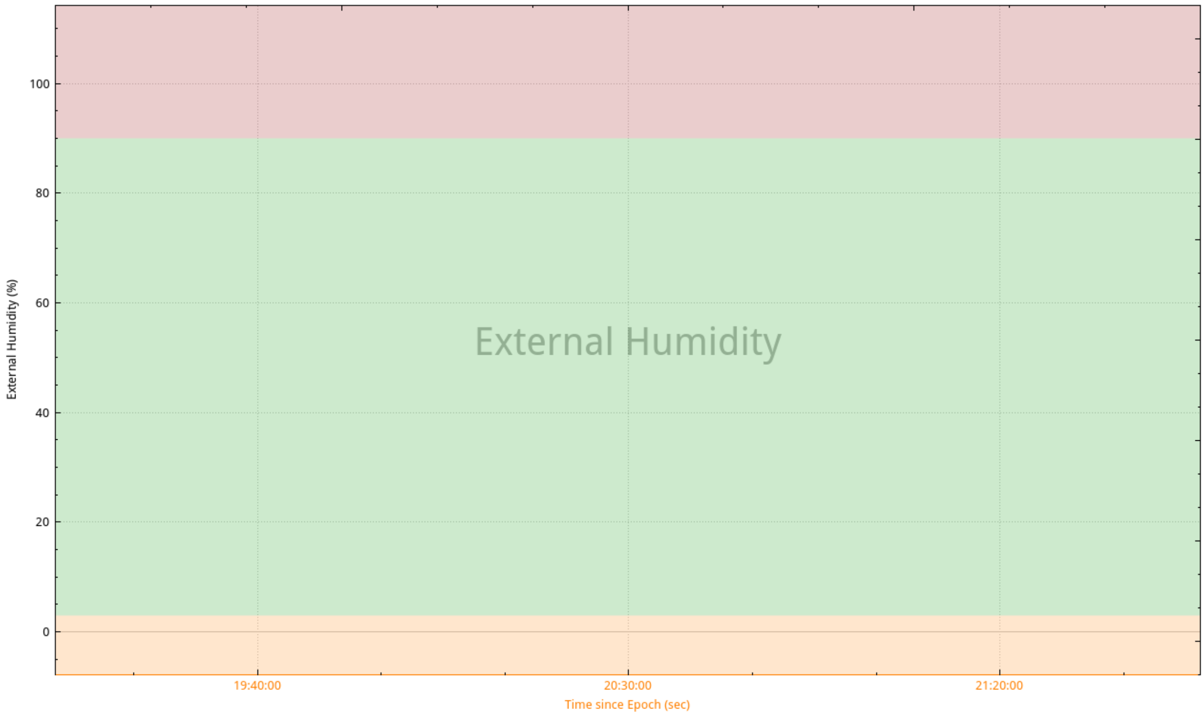

Figure 138: Graph depicting the environmental humidity threshold levels

The environmental humidity is calculated by applying a mathematical operation on the manifold humidity reading. Based on [100] the external and internal humidities are related through the dew point which is assumed to be common (this is indeed the case for low pressure changes). Calculation of the coefficient gamma for T = manifold temperature and RH = manifold relative humidity, leads to the deduction of the value of dew point Tdp for within the manifold in the following equations:

$$\gamma(T, RH) = \ln\left(\frac{RH}{100}\right) + \frac{bT}{c+T};$$

$$T_{dp} = \frac{c\gamma(T, RH)}{b - \gamma(T, RH)};$$

Where:

T = manifold temperature
RH = relative humidity in manifold
b = 17.67
c = 243.5oC

Consequently, the Tdp can be used to determine the relative humidity of the environment by using the environmental temperature and the above equations solved for RH.

Ultimately

```
Environmental RH = f(manifold & external temperature, manifold RH)
```

Carbon monoxide threshold sensor type

The carbon monoxide sensor has the following 2 thresholds, which separate the following 3 threshold zones

Table 58: Carbon monoxide thresholds and threshold zones

Threshold name	Default Value (ppm)	User - Defined / obtained from Training	zone	zone color	Zone Description
low	25	user - defined	low	green	
			signal	orange	

toxic	50	user – defined			
			toxic	red	

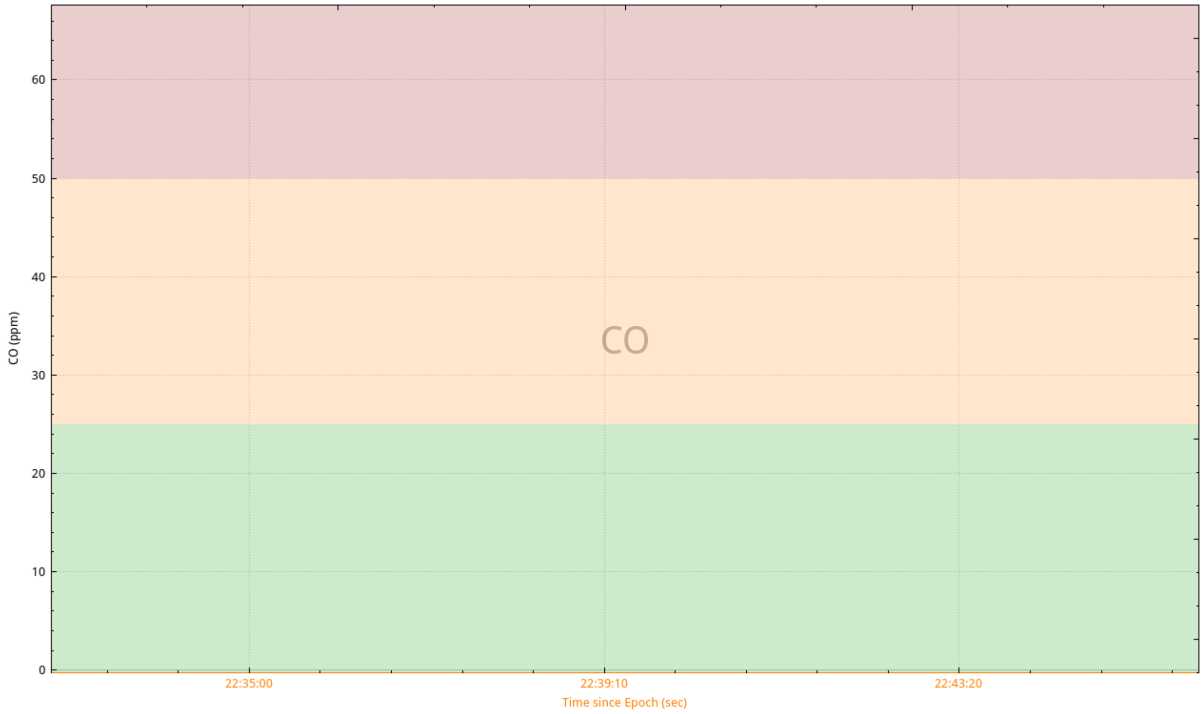

Figure 139: Graph depicting the carbon monoxide threshold levels

As far as toxic gases are concerned, it is expected that “low” zone is the normal operating condition. Anything above that condition is considered a hazard and is reported accordingly.

Hydrogen sulphide threshold sensor type

The hydrogen sulphide sensor has the following 2 thresholds, which separate the following 3 threshold zones

Table 59: Hydrogen sulphide thresholds and threshold zones

Threshold name	Default Value (ppm)	User - Defined / obtained from Training	zone	zone color	Zone Description
low	1	user - defined	low	green	
			signal	orange	
toxic	5	user - defined			
			toxic	red	

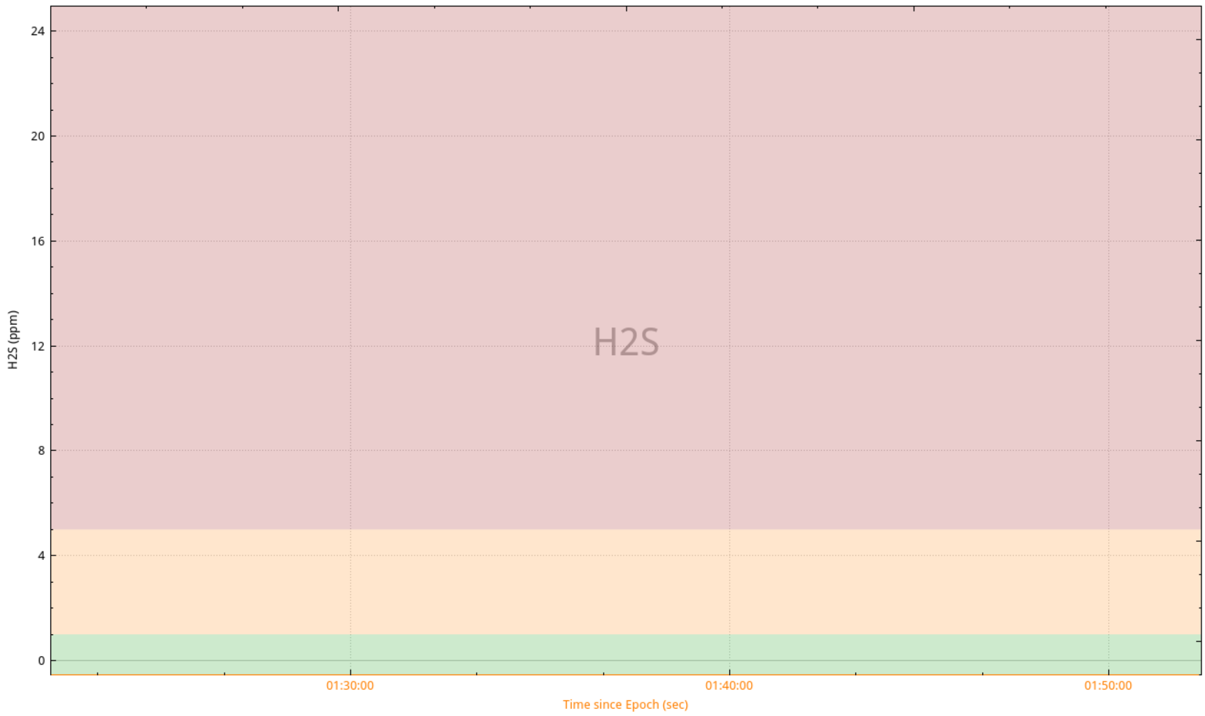

Figure 140: Graph depicting the hydrogen sulphide threshold levels

The hydrogen sulphide is also extremely toxic and thus even a 1ppm concentration will trigger it.

Combustibles and derivatives threshold sensor type
The combustibles and derivatives sensor has the following threshold, which separates the following 2 threshold zones

Table 60: combustibles and derivatives thresholds and threshold zones

Threshold name	Default Value (% concentration or %LEL)	User - Defined / obtained from Training	zone	zone color	Zone Description
signal	10	user - defined	zero	green	
			signal	orange	

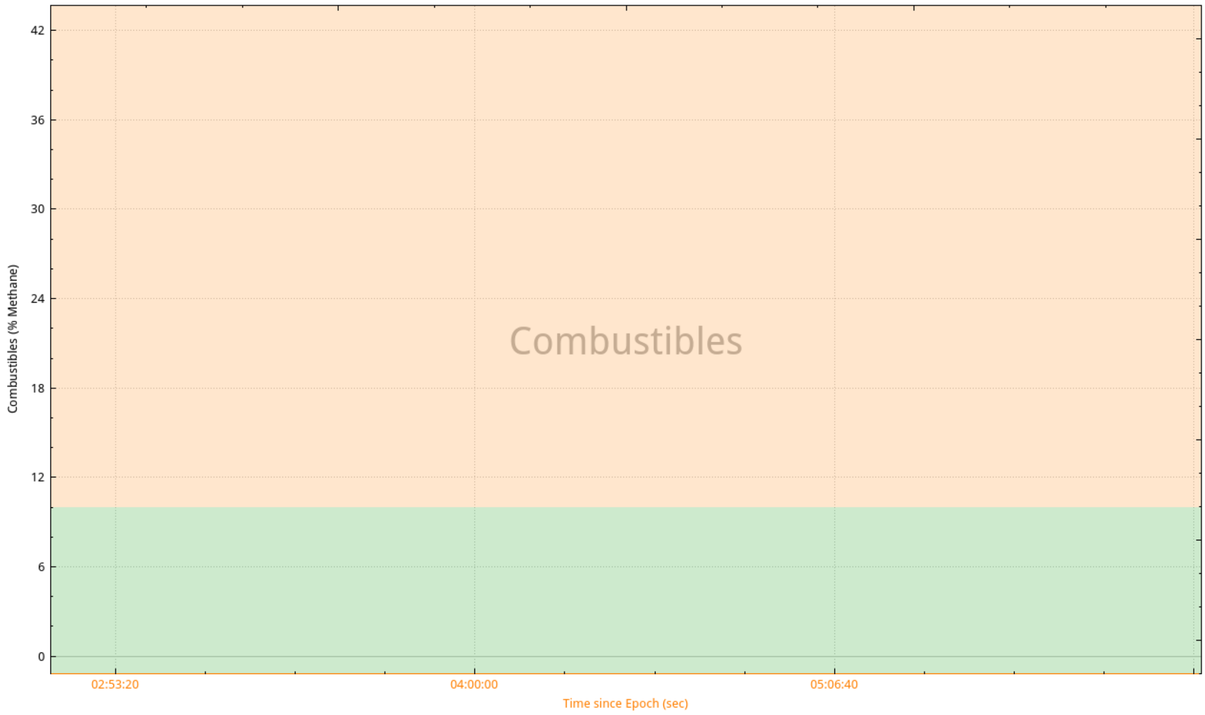

Figure 141: Graph depicting the combustibles and derivatives threshold levels

The combustibles and derivatives sensor is simply a gate between normal (green) and signal threshold levels. The incoming data are values for the percentage concentration of methane (methane % concentration). Based on this value the derivatives are calculated and saved in individual virtual sensor objects. The derivatives are the % LEL value for a number of flammable gases all of which are related to the value of methane % concentration. The formula used is the following

```
Gas %LEL = (methane % concentration)*100/(5*flammable gas coeff)
```

Where the "flammable gas coefficient" is the following for each gas

Table 61: Flammable Gas Coefficients for calculation of target gas %LEL based on methane % concentration

Derivative flammable gas sensor name	Flammable gas coefficient[101]
Methane	1
Propane	0.65
Butane	0.65
Pentane	0.55
Hexane	0.55
Heptane	0.45
Octane	0.35
Methanol	0.85
Ethanol	0.85
Isopropyl	0.65
Acetylene	0.9
Butadiene	0.6
CarbonMonox	1.2
Acetone	0.7
MethylEthylKetone	0.55
Toluene	0.4

EthylAcetate	0.55
Hydrogen	1.1
Ammonia	1.4
Cyclohexane	0.5

The derivate flammable gases are reported as individual sensors, but are only virtual representations that base their values on the original methane % concentration hardware sensor, whilst having their individual thresholds. It is noted that on every processing cycle, all the virtual sensors are updated along with the parent combustible sensor.

8.5.6. Global Indicators – calculation

The direct statistical analysis of the incoming measurements provides a good indication about the state of each sensor. It also helps to quantize time series signals into discrete states that are easier to comprehend by the user. However, due to the large number of sensors, the information that needs to be processed by the user at real time is still overwhelming. Additionally, identifying human presence should not be related to merely a single sensor signal. To be more precise, the human expiration footprint contains not only increased levels of CO_2, but also weakened levels of O_2. What is more, indicators of human presence can be strengthened by the presence of ammonia.

To aid in obtaining more reliable indications about human presence, approach, points of interest and others, the global indicators have been created. The idea is to establish a combinatory logic that establishes connections among the individual sensor indicators and resulting states that will be easily comprehended by the end-user.

What is more, these connections should be easy to update by the user so as to improve user experience and create sets of state connections for various scenarios. For example, the global human indicator should usually take into account data from CO_2, O_2 and NH_3 sensors as they can all pick up the footprint left by humans. When searching for human presence near known sources of ammonia, such as public restrooms, it may be useful to quiet down the NH_3 sensor.

In order to create the connections, a simple table is proposed. The sensor indicator states are used as inputs to the look-up table and their combination leads to specific output states. These are:

- Zero: means that there is no change of state, no indication of error or otherwise any cause for alarm.
- Weak: means that there is a change of which the user should be notified.
- Strong: means that there exist multiple non-conflicting sensor indicator states suggesting the same thing. This depends of the purpose of the indicator.

Such a table can easily be created in a spreadsheet application and imported into the core application as a simple ";" separated text file. The default tables are provided in APPENDIX: ADVANCED LOGIC UNIT - LOGIC TABLES (appendix 13). The standard form of the table is shown in Table 62: Typical global indicator state table.

Table 62: Typical global indicator state table

#indicator	Indication strength	Individual Sensor indicator input #1	Individual Sensor indicator input #2	…	Individual Sensor indicator input #N	State Description
Human	Zero	Noise	Noise	…	Normal	
Human	Weak	Signal	Noise	…	Low	
Human	Strong	Warning	low	…	High	
…	…	…	…	…	…	

Each row on this table describes exactly one state. On the 1st column one can observe the indicator name which is used to verify that the state described indeed belongs to a specific indicator. On the 2nd column the target output state is stored, while from column 3 onwards the input states (of the related individual sensors) are given. Finally, on the last column an explanatory description is provided for the output target state. This can be anything that the user wishes to see when the specific state is reached.

Global Indicator operation

Global indicators are implemented in such a way so as to be easily adaptable, without having to recompile the code. This means that on start-up each global indicator reads the corresponding table from the ".csv" file and populates internal structures. Then during runtime the individual sensor indicators are used to update the global indicator state which is reported upstream. The two phases of operation are described individually.

Start-up operation

In this stage the core application deals with reading the text file, performing sanity tests on the text file and populating the internal state table.

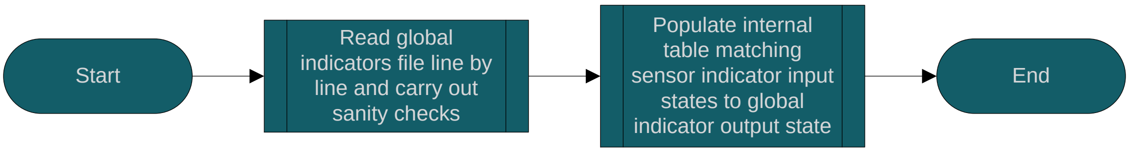
Start
Read global indicators file line by line and carry out sanity checks
Populate internal table matching sensor indicator input states to global indicator output state
End

Figure 142: Global indicators start-up operation

On start-up the core expects to find a corresponding csv file; otherwise it will exit. Comment lines start with # and will be skipped, but the 1st line must be a comment containing the titles for every column. Character ":" should not appear in the states' file because it can interfere with the inter-communication subsystem of the core algorithm. Additional sanity checks are performed which include checking that both input states and output states have the correct spelling so that there will no problem translating the text file into internal variable names.

Once all sanity checks have been passed, the text file is split according to lines (one line per changed input state) and the output state and related input states are populated in the state table.

Runtime operation

During runtime, and specifically after the individual sensor indicators have been updated, they are fed as input to the corresponding global indicator. The latter uses the state table as a reference to match the given inputs to an output state which is then reported upstream.

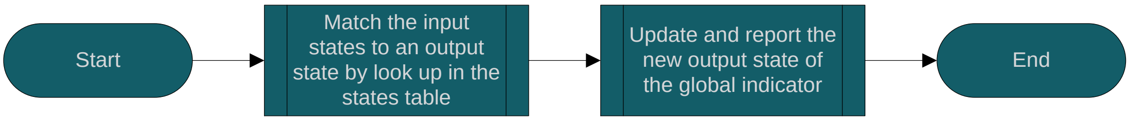
Start
Match the input states to an output state by look up in the states table
Update and report the new output state of the global indicator
End

Figure 143: Global indicators runtime operation

Please note that if no output state is given for the input states, the reported state is "invalid". Please also note that prior to training any indicators that need training to correctly report state will remain at "invalid" state, thus reminding the user that they should proceed with loading earlier trained data or commence a training operation.

Global Indicator types

A number of indicator types have been discussed and proposed by the developers and finalized with the end-users so as to create a system that is both easy to comprehend and analytical enough to give detailed information. To this extent six global indicators have been proposed which can be grouped in 2 categories

- 3 global indicators are related to human presence indication.
- 3 global indicators are related to e-nose and environmental status.

The exact purpose, related inputs and outputs of each are discussed in the following sections

Human Presence Global Indicator

The most direct way to sense a human in the vicinity is to check the reported levels of CO_2 and O_2. The human expiration footprint contains increased amounts of CO_2 and reduced amounts of O_2. Either of these 2 indications is interesting enough to necessitate that the user be notified of the difference, causing a weak indication to be raised. If both of them occur simultaneously then there is a strong indication that a human may be present, and it is reported as such to the user.

Unfortunately, one cannot be certain of all the scenarios and conditions that the e-nose may face. For example, increased CO_2 and reduced O_2 may also be the footprint of a fire. The cameras will definitely help the user analyze the situation better, but the e-nose will aid by using the temperature sensor to assess the situation. Thus, while for normal temperatures the indications are set, for higher than normal temperatures the output states are adjusted to account for that. Likewise, a low temperature in the manifold signifies that the system has not reached operating level yet.

Additionally, NH_3 presence is a strong indication of urine and the latter is a substance related to life. As a result its presence strengthens the human presence indication and it is reported as such.

In summary, the current states of CO_2, O_2, NH_3, manifold temperature and environmental temperature are used to determine the state of the human presence global indicator. The corresponding state table can be seen in Table 70.

Approach (a.k.a. trend, gradient) Global indicator

The movement of the robotic platform creates transient responses in the levels of the gases as it approaches or moves away from sources in its path. These cannot be registered just by looking at the current level of the concentrations. Instead, an observation into the past values will help realize the trend (i.e. the slope) of the gas concentration.

A graph showing past values will give an immediate view of the general trend to the end-user. However a graph is also an overwhelmingly feature-rich interface which is somewhat difficult to process in real time. The approach global indicator solves this issue by looking internally into the past values and reporting their trend. This happens for all monitored gases that are involved in human presence indication.

Specifically, the trends of CO_2, O_2 and NH_3 are included since these are vital for human presence tracking. Then, intuition is used to interpret each state. For example, an increase in CO_2 and/or NH_3 means that the e-nose is approaching a corresponding gas source. This may very well be a live subject (human, pet, etc.). If this increase happens simultaneously with a decrease in O_2, then the user gets a strong indication that they are approaching a live subject.

Apart from the main gas sensors, external humidity and environmental temperature are tracked. The reason for that is because human exhaling contains increased moisture and may also slightly increase the temperature of the cavity. If this happens, there are valid reasons to get a stronger indication that a live subject is in the vicinity, should indications from one of the 3 main sensors (CO_2, O_2, NH_3) exist.

Of course, there may arise situations that go against intuition. For example, an increase in both CO_2 and O_2 is not an expected state nor is an increase in humidity while NH_3 is dropping. Normally, either CO_2 will increase while O_2 decreases or vice-versa and NH_3 will not decrease with increasing humidity. Thus, the occurrence of such states is reported as conflicting and should not occur for prolonged durations. However, they may appear in the short run, as sensor response delay is different across the sensors (especially in the O_2 sensor) and can lead to the appearance of transient states. Additionally, if the e-nose is to be used in "special" locations, then the trend state table may need to be adjusted accordingly (such as catastrophic event near a location where one or more of the tracked gases exist in abnormal quantities).

In summary, if any two of the main sensors (CO_2, O_2 & NH_3) report non-conflicting trends, then a weak indication of "approaching" or "moving away" is reported. If all 3 provide nonconflicting trends, then a strong indication is reported. If on top of two main sensor nonconflicting trend indications at least one of the secondary sensors reports a nonconflicting trend, then a strong indication is reported.

On the other hand, If any of the main sensors report conflicting trends then the global indicator will remain quiet (state: zero). If the main sensors report non-conflicting trends, but at least one of the secondary sensors reports a conflicting trend, then the reported state will be zero. That is, even though the secondary sensors do not have the "strength" to set the output state of the trend global indicator to "strong" on their own, their conflicting (against main sensors) reports can quiet down (to zero) an otherwise weak or string indication. The corresponding state table can be found in Table 71.

Point of interest Global indicator

Point of interest global indicator is by definition a unique, short-lived trigger. If any one of the individual indicators has triggered "POI", then a weak indication at the global level will be reached. If two or more individual sensors trigger "POI", then this will be reported as a "strong" indication at the global indicator level. The individual sensors that have point of interest sensor functionality are CO_2, O_2 and NH_3.

Please note that due to the simplicity of this indicator, no file is associated with it. The functionality is hard-coded directly in the main loop execution.

Flammables Global Indicator

The flammables indicator belongs to the group of sensors that are not directly related to human presence, but aid in identifying locations where it would be hazardous for people to be trapped, or rescuers to enter. It tracks the current levels of the combustibles and O_2 sensors. The reason not only the combustibles sensor is monitored is because oxygen is an oxidizer and can help fuels burn. Therefore, oxygen reaching a level of "toxic" will trigger a weak indication to be reported to the end-user, while if any one (or more) of the combustibles sensor detects a signal (i.e. reaches "signal" level), then a strong indication will be reported to the user.

Please note that no explicit state table has been generated for this global indicator and all logic has been hard-coded in the main loop.

Toxic Gases Global Indicator

The toxic global indicator monitors all sensors having the potential to reach toxic levels. This includes CO_2, O_2, CO and H_2S sensors. It does not include the NH_3 sensor due to the extremely low range in which it can operate (up to 100ppm). The indicator will be quiet until any of the monitored gases reaches "toxic" level, at which time a strong indication will be reported.

E-nose environmental status Global Indicator

The environmental status indicator monitors the environmental and manifold temperatures, pressure and environmental humidity of the e-nose hardware to make sure that the system operates under normal conditions. All individual sensors should report "normal" level of operation for this sensor to remain quiet. Otherwise, a strong indication will be reported to the users. In some extremely unlikely case (for example when the environmental temperature is low, or the manifold temperature is only slightly higher than normal) a weak indication that something requires the attention of the user will be reported instead.

Pressure changes, possibly caused by blocking of the pneumatic systems entrance or exit, operation in too hot, extremely cold, or extremely humid environments, will all be monitored and reported to the user.

Hardware status Indicators

Apart from the environmental status indicator the e-nose also monitors and reports the state of the hardware. This includes:

- If the system has been calibrated
- If the system has been trained
- The status of the heating elements
- The status of the air pump

These are indications related to the health of the system and are updated constantly by monitoring the state flags of the e-nose (see Table 40).

Logging

The ENALU core application has been equipped with a powerful logging mechanism. The reason is twofold; on one hand all decisions, responses to user requests and actions should be reported and stored for future reference and, on the other hand, the entire session should be able to be played back for educational purposes. To fulfill the first requirement the logging mechanism has been implemented so as to report everything that is carried out in three outputs: the command line standard output, the user interface notification board, and the log files. For the latter, two log files have been proposed where the first logs all the notification messages as they appear in the command line stand output and user interface, while the second logs the input from the e-nose hardware directly.

8.5.7. Extended GUI of the 3rd prototype

The user interface of ENALU is an integral part of the system. The core application may continue to process incoming information without a GUI, but the user will usually only interact with the e-nose through the graphical user interface. It is important that the interface provides access to the information in a concise and direct way. For this reason an easy-to-comprehend layout is essential and color coding has been used wherever possible in order to provide a subconscious connection between specific states and colors. At the same time a more elaborate graphical user interface would help developers and power users get a more complete view of the situation. For this reason two separate GUIs were implemented.

Extended User Interface

The main graphical user interface presents all the information that is being processed by the core ENALU application. Namely, it shows current values, historical values (as plots), information about all sensor types and indicators for every sensor, as well as every global indicator. Additionally, it provides a configuration interface so that the user can configure the core ENALU application quickly using a familiar interface of buttons and drop-down menus (and minimal typing).

Main window

The initial view of ENALU GUI also happens to be the main window. It contains (from top to bottom):

- a menu bar,
- the graph widgets of the 13 main sensors,
- the notification board (where all the logged messages from core ENALU appear, just as they will be saved in the enosestate.log)
- quick access to several important functions (buttons on the left) and status of the hardware (colored labels on the right)
- the six global indicators

All of which can be seen in the following image:

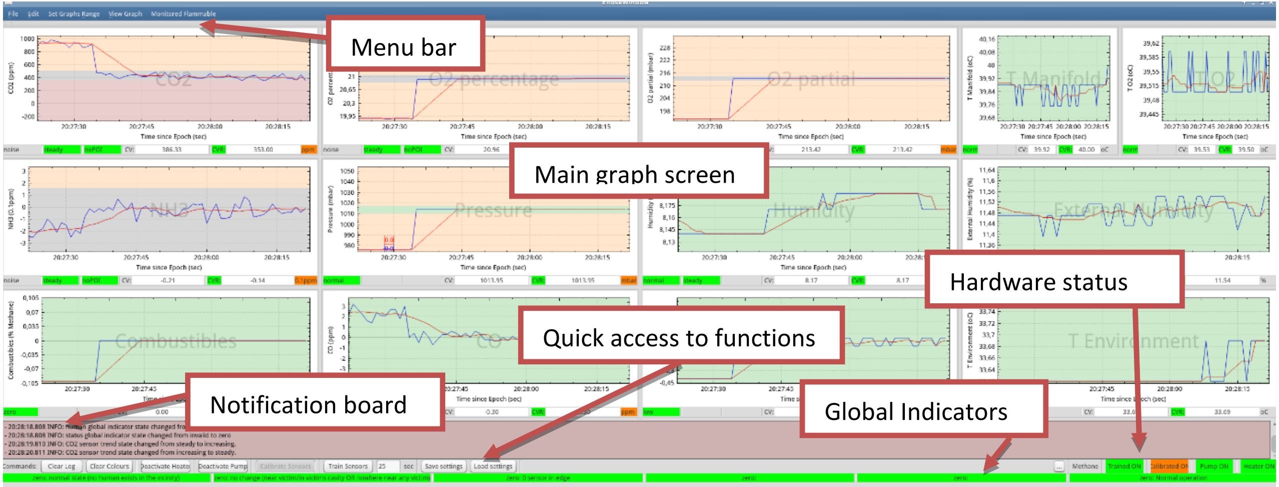
File
Edit
Set Graphs Range
View Graph
Monitored Flammable
Menu bar
CO2
O2 percentage
O2 partial
T Manifold
T O2
Main graph screen
NH3
Pressure
Humidity
External Humidity
Hardware status
Combustibles
CO
Quick access to functions
T Environment
Notification board
Global Indicators
Time since Epoch (sec)
Commands:
Clear Log
Clear Colours
Deactivate Heater
Deactivate Pump
Calibrate Sensors
Train Sensors
25
sec
Save settings
Load settings
Methane
Trained ON
Calibrated ON
Pump ON
Heater ON

```
- 20:28:18.808 INFO: human global indicator state changed fro
- 20:28:18.808 INFO: status global indicator state changed from invalid to zero
- 20:28:19.810 INFO: CO2 sensor trend state changed from steady to increasing.
- 20:28:20.811 INFO: CO2 sensor trend state changed from increasing to steady.
```

zero: normal state (no human exists in the vicinity)
zero: no change (near victim/in victims cavity OR nowhere near any victim)
zero: 0 sensor in edge
zero:
zero:
zero: Normal operation

Figure 144: ENALU GUI main window layout

Menu bar

The menu bar provides access to all commands of the ENALU core application. Specifically, it gives access to:

- the configuration window ("Edit" -> "Configuration")
- saving and reloading settings ("File" menu)
- changing the history buffer size that is viewable on each graph ("Set Graph Range")

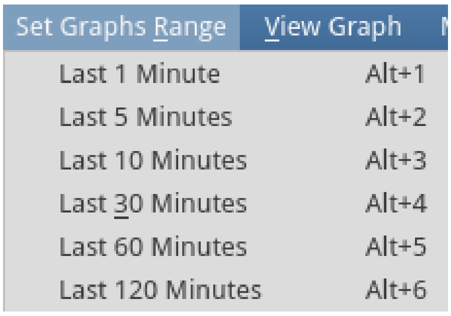
Set Graphs Range
View Graph
Last 1 Minute Alt+1
Last 5 Minutes Alt+2
Last 10 Minutes Alt+3
Last 30 Minutes Alt+4
Last 60 Minutes Alt+5
Last 120 Minutes Alt+6

Figure 145: "Set Graph Range" menu allows time window of graphs to be changed

- allows switching between different graph "screens" (that is main screen, combustibles graph screen and zoomed in view of each sensor)

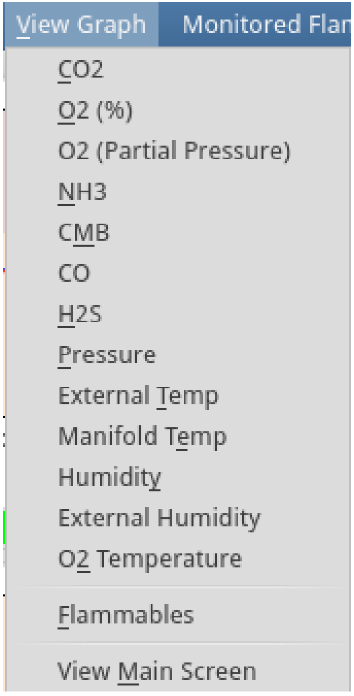
View Graph
Monitored Flan
CO2
O2 (%)
O2 (Partial Pressure)
NH3
CMB
CO
H2S
Pressure
External Temp
Manifold Temp
Humidity
External Humidity
O2 Temperature
Flammables
View Main Screen

Figure 146: "view graph" menu, which allows zooming in on a specific graph

- the selection menu for %LEL combustibles sensor:

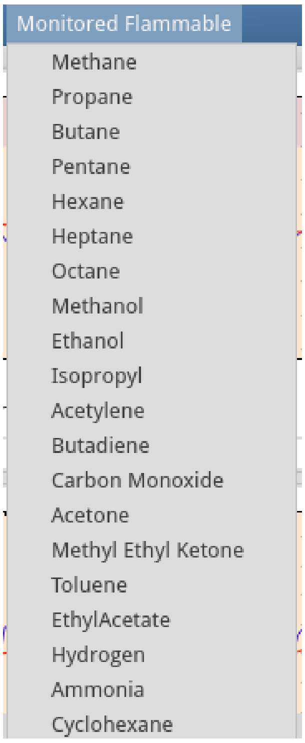
Monitored Flammable
Methane
Propane
Butane
Pentane
Hexane
Heptane
Octane
Methanol
Ethanol
Isopropyl
Acetylene
Butadiene
Carbon Monoxide
Acetone
Methyl Ethyl Ketone
Toluene
EthylAcetate
Hydrogen
Ammonia
Cyclohexane

Figure 147: Combustible selection graph, which allows selection of the primary flammables monitoring %LEL gas

Please note that when a flammable sensor is selected from the list, the selected sensor name should appear in the quick access and global indicators toolbar left of the "trained" status indicator.

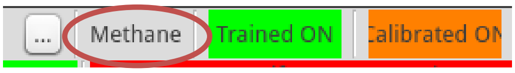
...
Methane
Trained ON
Calibrated ON

Figure 148: Currently monitored combustibles gas indicator

Main sensors screen

The main window shows the 13 main sensor graphs. Each sensor is identified by the large letters with its sensor name in the middle of the graph. The graphs have the following layout:

Table 63: Layout of the main sensors screen

CO2	O2 (%)	O2 (partial pressure)	Temperatures (manifold left and O2 sensor right)
NH3	Pressure	Humidity (internal)	Humidity (environmental)
Combustibles main sensor (methane % concentration, not %LEL)	CO	H2S	Environmental Temperature

Notification board

The notification board reports all messages sent from the ENALU core application. Usually the user should expect only informative messages tagged as "INFO". These are reported in black colored fonts and on white background.

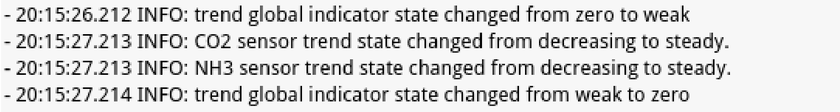

```
- 20:15:26.212 INFO: trend global indicator state changed from zero to weak
- 20:15:27.213 INFO: CO2 sensor trend state changed from decreasing to steady.
- 20:15:27.213 INFO: NH3 sensor trend state changed from decreasing to steady.
- 20:15:27.214 INFO: trend global indicator state changed from weak to zero
```

Figure 149: Notification board containing only INFO graded messages

Should a warning occur, the fonts will be colored orange.

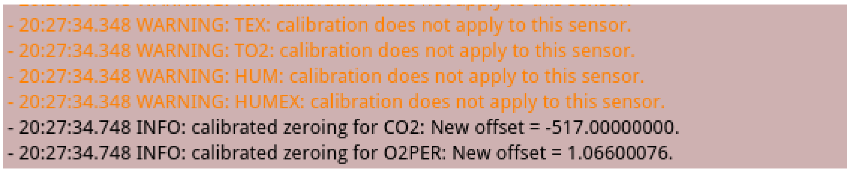

```
- 20:27:34.348 WARNING: TEX: calibration does not apply to this sensor.
- 20:27:34.348 WARNING: TO2: calibration does not apply to this sensor.
- 20:27:34.348 WARNING: HUM: calibration does not apply to this sensor.
- 20:27:34.348 WARNING: HUMEX: calibration does not apply to this sensor.
- 20:27:34.748 INFO: calibrated zeroing for CO2: New offset = -517.00000000.
- 20:27:34.748 INFO: calibrated zeroing for O2PER: New offset = 1.06600076.
```

Figure 150: Notification board containing WARNING (orange) graded messages

And if errors occur the messages will be colored red.

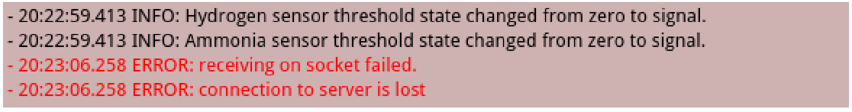

```
- 20:22:59.413 INFO: Hydrogen sensor threshold state changed from zero to signal.
- 20:22:59.413 INFO: Ammonia sensor threshold state changed from zero to signal.
- 20:23:06.258 ERROR: receiving on socket failed.
- 20:23:06.258 ERROR: connection to server is lost
```

Figure 151: Notification board containing ERROR (red) graded messages

When warnings or error messages appear, the background color will also be painted accordingly. The reason is so the user will not miss a warning or error message that has been quickly scrolled up because, in the meantime, many messages have appeared.

Once the user has scrolled up and viewed the warning/error messages, they can press the button “Clear Colors” in order to color the background of the notification board white again. Finally should the user require to clear the notification board, they can press “clear log” button.

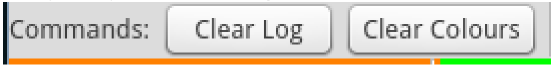

Figure 152: Buttons to clear log messages, or clear the background color of the notification board

Quick access buttons and global indicators

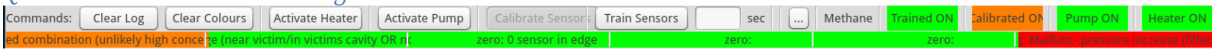

Figure 153: Detailed view of the quick access button and global indicators

The quick access buttons are shown in the top left corner and they include (from left to right):

- button to clear the messages in the notification board (“clear log”)
- button to clear only the background colors of the notification board (if non-white)
- an “activate-deactivate heater” toggle button
- an “activate-deactivate pump” toggle button
- a “calibrate sensors” button which performs zero calibration on all sensors
- a “train sensors” which can be used in the field on the right of this button contains a valid training duration (1-3600 seconds)
- a button with “…” which provides access to the configuration window

The indicators of the top row include:

- an indicator of the selected combustible gas %LEL virtual sensor (currently “methane”)
- an indicator for the training state of the system (green = trained, red = not trained)
- an indicator for the calibration state of the system (green = two point calibrated, orange= zero calibrated, red = not calibrated)
- pump status (green is ON, red = OFF, pressing “activate pump” button should turn this led green)
- heater status (green is ON, red = OFF, pressing “activate heater” button should turn this led green)
- color coded: trained, calibration and hardware status are shown on top right corner

Then, on the 2nd row, the 6 global indicators are shown (again from left to right), all of which have the following color code: green = zero (no indication), orange = weak indication, red = string indication:

- the human presence global indicator
- the approaching indication
- the point of interest (Hot Spot) indicator
- the toxic indicator
- the combustibles indicator
- the environmental status indicator

Enlarged window

The zoomed-in window refers to an enlarged version of the graph of any one of the sensor graphs from the main screen. The user can right-click on any of those graphs and the selected graph will occupy the whole main sensor graph screen. This way the user can get a clearer view of the specific sensor graph. It also possible to navigate to “view graph’ menu and select the sensor desired to get the same effect.
Enlarging is available for all the sensors of the main screen.
To return to the main sensors screen the user can right-click on the enlarged graph or navigate through “view graph” menu, or even press “m” on the keyboard.

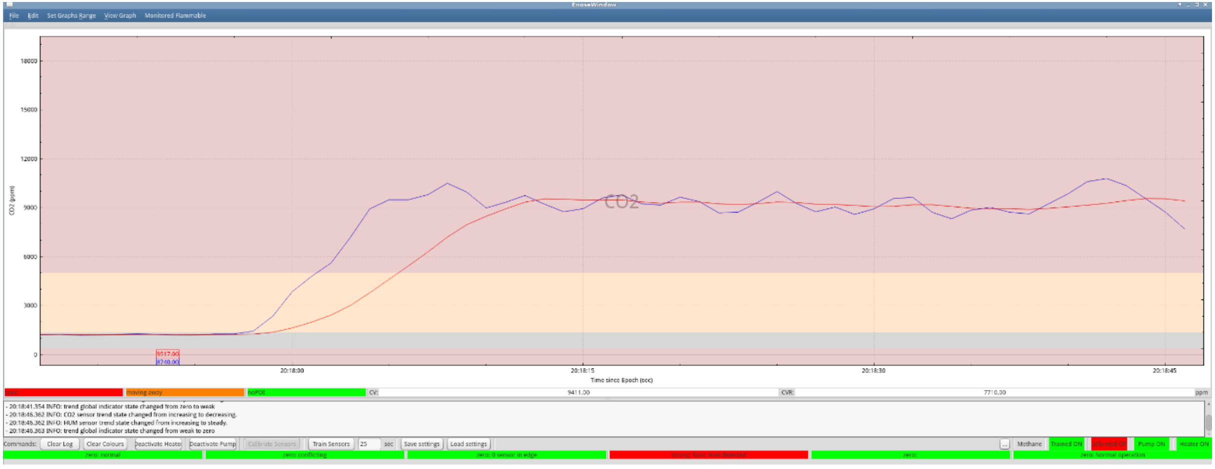
EnoseWindow
File
Edit
Set Graphs Range
View Graph
Monitored Flammable
18000
15000
12000
9000
6000
3000
0
CO2 (ppm)
CO2
9517.00
8740.00
20:18:00
20:18:15
20:18:30
20:18:45
Time since Epoch (sec)
toxic
moving away
noPOI
CV:
9411.00
CVR:
7710.00
ppm
Commands:
Clear Log
Clear Colours
Deactivate Heater
Deactivate Pump
Calibrate Sensors
Train Sensors
25
sec
Save settings
Load settings
...
Methane
Trained ON
Calibrated OFF
Pump ON
Heater ON
zero: normal
zero: conflicting
zero: 0 sensor in edge
strong: Toxic level detected
zero:
zero: Normal operation

```
- 20:18:41.354 INFO: trend global indicator state changed from zero to weak
- 20:18:46.362 INFO: CO2 sensor trend state changed from increasing to decreasing.
- 20:18:46.362 INFO: HUM sensor trend state changed from increasing to steady.
- 20:18:46.363 INFO: trend global indicator state changed from weak to zero
```

Figure 154: Enlarged sensor graph

Sensor graph widget

At the heart of the GUI the sensor widget contains all the information related to a single sensor. This includes:

- The current instantaneous value (CVR) and blue line in graph
- The current average value (CV) and red line in graph
- The units of values for this sensor
- The calibration state of the sensor (color coded on the units’ label. Red=non calibrated, orange= zero calibrated, green= two point (fully) calibrated)
- The training state of the sensor (color coded on the CVR label: red= not trained, green = trained)
- The threshold sensor type indicator (bottom left)
- The approach sensor type indicator (if applicable to specific sensor, empty otherwise)
- The point of interest sensor type indicator (if applicable to specific sensor, empty otherwise)
- The threshold levels related to the specific sensor (shown as colored horizontal strips in the graph).

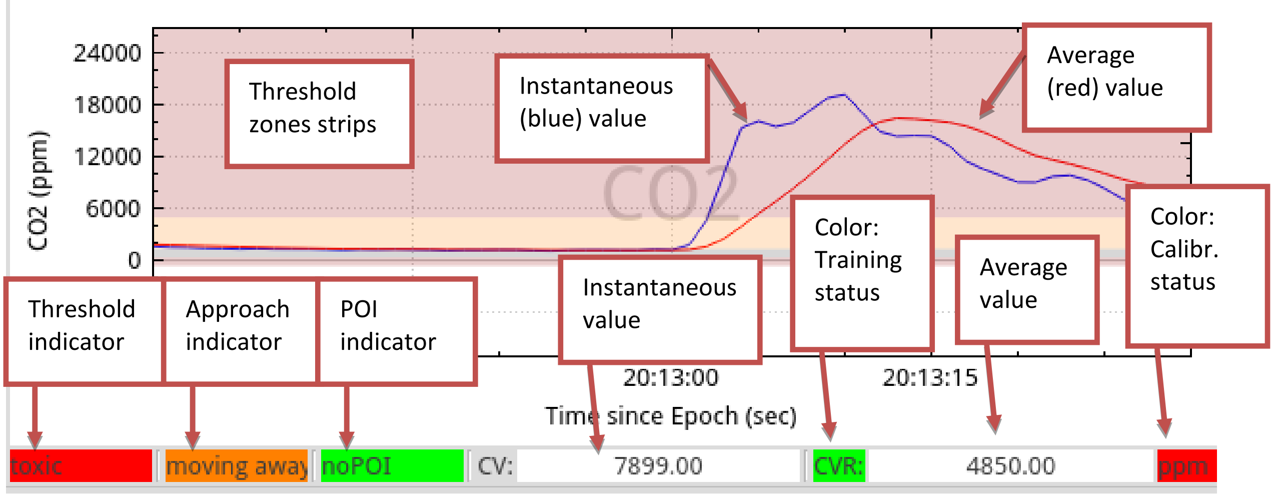
24000
18000
12000
6000
0
CO2 (ppm)
CO2
Threshold zones strips
Instantaneous (blue) value
Average (red) value
Color: Training status
Color: Calibr. status
Instantaneous value
Average value
Threshold indicator
Approach indicator
POI indicator
20:13:00
20:13:15
Time since Epoch (sec)
toxic
moving away
noPOI
CV:
7899.00
CVR:
4850.00
ppm

Figure 155: Typical sensor widget

Especially for the threshold horizontal in the graph above, the user can see that there are 4 levels as expected:

- “Zero” : with red color at the bottom

- “Noise”: with grey
- “Signal”: with orange/yellow
- “Toxic”: with red at the top
- The extremely low or high values (that are never expected to be travelled by graph lines are white

The user can hover with the mouse over the graph to see specific value of the graph exactly under the x-axis value of the mouse cursor as shown in the following figure. The graph values will appear in correspondingly color-coded boxes at the bottom left:

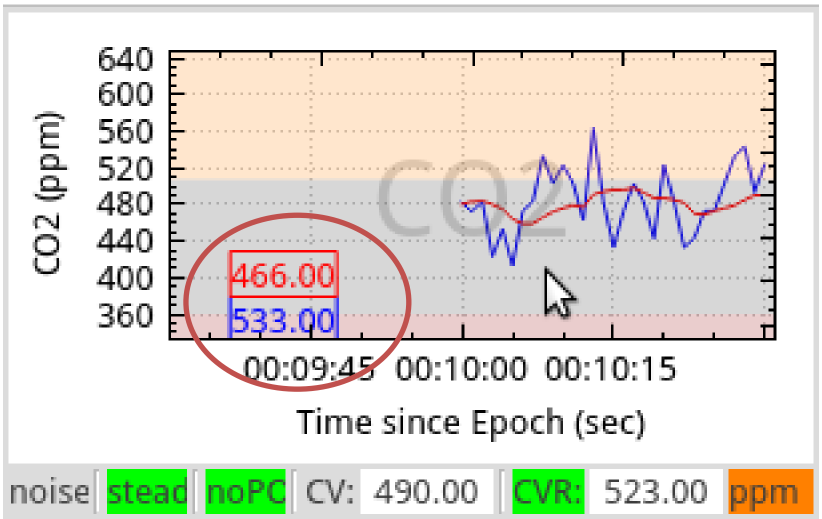

Figure 156: Hover with the mouse to find the current values at the x-axis location of the mouse

Color coding

Extremely important for the user is to understand the color coding of the graphs because ultimately this will help accelerate the process of quickly identifying if something is wrong. As a result, each color that appears on such a sensor widget has a certain “meaning” attached to it:

- Green: means “normal” , or that no hazardous levels have been reached for flammable and/or toxic gases
- Grey: means “uncertain if anything here”. This is because vales that have appeared during training as “non-significant” cannot be identified differently at a later stage by the e-nose.
- Red: means “(potential) hazard”, whether it is for the trapped subject, the rescue crew or even the e-nose electronics. This is different from the global indicators where red may indicate hazard, or strong indication that a trapped subject is present and e-nose has picked his/her signal up.
- Yellow/orange: means “operator attention is requested”. This is either because one of the human presence tracking indicators has spotted someone (or its threshold level is “signal”) or because one or more of the sensors are in “warning” state.

Viewing a different window size

By navigating to the menu “Set Graphs Range” , the user can view a variety of historical graph data. Available time ranges are: 1, 2, 5, 10, 30, 60 and 120 minutes.

Panning and zooming

By default the graphs track the latest value which appears at the right-most side of the graph and is updated every second (in real time). If the user wishes to view some part of the graph that has moved out of view, they need to first “disengage” the auto-shifting of the graph. To do that the user should double (left) click on the graph to disengage the graph auto-sifting. Pan (by left mouse dragging) and zoom (by mouse wheel) are now enabled. To return to auto-shifting state the user should double-click again on the graph.

In order to avoid forgetting when graph auto-shifting has been disabled, the x-axis of the specific sensor graph is painted yellow.

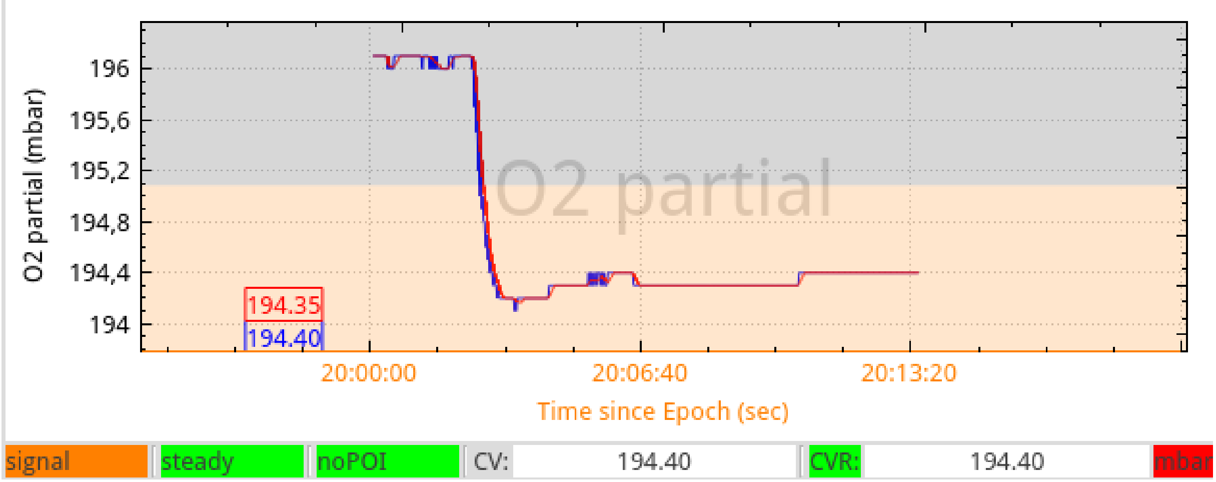

Figure 157: Disengaging the auto-shifting of the real-time graph in order to manually pan and zoom

Internal Communication (E-Nose, Advanced Logic Unit, GUI)

The e-nose follows a modular design in order to implement requirements. As a consequence, different systems must be connected and communicate. Different parts of the information path have different technical requirements, which in turn lead to different technologies being used. This is discussed briefly in the following sections

E-nose hardware to ENALU communication

Communication between the hardware and the core ENALU application is implemented as a “fire and forget” transmission from the e-nose point of view; the core ENALU is constantly listening for new data. The firmware on the hardware sends data to the core and expects that it will be received. A good communication channel is vital. Its absence means that no processing can be performed. It is thus important to maintain an open and established connection for the entire duration of a rescue operation. If the connection gets dropped, the e-nose will immediately be notified and will try to reconnect. Additionally, it is useful to secure the data transmission so as to avoid receiving erroneous values.

For these reasons it seemed preferable to use TCP protocol rather than a connectionless one. The established connection offered by the protocol ensures that the core application can “sense” the potential absence of the e-nose and report it immediately to the user. Simultaneously, it can continually try to re-establish the connection so that when the hardware becomes available again, it can continue from where it left off. Additionally, error checking that is inherent in this type of protocol will ensure that the correct data reaches the core ENALU application.

Moreover, the length of cabling that is necessary to provide enough “freedom” to the e-nose hardware renders the serial connection inadequate. To this extent a serial to Ethernet device (xport) has been used which buffers and translates serial streams into Ethernet ones. It provides full duplex communication and is permanently attached to the embedded system of the e-nose hardware.

ENALU to GUI communication

The connection between the ENALU core application and the user interface follows a radically different philosophy than the one between the core and the hardware. In this case, the requirement is for one-to-multiple communication receivers scheme where the source is the core ENALU application while the destinations can be one or many user interface units and one or more central storage facilities. These destinations may, or may not, exist for the full duration of the rescue mission, and even when present, they may appear and disappear as communication to those receivers may take place over wireless channels.

It was decided to use a connectionless protocol, namely UDP, which enables simple broadcasting of the data while closing the connection at the end of the transmission. To be more precise, the open sound control (OSC) protocol has been selected which offers a library (“oscpack”) that can be used to send primitive data types and strings over a UDP stream. The version of the library used (which has been compiled dynamically as a shared object) is 1.1.0.

8.6. Electronic nose testing (verification)

The following tests are performed to evaluate the hardware platform mostly and some aspects of the software. For this reason, the raw measurement values (CVR) and the filtered values (CV) are displayed in graphs (Y-axis in a volume concentration unit). The X-axis is time, a time stamp is used, but it also corresponds to seconds and sample number. In some tests, the sensor output was not zeroed so that a better understanding of sensor performance could be gained.

8.6.1. Victim localization tests

Breath-based detection Test 1 (approaching test)

This confined space test is the most realistic test performed in controlled, but close to realistic scenarios (from the perspective of air conditions). The test utilized a closet that was sealed with food wrap with a human test subject inside it. For safety reasons, a ventilation opening was always present that ensured adequate amounts of fresh air and no chance of suffocation of the test subject. The test subject was constantly under supervision and was provided with instructions and the means to escape any time he deemed it necessary. The setup and test procedure were very similar to the experiments carried out with the second prototype of the e-nose, with the following changes:

1. The Third prototype intended to be integrated in the robotic platform was used.
2. The completed graphical user interface was used (the version that provides full functionality and is intended for development, testing and training purposes)
3. The ventilation opening of the closet was connected to a ventilation tube (20cm diameter and about 90cm in length) to simulate the access path of a survival space under a pile of rubble.

The e-nose was operated in the full power mode (heater enabled), and a sampling tube was connected to the input interface to facilitate scanning. Prior to carrying out the measurements of the test procedure, the e-nose was left to warm up and reach the operational temperature of the full power mode. When warm, the sampling input was placed outside the window and the system was calibrated (1 point calibration – assuming the air outside the building had nominal concentration values). After completion, the sampling input was brought inside and the electronic nose was trained for three minutes (180 seconds) to automatically determine the noise and signal thresholds of the current location.

The following picture illustrates the setup.

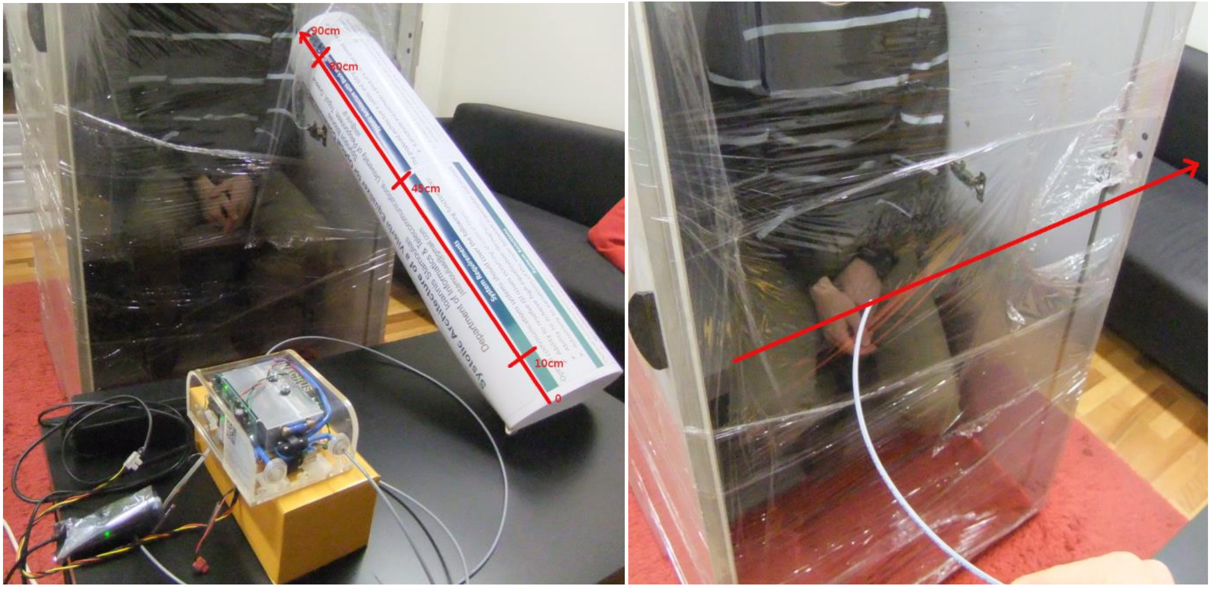

Figure 158. The confined space and breath-based victim localization test for the 3rd prototype of the e-nose

The experiment goals were the following:

1. Verify the victim localization capability of the e-nose.
2. Verify the functionality of the auto training.
3. Verify the functionality of the victim localization indicator signals, for individual sensors and the global indicators.

4. Measure the response of the e-nose in various positions inside a ventilation shaft (tube) of a confined space when a human is inside.
5. Measure the response of the electronic nose when crossing in front of a ventilation opening.

A summary of the experiment results when moving the sampling tube from the environment into the closet through the ventilation shaft are collected in the following table:

Table 64. Results summary for the experiment of going into a confined space via a ventilation tube

Location → Output ↓	Outside tube	10cm inside tube	50cm inside tube	80cm inside tube	Inside closet
CO_2 (ppm)	472	523	545	702	2081
O_2 (mbar) $[O_2]$ (%)	213.30 [20.95]	213.23 [20.94]	213.20 [20.93]	213.16 [20.93]	212.16 [20.82]
Human indicator	Normal	Normal	Normal	Weak: CO2...	Strong: ...CO2 + O2
Approaching ind.	Zero	Zero	Zero	Weak: approaching	Strong
Hot Spot ind.	Zero	Zero	Zero	Zero	Zero

The following picture illustrates an interface caption when the e-nose sampling tube was moved from 80cm inside the tube to inside the closet. Global indicators are on the bottom (left to right: human presence, approaching, Hot Spot, toxic, combustibles, status); individual indicators are on the bottom of each sensor's measurements plot; thresholds are displayed on the plots with different color coverage of the background. Color coding is the following: global indicators zero = green, weak = orange, red = strong. Thresholds – background color coding is the following. OK = green, noise or nothing = gray, signal = orange, hazard = red.

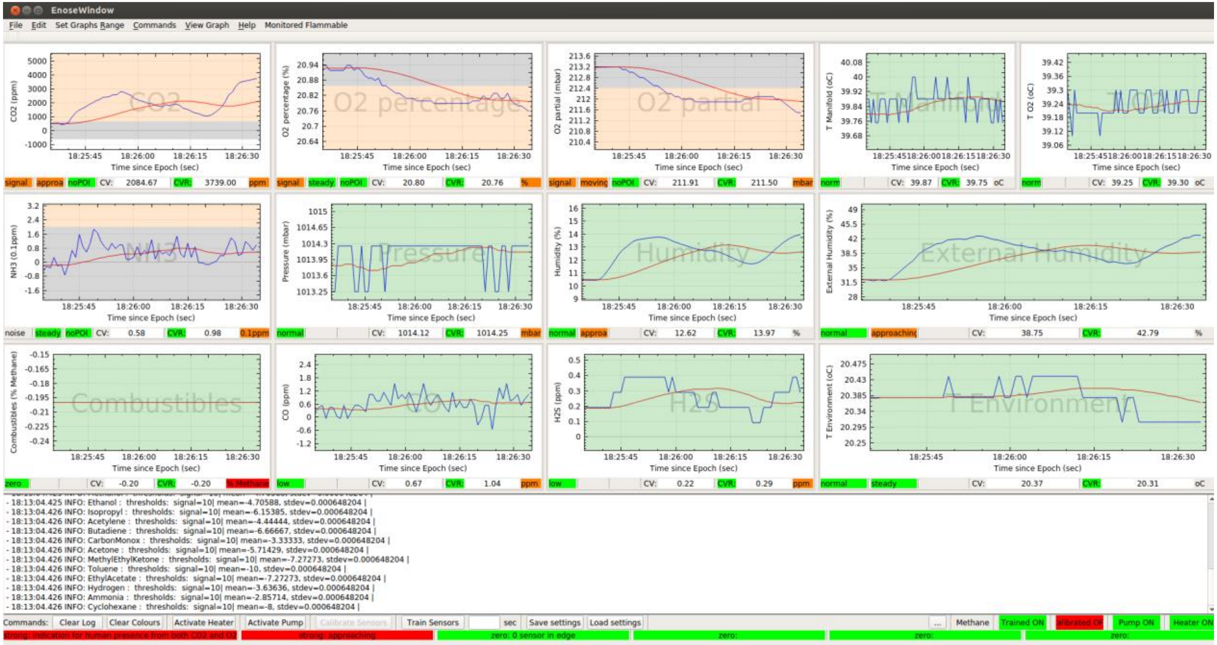
EnoseWindow
File Edit Set Graphs Range Commands View Graph Help Monitored Flammable
CO2
O2 percentage
O2 partial
T Manifold
T O2
NH3
Pressure
Humidity
External Humidity
Combustibles
CO
H2S
T Environment
Time since Epoch (sec)
Commands: Clear Log Clear Colours Activate Heater Activate Pump Calibrate Sensors Train Sensors sec Save settings Load settings
Methane Trained ON Calibrated OFF Pump ON Heater ON

```
- 18:13:04.425 INFO: Ethanol :  thresholds:  signal=10| mean=-4.70588, stdev=0.000648204 |
- 18:13:04.426 INFO: Isopropyl :  thresholds:  signal=10| mean=-6.15385, stdev=0.000648204 |
- 18:13:04.426 INFO: Acetylene :  thresholds:  signal=10| mean=-4.44444, stdev=0.000648204 |
- 18:13:04.426 INFO: Butadiene :  thresholds:  signal=10| mean=-6.66667, stdev=0.000648204 |
- 18:13:04.426 INFO: CarbonMonox :  thresholds:  signal=10| mean=-3.33333, stdev=0.000648204 |
- 18:13:04.426 INFO: Acetone :  thresholds:  signal=10| mean=-5.71429, stdev=0.000648204 |
- 18:13:04.426 INFO: MethylEthylKetone :  thresholds:  signal=10| mean=-7.27273, stdev=0.000648204 |
- 18:13:04.426 INFO: Toluene :  thresholds:  signal=10| mean=-10, stdev=0.000648204 |
- 18:13:04.426 INFO: EthylAcetate :  thresholds:  signal=10| mean=-7.27273, stdev=0.000648204 |
- 18:13:04.426 INFO: Hydrogen :  thresholds:  signal=10| mean=-3.63636, stdev=0.000648204 |
- 18:13:04.426 INFO: Ammonia :  thresholds:  signal=10| mean=-2.85714, stdev=0.000648204 |
- 18:13:04.426 INFO: Cyclohexane :  thresholds:  signal=10| mean=-8, stdev=0.000648204 |
```

```
strong: indication for human presence from both CO2 and O2 | strong: approaching | zero: 0 sensor in edge | zero: | zero: | zero:
```

Figure 159. Human presence and approaching indicator triggered when moving inside the confined space

The ventilation tube was removed and a single ventilation opening was present on the closet. The sampling tube was passed slowly in front of the opening. A summary of the experiment results when moving the sampling tube in front of the closet opening are collected in the following table:

Table 65. Results summary for the experiment of crossing a ventilation opening

Location → Output ↓	At Opening	At end of Opening	After Opening 1	After Opening 2	After Opening 3
CO_2 (ppm)	421	508	1211	471	458

Location → Output ↓	At Opening	At end of Opening	After Opening 1	After Opening 2	After Opening 3
O_2 (mbar) [O_2] (%)	213.40 [20.94]	213.39 [20.94]	212.25 [20.83]	212.73 [20.87]	213.13 [20.91]
Human indicator	Normal	Normal	Strong: ...CO2 + O2	Normal	Normal
Approaching ind.	Zero	Zero	Strong	Weak: moving away	Weak: moving away
Hot Spot ind.	Zero	Zero	Zero	Zero	Zero

The following picture illustrates an interface caption when the electronic nose sampling tube had reached the end of the ventilation opening.

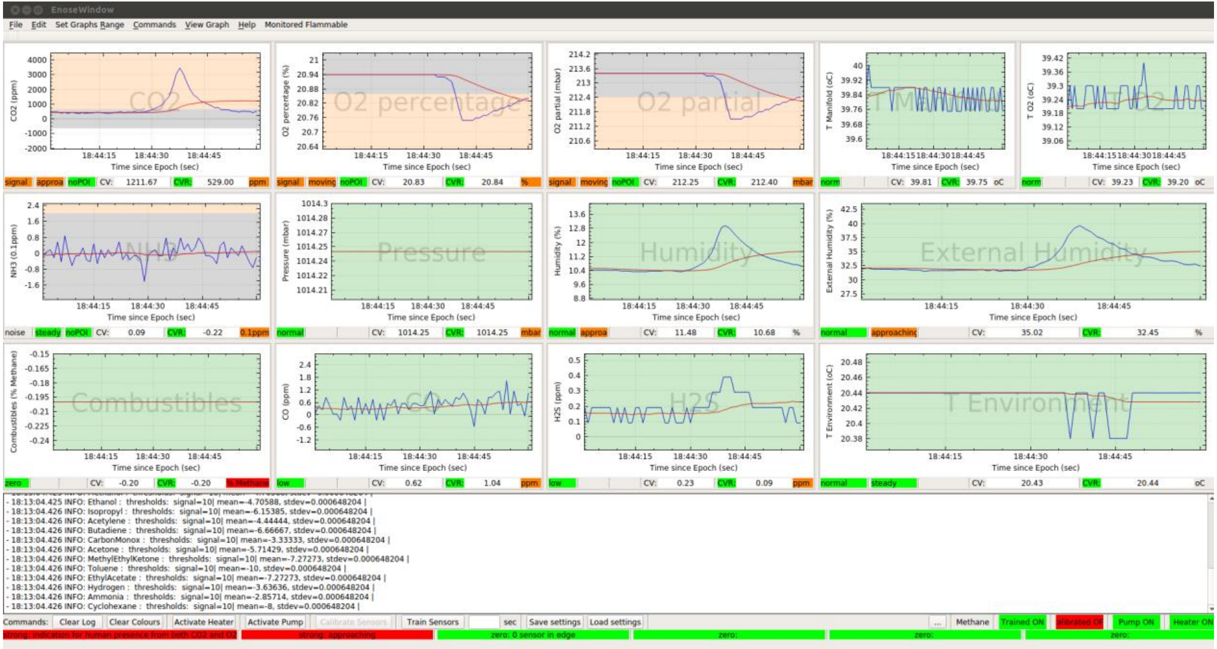
EnoseWindow
File Edit Set Graphs Range Commands View Graph Help Monitored Flammable
CO2
O2 percentage
O2 partial
T Manifold
T O2
NH3
Pressure
Humidity
External Humidity
Combustibles
CO
H2S
T Environment
Time since Epoch (sec)
18:44:15
18:44:30
18:44:45
Commands: Clear Log Clear Colours Activate Heater Activate Pump Calibrate Sensors Train Sensors sec Save settings Load settings
Methane Trained ON Pump ON Heater ON

```
- 18:13:04.425 INFO: Ethanol :  thresholds:  signal=10| mean=-4.70588, stdev=0.000648204 |
- 18:13:04.426 INFO: Isopropyl :  thresholds:  signal=10| mean=-6.15385, stdev=0.000648204 |
- 18:13:04.426 INFO: Acetylene :  thresholds:  signal=10| mean=-4.44444, stdev=0.000648204 |
- 18:13:04.426 INFO: Butadiene :  thresholds:  signal=10| mean=-6.66667, stdev=0.000648204 |
- 18:13:04.426 INFO: CarbonMonox :  thresholds:  signal=10| mean=-3.33333, stdev=0.000648204 |
- 18:13:04.426 INFO: Acetone :  thresholds:  signal=10| mean=-5.71429, stdev=0.000648204 |
- 18:13:04.426 INFO: MethylEthylKetone :  thresholds:  signal=10| mean=-7.27273, stdev=0.000648204 |
- 18:13:04.426 INFO: Toluene :  thresholds:  signal=10| mean=-10, stdev=0.000648204 |
- 18:13:04.426 INFO: EthylAcetate :  thresholds:  signal=10| mean=-7.27273, stdev=0.000648204 |
- 18:13:04.426 INFO: Hydrogen :  thresholds:  signal=10| mean=-3.63636, stdev=0.000648204 |
- 18:13:04.426 INFO: Ammonia :  thresholds:  signal=10| mean=-2.85714, stdev=0.000648204 |
- 18:13:04.426 INFO: Cyclohexane :  thresholds:  signal=10| mean=-8, stdev=0.000648204 |
```

```
strong: indication for human presence from both CO2 and O2 | strong: approaching | zero: 0 sensor in edge | zero: | zero: | zero:
```

Figure 160. E-nose system output when crossing the ventilation opening of a human-occupied confined space with the electronic nose.

Conclusions

The victim localization capabilities of the electronic nose were successfully verified for the 3rd prototype. The response of the e-nose inside a ventilation shaft is not linear as also observed in other experiments. This means that the e-nose might not always register human presence indicators at the beginning, or even at the middle of the access path to the void. To have conclusive results, the e-nose must be placed inside the cavity of interest where the conditions allow for the maximum response to be generated. The auto training functionality of the e-nose performed very well since the individual sensor indicators did not produce false positives and they correctly produced positives when they were expected to. The global indicators performed satisfactorily. The human presence indicator performed very well, always pointing out conditions where human presence signs were within detectable limits. The approaching indicator performed well for longer approaching events (when the human presence indicators rise for more than 20 seconds) correctly indicating weak and strong status. For short approaching events (when the human presence indicators rise for less than 20 seconds) the approaching indicator did not produce the strong status due to the underlying latency – response time of some of the sensors and the filter delay. The e-nose did not produce any Hot Spot indicator signals for the very short approaching events (passing fast in front of a ventilation opening) since it is configured not to do so when the human presence global indicator is not triggered. As a general rule of thumb, the human presence indicator is adequate for most situations. For situations where the human presence indicator is triggered in a large void or the access path towards a void, the approaching indicator will help determine the correct direction for movement. The Hot Spot indicator further assists the search pattern and localization by providing the detections of peaks of human presence. Another alternative would be to retrain the e-nose inside the system and only use the human indicator.

Breath-based detection test 2 (Hot spot test –with balloon)

This breath-based test is configured in such a way that the victim localization indicators, and especially the Hot Spot indicator, can be tested without having to place a human subject in a confined space. For this, the following apparatus is created. A balloon is inflated with exhaled air and is mounted on a tube that has a configurable flow control vane and an output nozzle. The vane and nozzle are configured so that a small amount of exhaled air is steadily released into the atmosphere, creating a small increase of the human presence indicators near the nozzle's output. This setup simulates the entrance of a confined space with a victim inside. The following picture illustrates the apparatus.

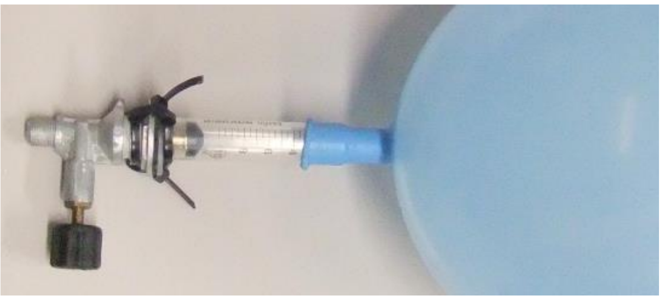

Figure 161. Apparatus for creating a small, steady and controlled exhaled air flow.

The experiment procedure was the following: The electronic nose was operated in the full power mode (heater enabled), and a sampling tube was connected to the input interface to facilitate scanning. Prior to carrying out the measurements of the test procedure, the e-nose was left to warm up and reach the operational temperature of the full power mode. When warm, the sampling input was placed outside the window and the system was calibrated (1 point calibration – assuming the air outside the building has nominal concentration values). After completion, the sampling input was left outside and the e-nose was trained for three minutes (180 seconds) to automatically determine the noise and signal thresholds of the current location (the external fresh air). It was performed this way so that when the sampling input was brought inside the office where people were present, the human presence indicators would be triggered. The goal was to have the human presence global indicator permanently triggered and test the Hot Spot indicator when increased human indicators are present momentarily by applying a more concentrated breath sample via the balloon. This was achieved by opening the valve controlling the air release from the balloon and momentarily bringing the e-nose's sampling input close to the nozzle and then moving it away. A summary of the experiment results when moving the sampling tube in front of the valve nozzle are collected in the following table:

Figure 162. Results summary for the experiment of detecting a Hot Spot

Location → Output ↓	Outside Office	Inside Office	Close to Nozzle	Away from Nozzle 1	Away from Nozzle 2
CO_2 (ppm)	412	861	1054	1121	1159
O_2 (mbar) [O_2] (%)	213.44 [20.96]	212.45 [20.86]	212.33 [20.85]	212.19 [20.84]	211.96 [20.82]
Human indicator	Normal	Strong: ...CO2 + O2	Strong: ...CO2 + O2	Strong: ...CO2 + O2	Strong: ...CO2 + O2
Approaching ind.	Zero	Zero	Zero: approaching	Weak: approaching	Weak: approaching
Hot Spot ind.	Zero	Zero	Strong: ...	Zero	Zero

The e-nose produced the indicator signals when close to the nozzle as illustrated in the following picture.

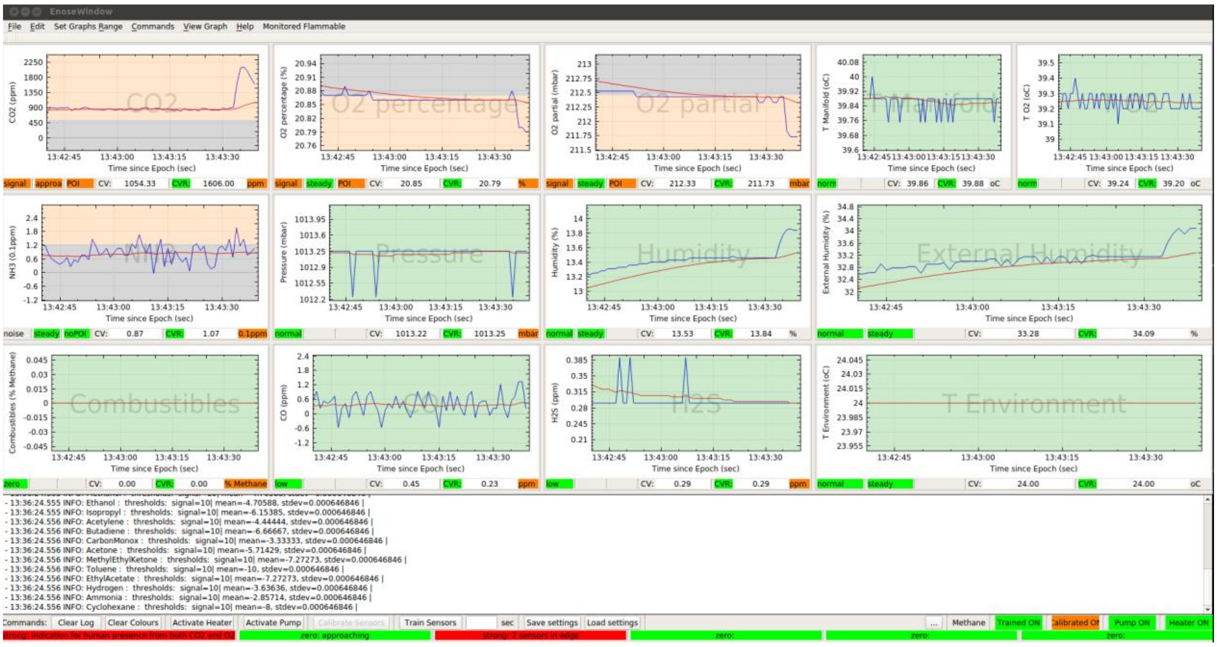
EnoseWindow
File Edit Set Graphs Range Commands View Graph Help Monitored Flammable
CO2
O2 percentage
O2 partial
T Manifold
T O2
NH3
Pressure
Humidity
External Humidity
Combustibles
CO
H2S
T Environment
Time since Epoch (sec)
Commands: Clear Log Clear Colours Activate Heater Activate Pump Calibrate Sensors Train Sensors sec Save settings Load settings
Methane Trained ON Calibrated ON Pump ON Heater ON
strong: indication for human presence from both CO2 and O2
zero: approaching
strong: 2 sensors in edge

```
- 13:36:24.555 INFO: Ethanol :  thresholds:  signal=10| mean=-4.70588, stdev=0.000646846 |
- 13:36:24.555 INFO: Isopropyl :  thresholds:  signal=10| mean=-6.15385, stdev=0.000646846 |
- 13:36:24.556 INFO: Acetylene :  thresholds:  signal=10| mean=-4.44444, stdev=0.000646846 |
- 13:36:24.556 INFO: Butadiene :  thresholds:  signal=10| mean=-6.66667, stdev=0.000646846 |
- 13:36:24.556 INFO: CarbonMonox :  thresholds:  signal=10| mean=-3.33333, stdev=0.000646846 |
- 13:36:24.556 INFO: Acetone :  thresholds:  signal=10| mean=-5.71429, stdev=0.000646846 |
- 13:36:24.556 INFO: MethylEthylKetone :  thresholds:  signal=10| mean=-7.27273, stdev=0.000646846 |
- 13:36:24.556 INFO: Toluene :  thresholds:  signal=10| mean=-10, stdev=0.000646846 |
- 13:36:24.556 INFO: EthylAcetate :  thresholds:  signal=10| mean=-7.27273, stdev=0.000646846 |
- 13:36:24.556 INFO: Hydrogen :  thresholds:  signal=10| mean=-3.63636, stdev=0.000646846 |
- 13:36:24.556 INFO: Ammonia :  thresholds:  signal=10| mean=-2.85714, stdev=0.000646846 |
- 13:36:24.556 INFO: Cyclohexane :  thresholds:  signal=10| mean=-8, stdev=0.000646846 |
```

Figure 163. E-nose system output when momentarily exposed to high human presence air conditions.

Conclusions

The Hot Spot indicator tested with the balloon setup performed well, indicating the position of the maximum human indicator signs (works on raw values –CVR). The human indicator performed as well as anticipated. The approaching indicator in this case performed as expected, indicated a weak approaching signal while the sampling input tube was moved away from the Hot Spot because it is based on the filtered values. This should have not been the output for the ideal response of the system which is to produce a moving away signal. This behavior, though, can be anticipated by the operator when he has knowledge of the operating topography that is provided by the optical cameras of the robotic platform. Also, this scenario is not the typical scenario and represents the most difficult case for victim localization (for the e-nose when human presence signs are elevated in a large cavity. This issue can easily be overcome by retraining the e-nose inside the confined space and using the e-nose with the human presence and approaching indicators. Another option, but not for the typical user, would be to monitor the raw values (CVR) of the sensor measurements in such difficult cases.

NH_3 detection test

A test of NH_3 gas detection was performed with the following procedure: A solution containing a small concentration of ammonia was brought close to the input interface of the e-nose. The ammonia solution used was a “15ml Salkano mosquito stick”. The e-nose was operated in the full power mode (with the heaters turned ON and the temperature of the manifold at the set point temperature). The sampling pump was operated for a while before momentarily exposing the electronic nose to the ammonia fumes. The following graphs illustrate the results.

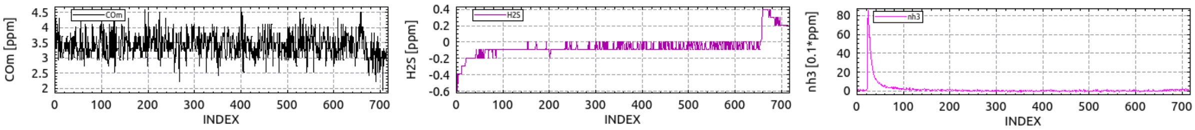

Figure 164. CO, H_2S and NH_3 sensor response to ammonia gas (mosquito bite stick)

Mosquitos Stick

Figure 165. Ammonia containing product used for testing

The sensor responds well to the ammonia fumes contained in the product. No cross-sensitivity is noticed in this experiment with other sensors of the system. The sensor also exhibits a good and fast recovery to the base signal levels after the excitation source is removed.

8.6.2. Hazardous conditions in the air detection tests

Carbon Monoxide (CO)

A test of CO gas detection was performed with the following procedure. The input interface of the e-nose was connected to a sampling tube so that air from a sampling bag could be directly fed into it. The e-nose was operated in the low power mode with the heaters turned OFF and the temperature of the manifold at the environmental temperature. A sampling bag (volume of approximately 1 liter) was filled with the exhaled smoke of a smoker (a puff of smoke originating from an unfiltered cigarette with aromatic tobacco). The e-nose was operated for some time (pump enabled) and then the sampling bag was connected to the sampling tube. The following graphs illustrate the results.

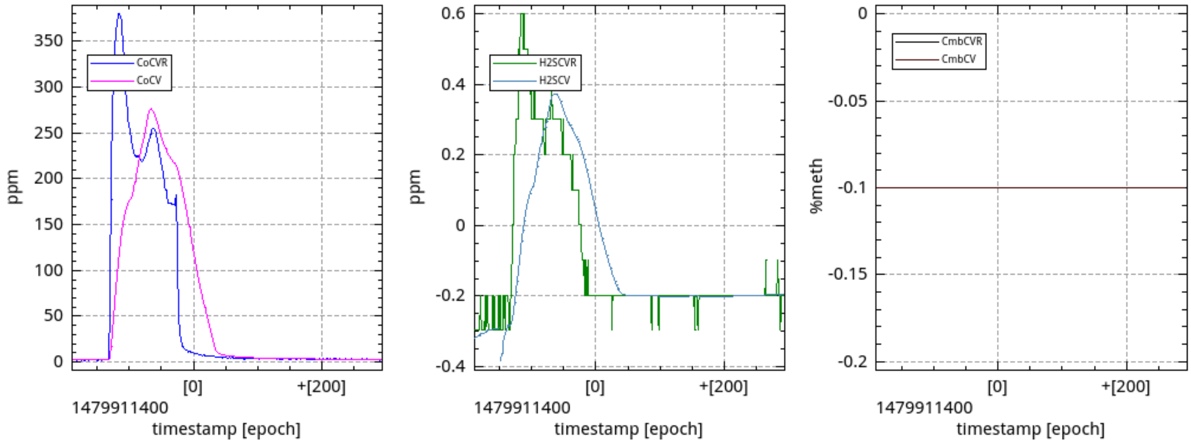

Figure 166. Left to right: Response of the CO, H_2S and Combustibles sensors to exhaled cigarette smoke

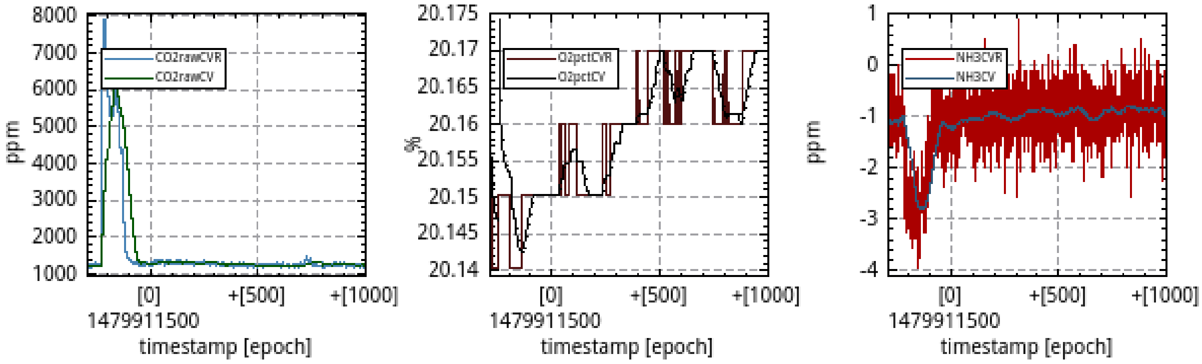

Figure 167. Left to right: Response of the CO_2, O_2 and NH_3 sensors to exhaled cigarette smoke

The figures illustrate a good response and exhibit the expected behavior. The CO sensor detects a large concentration of CO and, at the same time, the H_2S and NH_3 sensors show little cross-sensitivity. The H_2S sensor has a CO capturing filter for this purpose so that CO and H_2S can be distinguished. The NH_3 sensor's response to the CO is negative compared to the positive response to NH_3 gas and is not an issue for the system. The CO_2 and O_2 sensors correctly respond to the exhaled air.

Combustibles

A test of combustibles gas detection was performed with the following procedure. The e-nose was operated in the low power mode with the heaters turned OFF and the temperature of the manifold at the environmental temperature. A cigarette lighter was triggered to emit gas, without igniting it, directly into the air sampling input of the e-nose while the pump was active. The following graphs illustrate the results:

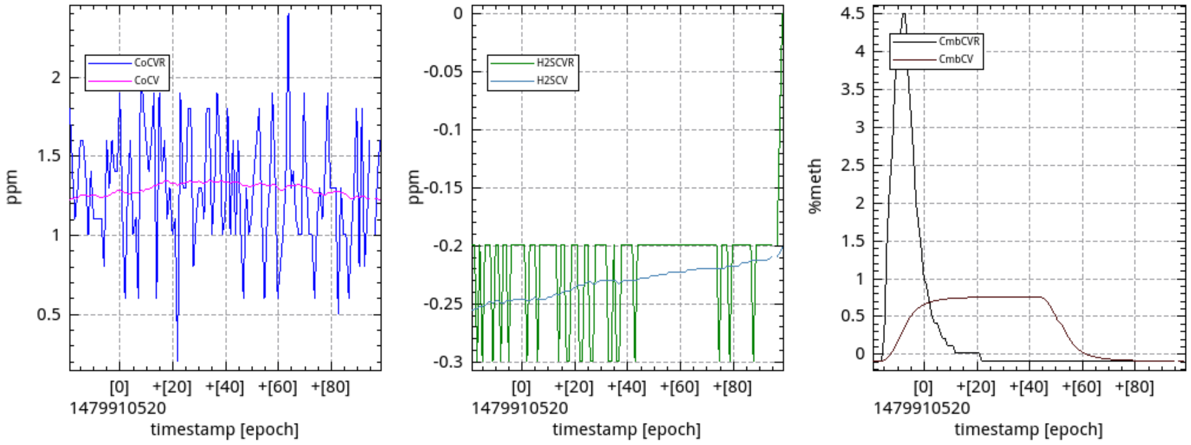

Figure 168. Left to right: Response of the CO, H_2S and Combustibles sensors to cigarette lighter gas

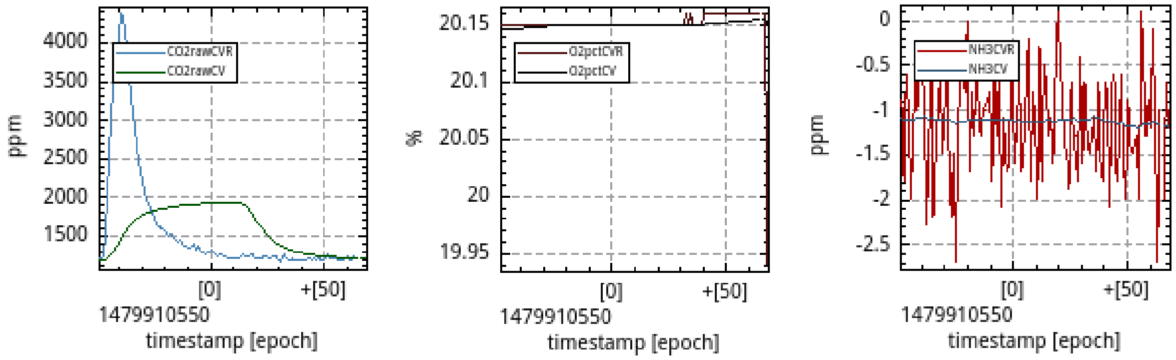

Figure 169. Left to right: Response of the CO_2, O_2 and NH_3 sensors to cigarette lighter gas

The figures illustrate a good response of the sensors to the gas (5% methane is 100%LEL) and expose the cross-sensitivity of the CO_2 sensor to the combustible gas used. This is not a problem for the system because the advanced logic unit can detect this case and report the correct output indicators.

Hydrogen Sulfide (H_2S)

The concept with these tests is to show the capability of detecting the target gases, but not necessarily in hazardous concentrations. The H_2S detection case required the e-nose to be portable so that a scan could be performed in various sewer/ gutter openings. A long sampling tube, an Android tablet, and a battery pack were connected to the e-nose. Only raw values were acquired, but this was not an issue for the type of experiment and operator/ developer. The user interface and advanced logic unit were not ported, and will not be, on this type of tablet.

The following picture illustrates the portable configuration for this test:

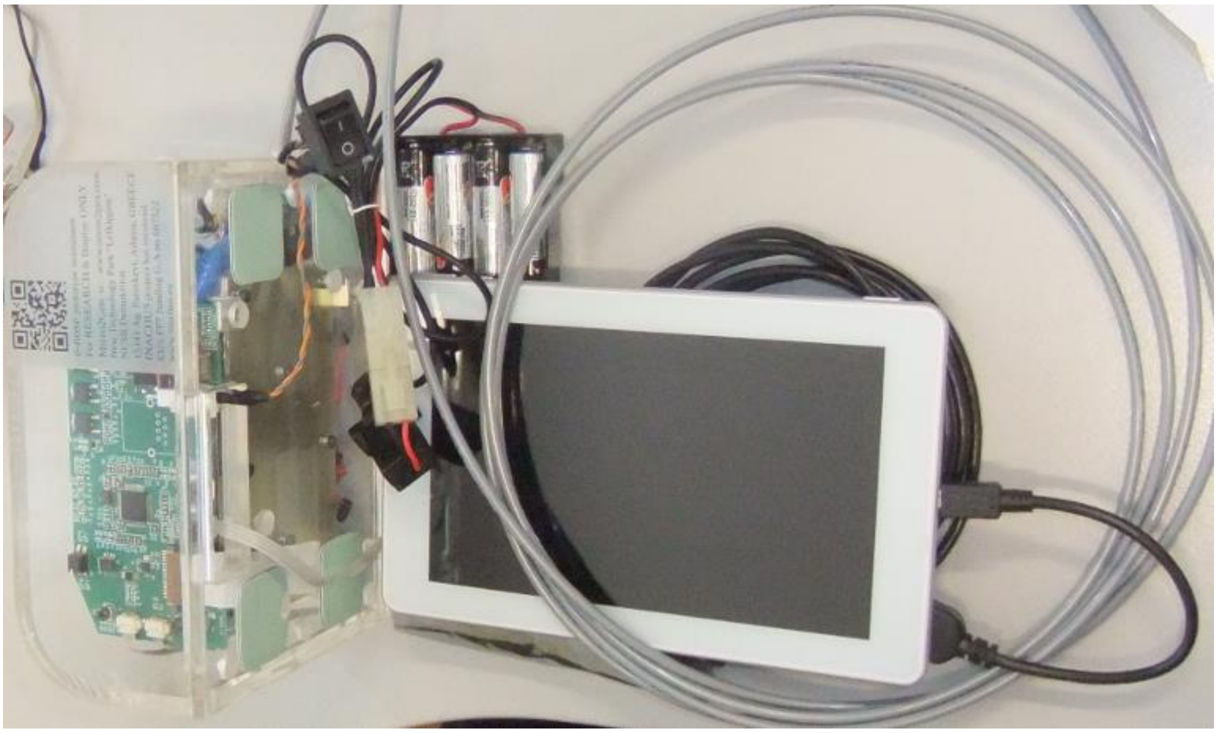

Figure 170. A portable e-nose configuration for scanning and acquiring measurements

The scanning of various potential areas was performed, but no H_2S was detected with either the e-nose or with the operator's sense of smell (H_2S has a rotten eggs odor). For this reason "stink bomb" vials (H_2S based) were used instead.

H_2S detection via stink ampoule

The tests with the stink ampoules were conducted outdoors for obvious reasons. The particular ampoule purchased (www.clevermarket.gr) contains a solution of ammonium sulfide.

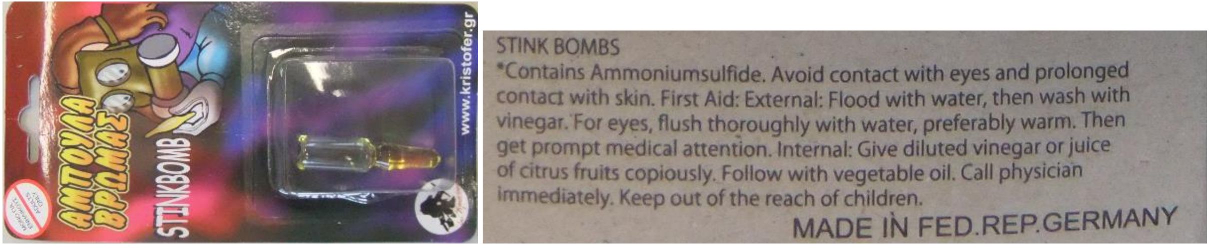

STINK BOMBS
*Contains Ammoniumsulfide. Avoid contact with eyes and prolonged contact with skin. First Aid: External: Flood with water, then wash with vinegar. For eyes, flush thoroughly with water, preferably warm. Then get prompt medical attention. Internal: Give diluted vinegar or juice of citrus fruits copiously. Follow with vegetable oil. Call physician immediately. Keep out of the reach of children.
MADE IN FED.REP.GERMANY

Figure 171. Ampoule with ammonium sulfide for H_2S testing

When the ampoule is broken, the release of ammonia and hydrogen sulphide is expected. The following procedure was followed for conducting the experiment:

The e-nose was used in the portable configuration to acquire measurements. The pump was operated constantly – ON. A 1.5 liter water bottle was cut so that a deep cup (gas chamber) was formed. A flat stone was placed on the bottom of the cup. The ampoule was placed on the stone. Another stone was used to cap the ampoule. The cup with the ampoule and stones was forced on the ground and the ampoule broke releasing its contents. The e-nose's sampling interface (extended via long tube) was brought close and was placed in the cup chamber.

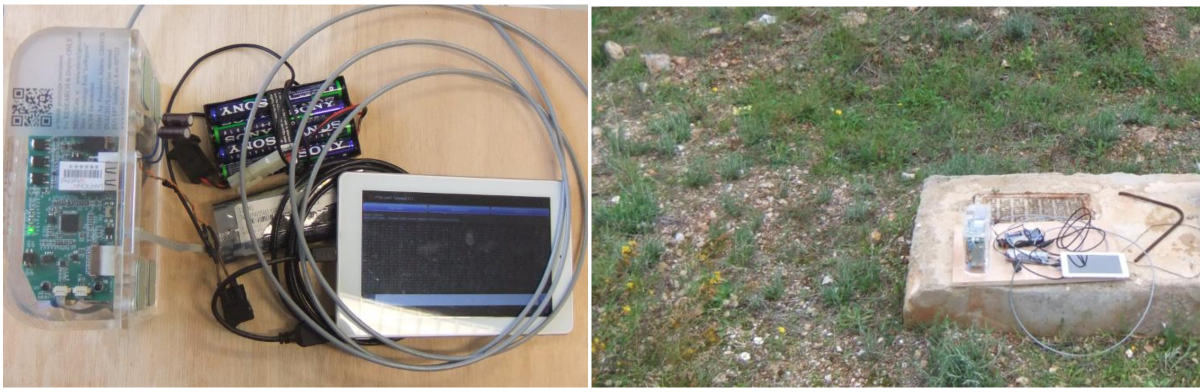

Figure 172. H_2S detection test apparatus

The following picture illustrates the measurements:

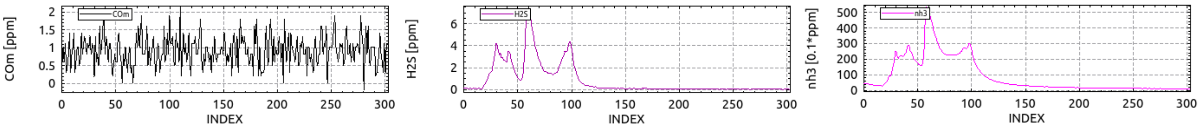

Figure 173. The CO, H_2S and NH_3 sensors response from exposure to a stink ampoule (ammonium sulfide solution)

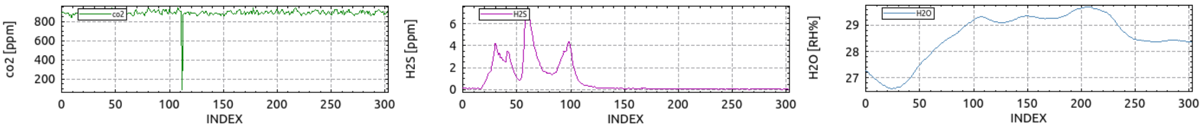

Figure 174. The CO_2, H_2S and Humidity sensors response from exposure to a stink ampoule (ammonium sulfide solution)

The H_2S measurement was not as high as expected compared to the ammonia sensor output. The other sensors did not exhibit any significant sensitivity. The release of H_2S was boosted by exposing the ammonium sulfide to a weak acid. A piece of orange was squeezed on the spot directly into the cup (orange juice) and the cup was covered by hand to momentarily increase the concentration. The following figures illustrate the results:

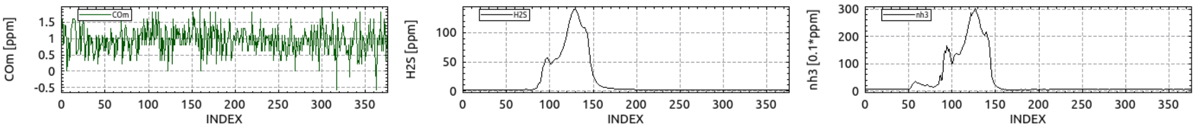

Figure 175. The CO, H_2S and NH_3 sensors response from exposure to a stink ampoule (ammonium sulfide solution)

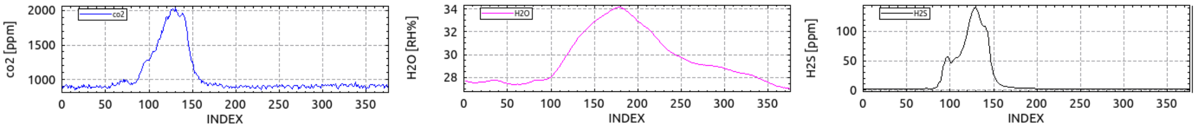

Figure 176. The CO_2, H_2S and Humidity sensors response from exposure to a stink ampoule (ammonium sulfide solution)

The sensor performed as expected, both ammonia and H_2S sensors produced a significant response. At very high H_2S concentrations, it seems the CO_2 sensor shows some sensitivity. This is not an issue for the system because detection of such high levels of H_2S indicates a very dangerous atmosphere and the survivability of trapped victims, especially for prolonged durations, is very unlikely. The carbon monoxide sensor did not register any noteworthy response. This experiment is considered successful and verifies the capability of the e-nose to detect and measure hydrogen sulfide gas.

Conclusions

The detection and measurement capability of the electronic nose for the specified hazardous gases was successfully verified with practical methods and off-the-shelf materials.

Power consumption in various modes of operation

The e-nose, without the Ethernet module installed, was tested to determine the actual power requirements in the available operating modes. The voltage applied was 12V in order to determine the requirements for a battery pack in case of making the device independent from the robotic platform. This configuration was used to power the e-nose for the H_2S tests. The following table lists the results:

Table 66. Power consumption in various operating modes

Condition	Voltage(V)	Current (mA)	Power (W)
Idle	12	90	1.08
Pump ON	12	150	1.8
Heater ON	12	210	2.52
Pump and Heater ON	12	270	3.24

According to these measurements, taking into account the AA energizer battery*, the e-nose could operate for at least three hours, in full load, until cell voltage reached 1.2V and the power supplies crossed the under voltage threshold and turned OFF (when using eight cells).
*http://data.energizer.com/PDFs/E91.pdf

8.7. Second field tests P3 – End-user Validation

The e-nose system was tested in a field test that took place in Weeze, Germany at a USaR training facility [102]. Here the system was tested stand-alone, as a physical device, and integrated considering its data intercommunication with the other higher level systems. In this work, only the detection and results presentation aspects of the stand-alone e-nose system are presented. The victim localization aspects were validated by searching for victims from the surface of the rubble pile. The e-nose system was stationary and a long air sampling tube was used to scan the openings in the rubble for human presence indicators. Figure 177

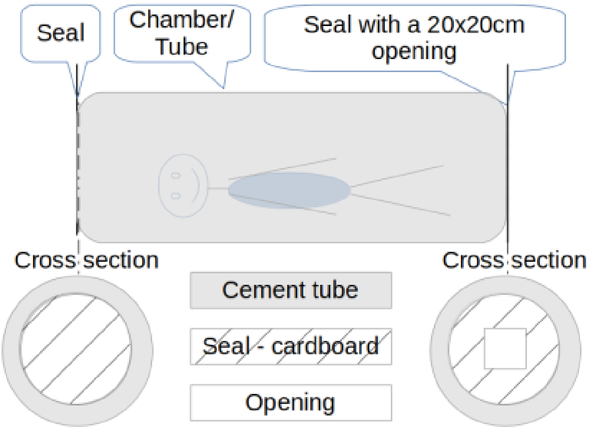

Figure 177. The victim's survival space used to test the e-nose victim localization capabilities.

illustrates the victim's placement. A large diameter concrete tube was used as the survival space. One end of the tube was sealed, while the other had a cardboard seal with an opening of about 20cm x 20cm that could easily be removed for the volunteer victim to enter and exit the space. The e-nose's air sampling input was connected to a 4m long air tube so that a scan could be performed on the surface of the rubble. The following picture illustrates the actual location.

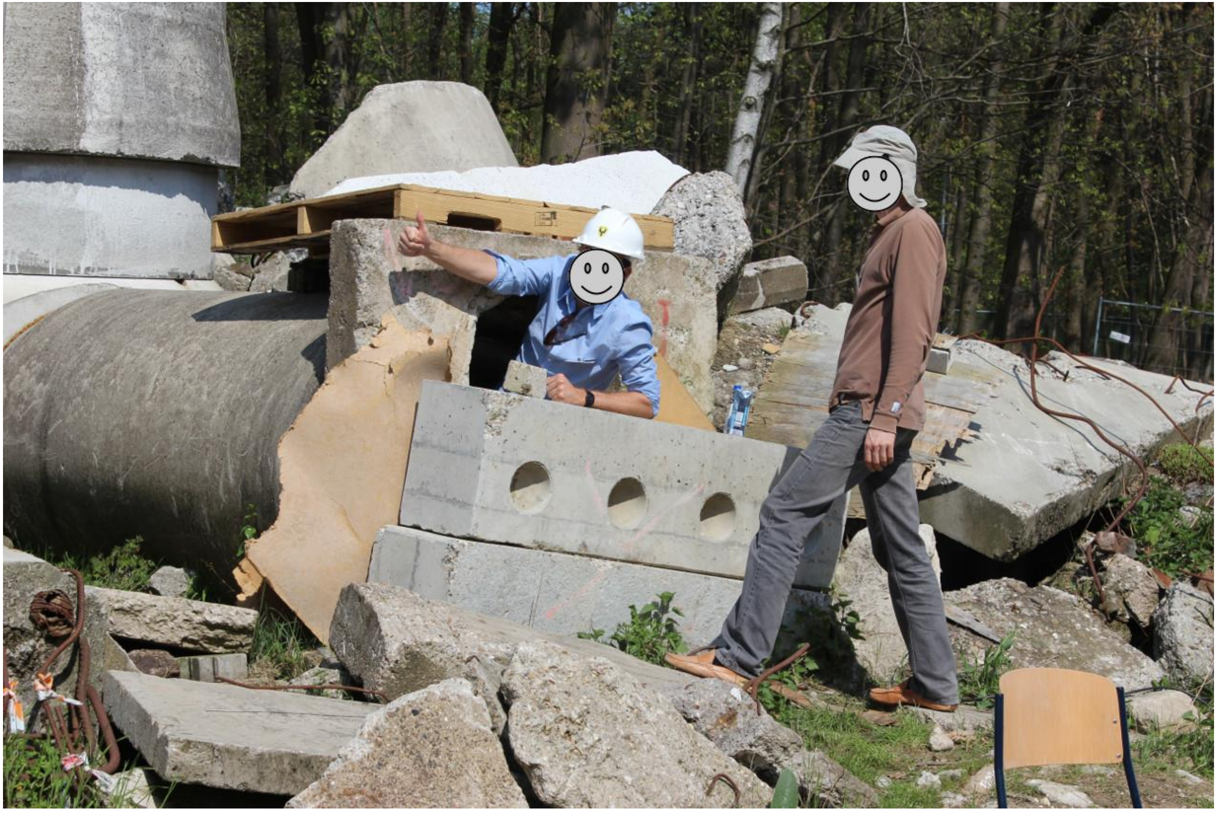

Figure 178. The volunteer "victim" while entering the confined space 20 minutes before the e-nose test and demonstration.

Placing the sampling tube in the opening of the chamber should trigger the e-nose victim detection indicator. Figure 178 illustrates the survival space and the volunteer victim entering it approximately 20 minutes before the demonstration. Figure 179 illustrates the presentation and demonstration configuration for the victim localization and hazardous detection tests. The e-nose system is the yellow block placed on the edge of the table seen in the centre of the picture. Next to it, on the right, is the control interface laptop. In front of it is a bottle with an orange cap used for H_2S gas testing. The confined space can be distinguished in the background behind the e-nose. The air sampling tube was used to scan the area of the rubble pile around the e-nose. Hazardous condition detection was performed with test gasses contained in air sample containers. No confined space had its air converted to a hazardous composition of any kind. The same approach was used for ammonia detection. H_2S was generated from a stink ampoule by breaking it inside the bottle with the orange cap. A combustible atmosphere was created with a gas cigarette lighter, and CO was tested with exhaled cigarette smoke. NH_3 was sourced from a mosquito bite stick that includes a small concentration of ammonia. The following picture illustrates the presentation/demonstration location.

Figure 179. The e-nose demonstration for victim localization and hazardous conditions detection capabilities.

The interface presented to the operators was the one for development and testing purposes (the same interface could be used for training and maintenance purposes) with the explicit directive to focus their attention on the global indicators portion of the screen and ignore the individual gas concentration plots. External, to the laptop interface, labels and viewing blanks were introduced in order to guide the observers to view the correct portion of the display.

Test scenario

The test and demonstration scenario had 7 distinct cases. These cases are the following:

Case (1)	Before deployment into the rubble the calibration parameters were applied and the e-nose trained to local conditions.
Case (2)	A search was performed near the area where the victim was entrapped, monitoring the output from the e-nose. The e-nose air sampling tube was placed near and inside the space with the trapped victim. Signs of human presence were detected. The e-nose was removed from the void.
Case (3)	The e-nose sampling tube was placed at the opening of a bottle containing a gas mixture of H_2S.
Case (4)	The e-nose sampling tube was placed at the nozzle of a cigarette lighter containing a combustible gas.
Case (5)	The e-nose sampling tube was blocked to simulate filter blockage.
Case (6)	Exhaled air was blown over the sampling tube to acquire toxic concentrations of CO_2.
Case (7)	Exhaled cigarette smoke was blown over the sampling tube to acquire toxic concentrations of CO.

Measurements and description

The following picture illustrates the measurements of the complete test and demonstration which includes all the aforementioned cases after their completion as seen in the e-nose interface. The timeframe was selected so that all events are displayed. Because of the large span of the measurements it is not very easy to distinguish detection events, especially those with a small gas concentration. Following the complete test and demonstration measurements are more detailed captions of the interface for each of the aforementioned cases of the scenario, indicated on the graphs as numbers in parenthesis (#), corresponding to case number. The interface includes the measurement plots, the individual indicators, the current value, the average value bellow each plot. On the bottom of the interface are the global indicators. For all plots, the most recent measurement is the rightmost value. Individual indicators are calculated based on the most recent data for the type of indicator. Global indicators are calculated based on the values of individual indicators at the current moment. For the human detection case, multiple interface plots are shown in order to illustrate, as much as possible, the actual response of the system while being tested without “knowing/seeing” future measurements in an effort to recreate the operator’s experience during the test. Table 67 summarizes the measurements and the ENALU output of the test.

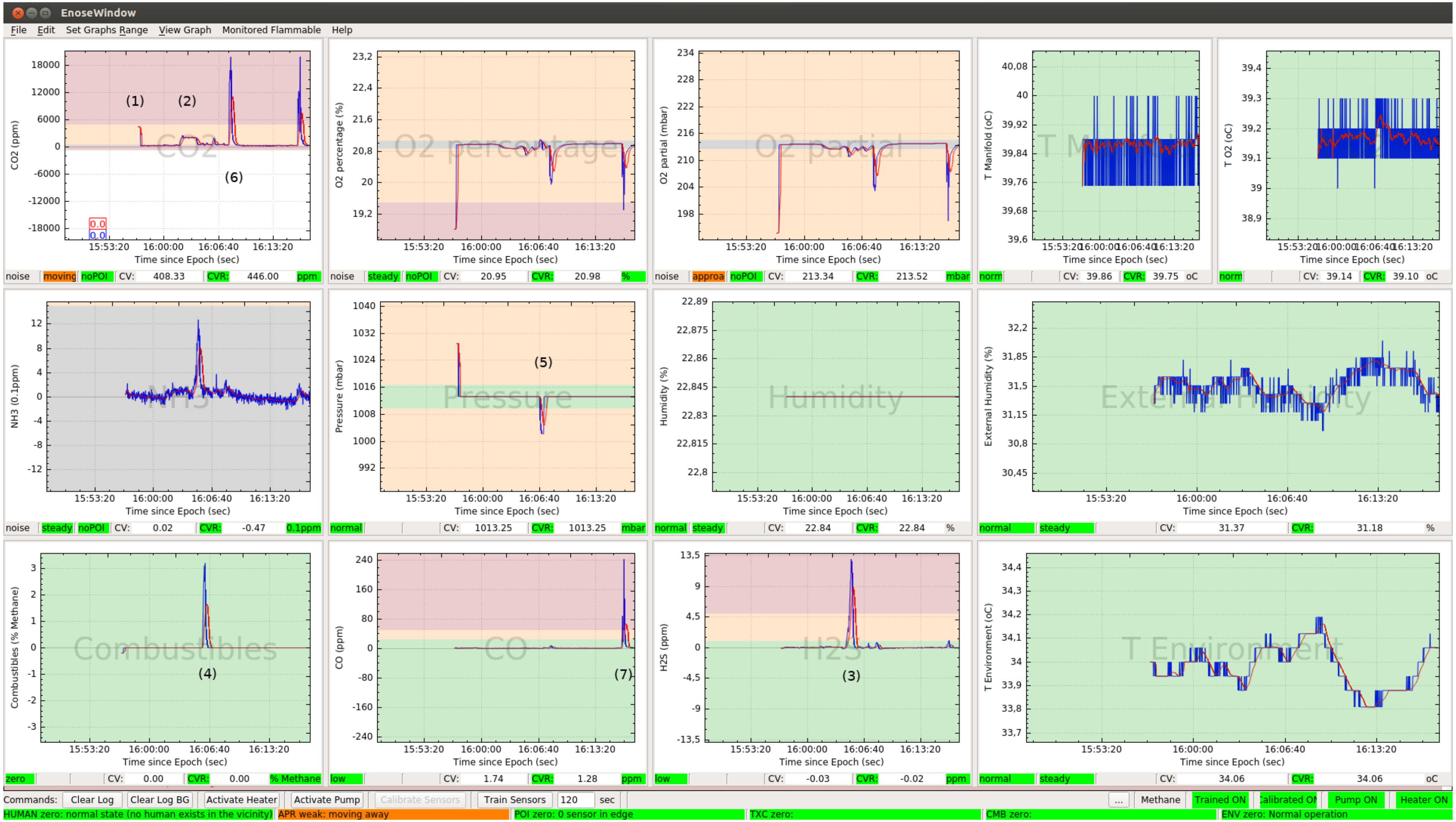
EnoseWindow
File
Edit
Set Graphs Range
View Graph
Monitored Flammable
Help
CO2 (ppm)
18000
12000
6000
0
-6000
-12000
-18000
(1)
(2)
(6)
CO2
0.0
0.0
O2 percentage (%)
23,2
22,4
21,6
20,8
20
19,2
O2 percentage
O2 partial (mbar)
234
228
222
216
210
204
198
O2 partial
T Manifold (oC)
40,08
40
39,92
39,84
39,76
39,68
39,6
T Manifold
T O2 (oC)
39,4
39,3
39,2
39,1
39
38,9
NH3 (0.1ppm)
12
8
4
0
-4
-8
-12
NH3
Pressure (mbar)
1040
1032
1024
1016
1008
1000
992
(5)
Pressure
Humidity (%)
22,89
22,875
22,86
22,845
22,83
22,815
22,8
Humidity
External Humidity (%)
32,2
31,85
31,5
31,15
30,8
30,45
External Humidity
Combustibles (% Methane)
3
2
1
0
-1
-2
-3
Combustibles
(4)
CO (ppm)
240
160
80
0
-80
-160
-240
CO
(7)
H2S (ppm)
13,5
9
4,5
0
-4,5
-9
-13,5
H2S
(3)
T Environment (oC)
34,4
34,3
34,2
34,1
34
33,9
33,8
33,7
T Environment
15:53:20
16:00:00
16:06:40
16:13:20
Time since Epoch (sec)
Commands:
Clear Log
Clear Log BG
Activate Heater
Activate Pump
Calibrate Sensors
Train Sensors
sec
...
Methane
Trained ON
Calibrated ON
Pump ON
Heater ON

noise | moving | noPOI | CV: 408.33 | CVR: 446.00 | ppm

noise | steady | noPOI | CV: 20.95 | CVR: 20.98 | %

noise | approa | noPOI | CV: 213.34 | CVR: 213.52 | mbar

norm | CV: 39.86 | CVR: 39.75 | oC

norm | CV: 39.14 | CVR: 39.10 | oC

noise | steady | noPOI | CV: 0.02 | CVR: -0.47 | 0.1ppm

normal | CV: 1013.25 | CVR: 1013.25 | mbar

normal | steady | CV: 22.84 | CVR: 22.84 | %

normal | steady | CV: 31.37 | CVR: 31.18 | %

zero | CV: 0.00 | CVR: 0.00 | % Methane

low | CV: 1.74 | CVR: 1.28 | ppm

low | CV: -0.03 | CVR: -0.02 | ppm

normal | steady | CV: 34.06 | CVR: 34.06 | oC

Train Sensors: 120 sec

HUMAN zero: normal state (no human exists in the vicinity)

APR weak: moving away

POI zero: 0 sensor in edge

TXC zero:

CMB zero:

ENV zero: Normal operation

Figure 180. All test scenario measurements are illustrated in this e-nose interface screenshot.

Case (1) – Application of calibration calculation to raw measurements. The sudden change (step response) of the measurements is a result of printing the corrected values after the uncorrected values. A large step indicates a large correction was applied to the raw sensor measurements. After loading calibration data, the e-nose can be retrained on the local air conditions to determine the detection thresholds that are not fixed values.

Case (2) - Victim localization captured progression is illustrated in the following pictures. The gases of interest for victim localization are CO_2, O_2 and NH_3. For a detailed description of the user interface and the calculation of the indicators see 8.5.6 Global Indicators – calculation and 8.5.7 Extended GUI of the 3rd prototype.

In Figure 181 the e-nose sampling tube was used to scan over the rubble pile where no victim was present. No indicators are triggered while the e-nose is properly configured and active. The interface's timeframe was configured to be 1 minute so that only the measurements of the last minute are displayed and affect the autoscaling of the vertical axis (concentration).

In Figure 182 the e-nose air sampling interface is brought close and then is inserted inside the cavity with the victim. A weak (global) approaching indicator is triggered, driven by the CO_2 (individual) approaching indicator. No human presence indicator is triggered yet because none of the human presence gases have reached the signal threshold levels indicated by the orange color section of the plot. To trigger the Human indicator the filtered-average value of the measurements indicated with the red line/trace must be in the orange region of the plot. The interface's timeframe was configured to be 1 minute.

In Figure 183 the e-nose sampling interface continues to sample air from inside the victim-occupied cavity. A weak human indicator is triggered, driven by the CO_2 signal indicator. The (global) approaching indicator continues to register a weak state. The Point of interest (global) indicator is triggered driven by the CO_2 (individual) POI indicator. The interface's timeframe was configured to be 1 minute.

In Figure 184 the e-nose sampling interface continues to sample air from inside the victim-occupied cavity. The human indicator continues to hold a weak state driven by the CO_2 signal indicator. The (global) approaching indicator continues to register a weak state. The Point of Interest (global) indicator continues to register a weak state driven by the CO_2 (individual) POI indicator. The interface's timeframe was configured to be 1 minute.

In Figure 185 the e-nose sampling interface continues to sample air from inside the victim-occupied cavity. A strong human indicator is triggered, driven by the CO_2 and O_2 signal indicator. The approaching and POI global indicators are cleared indicating that the air conditions inside the cavity are steady and that the sensors have settled/converged. The interface's timeframe was configured to be 3 minutes.

After this, the indicator states remained steady. The e-nose air sampling tube was removed from the victim-occupied cavity in order to proceed with the Hazardous condition detection tests. At this point the priority (validity) of the global indicators should be relisted: First, with the highest priority is the status indicator. If the e-nose for any of the mentioned conditions is not in optimal status, the e-nose outputs might not be valid. After the status indicator follows the combustibles indicator because high concentrations of combustible gases although cause only a small cross-sensitivity can create false positive human indicators. After the Combustibles indicator follows the Toxic indicator since high levels of some of the toxic gases can affect the human presence indicator. Last, with the lowest priority, are the Human presence indicator, the Approaching indicator and the Point of Interest indicators. Some of these priorities can be programmed in the indicator calculation logic as part of the Human indication text displayed to the operator.

Table 67. Summary of results for case (2): Searching outside the cavity and then moving inside. NH_3 readings did not measure significant change.

Location→ Output ↓	**Summary of victim detection results when entering inside an occupied confined space**				
	Away from opening	***Entrance of opening***	***1 Inside survival space***	***2 Inside survival space***	***3 Inside survival space***
Detailed measurements	Figure 181	Figure 182	Figure 183	Figure 184	Figure 185
CO_2 (ppm)	445	531	655	2050	2100
O_2(%) [O_2](mbar)	20.97 [213.55]	20.97 [213.52]	20.97 [213.5]	20.93 [213.06]	20.88 [212.55]
Human indicator	Normal	Normal	Weak: Transition state…	Weak: Transition state…	Strong: indications from…
Approaching indicator	Zero	Weak: Approaching	Weak: Approaching	Weak: Approaching	Zero
Hot Spot indicator	Zero	Zero	Weak	Zero	Zero

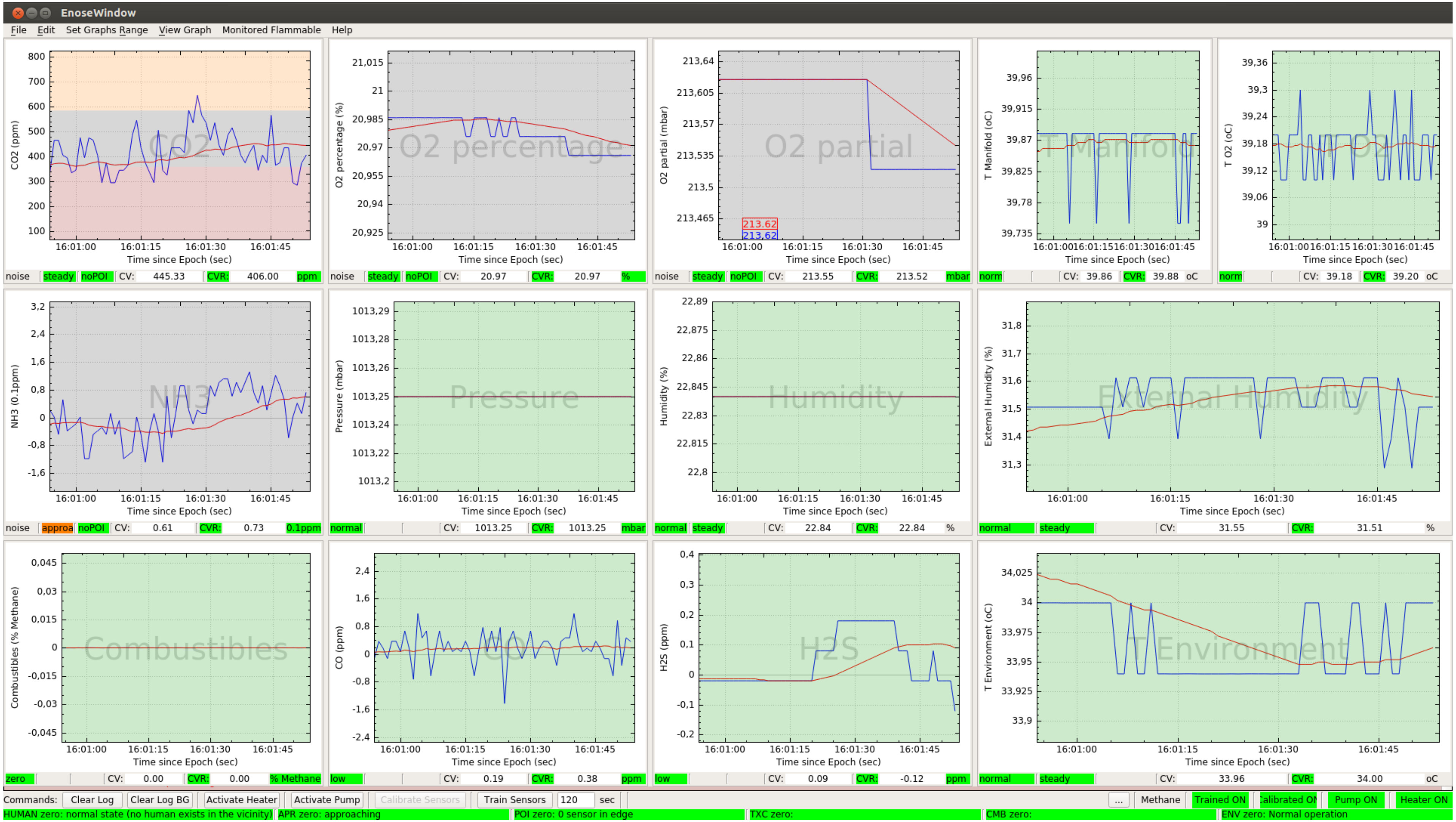
EnoseWindow
File Edit Set Graphs Range View Graph Monitored Flammable Help
CO2
CO2 (ppm)
800 700 600 500 400 300 200 100
O2 percentage
O2 percentage (%)
21,015 21 20,985 20,97 20,955 20,94 20,925
O2 partial
O2 partial (mbar)
213,64 213,605 213,57 213,535 213,5 213,465
213.62
213.62
T Manifold
T Manifold (oC)
39,96 39,915 39,87 39,825 39,78 39,735
T O2
T O2 (oC)
39,36 39,3 39,24 39,18 39,12 39,06 39
NH3
NH3 (0.1ppm)
3,2 2,4 1,6 0,8 0 -0,8 -1,6
Pressure
Pressure (mbar)
1013,29 1013,28 1013,26 1013,25 1013,24 1013,22 1013,2
Humidity
Humidity (%)
22,89 22,875 22,86 22,845 22,83 22,815 22,8
External Humidity
External Humidity (%)
31,8 31,7 31,6 31,5 31,4 31,3
Combustibles
Combustibles (% Methane)
0,045 0,03 0,015 0 -0,015 -0,03 -0,045
CO
CO (ppm)
2,4 1,6 0,8 0 -0,8 -1,6 -2,4
H2S
H2S (ppm)
0,4 0,3 0,2 0,1 0 -0,1 -0,2
T Environment
T Environment (oC)
34,025 34 33,975 33,95 33,925 33,9
16:01:00 16:01:15 16:01:30 16:01:45
Time since Epoch (sec)
Commands: Clear Log Clear Log BG Activate Heater Activate Pump Calibrate Sensors Train Sensors 120 sec ... Methane Trained ON Calibrated ON Pump ON Heater ON

noise | steady | noPOI | CV: 445.33 | CVR: 406.00 ppm
noise | steady | noPOI | CV: 20.97 | CVR: 20.97 %
noise | steady | noPOI | CV: 213.55 | CVR: 213.52 mbar
norm | CV: 39.86 | CVR: 39.88 oC
norm | CV: 39.18 | CVR: 39.20 oC
noise | approa | noPOI | CV: 0.61 | CVR: 0.73 0.1ppm
normal | CV: 1013.25 | CVR: 1013.25 mbar
normal | steady | CV: 22.84 | CVR: 22.84 %
normal | steady | CV: 31.55 | CVR: 31.51 %
zero | CV: 0.00 | CVR: 0.00 % Methane
low | CV: 0.19 | CVR: 0.38 ppm
low | CV: 0.09 | CVR: -0.12 ppm
normal | steady | CV: 33.96 | CVR: 34.00 oC

HUMAN zero: normal state (no human exists in the vicinity)
APR zero: approaching
POI zero: 0 sensor in edge
TXC zero:
CMB zero:
ENV zero: Normal operation

Figure 181. Case (2). Scanning far away from the survival space

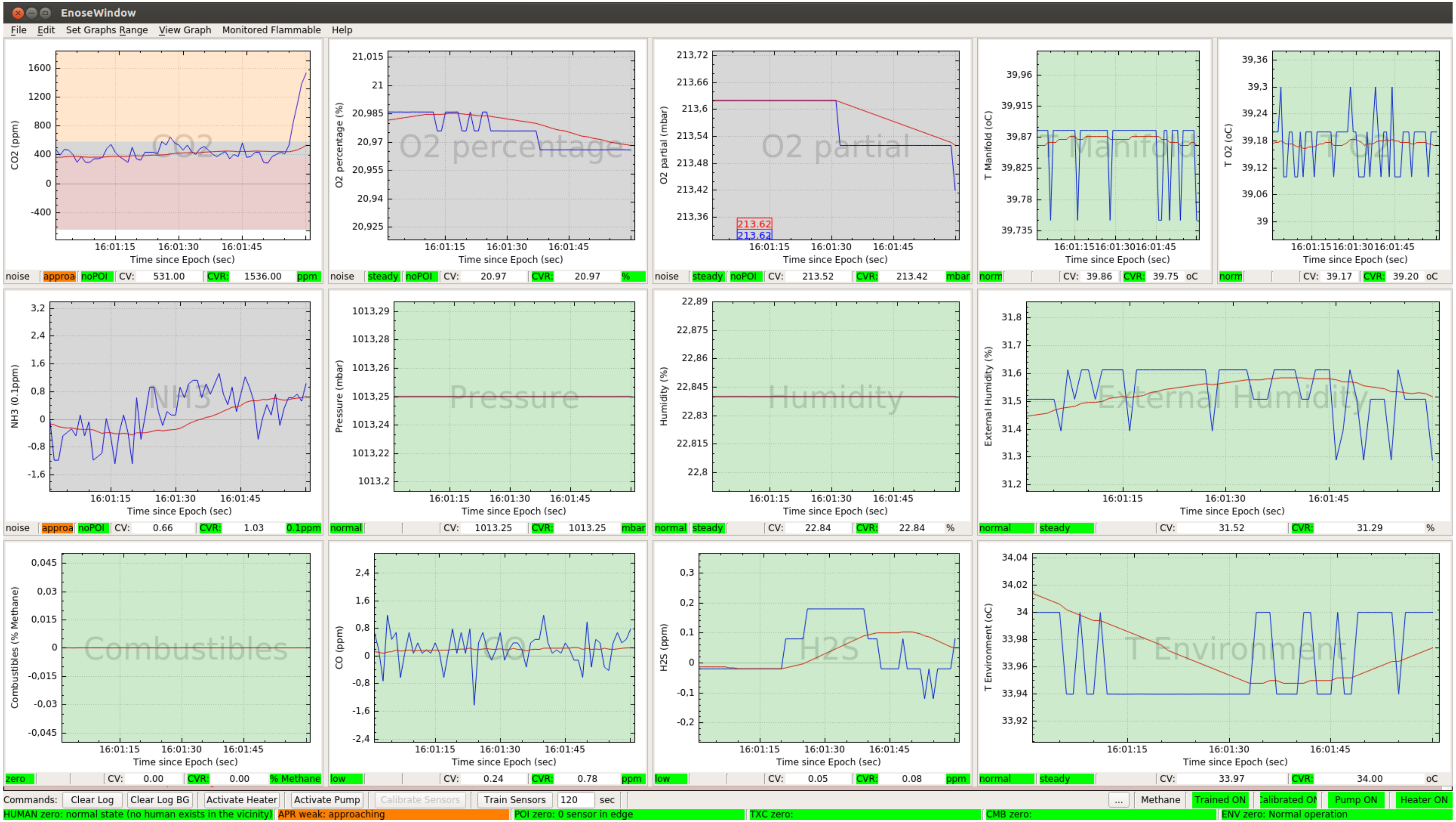
EnoseWindow
File Edit Set Graphs Range View Graph Monitored Flammable Help
CO2
CO2 (ppm)
1600
1200
800
400
0
-400
16:01:15
16:01:30
16:01:45
Time since Epoch (sec)
O2 percentage
O2 percentage (%)
21,015
21
20,985
20,97
20,955
20,94
20,925
O2 partial
O2 partial (mbar)
213,72
213,66
213,6
213,54
213,48
213,42
213,36
213.62
213.62
T Manifold
T Manifold (oC)
39,96
39,915
39,87
39,825
39,78
39,735
T O2
T O2 (oC)
39,36
39,3
39,24
39,18
39,12
39,06
39
NH3
NH3 (0.1ppm)
3,2
2,4
1,6
0,8
0
-0,8
-1,6
Pressure
Pressure (mbar)
1013,29
1013,28
1013,26
1013,25
1013,24
1013,22
1013,2
Humidity
Humidity (%)
22,89
22,875
22,86
22,845
22,83
22,815
22,8
External Humidity
External Humidity (%)
31,8
31,7
31,6
31,5
31,4
31,3
31,2
Combustibles
Combustibles (% Methane)
0,045
0,03
0,015
0
-0,015
-0,03
-0,045
CO
CO (ppm)
2,4
1,6
0,8
0
-0,8
-1,6
-2,4
H2S
H2S (ppm)
0,3
0,2
0,1
0
-0,1
-0,2
T Environment
T Environment (oC)
34,04
34,02
34
33,98
33,96
33,94
33,92
Commands: Clear Log Clear Log BG Activate Heater Activate Pump Calibrate Sensors Train Sensors 120 sec ... Methane Trained ON Calibrated ON Pump ON Heater ON

noise | approa | noPOI | CV: 531.00 | CVR: 1536.00 | ppm

noise | steady | noPOI | CV: 20.97 | CVR: 20.97 | %

noise | steady | noPOI | CV: 213.52 | CVR: 213.42 | mbar

norm | CV: 39.86 | CVR: 39.75 | oC

norm | CV: 39.17 | CVR: 39.20 | oC

noise | approa | noPOI | CV: 0.66 | CVR: 1.03 | 0.1ppm

normal | CV: 1013.25 | CVR: 1013.25 | mbar

normal | steady | CV: 22.84 | CVR: 22.84 | %

normal | steady | CV: 31.52 | CVR: 31.29 | %

zero | CV: 0.00 | CVR: 0.00 | % Methane

low | CV: 0.24 | CVR: 0.78 | ppm

low | CV: 0.05 | CVR: 0.08 | ppm

normal | steady | CV: 33.97 | CVR: 34.00 | oC

HUMAN zero: normal state (no human exists in the vicinity) | APR weak: approaching | POI zero: 0 sensor in edge | TXC zero: | CMB zero: | ENV zero: Normal operation

Figure 182. Case (2). Scanning the entrance and then inside the survival space. Approaching indicator is triggered

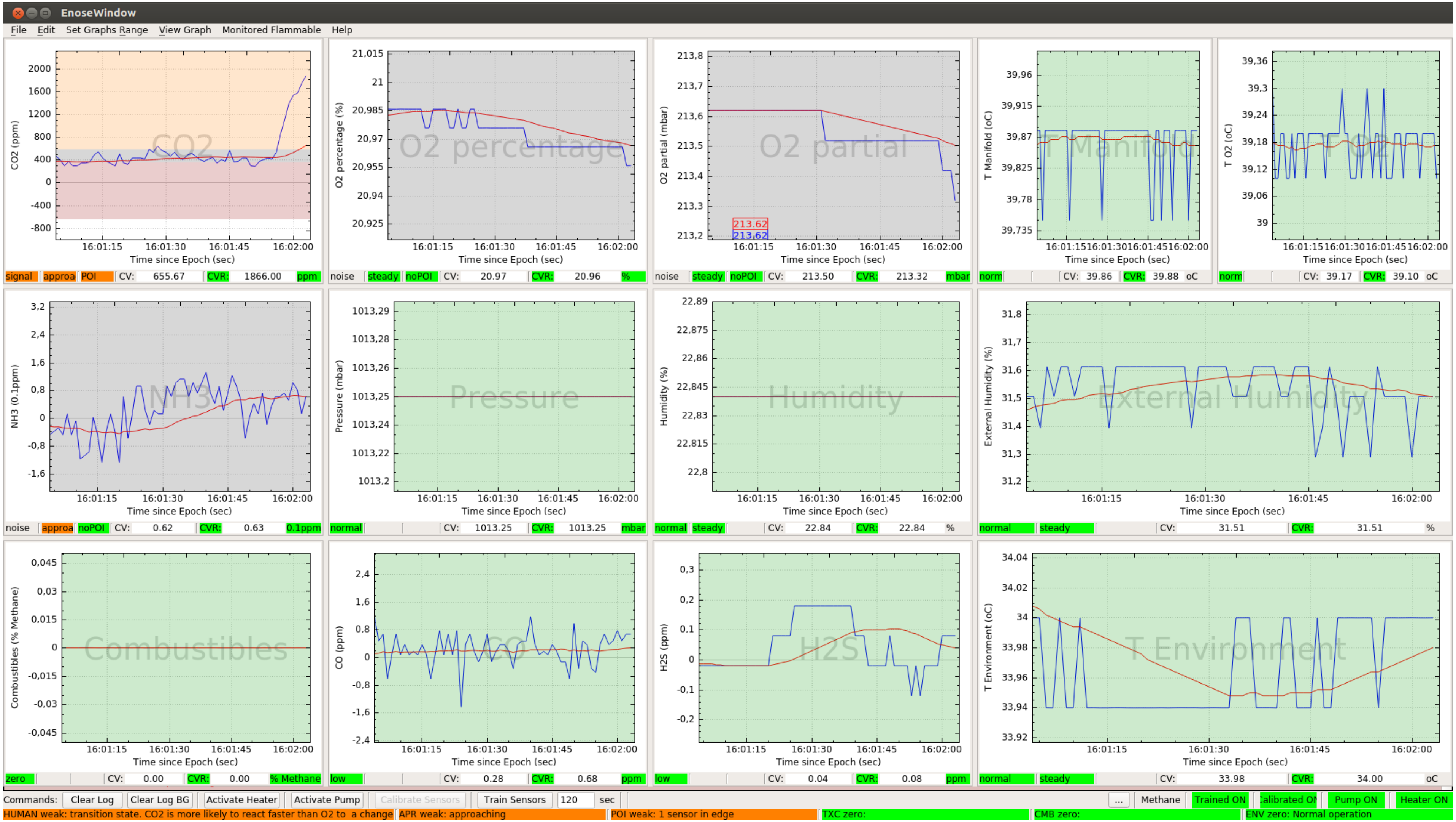
EnoseWindow
File Edit Set Graphs Range View Graph Monitored Flammable Help
CO2
CO2 (ppm)
2000
1600
1200
800
400
0
-400
-800
O2 percentage
O2 percentage (%)
21,015
21
20,985
20,97
20,955
20,94
20,925
O2 partial
O2 partial (mbar)
213,8
213,7
213,6
213,5
213,4
213,3
213,2
213.62
213.62
T Manifold
T Manifold (oC)
39,96
39,915
39,87
39,825
39,78
39,735
T O2
T O2 (oC)
39,36
39,3
39,24
39,18
39,12
39,06
39
NH3
NH3 (0.1ppm)
3,2
2,4
1,6
0,8
0
-0,8
-1,6
Pressure
Pressure (mbar)
1013,29
1013,28
1013,26
1013,25
1013,24
1013,22
1013,2
Humidity
Humidity (%)
22,89
22,875
22,86
22,845
22,83
22,815
22,8
External Humidity
External Humidity (%)
31,8
31,7
31,6
31,5
31,4
31,3
31,2
Combustibles
Combustibles (% Methane)
0,045
0,03
0,015
0
-0,015
-0,03
-0,045
CO
CO (ppm)
2,4
1,6
0,8
0
-0,8
-1,6
-2,4
H2S
H2S (ppm)
0,3
0,2
0,1
0
-0,1
-0,2
T Environment
T Environment (oC)
34,04
34,02
34
33,98
33,96
33,94
33,92
16:01:15
16:01:30
16:01:45
16:02:00
Time since Epoch (sec)
Commands:
Clear Log
Clear Log BG
Activate Heater
Activate Pump
Calibrate Sensors
Train Sensors
120
sec
...
Methane
Trained ON
Calibrated ON
Pump ON
Heater ON

signal approa POI CV: 655.67 CVR: 1866.00 ppm
noise steady noPOI CV: 20.97 CVR: 20.96 %
noise steady noPOI CV: 213.50 CVR: 213.32 mbar
norm CV: 39.86 CVR: 39.88 oC
norm CV: 39.17 CVR: 39.10 oC
noise approa noPOI CV: 0.62 CVR: 0.63 0.1ppm
normal CV: 1013.25 CVR: 1013.25 mbar
normal steady CV: 22.84 CVR: 22.84 %
normal steady CV: 31.51 CVR: 31.51 %
zero CV: 0.00 CVR: 0.00 % Methane
low CV: 0.28 CVR: 0.68 ppm
low CV: 0.04 CVR: 0.08 ppm
normal steady CV: 33.98 CVR: 34.00 oC

HUMAN weak: transition state. CO2 is more likely to react faster than O2 to a change
APR weak: approaching
POI weak: 1 sensor in edge
TXC zero:
CMB zero:
ENV zero: Normal operation

Figure 183. Case (2). Continuing to sample from inside the survival space. A weak Human presence is triggered.

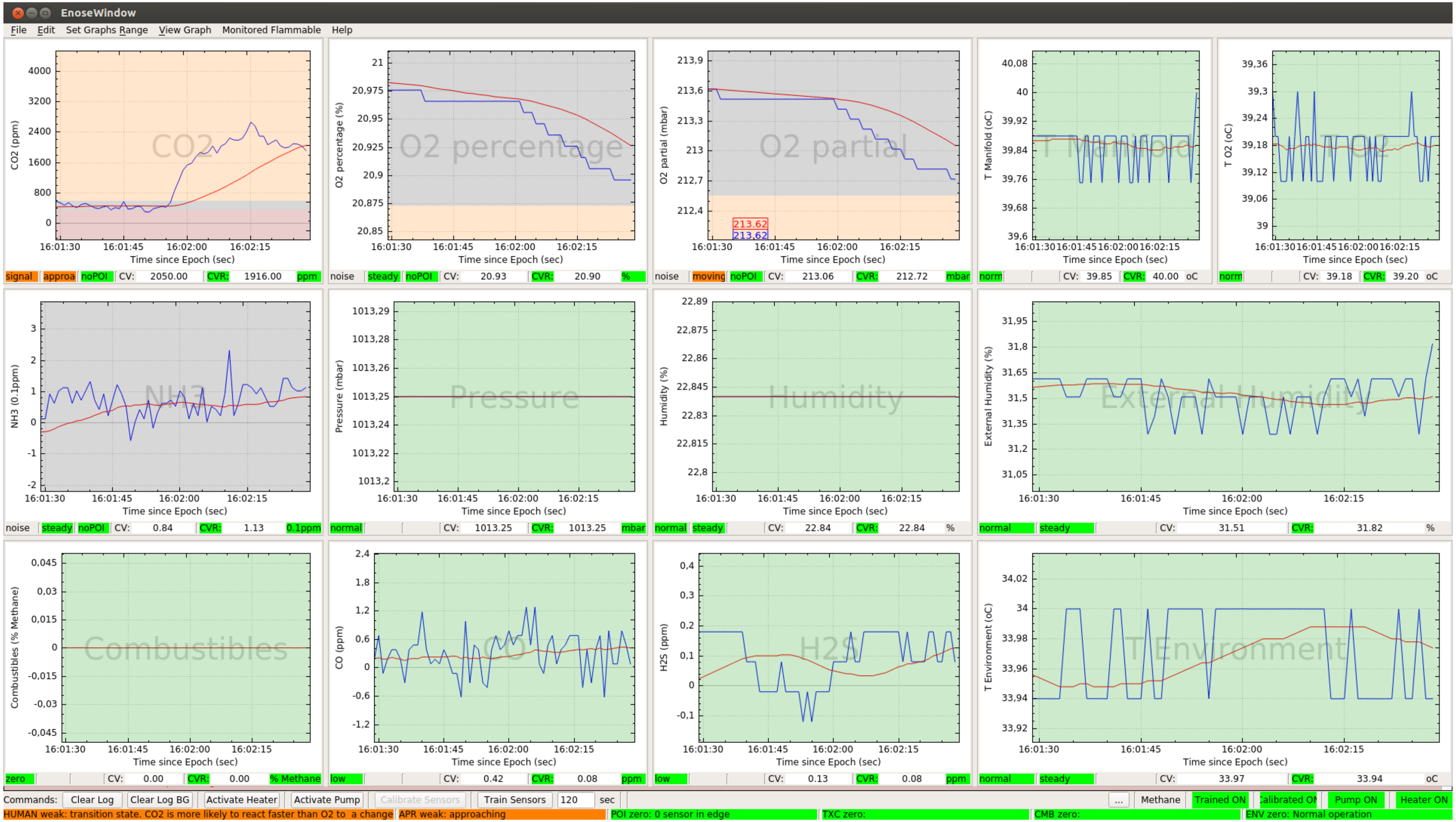
EnoseWindow
File
Edit
Set Graphs Range
View Graph
Monitored Flammable
Help
CO2
CO2 (ppm)
O2 percentage
O2 percentage (%)
O2 partial
O2 partial (mbar)
213.62
213.62
T Manifold
T Manifold (oC)
T O2
T O2 (oC)
NH3
NH3 (0.1ppm)
Pressure
Pressure (mbar)
Humidity
Humidity (%)
External Humidity
External Humidity (%)
Combustibles
Combustibles (% Methane)
CO
CO (ppm)
H2S
H2S (ppm)
T Environment
T Environment (oC)
16:01:30
16:01:45
16:02:00
16:02:15
Time since Epoch (sec)
Commands:
Clear Log
Clear Log BG
Activate Heater
Activate Pump
Calibrate Sensors
Train Sensors
120
sec
...
Methane
Trained ON
Calibrated ON
Pump ON
Heater ON

signal | approa | noPOI | CV: 2050.00 | CVR: 1916.00 ppm

noise | steady | noPOI | CV: 20.93 | CVR: 20.90 %

noise | moving | noPOI | CV: 213.06 | CVR: 212.72 mbar

norm | CV: 39.85 | CVR: 40.00 oC

norm | CV: 39.18 | CVR: 39.20 oC

noise | steady | noPOI | CV: 0.84 | CVR: 1.13 0.1ppm

normal | CV: 1013.25 | CVR: 1013.25 mbar

normal | steady | CV: 22.84 | CVR: 22.84 %

normal | steady | CV: 31.51 | CVR: 31.82 %

zero | CV: 0.00 | CVR: 0.00 % Methane

low | CV: 0.42 | CVR: 0.08 ppm

low | CV: 0.13 | CVR: 0.08 ppm

normal | steady | CV: 33.97 | CVR: 33.94 oC

HUMAN weak: transition state. CO2 is more likely to react faster than O2 to a change | APR weak: approaching | POI zero: 0 sensor in edge | TXC zero: | CMB zero: | ENV zero: Normal operation

Figure 184. Case (2). Sampling inside the survival space. Human presence indicator is still weak but the O_2 sensor is converging. This maintains the Approaching indicator

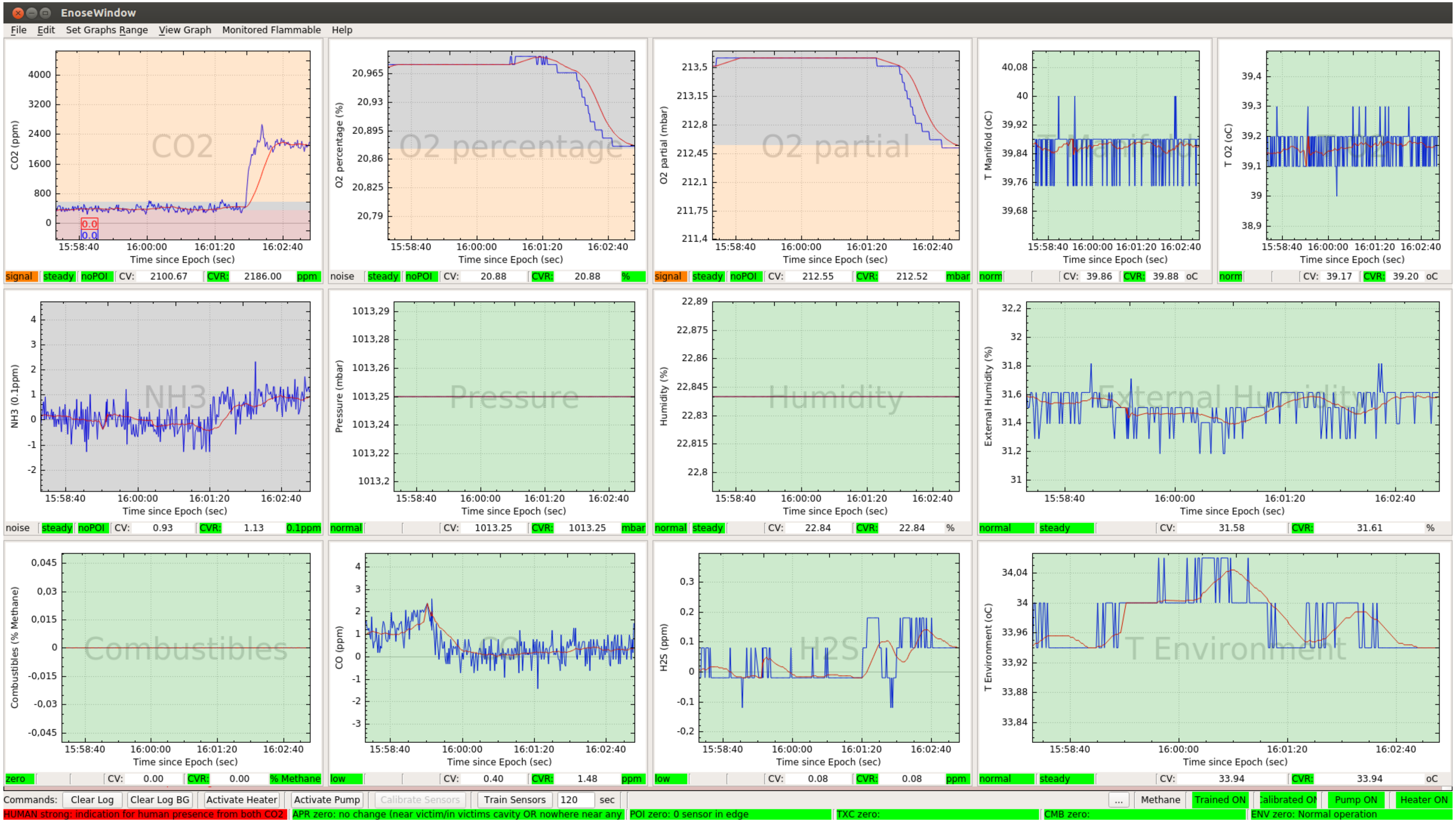
EnoseWindow
File
Edit
Set Graphs Range
View Graph
Monitored Flammable
Help
CO2
CO2 (ppm)
O2 percentage
O2 percentage (%)
O2 partial
O2 partial (mbar)
T Manifold (oC)
T O2 (oC)
NH3
NH3 (0.1ppm)
Pressure
Pressure (mbar)
Humidity
Humidity (%)
External Humidity
External Humidity (%)
Combustibles
Combustibles (% Methane)
CO (ppm)
H2S
H2S (ppm)
T Environment
T Environment (oC)
15:58:40
16:00:00
16:01:20
16:02:40
Time since Epoch (sec)
Commands:
Clear Log
Clear Log BG
Activate Heater
Activate Pump
Calibrate Sensors
Train Sensors
sec
...
Methane
Trained ON
Calibrated ON
Pump ON
Heater ON

CO2: signal | steady | noPOI | CV: 2100.67 | CVR: 2186.00 ppm
O2 percentage: noise | steady | noPOI | CV: 20.88 | CVR: 20.88 %
O2 partial: signal | steady | noPOI | CV: 212.55 | CVR: 212.52 mbar
T Manifold: norm | CV: 39.86 | CVR: 39.88 oC
T O2: norm | CV: 39.17 | CVR: 39.20 oC
NH3: noise | steady | noPOI | CV: 0.93 | CVR: 1.13 0.1ppm
Pressure: normal | CV: 1013.25 | CVR: 1013.25 mbar
Humidity: normal | steady | CV: 22.84 | CVR: 22.84 %
External Humidity: normal | steady | CV: 31.58 | CVR: 31.61 %
Combustibles: zero | CV: 0.00 | CVR: 0.00 % Methane
CO: low | CV: 0.40 | CVR: 1.48 ppm
H2S: low | CV: 0.08 | CVR: 0.08 ppm
T Environment: normal | steady | CV: 33.94 | CVR: 33.94 oC

Train Sensors 120 sec

HUMAN strong: indication for human presence from both CO2
APR zero: no change (near victim/in victims cavity OR nowhere near any
POI zero: 0 sensor in edge
TXC zero:
CMB zero:
ENV zero: Normal operation

Figure 185. Case (2). With the sampling tube inside the survival space, a strong Human presence indicator is triggered.

The following pictures illustrate the detection of hazardous conditions of case (3) to case (7).

In Figure 186, case (3) is illustrated. The e-nose sampling tube was inserted in a sample bottle that contained a mixture with H_2S and was removed after about 10 seconds. The timeframe of the plots was set to 5 minutes. The main plot of interest is that of H_2S. A strong (global) Toxic indicator was triggered driven by the H_2S sensor (individual) toxic indicator. A small increase in the measured NH_3 concentration can be observed which could be attributed to cross-sensitivity of the sensor, or that there was an actual presence of NH_3 in the sample mixture –stink ampoule. A small decrease of the O_2 concentration measurement with a small increase of the CO_2 can also be observed which caused the triggering of the (global) Human presence indicator and associated (global) Point of Interest and (global) Approaching indicators. This condition is not detrimental for the e-nose functionality. It is desirable to have knowledge of potential false positives which can be provided with this configuration. A solution for resuming the search for human presence signs in a space with a hazardous condition would be to retrain the e-nose in that space in order to recalculate the signal thresholds considering the background concentrations as noise. This strategy allows the continuation of the search for signs of human presence, but with a reduced “sensitivity”.

In Figure 187, case (4) is illustrated. The e-nose sampling tube was placed over the nozzle of a cigarette lighter that provided gas for about 10 seconds. The timeframe of the plots was set to 5 minutes. The main plot of interest is that of Combustibles. A strong (global) Combustibles indicator was triggered driven by the Combustibles, (individual) indicator. The Combustibles indicator was configured to monitor for the 10% Lower Explosive Limits LEL of methane. A small decrease of the O_2 concentration measurement with a small increase of the CO_2 can also be observed which caused the triggering of the (global) Human presence indicator and associated (global) Point of interest and (global) Approaching indicators. This condition is not detrimental for the e-nose functionality. It is desirable to have knowledge of potential false positives which can be provided with this configuration. A solution for resuming the search for human presence signs in a space with a hazardous condition would be to retrain the e-nose in that space in order to recalculate the signal thresholds considering the background concentrations as noise. This strategy allows the continuation of the search for signs of human presence but with a reduced “sensitivity”.

In Figure 188, case (5) is illustrated. The e-nose sampling tube input is blocked with a fingertip for about 20 seconds in order to simulate filter blockage. The timeframe of the plots was set to 5 minutes. The main plot of interest is that of pressure. A strong (global) Malfunction status indicator is triggered driven by the low pressure reading of the O_2 pressure sensor. With this state, the e-nose output cannot be considered valid. No remote action can be performed to rectify this issue. The e-nose filters have to be changed to restore proper operation.

In Figure 189, Case (6) is illustrated. The e-nose sampling tube was placed in front of a person’s mouth when exhaling, for about 20 seconds. The timeframe of the plots was set to 5 minutes. The main plots of interest are those of O_2 and CO_2. A strong (global) Toxic indicator is triggered driven by the hazardous levels of CO_2 that triggered its (individual) Toxic indicator. The (global) Human, Approaching and Point of interest indicators are also correctly triggered.

In Figure 190, case (7) is illustrated. The e-nose sampling tube was placed in front of a person’s mouth when exhaling cigarette smoke for about 10 seconds. The timeframe of the plots was set to 5 minutes. The main plots of interest are those of CO, CO_2 and O_2. A strong (global) Toxic indicator is triggered driven by the hazardous levels of CO and CO_2 indicated by their (individual) Toxic indicators. The (global) Human, Approaching and Point of interest indicators are also correctly triggered. Unfortunately, the case where the high levels of CO_2 and low levels of O_2 are not caused by exhaled breath, but fire, cannot be distinguished when there is CO. Although this is not ideal, again the condition in which a false positive can be produced is detected which is very important. Table 68 summarizes the measurements and the ENALU output of the test scenario.

Table 68. Summary of detection results for cases 3-7.

Case #→ Output ↓	**Summary of detection results for cases 3-7**				
	Case 3	***Case 4***	***Case 5***	***Case 6***	***Case 7***
Detailed measurements	Figure 186	Figure 187	Figure 188	Figure 189	Figure 190
CO$_2$ (ppm)	632	975	574	10422	6769
O$_2$(%) [O$_2$](mbar)	20.77 [211.44]	20.88 [212.63]	21.04 [212.64]	20.42 [207.68]	20.53 [208.83]
NH$_3$ (0.1ppm)	7.9	0.91	0.90	1.2	0.51
CO (ppm)	1.02	0.47	0.06	4.29	59.58
H$_2$S (ppm)	8.68	0.01	0.06	0.38	0.38
Combust. (%)	0	0.77	0	0	0
Human indicator	Strong: indications	Weak: Transition state	Zero	Weak: High CO$_2$ low O$_2$	Weak: High CO$_2$ low O$_2$
Approaching indicator	Weak: moving away	Zero: Conflicting	Zero	Strong: Approaching	Strong: Approaching
Hot spot indicator	Weak	Weak	Zero	Weak	Strong
Toxic Indicator	Strong	Zero	Zero	Strong	Strong
Combust. Indicator	Zero	Strong	Zero	Zero	Zero
Status Indicator	Zero	Zero	Strong: Filter blocked	Zero	Zero

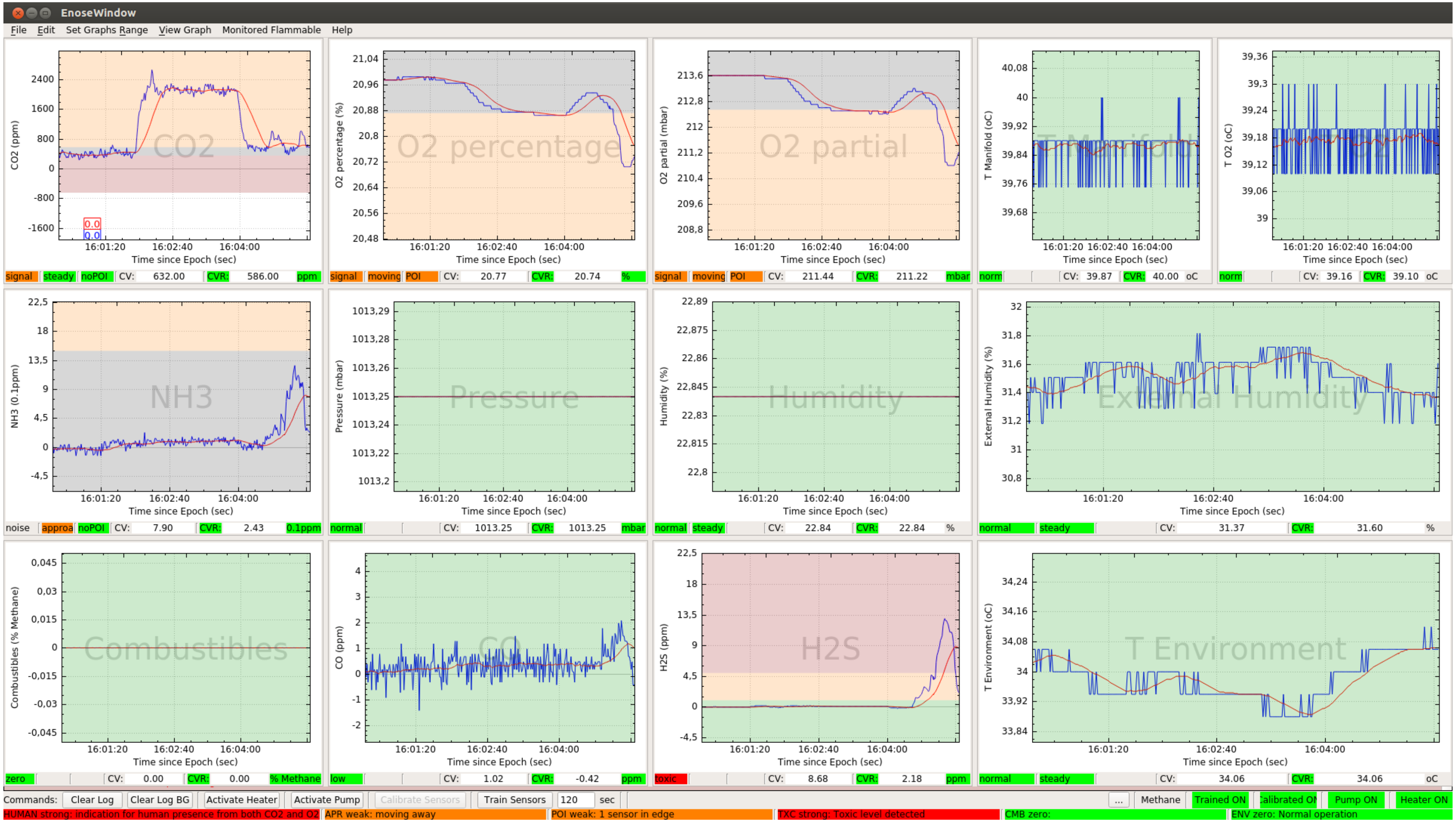
EnoseWindow
File Edit Set Graphs Range View Graph Monitored Flammable Help
CO2
CO2 (ppm)
O2 percentage
O2 percentage (%)
O2 partial
O2 partial (mbar)
T Manifold
T Manifold (oC)
T O2
T O2 (oC)
NH3
NH3 (0.1ppm)
Pressure
Pressure (mbar)
Humidity
Humidity (%)
External Humidity
External Humidity (%)
Combustibles
Combustibles (% Methane)
CO
CO (ppm)
H2S
H2S (ppm)
T Environment
T Environment (oC)
16:01:20 16:02:40 16:04:00
Time since Epoch (sec)
Commands: Clear Log Clear Log BG Activate Heater Activate Pump Calibrate Sensors Train Sensors 120 sec
... Methane Trained ON Calibrated ON Pump ON Heater ON

signal steady noPOI CV: 632.00 CVR: 586.00 ppm

signal moving POI CV: 20.77 CVR: 20.74 %

signal moving POI CV: 211.44 CVR: 211.22 mbar

norm CV: 39.87 CVR: 40.00 oC

norm CV: 39.16 CVR: 39.10 oC

noise approa noPOI CV: 7.90 CVR: 2.43 0.1ppm

normal CV: 1013.25 CVR: 1013.25 mbar

normal steady CV: 22.84 CVR: 22.84 %

normal steady CV: 31.37 CVR: 31.60 %

zero CV: 0.00 CVR: 0.00 % Methane

low CV: 1.02 CVR: -0.42 ppm

toxic CV: 8.68 CVR: 2.18 ppm

normal steady CV: 34.06 CVR: 34.06 oC

HUMAN strong: indication for human presence from both CO2 and O2

APR weak: moving away

POI weak: 1 sensor in edge

TXC strong: Toxic level detected

CMB zero:

ENV zero: Normal operation

Figure 186. Case (3). H_2S detection with the Toxic indicator being triggered.

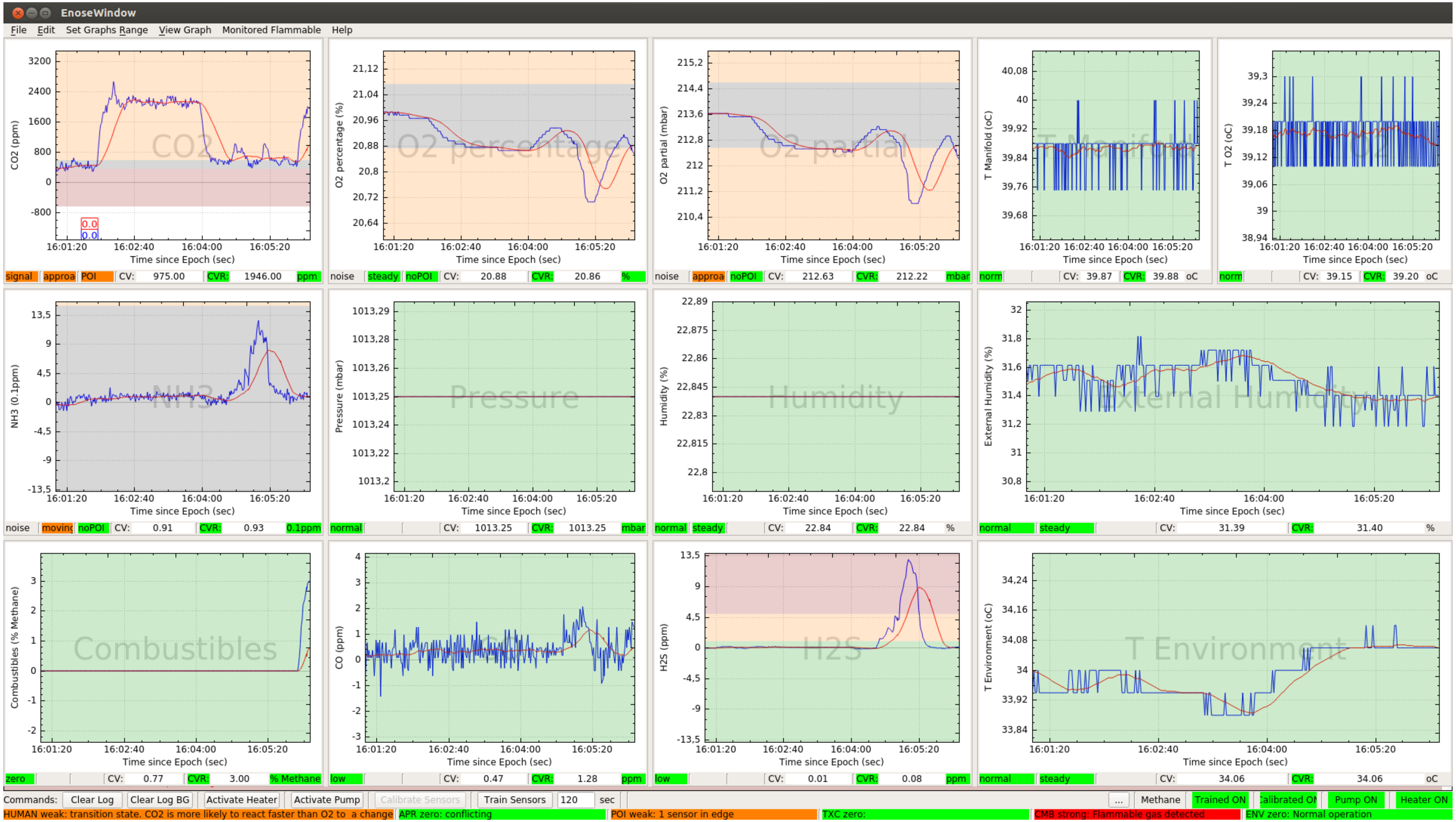
EnoseWindow
File Edit Set Graphs Range View Graph Monitored Flammable Help
CO2 (ppm)
3200
2400
1600
800
0
-800
0.0
0.0
CO2
O2 percentage (%)
21,12
21,04
20,96
20,88
20,8
20,72
20,64
O2 percentage
O2 partial (mbar)
215,2
214,4
213,6
212,8
212
211,2
210,4
O2 partial
T Manifold (oC)
40,08
40
39,92
39,84
39,76
39,68
T Manifold
T O2 (oC)
39,3
39,24
39,18
39,12
39,06
39
38,94
T O2
NH3 (0.1ppm)
13,5
9
4,5
0
-4,5
-9
-13,5
NH3
Pressure (mbar)
1013,29
1013,28
1013,26
1013,25
1013,24
1013,22
1013,2
Pressure
Humidity (%)
22,89
22,875
22,86
22,845
22,83
22,815
22,8
Humidity
External Humidity (%)
32
31,8
31,6
31,4
31,2
31
30,8
External Humidity
Combustibles (% Methane)
3
2
1
0
-1
-2
Combustibles
CO (ppm)
4
3
2
1
0
-1
-2
-3
CO
H2S (ppm)
13,5
9
4,5
0
-4,5
-9
-13,5
H2S
T Environment (oC)
34,24
34,16
34,08
34
33,92
33,84
T Environment
16:01:20
16:02:40
16:04:00
16:05:20
Time since Epoch (sec)
Commands:
Clear Log
Clear Log BG
Activate Heater
Activate Pump
Calibrate Sensors
Train Sensors
sec
...
Methane
Trained ON
Calibrated ON
Pump ON
Heater ON

signal | approa | POI | CV: 975.00 | CVR: 1946.00 | ppm

noise | steady | noPOI | CV: 20.88 | CVR: 20.86 | %

noise | approa | noPOI | CV: 212.63 | CVR: 212.22 | mbar

norm | CV: 39.87 | CVR: 39.88 | oC

norm | CV: 39.15 | CVR: 39.20 | oC

noise | moving | noPOI | CV: 0.91 | CVR: 0.93 | 0.1ppm

normal | CV: 1013.25 | CVR: 1013.25 | mbar

normal | steady | CV: 22.84 | CVR: 22.84 | %

normal | steady | CV: 31.39 | CVR: 31.40 | %

zero | CV: 0.77 | CVR: 3.00 | % Methane

low | CV: 0.47 | CVR: 1.28 | ppm

low | CV: 0.01 | CVR: 0.08 | ppm

normal | steady | CV: 34.06 | CVR: 34.06 | oC

Train Sensors: 120 sec

HUMAN weak: transition state. CO2 is more likely to react faster than O2 to a change

APR zero: conflicting

POI weak: 1 sensor in edge

TXC zero:

CMB strong: Flammable gas detected

ENV zero: Normal operation

Figure 187. Case (4). Combustible atmosphere detected, with the Combustibles indicator being triggered.

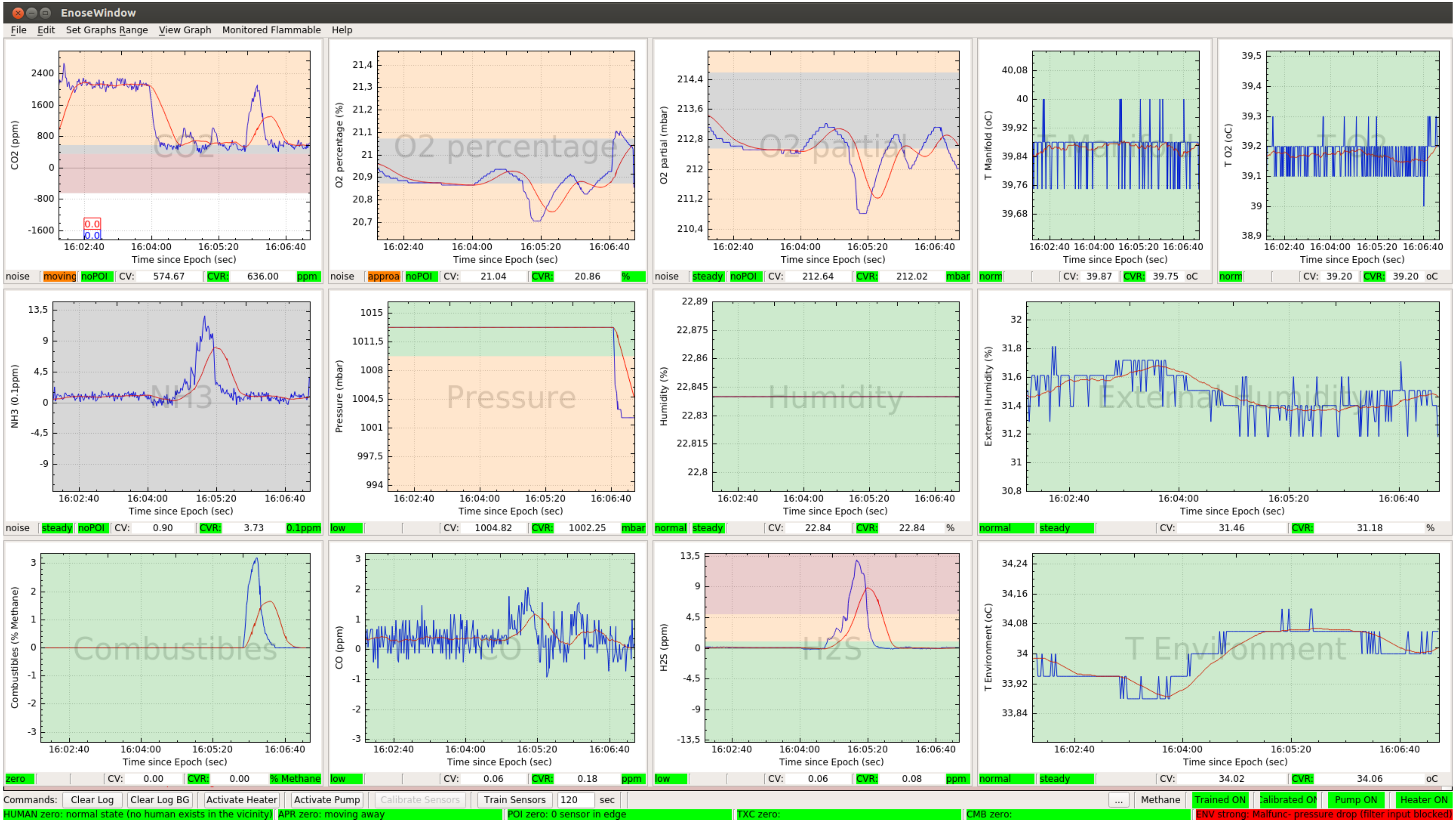
EnoseWindow
File Edit Set Graphs Range View Graph Monitored Flammable Help
CO2 (ppm)
2400
1600
800
0
-800
-1600
0.0
0.0
CO2
O2 percentage (%)
21,4
21,3
21,2
21,1
21
20,9
20,8
20,7
O2 percentage
O2 partial (mbar)
214,4
213,6
212,8
212
211,2
210,4
O2 partial
T Manifold (oC)
40,08
40
39,92
39,84
39,76
39,68
T Manifold
T O2 (oC)
39,5
39,4
39,3
39,2
39,1
39
38,9
T O2
NH3 (0.1ppm)
13,5
9
4,5
0
-4,5
-9
NH3
Pressure (mbar)
1015
1011,5
1008
1004,5
1001
997,5
994
Pressure
Humidity (%)
22,89
22,875
22,86
22,845
22,83
22,815
22,8
Humidity
External Humidity (%)
32
31,8
31,6
31,4
31,2
31
30,8
External Humidity
Combustibles (% Methane)
3
2
1
0
-1
-2
-3
Combustibles
CO (ppm)
3
2
1
0
-1
-2
-3
CO
H2S (ppm)
13,5
9
4,5
0
-4,5
-9
-13,5
H2S
T Environment (oC)
34,24
34,16
34,08
34
33,92
33,84
T Environment
16:02:40
16:04:00
16:05:20
16:06:40
Time since Epoch (sec)
Commands: Clear Log Clear Log BG Activate Heater Activate Pump Calibrate Sensors Train Sensors
120 sec
...
Methane
Trained ON
Calibrated ON
Pump ON
Heater ON

```
noise  moving  noPOI  CV:  574.67  CVR:  636.00  ppm
noise  approa  noPOI  CV:  21.04  CVR:  20.86  %
noise  steady  noPOI  CV:  212.64  CVR:  212.02  mbar
norm  CV:  39.87  CVR:  39.75  oC
norm  CV:  39.20  CVR:  39.20  oC
noise  steady  noPOI  CV:  0.90  CVR:  3.73  0.1ppm
low  CV:  1004.82  CVR:  1002.25  mbar
normal  steady  CV:  22.84  CVR:  22.84  %
normal  steady  CV:  31.46  CVR:  31.18  %
zero  CV:  0.00  CVR:  0.00  % Methane
low  CV:  0.06  CVR:  0.18  ppm
low  CV:  0.06  CVR:  0.08  ppm
normal  steady  CV:  34.02  CVR:  34.06  oC
HUMAN zero: normal state (no human exists in the vicinity)
APR zero: moving away
POI zero: 0 sensor in edge
TXC zero:
CMB zero:
ENV strong: Malfunc- pressure drop (filter input blocked)
```

Figure 188. Case (5). Air input sampling/Filter blockage detection with an error status indicator being triggered.

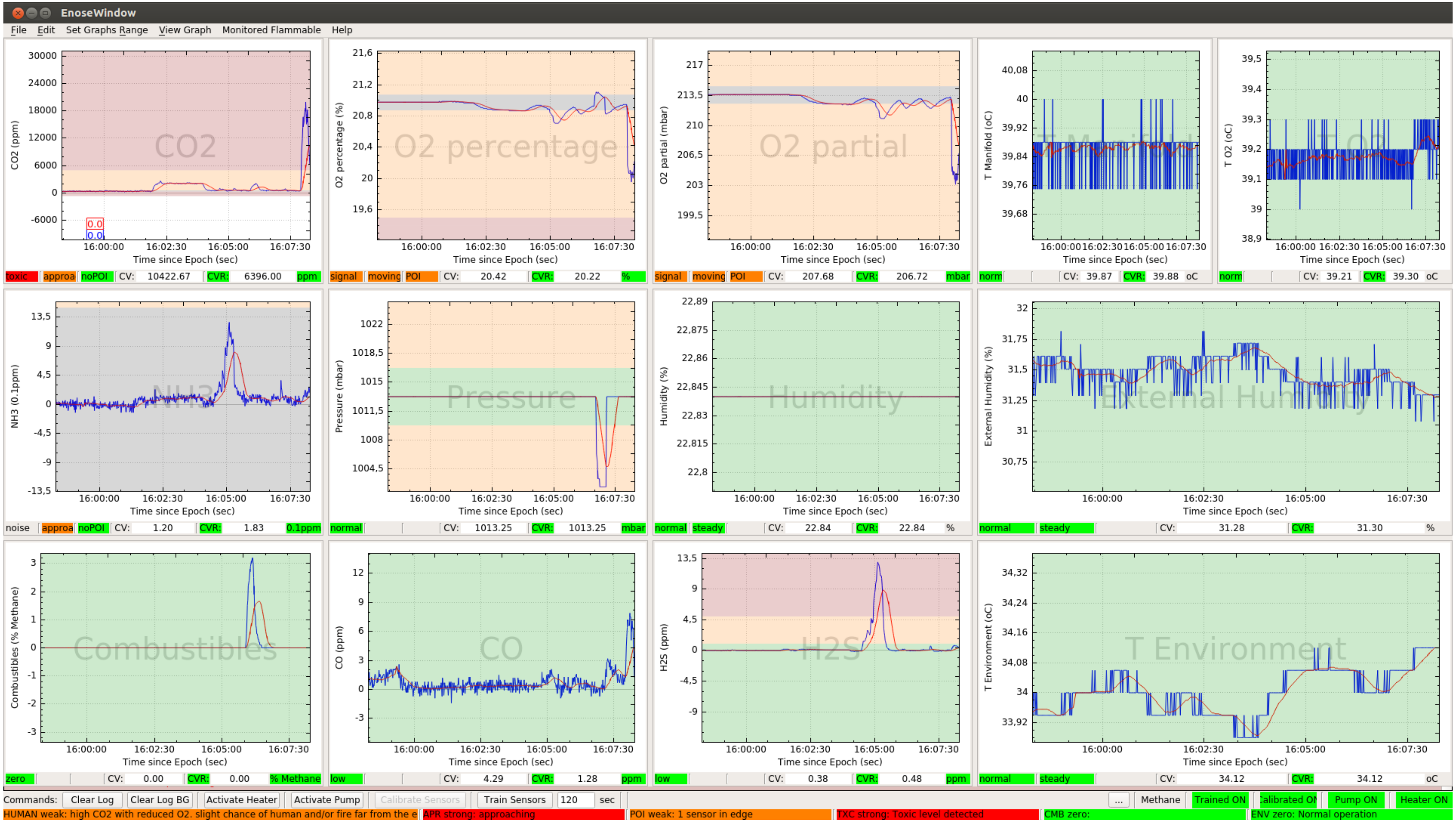
EnoseWindow
File
Edit
Set Graphs Range
View Graph
Monitored Flammable
Help
CO2
CO2 (ppm)
30000
24000
18000
12000
6000
0
-6000
0.0
0.0
O2 percentage
O2 percentage (%)
21,6
21,2
20,8
20,4
20
19,6
O2 partial
O2 partial (mbar)
217
213,5
210
206,5
203
199,5
T Manifold
T Manifold (oC)
40,08
40
39,92
39,84
39,76
39,68
T O2
T O2 (oC)
39,5
39,4
39,3
39,2
39,1
39
38,9
NH3
NH3 (0.1ppm)
13,5
9
4,5
0
-4,5
-9
-13,5
Pressure
Pressure (mbar)
1022
1018,5
1015
1011,5
1008
1004,5
Humidity
Humidity (%)
22,89
22,875
22,86
22,845
22,83
22,815
22,8
External Humidity
External Humidity (%)
32
31,75
31,5
31,25
31
30,75
Combustibles
Combustibles (% Methane)
3
2
1
0
-1
-2
-3
CO
CO (ppm)
12
9
6
3
0
-3
H2S
H2S (ppm)
13,5
9
4,5
0
-4,5
-9
T Environment
T Environment (oC)
34,32
34,24
34,16
34,08
34
33,92
16:00:00
16:02:30
16:05:00
16:07:30
Time since Epoch (sec)
Commands:
Clear Log
Clear Log BG
Activate Heater
Activate Pump
Calibrate Sensors
Train Sensors
sec
...
Methane
Trained ON
:alibrated ON
Pump ON
Heater ON

toxic | approa | noPOI | CV: 10422.67 | CVR: 6396.00 | ppm
signal | moving | POI | CV: 20.42 | CVR: 20.22 | %
signal | moving | POI | CV: 207.68 | CVR: 206.72 | mbar
norm | CV: 39.87 | CVR: 39.88 | oC
norm | CV: 39.21 | CVR: 39.30 | oC
noise | approa | noPOI | CV: 1.20 | CVR: 1.83 | 0.1ppm
normal | CV: 1013.25 | CVR: 1013.25 | mbar
normal | steady | CV: 22.84 | CVR: 22.84 | %
normal | steady | CV: 31.28 | CVR: 31.30 | %
zero | CV: 0.00 | CVR: 0.00 | % Methane
low | CV: 4.29 | CVR: 1.28 | ppm
low | CV: 0.38 | CVR: 0.48 | ppm
normal | steady | CV: 34.12 | CVR: 34.12 | oC

Train Sensors: 120 sec

HUMAN weak: high CO2 with reduced O2. slight chance of human and/or fire far from the e
APR strong: approaching
POI weak: 1 sensor in edge
TXC strong: Toxic level detected
CMB zero:
ENV zero: Normal operation

Figure 189. Case (6). A Toxic indicator being triggered by high levels of CO₂ from undiluted exhaled breath.

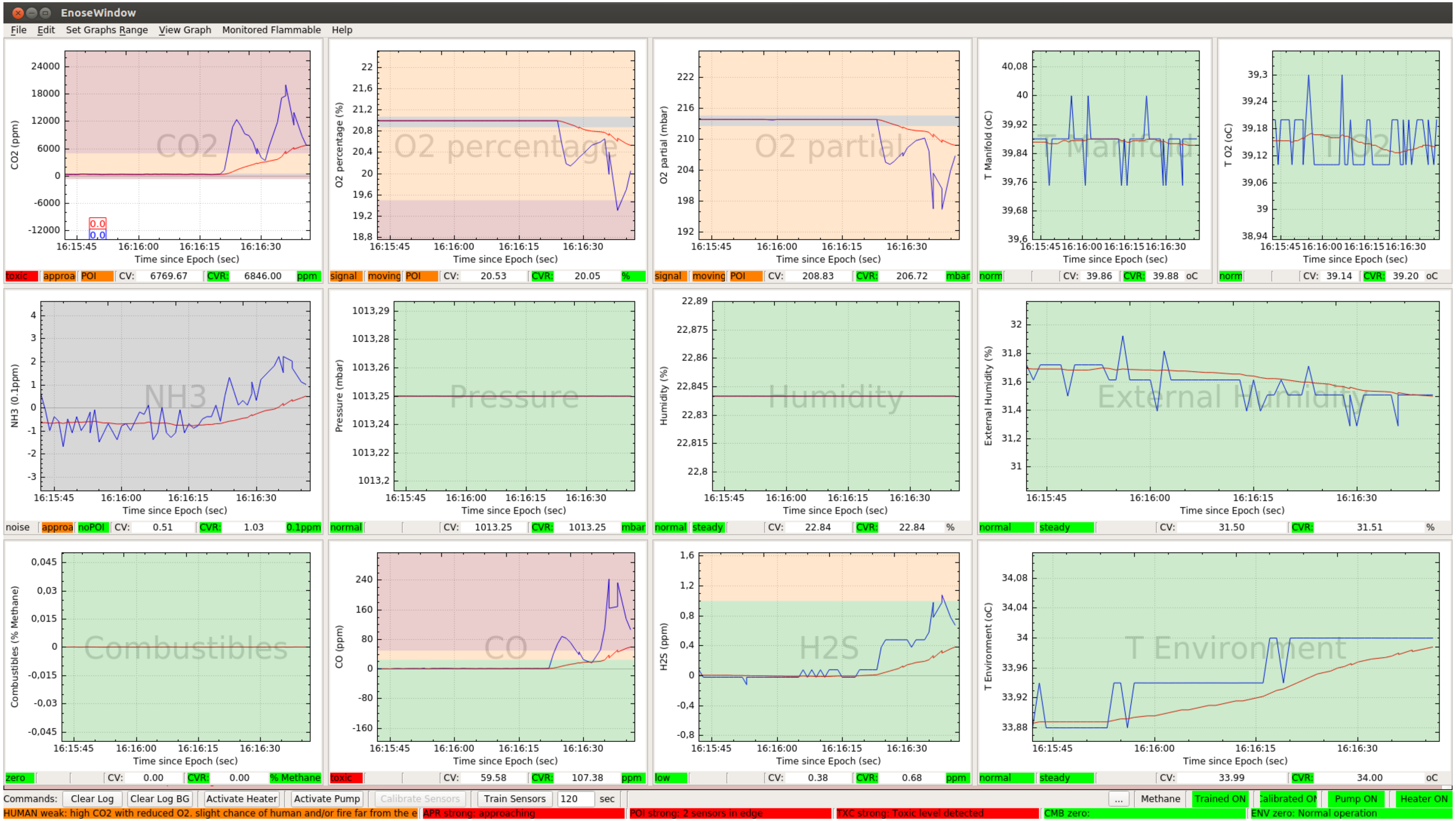
EnoseWindow
File
Edit
Set Graphs Range
View Graph
Monitored Flammable
Help
CO2
CO2 (ppm)
24000
18000
12000
6000
0
-6000
-12000
0.0
0.0
O2 percentage
O2 percentage (%)
22
21,6
21,2
20,8
20,4
20
19,6
19,2
18,8
O2 partial
O2 partial (mbar)
222
216
210
204
198
192
T Manifold
T Manifold (oC)
40,08
40
39,92
39,84
39,76
39,68
39,6
T O2
T O2 (oC)
39,3
39,24
39,18
39,12
39,06
39
38,94
NH3
NH3 (0.1ppm)
4
3
2
1
0
-1
-2
-3
Pressure
Pressure (mbar)
1013,29
1013,28
1013,26
1013,25
1013,24
1013,22
1013,2
Humidity
Humidity (%)
22,89
22,875
22,86
22,845
22,83
22,815
22,8
External Humidity
External Humidity (%)
32
31,8
31,6
31,4
31,2
31
Combustibles
Combustibles (% Methane)
0,045
0,03
0,015
0
-0,015
-0,03
-0,045
CO
CO (ppm)
240
160
80
0
-80
-160
H2S
H2S (ppm)
1,6
1,2
0,8
0,4
0
-0,4
-0,8
T Environment
T Environment (oC)
34,08
34,04
34
33,96
33,92
33,88
16:15:45
16:16:00
16:16:15
16:16:30
Time since Epoch (sec)
Commands:
Clear Log
Clear Log BG
Activate Heater
Activate Pump
Calibrate Sensors
Train Sensors
sec
...
Methane
Trained ON
:alibrated ON
Pump ON
Heater ON

toxic | approa | POI | CV: 6769.67 | CVR: 6846.00 | ppm
signal | moving | POI | CV: 20.53 | CVR: 20.05 | %
signal | moving | POI | CV: 208.83 | CVR: 206.72 | mbar
norm | CV: 39.86 | CVR: 39.88 | oC
norm | CV: 39.14 | CVR: 39.20 | oC
noise | approa | noPOI | CV: 0.51 | CVR: 1.03 | 0.1ppm
normal | CV: 1013.25 | CVR: 1013.25 | mbar
normal | steady | CV: 22.84 | CVR: 22.84 | %
normal | steady | CV: 31.50 | CVR: 31.51 | %
zero | CV: 0.00 | CVR: 0.00 | % Methane
toxic | CV: 59.58 | CVR: 107.38 | ppm
low | CV: 0.38 | CVR: 0.68 | ppm
normal | steady | CV: 33.99 | CVR: 34.00 | oC

Train Sensors 120 sec

HUMAN weak: high CO2 with reduced O2. slight chance of human and/or fire far from the e
APR strong: approaching
POI strong: 2 sensors in edge
TXC strong: Toxic level detected
CMB zero:
ENV zero: Normal operation

Figure 190. Case (7). Toxic indicator triggered from CO gas originating from exhaled cigarette smoke.

Conclusions

The e-nose system was tested in near real conditions with actual human (controlled) entrapment. The e-nose system was successful in detecting signs of human presence. The e-nose device operated successfully without any malfunctions or loss of performance in an outdoor environment for at least 2 full working days. The heuristic algorithm for generating (global) indicators performed well. The e-nose user interface was essential in verifying and validating the aforementioned research goals. A number of different end-users from different countries and with different roles and backgrounds were also present during some of the tests and demonstrations of the e-nose. Most of them were able to understand the instructions given regarding the interface and the location of the key information. They were convinced of the functionality of the e-nose regarding its victim localization capabilities and also its hazardous detection capabilities. Some users commented on the complexity of the interface that presents the output of the e-nose. Experienced end-users specifically trained in operating under the rubble and proficient in using gas detectors and other assistive technologies clearly understood the benefits of using this e-nose system. They even comprehended the more complicated aspects of the information presented on the interface. The research goal to generate simple outputs and a good interface was achieved. Another very important outcome from the interaction with the end-users during the live demonstrations was the understanding, from our side, of the importance of training and relevant training material. Although training cards were handed out during the demonstration, there was not enough time for the information to "sink in". Users already familiar with similar technologies focused on the extra capabilities and functionality available. As with any technology and tool, proper training is required to understand the principles of operation, capabilities, and limitations in order to maximize the potential benefits.

8.8. Third field tests P4 – Final Validation

The e-nose system was tested in a field test that took place in Roquebillière France at a temporary USaR training location. The following figure illustrates the location.

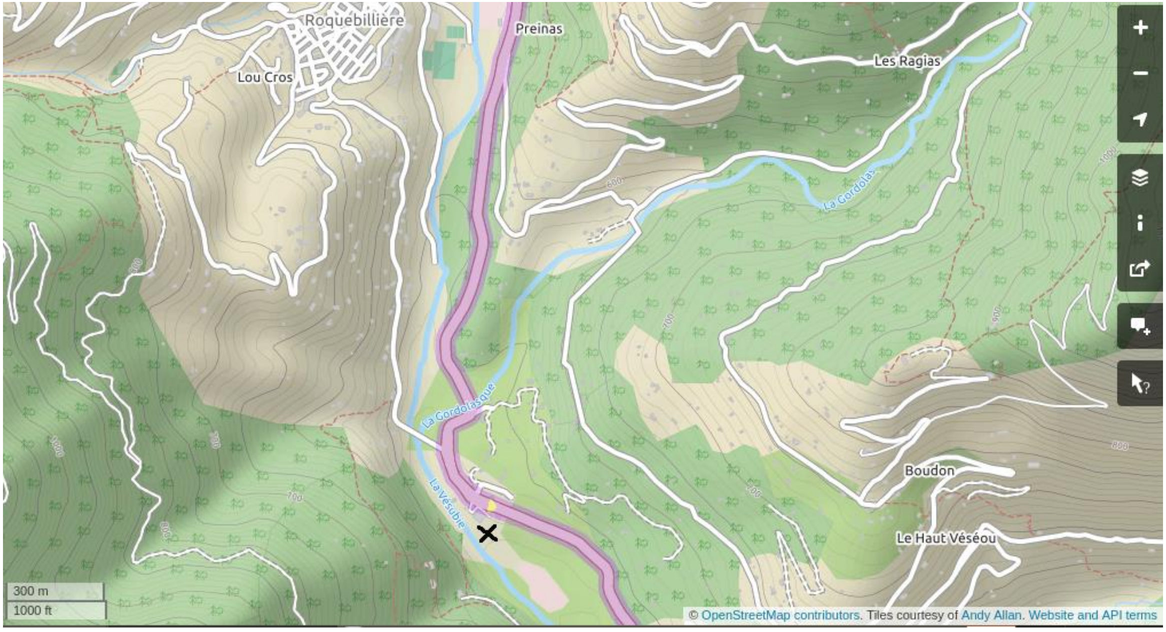

© OpenStreetMap contributors. Tiles courtesy of Andy Allan. Website and API terms

Figure 191. The location of the training site – Gordolon Worksite marked with a black X on the bottom centre of the map.

Here the system was tested as part of the sensor payload of a robotic platform. In this work, only the detection and results presentation aspects of the e-nose system are presented. The victim localization aspects were validated by searching for victims from inside/under the surface of the rubble pile. The field test location (worksite) was near the riverbed which is between two hillsides as can be seen on the map of Figure 191. The field test took place during a mildly cold and very humid day. The e-nose tests started in the morning and were performed until the afternoon. There was a mild, but constant, south – south east wind flowing at the test site and the temperature was not more than 10^{o}C. Figure 192 illustrates the test location with the picture taken with a south view orientation. The worksite has a number of rubble piles where various volunteer victims are hidden simulating entrapment. On the bottom right, the e-nose mounted on the robotic platform is halfway inside the rubble pile while the victim is located in the rubble pile seen on the bottom left.

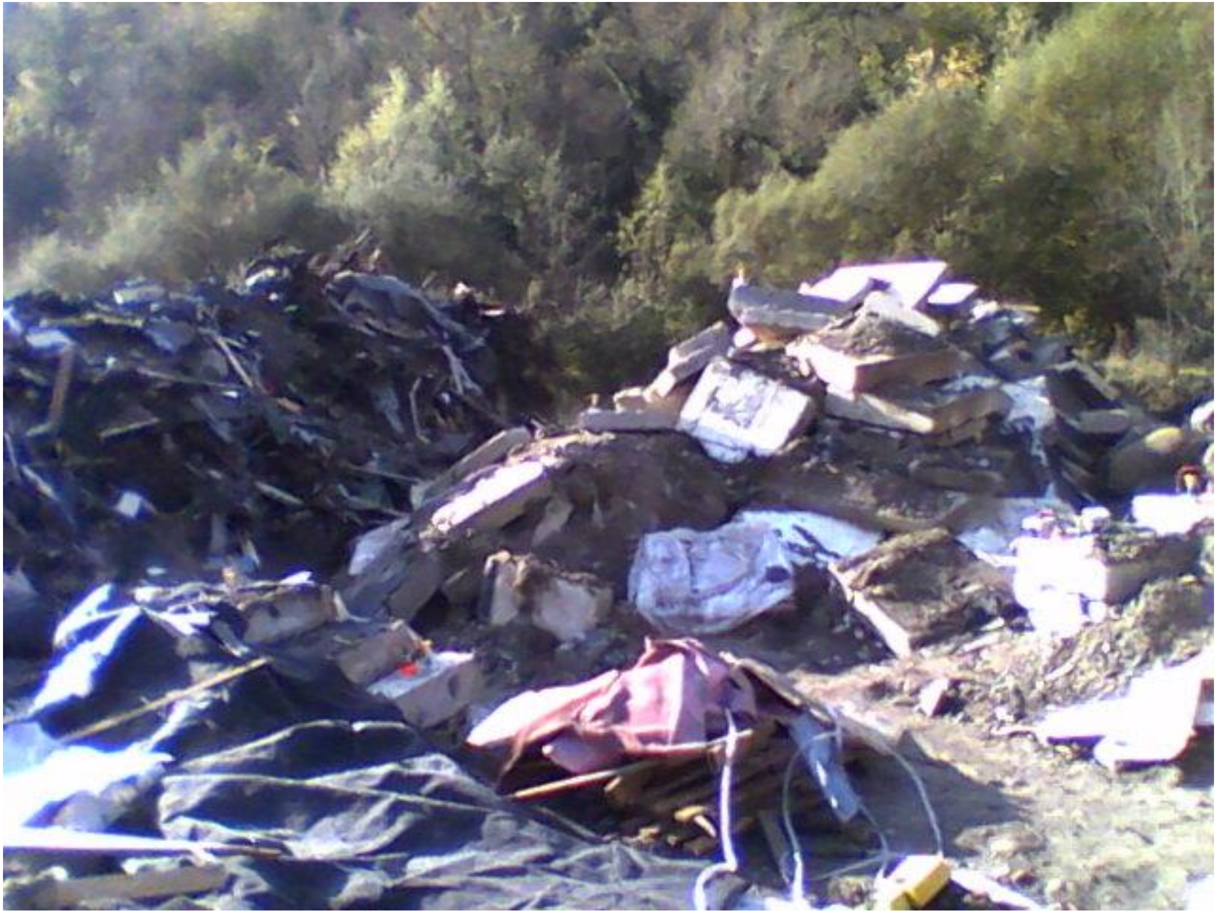

Figure 192. The test location with various rubble piles with hidden “survivors”. On the bottom right, the robotic platform is entering the rubble with a goal of reaching the area seen on the bottom left.

A better view of the robotic platform while entering the rubble pile can be seen in Figure 193. In this figure, the e-nose is on the middle compartment of the e-nose. The two air interface ports can be distinguished on the visible side of the compartment. The 2 light yellow squares which include the air interface ports can be removed by unscrewing the 4 screws so that the air filters can be changed on site. The input port is the one closer to the front of the robotic platform. A tube can be inserted in the air input sampling interface to facilitate scanning from the surface before entering the rubble. During the demonstration, the robotic platform travelled under the rubble pile and reached the area near the victim.

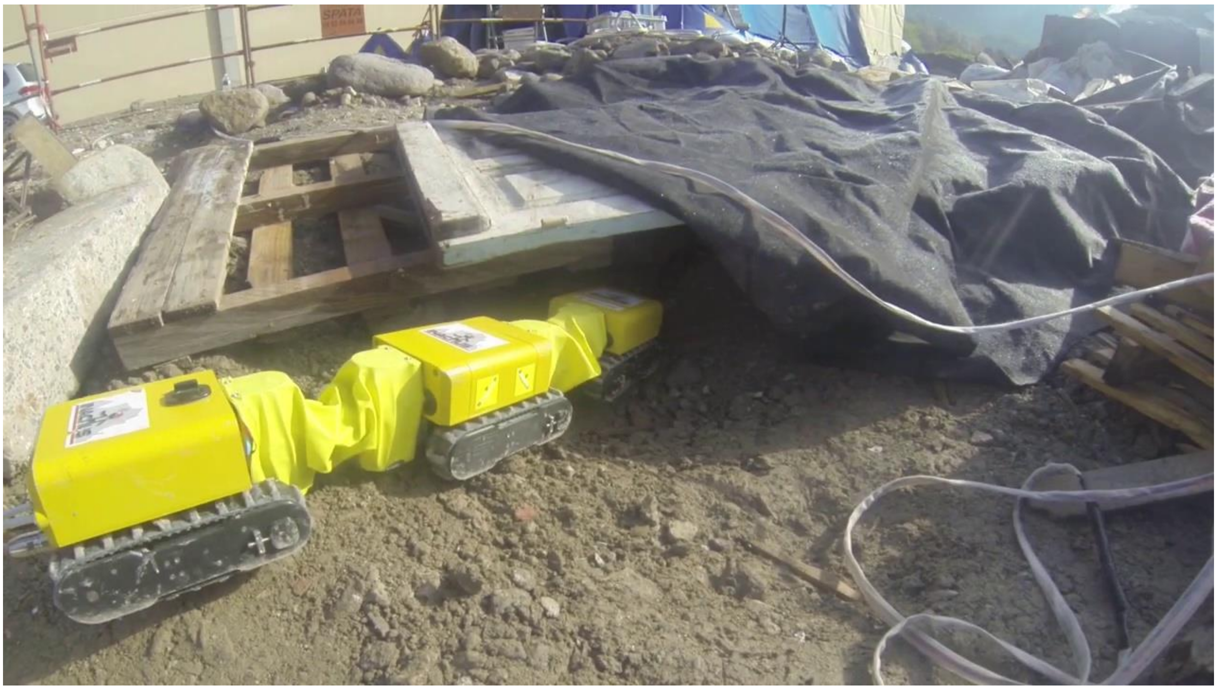

Figure 193. The search location. Entering the rubble pile, the e-nose is located on the central compartment. The air input and output interfaces can be distinguished on the side of the e-nose compartment.

The e-nose successfully indicated signs of human presence as can be see in Figure 194. In this picture, the e-nose Indicators have been integrated in the control interface of the robotic platform. The e-nose interface is located on the right side of the tablet. From top, where the finger is pointing, to the bottom, the following indicators can be distinguished on the e-nose section of the interface: Human indicator, Approaching indicator, Hot-spot indicator, Toxic indicator, Combustibles indicator, Status indicator. The Human presence indicator is red indicating strong signs of human presence. In this case the e-nose detection is also confirmed with the help of the (visible spectrum) camera seen on the centre of the interface and also by the infrared camera seen on the bottom right of the screen which detected the warmer face and hand of the victim. No confined space had its air converted or filled with a hazardous composition. For performing hazardous condition detection tests, sample gases were fed directly into the e-nose air input interface which was extended with a sampling tube.

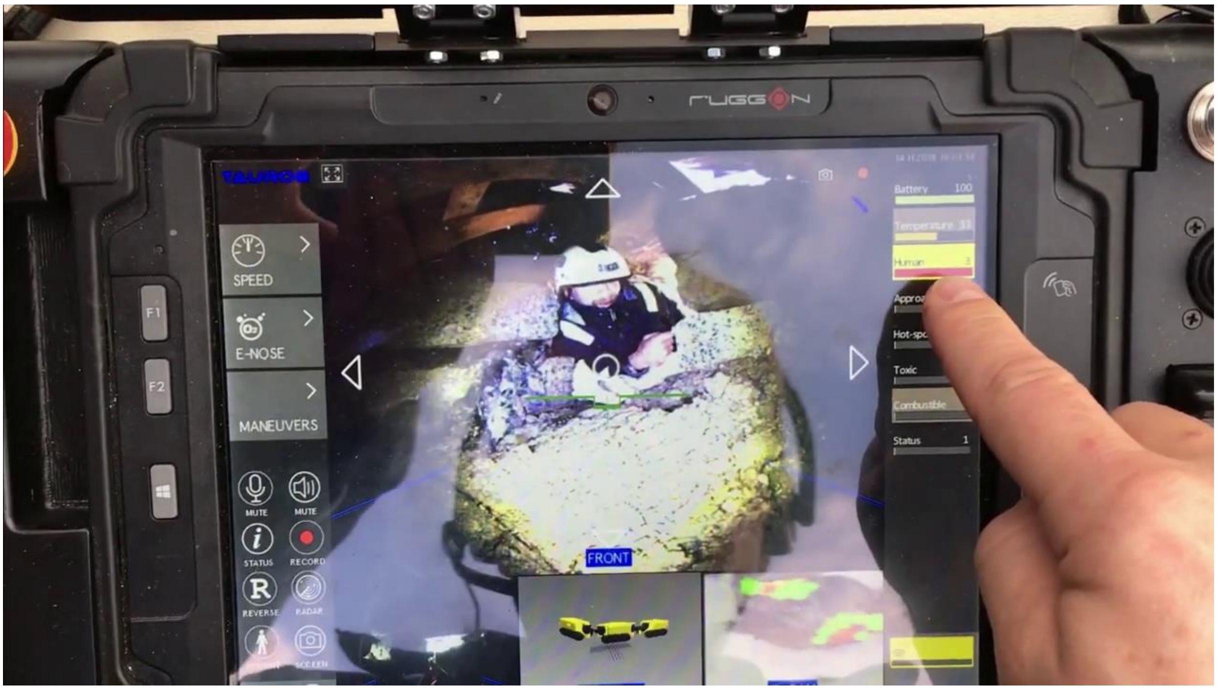
SPEED
E-NOSE
MANEUVERS
MUTE
MUTE
STATUS
RECORD
REVERSE
RADAR
SCREEN
F1
F2
Battery 100
Temperature 31
Human
Approa
Hot-spo
Toxic
Combustible
Status 1
FRONT

Figure 194. The robotic platform's control interface. On the right is the output of the e-nose, from top to bottom: Human indicator (red = strong indicator, person detected), Approaching indicator, Hot-spot indicator, Toxic indicator, Combustible indicator, Status indicator.

The detection of a combustible atmosphere was performed by placing a cigarette lighter in front of the sampling tube while the pump was sampling and pressing the gas release trigger without igniting it. The e-nose interface was capable of detecting this indicative hazardous atmosphere and the Combustibles indicator was triggered.

The detection of a poisonous atmosphere was performed by exhaling cigarette smoke in front of the sampling tube while the pump was sampling. The e-nose interface was capable of detecting this indicative hazardous atmosphere and the Toxic indicator was triggered. Figure 195 on the left illustrates the demonstrated scenario and Figure 195 on the right illustrates the interface output indicating the Toxic indicator. The Hot spot indicator was also activated. This is a correct output since two people were working over the sampling interface and the CO is included in exhaled breath.

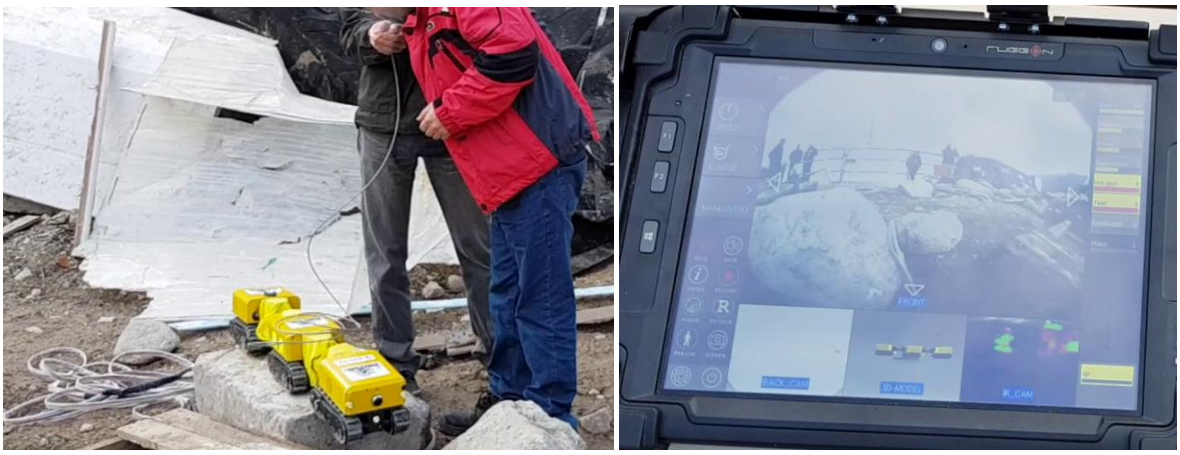
FRONT
BACK_CAM
3D MODEL
IR_CAM

Figure 195. Carbon monoxide detection test.

Human presence test scenario

The test and demonstration scenario had only one distinct case for victim localization under the rubble. It was orchestrated in such a way so that all sensor systems on the robotic platform could demonstrate their capabilities. This work focuses on the e-nose related test for human detection.

Measurements and description

Figure 196 illustrates the measurements of a complete human detection test and demonstration after its completion as seen in the development and testing e-nose interface. This interface was not demonstrated to the users during the field test. This interface is only used to show the detailed measurements and outputs that resulted in showing the output seen in Figure 194.

Table 69 summarizes the Global indicator states during the development of the scenario. The interface includes the measurement plots, the individual indicators, the current value, and the average value bellow each plot. On the bottom of the interface are the global indicators. For all plots, the most recent measurement is the rightmost value. Individual indicators are calculated based on the most recent data for the type of indicator. Global indicators are calculated based on the values of individual indicators at the current moment. For this human detection case, multiple interface plots are shown after this one in order to illustrate, as much as possible, the actual response of the system while being tested without “knowing/seeing” future measurements in an effort to recreate the operator’s experience during the test. The only outputs available to the operator of the robotic platform are the global indicators seen on the bottom. The first peak illustrated in the measurement plots is the application of the calibration parameters to the data. The second peak is the human detection event when the robot reached directly in front of the victim’s face and then was removed. Another peak is developing at the end as part of another test that followed, a combustible gas detection test which is not presented as it is similar to other tests already presented.

In Figure 197 the robotic platform has already entered the rubble and is moving toward the victim. The time frame of the measurement plots is 1 minute. The plots of interest are those of CO_2 and O_2. A weak (global) Approaching indicator is triggered driven by the (individual) Approaching indicators of the CO_2 and O_2 sensors.

In Figure 198 the robotic platform is getting closer to the victim. The time frame of the measurement plots is 1 minute. The plots of interest are those of CO_2 and O_2. A weak (global) Human presence indicator is triggered with the (global) Point of interest indicator. The Approaching (global) indicator is still in a weak state. The output of the Point of interest (global) indicator is driven by the fast response of the CO_2 sensor.

In Figure 199 the e-nose is close to the victim. The time frame of the measurement plots is 1 minute. The plots of interest are those of CO_2 and O_2. A strong Human (global) indicator is triggered driven by the newly triggered (individual) O_2 signal indicator and the existing CO_2 (individual) signal indicator. The Approaching (global) indicator remains at a weak approaching state while the Point of interest (global) indicator is zero.

In Figure 200 the e-nose has moved in front of the victim. The time frame of the measurement plots is 5 minutes. The plots of interest are those of CO_2 and O_2. A strong (global) Human presence indicator state is maintained driven by the O_2 and CO_2 individual indicator outputs. The Approaching indicator holds a zero state correctly indicating the e-nose being stationary in front of the victim while other sensor systems are being tested. The Point of interest global indicator was correctly not triggered because the movement of the robotic platform was relatively slow and the measurements did not change rapidly. From this point the e-nose is slowly moved away from the victim.

In Figure 201 the e-nose has moved away from the immediate vicinity of the victim. The time frame of the measurement plots is 1 minute. The plots of interest are those of CO_2 and O_2. A weak moving away (global) Approaching indicator is triggered by the CO_2 and O_2 sensors. The (global) Human presence indicator remains at a strong level.

In Figure 202 the e-nose is relatively far away from the vicinity of the victim. The time frame of the measurement plots is 1 minute. The plots of interest are those of CO_2 and O_2. The (global) Human indicator has transitioned to a weak state as the Approaching (global) indicator remains at a weak moving away state. Beyond this point, both Human and Approaching (global) indicators transition to a zero state after the e-nose exiting the rubble. Table 69 summarizes the measurements and the ENALU output of the test scenario.

Table 69. Summary of victim detection results when inside an occupied confined space.

Location→ Output ↓	**Summary of victim detection results when inside an occupied confined space**					
	Moving to victim	***1 Closer to victim***	***2 Closer to victim***	***In front of victim***	***Moving away***	***Far away***
Detailed measurements	Figure 197	Figure 198	Figure 199	Figure 200	Figure 201	Figure 202
CO2 (ppm)	490	810	1701	2184	1549	1093
O2(%) [O2](mbar)	20.95 [213.32]	20.94 [213.29]	20.91 [213.00]	20.86 [212.54]	20.90 [212.91]	20.91 [213.02]
Human indicator	Zero	Weak: Transition state…	Strong: indications from…	Strong: indications from…	Strong: indications from…	Weak: Transition state…
Approaching indicator	Weak: Approaching	Weak: Approaching	Weak: Approaching	zero	Weak: Moving away	Weak: Moving away
Hot spot indicator	Zero	Weak	Zero	Zero	Zero	Zero
Toxic indicator	Zero	Zero	Zero	Zero	Zero	Zero

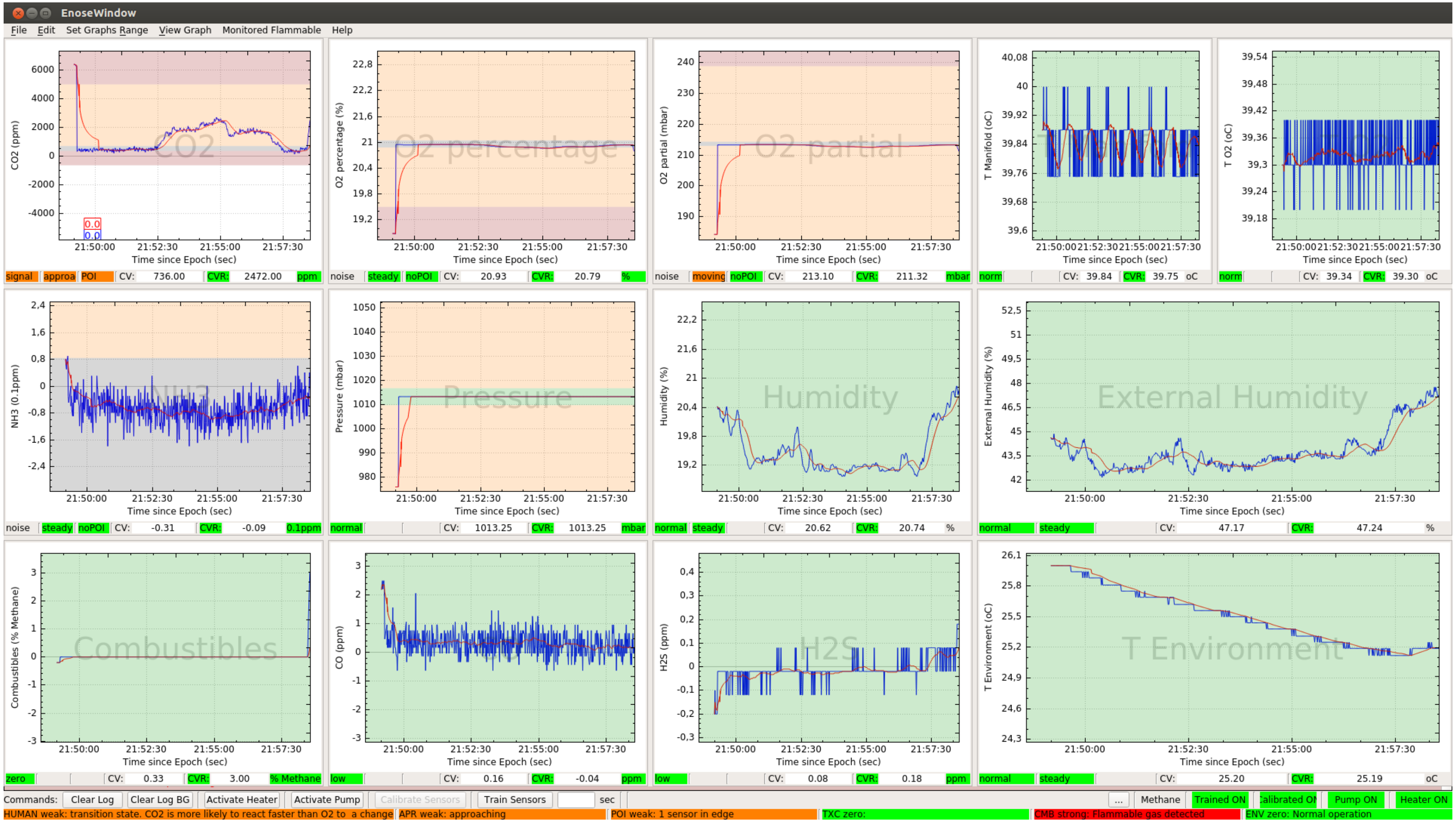
EnoseWindow
File Edit Set Graphs Range View Graph Monitored Flammable Help
CO2
CO2 (ppm)
Time since Epoch (sec)
signal approa POI CV: 736.00 CVR: 2472.00 ppm
O2 percentage
O2 percentage (%)
noise steady noPOI CV: 20.93 CVR: 20.79 %
O2 partial
O2 partial (mbar)
noise moving noPOI CV: 213.10 CVR: 211.32 mbar
T Manifold (oC)
norm CV: 39.84 CVR: 39.75 oC
T O2 (oC)
norm CV: 39.34 CVR: 39.30 oC
NH3
NH3 (0.1ppm)
noise steady noPOI CV: -0.31 CVR: -0.09 0.1ppm
Pressure
Pressure (mbar)
normal CV: 1013.25 CVR: 1013.25 mbar
Humidity
Humidity (%)
normal steady CV: 20.62 CVR: 20.74 %
External Humidity
External Humidity (%)
normal steady CV: 47.17 CVR: 47.24 %
Combustibles
Combustibles (% Methane)
zero CV: 0.33 CVR: 3.00 % Methane
CO
CO (ppm)
low CV: 0.16 CVR: -0.04 ppm
H2S
H2S (ppm)
low CV: 0.08 CVR: 0.18 ppm
T Environment
T Environment (oC)
normal steady CV: 25.20 CVR: 25.19 oC
21:50:00 21:52:30 21:55:00 21:57:30
Commands: Clear Log Clear Log BG Activate Heater Activate Pump Calibrate Sensors Train Sensors sec
... Methane Trained ON Calibrated ON Pump ON Heater ON

HUMAN weak: transition state. CO2 is more likely to react faster than O2 to a change

APR weak: approaching

POI weak: 1 sensor in edge

TXC zero:

CMB strong: Flammable gas detected

ENV zero: Normal operation

Figure 196: Human detection data with the e-nose mounted on the robotic platform. The robotic platform moved under the rubble to and then away from the victim.

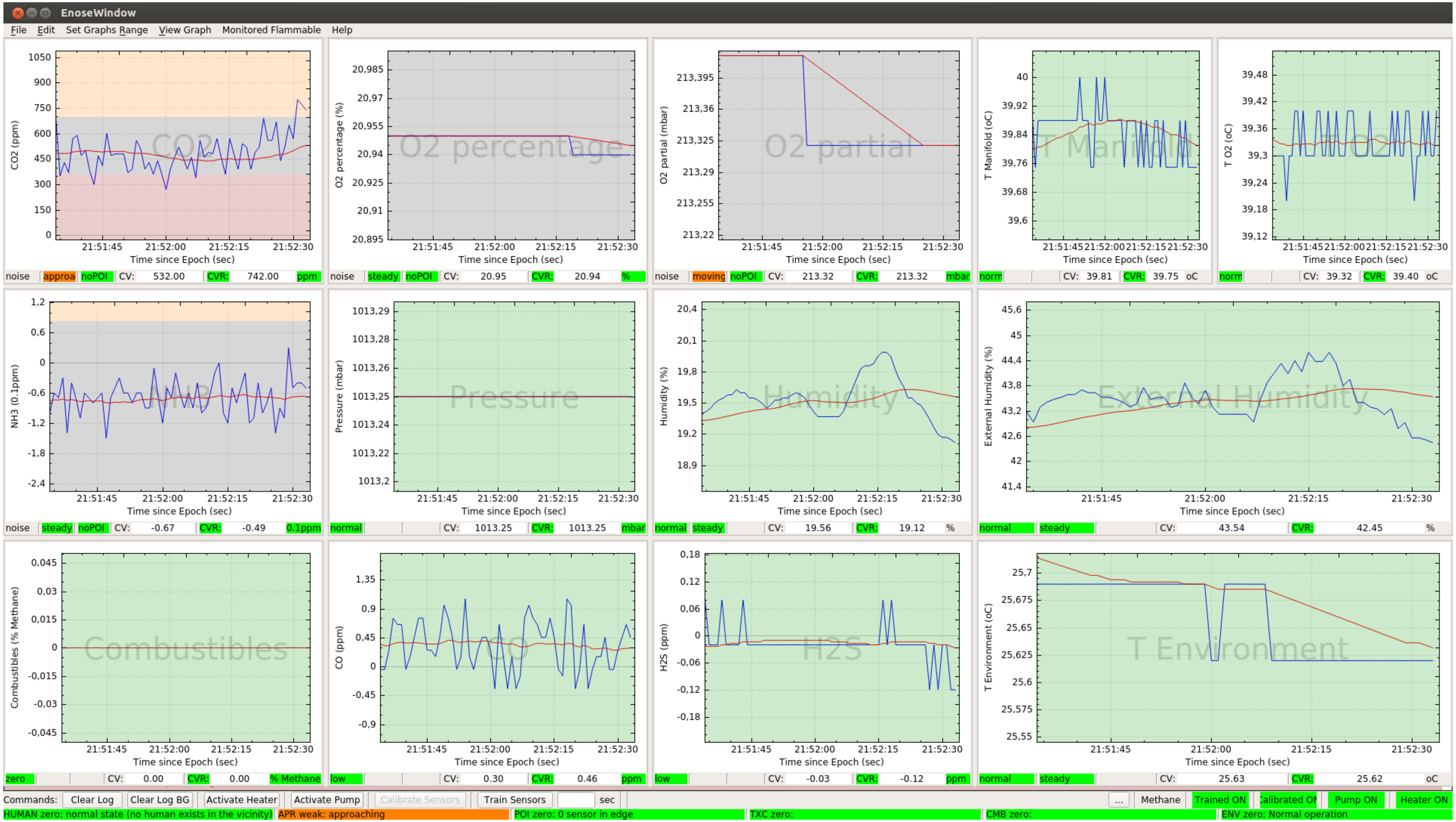
EnoseWindow
File Edit Set Graphs Range View Graph Monitored Flammable Help
CO2 (ppm)
1050 900 750 600 450 300 150 0
CO2
O2 percentage (%)
20,985 20,97 20,955 20,94 20,925 20,91 20,895
O2 percentage
O2 partial (mbar)
213,395 213,36 213,325 213,29 213,255 213,22
O2 partial
T Manifold (oC)
40 39,92 39,84 39,76 39,68 39,6
T Manifold
T O2 (oC)
39,48 39,42 39,36 39,3 39,24 39,18 39,12
T O2
NH3 (0.1ppm)
1,2 0,6 0 -0,6 -1,2 -1,8 -2,4
NH3
Pressure (mbar)
1013,29 1013,28 1013,26 1013,25 1013,24 1013,22 1013,2
Pressure
Humidity (%)
20,4 20,1 19,8 19,5 19,2 18,9
Humidity
External Humidity (%)
45,6 45 44,4 43,8 43,2 42,6 42 41,4
External Humidity
Combustibles (% Methane)
0,045 0,03 0,015 0 -0,015 -0,03 -0,045
Combustibles
CO (ppm)
1,35 0,9 0,45 0 -0,45 -0,9
CO
H2S (ppm)
0,18 0,12 0,06 0 -0,06 -0,12 -0,18
H2S
T Environment (oC)
25,7 25,675 25,65 25,625 25,6 25,575 25,55
T Environment
21:51:45 21:52:00 21:52:15 21:52:30
Time since Epoch (sec)
Commands: Clear Log Clear Log BG Activate Heater Activate Pump Calibrate Sensors Train Sensors sec ... Methane Trained ON Calibrated ON Pump ON Heater ON

noise approa noPOI CV: 532.00 CVR: 742.00 ppm
noise steady noPOI CV: 20.95 CVR: 20.94 %
noise moving noPOI CV: 213.32 CVR: 213.32 mbar
norm CV: 39.81 CVR: 39.75 oC
norm CV: 39.32 CVR: 39.40 oC
noise steady noPOI CV: -0.67 CVR: -0.49 0.1ppm
normal CV: 1013.25 CVR: 1013.25 mbar
normal steady CV: 19.56 CVR: 19.12 %
normal steady CV: 43.54 CVR: 42.45 %
zero CV: 0.00 CVR: 0.00 % Methane
low CV: 0.30 CVR: 0.46 ppm
low CV: -0.03 CVR: -0.12 ppm
normal steady CV: 25.63 CVR: 25.62 oC

HUMAN zero: normal state (no human exists in the vicinity) APR weak: approaching POI zero: 0 sensor in edge TXC zero: CMB zero: ENV zero: Normal operation

Figure 197: Human detection data with the e-nose mounted on the robotic platform. A weak approaching global indicator is triggered.

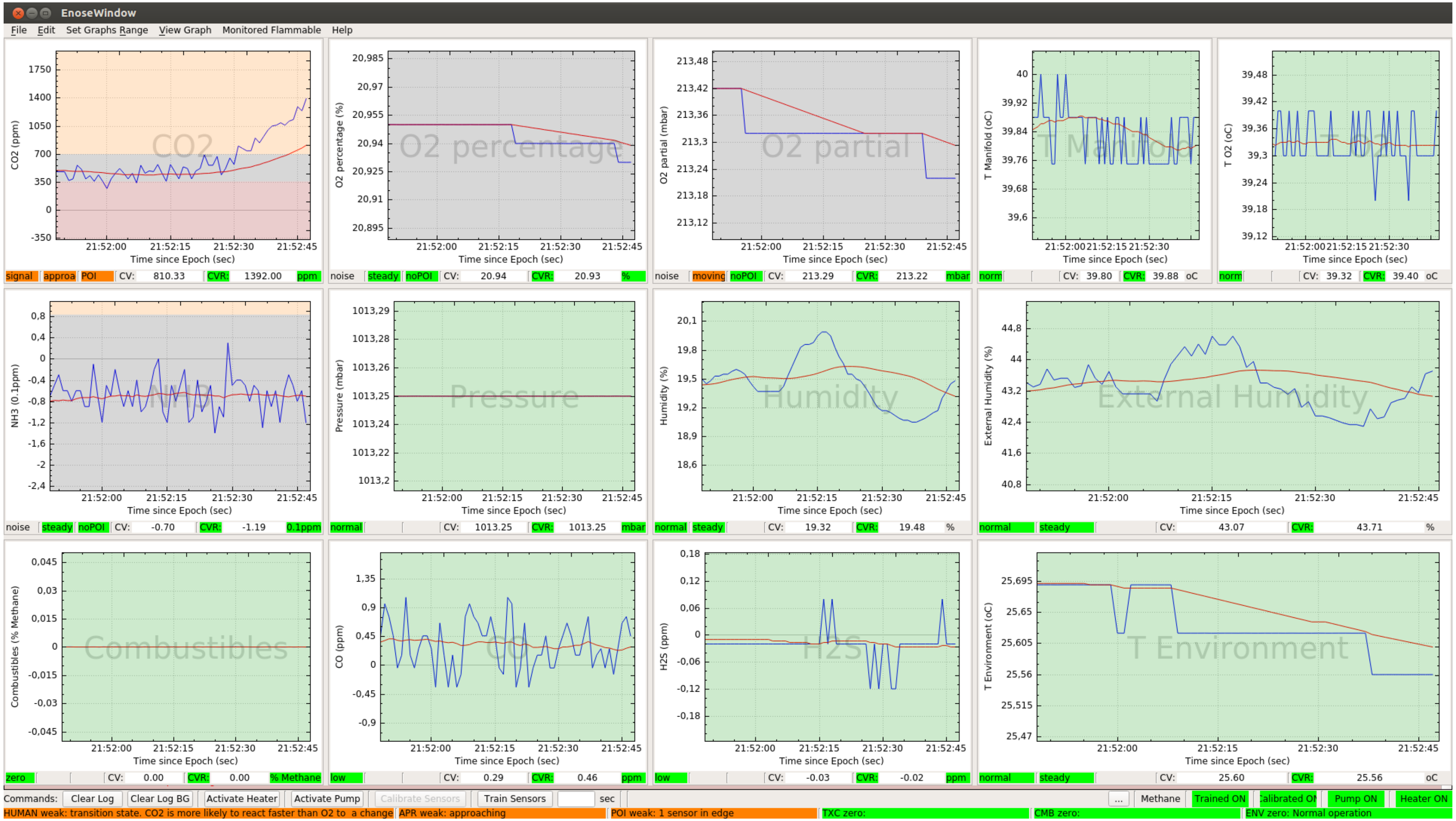
EnoseWindow
File
Edit
Set Graphs Range
View Graph
Monitored Flammable
Help
CO2
CO2 (ppm)
1750
1400
1050
700
350
0
-350
O2 percentage
O2 percentage (%)
20,985
20,97
20,955
20,94
20,925
20,91
20,895
O2 partial
O2 partial (mbar)
213,48
213,42
213,36
213,3
213,24
213,18
213,12
T Manifold
T Manifold (oC)
40
39,92
39,84
39,76
39,68
39,6
T O2
T O2 (oC)
39,48
39,42
39,36
39,3
39,24
39,18
39,12
NH3
NH3 (0.1ppm)
0,8
0,4
0
-0,4
-0,8
-1,2
-1,6
-2
-2,4
Pressure
Pressure (mbar)
1013,29
1013,28
1013,26
1013,25
1013,24
1013,22
1013,2
Humidity
Humidity (%)
20,1
19,8
19,5
19,2
18,9
18,6
External Humidity
External Humidity (%)
44,8
44
43,2
42,4
41,6
40,8
Combustibles
Combustibles (% Methane)
0,045
0,03
0,015
0
-0,015
-0,03
-0,045
CO
CO (ppm)
1,35
0,9
0,45
0
-0,45
-0,9
H2S
H2S (ppm)
0,18
0,12
0,06
0
-0,06
-0,12
-0,18
T Environment
T Environment (oC)
25,695
25,65
25,605
25,56
25,515
25,47
21:52:00
21:52:15
21:52:30
21:52:45
Time since Epoch (sec)
Commands:
Clear Log
Clear Log BG
Activate Heater
Activate Pump
Calibrate Sensors
Train Sensors
sec
...
Methane
Trained ON
Calibrated ON
Pump ON
Heater ON

signal | approa | POI | CV: 810.33 | CVR: 1392.00 | ppm

noise | steady | noPOI | CV: 20.94 | CVR: 20.93 | %

noise | moving | noPOI | CV: 213.29 | CVR: 213.22 | mbar

norm | CV: 39.80 | CVR: 39.88 | oC

norm | CV: 39.32 | CVR: 39.40 | oC

noise | steady | noPOI | CV: -0.70 | CVR: -1.19 | 0.1ppm

normal | CV: 1013.25 | CVR: 1013.25 | mbar

normal | steady | CV: 19.32 | CVR: 19.48 | %

normal | steady | CV: 43.07 | CVR: 43.71 | %

zero | CV: 0.00 | CVR: 0.00 | % Methane

low | CV: 0.29 | CVR: 0.46 | ppm

low | CV: -0.03 | CVR: -0.02 | ppm

normal | steady | CV: 25.60 | CVR: 25.56 | oC

HUMAN weak: transition state. CO2 is more likely to react faster than O2 to a change | APR weak: approaching | POI weak: 1 sensor in edge | TXC zero: | CMB zero: | ENV zero: Normal operation

Figure 198: Human detection data with the e-nose mounted on the robotic platform. A weak Human (global) indicator is triggered, the weak Approaching (global) indicator is active, a weak Point of interest (global) indicator is triggered.

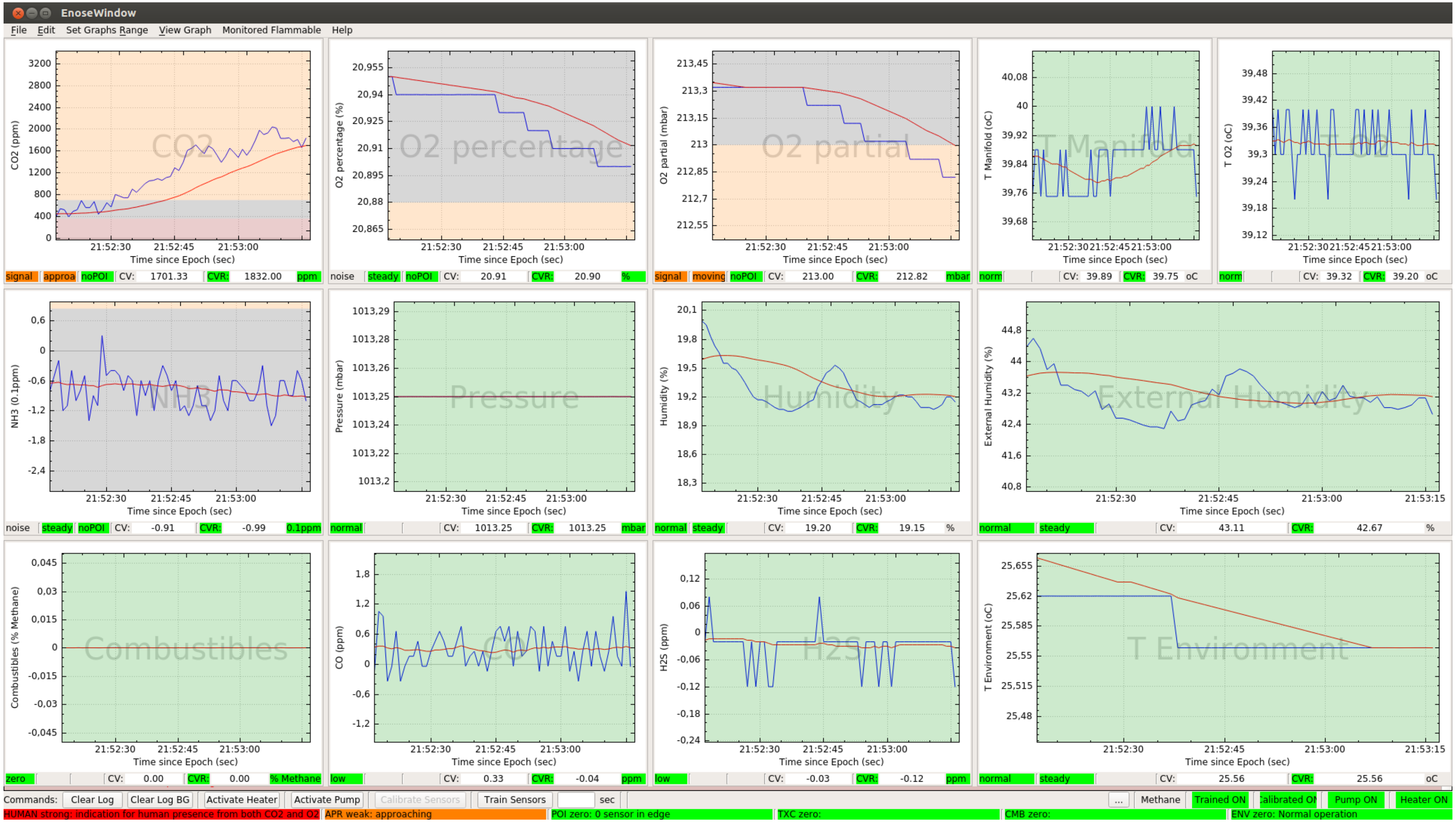
EnoseWindow
File
Edit
Set Graphs Range
View Graph
Monitored Flammable
Help
CO2 (ppm)
CO2
O2 percentage (%)
O2 percentage
O2 partial (mbar)
O2 partial
T Manifold (oC)
T Manifold
T O2 (oC)
T O2
NH3 (0.1ppm)
NH3
Pressure (mbar)
Pressure
Humidity (%)
Humidity
External Humidity (%)
External Humidity
Combustibles (% Methane)
Combustibles
CO (ppm)
CO
H2S (ppm)
H2S
T Environment (oC)
T Environment
Time since Epoch (sec)
21:52:30
21:52:45
21:53:00
21:53:15
Commands:
Clear Log
Clear Log BG
Activate Heater
Activate Pump
Calibrate Sensors
Train Sensors
sec
...
Methane
Trained ON
Calibrated ON
Pump ON
Heater ON

```
signal | approa | noPOI | CV: 1701.33 | CVR: 1832.00 | ppm
noise | steady | noPOI | CV: 20.91 | CVR: 20.90 | %
signal | moving | noPOI | CV: 213.00 | CVR: 212.82 | mbar
norm | CV: 39.89 | CVR: 39.75 | oC
norm | CV: 39.32 | CVR: 39.20 | oC
noise | steady | noPOI | CV: -0.91 | CVR: -0.99 | 0.1ppm
normal | CV: 1013.25 | CVR: 1013.25 | mbar
normal | steady | CV: 19.20 | CVR: 19.15 | %
normal | steady | CV: 43.11 | CVR: 42.67 | %
zero | CV: 0.00 | CVR: 0.00 | % Methane
low | CV: 0.33 | CVR: -0.04 | ppm
low | CV: -0.03 | CVR: -0.12 | ppm
normal | steady | CV: 25.56 | CVR: 25.56 | oC
HUMAN strong: indication for human presence from both CO2 and O2
APR weak: approaching
POI zero: 0 sensor in edge
TXC zero:
CMB zero:
ENV zero: Normal operation
```

Figure 199: Human detection data with the e-nose mounted on the robotic platform. A strong human (global) indicator is triggered while the approaching (global) indicator is still weak.

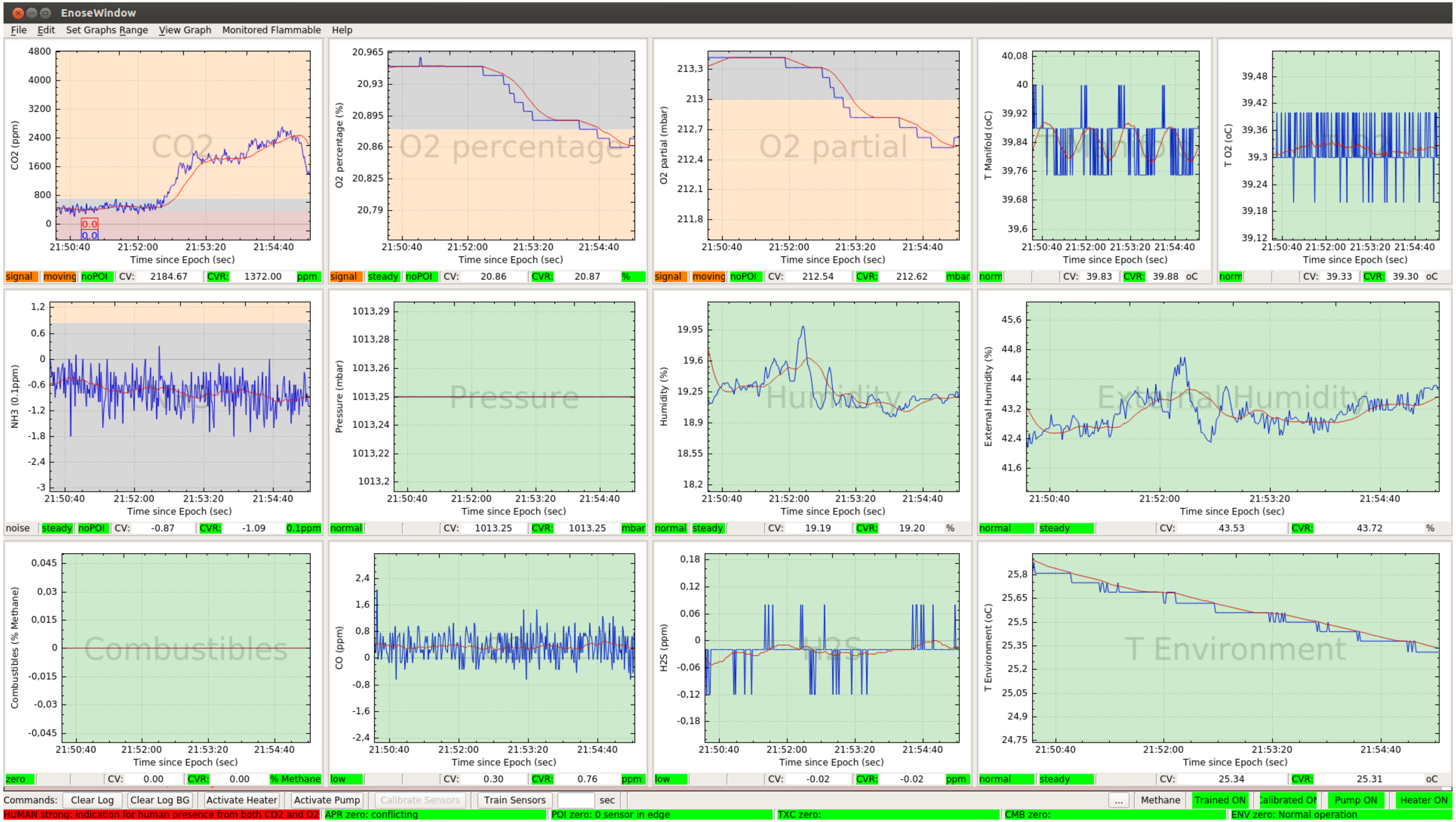
EnoseWindow
File
Edit
Set Graphs Range
View Graph
Monitored Flammable
Help
CO2
CO2 (ppm)
4800
4000
3200
2400
1600
800
0
0.0
0.0
O2 percentage
O2 percentage (%)
20,965
20,93
20,895
20,86
20,825
20,79
O2 partial
O2 partial (mbar)
213,3
213
212,7
212,4
212,1
211,8
T Manifold (oC)
40,08
40
39,92
39,84
39,76
39,68
39,6
T O2 (oC)
39,48
39,42
39,36
39,3
39,24
39,18
39,12
NH3 (0.1ppm)
1,2
0,6
0
-0,6
-1,2
-1,8
-2,4
-3
Pressure
Pressure (mbar)
1013,29
1013,28
1013,26
1013,25
1013,24
1013,22
1013,2
Humidity
Humidity (%)
19,95
19,6
19,25
18,9
18,55
18,2
External Humidity
External Humidity (%)
45,6
44,8
44
43,2
42,4
41,6
Combustibles
Combustibles (% Methane)
0,045
0,03
0,015
0
-0,015
-0,03
-0,045
CO (ppm)
2,4
1,6
0,8
0
-0,8
-1,6
-2,4
H2S
H2S (ppm)
0,18
0,12
0,06
0
-0,06
-0,12
-0,18
T Environment
T Environment (oC)
25,8
25,65
25,5
25,35
25,2
25,05
24,9
24,75
21:50:40
21:52:00
21:53:20
21:54:40
Time since Epoch (sec)
Commands:
Clear Log
Clear Log BG
Activate Heater
Activate Pump
Calibrate Sensors
Train Sensors
sec
...
Methane
Trained ON
Calibrated ON
Pump ON
Heater ON

signal | moving | noPOI | CV: 2184.67 | CVR: 1372.00 | ppm

signal | steady | noPOI | CV: 20.86 | CVR: 20.87 | %

signal | moving | noPOI | CV: 212.54 | CVR: 212.62 | mbar

norm | CV: 39.83 | CVR: 39.88 | oC

norm | CV: 39.33 | CVR: 39.30 | oC

noise | steady | noPOI | CV: -0.87 | CVR: -1.09 | 0.1ppm

normal | CV: 1013.25 | CVR: 1013.25 | mbar

normal | steady | CV: 19.19 | CVR: 19.20 | %

normal | steady | CV: 43.53 | CVR: 43.72 | %

zero | CV: 0.00 | CVR: 0.00 | % Methane

low | CV: 0.30 | CVR: 0.76 | ppm

low | CV: -0.02 | CVR: -0.02 | ppm

normal | steady | CV: 25.34 | CVR: 25.31 | oC

HUMAN strong: indication for human presence from both CO2 and O2

APR zero: conflicting

POI zero: 0 sensor in edge

TXC zero:

CMB zero:

ENV zero: Normal operation

Figure 200: Human detection data with the e-nose mounted on the robotic platform. A strong human (global) indicator is active while the approaching (global) indicator is zero.

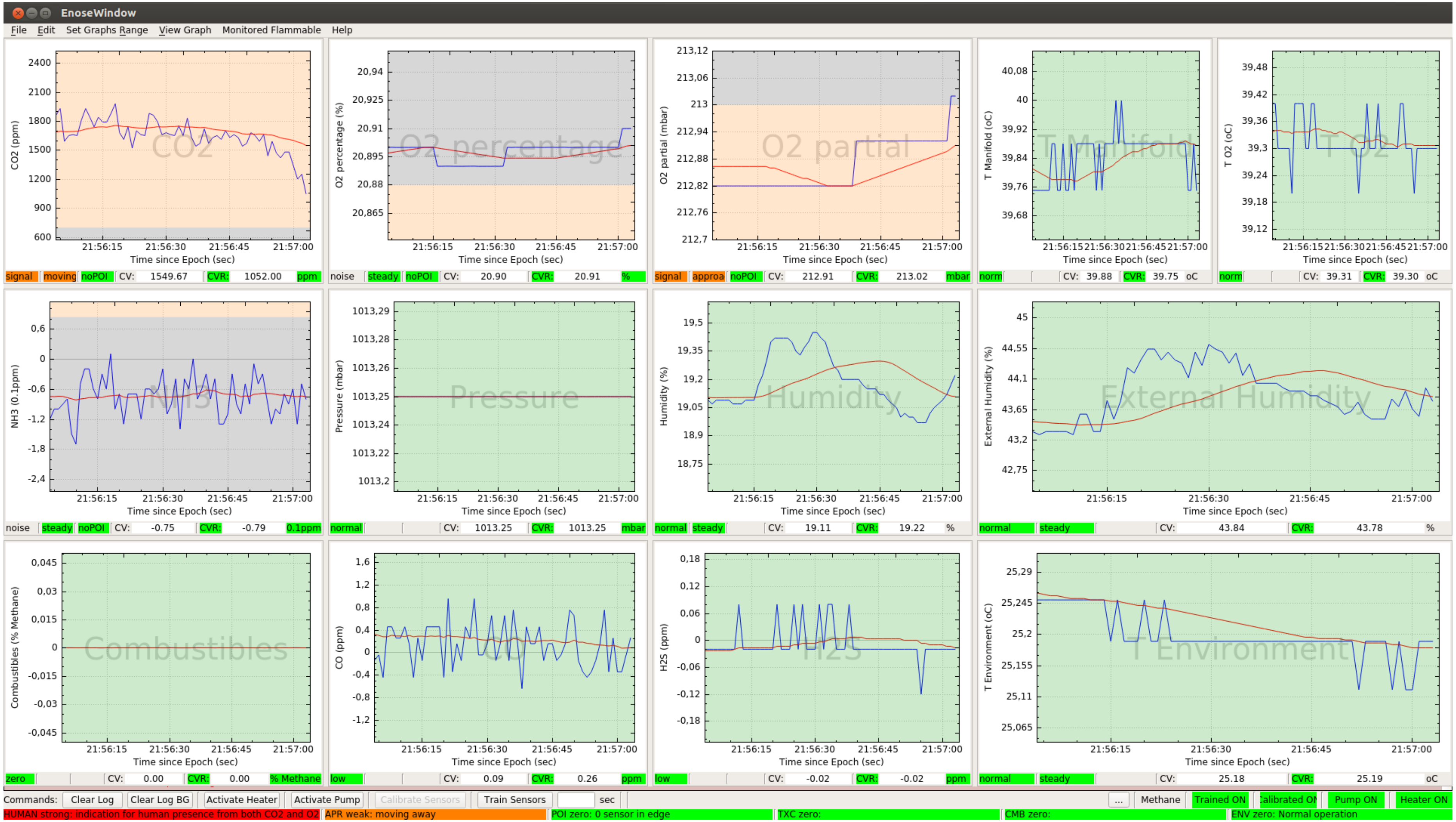
EnoseWindow
File
Edit
Set Graphs Range
View Graph
Monitored Flammable
Help
CO2
CO2 (ppm)
2400
2100
1800
1500
1200
900
600
O2 percentage
O2 percentage (%)
20,94
20,925
20,91
20,895
20,88
20,865
O2 partial
O2 partial (mbar)
213,12
213,06
213
212,94
212,88
212,82
212,76
212,7
T Manifold
T Manifold (oC)
40,08
40
39,92
39,84
39,76
39,68
T O2
T O2 (oC)
39,48
39,42
39,36
39,3
39,24
39,18
39,12
NH3
NH3 (0.1ppm)
0,6
0
-0,6
-1,2
-1,8
-2,4
Pressure
Pressure (mbar)
1013,29
1013,28
1013,26
1013,25
1013,24
1013,22
1013,2
Humidity
Humidity (%)
19,5
19,35
19,2
19,05
18,9
18,75
External Humidity
External Humidity (%)
45
44,55
44,1
43,65
43,2
42,75
Combustibles
Combustibles (% Methane)
0,045
0,03
0,015
0
-0,015
-0,03
-0,045
CO
CO (ppm)
1,6
1,2
0,8
0,4
0
-0,4
-0,8
-1,2
H2S
H2S (ppm)
0,18
0,12
0,06
0
-0,06
-0,12
-0,18
T Environment
T Environment (oC)
25,29
25,245
25,2
25,155
25,11
25,065
21:56:15
21:56:30
21:56:45
21:57:00
Time since Epoch (sec)
Commands:
Clear Log
Clear Log BG
Activate Heater
Activate Pump
Calibrate Sensors
Train Sensors
sec
...
Methane
Trained ON
Calibrated ON
Pump ON
Heater ON

signal | moving | noPOI | CV: 1549.67 | CVR: 1052.00 | ppm

noise | steady | noPOI | CV: 20.90 | CVR: 20.91 | %

signal | approa | noPOI | CV: 212.91 | CVR: 213.02 | mbar

norm | CV: 39.88 | CVR: 39.75 | oC

norm | CV: 39.31 | CVR: 39.30 | oC

noise | steady | noPOI | CV: -0.75 | CVR: -0.79 | 0.1ppm

normal | CV: 1013.25 | CVR: 1013.25 | mbar

normal | steady | CV: 19.11 | CVR: 19.22 | %

normal | steady | CV: 43.84 | CVR: 43.78 | %

zero | CV: 0.00 | CVR: 0.00 | % Methane

low | CV: 0.09 | CVR: 0.26 | ppm

low | CV: -0.02 | CVR: -0.02 | ppm

normal | steady | CV: 25.18 | CVR: 25.19 | oC

HUMAN strong: indication for human presence from both CO2 and O2

APR weak: moving away

POI zero: 0 sensor in edge

TXC zero:

CMB zero:

ENV zero: Normal operation

Figure 201: Human detection data with the e-nose mounted on the robotic platform. A strong Human (global) indicator is active while the Approaching (global) indicator is weak - moving away.

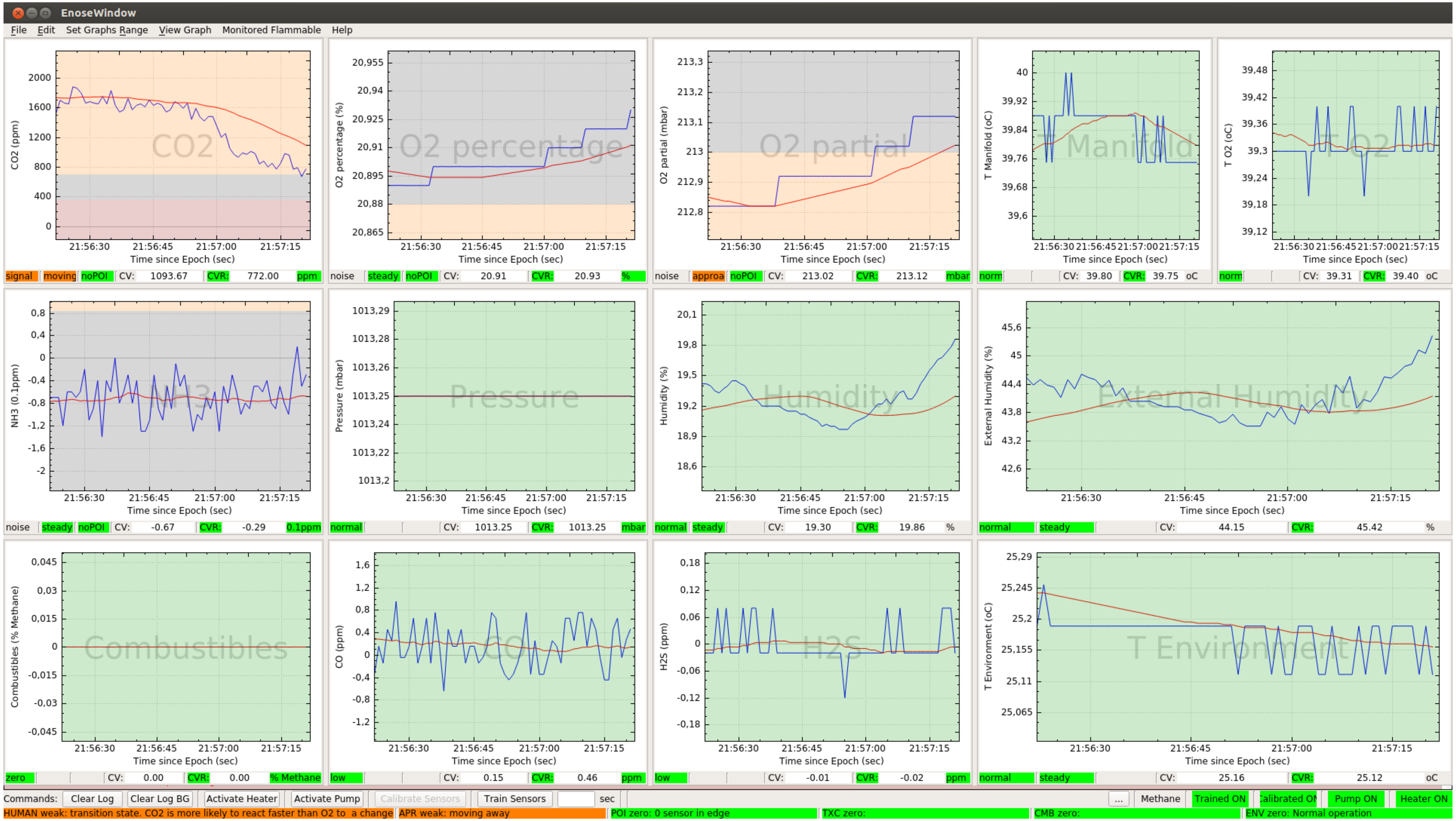
EnoseWindow
File
Edit
Set Graphs Range
View Graph
Monitored Flammable
Help
CO2
CO2 (ppm)
2000
1600
1200
800
400
0
O2 percentage
O2 percentage (%)
20,955
20,94
20,925
20,91
20,895
20,88
20,865
O2 partial
O2 partial (mbar)
213,3
213,2
213,1
213
212,9
212,8
T Manifold
T Manifold (oC)
40
39,92
39,84
39,76
39,68
39,6
T O2
T O2 (oC)
39,48
39,42
39,36
39,3
39,24
39,18
39,12
NH3
NH3 (0.1ppm)
0,8
0,4
0
-0,4
-0,8
-1,2
-1,6
-2
Pressure
Pressure (mbar)
1013,29
1013,28
1013,26
1013,25
1013,24
1013,22
1013,2
Humidity
Humidity (%)
20,1
19,8
19,5
19,2
18,9
18,6
External Humidity
External Humidity (%)
45,6
45
44,4
43,8
43,2
42,6
Combustibles
Combustibles (% Methane)
0,045
0,03
0,015
0
-0,015
-0,03
-0,045
CO
CO (ppm)
1,6
1,2
0,8
0,4
0
-0,4
-0,8
-1,2
H2S
H2S (ppm)
0,18
0,12
0,06
0
-0,06
-0,12
-0,18
T Environment
T Environment (oC)
25,29
25,245
25,2
25,155
25,11
25,065
21:56:30
21:56:45
21:57:00
21:57:15
Time since Epoch (sec)
Commands:
Clear Log
Clear Log BG
Activate Heater
Activate Pump
Calibrate Sensors
Train Sensors
sec
...
Methane
Trained ON
:alibrated ON
Pump ON
Heater ON

signal | moving | noPOI | CV: 1093.67 | CVR: 772.00 ppm

noise | steady | noPOI | CV: 20.91 | CVR: 20.93 %

noise | approa | noPOI | CV: 213.02 | CVR: 213.12 mbar

norm | CV: 39.80 | CVR: 39.75 oC

norm | CV: 39.31 | CVR: 39.40 oC

noise | steady | noPOI | CV: -0.67 | CVR: -0.29 0.1ppm

normal | CV: 1013.25 | CVR: 1013.25 mbar

normal | steady | CV: 19.30 | CVR: 19.86 %

normal | steady | CV: 44.15 | CVR: 45.42 %

zero | CV: 0.00 | CVR: 0.00 % Methane

low | CV: 0.15 | CVR: 0.46 ppm

low | CV: -0.01 | CVR: -0.02 ppm

normal | steady | CV: 25.16 | CVR: 25.12 oC

HUMAN weak: transition state. CO2 is more likely to react faster than O2 to a change

APR weak: moving away

POI zero: 0 sensor in edge

TXC zero:

CMB zero:

ENV zero: Normal operation

Figure 202: Human detection data with the e-nose mounted on the robotic platform. A weak Human (global) indicator is triggered while the Approaching (global) indicator is weak - moving away...

Conclusions and discussion

The e-nose system was tested in near real conditions with actual human (controlled) entrapment. The e-nose system was successful in detecting signs of human presence when transported inside the rubble as part of the sensor payload of a robotic platform. The e-nose device operated successfully without any malfunctions or loss of performance in a harsh outdoor environment for at least 2 full working days. The heuristic algorithm for generating (global) indicators performed well. The performance of the Approaching and Point of interest global indicators was very good at typical search/scanning speeds. At fast scanning speeds their performance was satisfactory; namely, a delayed response was noticed in relation to the actual human position. Their delayed response can be attributed to the very fast scan speed the robotic platform achieved in the prepared and practiced path to the survival space.

The performance of the victim localization capabilities of the e-nose when hazardous conditions are present inside the rubble are estimated to be similar with that when tested outside the rubble; small cross sensitivity of the victim localization sensors with high concentrations of hazardous gases trigger false alarms. By retraining the system with those conditions present the e-nose can resume searching but with a reduced “sensitivity”.

There are some poisons and contaminants that affect some of the e-nose sensors’ performance and longevity. See 14. APPENDIX: ELECTRONIC NOSE SENSOR POISONS AND CONTAMINANTS for indicative precautions.

The e-nose’s victim localization capabilities were also demonstrated to interested end-users. The simple interface was considered successful in fulfilling its purpose in conjunction with all the other sensor technologies available on the robotic platform. End-user feedback commented on the lack of information about exactly which gas triggered a toxic indicator on the robotic platform interface. Regarding this remark, as a future development, this information is available from the advanced logic unit of the e-nose and only needs to be changed in the text message implemented in the global indicator look-up table.

9. Alternative uses of the e-nose

9.1. Fixed position stand-alone e-nose system

The utilization of the e-nose as a stand-alone module for search and rescue operations was examined. A stand-alone e-nose could be placed at a fixed location to monitor the status of a specific void in the rubble. A sampling tube would be placed in the cavity through a natural or drilled hole. The following block diagram illustrates the required components for implementing the core functionality. The picture on the right illustrates the approximate volume and position of the various components

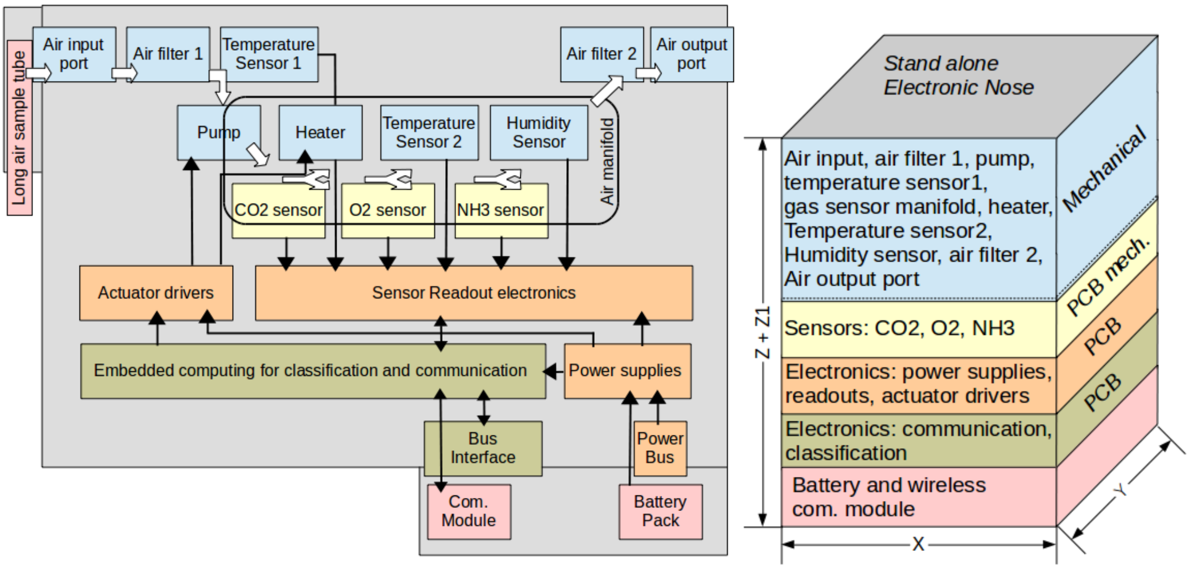
Long air sample tube
Air input port
Air filter 1
Temperature Sensor 1
Air filter 2
Air output port
Pump
Heater
Temperature Sensor 2
Humidity Sensor
Air manifold
CO2 sensor
O2 sensor
NH3 sensor
Actuator drivers
Sensor Readout electronics
Embedded computing for classification and communication
Power supplies
Bus Interface
Power Bus
Com. Module
Battery Pack
Stand alone Electronic Nose
Air input, air filter 1, pump, temperature sensor1, gas sensor manifold, heater, Temperature sensor2, Humidity sensor, air filter 2, Air output port
Sensors: CO2, O2, NH3
Electronics: power supplies, readouts, actuator drivers
Electronics: communication, classification
Battery and wireless com. module
Mechanical
PCB mech.
PCB
PCB
Z + Z1
X
Y

Figure 203. The system implementing the basic functionality but independently from the snake robot

From a hardware perspective, only an extra component containing a battery pack and a wireless communication module are required, not including the interfacing device, most possibly a laptop or tablet. From a software perspective, a program running on the interfacing device would have to be developed to substitute the robotic platform's operator interface for the e-nose.

9.2. PORTABLE STAND-ALONE ELECTRONIC NOSE

The e-nose is designed to operate in the robotic platform and utilize the provided resources. To obtain a functional stand-alone version of the e-nose (requested by the end-users), the resources provided by the robotic platform must be somehow provided or integrated in the e-nose itself. These resources are:

1. A power supply,
2. A user interface,
3. A platform for the Advanced Logic Unit to run on.

The e-nose and the robotic platform are both designed so that it is possible to detach the e-nose from the robotic platform while maintaining a sufficiently protective cover, exposing only the interfaces for communications and power and air sampling.

9.2.1. Power supply

The e-nose is designed so that it can operate from a wide range of Direct Current Voltage rails (10V-28V), but it is optimized to operate in the (18V-24V) range. Operating in the low voltage range (10V-18V) without any configuration/optimization will only induce an increased start-up time. Circuit protection will still be within operational limits but closer to the upper/ over current limit. It is therefore possible to provide the required power from an external battery module, or even a battery pack that is electrically connected to the e-nose. The battery module could be physically attached to the e-nose from the same mounting points used for the robotic platform, or could be placed somewhere more convenient like in a backpack. Since the e-nose is meant to be a portable device for searching by executing a search pattern, a low weight battery pack would make more sense, with battery cells of choice being disposable alkaline cells or rechargeable NiCad - NiMH cells. Lithium based batteries are not advised because of travelling restrictions on commercial airlines. For practical reasons and with this guideline in mind, the battery module voltage would be around 12V. In the configuration for 12), a battery pack with ten batteries connected in series should be used to cover both alkaline (cell voltage ~1.5V) and rechargeable (Cell voltage ~1.2V) configurations. Expected Battery life (with AA size, 1000-2000mAh) would be more than one hour but not more than three hours, depending on usage and environmental conditions. Since in this configuration it is not anticipated that the e-nose will get very close to survival spaces with victims, where the humidity might be around 100%RH, the device can be operated with the heating disabled to reduce power consumption. In the stand-alone use of the electronic device, the operator will be more attentive to the operation of the device so the pump function could be controlled by him and used only when actually scanning, thus conserving power and prolonging battery life.

9.2.2. User interface and Advanced Logic Unit

There are two possible configurations for a stand-alone user interface of the e-nose intended for the field. The first solution is very similar or almost identical to the user interface integrated in the robotic platform. In this configuration a Windows tablet is used as the interface. The modifications required include porting the Advanced Logic Unit software to the tablet and adapting it to accept the measurement stream from a different source, a USB (or emulated serial over USB) connection. This configuration could be a completely stand-alone solution and at the same time be compatible with the INACHUS framework

The second solution is more suitable for creating a truly stand-alone and rugged e-nose device. In this configuration though, certain compromises have to be made so that the interface is robust and at the same time functional. The interfacing would be achieved through a small number of actual buttons for sending control commands and the outputs would be provided via a combination of light indicators and audible signals via a buzzer/speaker. A small backlight LCD could also be used. The operation would be similar to that of a Geiger counter, but the output sound would be coded to provide more information. The main reporting function is audio so that the operator can use his eyes to navigate the terrain and stick the air sampling probe into the rubble. Audible output would be created based on the CO_2 measurement. Scrolling through the other sensor values would be possible by pressing the corresponding button. It would also be possible to automatically cycle and audibly report all the measurements' values. The combined outputs (Human presence indicator, Trend indicator and Edge indicator) will not be ported to the microcontroller since there is not such a need; the operator is dedicated to the e-nose. The output coding of the results of each sensor will be a periodic sweep of two values of concentration, the reference value and the current value. The values will be converted into frequencies with an exponential function so they are separated enough and can easily be distinguished by the operator. When the first frequency is lower than the second one, the current value measured was larger than the reference measurement. The higher the frequency, the larger the concentration is. Hazardous alarms would interrupt this audio reporting with a different single tone. The sensor that triggered the alarm will be indicated with a light indicator or printed on the screen. The screen used should be a single color numeric or alphanumeric LCD type with a backlight so that it can be visible both under the bright sun and in the dark.

The implementation of the second configuration of the interface requires some HW development and also plenty of low level firmware development. The advanced Logic Unit software cannot be easily ported to the microcontroller but that is not a problem since most of it will not be used. Its functionality is tasked to the operator of the device. Training requirements for this configuration of the tool will be more demanding, but this will be a more powerful tool in the hands of a capable operator. Getting the feel of the tool and the output can be achieved indoors, by using in parallel, the complete full version interface developed for testing purposes of the prototype device and the stand-alone field interface.

9.2.3. Suitable components

The following list contains the components that could be utilized to build an add-on module for operating the e-nose as a standalone device.

1. Battery Holder: Bolayu New 10 AA 2A Battery 15V Clip Holder Box Case Storage With Wire Leads Black (https://www.amazon.com/Bolayu-Battery-Holder-Storage-Leads/dp/B01FRXZX2O%3FSubscriptionId%3DAKIAILSHYYTFIVPWUY6Q%26tag%3Dduckduckgo-d-20%26linkCode%3Dxm2%26camp%3D2025%26creative%3D165953%26creativeASIN%3DB01FRXZX2O)
2. LCD Display: MIDAS MCCOG21605D6W-SPTLYI Alphanumeric LCD, 16 x 2, Black on Yellow / Green, 3V to 5V, I^2C, English, Japanese, Transflective (http://export.farnell.com/midas/mccog21605d6w-sptlyi/lcd-cog-2x16-stn-y-grn-b-l-i2c/dp/2063205)
3. Light Indicators: CML INNOVATIVE TECHNOLOGIES 192D1001 LED Panel Mount Indicator, Black Chrome Bezel, Green, 12 mm, 2.2 VDC, 20 mA, 40 mcd, IP67 (http://export.farnell.com/cml-innovative-technologies/192d1001/led-indicator-8mm-green/dp/1139529)
4. Control Buttons: MULTICOMP MCAK304NWWB Keypad, 20 mA, 24 V, 3 x 4, Matrix, 12 (http://export.farnell.com/multicomp/mcak304nwwb/keypad-3x4-array-plastic/dp/1182235)
5. Power Switch: TE CONNECTIVITY / ALCOSWITCH AV1911P524Q04 Illuminated Pushbutton Switch, Alcoswitch, AV19 Anti-Vandal Series, SPDT, Push On-Push Off, 3 A(http://export.farnell.com/te-connectivity-alcoswitch/av1911p524q04/pb-switch-spdt-yel-250v-quickconnect/dp/2565073)
6. Speaker-buzzer: Headphones could be used or a dedicated waterproof speaker: VISATON 2912 LOUDSPEAKER, MINI, WATERPROOF, 8 OHM (http://export.farnell.com/visaton/2912/loudspeaker-mini-waterproof-8/dp/1675520?ost=1675520&selectedCategoryId=&categoryNameResp=All%2BCategories&searchView=table&iscrfnonsku=false)

The following pictures illustrate the selected devices:

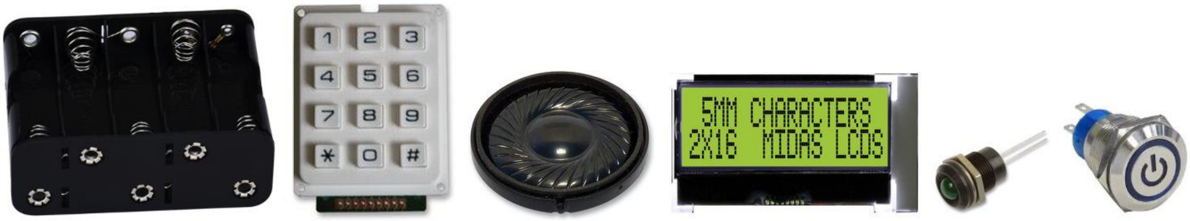

Figure 204: From left to right, battery holder, keypad, speaker, LCD screen, LED indicator, ON/OFF push button.

9.3. People detector

The e-nose can be used to detect people in poorly ventilated and confined spaces other than building rubble. An area where this could be realized is in international cargo transportation for the detection of hidden people trying to cross borders without the required documents. Another case is in the field of road transportation of goods in trucks. There are two configurations the e-nose can be adapted for, fixed applications and portable. In the fixed position configuration the e-nose would be permanently installed in a truck while in a portable configuration it would be used to test different trucks at a check point.

9.3.1. Fixed position people detector

The e-nose can be installed in fixed positions in buildings or in transportation compartments for goods where people are normally not supposed to be located. The owners or people in charge of those spaces would install the e-nose-based people detector in order to avoid any legal ramifications in case someone is able to slip through security and occupy one of those spaces. The utilization of the e-nose in such a case would be similar to that of the installation in the robotic platform. Not many changes are required in order to use the e-nose in such situations. The e-nose could be used to monitor multiple positions near the position where it is installed. This could be achieved with a network of low-cost, low profile sampling tubes connected to the e-nose via a sample tube selector. This selector would be a cluster of valves opening the path to a single space at a time enough to sample air and take measurements. The control of the sampler could be implemented in the e-nose logic. For this type of application, all the capabilities of the e-nose would have to be utilized except for the aspect regarding hazardous gas detection. The following block diagram illustrates the components to be utilized:

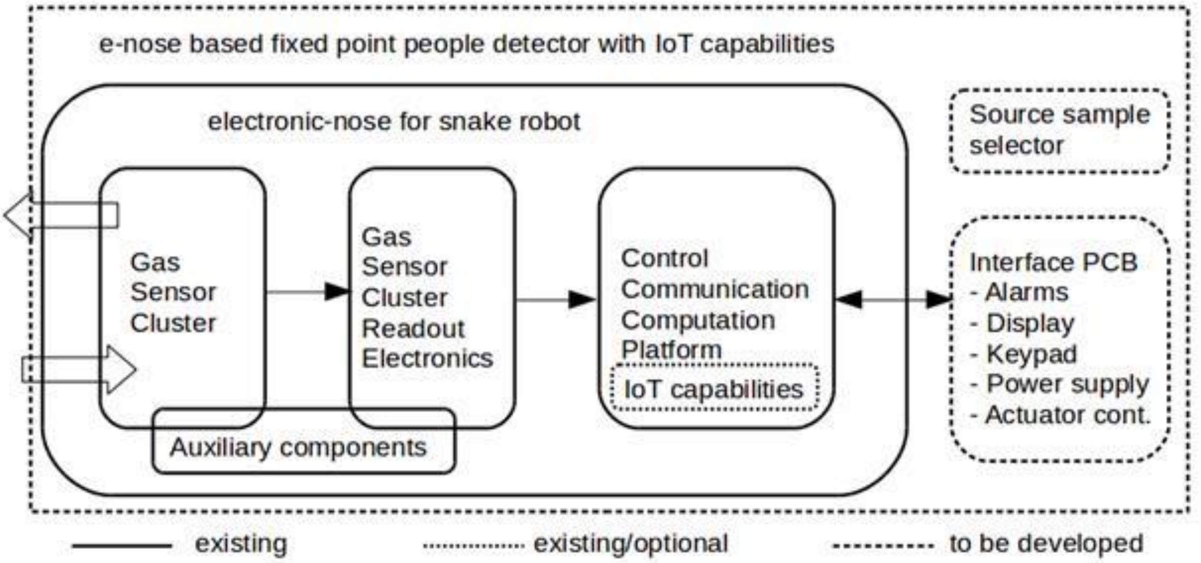
e-nose based fixed point people detector with IoT capabilities
electronic-nose for snake robot
Source sample selector
Gas Sensor Cluster
Gas Sensor Cluster Readout Electronics
Control Communication Computation Platform
IoT capabilities
Interface PCB
- Alarms
- Display
- Keypad
- Power supply
- Actuator cont.
Auxiliary components
existing
existing/optional
to be developed

Figure 205. Block diagram of a fixed point people detector with IoT and multi-source capabilities based on the e-nose.

The following diagram illustrates a 6 source sample selector based on 2way solenoid valves

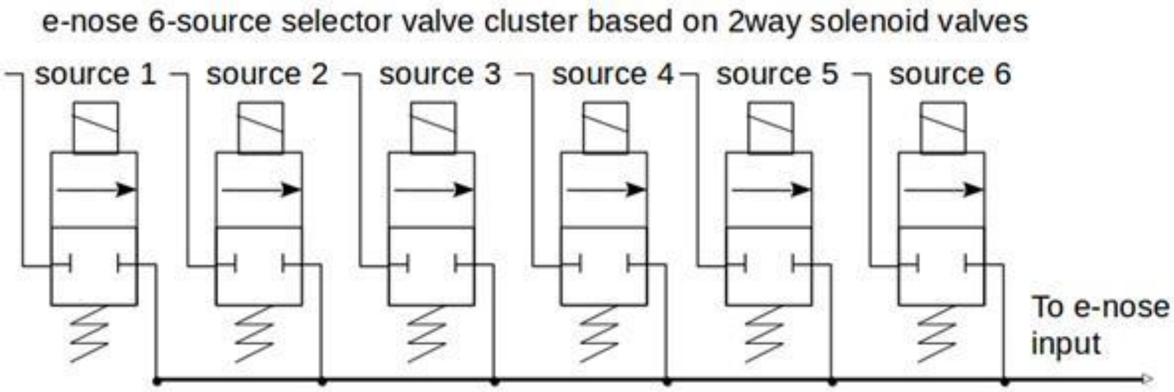
e-nose 6-source selector valve cluster based on 2way solenoid valves
source 1
source 2
source 3
source 4
source 5
source 6
To e-nose input

Figure 206. Block diagram of the implementation of the multi-source sampling solution for the fixed point people detector based on the e-nose.

The control of the source selector can be implemented in the e-nose control logic and the driving electronics can be placed in the interface PCB. A 6 source valve cluster device could fit in one of the generic instrument boxes.

9.3.2. Portable people detector

The e-nose can also be used as a portable people detector in cases other than building rubble. Such a scenario could involve testing cargo trucks for undocumented human passengers hidden in the cargo area of the truck. The e-nose could be used for this type of search with few modifications and additions. Since the device would not be used as a hazardous detector, some safety design aspects would not have to be followed. The e-nose could be paired with a mobile phone as the user interface and a battery pack as a power source. The e-nose sampling port would have to be connected to a small probe to be able to more easily facilitate the sampling of air from specific high value air samples, close to doors when they are just slightly open. A different type of probe could be a large one to facilitate the sampling of air far inside the cargo hold of a truck. This large sampling probe would essentially be a long flexible tube suspended by a means to support it a fairly long distance from just one end. This could be a mechanical support like a fishing rod. For this configuration, all the components of the e-nose are required. Also, the sampling pump function could be boosted to 100% to increase the transfer of the sampled air as fast as possible through the long sampling tube to the e-nose so the result could be available shortly.

9.4. Smoking detector

The e-nose can be used to detect the presence of smoke from a cigarette, by detecting some of the constituents of cigarette smoke, CO and CO_2. This functionality could be included in any of the other devices listed in other sections of this chapter as long as the necessary sensors are included. In a simple fixed position gas detector installation in an office building a unique alarm tone could be triggered to indicate smoking in a non-smoking area was detected. If the controller has IoT capabilities, management could also be informed to handle further action. If the device has control over a ventilation actuator, it could be enabled to clear the air or if the device is connected to an advanced inverter actuator, it could increase the output to speed up the air renewal and remove the disturbance according to pre-programmed timeframe parameters.

9.5. Capnography

Capnograghy is a breath-based metabolism monitoring method. It monitors the amount of exhaled CO_2 which indicates metabolic activity. The e-nose could be adapted to function as a capnography instrument with the following two modifications/additions. First, a suitable sampling mask would have to be adapted to the e-nose sampling input. Second, the CO_2 sensor readings would have to be filtered and processed differently. Absolute CO_2 concentration value is important so 2 point calibration is mandatory. A different interface would be required for implementing the capnography specific interface requirements.

10.CONCLUSIONS

The main objective and goal of this research work was to improve the methods and tools used in the detection of trapped victims during Urban Search and Rescue (USaR) operations from an air-based detection perspective that is implemented with e-nose systems. The e-nose system and detection concept for victim localization and air related hazard detection in confined spaces presented in this work was successfully tested in realistic conditions. The performance of the e-nose system indicates that it can be used as part of USaR operations inside a relatively poorly ventilated, confined space to determine human presence and hazardous conditions in the air. The volume, weight, simplicity and power consumption of the system are considered contributing factors for its adoption. The device can operate in a wide range of environmental conditions. The presence of the carefully selected sensors for measuring the concentration of typical hazardous conditions improves the victim localization capabilities of the system. It indicates survivable atmospheres and also detects conditions that cause interference with the victim detection sensors and indicates that potentially false positive detections might be displayed. This thesis improved the state of the art by introducing a low-cost and mobile e-nose system capable of searching for signs of human presence from the surface, but most importantly from inside the rubble when transported on a robotic platform as part of its sensor payload. User interface aspects were also thoroughly investigated. To this end, a heuristic algorithm was formulated for producing simple output combining all the sensor readings. The output also includes information that assists the operator in performing the search during a rescue operation. Methods and practices for reducing false output (positive and negative) were conceived and implemented. Also included in the implemented system is the detection of hazardous conditions in order to improve the working conditions of the rescuers from a safety perspective, and at the same time improve the victim detection aspects regarding the survivability in a space. The implemented system was tested and verified in controlled and near real conditions. The e-nose system performed very well in the intended environment inside the rubble pile. The heuristic algorithm for generating simple outputs performed very well. Scanning speed can be drastically increased at the expense of noise immunity performance if such a need arises. The capabilities of the final system were also demonstrated to end-users and its capabilities were validated by them, too. End-users provided useful feedback regarding the usability of the interface and the system which will be considered in (potential) future work. The resulting e-nose system can be said to have reached, according to the European Union’s (EU) Technology Readiness Level (TRL) definitions, TRL 7 – “System prototype demonstration in operational environment”. The system proposed in this research work, could be commercially manufactured and certified (CE and ATEX), if another design cycle is performed.

The findings of the theoretical analysis and its validation quantify the influence of the studied parameters, concerning the concentration of CO_2 and O_2 inside a rubble void and estimate the expected human presence detection limits of a system with gas sensors with specific sensor characteristics. It shows that a system with gas sensors can indeed detect human presence in a plethora of scenarios. It also theoretically shows that a system with gas sensors is not the ideal human detection system and cannot detect human presence in all scenarios, but the basis for determining such cases was established. This work could be the foundation for the development of a tool that evaluates the expected performance of gas sensor-based systems. This can be in the early conception stages of a system as a feasibility study or real-time at a USaR operations worksite.

In a future work the output messages for the global toxic indicator could be made more informative. A study and test implementation for evaluating the priority of the global indicators and their cross-correlated status should be performed. In such a study the possibility of implementing a single (global) output could be examined. Even though the start-up procedure for the system is simple, considering all facts regarding hazardous conditions, the warm-up time of the 3rd prototype system which depends on the initial temperature of the e-nose device could be improved. A future research activity could be to train an AI system for updating the indicators and compare the performance with the current configuration of the system.

11.REFERENCES

[1] https://www.fireservice.gr/el/periphereiakes-yperesies

[2] http://www.hrt.org.gr/

[3] http://www.insarag.org/

[4] J. Tran, et al., "Canine assisted robot deployment for urban search and rescue.," presented at the IEEE International Workshop on Safety Security and Rescue Robotics (SSRR), 2010.

[5] N. Thi Phuoc Van, L. Tang, V. Demir, S. F. Hasan, N. Duc Minh, and S. Mukhopadhyay, "Review-Microwave Radar Sensing Systems for Search and Rescue Purposes," *Sensors,* vol. 19, p. 2879, 2019.

[6] P. Agrafiotis, et al., "Real Time Earthquake's Survivor Detection using a Miniaturized LWIR Camera," in *9th ACM International Conference on PErvasive Technologies Related to Assistive Environments*, 2016.

[7] M. Korkalainen, A. P. Mäyrä, and K. Känsälä, "An open communication and sensor platform for urban search and rescue operations," in *Unmanned/Unattended Sensors and Sensor Networks IX*, 2012, p. 85400O.

[8] M. Konyo, Y. Ambe, H. Nagano, Y. Yamauchi, S. Tadokoro, Y. Bando*, et al.*, "ImPACT-TRC thin serpentine robot platform for urban search and rescue," in *Disaster robotics*, ed: Springer, 2019, pp. 25-76.

[9] F. van Breugel, J. Riffell, A. Fairhall, and M. H. Dickinson, "Mosquitoes Use Vision to Associate Odor Plumes with Thermal Targets," *Current Biology,* vol. 25, pp. 2123-2129, Aug 17 2015.

[10] R. Huo, A. Agapiou, V. Bocos-Bintintan, L. J. Brown, C. Burns, C. S. Creaser*, et al.*, "The trapped human experiment," *Journal of Breath Research,* vol. 5, Dec 2011.

[11] A. Anyfantis and S. Blionas, "Indoor air quality monitoring sensors for the design of a simple, low cost, mobile e-nose for real time victim localization," presented at the PACET 2019, Volos, Greece, 2019.

[12] A. Anyfantis and S. Blionas, "Proof of concept apparatus for the design of a simple, low cost, mobile e-nose for real-time victim localization (human presence) based on indoor air quality monitoring sensors," *Sensing and Bio-Sensing Research,* vol. 27, p. 100312, 2020.

[13] A. Anyfantis and S. Blionas, "Design and Development of a Mobile e-nose platform for Real Time Victim Localization in Confined Spaces During USaR Operations," in *2020 IEEE International Instrumentation and Measurement Technology Conference (I2MTC)*, 2020, pp. 1-6.

[14] J. Huang and J. Wu, "Robust and Rapid Detection of Mixed Volatile Organic Compounds in Flow Through Air by a Low Cost Electronic Nose," *Chemosensors,* vol. 8, p. 73, 2020.

[15] A. T. Güntner, N. J. Pineau, P. Mochalski, H. Wiesenhofer, A. Agapiou, C. A. Mayhew*, et al.*, "Sniffing entrapped humans with sensor arrays," *Analytical chemistry,* vol. 90, pp. 4940-4945, 2018.

[16] K. Känsälä, M. Korkalainen, and A. Mäyrä, "A versatile sensor network for urban search and rescue operations," in *Unmanned/unattended sensors and sensor networks VIII*, 2011, p. 81840H.

[17] H. Fan, V. Hernandez Bennetts, E. Schaffernicht, and A. J. Lilienthal, "Towards gas discrimination and mapping in emergency response scenarios using a mobile robot with an electronic nose," *Sensors,* vol. 19, p. 685, 2019.

[18] S. J. Patil, A. V. Patil, C. G. Dighavkar, K. S. Thakare, R. Y. Borase, S. J. Nandre*, et al.*, "Semiconductor metal oxide compounds based gas sensors: A literature review," *Frontiers of Materials Science,* vol. 9, pp. 14-37, Mar 2015.

[19] Anyfantis, A., & Blionas, S. (2021). An analysis on the performance of a mobile platform with gas sensors for real time victim localization. *Sensors*, 21(6), 2018.

[20] Anyfantis, A., Silis, A., & Blionas, S. (2021). A low cost, mobile e-nose system with an effective user interface for real time victim localization and hazard detection in USaR operations. *Measurement: Sensors*, 100049.

[21] Monks, P. S., et al. "Atmospheric composition change–global and regional air quality." *Atmospheric Environment* 43.33 (2009): 5268-5350.

[22] Colbeck, I. (1987), "Air: Composition and Chemistry. By Peter Brimblecombe." *Weather*, 42: 56–57. doi: 10.1002/j.1477-8696.1987.tb06920.x

[23] Ed Dlugokencky and Pieter Tans, "Recent Global CO_2." NOAA/ESRL *http://www.esrl.noaa.gov/gmd/ccgg/trends/global.html*

[24] ASHRAE 2009 Handbook, Ch1,1.2, (9a)

[25] Rolf Brugger. "Humidity and Dew Point Table." *http://rolfb.ch/tools/thtable.php*

[26] SENSIRION. "Introduction to Relative Humidity and Temperature Sensors." *https://www.sensirion.com/en/products/digital-humidity-sensors-for-reliable-measurements/all-documents-of-sensirions-humidity-sensors-for-download/*

[27] SENSIRION. "Humidity and Temperature at a Glance." https://www.sensirion.com/en/products/digital-humidity-sensors-for-reliable-measurements/all-documents-of-sensirions-humidity-sensors-for-download/

[28] Seco, Roger, Josep Penuelas, and Iolanda Filella. "Short-chain oxygenated VOCs: Emission and uptake by plants and atmospheric sources, sinks, and concentrations." *Atmospheric Environment* 41.12 (2007): 2477-2499.

[29] Taalman, Rob DFM. "Isoprene: background and issues." *Toxicology* 113.1 (1996): 242-246.

[30] Loreto, F. and Sharkey, T.D. (1993) Isoprene emission by plants is affected by transmissible wound signals. Plants Cell Environ. 16, 563-570.

[31] Zimmerman, P.R., Chatfield, R.B., Fishman, J., Crutzen, P.J. and Hanst, P.L. (1978) Estimates on the production of CO and H, from the oxidation of hydrocarbon emmisions from vegetation. Geophys. Res. Lett. 5, 679-682.

[32] Gelmont, D., Stein, R.D. and Mead, J.F. (198 1) Isoprene: the main hydrocarbon in human breath. Biochem. Biophys. Res. Commun. 99, 1456- 1460.

[33] Taalman, Rob DFM. "Isoprene: background and issues." *Toxicology* 113.1 (1996): 242-246.

[34] Borbon, Agnès, et al. "An investigation into the traffic-related fraction of isoprene at an urban location." *Atmospheric Environment* 35.22 (2001): 3749-3760.

[35] Chang, Chih-Chung, et al. "Seasonal characteristics of biogenic and anthropogenic isoprene in tropical–subtropical urban environments." *Atmospheric Environment* 99 (2014): 298-308.

[36] Richard M. Effros, Marshall B. Dunning III, Julie Biller, Reza Shaker. "The promise and perils of exhaled breath condensates." *American Journal of Physiology - Lung Cellular and Molecular Physiology* Published 1 December 2004 Vol. 287 no. 6, L1073-L1080 DOI: 10.1152/ajplung.00069.2004

[37] Martinez-Lozano Sinues, Pablo, Malcolm Kohler, and Renato Zenobi. "Human breath analysis may support the existence of individual metabolic phenotypes." *PloS one* 8.4 (2013): e59909.

[38] Buszewski, Bogusław, et al. "Human exhaled air analytics: biomarkers of diseases." Biomedical chromatography 21.6 (2007): 553-566.

[39] Wang, Chuji, and Peeyush Sahay. "Breath analysis using laser spectroscopic techniques: breath biomarkers, spectral fingerprints, and detection limits." Sensors 9.10 (2009): 8230-8262.

[40] Fenske, Jill D., and Suzanne E. Paulson. "Human breath emissions of VOCs." *Journal of the Air & Waste Management Association* 49.5 (1999): 594-598.

[41] Huo, R., et al. "The trapped human experiment." Journal of breath research 5.4 (2011): 046006.

[42] "Second Generation Locator for Urban Search and Rescue Operations." *http://www.sgl-eu.org/*

[43] Glindemann, Dietmar, et al. "The two odors of iron when touched or pickled: (skin) carbonyl compounds and organophosphines." *Angewandte Chemie International Edition* 45.42 (2006): 7006-7009.

[44] Beach, Huntington. "COMPOSITION AND CONCENTRATIVE PROPERTIES OF HUMAN URINE." (1971).

[45] Smith, Stephen, et al. "A comparative study of the analysis of human urine headspace using gas chromatography–mass spectrometry." *Journal of breath research* 2.3 (2008): 037022.

[46] Mochalski, Paweł, et al. "Permeation profiles of potential urine-borne biomarkers of human presence over brick and concrete." *Analyst* 137.14 (2012): 3278-3285.

[47] Urease. *https://en.wikipedia.org/wiki/Urease*

[48] Karplus, P. Andrew, Matthew A. Pearson, and Robert P. Hausinger. "70 years of crystalline urease: what have we learned?." *Accounts of chemical research* 30.8 (1997): 330-337.

[49] Benini, Stefano, Francesco Musiani, and Stefano Ciurli. "Urease." *Encyclopedia of Metalloproteins*. Springer New York, 2013. 2287-2292.

[50] Callahan, Brian P., Yang Yuan, and Richard Wolfenden. "The burden borne by urease." *Journal of the American Chemical Society* 127.31 (2005): 10828-10829.

[51] Callahan BP, Yuan Y, Wolfenden R (2005) The burden borne by urease. J Am Chem Soc 127:10828–10829

[52] Smeets, Monique AM, et al. "Odor and irritation thresholds for ammonia: a comparison between static and dynamic olfactometry." *Chemical Senses* 32.1 (2007): 11-20.

[53] Norberg, A., et al. "The urine smell around patients with urinary incontinence." *Gerontology* 30.4 (1984): 261-266.

[54] Röck, Frank, Nicolae Barsan, and Udo Weimar. "Electronic nose: current status and future trends." *Chemical reviews* 108.2 (2008): 705-725.

[55] CO_2Meter. "NDIR CO_2 Sensor." *http://www.co2meter.com/collections/co2-sensors/products/s8-miniature-co2-sensor*

[56] International Light TECHNOLOGIES. "Light Sources for use in NDIR Gas Sensors." *http://www.intl-lighttech.com/applications/light-sources/ndir-gas-sensor-lamps*

[57] *https://en.wikipedia.org/wiki/Nondispersive_infrared_sensor*

[58] Cheeke, J. D. N., and Z. Wang. "Acoustic wave gas sensors." *Sensors and Actuators B: Chemical* 59.2 (1999): 146-153.

[59] Bill Drafts. "Acoustic Wave Technology Sensors." sensors ONLINE. October 1, 2000 *http://www.sensorsmag.com/sensors/acoustic-ultrasound/acoustic-wave-technology-sensors-936*

[60] Micronas. "Capacitive Coupled Field Effect Transistor sensor." *http://www.micronas.com/en/products/gas-sensors*

[61] ThermoSCIENTIFIC. "MIRAN SapphIRe Portable Ambient Analyzers." *http://www.thermoscientific.com/en/product/miran-sapphire-portable-ambient-analyzers-1.html*

[62] American Society for Mass Spectrometry. "About mass Spectrometry." *http://www.asms.org/about/about-mass-spectrometry*

[63] ThermoSCIENTIFIC. "Mass Spectrometry." *http://www.thermoscientific.com/content/tfs/en/products/mass-spectrometry.html*

[64] "Gas Chromatography." *http://www.gas-chromatography.net/*

[65] CBRNE TECH INDES. "Flame photometric Detection (FPD)." *http://www.cbrnetechindex.com/Chemical-Detection/Technology-CD/Sensors-CD-T/Flame-Photometric-Detection-CD-S*

[66] Center for Public Environmental Oversight "Photo Ionization Detector." *http://www.cpeo.org/techtree/ttdescript/photion.htm*

[67] ION science. "Tiger Handheld VOC Gas Detector." *http://www.ionscience.com/products/tiger-handheld-voc-gas-detector*

[68] LCGC magazine. "The Flame Ionization Detector." *http://www.chromatographyonline.com/flame-ionization-detector*

[69] GOW-MAC Instrument. "The Thermal Conductivity Detector (TCD)." *http://www.gow-mac.com/Products/GCDetectorsandFilaments/ThermalConductivityDetectors/TCDsGeneral.aspx*

[70] Bondavalli, Paolo, Pierre Legagneux, and Didier Pribat. "Carbon nanotubes based transistors as gas sensors: state of the art and critical review." *Sensors and Actuators B: Chemical* 140.1 (2009): 304-318.

[71] VAPORSENS. "vSENS conductive polymer electronic nose." *http://www.vaporsens.com/gas-vapor-sensors/*

[72] Environics. "Chemical detection (AIMS)." *http://www.environics.fi/technologies/chemical-detection/*

[73] RAE SYSTEMS. "MultiRAE Datasheet." *http://www.raesystems.com/customer-care/resource-center/multirae-datasheet*

[74] D. Colinetlagneaux and J. Troquet, "Development of Gaseous Composition of Exhaled Air in Man during Calm and Forced Breathing," *Archives Internationales De Physiologie Et De Biochimie,* vol. 80, pp. 775-+, 1972.

[75] G. M. Saidel and J. S. Lin, "Transport Abnormalities from Single-Breath Dynamics of Ar, Co2 and O2," *Respiration Physiology,* vol. 64, pp. 253-266, Jun 1986.

[76] S. J. Aukburg, G. R. Neufeld, S. Levine, and P. W. Scherer, "Effective Diffusing Area (Eda) Derived from Single Breath O-2 and Co-2 Exhalation Curves Compared," *Federation Proceedings,* vol. 44, pp. 1581-1581, 1985.

[77] J. H. Wang, S. G. Wang, T. F. Zhang, and F. Battaglia, "Assessment of single-sided natural ventilation driven by buoyancy forces through variable window configurations," *Energy and Buildings,* vol. 139, pp. 762-779, Mar 15 2017.

[78] E. ToolBox. (2004, 1/08/2019). Carbon Dioxide Concentrations in Rooms with People. Available: https://www.engineeringtoolbox.com/pollution-concentration-rooms-d_692.html

[79] A. A. Shusterman, V. E. Teige, A. J. Turner, C. Newman, J. Kim, and R. C. Cohen, "The BErkeley Atmospheric CO2 Observation Network: initial evaluation," *Atmospheric Chemistry and Physics,* vol. 16, pp. 13449-13463, Oct 31 2016.

[80] https://en.wikipedia.org/wiki/Respiratory_rate

[81] https://en.wikipedia.org/wiki/Spirometry

[82] http://posizyr.prv.pl/baby-development-chart-in-whoom.php

[83] http://www.chartsgraphsdiagrams.com/HealthCharts/weight-birth-36-boys.html

[84] http://www.ichartmybaby.com/

[85] http://www.weightcruncher.com/height-and-weight-charts.html

[86] http://halls.md/average-weight-women/

[87] http://forum.bulletproofexec.com/index.php?/topic/14425-frame-sizes-body-shape-in-people/

[88] Brimblecombe, P. *Air: Composition & Chemistry*; Cambridge Cambridgeshire; Cambridge University Press: New York, NY, USA, 1986.

[89] Colinetlagneaux, D.; Troquet, J. Development of Gaseous Composition of Exhaled Air in Man during Calm and Forced Breathing. *Arch. Int. Physiol. Biochim.* 1972, *80*, 775.

[90] Saidel, G.M.; Lin, J.S. Transport Abnormalities from Single-Breath Dynamics of Ar, CO_2 and O_2. *Respir. Physiol.* 1986, *64*, 253–266.

[91] Shusterman, A.A.; Teige, V.E.; Turner, A.J.; Newman, C.; Kim, J.; Cohen, R.C. The BErkeley Atmospheric CO2 Observation Network: Initial evaluation. *Atmos. Chem. Phys.* 2016, *16*, 13449–13463.

[92] http://www.aqua-calc.com/page/density-table/substance/aluminum

[93] http://cdiac.ornl.gov/pns/current_ghg.html

[94] https://en.wikipedia.org/wiki/Atmosphere_of_Earth

[95] https://www.easycalculation.com/medical/pressure-of-inspired-oxygen.php

[96] https://books.google.gr/books?id=E8ZkDAAAQBAJ&pg=PA71&lpg=PA71&dq=nh3+concentration+sea+level&source=bl&ots=m8XK0imdi1&sig=1uuLgBBm-nCPZUetXD8oY38KODQ&hl=el&sa=X&ved=0ahUKEwim-oa45enQAhVC7xQKHShnBpcQ6AEIHzAA#v=onepage&q=nh3%20concentration%20sea%20level&f=false

[97] https://en.wikipedia.org/wiki/Carbon_monoxide

[98] https://en.wikipedia.org/wiki/Hydrogen_sulfide

[99] http://cdiac.ornl.gov/pns/current_ghg.html

[100] https://en.wikipedia.org/wiki/Dew_point

[101] http://www.citytech.com.cn/PDF-Datasheets/4p75.pdf

[102] https://www.tb-weeze.de/en/

[103] (1963), Conversion Factors. *Weed Research*, 3: 78. doi: 10.1111/j.1365-3180.1963.tb00225.x

12.APPENDIX: ATMOSPHERIC AIR CONSTITUENTS –SUPPLEMENTARY DATA

12.1. Conversion factors for converting parts per million for some constituents

In the referenced work, conversion factors for converting parts per million to ugm-3 at 0°C can be found. The weight is that of the total molecule, except where marked otherwise. These conversion factors can be corrected for different temperatures by multiplying K by 273/T, where T is the absolute temperature [103]

The general form to convert between volume concentration and mass concentration for gas mixtures is the following

ppm = (mg/m3 value)(24.45)/(molecular weight)
mg/m3 = (ppm value)(molecular weight)/24.45
24.45 is a conversion factor that represents the volume of one mole of gas.
To determine the molecular weight of a particular substance, add the atomic weights (look at the MSDS of the particular substance) of each atom present in the chemical formula of that particular substance.
Note: This calculation assumes a temperature of 25°C (77°F) and a pressure of 1 atmosphere (760 torr or 760 mm Hg).

13.APPENDIX: ADVANCED LOGIC UNIT - LOGIC TABLES

The advanced logic unit's task is to generate the alarms and indicators. The alarms and indicators that are presented to the user are limited to those requested by the end-users. Other conditions or states are detected and can be distinguished by the logic. The classification of the measurements is based on logic operations that would be performed by an experienced scientist when investigating the available measurements. The methodology has similarities with fuzzy logic in the sense that the measurements are organized in ranges, for example- Zero, Low, High. A range description value is assigned to each individual sensor. For every alarm and indicator, the range description of the sensors that can provide information about that alarm or indicator are evaluated. The evaluation is based on deterministic logic functions and the output of the evaluation is also a range description for that alarm or indicator. The logic provides an output for all the possible combinations of inputs which affect that alarm or indicator. The logic is designed to anticipate not optimal operating conditions, and detect when sources of interference are present. The logic can be changed without having to recompile the code (Human indicator only) since some cases are ambiguous. No training or optimization procedure is required for new sensors other than initial calibration (standard procedure for gas monitors). Training of the system is required at the site of an operation just before deployment in the sense of collecting enough measurements to determine the background levels. This sampling is automated and relatively quick. The thresholds for most of the description values for the zero range are determined this way. The typical criteria is average + 3*standard deviation.

The advanced logic unit implemented logic is listed in the following tables:

The following table lists a sample of the Logic implemented for the Human presence Indicator.

Table 70: Implemented logic for generating the Human Indicator

Indication strength (zero/weak/ strong)	CO_2 (noise, signal, toxic)	O_2 (zero, signal, noise, warning, toxic)	NH_3 (zero, signal)	CO (low, toxic)	H_2S (low, toxic)	Combustibles (zero, signal)	Humidity (normal, high)	Pressure (low, normal, high)	Temperature - System (low, normal, high)	Temperature - Environment (low, working conditions, high = above 40(°C)	Comments
Zero	noise	noise	noise	x	x	x	x	X	normal	x	**normal state (when no human exists in the vicinity we should be here)**
Weak	signal	noise	noise	x	x	x	x	X	normal	x	transition state. CO_2 is more likely to react faster than O_2 to a change
Zero	toxic	noise	noise	x	x	x	x	X	normal	x	undefined combination (unlikely high concentration of CO_2 in an otherwise normal environment)
Weak	noise	signal	noise	x	x	x	x	X	normal	x	undefined combination
Strong	signal	signal	noise	x	x	x	x	X	normal	x	indication for human presence from both CO_2 and O_2
Weak	toxic	signal	noise	x	x	x	x	X	normal	x	high CO_2 with reduced O_2. slight chance of human and/or fire far from the e-nose
Zero	noise	zero	noise	x	x	x	x	X	normal	x	undefined combination
Weak	signal	zero	noise	x	x	x	x	X	normal	x	undefined combination
Zero	toxic	zero	noise	x	x	x	x	X	normal	x	if human presence exists, then they wouldn't be alive due to O_2 and CO_2
Zero	noise	warning	noise	x	x	x	x	X	normal	x	likely to occur only near O_2 generators
Weak	signal	warning	noise	x	x	x	x	X	normal	x	undefined combination (unlikely high concentration of CO_2 and O_2)
.	.	.	.	.	.	.	.	.	.	.	.
.	.	.	.	.	.	.	.	.	.	.	.
.	.	.	.	.	.	.	.	.	.	.	.
Zero	toxic	warning	signal	x	x	x	x	X	high	x	undefined combination (unlikely high concentration of CO_2 and O_2 in heated environment)
Zero	noise	toxic	signal	x	x	x	x	X	high	x	undefined combination
Weak	signal	toxic	signal	x	x	x	x	X	high	x	undefined combination
Zero	toxic	toxic	signal	x	x	x	x	X	high	x	undefined combination
Zero	x	x	x	x	x	x	x	X	low	x	**manifold is warming up. Human indicator is silenced during this time.**

.

The following table lists a sample of the Approaching (Trend) Indicator logic.

Table 71: Implemented logic for generating the Approaching (Trend) Indicator

Indication strength (zero/weak/strong)	CO_2 (increasing, steady, decreasing)	O_2 (increasing, steady, decreasing)	NH_3 (increasing, steady, decreasing)	CO (low, toxic)	H_2S (low, toxic)	Combustibles (zero, signal)	Humidity (increasing, steady, decreasing)	Pressure (low,normal, high)	Temperature - system(low,normal, high)	Temperature - Environment (increasing, steady, decreasing)	comment / scenario (approaching or moving away)
zero	steady	steady	Steady	x	x	x	steady	X	x	steady	no change (near victim/in victims cavity OR nowhere near any victim)
zero	increasing	steady	Steady	x	x	x	steady	X	x	steady	approaching
zero	decreasing	steady	Steady	x	x	x	steady	X	x	steady	moving away
zero	steady	increasing	Steady	x	x	x	steady	X	x	steady	moving away
zero	increasing	increasing	Steady	x	x	x	steady	X	x	steady	conflicting
weak	decreasing	increasing	Steady	x	x	x	steady	X	x	steady	moving away
zero	steady	decreasing	Steady	x	x	x	steady	X	x	steady	approaching
.	.	.	.	.	.	.	.	.	.	.	.
.	.	.	.	.	.	.	.	.	.	.	.
.	.	.	.	.	.	.	.	.	.	.	.
zero	Increasing	increasing	decreasing	x	x	x	decreasing	X	x	decreasing	conflicting
strong	Decreasing	increasing	decreasing	x	x	x	decreasing	X	x	decreasing	moving away (strongest possible insurance)
strong	Steady	decreasing	decreasing	x	x	x	decreasing	X	x	decreasing	moving away
zero	Increasing	decreasing	decreasing	x	x	x	decreasing	X	x	decreasing	conflicting
zero	Decreasing	decreasing	decreasing	x	x	x	decreasing	X	x	decreasing	conflicting

The following table lists the hot spot (Edge) Indicator logic.

Table 72: Implemented logic for generating the Hot spot (Edge) indicator.

Indication strength (zero/weak/strong)	CO_2 (no peak, peak)	O_2 (no crest, crest)	NH_3 (no peak, peak)	CO (no peak, peak)	H_2S (no peak, peak)	Combustibles (no peak, peak)	Humidity (no peak, peak)	Pressure (no peak, peak)	Temperature – system (no peak, peak)	Temperature - Environment (no peak, peak)	comment / scenario (approaching or moving away)
zero	no peak	no crest	no peak	x	X	x	x	X	x	x	
strong (peak)	Peak	x	Peak	x	X	x	x	X	x	x	either sensor that gets a peak, triggers the edge alarm
strong (crest)	X	crest	X	x	X	x	x	X	x	x	the only sensor that can get a significant crest is the O_2

The following table lists the Toxic Alarm logic.

Table 73: Implemented logic for generating the Toxic Alarm

Indication strength (zero/weak/strong)	CO_2 (noise, signal, toxic)	O_2 (zero, signal, noise, warning, toxic)	NH_3 (zero, signal)	CO (zero, low, toxic)	H_2S (zero, low, toxic)	Combustibles (zero, low, signal)	Humidity (normal ,high)	Pressure (low, normal, high)	Temperature – system (low, normal, high)	Temperature - Environment (low, normal, high)	comment / scenario (approaching or moving away)
strong	Toxic	toxic	X	toxic	toxic	x	x	X	x	x	if any sensor reports in the toxic zone, the indicator is triggered
weak	X	warning	X	low	low	x	x	X	x	x	if any sensor reports in the weak (warning or low) zone, the indicator is triggered
zero	non toxic	non toxic	X	non-toxic	non-toxic	x	x	X	x	x	

The following table lists the Combustibles Alarm logic.

Table 74: Implemented logic for generating the Combustibles Alarm.

Indication strength (zero/weak/strong)	CO$_2$ (noise, signal, toxic)	O$_2$ (zero, signal, noise, warning, toxic)	NH$_3$ (zero, signal)	CO (zero, low, toxic)	H$_2$S (zero, low, toxic)	Combustibles (zero, low, signal)	Humidity (normal ,high)	Pressure (low, normal, high)	Temperature – system (low, normal, high)	Temperature - Environment (low, normal, high)	comment / scenario (approaching or moving away)
zero	X	zero	X	x	x	zero	x	X	x	x	
zero	X	signal	X	x	x	zero	x	X	x	x	
zero	X	noise	X	x	x	zero	x	X	x	x	
zero	X	warning	X	x	x	zero	x	X	x	x	
weak	X	toxic	X	x	x	zero	x	X	x	x	flammable indicator is not triggered but there is high O$_2$ concentration (>30%)
strong	X	x	X	x	x	signal	x	X	x	x	flammable indicator is triggered
weak	X	signal	X	x	x	low	x	X	x	x	flammable indicator is triggered
weak	X	noise	X	x	x	low	x	X	x	x	flammable indicator is triggered
Weak	X	warning	X	x	x	low	x	X	x	x	flammable indicator is triggered
Weak	X	toxic	X	x	x	low	x	X	x	x	flammable indicator is triggered

14.APPENDIX: ELECTRONIC NOSE SENSOR POISONS AND CONTAMINANTS

Sensor Poisons and Contaminants

Several cleaners, solvents and lubricants can contaminate and cause permanent damage to sensors. Before using cleaners, solvents, and lubricants in close proximity to the device, read the following caution and table. **Caution: Use only the following products and procedures recommended:**

- **Use water-based cleaners.**
- **Use non-alcohol-based cleaners.**
- **Clean the exterior with a soft, damp cloth.**
- **Do not use soaps, polishes, or solvents.**

The following table lists common products to avoid using around sensors:

Cleaners and Lubricants	**Silicones**	**Aerosols**
Brake cleaners	Silicone cleaners and protectants	Bug repellents and sprays
Lubricants	Silicone based adhesives, sealants, and gels	Lubricants
Rust inhibitors	Hand/body and medicinal creams that contain silicone	Rust inhibitors
Window and glass cleaners	Tissues containing silicone	Window cleaners
Dish soaps Mold releasing agents	Mold releasing agents	
Citrus-based cleaners	Polishes	
Alcohol-based cleaners		
Hand sanitizer		
Anionic detergents		
Methanol (fuels and antifreezes)		

15.APPENDIX: A COST ESTIMATION FOR THE e-nose DEVICE

The cost of a single electronic nose is calculated based on the estimation for the cost of the individual components when having low volume manufacturing in mind (<100). The following table lists the component categories and their cost. The labor and cost of procurement is not included in the following estimation.

Table 75. e-nose cost estimation

Component Category	Cost	Units	Notes
TOTAL (Materials)	3500	€	Assembly labor not included
Assembly	7	Days	1 person (can be improved)
Testing (LAB)	1000	€	More data points than simple Calibration requires
Licenses (commercial use)	300	€	License for software module - per device

These components are acquired from multiple manufactures and suppliers (more than 10). Better prices could be achieved if larger quantities (100+) were to be manufactured.